ZooKeys 1232: 1–95 (2025)
DOI: 10.3897/zookeys.1232.143989

Research Article

Progress toward a list of saproxylic beetles (Coleoptera) in the southeastern USA

Clayton R. Traylor[1,2], Michael D. Ulyshen[3], J. Winston Cornish[1], Gabriel Tigreros[1,4], Joseph V. McHugh[1]

1 *Department of Entomology, University of Georgia, Athens, GA 30602, USA*
2 *Department of Biology, Temple University, Philadelphia, PA 19130, USA*
3 *USDA Forest Service, Southern Research Station, Athens, GA 30602, USA*
4 *The Jones Center at Ichauway, Newton, GA 39870, USA*
Corresponding author: Clayton R. Traylor (clayton.r.traylor@gmail.com)

Abstract

Deadwood-dependent (saproxylic) insects represent a large proportion of forest biodiversity, are major contributors to ecosystem processes, and are conservation priorities due to their sensitivity to changing forest conditions. Despite relevance across much of the world, research on saproxylic biodiversity has been concentrated in Europe where interest was first generated. A major impediment for this field elsewhere is a lack of resources to determine which species are saproxylic. Here, we attempt to facilitate research on saproxylic beetles (Coleoptera) in the southeastern USA by compiling information from 18 published studies and theses in the region. A list of 1,393 taxa (species or genera) from 74 families is provided with deadwood associations. This includes 891 taxa from 71 families that were reared or emerged from deadwood, and 831 taxa from 61 families that were collected from bulk trapping methods and considered to be saproxylic, or were previously included in a list of regional deadwood taxa. Additionally, for 293 taxa from non-economically important families that were considered to be saproxylic in a recently published study, known saproxylic habits, microhabitat associations, and conservation notes are listed. Sixty-eight of these species represent new state records in Georgia, USA. Although a checklist of saproxylic species is needed for the southeastern USA, it is precluded by a dearth of knowledge about the natural history and distribution of species in the region. Increasing our understanding of these species' habitat requirements is essential for understanding biodiversity responses to changing forest conditions and assessing conservation needs.

Key words: Coastal Plain, forest entomology, forest management, oak-pine forest, Piedmont, southern Appalachian Mountains, southern pine forest

Academic editor: Christopher Majka
Received: 9 December 2024
Accepted: 21 February 2025
Published: 14 March 2025

ZooBank: https://zoobank.org/E7F3DF85-80E1-41FB-8DB4-25E9460FCC9F

Citation: Traylor CR, Ulyshen MD, Cornish JW, Tigreros G, McHugh JV (2025) Progress toward a list of saproxylic beetles (Coleoptera) in the southeastern USA. ZooKeys 1232: 1–95. https://doi.org/10.3897/zookeys.1232.143989

Introduction

Saproxylic insects, those dependent on deadwood and associated resources for all or part of their life-cycle, are important contributors to ecosystem processes and account for a large portion of biodiversity within forests (Stokland et al. 2012). Many of these species aid in wood decomposition and nutrient cycling within forests (Ulyshen 2016), although assemblages are composed of species occupying a variety of functional roles, including phloeophages, xylophages, mycophages, and predators (Ulyshen and Šobotník 2018). Outside of deadwood, many saproxylic insects additionally perform, or are involved in, other ecosystem processes, such as pollination (Ulyshen et al. 2023). Estimates from northern and central Europe suggest that saproxylic species comprise approximately 20–25% of all invertebrates within forests (Siitonen 2001; Graf et al. 2022), although estimates are higher within some taxonomic groups (e.g., 42–65% for Coleoptera; Köhler 2000; Martikainen et al. 2000; Stenbacka et al. 2010; Gibb et al. 2013). Furthermore, many species facultatively use deadwood, increasing the proportion of forest invertebrate species utilizing this resource to 50–70% (Graf et al. 2022). Outside of Europe, the proportion of saproxylic species within forests has only been estimated for Coleoptera in the Atlantic Canada region: 63–79% (Majka 2009). Although saproxylic species occur in most insect orders (Ulyshen 2018), beetles (Coleoptera) are the most studied due to their taxonomic and ecological diversity (Gimmel and Ferro 2018).

Since the seminal work of Speight (1989) documenting the decline of saproxylic insects from intensive forest management and land-use change across Europe, great attention has been devoted to assessing the conservation status of saproxylic insects in the region (Seibold et al. 2015a; Cálix et al. 2018; Hagge et al. 2021) and documenting their basic habitat requirements and ecology (Siitonen and Saaristo 2000; Harvey et al. 2011; Horák et al. 2011; Lindman et al. 2023). Saproxylic communities are sensitive to the amounts and diversity of deadwood resources, and the quality and age of forest habitat more generally (Stenbacka et al. 2010; Gibb et al. 2013; Janssen et al. 2016, 2017; Seibold et al. 2016, 2017). Thus, much effort has been spent developing forest management practices that benefit these species, including deadwood retention or imitation of natural tree mortality dynamics (Thorn et al. 2014; Gossner et al. 2016; Heikkala et al. 2016; Roth et al. 2019; Ekström et al. 2021). Moreover, minimum thresholds of deadwood volume, under which certain species decline, have been determined for certain forest types (Müller and Bütler 2010; Lachat et al. 2012; Gossner et al. 2013). Overall, these efforts have provided evidence-based recommendations for saproxylic insect conservation in Europe.

Although saproxylic insects throughout the world are facing threats of deforestation and intensive forest management, research has been concentrated in Europe where awareness was first generated. But interest is rising in other regions where forests are the dominant vegetation (Davies et al. 2008; Seibold et al. 2015b). For example, researchers in Canada have devoted effort to this field (reviewed in Langor et al. 2008) and have produced conservation-priority lists of saproxylic species (Majka 2007). Similarly, there has been an increase in attention in the southeastern USA to assess host usage and habitat quality (e.g., Campbell et al. 2008a, b; Ulyshen and Hanula 2009a, 2010; Klepzig et al. 2012; Ferro et al. 2012a, b; Traylor et al. 2022a, 2023a, 2024). A global representation of saproxylic research is needed, as deadwood dynamics—to which saproxylic fauna are adapted—vary regionally from climatic and biotic differences (e.g., temperature and termites; Zanne et al. 2022), and the ecological relationships that guide conservation recommendations may change from these biogeographical differences. For example, the relationship between saproxylic insect biodiversity and deadwood volume may change in different climates (Lassauce et al. 2011; Lachat et al. 2012; Seibold and Thorn 2018), as ectothermic larvae can develop within smaller amounts of deadwood in warmer climates (Müller et al. 2015). Thus, it is important for management recommendations to be developed separately for each region based on the sensitivities and ecological roles of the endemic fauna within the context of local climatic conditions.

A major impediment to studying saproxylic insect biodiversity is simply recognizing which species are saproxylic. Decisions about inclusion or exclusion of species from analyses of saproxylic communities may influence the results, as well as the management practices drawn from them. This problem is especially relevant when biodiversity is assessed from trap samples, which collect a wider range of species and functional guilds than sampling directly from substrates (Micó et al. 2020). Currently, regional checklists of saproxylic species have been produced for Europe (Köhler 2000; Schmidl and Bußler 2004) and portions of Canada (e.g., Majka and Pollock 2006; Majka 2007; references cited in Langor et al. 2008). Additionally, resources are available for a few better-known and economically important insect groups in the USA, such as bark beetles (Curculionidae: Scolytinae; Wood 1982), woodboring beetles (Cerambycidae; Lingafelter 2007), and jewel beetles (Buprestidae; Nelson et al. 2008). Aside from these examples, few resources are available to aid in this task in North America as regional checklists with annotated saproxylic associations simply do not exist. Thus, studies of saproxylic biodiversity using trap samples are burdened with finding scattered primary literature documenting the natural history of each species (if any exist). Otherwise, decisions about saproxylic status must be presumed based on current classification and patterns of known natural history for congeneric or confamilial species.

Here, we provide two resources to aid research on saproxylic beetles in the southeastern USA. First, from published studies or theses in the southeastern region, we provide a list of taxa (species or genera) that either 1) emerged or were hand-collected directly from deadwood, 2) were considered to be saproxylic based on a classification process, or 3) were previously included in a regional list of common deadwood taxa. Secondly, we provide a summary of the known deadwood associations of 293 taxa from non-economically important families collected in a survey of saproxylic beetles in Georgia, USA (Traylor et al. 2023a). These resources should facilitate studies of saproxylic biodiversity in the southeastern USA and elsewhere in North America and form the foundation for a regional saproxylic checklist.

Methods

Saproxylic definition

The definition of “saproxylic” has evolved over time to fit a growing understanding of deadwood resources and the species that depend on them (Alexander 2008; Graf et al. 2022). Today, a saproxylic species is considered “any species that depends, during some part of its life cycle, upon wounded or decaying woody material from living, weakened or dead trees” (Stokland et al. 2012: 6). In addition to species dependent on wood, this definition broadly includes species dependent on non-wood resources found in or on living, weakened, or dead trees, such as the inner bark (phloem), sap runs, or slime fluxes in tree wounds. While it may seem bizarre for saproxylic species to use resources in living trees, it is widely recognized that important microhabitats can occur and accumulate over a tree's life, such as dead branches in the canopy or interior rot forming tree hollows (Micó 2018; Seibold et al. 2018). Additionally, this definition includes species that depend indirectly on saproxylic resources. For example, species dependent on wood-decaying fungi are considered saproxylic, as well as species representing higher trophic levels (e.g., predators, parasitoids, and parasites) that are dependent on other saproxylic species as hosts or prey (Stokland et al. 2012). Moreover, species that do not consume wood or other saproxylic organisms may still be saproxylic, such as bees that nest in deadwood or tree cavities (Ulyshen 2018).

An important distinction exists between species that are obligately dependent on deadwood and associated resources, versus those that use these habitats facultatively. In general, saproxylic species are those that are obligately dependent, and thus would disappear if those resources were removed from forests (Stokland et al. 2012). However, distinguishing facultative or obligative use of deadwood (i.e., non-saproxylic vs saproxylic) can be difficult and largely depends on incomplete information known about a species' biology.

List of saproxylic Coleoptera compiled from previous studies

From 18 published studies and theses in the southeastern USA (Table 1), we compiled a list of coleopteran taxa (species and genera) that either 1) emerged or were hand-collected directly from deadwood, 2) were considered saproxylic following some explicit determination process, or 3) were included in a previous regional list of common deadwood insects. Fifteen of these studies provided species lists of Coleoptera that either emerged or were hand-collected directly from deadwood in experimental methods (Table 1). Two studies provided lists of species that were considered to be saproxylic after a determination process. Klepzig et al. (2012) used pitfall trapping to collect insects and considered beetle species as saproxylic, non-saproxylic ground beetles, or other based on familiarity with the taxa and published natural history. Traylor et al. (2023a) collected beetles with flight intercept traps and litter-sifting and classified the collected species as saproxylic or not (see below). Finally, one study created a list of wood-feeding beetles that are commonly collected in the southern USA (Hanula 1996). Many other, often older, publications provide accounts of deadwood associations based on field observations (e.g., Savely 1939; Howden and Vogt 1951), but those are not included here. Other studies assumed saproxylic status based on the known natural history of closely related taxa, but did not go through any explicit determination process (e.g., Campbell et al. 2008a, b); therefore, they were not included.

Only species or generic determinations (including subgeneric distinctions, when possible) were included in our lists; morphospecies at the tribe, subfamily, or family rank were excluded. We checked the validity of all taxonomic names using the Integrated Taxonomic Information System (www.ITIS.gov), or with the most recent taxonomic revision of the group or other published literature.

Table 1. Experimental studies providing species lists of Coleoptera with deadwood associations. Coleoptera were emergent from deadwood (method = E), hand-collected from deadwood (H), or classified (C) as saproxylic in the southeastern United States. The state(s) and ecoregion(s) sampled from each study are provided. Level III Ecoregions follow https://www.epa.gov/eco-research/ecoregions-north-america. The list of Coleoptera can be found in Suppl. material 1.

Study	State	Type III Ecoregion(s)	Method
Ferro and Gimmel 2014	LA	8.3.6 (Mississippi Valley Loess Plains)	E
Ferro and Nguyen 2016	LA	8.3.5 (Southeastern Plains); 8.3.6 (Mississippi Valley Loess Plains); 8.3.7 (South Central Plains); 8.5.2 (Mississippi Alluvial Plain); 8.5.3 (Southern Coastal Plain); 9.5.1 (Western Gulf Coastal Plain)	E
Ferro et al. 2009	LA	8.3.6 (Mississippi Valley Loess Plains)	E
Ferro et al. 2012a	TN	8.4.4 (Blue Ridge)	E
Ferro et al. 2012b	TN	8.4.4 (Blue Ridge)	E
Garrick et al. 2019	AL, NC, TN	8.4.4 (Blue Ridge); 8.4.9 (Southwestern Appalachians)	H
Gil 2008	LA	8.3.6 (Mississippi Valley Loess Plains)	H
Hanula 1996	southern region		C
Klepzig et al. 2012	LA, MS, NC, TX	8.3.5 (Southeastern Plains); 8.3.7 (South Central Plains); 8.5.1 (Middle Atlantic Coastal Plain)	C
Tigreros 2024	GA	8.3.5 (Southeastern Plains)	E
Traylor et al. 2023a	GA	8.3.4 (Piedmont)	C
Ulyshen 2014	MS	8.3.5 (Southeastern Plains)	E
Ulyshen and Hanula 2009a	SC	8.3.5 (Southeastern Plains)	E
Ulyshen and Hanula 2009b	SC	8.3.5 (Southeastern Plains)	E
Ulyshen and Hanula 2010	SC	8.3.5 (Southeastern Plains)	E
Ulyshen et al. 2010	GA	8.3.4 (Piedmont)	E
Ulyshen et al. 2020	MS	8.3.5 (Southeastern Plains)	E
Ulyshen et al. 2024	SC	8.3.5 (Southeastern Plains)	E

Annotated list of saproxylic Coleoptera

We summarized saproxylic habits of 293 coleopteran taxa considered to be saproxylic from Traylor et al. (2023a). Briefly, from March–September 2020 in Clarke County, Georgia, USA, beetles were collected from forests using two methods: 1) a flight intercept trap (two clear, intersecting panels attached over a white bucket) suspended 5 m aboveground and baited with ethanol, and 2) leaf litter sifting and extraction via a Berlese funnel (see Traylor et al. 2022b, 2023a for details). For each species, we provide summary statistics of collection data. Full data of species' abundance per sampling location, species' abundance per sampling period for each collection method, and forest details are publicly available at a repository (Traylor et al. 2023b).

The saproxylic determination process was as follows. Species were identified and considered as saproxylic or not based on known natural history information indicating that they either develop in, or are primarily found within, deadwood or other saproxylic habitats. We used Gimmel and Ferro (2018) to exclude some families and subfamilies from saproxylic consideration. Species and morphospecies with no known natural history information were also considered saproxylic if all their congeners with known natural history could be considered saproxylic. See Traylor et al. (2023a) for more information.

Here, we assembled known natural history information for each saproxylic species (or genus for morphospecies) based on published accounts, rearing/emergence records, or verifiable images with documented natural history information from Bugguide (www.bugguide.net). Additionally, we provide specific information on microhabitat usage (if known) and conservation notes (if applicable). Unless stated otherwise, we also provide general distributions for each species from occurrences recorded in the Global Biodiversity Information Facility (GBIF; www.gbif.org) and BugGuide (www.bugguide.net). Non-mutually exclusive distribution categories are defined as follows: the southeastern United States (Virginia south to Florida, west to Arkansas and eastern Texas), the eastern United States (Minnesota south to Louisiana, and eastward), eastern North America (the eastern United States and Canada, Ontario and eastward), central United States (the "plain states", i.e., Wisconsin south to Texas, and west to Montana and New Mexico), central North America (central United States and Canada, Manitoba west to Alberta). The assembled information is not intended to be a full review of each species' natural history. Instead, the information is meant to provide a summary of deadwood associations and saproxylic habits exhibited by each species that can be used to aid researchers in classifying species as saproxylic or not and to give some background on required habitats or wood types. Natural history information unrelated to deadwood was not included (e.g., that adult Mordellidae visit flowers). Because natural history and host record reviews already exist for economically important groups in this region, such as Buprestidae (Nelson et al. 2008), Cerambycidae (Lingafelter 2007), and Curculionidae: Scolytinae (Wood 1982), we do not include these taxa below unless they are new state records in Georgia, USA.

Results

In total, 1,393 beetle taxa (species or genera) from 74 families had deadwood associations recorded in the 18 studies or theses (Suppl. material 1). This includes 891 taxa from 71 families that were reared or emerged from deadwood, and 831 taxa from 61 families that were collected from bulk trapping methods and considered to be saproxylic or were listed as common associates of deadwood. We urge readers to be cautious in the use of this list, as some species that were reared or emerged from deadwood are likely to be facultatively saproxylic. Additionally, some taxa considered to be saproxylic could be reclassified as facultative users of deadwood if more detailed knowledge of their natural history became available and supported the change.

Below, we provide the deadwood habitat associations of 293 saproxylic beetle taxa (281 species and 12 genera for which only morphospecies were assigned) collected from 40 sites during a survey conducted in the Piedmont region of Georgia, USA (Traylor et al. 2023a). Natural history data relevant to saproxylic habits are summarized for each species, and bionomic information is included when possible. All taxa were considered obligately saproxylic, but as before, additional information learned about the listed taxa in the future may require that some be considered facultative. Sixty-eight species are new state records in Georgia, USA and have been marked as such (* indicates that museum specimens exist from Georgia, but they are not formally published: An Annotated List of the Coleoptera of Georgia, v. 1.0; https://site.caes.uga.edu/ugca/turnbow-and-smith/). Abundance for each species per site with geographic coordinates, per sampling method, and per collection date can be found in a data repository (Traylor et al. 2023b).

Aderidae

Cnopus impressus (LeConte, 1875)

Collection information. USA: **Georgia (new state record*)**: Clarke Co.: 22 individuals from 15 sites. Caught in flight trap from 6 May–27 July 2020.

Distribution. Eastern North America, possibly further west.

Saproxylic habits. Emerged from and associated with loblolly pine (*Pinus taeda* L. (Pinaceae)), also emerged from sweetgum (*Liquidambar styraciflua* L. (Altingiaceae)) (Ulyshen and Hanula 2009a); adults occur in dead tree trunks (Ciegler 2014).

Conservation. In the Piedmont, significantly associated with forests within highly forested landscapes (> 50% forest; Traylor et al. 2023a) and occurrence probability increases with the amount of landscape forest cover (Traylor et al. 2024).

Ganascus ventricosus (LeConte, 1875)

Collection information. USA: Georgia: Clarke Co.: five individuals from five sites. Caught in flight trap from 6 May–14 July 2020.

Distribution. Eastern North America.

Saproxylic habits. Emerged from loblolly pine and sweetgum logs (Ulyshen and Hanula 2009a); adults occur in rotten wood, such as black oak (*Quercus velutina* Lam. (Fagaceae)) (Palmer 2017).

Pseudariotus notatus (LeConte, 1855)

Collection information. USA: Georgia: Clarke Co.: two individuals from two sites. Caught in flight trap from 14–27 July 2020.

Distribution. Southeastern United States.

Saproxylic habits. Emerged from loblolly pine, including logs dead for five years, as well as burned and unburned logs (Ulyshen and Hanula 2010; Ulyshen et al. 2010).

Anamorphidae

Genus *Anamorphus* LeConte, 1878

Collection information. USA: Georgia: Clarke Co.: two individuals from two sites. Caught in flight trap from 19 May–14 July 2020. Specimens unable to be identified to species.

Saproxylic habits. Species of *Anamorphus* have emerged from hardwood twigs (*Anamorphus waltoni* Blatchley, 1918) (Ferro and Nguyen 2016).

Clemmus minor (Crotch, 1873)

Collection information. USA: Georgia: Clarke Co.: a single individual from one site. Caught in flight trap from 21 April–6 May 2020.

Distribution. Southeastern and central United States.

Saproxylic habits. Emerged from hardwood twigs (Ferro and Nguyen 2016); adults occur under and inside fallen, rotting logs (Gruber 2008).

Micropsephodes lundgreni Leschen and Carlton, 2000

Collection information. USA: Georgia: Clarke Co.: seven individuals from five sites. Caught in flight trap from 21 April–26 August 2020.

Distribution. Southeastern United States.

Saproxylic habits. Emerged from sweetgum logs and snags (standing dead trees) (Ulyshen and Hanula 2009a), recently dead coarse woody debris (Ferro et al. 2012a), and twig bundles of southern red oak (*Quercus falcata* Michx.) (Ferro and Gimmel 2014); for more information see Shockley et al. (2008).

Anthribidae

Choragus zimmermanni LeConte, 1876

Collection information. USA: **Georgia (new state record)**: Clarke Co.: two individuals from two sites. Caught in flight trap from 16 June–14 July 2020.

Distribution. Eastern North America (Valentine 1998).

Saproxylic habits. Breed in deadwood, such as sweetgum (Brues 1927); species of *Choragus* Kirby, 1819 feed on ascomycete fungi (Xylariaceae and Diatrypaceae) (Valentine 1998).

Euparius marmoreus (Olivier, 1795)

Collection information. USA: Georgia: Clarke Co.: a single individual from one site. Caught in flight trap from 27 July–11 August 2020.

Distribution. Eastern and central North America.

Saproxylic habits. Feeds on a variety of polypore fungi, including *Trametes* Fr. (Polyporaceae), *Megasporoporia setulosa* (Henn.) (Polyporaceae), *Trichaptum* Murrill (Hymenochaetales), *Scopuloides hydnoides* (Cooke and Massee) Hjortstam and Ryvarden (Meruliaceae), *Panus rudis* Fr. (Polyporaceae), and *Perenniporia medulla-panis* (Jacq.) Donk (Polyporaceae) (Valentine 1998).

Eusphyrus walshi LeConte, 1876

Collection information. USA: Georgia: Clarke Co.: eight individuals from six sites. Caught in flight trap from 19 May–9 September 2020.

Distribution. Eastern North America.

Saproxylic habits. Emerged from poison ivy vines (*Toxicodendron* Mill. (Anacardiaceae), and adults occur on dead hardwood branches and under bark, such as oak (*Quercus* L.) (Valentine 1998).

Euxenus jordani Valentine, 1991

Collection information. USA: **Georgia (new state record)**: Clarke Co.: two individuals from a single site. Caught in flight trap from 2 June–26 August 2020.

Distribution. Eastern North America (Valentine 1998).

Saproxylic habits. Emerged from the fungus *Biscogniauxia atropunctata* (Schwein.) Pouzar (Graphostromataceae) (Valentine 1998).

Euxenus punctatus LeConte, 1876

Collection information. USA: **Georgia (new state record)**: Clarke Co.: seventeen individuals from 13 sites. Caught in flight trap from 30 June–26 August 2020.

Distribution. Eastern North America.

Saproxylic habits. Emerged from *Hypoxylon perforatum* (Schwein.) Fr. (Hypoxylaceae) and adults occur on similar fungi growing on dead branches (Valentine 1998).

Conservation. Occurrence probability increases with the amount of landscape forest cover in the Piedmont (Traylor et al. 2024).

Goniocloeus bimaculatus (Olivier, 1795)

Collection information. USA: Georgia: Clarke Co.: a single individual from one site. Caught in flight trap from 6–19 May 2020.

Distribution. Eastern North America.

Saproxylic habits. Adults occur under bark and on various fungi growing on hardwood trees, including *Biscogniauxia* Kuntze, *Xylaria* Hill ex Schrank (Xylariaceae), and *Diatrype* Fr. (Diatrypaceae) (Valentine 1998).

Ischnocerus infuscatus Fåhraeus, 1839

Collection information. USA: **Georgia (new state record*)**: Clarke Co.: three individuals from two sites. Caught in flight trap from 16 June–26 August 2020.

Distribution. Southeastern United States to Central America, and Caribbean islands.

Saproxylic habits. Emerged from deadwood of several hardwood trees, apparently without fungi (Valentine 1998).

Ormiscus saltator LeConte, 1876

Collection information. USA: **Georgia (new state record*)**: Clarke Co.: a single individual from one site. Caught in flight trap from 19 May–2 June 2020.

Distribution. Eastern North America.

Saproxylic habits. Breeds in dead wood of deciduous trees (Pierce 1930).

Piesocorynus moestus **(LeConte, 1824)**

Collection information. USA: Georgia: Clarke Co.: a single individual from one site. Caught in flight trap from 30 June–14 July 2020.

Distribution. Eastern North America.

Saproxylic habits. Adults and larvae of *Piesocorynus* Dejean, 1834 feed on various fungi in the order Xylariales (e.g., *Hypoxylon* Bull.) (Valentine 1998); adults occur on old logs and under bark (Pierce 1930).

Piesocorynus plagifer **Jordan, 1904**

Collection information. USA: Georgia: Clarke Co.: a single individual from one site. Caught in flight trap from 11–26 August 2020.

Distribution. Eastern North America into Central America.

Saproxylic habits. Adults and larvae of *Piesocorynus* feed on various fungi in the order Xylariales (e.g., *Hypoxylon*) (Valentine 1998); adults occur on fungus growing on dead tree trunks and under loose bark (Pierce 1930).

Toxonotus cornutus **(Say, 1831)**

Collection information. USA: Georgia: Clarke Co.: 10 individuals from nine sites. Caught in flight trap from 9 March–14 July 2020.

Distribution. Eastern North America.

Saproxylic habits. Bores into dead wood, such as persimmon (*Diospyros* L. (Ebenaceae)), and adults also occur on dead trees, including white oak (*Quercus alba* L.) stems (Valentine 1998).

Bostrichidae

Lichenophanes bicornis **(Weber, 1801)**

Collection information. USA: Georgia: Clarke Co.: a single specimen from one site. Caught in flight trap from 19 May–2 June 2020.

Distribution. Eastern and central North America.

Saproxylic habits. Emerged from hardwood twigs and branches (Hoffmann 1942; Ferro and Nguyen 2016); adults occur under bark of dead hardwood trees (Downie and Arnett 1996).

Conservation. Rare in the Maritime Provinces of Canada, possibly due to the history of intensive forest management in the region altering forest composition and structure (Majka 2007).

Micrapate cristicauda **Casey, 1898**

Collection information. USA: **Georgia (new state record)**: Clarke Co.: a single individual from one site. Caught in flight trap from 21 April–6 May 2020.

Distribution. Southeastern United States.

Saproxylic habits. Emerged and adults collected from dead muscadine vine (*Vitis rotundifolia* Michx. (Vitaceae)) (Fischer 1950; Beiriger 2008).

Xylobiops basilaris (Say, 1824)

Collection information. USA: Georgia: Clarke Co.: 147 individuals from 25 sites. Caught in flight trap from 9 March–9 September 2020.

Distribution. Eastern North America, west to southern California and south to Mexico.

Saproxylic habits. Larvae bore into the sapwood of a wide variety of dead and dying hardwood trees, and occasionally conifers (Solomon 1995); prefers smaller branches (Hoffmann 1942).

Bothrideridae

Bothrideres cryptus Stephan, 1989

Collection information. USA: **Georgia (new state record*)**: Clarke Co.: two individuals from two sites. Caught in flight trap from 21 April–2 June 2020.

Distribution. Eastern North America (Stephan 1989).

Saproxylic habits. Occur under the dry bark of dead oaks, where it parasitizes cerambycid larvae of the genus *Parelaphidion* Skiles, 1985 (Stephan 1989).

Bothrideres geminatus (Say, 1826)

Collection information. USA: Georgia: Clarke Co.: four individuals from four sites. Caught in flight trap from 9 March–16 June 2020.

Distribution. Eastern and central North America.

Saproxylic habits. Larvae occur under the dry bark of dead hardwood trees (Stephan 1989), parasitizing the larvae of *Chrysobothris* Eschscholtz, 1829 (Buprestidae) (Craighead 1920).

Conservation. Significantly associated with old forests (predating 1938 and oak dominated) in highly forested landscapes (> 50% forest) in the Piedmont (Traylor et al. 2023a).

Carabidae

Mioptachys flavicauda (Say, 1823)

Collection information. USA: Georgia: Clarke Co.: two individuals from two sites. Caught in flight trap from 21 April–11 August 2020.

Distribution. North America.

Saproxylic habits. Predator of small arthropods under bark (Ferro et al. 2012a); emerged from a wide variety of deadwood substrates, including logs, standing dead trees, and coarse and fine woody debris of loblolly pine, sweetgum, oak and various hardwoods (Ulyshen and Hanula 2009a; Ferro et al. 2012a; Ferro and Nguyen 2016); emerged from burned and unburned loblolly pine logs (Ulyshen et al. 2010), and loblolly pine and hardwoods across decomposition stages (Ulyshen and Hanula 2010; Ferro et al. 2012a); associated with logs and portions of standing dead trees near to the ground (Ulyshen and Hanula 2009a).

Cerambycidae

Saperda imitans Felt and Joutel, 1904

Collection information. USA: **Georgia (new state record*)**: Clarke Co.: two individuals from two sites. Caught in flight trap from 19 May–30 June 2020.

Distribution. Eastern North America.

Saproxylic habits. Larvae feed in various hardwood trees such as hickory (*Carya* Nutt. (Juglandaceae)), cherry (*Prunus* L. (Rosaceae)), and willow (*Salix* L. (Salicaceae)) (Lingafelter 2007); in black cherry (*Prunus serotina* Ehrh.), *S. Imitans* prefers larger diameter branches with phloem still present (DiGirolomo et al. 2011).

Cerylonidae

Cerylon castaneum (Say, 1826)

Collection information. USA: Georgia: Clarke Co.: four individuals from three sites. Caught in flight trap from 9 March–19 May 2020.

Distribution. Eastern North America, transcontinental in the north.

Saproxylic habits. Feed on spores and hyphae of fungi growing on and under the bark of dead trees (Lawrence and Stephan 1975); emerged from hardwood logs (Ferro et al. 2012a), and adults occur under bark after four to six years of decomposition (in hickory, Blackman and Stage 1924).

Conservation. Significantly higher abundance in primary (= old-growth) than secondary (= second-growth) forests in the southern Appalachian Mountains (Ferro et al. 2012a).

Cerylon unicolor (Ziegler, 1845)

Collection information. USA: Georgia: Clarke Co.: 13 individuals from 10 sites. Caught in flight trap from 25 March–9 September 2020.

Distribution. North America.

Saproxylic habits. Adults occur under the bark of various dead hardwood and conifer trees and on fungi, and larvae develop under the bark of hardwoods (Lawrence and Stephan 1975); emerged from loblolly pine, water oak (*Quercus nigra* L.), and especially sweetgum, and associated with portions of dead trees close to the ground (Ulyshen and Hanula 2009a).

Ciidae

Genus *Cis* Latreille, 1797

Collection information. USA: Georgia: Clarke Co.: 36 individuals from 25 sites. Caught in flight trap and sifted from leaf litter from 9 March–26 August 2020. Includes 10 morphospecies that were not determined to species-level.

Saproxylic habits. Larvae and adults live and feed on wood-decomposing bracket fungi (Thayer and Lawrence 2002); although *Cis* can be found in a wide variety of bracket fungi, species typically have a narrow range of related fungal hosts (Orledge and Reynolds 2005), and host use for North American species is reviewed in Lawrence (1973).

Genus *Octotemnus* Mellié, 1847

Collection information. USA: Georgia: Clarke Co.: three individuals from three sites. Caught in flight trap from 9 March–27 July 2020. Includes one morphospecies that was not determined to species-level.

Saproxylic habits. Larvae and adults live and feed on wood-decomposing, bracket fungi (Thayer and Lawrence 2002); most *Octotemnus* have a narrow range of related fungal hosts and fall within the *Trametes* ciid host-group (Lawrence 1973; Orledge and Reynolds 2005).

Genus *Orthocis* Casey, 1898

Collection information. USA: Georgia: Clarke Co.: a single individual from one site. Caught in flight trap from 21 April–6 May 2020. Includes one morphospecies that was not determined to species-level.

Saproxylic habits. Larvae and adults live and feed on wood-decomposing, bracket fungi (Thayer and Lawrence 2002); *Orthocis* have a narrow range of related fungal hosts and fall within the *Auricularia* Bull. (Auriculariaceae) ciid host-group (Lawrence 1973; Orledge and Reynolds 2005).

Cleridae

Chariessa pilosa (Forster, 1781)

Collection information. USA: Georgia: Clarke Co.: 25 individuals from 13 sites. Caught in flight trap from 21 April–14 July 2020.

Distribution. Eastern and central North America.

Saproxylic habits. Larvae and adults prey upon bark and woodboring beetles (Blackman and Stage 1924; Savely 1939; Hoffmann 1942); emerged from a wide variety of hardwood trees, and frequently occur on downed logs (Opitz 2017).

Conservation. Significantly associated with, and occurrence probability increases in, old forests (predating 1938 and oak dominated) in the Piedmont (Traylor et al. 2023a, 2024).

Cregya mixta (LeConte, 1866)

Collection information. USA: Georgia: Clarke Co.: 11 individuals from seven sites. Caught in flight trap from 16 June–9 September 2020.

Distribution. Eastern United States.

Saproxylic habits. Prey upon bostrichid beetles boring through dry, seasoned hardwoods, such as *Xylobiops* Casey, 1898 (Knull 1951), and occurs in association with others such as *Lyctus* Fabricius, 1792 (Opitz 2019).

Cregya oculata (Say, 1835)

Collection information. USA: Georgia: Clarke Co.: 34 individuals from 19 sites. Caught in flight trap from 19 May–26 August 2020.

Distribution. Eastern North America.

Saproxylic habits. Prey upon bark and woodboring beetles in pine (*Pinus* L. (Pinaceae)) and various hardwoods (Knull 1951; Opitz 2019).

Conservation. Occurrence probability increases with the amount of landscape forest cover in the Piedmont (Traylor et al. 2024).

Cymatodera bicolor (Say, 1825)

Collection information. USA: Georgia: Clarke Co.: a single individual from one site. Caught in flight trap from 9–21 April 2020.

Distribution. Eastern North America.

Saproxylic habits. Prey upon bark and woodboring beetles and occurs under bark of various hardwoods, including hickory, and “cedar” (presumably *Juniperus* L. (Cupressaceae)) (Hopkins 1893; Knull 1951; Dorshorst and Young 2008).

Cymatodera inornata (Say, 1835)

Collection information. USA: Georgia: Clarke Co.: three individuals from three sites. Caught in flight trap from 21 April–2 June 2020.

Distribution. Eastern United States.

Saproxylic habits. Likely a predator of woodboring beetles; it has emerged from hickory logs and oak twigs (Blackman and Stage 1924; Ferro and Gimmel 2014), and under bark of pine (Hopkins 1893).

Enoclerus ichneumoneus (Fabricius, 1777)

Collection information. USA: Georgia: Clarke Co.: 17 individuals from 13 sites. Caught in flight trap from 9 March–27 July 2020.

Distribution. Eastern North America.

Saproxylic habits. Larvae and adults prey upon bark and woodboring beetles, and occur under bark and within host galleries in a number of hardwood trees and *Juniperus* (Böving and Champlain 1920; Knull 1951).

Conservation. Occurrence probability increases in old forests (predating 1938 and oak dominated) and with the amount of landscape forest cover in the Piedmont (Traylor et al. 2024).

Enoclerus nigripes (Say, 1823)

Collection information. USA: Georgia: Clarke Co.: 10 individuals from nine sites. Caught in flight trap from 9 March–19 May 2020.

Distribution. Eastern and Central North America.

Saproxylic habits. Larvae and adults prey uopn bark and woodboring beetles and occur under bark and on logs infested with prey, including oak, hickory, cedar, spruce (*Picea* A.Dietr. (Pinaceae)), and especially pine (Knull 1951; Majka 2006; Dorshorst and Young 2008).

Conservation. Occurrence probability increases with the amount of landscape forest cover in the Piedmont (Traylor et al. 2024).

Madoniella dislocata (Say, 1825)

Collection information. USA: Georgia: Clarke Co.: 86 individuals from 31 sites. Caught in flight trap from 21 April–26 August 2020.

Distribution. Eastern North America.

Saproxylic habits. Prey upon bark and woodboring beetles, and occurs within host galleries and under bark, including a wide variety of hardwood and conifers (Knull 1951; Majka 2006; Dorshorst and Young 2008).

Conservation. Occurrence probability increases in old forests (predating 1938 and oak dominated) in the Piedmont (Traylor et al. 2024).

Neorthopleura thoracica (Say, 1823)

Collection information. USA: Georgia: Clarke Co.: 11 individuals from seven sites. Caught in flight trap from 6 May–14 July 2020.

Distribution. Eastern North America.

Saproxylic habits. Larvae and adults prey on bark and woodboring beetles in various hardwood trees, especially oak (Böving and Champlain 1920; Ulyshen and Hanula 2009a).

Conservation. Occurrence probability increases with the amount of landscape forest cover in the Piedmont (Traylor et al. 2024).

Phyllobaenus humeralis (Say, 1823)

Collection information. USA: Georgia: Clarke Co.: six individuals from two sites. Caught in flight trap from 9 April–16 June 2020.

Distribution. Eastern and central North America.

Saproxylic habits. Larvae develop within dead trees and shrubs, including oak, hickory, and sweetfern (*Comptonia peregrina* (L.) Coult. (Myricaceae))

(Pulaski 1979; Mawdsley 2002), and adults commonly occur on oak (Dorshorst and Young 2008).

Phyllobaenus pallipennis (Say, 1825)

Collection information. USA: **Georgia (new state record*)**: Clarke Co.: 40 individuals from 13 sites. Caught in flight trap from 16 June–9 September 2020.

Distribution. Eastern North America.

Saproxylic habits. Develop within branches and trunks of oaks and hickories (Mawdsley 2002).

Phyllobaenus unifasciatus (Say, 1825)

Collection information. USA: Georgia: Clarke Co.: a single individual from one site. Caught in flight trap from 6–19 May 2020.

Distribution. Eastern United States.

Saproxylic habits. Adults and larvae are predaceous on bark and woodboring beetles and occur under bark and in prey galleries primarily in hardwood trees (Böving and Champain 1920; Knull 1951; Dolphin et al. 1972; Mawdsley 2002); larvae additionally occur within woodier stem galls of cynipid wasps on oak, although food sources in this microhabitat are uncertain (e.g., Eliason and Potter 2000).

Phyllobaenus verticalis (Say, 1835)

Collection information. USA: Georgia: Clarke Co.: 65 individuals from 24 sites. Caught in flight trap from 21 April–30 June 2020.

Distribution. Eastern North America.

Saproxylic habits. Develops within and prey upon woodboring beetles in dead hardwoods (Knull 1932; Mawdsley 2002); larvae additionally occur within woodier stem galls of cynipid wasps on oak, although food sources in this microhabitat are uncertain (e.g., Eliason and Potter 2000).

Placopterus thoracicus (Olivier, 1795)

Collection information. USA: Georgia: Clarke Co.: 40 individuals from 25 sites. Caught in flight trap from 25 March–19 May 2020.

Distribution. Eastern North America.

Saproxylic habits. Larvae and adults prey upon bark beetles, woodboring beetles, and twig nesting wasps in small dead branches of hardwood trees and shrubs (Böving and Champlain 1920; Knull 1932; Foster and Barr 1972); larvae additionally occur within woodier stem galls of cynipid wasps on oak, although food sources in this microhabitat are uncertain (e.g., Eliason and Potter 2000).

Pyticeroides laticornis (Say, 1835)

Collection information. USA: Georgia: Clarke Co.: 31 individuals from 17 sites. Caught in flight trap from 9 April–26 August 2020.

Distribution. Eastern North America.

Saproxylic habits. Larvae and adults prey upon bark beetles within a variety of hardwoods and cedar (Böving and Champlain 1920; Knull 1951).

Cucujidae

Pediacus subglaber LeConte, 1854

Collection information. USA: Georgia: Clarke Co.: three individuals from three sites. Caught in flight trap from 9–25 March 2020.

Distribution. Eastern North America (Thomas 2003).

Saproxylic habits. Little known; adults occur under bark of dead conifers (Thomas 2003), including freshly killed loblolly pine and southern red oak (Gil 2008).

Cupedidae

Tenomerga cinerea (Say, 1831)

Collection information. USA: Georgia: Clarke Co.: five individuals from five sites. Caught in flight trap from 16 June–14 July 2020.

Distribution. Eastern and central North America.

Saproxylic habits. Larvae bore through rotten oak and pine, and adults occur under bark and in dead wood (Downie and Arnett 1996).

Curculionidae

Acalles carinatus LeConte, 1876

Collection information. USA: Georgia: Clarke Co.: a single individual from one site. Sifted from leaf litter from 27–28 July 2020.

Distribution. Eastern North America.

Saproxylic habits. Emerged from small diameter, dead hardwoods (Ferro et al. 2012a); adults occur under bark of dead trees, such as sugar maple (*Acer saccharum* Marshall (Sapindaceae)) (Blatchley 1925).

Acalles clavatus (Say, 1831)

Collection information. USA: **Georgia (new state record)**: Clarke Co.: 28 individuals from 14 sites. Sifted from leaf litter from 29 June–31 August 2020.

Distribution. Southeastern United States.

Saproxylic habits. Emerged from twigs of hardwood trees (Ferro and Nguyen 2016), including southern red oak (Ferro et al. 2009).

Conservation. Significantly associated with, and occurrence probability increases in, old forests (predating 1938 and oak dominated) in the Piedmont (Traylor et al. 2023a, 2024).

Acamptus rigidus LeConte, 1876

Collection information. USA: Georgia: Clarke Co.: two individuals from two sites. Caught in flight trap from 2–16 June 2020.

Distribution. Eastern and central North America.

Saproxylic habits. Little known, occur in red-rotten wood (Hanula 1996); larvae of *Acamptus* LeConte, 1876 develop under bark, in dead branches, and in tree wounds (Anderson 1952); species of *Acamptus* are associated with dead wood, tree wounds, and dead portions of living trees, such as rotten tree hollows (Kissinger 1964; Anderson 2002).

Apteromechus ferratus (Say, 1831)

Collection information. USA: Georgia: Clarke Co.: 26 individuals from 14 sites. Caught in flight trap from 25 March–26 August 2020.

Distribution. Eastern North America.

Saproxylic habits. Larvae mine the inner bark of recently dead trees, including *Sassafras* Presl (Lauraceae) (Kissinger 1963); emerged from freshly dead hardwood twigs and branches (Ferro et al. 2012a).

Conservation. Significantly higher abundance in secondary (= second-growth) than primary (= old-growth) forests in the southern Appalachian Mountains (Ferro et al. 2012a).

Apteromechus pumilus (Boheman, 1837)

Collection information. USA: Georgia: Clarke Co.: five individuals from four sites. Caught in flight trap from 25 March–16 June 2020.

Distribution. Southeastern United States (Ciegler 2010).

Saproxylic habits. unknown; larvae of *Apteromechus* Faust, 1896 mine the bark of recently dead trees (Kissinger 1963).

Cophes fallax (LeConte, 1876)

Collection information. USA: **Georgia (new state record*)**: Clarke Co.: five individuals from four sites. Caught in flight trap and sifted from leaf litter from 2 June–9 September 2020.

Distribution. Eastern North America.

Saproxylic habits. Emerged from a variety of hardwood twigs and branches (Blatchley and Leng 1916; Ferro and Gimmel 2014; Ferro and Nguyen 2016) and associated with fresh, small-diameter wood (Ferro et al. 2012a).

Conservation. Significantly higher abundance in primary (= old-growth) than secondary (= second-growth) forests in the southern Appalachian Mountains (Ferro et al. 2012a).

Cophes oblongus (LeConte, 1876)

Collection information. USA: Georgia: Clarke Co.: three individuals from two sites. Caught in flight trap from 27 July–26 August 2020.

Distribution. Southeastern United States and Caribbean islands.

Saproxylic habits. Emerged from hardwood twigs (Ferro and Gimmel 2014; Ferro and Nguyen 2016) and hackberry logs (presumably *Celtis* L. (Cannabaceae)) (Fox 2009).

Cophes obtentus (Herbst, 1797)

Collection information. USA: **Georgia (new state record*)**: Clarke Co.: two individuals from two sites. Caught in flight trap from 21 April–11 August 2020.

Distribution. Eastern North America into Central America, west to Arizona.

Saproxylic habits. Emerged from hardwood twigs (Ferro et al. 2012a; Ferro and Nguyen 2016); adults occur under bark and in hollow trees (Ciegler 2010).

Cossonus corticola Say, 1831

Collection information. USA: Georgia: Clarke Co.: two individuals from two sites. Caught in flight trap from 2 June–11 August 2020.

Distribution. Eastern North America to Central America.

Saproxylic habits. Larvae develop, and adults occur in dead pine logs (Anderson 1952; Moser et al. 1971; Gil 2008).

Cossonus impressifrons Boheman, 1838

Collection information. USA: Georgia: Clarke Co.: 25 individuals from 13 sites. Caught in flight trap from 19 May–11 August 2020.

Distribution. Eastern North America.

Saproxylic habits. Occur under bark and in logs of various hardwoods and pine (Blackman and Stage 1924; O'Brien 1997), although it may prefer hardwoods (e.g., oak) to pine (Gil 2008).

Cryptorhynchus fuscatus LeConte, 1876

Collection information. USA: Georgia: Clarke Co.: two individuals from two sites. Caught in flight trap from 6 May–26 August 2020.

Distribution. Eastern North America.

Saproxylic habits. Emerged from poison ivy vines and adults occur under bark of dead trees, such as pecan (*Carya illinoinensis* (Wangenh.) K.Koch) (Anderson 2008a), and in hollow trees (Ciegler 2010).

Dryophthorus americanus Bedel, 1885

Collection information. USA: Georgia: Clarke Co.: 11 individuals from nine sites. Caught in flight trap and sifted from leaf litter from 21 April–30 June 2020.

Distribution. Eastern North America.

Saproxylic habits. Consumes decayed woody material and occurs under bark and in rotting wood (Blackman and Stage 1918; Anderson 2002); conifers are listed as primary hosts (including pine and larch (*Larix* Mill. (Pinaceae)) (Blackman and Stage 1918; Blatchley 1928; Ciegler 2010), although it has also emerged in numbers from dead hickory and other hardwoods (Blackman and Stage 1924; Ferro et al. 2012a); highest abundance emerged from logs in intermediate- and late-decay stages (Blackman and Stage 1924; Ulyshen and Hanula 2010; Ferro et al. 2012a, b).

Conservation. Significantly higher abundance in primary (= old-growth) than secondary (= second-growth) forests in the southern Appalachian Mountains (Ferro et al. 2012a).

Eubulus bisignatus (Say, 1831)

Collection information. USA: Georgia: Clarke Co.: four individuals from three sites. Caught in flight trap from 25 March–14 July 2020.

Distribution. Eastern North America.

Saproxylic habits. Emerged from dead wood of peach (*Prunus persica* (L.) Batsch) (Dolphin et al. 1972); adults occur on dead branches and trunks of hardwood trees (Anderson 2008b; Ciegler 2010); larvae likely mine below bark and in the sapwood, as does *Eubulus parochus* (Herbst, 1797) (Halik and Bergdahl 2006).

Eubulus obliquefasciatus (Boheman, 1844)

Collection information. USA: Georgia: Clarke Co.: four individuals from four sites. Caught in flight trap from 25 March–30 June 2020.

Distribution. Eastern United States.

Saproxylic habits. Adults occur on dead trees, such as oak and sweetgum (Anderson 2008b); larvae likely mine below bark and in the sapwood, as does *E. Parochus* (Halik and Bergdahl 2006).

Eulechriops minuta (LeConte, 1824)

Collection information. USA: Georgia: Clarke Co.: three individuals from two sites. Caught in flight trap from 6 May–14 July 2020.

Distribution. Eastern United States.

Saproxylic habits. unknown, although associated with oaks (Sleeper 1963; Hespenheide 2003a); neotropical *Eulechriops* Faust, 1896 bore into woody materials (Jordal and Kirkendall 1998).

Himatium errans LeConte, 1876

Collection information. USA: Georgia: Clarke Co.: four individuals from four sites. Caught in flight trap from 21 April–27 July 2020.

Distribution. Eastern North America.

Saproxylic habits. Occur under bark and within bark beetle galleries in pine (O'Brien 1997; Ciegler 2010); emerged from dead loblolly pine and black walnut (*Juglans nigra* L. (Juglandaceae)) (Ulyshen and Hanula 2009a; Reed et al. 2015); may vector the pathogen of thousand cankers disease (*Geosmithia morbida* Kolařík, Freeland, Utley and Tisserat (Bionectriaceae)) (Moore et al. 2019).

Hylobius aliradicis Warner, 1966

Collection information. USA: Georgia: Clarke Co.: a single individual from one site. Caught in flight trap from 6–19 May 2020.

Distribution. Southeastern United States.

Saproxylic habits. Larvae develop in the roots of young, dying slash pines (*Pinus elliottii* Engelm.), and have been collected from pine bolts (Warner 1966); although Warner (1966) suggests that the larvae were the primary cause of tree death, more recent work suggests that *H. Aliradicis* and related pine weevils principally colonize already stressed trees (Helbig et al. 2016).

Hylocurus harnedi (Blackman, 1920)

Collection information. USA: **Georgia (new state record)**: Clarke Co.: one individual from one site. Caught in flight trap from 25 March–9 April 2020.

Distribution. Southeastern United States (Wood 1982).

Saproxylic habits. Larvae are xylophagous within dead branches of hickory (Wood 1982).

Laemosaccus obrieni Hespenheide, 2019

Collection information. USA: Georgia: Clarke Co.: two individuals from one site. Caught in flight trap from 21 April–6 May 2020.

Distribution. Eastern North America (Hespenheide 2019).

Saproxylic habits. Bores into twigs and stems, and has emerged from various oaks, hickories, and American chestnut (*Castanea dentata* (Marshall) Borkh. (Fagaceae)) (Hespenheide 2019).

Lechriops oculata (Say, 1824)

Collection information. USA: Georgia: Clarke Co.: 838 individuals from 36 sites. Caught in flight trap from 9 March–9 September 2020.

Distribution. Eastern North America.

Saproxylic habits. Adults occur under bark (Ott 2011a); western species of *Lechriops* develop under the bark of conifers (Hespenheide 2003b), although *L. oculata* is associated with hardwood trees (Sleeper 1963).

Magdalis barbita (Say, 1831)

Collection information. USA: Georgia: Clarke Co.: four individuals from four sites. Caught in flight trap from 9 April–6 May 2020.

Distribution. Eastern North America.

Saproxylic habits. Larvae feed on the inner bark and sapwood of unhealthy and dying elms (*Ulmus* L. (Ulmaceae)) (Baker 1972); emerged from slippery elm (*Ulmus rubra* Muhl.) and American elm (*Ulmus americana* L.) (Webster et al. 2012a; Haack 2020); adults also occur under bark of recently dead hardwoods, such as oak and hickory (Blatchley and Leng 1916).

Magdalis perforata Horn, 1873

Collection information. USA: Georgia: Clarke Co.: two individuals from two sites. Caught in flight trap from 21 April–26 August 2020.

Distribution. Eastern North America.

Saproxylic habits. Emerged from loblolly pine (Helbig et al. 2016); larvae likely feed on the inner bark and sapwood as do other species of *Magdalis* Germar, 1817 (Baker 1972).

Micromimus corticalis (Boheman, 1845)

Collection information. USA: **Georgia (new state record)**: Clarke Co.: 19 individuals from six sites. Caught in flight trap from 21 April–14 July 2020.

Distribution. Southeastern United States (Ciegler 2010).

Saproxylic habits. Emerged from hardwood woody debris (Ferro et al. 2012a); adults occur under bark (Ciegler 2010).

Phaenomerus foveipennis (Morimoto, 1961)

Collection information. USA: Georgia: Clarke Co.: a single individual from one site. Caught in flight trap from 2–16 June 2020.

Distribution. Eastern Palearctic, adventive in the southeastern United States (Schnepp and Anderson 2021).

Saproxylic habits. Occurs under bark in its native range (Morimoto 1961); other species of *Phaenomerus* Schönherr, 1836 are found in association with ambrosia beetles or have emerged from wood packaging (Thompson 1996; Schnepp and Anderson 2021).

Pissodes nemorensis Germar, 1824

Collection information. USA: Georgia: Clarke Co.: four individuals from three sites. Caught in flight trap from 9 March–2 June 2020.

Distribution. Eastern North America.

Saproxylic habits. Larvae feed in the phloem and sapwood of weakened or freshly killed pine (Atkinson et al. 1988); while generally considered a pest of pines (e.g., Ollieu 1971), more recent work suggests *P. Nemorensis* and related pine weevils principally colonize already stressed trees (Helbig et al. 2016).

Plocamus echidna (LeConte, 1876)

Collection information. USA: **Georgia (new state record)**: Clarke Co.: two individuals from two sites. Caught in flight trap from 19 May–2 June 2020.

Distribution. Eastern North America into Central America.

Saproxylic habits. Adults occur on dead beech (*Fagus grandifolia* Ehrh. (Fagaceae)) (Beutenmuller 1893; de Tonnancour et al. 2017) and may consume hickory as well (Blatchley and Leng 1916).

Plocamus hispidulus LeConte, 1876

Collection information. USA: Georgia: Clarke Co.: two individuals from two sites. Caught in flight trap from 25 March–11 August 2020.

Distribution. Eastern United States.

Saproxylic habits. Breeds in dead branches of "locust" trees (presumably *Robinia* L. or *Gleditsia* L. (both in Fabaceae)) (Beutenmuller 1893), and also emerged from black walnut (Reed et al. 2015).

Pseudopentarthrum simplex Casey, 1892

Collection information. USA: **Georgia (new state record*)**: Clarke Co.: a single individual from one site. Caught in flight trap from 16–30 June 2020.

Distribution. Eastern North America.

Saproxylic habits. Reared from a wound in a maple tree (*Acer* L.) and adults occur on dead trees and shrubs, such as wax myrtle (*Morella cerifera* (L.) Small (Myricaceae)) (Ciegler 2010); species of *Pseudopentarthrum* Wollaston, 1873 are associated with dead wood and various microhabitats (e.g., tree hollows; Anderson 2002).

Rhyncolus discors Casey, 1892

Collection information. USA: Georgia: Clarke Co.: 11 individuals from eight sites. Caught in flight trap from 25 March–2 June 2020.

Distribution. Eastern United States.

Saproxylic habits. Adults occur under bark and in wood of pine snags (Howden and Vogt 1951); larvae of *Rhyncolus* Germar, 1817 develop in dead wood (Anderson 1952).

Stenomimus pallidus (Boheman, 1845)

Collection information. USA: **Georgia (new state record)**: Clarke Co.: two individuals from one site. Caught in a flight trap from 21 April–6 May 2020.

Distribution. Eastern North America.

Saproxylic habits. Larvae develop under the bark of wounded and dead oak, hickory, and black walnut (Anderson 1952; Ciegler 2010); known to vector the pathogen of thousand cankers disease (*G. morbida*, Juzwik et al. 2015).

Stenoscelis andersoni Buchanan, 1948

Collection information. USA: Georgia: Clarke Co.: 19 individuals from 16 sites. Caught in flight trap from 21 April–16 June 2020.

Distribution. Eastern United States.

Saproxylic habits. Larvae develop in rotting birch (*Betula* L. (Betulaceae)) (Anderson 1952) and adults occur in soft dead wood (Kissinger 1955); emerged from burned and unburned loblolly pine logs (Ulyshen et al. 2010); associated with snags in bottomland forests (Ulyshen and Hanula 2009a).

Stenoscelis brevis (Boheman, 1845)

Collection information. USA: Georgia: Clarke Co.: 19 individuals from 10 sites. Caught in flight trap from 6 May–16 June 2020.

Distribution. Eastern North America.

Saproxylic habits. Larvae develop, and adults occur gregariously in decaying wood of many hardwoods and larch, including dead portions and exposed wood in living trees (Blackman and Stage 1918, 1924; Anderson 1952); adults also occur in solid, dry wood and old stumps (Beutenmuller 1893; Hoffmann 1942); associated with moderately decayed wood (Ferro et al. 2012a).

Conservation. Significantly higher abundance in secondary (= second-growth) than primary (= old-growth) forests in the southern Appalachian Mountains (Ferro et al. 2012a); rare in the Maritime Provinces of Canada, possibly due to the history of intensive forest management in the region altering forest composition and structure (Majka 2007).

Tomolips quercicola **(Boheman, 1845)**

Collection information. USA: Georgia: Clarke Co.: eight individuals from eight sites. Caught in flight trap from 21 April–30 June 2020.

Distribution. Eastern North America south to Central America.

Saproxylic habits. Emerged from loblolly pine, water oak, and sweetgum in bottomland forests (Ulyshen and Hanula 2009a); adults occur in rotten deadwood, tree hollows, and under bark of various trees, including beech and magnolia (*Magnolia* L. (Magnoliaceae)) (Blatchley 1928; Kissinger 1955; Ciegler 2010).

Xyleborus pfeilii **(Ratzeburg, 1837)**

Collection information. USA: **Georgia (new state record)**: Clarke Co.: two individuals from two sites. Caught in flight trap from 30 June–14 July 2020.

Distribution. Introduced across the world, adventive in North America (Gomez et al. 2018).

Saproxylic habits. Larvae are ambrosial feeders and polyphagous in tree-hosts (Wood 1982; Wood and Bright 1992).

Dermestidae

Orphilus ater **Erichson, 1846**

Collection information. USA: Georgia: Clarke Co.: 27 individuals from 15 sites. Caught in flight trap from 9 March–16 June 2020.

Distribution. Eastern North America.

Saproxylic habits. unknown; larvae of *Orphilus* Erichson, 1846 develop within dry, fungus-infested branches (Beal 1985; Pushkin and Mykhailovych 2019).

Conservation. Occurrence probability increases in old forests (predating 1938 and oak dominated) in the Piedmont (Traylor et al. 2024).

Disteniidae

Elytrimitatrix undata **(Fabricius, 1775)**

Collection information. USA: Georgia: Clarke Co.: four individuals from three sites. Caught in flight trap from 14–27 July 2020.

Distribution. Eastern and central United States.

Saproxylic habits. Larvae develop within a variety of hardwoods and pine (Lingafelter 2007).

Elateridae

Alaus myops **(Fabricius, 1801)**

Collection information. USA: Georgia: Clarke Co.: a single individual from one site. Caught in flight trap from 2–16 June 2020.

Distribution. Eastern North America.

Saproxylic habits. Larvae are predators of woodboring insects in dead pine logs and stumps (Frost 1916; Savely 1939); occupies logs throughout decomposition (Savely 1939; Ulyshen and Hanula 2010).

Genus *Ampedus* Dejean, 1833

Collection information. See inidivudal species below.

Saproxylic habits. Little is known about specific habits of each species, but larvae of *Ampedus* develop in decomposing wood where they are thought to prey on other invertebrates (Ramberg 1979).

Ampedus areolatus (Say, 1823)

Collection information. USA: Georgia: Clarke Co.: nine individuals from eight sites. Caught in flight trap from 9 April–14 July 2020.

Distribution. Eastern and central North America.

Saproxylic habits. Emerged from loblolly pine logs throughout decomposition (Ulyshen and Hanula 2010); emerged from dead hardwoods and associated with larger diameter, moderately decayed pieces (Ferro et al. 2012a); adults occur under bark (Mathison 2021).

Conservation. Significantly higher abundance in primary (= old-growth) than secondary (= second-growth) forests in the southern Appalachian Mountains (Ferro et al. 2012a).

Ampedus collaris (Say, 1825)

Collection information. USA: Georgia: Clarke Co.: 84 individuals from 21 sites. Caught in flight trap from 9 March–30 June 2020.

Distribution. Eastern North America.

Saproxylic habits. Emerged from white spruce (*Picea glauca* (Moench) Voss (Pinaceae)) (Majka and Johnson 2008); adults occur in rotting wood, including hickory, white spruce, and eastern white pine (*Pinus strobus* L.) (Ramberg 1979).

Conservation. Significantly associated with young forests (regrown since 1938 and pine dominated) in the Piedmont (Traylor et al. 2023a).

Ampedus fuscatus (Melsheimer, 1845)

Collection information. USA: Georgia: Clarke Co.: six individuals from six sites. Caught in flight trap from 25 March–27 July 2020.

Distribution. Eastern North America.

Saproxylic habits. Adults occur in rotting wood and under bark, including hickory, cypress (*Cupressus* L. (Cupressaceae)), American sycamore

(*Platanus occidentalis* L. (Platanaceae)), pine, and blackjack oak (*Quercus marilandica* (Münchh.)) (Ramberg 1979; Mathison 2021).

Conservation. Significantly associated with young forests (regrown since 1938 and pine dominated) in highly forested landscapes (> 50% forest) in the Piedmont (Traylor et al. 2023a).

Ampedus melanotoides **Brown, 1933**

Collection information. USA: Georgia: Clarke Co.: 74 individuals from 26 sites. Caught in flight trap from 9 March–9 September 2020.

Distribution. Eastern North America.

Saproxylic habits. Adults occur in rotting wood, including hickory and willow (Ramberg 1979).

Ampedus melsheimeri **(Leng, 1918)**

Collection information. USA: Georgia: Clarke Co.: six individuals from four sites. Caught in flight trap from 21 April–11 August 2020.

Distribution. Eastern North America.

Saproxylic habits. Unknown.

Ampedus militaris **(Harris, 1836)**

Collection information. USA: Georgia: Clarke Co.: a single individual from one site. Caught in flight trap from 21 April–6 May 2020.

Distribution. Eastern North America.

Saproxylic habits. Little known, but adults occur under bark (Kelly 2011) and under decomposing logs (Webb 2019).

Ampedus nigricollis **(Herbst, 1801)**

Collection information. USA: Georgia: Clarke Co.: four individuals from four sites. Caught in flight trap from 9 March–2 June 2020.

Distribution. Eastern North America.

Saproxylic habits. Adults occur under bark and in rotting wood, including pine, hemlock (*Tsuga* (Endl.) Carrière (Pinaceae)), and a variety of hardwoods (Ramberg 1979; Mathison 2021).

Ampedus pedalis **(Germar, 1843)**

Collection information. USA: Georgia: Clarke Co.: 149 individuals from 27 sites. Caught in flight trap from 25 March–30 June 2020.

Distribution. Eastern North America.

Saproxylic habits. Adults occur in rotting wood, such as elm (Ramberg 1979).

Ampedus pusio Germar, 1844

Collection information. USA: Georgia: Clarke Co.: 102 individuals from 30 sites. Caught in flight trap from 16 June–9 September 2020.

Distribution. Eastern United States.

Saproxylic habits. Adults occur in snags and rotten stumps of pine (Ramberg 1979; Mathison 2021).

Ampedus rubricollis (Herbst, 1806)

Collection information. USA: Georgia: Clarke Co.: four individuals from four sites. Caught in flight trap from 9 March–19 May 2020.

Distribution. Eastern North America.

Saproxylic habits. Adults occur under bark of dead trees, such as pine (Ramberg 1979; Mathison 2021).

Ampedus sanguinipennis (Say, 1823)

Collection information. USA: Georgia: Clarke Co.: seven individuals from one site. Caught in flight trap from 19 May–30 June 2020.

Distribution. Eastern and central North America.

Saproxylic habits. Adults occur in rotting wood and under bark, including cypress, pine, oak, willow, and pear (*Pyrus* L. (Rosaceae)) (Ramberg 1979; Mathison 2021).

Athous cucullatus (Say, 1825)

Collection information. USA: Georgia: Clarke Co.: 24 individuals from 19 sites. Caught in flight trap from 16 June–9 September 2020.

Distribution. Eastern North America.

Saproxylic habits. Larvae occur in dead wood where they prey upon wood-boring larvae (Kirk 1922; Glen 1950); emerged from decayed loblolly pine, hickory, elm, and various hardwoods (Blackman and Stage 1924; Hoffmann 1942; Ulyshen and Hanula 2010; Ferro et al. 2012a).

Conservation. Occurrence probability increases in old forests (predating 1938 and oak dominated) in the Piedmont (Traylor et al. 2024).

Dipropus soleatus (Say, 1839)

Collection information. USA: Georgia: Clarke Co.: 11 individuals from nine sites. Caught in flight trap from 30 June–26 August 2020.

Distribution. Eastern United States (Mathison 2021).

Saproxylic habits. Larvae develop in soft decaying wood, including maple and cherry (Jewett 1946).

Conservation. Occurrence probability increases in old forests (predating 1938 and oak dominated) in the Piedmont (Traylor et al. 2024).

***Drapetes exstriatus* (Say, 1834)**

Collection information. USA: Georgia: Clarke Co.: two individuals from one site. Caught in flight trap from 30 June–11 August 2020.

Distribution. Eastern United States.

Saproxylic habits. Adults occur under bark, including oak and a long-dead fallen tree (Wilson 2012; Mathison 2021); larvae of *Drapetes* (Dejean, 1821) develop under loose bark or in decaying wood (Johnson 2015).

***Drapetes quadripustulatus* Bonvouloir, 1859**

Collection information. USA: Georgia: Clarke Co.: a single individual from one site. Caught in flight trap from 26 August–9 September 2020.

Distribution. Eastern United States (Mathison 2021).

Saproxylic habits. Emerged from loblolly pine throughout decomposition and in both burned and unburned logs (Ulyshen and Hanula 2010; Ulyshen et al. 2010), and also occur on southern red oak logs (Gil 2008); larvae of *Drapetes* develop under loose bark or in decaying wood (Johnson 2015).

***Lacon avitus* (Say, 1839)**

Collection information. USA: Georgia: Clarke Co.: a single individual from one site. Caught in flight trap from 14–27 July 2020.

Distribution. Eastern United States.

Saproxylic habits. unknown; species of *Lacon* Laporte, 1838 commonly occur under bark (Mathison 2021).

***Lacon discoideus* (Weber, 1801)**

Collection information. USA: Georgia: Clarke Co.: 18 individuals from nine sites. Caught in flight trap from 25 March–26 August 2020.

Distribution. Eastern North America.

Saproxylic habits. Adults occur in rotting logs; under bark (pine, magnolia, and oak), and within tree-hollow litter (Mathison 2021).

***Lacon marmoratus* (Fabricius, 1801)**

Collection information. USA: Georgia: Clarke Co.: three individuals from two sites. Caught in flight trap from 21 April–9 September 2020.

Distribution. Eastern North America.

Saproxylic habits. Adults occur under bark of decayed oak and pine trunks (Dozier 1918).

Orthostethus infuscatus (Germar, 1844)

Collection information. USA: Georgia: Clarke Co.: 173 individuals from 18 sites. Caught in flight trap from 2 June–9 September 2020.

Distribution. Eastern North America, west to Arizona, south to South America.

Saproxylic habits. Larvae inhabit decaying logs (Dozier 1918), apparently feeding on rotting wood (Savely 1939); emerged from decayed loblolly pine and oak (Savely 1939; Ulyshen and Hanula 2010); adults have been found within decayed interiors of living trees (Hepting 1935).

Conservation. Occurrence probability increases in old forests (predating 1938 and oak dominated) in the Piedmont (Traylor et al. 2024).

Parallelostethus attenuatus (Say, 1825)

Collection information. USA: Georgia: Clarke Co.: two individuals from two sites. Caught in flight trap from 30 June–27 July 2020.

Distribution. Eastern North America.

Saproxylic habits. Occurs in decayed wood, stumps, and tree-hollows of maple, oak, hackberry, and sycamore (*Platanus* L.) (Jewett 1946); feeds on rotten wood material (Kirk 1922).

Endecatomidae

Endecatomus rugosus (Randall, 1838)

Collection information. USA: Georgia: Clarke Co.: six individuals from two sites. Caught in flight trap from 9 March–9 April 2020.

Distribution. Eastern North America.

Saproxylic habits. Larvae develop within the shelf fungus *Fuscoporia gilva* (Schwein.) T. Wagner and M. Fisch. (Hymenochaetaceae) (Fisher 1950; Crowson 1961); also emerged from living polypores of *Fomes fomentarius* (L.) Fr. (Polyporaceae) (Matthewman and Pielou 1971).

Endomychidae

Stenotarsus hispidus (Herbst, 1799)

Collection information. USA: Georgia: Clarke Co.: a single individual from one site. Caught in flight trap from 21 April–6 May 2020.

Distribution. Eastern United States.

Saproxylic habits. Little known, adults occur under bark (Ott 2011b); adults and larvae are likely mycophagous on larger basidiomycete fungi (Skelley and Leschen 2002); adults of some *Stenotarsus* Perty, 1832 aggregate on their host fungi (Shockley et al. 2009).

Erotylidae

***Dacne quadrimaculata* (Say, 1835)**

Collection information. USA: Georgia: Clarke Co.: 21 individuals from 13 sites. Caught in flight trap from 9 March–6 May 2020.

Distribution. Eastern North America.

Saproxylic habits. Larvae develop, and adults occur in a variety of polypore fungi, but primarily dryad's saddle (*Cerioporus squamosus* (Huds.) Quél. (Polyporaceae)) and oyster mushroom (*Pleurotus* (Fr.) P. Kumm. (Pleurotaceae)) (Skelley et al. 1991).

Conservation. Occurrence probability increases with the amount of landscape forest cover in the Piedmont (Traylor et al. 2024).

***Ischyrus quadripunctatus* (Olivier, 1791)**

Collection information. USA: Georgia: Clarke Co.: two individuals from two sites. Caught in flight trap from 25 March–26 August 2020.

Distribution. Eastern North America, west to Arizona, south to South America.

Saproxylic habits. Emerged from *Irpex latemarginatus* (Durieu and Mont.) C.C. Chen and Sheng H. Wu, 2021 (Irpicaceae), and adults feed on other soft polypores (Skelley et al. 1991; Goodrich and Springer 1999).

***Megalodacne fasciata* (Fabricius, 1777)**

Collection information. USA: Georgia: Clarke Co.: a single individual from one site. Caught in flight trap from 26 August–9 September 2020.

Distribution. Eastern North America, likely introduced in the western United States (Goodrich and Springer 1999).

Saproxylic habits. Larvae develop within polypores of *Ganoderma lucidum* (Curtis) P. Karst. (Ganodermataceae), and adults feed on a wider range of polypores (Skelley et al. 1991).

***Triplax festiva* Lacordaire, 1842**

Collection information. USA: Georgia: Clarke Co.: three individuals from two sites. Caught in flight trap from 9–25 March 2020.

Distribution. Eastern North America.

Saproxylic habits. Larvae develop within polypores of *Inonotus* P. Karst. (Hymenochaetaceae) (Skelley et al. 1991).

***Triplax frontalis* Horn, 1862**

Collection information. USA: Georgia: Clarke Co.: three individuals from two sites. Caught in flight trap from 9 March–9 April 2020.

Distribution. Eastern and central United States.

Saproxylic habits. Larvae develop within *Xanthoporia andersonii* (Ellis and Everh.) Murrill (Hymenochaetaceae), and adults occur on species of *Inonotus* as well (Skelley et al. 1991).

Tritoma atriventris LeConte, 1847

Collection information. USA: Georgia: Clarke Co.: two individuals from two sites. Caught in flight trap and sifted from leaf litter from 2 June–31 August 2020.

Distribution. Southeastern and south-central United States (Goodrich and Springer 1999).

Saproxylic habits. Larvae develop in a variety of fungi growing on dead and dying wood, including *Desarmillaria tabescens* (Scop.) R.A. Koch and Aime (Physalacriaceae), *Lentinus arcularius* (Batsch) Zmitr. (Polyporaceae), *Omphalotus illudens* (Schwein.) Bresinsky and Besl (Omphalotaceae), and *Pluteus* Fr. (Plutaceae), and adults occur on numerous other fungi (Skelley et al. 1991).

Tritoma sanguinipennis (Say, 1825)

Collection information. USA: Georgia: Clarke Co.: four individuals from three sites. Caught in flight trap from 21 April–30 June 2020.

Distribution. Eastern North America.

Saproxylic habits. Larvae develop in *Lentinus arcularius*, and adults occur on several other fungi (Skelley et al. 1991).

Eucinetidae

Eucinetus strigosus LeConte, 1875

Collection information. USA: Georgia: Clarke Co.: a single individual from one site. Sifted from leaf litter from 27–28 July 2020.

Distribution. Eastern United States.

Saproxylic habits. unknown; species of *Eucinetus* Germar, 1818 breed in slime molds and basidiomycete fungi growing on dead wood, and often occur under bark or in decaying wood (Wheeler and Hoebeke 1984).

Eucnemidae

Adelothyreus dejeani Bonvouloir, 1872

Collection information. USA: Georgia: Clarke Co.: a single individual from one site. Caught in flight trap from 19 May–2 June 2020.

Distribution. Southeastern United States (Otto and Karns 2017).

Saproxylic habits. Emerged from hardwood twigs (Ferro and Nguyen 2016).

Deltometopus amoenicornis (Say, 1836)

Collection information. USA: Georgia: Clarke Co.: a single individual from one site. Caught in flight trap from 30 June–14 July 2020.

Distribution. Eastern North America.

Saproxylic habits. Larvae develop in white-rotted or otherwise unspecified decayed wood, including maple, hickory, American beech, and possibly conifers (Knull 1947; Muona 2000; Otto 2012a).

Dirrhagofarsus lewisi (Fleutiaux, 1900)

Collection information. USA: Georgia: Clarke Co.: 104 individuals from 32 sites. Caught in flight trap from 25 March–9 September 2020.

Distribution. Native to Japan, adventive in the eastern United States (Ford and Spilman 1979; Otto and Karns 2017).

Saproxylic habits. Larvae develop in the wet sapwood of American beech (Ford and Spilman 1979); emerged from moderately decayed hardwood logs (Ferro et al. 2012a) and occur on southern red oak (Gil 2008).

Dromaeolus badius (Melsheimer, 1844)

Collection information. USA: Georgia: Clarke Co.: five individuals from four sites. Caught in flight trap from 16 June–27 July 2020.

Distribution. Eastern North America, west to Arizona, Utah, and Idaho (Muona 2000).

Saproxylic habits. Larvae develop in decayed oak stumps (Osten Sacken 1862) and have also emerged from decayed tulip poplar (*Liriodendron tulipifera* L. (Magnoliaceae)), hickory, and aspen (*Populus* L. (Saliceae)arn 1909; Kirk 1922; Muona 2000).

Dromaeolus turnbowi Muona, 2000

Collection information. USA: Georgia: Clarke Co.: a single individual from one site. Caught in flight trap from 2–16 June 2020.

Distribution. Eastern United States (Otto 2022).

Saproxylic habits. unknown; species of *Dromaeolus* Kiesenwetter, 1858 develop within decaying wood (Muona 2000).

Entomophthalmus rufiolus (LeConte, 1866)

Collection information. USA: Georgia: Clarke Co.: 12 individuals from eight sites. Caught in flight trap from 19 May–9 September 2020.

Distribution. Eastern North America.

Saproxylic habits. Larvae develop within decayed, white-rotted hardwoods, including oak, maple, and basswood (*Tilia* L. (Malvaceae)), usually in sections of logs with little moisture (Ferro et al. 2012a; Otto 2014).

Hylis terminalis (LeConte, 1866)

Collection information. USA: Georgia: Clarke Co.: 11 individuals from eight sites. Caught in flight trap from 21 April–16 June 2020.

Distribution. Eastern North America.

Saproxylic habits. Emerged from hickory limbs and a moist, decayed American beech log (Horn 1886; Knull 1946; Muona 2000)

Isorhipis obliqua (Say, 1836)

Collection information. USA: Georgia: Clarke Co.: 866 individuals from 38 sites. Caught in flight trap from 21 April–11 August 2020.

Distribution. Eastern North America.

Saproxylic habits. Larvae develop in the heartwood of decayed hardwoods (e.g., maple; Peterson 1960), and have emerged from dry, dead wood of various hardwoods (Knull 1946; Muona 2000); associated with moderately decayed logs (Ferro et al. 2012a).

Conservation. Significantly higher abundance in secondary (= second-growth) than primary (= old-growth) forests in the southern Appalachian Mountains (Ferro et al. 2012a); significantly associated with old forests (predating 1938 and oak dominated) in the Piedmont (Traylor et al. 2023a).

Melasis pectinicornis Melsheimer, 1844

Collection information. USA: Georgia: Clarke Co.: 44 individuals from 24 sites. Caught in flight trap from 9 March–21 April 2020.

Distribution. Eastern United States (Muona 2000).

Saproxylic habits. Larvae develop under bark (Peterson 1960) and bore through wood (McClarin 2007); develops within a variety of hardwood trees of various decomposition stages, but may prefer maple as a host and moderately decayed logs (Muona 2000; Ferro et al. 2012a).

Conservation. Significantly higher abundance in secondary (= second-growth) than primary (= old-growth) forests in the southern Appalachian Mountains (Ferro et al. 2012a).

Microrhagus audax Horn, 1886

Collection information. USA: Georgia: Clarke Co.: a single individual from one site. Caught in flight trap from 19 May–2 June 2020.

Distribution. Eastern North America.

Saproxylic habits. Larvae develop within rotten elm (Otto 2015) and adults have emerged from hardwood twigs (Ferro and Nguyen 2016).

Microrhagus brunneus Otto, 2013

Collection information. USA: Georgia: Clarke Co.: a single individual from one site. Caught in flight trap from 21 April–6 May 2020.

Distribution. Eastern United States (Otto 2022).

Saproxylic habits. Larvae develop within the wood of rotten oak logs (Otto 2015).

Microrhagus carinicollis Otto, 2015

Collection information. USA: Georgia: Clarke Co.: 18 individuals from 14 sites. Caught in flight trap from 19 May–9 September 2020.

Distribution. Eastern United States (Otto 2022).

Saproxylic habits. Larvae develop within white-rotted, moist maple logs, and adults occur in oak stumps and branch debris (Otto 2015).

Microrhagus triangularis (Say, 1823)

Collection information. USA: Georgia: Clarke Co.: seven individuals from five sites. Caught in flight trap from 16 June–9 September 2020.

Distribution. Eastern North America.

Saproxylic habits. Larvae develop in moist, white-rotted logs, including maple and aspen (Otto 2015); adults also occur on dogwood logs (*Cornus* L. (Cornaceae)) (Muona 2000).

Conservation. Rare in the Maritime Provinces of Canada, possibly due to the history of intensive forest management in the region altering forest composition and structure (Majka 2007).

Nematodes atropos (Say, 1836)

Collection information. USA: Georgia: Clarke Co.: 36 individuals from 19 sites. Caught in flight trap from 19 May–27 July 2020.

Distribution. Eastern North America and Mexico.

Saproxylic habits. larvae, pupae, and adults have been found together within the base of a dead black oak (Van Horn 1909); emerged from water oak logs (Ulyshen and Hanula 2009a), hardwood twigs (Ferro and Nguyen 2016), and American beech, elm, and maple (Dury 1904).

Nematodes penetrans (LeConte, 1852)

Collection information. USA: Georgia: Clarke Co.: 130 individuals from 12 sites. Caught in flight trap from 19 May–30 June 2020.

Distribution. Eastern North America.

Saproxylic habits. Hypermetamorphic larvae develop within firm sections of rotten branches and trunks, including sugar maple (Otto 2017); also emerged from American beech, elm, and maple (Dury 1904; Knull 1947).

Conservation. Rare in the Maritime Provinces of Canada, possibly due to the history of intensive forest management in the region altering forest composition and structure (Majka 2007).

Rhagomicrus bonvouloiri **(Horn, 1886)**

Collection information. USA: Georgia: Clarke Co.: 12 individuals from 10 sites. Caught in flight trap from 19 May–26 August 2020.

Distribution. Eastern North America (Otto 2022).

Saproxylic habits. Larvae develop within white-rotted maple and wet, rotted aspen (Otto 2012b); adults also occur on pine stumps (Muona 2000) and have been found burrowing in a wet, rotting oak log (Otto 2012b).

Schizophilus subrufus **(Randall, 1838)**

Collection information. USA: **Georgia (new state record)**: Clarke Co.: two individuals from one site. Caught in flight trap from 14 July–11 August 2020.

Distribution. Eastern North America.

Saproxylic habits. Larvae develop within red-rotted oak logs (Otto and Young 1998).

Thambus horni **Muona, 2000**

Collection information. USA: **Georgia (new state record)**: Clarke Co.: three individuals from three sites. Caught in flight trap from 19 May–14 July 2020.

Distribution. Eastern North America.

Saproxylic habits. unknown; larvae are likely in deadwood, as typical for the family (Muona 2000).

Histeridae

Acritus exiguous **(Erichson, 1834)**

Collection information. USA: Georgia: Clarke Co.: 45 individuals from 25 sites. Caught in flight trap from 25 March–9 September 2020.

Distribution. Eastern North America.

Saproxylic habits. Feed on fungi under dead bark, including oak and elm (Savely 1939; Hoffmann 1942); emerged from oak, pine, and especially sweetgum logs and snags (Gil 2008; Ulyshen and Hanula 2009a).

Aeletes floridae **(Marseul, 1862)**

Collection information. USA: **Georgia (new state record*)**: Clarke Co.: a single individual from one site. Caught in flight trap from 14–27 July 2020.

Distribution. Eastern North America.

Saproxylic habits. Emerged from sweetgum (Ulyshen and Hanula 2009a) and loblolly pine dead for five years (Ulyshen and Hanula 2010); species of *Aeletes* Horn, 1873 are often found in association with rotting tree trunks and occasionally leaf litter (Kovarik and Caterino 2005).

Bacanius punctiformis **(LeConte, 1853)**

Collection information. USA: **Georgia (new state record*)**: Clarke Co.: nine individuals from six sites. Caught in flight trap from 19 May–26 August 2020.

Distribution. Eastern North America.

Saproxylic habits. Adults occur under bark and are suggested to feed on fungi (Savely 1939); emerged in great numbers from loblolly pine (throughout decomposition), sweetgum, and water oak, and was particularly associated with deadwood items near to the ground (Ulyshen and Hanula 2009a, 2010); additionally emerged from hardwood twigs (Ferro and Nguyen 2016).

Conservation. Significantly associated with forests in highly forested landscapes (> 50% forest) in the Piedmont (Traylor et al. 2023a).

Epierus pulicarius **Erichson, 1834**

Collection information. USA: Georgia: Clarke Co.: a single individual from one site. Caught in flight trap from 19 May–2 June 2020.

Distribution. Eastern North America.

Saproxylic habits. Emerged from moist wood of a decayed sweetgum stump (Snow 1958), loblolly pine logs throughout decomposition (Ulyshen and Hanula 2010), hardwood twigs (Ferro and Nguyen 2016).

Platysoma aequum **(LeConte, 1863)**

Collection information. USA: Georgia: Clarke Co.: a single individual from one site. Caught in flight trap from 9–25 March 2020.

Distribution. Eastern United States.

Saproxylic habits. Unknown; likely prey upon dipteran larvae under bark of dead trees as do similarly shaped species of *Platysoma* Leach, 1817 (Kovarik and Caterino 2005).

Platysoma aurelianum (Horn, 1873)

Collection information. USA: **Georgia (new state record*)**: Clarke Co.: nine individuals from seven sites. Caught in flight trap from 9 March–11 August 2020.

Distribution. Eastern North America.

Saproxylic habits. unknown; likely prey upon dipteran larvae under bark of dead trees as do similarly shaped species of *Platysoma* (Kovarik and Caterino 2005).

Platysoma leconti Marseul, 1853

Collection information. USA: Georgia: Clarke Co.: two individuals from two sites. Caught in flight trap from 21 April–14 July 2020.

Distribution. North America.

Saproxylic habits. Adults occur under bark of hardwood trees (Downie and Arnett 1996; Webster et al. 2012b); emerged from loblolly pine, water oak, and especially sweetgum (Ulyshen and Hanula 2009a), as well as hardwood twigs (Ferro and Nguyen 2016) and the non-native mimosa (*Albizia julibrissin* (Durazz.) (Fabaceae)) (Ulyshen et al. 2018).

Platysoma parallelum (Say, 1825)

Collection information. USA: Georgia: Clarke Co.: a single individual from one site. Caught in flight trap from 25 March–9 April 2020.

Distribution. Eastern North America.

Saproxylic habits. Predator of bark beetles in pine (Shepherd and Goyer 2005), and adults also occur under decaying elm bark (Hoffmann 1942); emerged from and associated with fresh loblolly pine logs (Ulyshen and Hanula 2010).

Hybosoridae

Ceratocanthus aeneus (MacLeay, 1819)

Collection information. USA: Georgia: Clarke Co.: two individuals from two sites. Caught in flight trap from 27 July–26 August 2020.

Distribution. Southeastern United States.

Saproxylic habits. Larvae develop within the moist, rotting contents of hollow trees (Choate 1987); adults also occur under bark (Hoffman 2006).

Germarostes aphodioides (Illiger, 1800)

Collection information. USA: Georgia: Clarke Co.: three individuals from three sites. Caught in flight trap from 21 April–14 July 2020.

Distribution. Eastern United States, south to Central America.

Saproxylic habits. Adults occur under bark of dead oaks (Robinson 1918), and in dying, fungus covered trees, such as tulip tree (Evans 2009); emerged from water oak and sweetgum typically at higher strata in the canopy but also associated with water oak and snags (Ulyshen and Hanula 2009a).

Ischaliidae

Ischalia costata (LeConte, 1861)

Collection information. USA: **Georgia (new state record*)**: Clarke Co.: a single individual from one site. Sifted from leaf litter from 27–28 July 2020.

Distribution. Northeastern North America, south to Georgia and Alabama.

Saproxylic habits. Larvae and adults of *Ischalia* Pascoe, 1860 feed on fungal mycelia growing on rotting stumps and downed logs (Young 1985); adults are flightless (Majka 2011).

Laemophloeidae

Charaphloeus adustus (LeConte, 1854)

Collection information. USA: **Georgia (new state record*)**: Clarke Co.: 13 individuals from 10 sites. Caught in flight trap from 9 March–16 June 2020.

Distribution. Eastern North America.

Saproxylic habits. Emerged from ash limbs (*Fraxinus* L. (Oleaceae)) (Ulyshen et al. 2012); adults occur under bark and on dead branches (Thomas 1993; Kim 2009).

Charaphloeus convexulus (LeConte, 1879)

Collection information. USA: **Georgia (new state record*)**: Clarke Co.: seven individuals from seven sites. Caught in flight trap from 9 March–9 April 2020.

Distribution. Eastern North America, west to Texas and North Dakota.

Saproxylic habits. Very little known; adults occur under bark (Thomas 1993).

Dysmerus basalis Casey, 1884

Collection information. USA: **Georgia (new state record)**: Clarke Co.: 11 individuals from eight sites. Caught in flight trap from 9 March–27 July 2020.

Distribution. Eastern and central United States, and Caribbean islands.

Saproxylic habits. Occur under bark and in bark beetle galleries, and emerged from bark beetle infested twigs, including sweetgum, poison ivy, and poisonwood (*Metopium toxiferum* (L.) Krug and Urb. (Anacardiaceae)) (Thomas 2009).

Laemophloeus biguttatus (Say, 1827)

Collection information. USA: Georgia: Clarke Co.: 24 individuals from 13 sites. Caught in flight trap from 9 March–26 August 2020.

Distribution. North America.

Saproxylic habits. Larvae develop under the bark of standing dead oaks (e.g., *Quercus hemisphaerica* W.Bartram ex Willd.) infested with the fungi *Biscogniauxia atropunctata*, and apparently jump when disturbed (Bertone et al. 2022); adults also occur under bark (Thomas 1993).

Conservation. Occurrence probability increases in old forests (predating 1938 and oak dominated) in the Piedmont (Traylor et al. 2024).

Laemophloeus fasciatus Melsheimer, 1846

Collection information. USA: Georgia: Clarke Co.: three individuals from three sites. Caught in flight trap from 9 March–26 August 2020.

Distribution. Eastern North America.

Saproxylic habits. Adults occur under bark (Thomas 1993).

Genus *Lathropus* Erichson, 1846

Collection information. USA: Georgia: Clarke Co.: 18 individuals from 13 sites. Caught in flight trap from 9 March–9 September 2020.

Saproxylic habits. Species of *Lathropus* occur under bark and in association with bark beetles (Thomas 1993); however, some evidence suggests the association is incidental and that *Lathropus* feed on fungi (Uliana 2003; Thomas 2010).

Phloeolaemus chamaeropis (Schwarz, 1878)

Collection information. USA: Georgia: Clarke Co.: two individuals from two sites. Caught in flight trap from 16 June–14 July 2020.

Distribution. Southeastern United States (Thomas 1993).

Saproxylic habits. Adults occur under the bark of hardwood logs (sometimes freshly dead with fermenting phloem), especially oak, and apparently feed on fungi (Thomas 1993); emerged from water oak and sweetgum logs (Ulyshen and Hanula 2009a) and occur on freshly dead southern red oak (Gil 2008).

Placonotus zimmermanni (LeConte, 1854)

Collection information. USA: Georgia: Clarke Co.: five individuals from five sites. Caught in flight trap from 9 March–14 July 2020.

Distribution. Eastern North America.

Saproxylic habits. Emerged from oaks, sweetgum, loblolly pine, and non-native mimosa, and especially associated with oak logs (Gil 2008; Ulyshen and Hanula 2009a; Ulyshen et al. 2018).

Lampyridae

Lucidota atra (Olivier, 1790)

Collection information. USA: Georgia: Clarke Co.: two individuals from one site. Caught in flight trap from 19 May–30 June 2020.

Distribution. Eastern North America.

Saproxylic habits. Larvae inhabit damp, rotting logs, but may also wander outside of this habitat (Branham and Archangelsky 2000).

Latridiidae

Enicmus aterrimus Motschulsky, 1866

Collection information. USA: **Georgia (new state record)**: Clarke Co.: 35 individuals from 19 sites. Caught in flight trap from 9 March–9 September 2020.

Distribution. North America.

Saproxylic habits. Adults and larvae of most *Enicmus* Thomson, 1859 feed on slime molds (Myxomycetes) (Andrews 2002), but it is unclear whether this is true for *E. Aterrimus* (Lawrence and Newton 1980).

Enicmus maculatus (LeConte, 1878)

Collection information. USA: Georgia: Clarke Co.: 289 individuals from 33 sites. Caught in flight trap from 9 March–9 September 2020.

Distribution. Eastern United States.

Saproxylic habits. Larvae develop in, and adults occur on *Hypoxylon* growing on oaks, including live oak (*Quercus virginiana* Mill.) and southern red oak, apparently feeding on conidia (Lawrence 1977; Gil 2008).

Conservation. Occurrence probability increases in old forests (predating 1938 and oak dominated) in the Piedmont (Traylor et al. 2024).

Enicmus tenuicornis LeConte, 1878

Collection information. USA: **Georgia (new state record)**: Clarke Co.: six individuals from four sites. Caught in flight trap from 6 May–30 June 2020.

Distribution. North America.

Saproxylic habits. Feeds on slime molds in the genus *Stemonitis* Gleditsch (Stemonitaceae) (Lawrence and Newton 1980); emerged from spruce (*Picea* A.Dietr), fir (*Abies* Mill.), and pine (all in Pinaceae) in the Pacific northwest (Hatch 1961), and mainly associated with coniferous forests in Atlantic Canada (Majka et al. 2009).

Leiodidae

Genus *Agathidium* Panzer, 1797

Collection information. USA: Georgia: Clarke Co.: 69 individuals from 21 sites, not identified to species-level. Caught in flight trap and sifted from leaf litter from 9 March–9 September 2020.

Saproxylic habits. Species of *Agathidium* are specialist consumers of slime molds (Lawrence and Newton 1980) and commonly occur under bark, in wood, or on fungi (Downie and Arnett 1996).

Conservation. Significantly higher abundance in primary (= old-growth) than secondary (= second-growth) forests in the southern Appalachian Mountains (Ferro et al. 2012a).

Genus *Anisotoma* Panzer, 1797

Collection information. USA: Georgia: Clarke Co.: a single individual from one site, not identified to species-level. Caught in flight trap from 19 May–2 June 2020.

Saproxylic habits. Species of *Anisotoma* are specialist consumers of slime molds (Lawrence and Newton 1980) and occur in decaying wood (Wheeler 1979).

Lucanidae

Platycerus quercus (Weber, 1801)

Collection information. USA: Georgia: Clarke Co.: a single individual from one site. Caught in flight trap from 25 March–9 April 2020.

Distribution. Eastern North America.

Saproxylic habits. Larvae feed on decaying wood and develop within rotting oak and hickory logs (Hoffmann 1937; Savely 1939).

Lycidae

Eros humeralis (Fabricius, 1801)

Collection information. USA: Georgia: Clarke Co.: a single individual from one site. Caught in flight trap from 25 March–9 April 2020.

Distribution. Eastern North America.

Saproxylic habits. Larvae develop within decaying wood (Bocak and Matsuda 2003; Fleming 2011) and adults sometimes aggregate under bark of stumps, such as pine (Frost 1945).

Lymexylidae

Melittomma sericeum (Harris, 1841)

Collection information. USA: **Georgia (new state record*)**: Clarke Co.: four individuals from three sites. Caught in flight trap from 16 June–27 July 2020.

Distribution. Eastern North America.

Saproxylic habits. Larvae bore through wounded wood, broken branches, dying trees, stumps, and freshly cut logs of oak, primarily white oak (Solomon 1995); adult females transport a symbiotic ambrosial fungus to new hosts with mycangia near their ovipositor, and this fungus grows on the walls of larval tunnels (Young 2002a); historically, *M. Sericeum* preferred American chestnut (Hopkins 1893).

Melandryidae

Anisoxya glaucula LeConte, 1866

Collection information. USA: **Georgia (new state record)**: Clarke Co.: two individuals from one site. Caught in flight trap from 2–30 June 2020.

Distribution. Eastern North America.

Saproxylic habits. Very little known; adults occur under bark (Staines and Staines 2021); species of *Anisoxya* Mulsant, 1856 from other regions develop within dead branches and stems of hardwood trees (Nikitsky and Pollock 2010).

Dircaea liturata LeConte, 1866

Collection information. USA: Georgia: Clarke Co.: 78 individuals from 31 sites. Caught in flight trap from 21 April–9 September 2020.

Distribution. Eastern North America, west to Alberta in Canada.

Saproxylic habits. Emerged from moderately decayed hardwood logs (Ferro et al. 2012a) and adults occur on a variety of dead hardwood trees (Majka and Pollock 2006); larvae of *Dircaea* Fabricius, 1798 develop within soft, white-rotten wood (Nikitsky and Pollock 2010).

Conservation. Significantly higher abundance in primary (= old-growth) than secondary (= second-growth) forests in the southern Appalachian Mountains (Ferro et al. 2012a).

Microscapha clavicornis LeConte, 1866

Collection information. USA: Georgia: Clarke Co.: five individuals from four sites. Caught in flight trap from 21 April–26 August 2020.

Distribution. Eastern North America.

Saproxylic habits. Emerged from hardwood twigs (Ferro and Nguyen 2016); adults feed on fungi growing on rotting wood (Luk 2012).

Microtonus sericans LeConte, 1862

Collection information. USA: Georgia: Clarke Co.: 71 individuals from 25 sites. Caught in flight trap from 25 March–27 July 2020.

Distribution. Eastern North America.

Saproxylic habits. Emerged from dead hardwood pieces of a variety of sizes and decomposition stages (Ferro et al. 2012a), including southern red oak twigs (Ferro et al. 2009; Ferro and Gimmel 2014); adults also occur on dead trees and shrubs, such as hawthorn (*Crataegus* L. (Rosaceae)) (Majka and Pollock 2006).

Conservation. In the Piedmont, significantly associated with forests within sparsely forested landscapes (<50% forest; Traylor et al. 2023a) and occurrence probability decreases with the amount of landscape forest cover (Traylor et al. 2024).

Orchesia castanea Melsheimer, 1846

Collection information. USA: **Georgia (new state record*)**: Clarke Co.: a single individual from one site. Caught in flight trap from 19 May–2 June 2020.

Distribution. Eastern North America, transcontinental in north.

Saproxylic habits. Breeds in a variety of polypore fungi, including *Trametes*, *Inonotus hispidus* (Bull.) P. Karst, and *Gloeophyllum sepiarium* (Wulfen) P. Karst (Gloeophyllaceae) (Weiss and West 1920); additionally emerged from rotting hickory branches dead for two to four years (Blackman and Stage 1924).

Orchesia cultriformis Laliberté, 1967

Collection information. USA: **Georgia (new state record*)**: Clarke Co.: a single individual from one site. Caught in flight trap from 25 March–9 April 2020.

Distribution. Eastern North America, transcontinental in north.

Saproxylic habits. Develop within decaying polypores of parasitic fungi, including *Inocutis dryophila* (Berk.) Fiasson and Niemelä (Hymenochaetaceae) growing on oaks (Hinson 2016) and *Inonotus obliquus* (Fr.) Pilát growing on birch (Bunyard 2015).

Genus *Phloiotrya* Stephens, 1832

Collection information. USA: Georgia: Clarke Co.: 22 individuals from 13 sites, unable to identify to species-level. Caught in flight trap from 21 April–30 June 2020.

Saproxylic habits. Species of *Phloiotrya* develop within firm wood of deciduous trees and adults feed on fungi (Nikitsky and Pollock 2010).

Spilotus quadripustulatus (Melsheimer, 1846)

Collection information. USA: **Georgia (new state record*)**: Clarke Co.: two individuals from two sites. Caught in flight trap from 9 April–6 May 2020.

Distribution. Eastern North America.

Saproxylic habits. Very little known; emerged from maple wood (DiGirolomo 2015) and associated with hardwood forests in Canada (Webster et al. 2012c).

Conservation. Rare in the Maritime Provinces of Canada, possibly due to the history of intensive forest management in the region altering forest composition and structure (Majka 2007).

***Symphora flavicollis* (Haldeman, 1848)**

Collection information. USA: Georgia: Clarke Co.: six individuals from four sites. Caught in flight trap from 21 April–2 June 2020.

Distribution. Eastern North America.

Saproxylic habits. unknown; other species of *Symphora* LeConte, 1866 emerged from dead hardwoods (Ferro et al. 2012a).

***Symphora rugosa* (Haldeman, 1848)**

Collection information. USA: Georgia: Clarke Co.: 31 individuals from 19 sites. Caught in flight trap from 6 May–11 August 2020.

Distribution. Eastern North America.

Saproxylic habits. Emerged from moderately decayed hardwood pieces (Ferro et al. 2012a).

Micromalthidae

***Micromalthus debilis* LeConte, 1878**

Collection information. USA: **Georgia (new state record)**: Clarke Co.: a single individual from one site. Caught in flight trap from 14–27 July 2020.

Distribution. Eastern North America, but spread to other regions (Philips and Young 2000).

Saproxylic habits. Develops within red-rotted hardwoods, especially oak and chestnut (Philips and Young 2000); displays a unique and complicated life cycle with separate phases of paedogenesis and parthenogenesis (see Philips and Young (2000) for overview and Barber (1913a, b) for original description).

Monotomidae

Genus *Bactridium* LeConte, 1861

Collection information. USA: Georgia: Clarke Co.: 11 individuals from nine sites, unable to identify to species-level. Caught in flight trap from 9 March–11 August 2020.

Saproxylic habits. Species of *Bactridium* occur under bark of hardwoods and feed on ascomycete fungi (McElrath and McHugh 2018).

***Rhizophagus sayi* Schaeffer, 1913**

Collection information. USA: Georgia: Clarke Co.: three individuals from two sites. Caught in flight trap from 9–25 March 2020.

Distribution. Eastern North America.

Saproxylic habits. Occur under the bark of deciduous trees where it is a predator and likely fungivore (Bousquet 1990); found in association with bark beetles (McElrath and McHugh 2018).

Conservation. Significantly associated with young forests (regrown since 1938 and pine dominated) in highly forested landscapes (> 50% forest) in the Piedmont (Traylor et al. 2023a).

Mordellidae

Falsomordellistena discolor (Melsheimer, 1846)

Collection information. USA: Georgia: Clarke Co.: three individuals from three sites. Caught in flight trap from 19 May–30 June 2020.

Distribution. Eastern North America.

Saproxylic habits. unknown; other species of *Falsomordellistena* Ermisch have been reared from dead wood (Ferro et al. 2009; Ferro et al. 2012a).

Falsomordellistena hebraica (LeConte, 1862)

Collection information. USA: Georgia: Clarke Co.: 13,688 individuals from 40 sites. Caught in flight trap from 9 April–9 September 2020.

Distribution. Eastern North America.

Saproxylic habits. Emerged from southern red oak twigs (Ferro et al. 2009).

Falsomordellistena pubescens (Fabricius, 1798) (treated as a species complex)

Collection information. USA: Georgia: Clarke Co.: 9,313 individuals from 40 sites, including many specimens more appropriately determinable as Falsomordellistena bihamata (Melsheimer, 1846), and several types of intermediate forms of the two species. Because of the sheer number of specimens and the clear gradient between the two species observed, they were treated as a collective here. Caught in flight trap from 9 April–26 August 2020.

Distribution. Eastern North America, south to Central America.

Saproxylic habits. *Falsomordellistena bihamata* has emerged from small pieces of moderately decayed hardwoods (Ferro et al. 2012a).

Glipodes sericans (Melsheimer, 1846)

Collection information. USA: Georgia: Clarke Co.: three individuals from three sites. Caught in flight trap from 30 June–9 September 2020.

Distribution. Southeastern United States, south to Mexico.

Saproxylic habits. Larvae develop in rotten oak logs, where they feed on the decaying wood (Savely 1939).

Hoshihananomia octopunctata (Fabricius, 1775)

Collection information. USA: Georgia: Clarke Co.: 18 individuals from 13 sites. Caught in flight trap from 19 May–11 August 2020.

Distribution. Eastern North America.

Saproxylic habits. Larvae develop within dead oak, hickory, and American beech (Felt 1906; Leng and Davis 1924; Ford and Jackman 1996; Jackman and Lu 2002).

Mordella atrata Melsheimer, 1846

Collection information. USA: Georgia: Clarke Co.: 11 individuals from eight sites. Caught in flight trap from 19 May–14 July 2020.

Distribution. North America.

Saproxylic habits. Emerged from a loblolly pine log (MU pers. obs.; Traylor et al. 2023c).

Mordella lunulata Helmuth, 1865

Collection information. USA: Georgia: Clarke Co.: 42 individuals from 18 sites. Caught in flight trap from 19 May–27 July 2020.

Distribution. Eastern United States.

Saproxylic habits. unknown, except adults beat from dead hardwood limbs (Downie and Arnett 1996); other species of *Mordella* L., 1758 develop within various types of decaying wood (reviewed in Traylor et al. 2023c).

Mordella marginata Melsheimer, 1846

Collection information. USA: Georgia: Clarke Co.: 158 individuals from 36 sites. Caught in flight trap from 21 April–27 July 2020.

Distribution. Eastern North America.

Saproxylic habits. Emerged from a variety of sizes and types of dead wood from hardwood trees (Dolphin et al. 1972; Ford and Jackman 1996; Ferro et al. 2012a; Ferro and Nguyen 2016); emerged from the fungus *Gloeophyllum sepiarium* although this is an unlikely host (Weiss 1920).

Mordella obliqua LeConte, 1878

Collection information. USA: Georgia: Clarke Co.: three individuals from three sites. Caught in flight trap from 2–30 June 2020.

Distribution. Eastern United States.

Saproxylic habits. unknown, except adults beat from dead hardwood limbs (Downie and Arnett 1996); other species of *Mordella* develop within various types of decaying wood (reviewed in Traylor et al. 2023c).

Mordellaria fascifera (LeConte, 1878)

Collection information. USA: Georgia: Clarke Co.: 16 individuals from 13 sites. Caught in flight trap from 2 June–11 August 2020.

Distribution. Southeastern United States (Liljeblad 1945).

Saproxylic habits. unknown; other species of *Mordellaria* Ermisch, 1950 develop within various types of decaying wood (reviewed in Traylor et al. 2023c).

Mordellaria serval (Say, 1835)

Collection information. USA: Georgia: Clarke Co.: 122 individuals from 37 sites. Caught in flight trap from 19 May–11 August 2020.

Distribution. Eastern North America.

Saproxylic habits. Emerged from moderately decayed hardwood logs (Ferro et al. 2012a); adults occur on various deadwood pieces, including dead pine, "ironwood" stumps, and dead American beech (Brimley 1951; Lisberg and Young 2003).

Mordellaria undulata (Melsheimer, 1846)

Collection information. USA: **Georgia (new state record*)**: Clarke Co.: 233 individuals from 36 sites. Caught in flight trap from 19 May–9 September 2020.

Distribution. Eastern North America, not yet recorded from much of the southeast.

Saproxylic habits. Develops within rotting elm (Hoffmann 1942); adults occur on dead hardwood branches (Downie and Arnett 1996).

Mordellistena liturata (Melsheimer, 1846)

Collection information. USA: Georgia: Clarke Co.: 277 individuals from 37 sites. Caught in flight trap from 19 May–9 September 2020.

Distribution. Eastern North America.

Saproxylic habits. Emerged from fresh swamp white oak logs (*Quercus bicolor* Willd.) (Powell et al. 2016, G.S. Powell in litt.), and from moderately decayed loblolly pine logs (Ulyshen et al. 2020; Traylor et al. 2023c).

Conservation. Significantly associated with forests in highly forested landscapes (> 50% forest) in the Piedmont (Traylor et al. 2023a).

Mordellistena masoni Liljeblad, 1918

Collection information. USA: **Georgia (new state record*)**: Clarke Co.: 98 individuals from 27 sites. Caught in flight trap from 2 June–11 August 2020.

Distribution. Eastern North America.

Saproxylic habits. Emerged from freshly cut loblolly pine logs (MU pers. obs.; Traylor et al. 2023c).

Conservation. In the Piedmont, significantly associated with forests within highly forested landscapes (> 50% forest; Traylor et al. 2023a) and occurrence probability increases with the amount of landscape forest cover (Traylor et al. 2024).

Mordellistena militaris LeConte, 1862

Collection information. USA: **Georgia (new state record*)**: Clarke Co.: 24 individuals from 12 sites. Caught in flight trap from 19 May–11 August 2020.

Distribution. Eastern North America.

Saproxylic habits. Emerged from decaying loblolly pine logs (Ulyshen et al. 2020; Traylor et al. 2023c).

Mordellistena picipennis Smith, 1882

Collection information. USA: Georgia: Clarke Co.: six individuals from two sites. Caught in flight trap from 2–16 June 2020.

Distribution. Eastern United States (Liljeblad 1945).

Saproxylic habits. Breeds in chestnut (Liljeblad 1945).

Mordellistena tosta LeConte, 1862

Collection information. USA: Georgia: Clarke Co.: 16 individuals from nine sites. Caught in flight trap from 19 May–30 June 2020.

Distribution. Eastern North America.

Saproxylic habits. Emerged from decayed loblolly pine logs (Ulyshen et al. 2020; Traylor et al. 2023c), and from alder (*Alnus* Mill. (Betulaceae)) (Liljeblad 1945).

Conservation. Significantly associated with, and occurrence probability increases in, young forests (regrown since 1938 and pine dominated) in the Piedmont (Traylor et al. 2023a, 2024).

Mordellistena trifasciata (Say, 1826)

Collection information. USA: Georgia: Clarke Co.: 305 individuals from 39 sites. Caught in flight trap from 21 April–9 September 2020.

Distribution. Eastern North America, south to Central America.

Saproxylic habits. Emerged from a sweetgum log (Ulyshen and Hanula 2009a; Traylor et al. 2023c).

Mordellochroa scapularis (Say, 1824)

Collection information. USA: **Georgia (new state record)**: Clarke Co.: 352 individuals from 38 sites. Caught in flight trap from 9 March–16 June 2020.

Distribution. Eastern North America, transcontinental in the north.

Saproxylic habits. Emerged from fresh hardwood logs (Ferro et al. 2012a).

Paramordellaria triloba **(Say, 1824)**

Collection information. USA: **Georgia (new state record*)**: Clarke Co.: six individuals from four sites. Caught in flight trap from 2 June–27 July 2020.

Distribution. Eastern North America.

Saproxylic habits. Emerged from a small diameter, decaying hardwood (Ferro et al. 2012a); adults occur on dead hardwoods, including "ironwood" and black cherry (Brimley 1951).

Yakuhananomia bidentata **(Say, 1824)**

Collection information. USA: Georgia: Clarke Co.: two individuals from two sites. Caught in flight trap from 2 June–27 July 2020.

Distribution. Eastern North America.

Saproxylic habits. Emerged from fungus-infested wood (Hoffmann 1942); adults occur on dead and dying hardwood trees including oak, hickory, and American beech (Leng and Davis 1924; Brimley 1951; Downie and Arnett 1996).

Murmidiidae

Mychocerinus depressus **(LeConte, 1866)**

Collection information. USA: Georgia: Clarke Co.: a single individual from one site. Caught in flight trap from 21 April–6 May 2020.

Distribution. Eastern North America.

Saproxylic habits. Adults occur under fungus-covered bark of oak, beech, and hickory (Lawrence and Stephan 1975); emerged from water oak, loblolly pine, and sweetgum, and associated with standing dead trees (Ulyshen and Hanula 2009a).

Mycetophagidae

Litargus sexpunctatus **(Say, 1826)**

Collection information. USA: Georgia: Clarke Co.: 12 individuals from nine sites. Caught in flight trap from 9 March–11 August 2020.

Distribution. Eastern North America.

Saproxylic habits. Larvae develop, and adults occur on *Hypoxylon* growing on oak, where they feed on conidia (Lawrence 1977); adults also occur on other fungi, such as *Pleurotus ostreatus* (Jacq.) P. Kumm. (Cline and Leschen 2005); emerged from and associated with dead oaks in upland forests (Ulyshen and Hanula 2009a).

Conservation. In the Piedmont, significantly associated with forests within highly forested landscapes (> 50% forest; Traylor et al. 2023a) and occurrence probability increases with the amount of landscape forest cover (Traylor et al. 2024).

Mycetophagus pluripunctatus **LeConte, 1856**

Collection information. USA: **Georgia (new state record*)**: Clarke Co.: two individuals from two sites. Caught in flight trap from 9 March–9 April 2020.

Distribution. Eastern North America.

Saproxylic habits. Adults occur in or on fleshy and gilled polypore fungi on standing dead trees and logs (Ciegler 2014), including *Climacodon septentrionalis* (Fr.) P. Karst (Meruliaceae) (Webster et al. 2012c).

Nitidulidae

Amphicrossus ciliatus **(Olivier, 1811)**

Collection information. USA: Georgia: Clarke Co.: 420 individuals from 39 sites. Caught in flight trap from 9 March–9 September 2020.

Distribution. Eastern North America.

Saproxylic habits. Larvae develop within slime fluxes (fermenting sap flows) on tree injuries, and adults occur in this habitat too (Cole and Streams 1970); adults occur at sap flows on oaks and maples, and on fleshy fungus (Price and Young 2006).

Conservation. Occurrence probability increases in old forests (predating 1938 and oak dominated) in the Piedmont (Traylor et al. 2024).

Nosodendridae

Nosodendron unicolor **Say, 1824**

Collection information. USA: Georgia: Clarke Co.: 15 individuals from 12 sites. Caught in flight trap from 9 March–26 August 2020.

Distribution. Eastern United States.

Saproxylic habits. Larvae develop within slime fluxes on hardwood trees, and adults occur in this habitat as well (Hayes and Chu 1946); the beetles feed on fermenting sap enriched with microorganisms and any predation is likely facultative (Ivie 2002a).

Conservation. Occurrence probability increases in old forests (predating 1938 and oak dominated) in the Piedmont (Traylor et al. 2024).

Passandridae

Catogenus rufus **(Fabricius, 1798)**

Collection information. USA: Georgia: Clarke Co.: seven individuals from six sites. Caught in flight trap from 25 March–26 August 2020.

Distribution. Eastern North America, south to Central America.

Saproxylic habits. Larvae parasitize the pupae of woodboring beetles, and adults can occur under loose bark of dead and dying hardwood and conifer trees (Dimmock 1882; Fiske 1905).

Ptinidae

Byrrhodes fallax (Fall, 1905)

Collection information. USA: **Georgia (new state record*)**: Clarke Co.: 10 individuals from nine sites. Caught in flight trap from 19 May–26 August 2020.

Distribution. Southeastern United States (White 1982).

Saproxylic habits. Unknown; species of *Byrrhodes* Leconte, 1878 occur in hard (persistent) tree fungi (Lawrence and de Viedma 1991; Philips 2002).

Byrrhodes incomptus (LeConte, 1865)

Collection information. USA: **Georgia (new state record*)**: Clarke Co.: 59 individuals from 20 sites. Caught in flight trap from 21 April–27 July 2020.

Distribution. Eastern North America (White 1982).

Saproxylic habits. Very little known; emerged from fungus (Arango and Young 2012).

Byrrhodes intermedius (LeConte, 1878)

Collection information. USA: **Georgia (new state record*)**: Clarke Co.: 37 individuals from 17 sites. Caught in flight trap from 9 April–26 August 2020.

Distribution. Eastern North America (White 1982).

Saproxylic habits. Emerged from *Ganoderma applanatum* (Pers.) Pat. Growing on a dead elm (Arango and Young 2012), and adults also occur on other shelf fungi, including *Fomes fomentarius* (Böving 1954).

Conservation. Rare in the Maritime Provinces of Canada, possibly due to the history of intensive forest management in the region altering forest composition and structure (Majka 2007).

Byrrhodes tristriatus (LeConte, 1878)

Collection information. USA: Georgia: Clarke Co.: 15 individuals from 11 sites. Caught in flight trap from 21 April–9 September 2020.

Distribution. Eastern North America.

Saproxylic habits. Reproduce in old brackets of *Inonotus cuticularis* (Bull.) P.Karst. (Weiss and West 1922).

Calymmaderus nitidus (LeConte, 1865)

Collection information. USA: Georgia: Clarke Co.: three individuals from three sites. Caught in flight trap from 2 June–14 July 2020.

Distribution. Eastern North America.

Saproxylic habits. Emerged from southern red oak and other hardwood twigs (Ferro et al. 2009; Ferro and Nguyen 2016).

Dorcatoma falli White, 1965

Collection information. USA: **Georgia (new state record)**: Clarke Co.: 35 individuals from 13 sites. Caught in flight trap from 9 April–2 June 2020.

Distribution. Eastern North America.

Saproxylic habits. unknown; species of *Dorcatoma* Hebrst, 1972 occur in large, persistent, and often woody polypore fungi (Lawrence and de Viedma 1991; Philips 2002).

Eucrada humeralis (Melsheimer, 1846)

Collection information. USA: **Georgia (new state record)**: Clarke Co.: a single individual from one site. Caught in flight trap from 9–21 April 2020.

Distribution. Eastern North America.

Saproxylic habits. Mine under bark of dead oak trees (Rozen 1958).

Euvrilletta mucorea (LeConte, 1865)

Collection information. USA: **Georgia (new state record)**: Clarke Co.: a single individual from one site. Caught in flight trap from 2–16 June 2020.

Distribution. Southeastern United States.

Saproxylic habits. unknown; species of *Euvrilleta* Van Dyke, 1946 develop within decayed wood of both hardwood and conifer trees (Baker 1972; Arango and Young 2012).

Euvrilletta peltata (Harris, 1836)

Collection information. USA: Georgia: Clarke Co.: five individuals from five sites. Caught in flight trap from 2 June–30 June 2020.

Distribution. Eastern North America.

Saproxylic habits. Bores through the rotten sapwood and heartwood of hardwoods and conifers (Baker 1972).

Conservation. Rare in the Maritime Provinces of Canada, possibly due to the history of intensive forest management in the region altering forest composition and structure (Majka 2007).

Hadrobregmus notatus (Say, 1825)

Collection information. USA: Georgia: Clarke Co.: a single individual from one site. Caught in flight trap from 25 March–9 April 2020.

Distribution. Eastern North America.

Saproxylic habits. Larvae develop within dead and rotten oak, ash, chestnut, and pine (Böving 1954; White 1982).

***Hemicoelus carinatus* (Say, 1823)**

Collection information. USA: **Georgia (new state record*)**: Clarke Co.: a single individual from one site. Caught in flight trap from 6–19 May 2020.

Distribution. Eastern North America, transcontinental in the north.

Saproxylic habits. Develops within a variety of dead hardwood and conifer trees (Simeone 1960), including freshly-dead and decayed wood (Arango and Young 2012).

***Oligomerus alternans* LeConte, 1865**

Collection information. USA: **Georgia (new state record*)**: Clarke Co.: a single individual from one site. Caught in flight trap from 19 May–2 June 2020.

Distribution. Eastern North America (Arango and Young 2012).

Saproxylic habits. Unknown; species of *Oligomerus* Redtenbacher, 1849 have been reared from various hardwoods (Philips 2002; Arango and Young 2012).

***Oligomerus sericans* (Melsheimer, 1846)**

Collection information. USA: Georgia: Clarke Co.: a single individual from one site. Caught in flight trap from 2–16 June 2020.

Distribution. Eastern North America.

Saproxylic habits. Not well known, hosts are thought to be walnut (*Juglans* L.), chestnut, and white oak (Fall 1905; Böving 1954; White 1982).

***Petalium bistriatum* (Say, 1825)**

Collection information. USA: Georgia: Clarke Co.: 488 individuals from 35 sites. Caught in flight trap from 21 April–9 September 2020.

Distribution. Eastern North America.

Saproxylic habits. Emerged from dry sections of black oak and bear oak (*Quercus ilicifolia* Wangenh.), with the bear oak record apparently coming from outer bark of a living tree (Ford 1973).

Conservation. Significantly associated with old forests (predating 1938 and oak dominated) in the Piedmont (Traylor et al. 2023a).

***Petalium debile* Fall, 1905**

Collection information. USA: Georgia: Clarke Co.: a single individual from one site. Caught in flight trap from 2–16 June 2020.

Distribution. Eastern United States.

Saproxylic habits. Emerged from southern red oak twigs (Ferro et al. 2009; Ferro and Gimmel 2014).

Petalium incisum **Ford, 1973**

Collection information. USA: Georgia: Clarke Co.: 176 individuals from 28 sites. Caught in flight trap and sifted from leaf litter from 19 May–9 September 2020.

Distribution. Eastern North America.

Saproxylic habits. Emerged from dead, dry sections of poison ivy, black locust (*Robinia pseudoacacia* L.), and staff vine (*Celastrus* L. (Celastraceae)) (Ford 1973).

Petalium whitei **Ford, 1973**

Collection information. USA: Georgia: Clarke Co.: 13 individuals from 11 sites. Caught in flight trap from 9 March–30 June 2020.

Distribution. Eastern North America.

Saproxylic habits. unknown; other species of *Petalium* LeConte reproduce in dry deadwood (Ford 1973).

Priobium sericeum **(Say, 1825)**

Collection information. USA: Georgia: Clarke Co.: two individuals from two sites. Caught in flight trap from 16–30 June 2020.

Distribution. Eastern North America.

Saproxylic habits. Larvae develop within dead branches of oak, cherry, hickory, holly (*Ilex* L. (Aquifoliaceae)), and mountain laurel (*Kalmia latifolia* L. (Ericaceae)) (White 1982), and apparently use very dry wood (McClarin 2005); emerged from large and small hardwood pieces and associated with fresh wood (Ferro et al. 2012a; Ferro and Nguyen 2016).

Conservation. Significantly higher abundance in primary (= old-growth) than secondary (= second-growth) forests in the southern Appalachian Mountains (Ferro et al. 2012a).

Genus *Ptilinus* Mueller, 1764

Collection information. USA: Georgia: Clarke Co.: five individuals from four sites, not identified to species-level (females). Caught in flight trap from 21 April–19 May 2020.

Saproxylic habits. Larvae of *Ptilinus* feed in dead hardwood trees and shrubs (White 1982).

Trichodesma gibbosa **(Say, 1825)**

Collection information. USA: Georgia: Clarke Co.: four individuals from four sites. Caught in flight intercept trap from 21 April–2 June 2020.

Distribution. Eastern North America.

Saproxylic habits. Larvae develop within a variety of dead hardwood trees (White 1982); emerged from both fresh and decayed hickory, including the decaying walls of a tree hollow (Blackman and Stage 1924; Holland 2009).

Trichodesma klagesi **Fall, 1905**

Collection information. USA: **Georgia (new state record*)**: Clarke Co.: a single individual from one site. Caught in flight trap from 2–16 June 2020.

Distribution. Eastern North America (Hinson and Blinn 2018).

Saproxylic habits. Emerged from hickory and dead stems of spice bush (*Lindera benzoin* (L.) Blume (Lauraceae)) (White 1982), as well as dead hardwood pieces of various diameter and decomposition stages (Ferro et al. 2012a).

Tricorynus gracilis **(Fall, 1905)**

Collection information. USA: **Georgia (new state record)**: Clarke Co.: a single individual from one site. Caught in flight trap from 25 March–9 April 2020.

Distribution. Eastern North America (White 1982).

Saproxylic habits. Larvae and adults collected from the fungus *Camillea tinctor* (Berk.) Læssøe, J.D. Rogers and Whalley (Xylariaceae) growing on the bark of a dead maple (Böving 1954; White 1963).

Tricorynus nigritulus **(LeConte, 1865)**

Collection information. USA: **Georgia (new state record*)**: Clarke Co.: 18 individuals from 10 sites. Caught in flight trap from 19 May–26 August 2020.

Distribution. Eastern North America (White 1982).

Saproxylic habits. Emerged from dead wood of elm and dead vines of *Wisteria* Nutt. (Fabaceae) (Böving 1954; White 1963).

Tricorynus punctatus **(LeConte, 1865)**

Collection information. USA: Georgia: Clarke Co.: 262 individuals from 40 sites. Caught in flight trap from 21 April–11 August 2020.

Distribution. Eastern North America (White 1982).

Saproxylic habits. Emerged from old sycamore logs and grape vines (*Vitis* L.) (White 1963).

Pyrochroidae

Dendroides canadensis **Latreille, 1810**

Collection information. USA: Georgia: Clarke Co.: a single individual from one site. Caught in flight trap from 19 May–2 June 2020.

Distribution. Eastern North America.

Saproxylic habits. Larvae develop under loose bark on the upper side of decaying logs (Young 2002b).

Conservation. Significantly higher abundance in primary (= old-growth) than secondary (= second-growth) forests in the southern Appalachian Mountains (Ferro et al. 2012a).

Neopyrochroa femoralis **(LeConte, 1855)**

Collection information. USA: Georgia: Clarke Co.: two individuals from two sites. Caught in flight trap from 25 March–9 April 2020.

Distribution. Eastern North America.

Saproxylic habits. Larvae develop under bark and in decayed wood of standing dead trees (Young 2002b).

Conservation. Rare in the Maritime Provinces of Canada, possibly due to the history of intensive forest management in the region altering forest composition and structure (Majka 2007).

Neopyrochroa flabellata **(Fabricius, 1787)**

Collection information. USA: Georgia: Clarke Co.: a single individual from one site. Caught in flight trap from 2–16 June 2020.

Distribution. Eastern North America.

Saproxylic habits. Larvae develop under bark and in decaying wood of logs, usually on the underside that is resting on the soil (Young 2002b).

Salpingidae

Inopeplus reclusa **(LeConte, 1880)**

Collection information. USA: **Georgia (new state record*)**: Clarke Co.: two individuals from two sites. Caught in flight trap from 19 May–2 June 2020.

Distribution. Southeastern United States.

Saproxylic habits. Emerged from loblolly pine logs (Ulyshen 2014); adults beaten from dead branches of a button bush (probably *Cephalanthus* L. (Rubiaceae)) (Blatchley 1918).

Scarabaeidae

Gnorimella maculosa **(Knoch, 1801)**

Collection information. USA: Georgia: Clarke Co.: eight individuals from eight sites. Caught in flight trap from 25 March–9 April 2020.

Distribution. Eastern North America.

Saproxylic habits. Emerged from moderately to well-decayed hardwood substrates, such as the hollowed interior of a redbud (*Cercis* L. (Fabaceae)) trunk or rotten logs (Ritcher 1966; Ferro et al. 2012a); adults occur on dead trees, such as red maple (*Acer rubrum* L.) (Staines 1984).

Conservation. Occurrence probability increases in old forests (predating 1938 and oak dominated) in the Piedmont (Traylor et al. 2024).

Valgus canaliculatus (Olivier, 1789)

Collection information. USA: Georgia: Clarke Co.: 480 individuals from 37 sites. Caught in flight trap from 25 March–27 July 2020.

Distribution. Eastern United States.

Saproxylic habits. Associated with subterranean termites (*Reticulitermes flavipes* (Kollar, 1837) (Blattodea: Rhinotermitidae)), and larvae develop by feeding on the walls of the termite galleries (Ritcher 1958); adults occur under bark of standing dead trees, such as mockernut hickory (*Carya tomentosa* Nutt.) and pine (Howden and Vogt 1951; Steury and Paulsen 2022).

Valgus seticollis (Palisot de Beauvois, 1805)

Collection information. USA: Georgia: Clarke Co.: two individuals from two sites. Caught in flight trap from 9 March–21 April 2020.

Distribution. Eastern United States.

Saproxylic habits. Associated with subterranean termites (*R. flavipes*), and larvae develop by feeding on the walls of termite galleries (Ritcher 1958).

Scraptiidae

Canifa pallipes (Melsheimer, 1846)

Collection information. USA: **Georgia (new state record*)**: Clarke Co.: 63 individuals from 28 sites. Caught in flight trap from 25 March–14 July 2020.

Distribution. Eastern North America, transcontinental in the north.

Saproxylic habits. Emerged from dead hardwood trees, such as elm (Hoffmann 1942) and oak dead for 2–3 years (McClarin 2008a); also emerged in numbers from black knot fungus (*Apiosporina morbosa* (Schwein.) Arx (Venturiaceae)) growing on cherry trees (Melvin et al. 1967).

Conservation. Occurrence probability increases in old forests (predating 1938 and oak dominated) in the Piedmont (Traylor et al. 2024).

Canifa plagiata (Melsheimer, 1846)

Collection information. USA: Georgia: Clarke Co.: 10 individuals from five sites. Caught in flight trap from 9 April–2 June 2020.

Distribution. Eastern North America.

Saproxylic habits. unknown; larvae of *Canifa* LeConte, 1866 develop under the bark of dead logs (Pollock 2002).

Conservation. Occurrence probability increases with the amount of landscape forest cover in the Piedmont (Traylor et al. 2024).

Canifa pusilla (Haldeman, 1848)

Collection information. USA: **Georgia (new state record*)**: Clarke Co.: four individuals from three sites. Caught in flight trap from 16 June–14 July 2020.

Distribution. Eastern North America.

Saproxylic habits. unknown; larvae of *Canifa* develop under the bark of dead logs (Pollock 2002).

Pentaria trifasciata (Melsheimer, 1846)

Collection information. USA: **Georgia (new state record*)**: Clarke Co.: a single individual from one site. Caught in flight trap from 19 May–2 June 2020.

Distribution. North America.

Saproxylic habits. Adults occur under rotting logs (Schneider 2017) and among other habitats (e.g., flowers, Downie and Arnett 1996).

Silvanidae

Cathartosilvanus imbellis (LeConte, 1854)

Collection information. USA: Georgia: Clarke Co.: five individuals from three sites. Caught in flight trap from 19 May–11 August 2020.

Distribution. Eastern North America.

Saproxylic habits. Occur almost exclusively under bark, especially of oaks (Thomas 1993); emerged from loblolly pine, water oak, southern red oak, ash, and sweetgum (Gil 2008; Ulyshen and Hanula 2009a, 2010; Ulyshen et al. 2012); may rapidly colonize freshly burned logs (Ulyshen et al. 2010).

Nausibius major Zimmermann, 1869

Collection information. USA: Georgia: Clarke Co.: 34 individuals from eight sites. Caught in flight trap from 25 March–26 August 2020.

Distribution. Eastern United States, west to Arizona, and south to Mexico.

Saproxylic habits. Adults occur under the bark of old oaks and rotten trees, and at slime fluxes on oaks (Thomas 1993; Valentine 2007).

Conservation. In the Piedmont, significantly associated with old forests (predating 1938 and oak dominated) in highly forested landscapes (> 50% forest; Traylor et al. 2023a) and occurrence probability increases in old forests (predating 1938 and oak dominated) and with landscape forest cover (Traylor et al. 2024).

Nausibius repandus LeConte, 1866

Collection information. USA: **Georgia (new state record)**: Clarke Co.: a single individual from one site. Caught in flight trap from 6–19 May 2020.

Distribution. Southeastern United States.

Saproxylic habits. Emerged from and occur in pines infested with bark beetles (Moser et al. 1971; Thomas 1993), including a recently dead longleaf pine (*Pinus palustris* Mill.) (Davis and Leng 1912).

Silvanus muticus Sharp, 1899

Collection information. USA: Georgia: Clarke Co.: six individuals from six sites. Caught in flight trap from 25 March–26 August 2020.

Distribution. Eastern North America.

Saproxylic habits. Adults occur under bark of various trees (pine, maple, oak, chestnut, and juniper (*Juniperus*)), likely feeding on fungal spores (Halstead 1973); emerged and collected from loblolly pine and southern red oak logs throughout decomposition (Gil 2008; Ulyshen and Hanula 2010), as well as hardwood twigs (Ferro and Nguyen 2016); associated with deadwood in upland forests (Ulyshen and Hanula 2009a).

Sphindidae

Sphindus americanus LeConte, 1866

Collection information. USA: **Georgia (new state record)**: Clarke Co.: 15 individuals from 11 sites. Caught in flight trap and sifted from leaf litter from 25 March–9 September 2020.

Distribution. North America.

Saproxylic habits. All life stages are dependent on slime molds growing on dead wood (Lawrence and Newton 1980; Stephenson et al. 1994; Majka 2010).

Synchroidae

Synchroa punctata Newman, 1838

Collection information. USA: **Georgia (new state record)**: Clarke Co.: eight individuals from seven sites. Caught in flight trap from 2 June–9 September 2020.

Distribution. Eastern North America.

Saproxylic habits. Larvae consume fungal material and rotting wood (Payne 1931; Savely 1939); adults occur in deadwood of numerous hardwoods and pine (Blackman and Stage 1924).

Tenebrionidae

Genus *Adelina* Dejean, 1835

Collection information. USA: Georgia: Clarke Co.: two individuals from two sites, not identified to species (females). Caught in flight trap from 9 March–9 April 2020.

Saproxylic habits. Larvae and adults of *Adelina* occur under bark (Doyen 1988; Ulyshen and Hanula 2009a; Ciegler 2014).

Androchirus femoralis (Olivier, 1795)

Collection information. USA: Georgia: Clarke Co.: 11 individuals from eight sites. Caught in flight trap from 19 May–14 July 2020.

Distribution. Eastern United States.

Saproxylic habits. Little known, adults have been found on stumps (Blatchley 1910); larvae of *Androchirus* LeConte, 1862 develop within dead bracket fungi (Luk 2007).

Diaperis maculata Olivier, 1791

Collection information. USA: Georgia: Clarke Co.: a single individual from one site. Caught in flight trap from 11–26 August 2020.

Distribution. Eastern North America, south to Central America, and Caribbean islands.

Saproxylic habits. Larvae develop within polypore fungi and adults occur in fungi or under bark (Park 1931; Wolcott and Montgomery 1933; Daggy 1946; Graves 1960).

Conservation. Occurrence apparently stable from 1900–present on Plummers Island, Maryland, despite losses of other species possibly due to changing forest conditions (Steiner 2008).

Genus *Hymenorus* Mulsant, 1852

Collection information. See individual species below.

Saproxylic habits. Little is known about the specific habits of each species, however, larvae of *Hymenorus* develop in decaying wood of both hardwoods and conifers, including tree knots and dead portions of living trees (Wolcott and Montgomery 1933; White 1983; Majka et al. 2008; Ferro et al. 2012a), and adults often occur under bark (Fall 1931; Dunford and Young 2004; Ciegler 2014).

Hymenorus discretus Casey, 1891

Collection information. USA: Georgia: Clarke Co.: two individuals from two sites. Caught in flight trap from 16 June–14 July 2020.

Distribution. Eastern United States.

Saproxylic habits. unknown; an association with leaf-cutting ants (*Atta texana* (Buckley, 1860) (Hymenoptera: Formicidae)) (Walter et al. 1938) is in error (Waller and Moser 1990).

Hymenorus humeralis LeConte, 1866

Collection information. USA: **Georgia (new state record)**: Clarke Co.: two individuals from two sites. Caught in flight trap from 16 June–14 July 2020.

Distribution. Eastern United States.

Saproxylic habits. Unknown.

Conservation. Apparently recently colonized Plummers Island, Maryland, since the early 1900s, despite the losses of other species possibly due to changing forest conditions (Steiner 2008).

Hymenorus illusus Fall, 1931

Collection information. USA: Georgia: Clarke Co.: two individuals from two sites. Caught in flight trap from 16 June–14 July 2020.

Distribution. Eastern United States.

Saproxylic habits. Adult occur in fungi (Fall 1931).

Conservation. Apparently lost after 1925 from the fauna of Plummers Island, Maryland, possibly due to changing forest conditions (Steiner 2008).

Hymenorus niger (Melsheimer, 1846)

Collection information. USA: Georgia: Clarke Co.: 40 individuals from 19 sites. Caught in flight trap from 6 May–26 August 2020.

Distribution. Eastern North America.

Saproxylic habits. unknown.

Conservation. Apparently recently colonized Plummers Island, Maryland, since the early 1900s, despite the losses of other species possibly due to changing forest conditions (Steiner 2008).

Hymenorus obesus Casey, 1891

Collection information. USA: Georgia: Clarke Co.: three individuals from two sites. Caught in flight trap from 30 June–14 July 2020.

Distribution. Eastern North America.

Saproxylic habits. Adults occur under loose bark (Fall 1931).

Conservation. Apparently recently colonized Plummers Island, Maryland, since the early 1900s, despite the losses of other species possibly due to changing forest conditions (Steiner 2008).

Hymenorus perforatus Casey, 1891

Collection information. USA: Georgia: Clarke Co.: 41 individuals from 17 sites. Caught in flight trap from 19 May–26 August 2020.

Distribution. Eastern United States.

Saproxylic habits. unknown.

Conservation. Apparently recently colonized Plummers Island, Maryland, since the early 1900s, despite the losses of other species possibly due to changing forest conditions (Steiner 2008); occurrence probability increases in old forests (predating 1938 and oak dominated) in the Piedmont (Traylor et al. 2024).

Hymenorus picipennis Casey, 1891

Collection information. USA: **Georgia (new state record)**: Clarke Co.: three individuals from two sites. Caught in flight trap from 2 June–14 July 2020.

Distribution. Eastern North America.

Saproxylic habits. Emerged from red oak (*Quercus rubra* L.) (Majka et al. 2008) and eastern white pine (Fall 1931); adults occur in rotting hardwood logs (Dunford and Young 2004; Garrick et al. 2019).

Hymenorus pilosus (Melsheimer, 1846)

Collection information. USA: Georgia: Clarke Co.: 16 individuals from 10 sites. Caught in flight trap from 2 June–11 August 2020.

Distribution. Eastern North America.

Saproxylic habits. unknown.

Conservation. Apparently recently colonized Plummers Island, Maryland, since the early 1900s, despite the losses of other species possibly due to changing forest conditions (Steiner 2008).

Lobopoda erythrocnemis (Germar, 1824)

Collection information. USA: Georgia: Clarke Co.: 72 individuals from 22 sites. Caught in flight trap from 9 March–9 September 2020.

Distribution. Southeastern United States.

Saproxylic habits. Emerged from loblolly pine logs 1–5 years after tree death (Ulyshen and Hanula 2009a, 2010); adults occur under bark and on dead standing pines (Campbell 1966).

Lobopoda punctulata (Melsheimer, 1846)

Collection information. USA: Georgia: Clarke Co.: 22 individuals from eight sites. Caught in flight trap from 19 May–11 August 2020.

Distribution. Eastern United States.

Saproxylic habits. Larvae develop within the rotting interior of living trees (Craighead 1950); adults feed on fungal spores and occur on dead oak limbs and under bark (Campbell 1966).

Conservation. Apparently lost after 1925 from the fauna of Plummers Island, Maryland, possibly due to changing forest conditions (Steiner 2008).

Mycetochara fraterna (Say, 1824)

Collection information. USA: **Georgia (new state record*)**: Clarke Co.: four individuals from four sites. Caught in flight trap from 21 April–2 June 2020.

Distribution. Eastern United States, transcontinental in Canada.

Saproxylic habits. Adults occur under bark of aspen (Campbell 1978); species of *Mycetochara* Berthold, 1827 have been reared from the decaying interior of a living maple tree (McClarin 2008b).

Conservation. Apparently lost after 1925 from the fauna of Plummers Island, Maryland, possibly due to changing forest conditions (Steiner 2008).

Genus *Neomida* Latreille, 1829

Collection information. USA: Georgia: Clarke Co.: a single individual from one site, unable to be identified to species-level due to damage. Caught in flight trap from 9–25 March 2020.

Saproxylic habits. All life stages occur in various fungi where the larvae develop, and adults also occur under bark of pine and oak (Ciegler 2014).

Platydema ellipticum (Fabricius, 1798)

Collection information. USA: Georgia: Clarke Co.: a single individual from one site. Caught in flight trap from 25 March–9 April 2020.

Distribution. Eastern United States.

Saproxylic habits. Larvae develop within the shelf fungus *F. Gilva* (Weiss 1919).

Conservation. Occurrence apparently stable from 1900–present on Plummers Island, Maryland, despite losses of other species possibly due to changing forest conditions (Steiner 2008).

Platydema micans Zimmermann, 1870

Collection information. USA: Georgia: Clarke Co.: two individuals from two sites. Sifted from leaf litter from 29 June–31August 2020.

Distribution. Eastern United States, Central America, and Caribbean Islands.

Saproxylic habits. Adults occur in decaying fleshy fungi (Blatchley 1910) and under rotten wood (Triplehorn 1965).

Platydema picilabrum Melsheimer, 1846

Collection information. USA: Georgia: Clarke Co.: two individuals from two sites. Caught in flight trap from 9 March–11 August 2020.

Distribution. Eastern United States.

Saproxylic habits. Emerged from a standing dead water oak (Ulyshen and Hanula 2009a); adults also occur within dead tree trunks (Ciegler 2014).

Conservation. Apparently lost after 1925 from the fauna of Plummers Island, Maryland, possibly due to changing forest conditions (Steiner 2008).

Platydema subcostatum **Laporte and Brullé, 1831**

Collection information. USA: Georgia: Clarke Co.: a single individual from one site. Caught in flight trap from 25 March–9 April 2020.

Distribution. Eastern North America.

Saproxylic habits. Emerged from water oak and sweetgum (Ulyshen and Hanula 2009a); adults aggregate under bark, feeding on fungi (Savely 1939), as well as in dead logs and tree trunks (Ciegler 2014).

Conservation. Apparently lost after 1925 from the fauna of Plummers Island, Maryland, possibly due to changing forest conditions (Steiner 2008).

Platydema teleops **Triplehorn, 1965**

Collection information. USA: **Georgia (new state record*)**: Clarke Co.: 16 individuals from nine sites. Caught in flight trap from 9 March–30 June 2020.

Distribution. Eastern North America.

Saproxylic habits. Adults occur under bark, on deadwood debris, and on fungi (Dunford and Young 2004; Webster et al. 2012d; Ciegler 2014).

Conservation. Apparently lost after 1925 from the fauna of Plummers Island, Maryland, possibly due to changing forest conditions (Steiner 2008).

Polypleurus perforatus **(Germar, 1824)**

Collection information. USA: Georgia: Clarke Co.: a single individual from one site. Sifted from leaf litter from 27–28 July 2020.

Distribution. Southeastern United States.

Saproxylic habits. Larvae develop within smaller, dry branches, and adults are flightless (Steiner 1999); adults occur under dead bark and logs, including oak and pine (Ciegler 2014).

Conservation. Apparently lost after 1925 from the fauna of Plummers Island, Maryland, possibly due to changing forest conditions (Steiner 2008); considered an indicator of undisturbed, open forest conditions (Steiner 1999).

Rhipidandrus paradoxus **(Beauvois, 1820)**

Collection information. USA: Georgia: Clarke Co.: a single individual from one site. Caught in flight trap from 25 March–9 April 2020.

Distribution. Eastern North America.

Saproxylic habits. Adults occur on oyster mushrooms (Cline and Leschen 2005) and toothed fungi (*Hericium* Pers. (Hericiaceae) and *Hydnellum* P.Karst (Thelephoraceae)) (Ciegler 2014).

Conservation. Apparently lost after 1925 from the fauna of Plummers Island, Maryland, possibly due to changing forest conditions (Steiner 2008).

Strongylium tenuicolle **(Say, 1827)**

Collection information. USA: Georgia: Clarke Co.: two individuals from two sites. Caught in flight trap from 19 May–30 June 2020.

Distribution. Eastern North America, west to Arizona (Johnston and Cortés Hernández 2021).

Saproxylic habits. Larvae develop within decaying wood of various hardwood trees, including rotting portions of living trees (Triplehorn and Spilman 1973).

Conservation. Occurrence apparently stable from 1900–present on Plummers Island, Maryland, despite the loss of other species possibly due to changing forest conditions (Steiner 2008).

Uloma mentalis **Horn, 1870**

Collection information. USA: Georgia: Clarke Co.: a single individual from one site. Caught in flight trap from 2–16 June 2020.

Distribution. Eastern North America.

Saproxylic habits. Emerged from hardwood twigs (Ferro and Nguyen 2016); adults occur under bark (Ciegler 2014).

Conservation. Apparently lost after 1975 from the fauna of Plummers Island, Maryland, possibly due to changing forest conditions (Steiner 2008).

Tetratomidae

Eustrophopsis bicolor **(Fabricius, 1798)**

Collection information. USA: Georgia: Clarke Co.: a single individual from one site. Caught in flight trap from 30 June–14 July 2020.

Distribution. North America.

Saproxylic habits. Adults occur under bark, in decaying wood or in hollows of a variety of trees, as well as in or on polypore fungi (Pollock 2012; Ciegler 2014).

Eustrophus tomentosus **Say, 1827**

Collection information. USA: Georgia: Clarke Co.: 105 individuals from 23 sites. Caught in flight trap from 25 March–9 September 2020.

Distribution. North America.

Saproxylic habits. Adults occur under bark, in decaying wood or in hollows of a variety of trees, in addition to in or on polypore fungi (Pollock 2012; Ciegler 2014).

Conservation. Rare in the Maritime Provinces of Canada, possibly due to the history of intensive forest management in the region altering forest composition and structure (Majka 2007).

Tetratoma tessellata Melsheimer, 1844

Collection information. USA: **Georgia (new state record*)**: Clarke Co.: three individuals from two sites. Caught in flight trap from 9 April–6 May 2020.

Distribution. Eastern North America.

Saproxylic habits. Occur on fungi growing on dead trees (birch, maple, oak) (Chantal 1985; Majka and Pollock 2006), including a dried oyster mushroom growing on a sugar maple (Webster et al. 2012c).

Throscidae

Aulonothroscus convergens (Horn, 1885)

Collection information. USA: Georgia: Clarke Co.: 45 individuals from 19 sites. Caught in flight trap from 9 March–9 September 2020.

Distribution. Eastern United States (Blanchard 1917).

Saproxylic habits. Emerged from loblolly pine throughout decomposition (Ulyshen and Hanula 2010) and hardwood twigs (Ferro and Nguyen 2016).

Aulonothroscus distans Blanchard, 1917

Collection information. USA: **Georgia (new state record)**: Clarke Co.: two individuals from two sites. Caught in flight trap from 21 April–6 May 2020.

Distribution. Eastern North America.

Saproxylic habits. Emerged in number from dead hardwoods and associated with freshly dead wood (Ferro et al. 2012a).

Conservation. Significantly higher abundance in secondary (= second-growth) than primary (= old-growth) forests in the southern Appalachian Mountains (Ferro et al. 2012a).

Aulonothroscus parallelus Blanchard, 1917

Collection information. USA: **Georgia (new state record*)**: Clarke Co.: 25 individuals from 12 sites. Caught in flight trap from 25 March–27 July 2020.

Distribution. Southeastern United States (previously known from Virginia and unspecified “southern” localities (Blanchard 1917)).

Saproxylic habits. Unknown; species of *Aulonothruscus* Horn, 1890 emerged from deadwood and adults occur under bark of dead hardwoods and conifers, including standing dead trees (Howden and Vogt 1951; Ulyshen and Hanula 2010; Ferro et al. 2012a).

Trogossitidae

Airora cylindrica (Audinet-Serville, 1828)

Collection information. USA: Georgia: Clarke Co.: a single individual from one site. Caught in flight trap from 16–30 June 2020.

Distribution. Eastern North America.

Saproxylic habits. Adults occur under bark of pine, oak, and hickory (Barron 1971); emerged from loblolly pine, water oak, and sweetgum, and associated with pine and snags (Ulyshen and Hanula 2009a).

Corticotomus cylindricus (LeConte, 1863)

Collection information. USA: Georgia: Clarke Co.: three individuals from two sites. Caught in flight trap from 25 March–19 May 2020.

Distribution. Eastern United States.

Saproxylic habits. Predator and associate of bark and ambrosia beetles (Blackman 1922; Thatcher 1960; Barron 1971); reared from, and occur on a variety of dead hardwoods and pine (Barron 1971).

Corticotomus parallelus (Melsheimer, 1844)

Collection information. USA: Georgia: Clarke Co.: two individuals from two sites. Caught in flight trap from 25 March–19 May 2020.

Distribution. Eastern United States.

Saproxylic habits. Mostly unknown, occur under bark of pine and emerged from sumac (*Rhus* L. (Anacardiaceae)) (Barron 1971).

Temnoscheila acuta (LeConte, 1858)

Collection information. USA: **Georgia (new state record)**: Clarke Co.: two individuals from two sites. Caught in flight trap from 16 June–14 July 2020.

Distribution. Eastern United States and Mexico (Barron 1971).

Saproxylic habits. Adults occur under dead bark and on logs, including pine (Barron 1971; Dajoz 1989); adults and larvae of *Temnoscheila* Westwood, 1830 are predatory on woodboring beetle larvae under the bark of dead trees and shrubs (Kolibáč 2013).

Tenebroides bimaculatus (Melsheimer, 1844)

Collection information. USA: Georgia: Clarke Co.: six individuals from four sites. Caught in flight trap from 21 April–14 July 2020.

Distribution. Eastern United States.

Saproxylic habits. Larvae are predators of woodboring larvae (Champlain and Knull 1923); emerged from water oak (Ulyshen and Hanula 2009a); adults and larvae also occur under bark, including oak and elm (Hoffmann 1942; Barron 1971).

Tenebroides corticalis (Melsheimer, 1844)

Collection information. USA: Georgia: Clarke Co.: nine individuals from eight sites. Caught in flight trap from 9 March–9 September 2020.

Distribution. North and Central America.

Saproxylic habits. Adults and larvae occur within a wide variety of tree species, decomposition stages, and sizes of deadwood, where they are predators of woodboring insects and bark beetles (Blackman and Stage 1924; Hoffmann 1942; Barron 1971); associated with logs and lower boles of dead trees (Ulyshen and Hanula 2009a).

Tenebroides laticollis (Horn, 1862)

Collection information. USA: Georgia: Clarke Co.: two individuals from two sites. Caught in flight trap from 14 July–26 August 2020.

Distribution. Eastern North America.

Saproxylic habits. Emerged from and associated with water oak (Ulyshen and Hanula 2009a); adults occur under bark of dead oak and apple (*Malus* Mill. (Rosaceae)), and on the fungus *Laetiporus sulphureus* (Bull.) Murrill (Laetiporaceae) (Barron 1971).

Tenebroides rugosipennis (Horn, 1862)

Collection information. USA: Georgia: Clarke Co.: 50 individuals from 19 sites. Caught in flight trap from 9 March–19 May 2020.

Distribution. Eastern United States, west to Arizona (Barron 1971).

Saproxylic habits. Occur under bark of dead oaks (Barron 1971).

Conservation. Occurrence probability increases in old forests (predating 1938 and oak dominated) in the Piedmont (Traylor et al. 2024).

Tenebroides semicylindricus (Horn, 1862)

Collection information. USA: Georgia: Clarke Co.: a single individual from one site. Caught in flight trap from 14–27 July 2020.

Distribution. Eastern United States.

Saproxylic habits. Emerged from water oak, loblolly pine, and sweetgum, and was associated with the crowns of standing dead trees (Ulyshen and Hanula 2009a).

Thymalus marginicollis Chevrolat, 1842

Collection information. USA: Georgia: Clarke Co.: three individuals from three sites. Caught in flight trap from 21 April–19 May 2020.

Distribution. Eastern North America, transcontinental in Canada.

Saproxylic habits. Larvae develop within polypore fungi (e.g., the birch polypore (*Fomitopsis betulina* (Bull.) B.K. Cui, M.L. Han and Y.C. Dai (Fomitopsidaceae)), and adults occur in association with it as well (Brues 1927; Minch 1952); adults also occur on other fungi, including *Daedalea confragosa* Berk. (Fomitopsidaceae), *Cerrena unicolor* (Bull.) Murrill (Cerrenaceae), and *Trametes versicolor* (L.) Lloyd (Barron 1971).

Zopheridae

Aulonium parallelopipedum (Say, 1826)

Collection information. USA: Georgia: Clarke Co.: two individuals from two sites. Caught in flight trap from 19 May–16 June 2020.

Distribution. Eastern United States.

Saproxylic habits. Emerged from sweetgum and water oak snags (Ulyshen and Hanula 2009a); adults occur on dead logs or under bark, including oak, beech, and elm (Hopkins 1893; Robinson 1918; Hoffmann 1942; Gil 2008); species of *Aulonium* Erichson, 1845 are likely fungivores that facultatively prey upon bark beetles (Ivie 2002b).

Bitoma quadricollis (Horn, 1885)

Collection information. USA: Georgia: Clarke Co.: 25 individuals from 15 sites. Caught in flight trap from 9 March–11 August 2020.

Distribution. Eastern North America.

Saproxylic habits. Larvae develop in *Hypoxylon* fungus growing on oaks, where they were consuming fungal tissue (Lawrence 1977); emerged from pine and especially oaks (Ulyshen and Hanula 2009a); adults most commonly reside under bark of freshly killed oaks, but also maple and beech (Stephan 1989; Gil 2008).

Conservation. Significantly associated with, and occurrence probability increases in, old forests (predating 1938 and oak dominated) in the Piedmont (Traylor et al. 2023a, 2024).

Bitoma quadriguttata (Say, 1826)

Collection information. USA: Georgia: Clarke Co.: 24 individuals from 15 sites. Caught in flight trap from 9 March–11 August 2020.

Distribution. Eastern North America.

Saproxylic habits. Emerged from sweetgum, loblolly pine, and especially oak in upland forests (Ulyshen and Hanula 2009a, 2010); adults occur under bark of various hardwoods and occasionally pines (Stephan 1989).

Colydium lineola Say, 1826

Collection information. USA: Georgia: Clarke Co.: 11 individuals from nine sites. Caught in flight trap from 25 March–11 August 2020.

Distribution. Eastern and coastal western North America.

Saproxylic habits. Adults and larvae inhabit bark beetle tunnels (Hopkins 1893; Hoffmann 1942), although reported predation may be circumstantial or facultative (Ivie 2002b); prefers deadwood at the base of trees (Stephan 1989; Ulyshen and Hanula 2009a); emerged from oaks, loblolly pine, hickory, and various other hardwoods (Blackman and Stage 1924; Stephan 1989; Gil 2008; Ulyshen and Hanula 2009a).

Endeitoma dentata (Horn, 1885)

Collection information. USA: Georgia: Clarke Co.: a single individual from one site. Sifted from leaf litter from 29–30 June 2020.

Distribution. Southeastern United States.

Saproxylic habits. Adults occur in rotting pine logs and under bark of oaks (Stephan 1989); rapidly colonizes burned loblolly pine logs (Ulyshen et al. 2010).

Endeitoma granulata (Say, 1826)

Collection information. USA: Georgia: Clarke Co.: 10 individuals from eight sites. Caught in flight trap from 25 March–2 June 2020.

Distribution. Eastern North America.

Saproxylic habits. Emerged from loblolly pine logs (Ulyshen and Hanula 2009a) and hardwood twigs (Ferro and Nguyen 2016); adults occur where mold is growing under loose bark of hardwoods (especially oaks) and pines (Stephan 1989; Gil 2008).

Namunaria guttulata (LeConte, 1863)

Collection information. USA: Georgia: Clarke Co.: seven individuals from seven sites. Caught in flight trap from 27 July–9 September 2020.

Distribution. Eastern North America.

Saproxylic habits. Occur on fungal growth under the bark of dead hardwoods (e.g., beech) and pines, including snags (Hopkins 1893; Howden and Vogt 1951; Stephan 1989); emerged from loblolly pine, sweetgum, and water oak logs and snags (Ulyshen and Hanula 2009a), and from ash limbs in the canopy (Ulyshen et al. 2012).

Conservation. Significantly associated with old forests (predating 1938 and oak dominated) in highly forested landscapes (> 50% forest) in the Piedmont (Traylor et al. 2023a).

Paha laticollis (LeConte, 1863)

Collection information. USA: Georgia: Clarke Co.: six individuals from six sites. Caught in flight trap and sifted from leaf litter from 9 March–30 June 2020.

Distribution. Eastern United States.

Saproxylic habits. Emerged from smaller hardwood branches and twigs (Ferro et al. 2012a; Ferro and Nguyen 2016) and collected from loblolly pine logs (Gil 2008); adults occur in white-rotten logs, in tree holes, and under bark, especially at the base of oaks (Stephan 1989).

Pycnomerus haematodes (Fabricius, 1801)

Collection information. USA: Georgia: Clarke Co.: four individuals from four sites. Caught in flight trap from 21 April–30 June 2020.

Distribution. Eastern United States.

Saproxylic habits. Adults and larvae occur under bark and in the wood of moist, rotting pines, and occasionally in bark beetle galleries (Savely 1939; Howden and Vogt 1951; Stephan 1989); emerged and collected from pine, oak, and sweetgum, but associated with pines and occurred throughout decomposition (Gil 2008; Ulyshen and Hanula 2009a, 2010); emerged from burned and unburned loblolly pine logs (Ulyshen et al. 2010).

Pycnomerus reflexus (Say, 1826)

Collection information. USA: Georgia: Clarke Co.: nine individuals from eight sites. Caught in flight trap from 25 March–9 September 2020.

Distribution. Eastern North America.

Saproxylic habits. Adults and larvae occur under bark of rotting oaks and pine (Savely 1939; Stephan 1989; Gil 2008); emerged from loblolly pine, sweetgum, and especially oaks, and associated with logs at base of dead trees (Ulyshen and Hanula 2009a).

Pycnomerus sulcicollis LeConte, 1863

Collection information. USA: Georgia: Clarke Co.: three individuals from three sites. Caught in flight trap from 2 June–26 August 2020.

Distribution. Eastern United States.

Saproxylic habits. Under bark and in moist, rotting wood of hardwoods (especially oaks and hickory), and occasionally pines (Stephan 1989; Gil 2008); emerged from oaks, loblolly pine, sweetgum logs and hardwood twigs (Ulyshen and Hanula 2009a; Ferro and Nguyen 2016); emerged throughout loblolly pine decomposition and associated with the base and fallen logs of dead pine trees (Ulyshen and Hanula 2009a, 2010).

Conservation. Significantly associated with young forests (regrown since 1938 and pine dominated) in highly forested landscapes (> 50% forest) in the Piedmont (Traylor et al. 2023a).

Synchita fuliginosa **Melsheimer, 1846**

Collection information. USA: Georgia: Clarke Co.: 47 individuals from 26 sites. Caught in flight trap from 21 April–9 September 2020.

Distribution. Eastern North America.

Saproxylic habits. Larvae and adults occur under bark and feed on fungal growth, including chestnut blight (*Cryphonectria parasitica* (Murrill.) Barr (Cryphonectriaceae) (Craighead 1920); emerged from, and occurs under bark of dead elm, maple, oak, pine, hickory, and birch (Savely 1939; Hoffmann 1942; Stephan 1989; Gil 2008), and associated with the wood at the base of dead sweetgums (Ulyshen and Hanula 2009a).

Synchita parvula **Guérin-Méneville, 1844**

Collection information. USA: Georgia: Clarke Co.: 567 individuals from 40 sites. Caught in flight trap from 9 March–9 September 2020.

Distribution. Eastern United States.

Saproxylic habits. Emerged and collected from oaks (southern red oak and water oak) (Gil 2008; Ulyshen and Hanula 2009a) and associated with dead oaks (Stephan 1989).

Conservation. significantly associated with old forests (predating 1938 and oak dominated) in the Piedmont (Traylor et al. 2023a).

Discussion

The Coleoptera lists provided here join others in assembling the natural history information of saproxylic invertebrates in the southeastern USA. Hanula (1996) provided a partial list of wood-feeding insects (Blattodea: Termitoidea, Coleoptera, Lepidoptera, and Hymenoptera) for the region, and others assembled similar lists for earthworms (Oligochaeta; Hendrix 1996); mites (Orbatida, Prostigmata, and Mesostigmata; Johnston and Crossley 1996); and millipedes (Diplopoda), centipedes (Chilopoda), and land-snails (various Gastropoda; Caldwell 1996). Snider (1996) compiled an overview of southeastern Collembola occurring in deadwood. Ferro et al. (2012a) provided habitat details and photographs of 71 Coleoptera species associated with various deadwood types and/or forest disturbance categories in Great Smoky Mountains National Park. Ferro et al. (2012a) additionally reviewed the saproxylic literature for the region and wrote a brief history of worldwide saproxylic research. Moreover, published works providing habitat associations and distributional information are available for better known and economically important groups such as Buprestidae (Nelson et al. 2008), Cerambycidae (Lingafelter 2007), and Curculionidae: Scoyltinae (Wood 1982). Aside from those referenced above, few resources exist for classifying invertebrate species as saproxylic, which may be a major impediment for deadwood-biodiversity research in the region. Thus, the lists that we present add to the foundation of knowledge about the region's saproxylic fauna, which will hopefully facilitate further biodiversity research.

An efficient way of gaining knowledge about host range and microhabitat usage for a wide variety of species is emergence experiments, where deadwood pieces are either created or chosen in the field, typically removed from the field after a period of time, and placed into chambers where insects will eventually emerge (methods reviewed in Ferro and Carlton 2011). These types of experiments are useful for inventorying the species using specific types of resources and comparing biodiversity patterns along environmental, spatial, or temporal gradients. For example, studies have examined the saproxylic fauna inhabiting deadwood in response to tree species, decomposition stage, diameter class, vertical stratification, seasonality, sun exposure, flooding, fire exposure, and native/non-native status (Ulyshen and Hanula 2009a, 2010; Ferro et al. 2009, 2012a; Ulyshen et al. 2010, 2012, 2018, 2020; Ferro and Gimmel 2014; Ulyshen 2014; Seibold et al. 2016; Seibold et al. 2018; Vogel et al. 2020; Lettenmaier et al. 2022). Much of the natural history information and species records included in our lists was partially or entirely learned from emergence studies. Such studies are invaluable for providing information about a species' use of particular habitats. For example, no habitat information was known of the canopy specialist, *Tenebroides semicylindricus* (Trogossitidae), until it emerged in numbers from dead wood removed from tree crowns (Ulyshen and Hanula 2009a). These studies, however, should be used to complement more thorough investigations of a species' biology, and documenting the detailed natural history of species should be prioritized when opportunities arise. For example, the fascinating and possibly unique life cycle of *Micromalthus debilis* (Micromalthidae) would have gone unnoticed were it not for the curiosity and careful study of Barber (1913a, b).

Producing a regional annotated checklist for saproxylic invertebrates would be a great goal for future researchers and would greatly facilitate research in this field. However, we are far from understanding the southeastern fauna well enough to accomplish this, and this is likely the case for other regions as well. From the 293 taxa for which we provide saproxylic habits, 29 species (9.9%) are considered saproxylic solely on taxonomic placement (i.e., no information exists but all congeners with known biology are saproxylic), and 68 species (23.2%) are recorded for the first time in the state of Georgia. Moreover, the extent of natural history known for many species included in our list is limited to a single rearing or emergence event. Thus, very basic biological and distributional information about saproxylic Coleoptera is lacking, and the same applies for other invertebrate groups as well. Filling this information gap is essential for understanding the responses of biodiversity to changing forest conditions and assessing conservation needs.

Acknowledgements

We thank Robert Turnbow and Cecil Smith for early access to their work, An Annotated List of the Coleoptera of Georgia (https://site.caes.uga.edu/ugca/turnbow-and-smith/). We thank two reviewers for their careful reading and comments to improve this manuscript.

Additional information

Conflict of interest

The authors have declared that no competing interests exist.

Ethical statement

No ethical statement was reported.

Funding

This study was funded through Presidential Early Career Award (PECASE) funds awarded to MD Ulyshen and USDA National Institute of Food and Agriculture Hatch project GEO00886 awarded to JV McHugh.

Author contributions

Clayton R. Traylor – Conceptualization, Data curation, Investigation, Methodology, Project administration, Writing – original draft, Writing – review and editing. Michael D Ulyshen – Conceptualization, Funding acquisition, Resources, Writing – review and editing. J. Winston Cornish – Data curation, Investigation, Methodology, Writing – review and editing. Gabriel Tigreros – Data curation, Writing – review and editing. Joseph V. McHugh – Conceptualization, Funding acquisition, Resources, Writing – review and editing.

Author ORCIDs

Clayton R. Traylor https://orcid.org/0000-0001-7798-7198
J. Winston Cornish https://orcid.org/0009-0002-3819-2936
Joseph V. McHugh https://orcid.org/0000-0002-7954-6254

Data availability

All of the data that support the findings of this study are available in the main text or Supplementary Information.

References

Alexander KNA (2008) Tree biology and saproxylic coleoptera: issues of definitions and conservation language. Revue d'Ecologie (La Terre et La Vie) 10: 9–13. https://doi.org/10.3406/revec.2008.1455

Anderson WH (1952) Larvae of some genera of Cossoninae (Coleoptera: Curculionidae). Annals of the Entomological Society of America 45: 281–309. https://doi.org/10.1093/aesa/45.2.281

Anderson RS (2002) Curculionidae Latreille 1802. In: Arnett RH, Thomas MC, Skelley PE, Frank JH (Eds) American Beetles. Polyphaga: Scarabaeoidea through Curculionoidea. CRC Press, Boca Raton, 722–815.

Anderson RS (2008a) A review of the genus *Cryptorhynchus* Illiger 1807 in the United States and Canada (Curculionidae: Cryptorhynchinae). The Coleopterists Bulletin 62: 168–180. https://doi.org/10.1649/1065.1

Anderson RS (2008b) A review of the genus *Eubulus* Kirsch 1869 in the United States and Canada (Curculionidae: Cryptorhynchinae). The Coleopterists Bulletin 62: 287–296. https://doi.org/10.1649/1064.1

Andrews FG (2002) Latridiidae Erichson 1842. In: Arnett RH, Thomas MC, Skelley PE, Frank JH (Eds) American Beetles. Polyphaga: Scarabaeoidea through Curculionoidea. CRC Press, Boca Raton, 395–398.

Arango RA, Young DK (2012) Death-watch and spider beetles of Wisconsin—Coleoptera: Ptinidae. General Technical Report FPL-GTR-209. United States Department of Agriculture, Forest Service, Forest Products Laboratory, Madison, 158 pp. https://doi.org/10.2737/FPL-GTR-209

Atkinson TH, Foltz JL, Connor MD (1988) Bionomics of *Pissodes nemorensis* Germar (Coleoptera: Curculionidae) in Northern Florida. Annals of the Entomological Society of America 81: 255–261. https://doi.org/10.1093/aesa/81.2.255

Baker WL (1972) Eastern forest insects. Miscellaneous Publication no. 1175. United States Department of Agriculture, Forest Service, Washington D.C., 642 pp. https://doi.org/10.5962/bhl.title.65893

Barber HS (1913a) Observations on the life history of *Micromalthus debilis* Lec. (Coleoptera). Proceedings of the Entomological Society of Washington 15: 31–38. https://biostor.org/reference/66179

Barber HS (1913b) The remarkable life-history of a new family (Micromalthidae) of beetles. Proceedings of the Biological Society of Washington 26: 185–190. https://biostor.org/reference/81590

Barron JR (1971) A revision of the Trogositidae of America North of Mexico (Coleoptera: Cleroidea). Memoirs of the Entomological Society of Canada 103: 1–143. https://doi.org/10.4039/entm10375fv

Beal RS (1985) Review of Nearctic species of *Orphilus* (Coleoptera: Dermestidae) with description of the larva of *O. subnitidus* LeConte. The Coleopterists Bulletin 39: 265–271. https://www.jstor.org/stable/4008285

Beiriger RL (2008) *Micrapate cristicauda* Casey (Coleoptera: Bostrichidae) in Florida. The Coleopterists Bulletin 62: 419–420. https://doi.org/10.1649/1101.1

Bertone MA, Gibson JC, Seago AE, Yoshida T, Smith AA (2022) A novel power-amplified jumping behavior in larval beetles (Coleoptera: Laemophloeidae). PLoS ONE 17: e0256509. https://doi.org/10.1371/journal.pone.0256509

Beutenmuller W (1893) On the food habits of North American Rhynchophora. Journal of the New York Entomological Society 1: 80–88. https://www.jstor.org/stable/25002559

Blackman MW (1922) Mississippi Bark Beetles. Technical Bulletin No. 11. Mississippi Agricultural Experiment Station, Agricultural College, 130 pp.

Blackman MW, Stage HH (1918) Notes on Insects Bred from the Bark and Wood of the American Larch. New York State College of Forestry at Syracuse University, Technical Publication No. 10. 18: 11–115. https://doi.org/10.5962/bhl.title.40923

Blackman MW, Stage HH (1924) On the succession of insects living in the bark and wood of dying, dead and decaying hickory New York State College of Forestry at Syracuse University, Technical Publication No. 17. 24: 3–269.

Blanchard F (1917) Revision of the Throscidae of North America (Coleoptera). Transactions of the American Entomological Society 43: 1–26. https://www.jstor.org/stable/25076962

Blatchley WS (1910) An illustrated descriptive catalogue of the Coleoptera or beetles (exclusive of the Rhynchophora) known to occur in Indiana. The Nature Publishing Co., Indianapolis, 1386 pp. https://doi.org/10.5962/bhl.title.56580

Blatchley WS (1918) Some new or scarce Coleoptera from western and southern Florida. The Canadian Entomologist 50: 416–424. https://doi.org/10.4039/Ent50416-12

Blatchley WS (1925) Notes on the Rhynchophora of Eastern North America with Descriptions of New Species, III. Journal of the New York Entomological Society 33: 87–113. https://www.jstor.org/stable/25004076

Blatchley WS (1928) Notes on the Rhynchophora of Eastern North America with Descriptions of New Species, IV. Journal of the New York Entomological Society 36: 235–262. https://www.jstor.org/stable/25004261

Blatchley WS, Leng CW (1916) Rhynchophora or weevils of north eastern America. The Nature Publishing Company, Indianapolis, 682 pp. https://doi.org/10.5962/bhl.title.1557

Bocak L, Matsuda K (2003) Review of the immature stages of the family Lycidae (Insecta: Coleoptera). Journal of Natural History 37: 1463–1507. https://doi.org/10.1080/00222930210125362

Bousquet Y (1990) A review of the North American species of *Rhizophagus* Herbst and a revision of the Nearctic members of the subgenus *Anomophagus* Reitter (Coleoptera: Rhizophagidae). The Canadian Entomologist 122: 131–171. https://doi.org/10.4039/Ent122131-1

Böving AG (1954) Mature larvae of the beetle family Anobiidae. Det Kongelige Danske Videnskabernes Selskab Biologiske Meddelelser 22: 1–298.

Böving AG, Champlain AB (1920) Larvae of North American beetles of the family Cleridae. Proceedings of the United States National Museum 57: 575–649. https://doi.org/10.5479/si.00963801.57-2323.575

Branham MA, Archangelsky M (2000) Description of the last larval instar and pupa of *Lucidota atra* (G. A. Olivier 1790) (Coleoptera: Lampyridae), with a discussion of abdominal segment homology across life stages. Proceedings of the Entomological Society of Washington 102: 869–877. https://biostor.org/reference/57037

Brimley JF (1951) Mordellidae of Prince Edward County, Ontario (Coleoptera). The Canadian Entomologist 83: 278–279. https://doi.org/10.4039/Ent83278-10

Brues CT (1927) Observations on wood-boring insects, their parasites and other associated species. Psyche 34: 73–90. https://doi.org/10.1155/1927/78738

Bunyard BA (2015) First record of insect mycophagy of the commercially-important “Chaga” fungus *Inonotus obliquus* (Ach. Ex Pers.) Pilát (Hymenochaetales: Hymenochaetaceae) in North America. Proceedings of the Entomological Society of Washington 117: 452–457. https://doi.org/10.4289/0013-8797.117.4.452

Caldwell RS (1996) Macroinvertebrates and their relationship to coarse woody debris: With Special reference to land snails. In: Biodiversity and Coarse Woody Debris in Southern Forests. General Technical Report SE-94. Proceedings of the Workshop on Coarse Woody Debris in Southern Forests: Effects on Biodiversity, Athens, Georgia (USA), October 1993. United States Department of Agriculture, Forest Service, Southern Research Station, Asheville, 49–54.

Cálix M, Alexander KNA, Nieto A, Dodelin B, Soldati F, Telnov D, Vazquez-Albalate X, Aleksandrowicz O, Audisio P, Istrate P, Jansson N, Legakis A, Liberto A, Makris C, Merkl O, Mugerwa Pettersson R, Schlaghamersky J, Bologna MA, Brustel H, Buse J, Novák V, Purchart L (2018) European Red List of Saproxylic Beetles. IUCN: Brussels, Belgium, 21 pp. https://portals.iucn.org/library/node/47296

Campbell JM (1966) A revision of the genus *Lobopoda* (Coleoptera: Alleculidae) in North America and the West Indies. Illinois Biological Monographs vol. 37, University of Illinois Press, Urbana, 203 pp. https://doi.org/10.5962/bhl.title.50292

Campbell JM (1978) A review of the North American species of *Mycetochara* Berthold (Coleoptera: Alleculidae). The Canadian Entomologist 110: 921–948. https://doi.org/10.4039/Ent110921-9

Campbell JW, Hanula JL, Outcalt KW (2008a) Effects of prescribed fire and other plant community restoration treatments on tree mortality, bark beetles, and other saproxylic Coleoptera of longleaf pine, *Pinus palustris* Mill., on the Coastal Plain of Alabama. Forest Ecology and Management 254: 134–144. https://doi.org/10.1016/j.foreco.2007.07.032

Campbell JW, Hanula JL, Waldrop TA (2008b) Effects of prescribed fire and fire surrogates on saproxylic Coleoptera in the southern Appalachians of North Carolina. Journal of Entomological Science 43: 57–75. https://doi.org/10.18474/0749-8004-43.1.57

Champlain AB, Knull JN (1923) Fragmentary notes on forest Coleoptera. The Canadian Entomologist 55: 112–115. https://doi.org/10.4039/Ent55112-5

Chantal C (1985) Les Tetratomidae (Coleoptera) du Québec. Fabreries 11: 43–66.

Choate PM (1987) Biology of *Ceratocanthus aeneus* (Coleoptera: Scarabaeidae: Ceratocanthinae). The Florida Entomologist 70: 301–305. https://doi.org/10.2307/3495061

Ciegler JC (2010) Weevils of South Carolina (Coleoptera: Nemonychidae, Attelabidae, Brentidae, Ithyceridae, and Curculionidae). Biota of South Carolina Vol 6. Clemson University Public Service Publishing, Clemson, 276 pp.

Ciegler JC (2014) Tenebrionoidea of South Carolina (Coleoptera: Mycetophagidae, Archaeocrypticidae, Tetratomidae, Melandryidae, Mordellidae, Riphiphoridae, Zopheridae, Tenebrionidae, Synchroidae, Oedemeridae, Stenotrachelidae, Meloidae, Mycteridae, Boridae, Pythidae, Pyrochroidae, Salpingidae, Anthicidae, Ischaliidae, and Aderidae). Biota of South Carolina Vol 8. Clemson University Public Service Publishing, Clemson, 243 pp.

Cline AR, Leschen RAB (2005) Coleoptera associated with the oyster mushroom, *Pleurotus ostreatus* Fries, in North America. Southeastern Naturalist 4: 409–420. https://doi.org/10.1656/1528-7092(2005)004[0409:CAWTOM]2.0.CO;2

Cole EJ, Streams FA (1970) Insects emerging from brown slime fluxes in southern New England. The Canadian Entomologist 102: 321–333. https://doi.org/https://doi.org/10.4039/Ent102321-3

Craighead FC (1920) Biology of some Coleoptera of the families Colydiidae and Bothrideridae. Proceedings of the Entomological Society of Washington 22: 1–13. https://biostor.org/reference/66815

Craighead FC (1950) Insect Enemies of Eastern Forests. Miscellaneous Publications No. 657, United States Department of Agriculture, Washington D.C., 679 pp. https://doi.org/10.5962/bhl.title.65598

Crowson RA (1961) Considerations on the genera *Endecatomus* Mellié and *Euderia* Broun (Coleoptera: Bostrychidae) with descriptions of their larvae. Proceedings of the Royal Entomological Society of London 30: 113–120. https://doi.org/10.1111/j.1365-3113.1961.tb00177.x

Daggy T (1946) Notes on the ecology and taxonomy of certain pupae of the family Tenebrionidae (Coleoptera). Proceedings of the Indiana Academy of Science 56: 253–260.

Dajoz R (1989) *Uleiota texana* (Coleoptera Cucujidae), une espèce nouvelle du Texas. Bulletin mensuel de la Société linnéenne de Lyon 58: 198–200. https://doi.org/10.3406/linly.1989.10882

Davies ZG, Tyler C, Stewart GB, Pullin AS (2008) Are current management recommendations for saproxylic invertebrates effective? A systematic review. Biodiversity and Conservation 17: 209–234. https://doi.org/10.1007/s10531-007-9242-y

Davis WT, Leng CW (1912) Insects on a recently felled tree. Journal of the New York Entomological Society 20: 119–121. https://biostor.org/reference/72252

de Tonnancour P, Anderson RS, Bouchard P, Chantal C, Dumont S, Vigneault R (2017) New Curculionoidea (Coleoptera) records for Quebec, Canada. ZooKeys 681: 95–117. https://doi.org/10.3897/zookeys.681.12469

DiGirolomo M (2015) Melandryid? - *Spilotus quadripustulatus*. https://bugguide.net/node/view/1050538/bgimage [accessed 30 June 2023]

DiGirolomo MF, Allen DC, Stehman SV (2011) Notes on the biology of *Saperda imitans* infesting wind-damaged black cherry in Allegheny hardwood stands. The Great Lakes Entomologist 44: 177–189. https://doi.org/10.22543/0090-0222.2231

Dimmock G (1882) Notes on *Catogenus rufus*. Psyche 3: 341–342. https://doi.org/10.1155/1882/37610

Dolphin RE, Mouzin TE, Cleveland ML (1972) Insects associated with peach wood in eastern United States. The Canadian Entomologist 104: 1593–1608. https://doi.org/10.4039/Ent1041593-10

Dorshorst JJ, Young DK (2008) An annotated checklist of Wisconsin checkered beetles (Coleoptera: Cleridae and Thanerocleridae). The Great Lakes Entomologist 41: 169–185.

Downie NM, Arnett RH (1996) Beetles of Northeastern North America, Volume 2. The Sandhill Crane Press, Gainesville, Florida, 1721 pp.

Doyen JT (1988) Descriptions of some phylogenetically important larvae of Tenebrionidae (Coleoptera). The Coleopterists Bulletin 42: 285–301. https://www.jstor.org/stable/4008496

Dozier HL (1918) An annotated list of Gainesville, Florida, Coleoptera. Entomological News 29: 295–298, 331–335. https://biostor.org/reference/3681

Dunford JC, Young DK (2004) An annotated checklist of Wisconsin darkling beetles (Coleoptera: Tenebrionidae) with comparisons to the western Great Lakes fauna. Transactions of the American Entomological Society 130: 57–76. https://www.jstor.org/stable/25078836

Dury C (1904) Notes on Coleoptera. Entomological News 15: 52–53.

Ekström AL, Bergmark P, Hekkala A-M (2021) Can multifunctional forest landscapes sustain a high diversity of saproxylic beetles? Forest Ecology and Management 490: 119107. https://doi.org/10.1016/j.foreco.2021.119107

Eliason EA, Potter DA (2000) Biology of *Callirhytis cornigera* (Hymenoptera: Cynipidae) and the arthropod community inhabiting its galls). Environmental Entomology 29: 551–559. https://doi.org/10.1603/0046-225X-29.3.551

Evans AV (2009) *Hybosorus illigeri* Reiche confirmed as part of the Virgina beetle fauna, with notes on *Germarostes* (Coleoptera: Hybosoridae). Banisteria 33: 43–46. https://biostor.org/reference/255828

Fall HC (1905) Revision of the Ptinidae of Boreal America. Transactions of the American Entomological Society 31: 97–296. https://www.jstor.org/stable/pdf/25076791

Fall HC (1931) The North American species of *Hymenorus* (Coleoptera: Alleculidae). Transactions of the American Entomological Society 57: 161–247. https://www.jstor.org/stable/25077260

Felt EP (1906) Insects Affecting Park and Woodland Trees. Annual Report of the New York State Museum, Report 59, Memoir 8. New York State Education Department, Albany, NY, 546 pp. https://doi.org/10.5962/bhl.title.8979

Ferro ML, Carlton CE (2011) A practical emergence chamber for collecting Coleoptera from rotting wood, with a review of emergence chamber designs to collect saproxylic insects. The Coleopterists Bulletin 65: 115–124. https://doi.org/10.1649/072.065.0202

Ferro ML, Gimmel ML (2014) Season of fine woody debris death affects colonization of saproxylic Coleoptera. The Coleopterists Bulletin 68: 681–685. https://doi.org/10.1649/0010-065X-68.4.681

Ferro ML, Nguyen NH (2016) Survey of twig-inhabiting Coleoptera in Louisiana, USA. The Coleopterists Bulletin 70: 551–558. https://doi.org/10.1649/0010-065X-70.3.551

Ferro ML, Gimmel ML, Harms KE, Carlton CE (2009) The beetle community of small oak twigs in Louisiana, with a literature review of Coleoptera from fine woody debris. The Coleopterists Bulletin 63: 239–263. https://doi.org/10.1649/1141.1

Ferro ML, Gimmel ML, Harms KE, Carlton CE (2012a) Comparison of Coleoptera emergent from various decay classes of downed coarse woody debris in Great Smoky Mountains National Park, USA. Insecta Mundi 0260: 1–80. https://journals.flvc.org/mundi/article/view/0260

Ferro ML, Gimmel ML, Harms KE, Carlton CE (2012b) Comparison of the Coleoptera communities in leaf litter and rotten wood in Great Smoky Mountains National Park, USA. Insecta Mundi 0259: 1–58. https://journals.flvc.org/mundi/article/view/0259

Fischer WS (1950) A revision of the North American species of beetles belonging to the family Bostrichidae. Miscellaneous publication no. 698. United Stated Department of Agriculture, Washington D.C., 157 pp. https://doi.org/10.5962/bhl.title.65663

Fiske WF (1905) *Catogenus rufus*, a coleopterous parasite. Proceedings of the Entomological Society of Washington 7: 90–92. https://biostor.org/reference/65424

Fleming K (2011) beetle pupa - *Eros humeralis*. https://bugguide.net/node/view/499226 [accessed 29 June 2023]

Ford EJ (1973) A revision of the genus *Petalium* LeConte in the United States, Greater Antilles, and the Bahamas. (Coleoptera: Anobiidae). Technical Bulletin No. 1467. United States Department of Agriculture, Agricultural Research Service, Washington D.C., 40 pp.

Ford EJ, Jackman JA (1996) New larval host plant associations of tumbling flower beetles (Coleoptera: Mordellidae) in North America. The Coleopterists Bulletin 50: 361–368. https://www.jstor.org/stable/4009273

Ford EJ, Spilman TJ (1979) Biology and immature stages of *Dirrhagofarsus lewisi*, a species new to the United States (Coleoptera, Eucnemidae). The Coleopterists Bulletin 33: 75–84. https://doi.org/10.5962/p.371761

Foster DE, Barr WF (1972) Notes on the distribution and bionomics of some North American Cleridae. Journal of the Kansas Entomological Society 45: 122–125. https://www.jstor.org/stable/25082471

Fox M (2009) Weevil emerged from hackberry log - *Cophes oblongus*. https://bugguide.net/node/view/273657/bgimage [Accessed 22 June 2023]

Frost CA (1916) Collecting notes and random observations on the Maine Coleoptera. The Canadian Entomologist 48: 381–390. https://doi.org/10.4039/Ent48381-11

Frost CA (1945) Note on Maine Coleoptera. Psyche 52: 177. https://doi.org/10.1155/1945/42754

Garrick RC, Reppel DK, Morgan JT, Burgess S, Hyseni C, Worthington RJ, Ulyshen MD (2019) Trophic interactions among dead-wood-dependent forest arthropods in the southern Appalachian Mountains, USA. Food Webs 18: e00112. https://doi.org/10.1016/j.fooweb.2018.e00112

Gibb H, Johansson T, Stenbacka F, Hjältén J (2013) Functional roles affect diversity-succession relationships for boreal beetles. PLoS ONE 8: e72764. https://doi.org/10.1371/journal.pone.0072764

Gil S (2008) Succession of Coleoptera on frshly killed loblolly pine (*Pinus taeda* L.) and southern read oak (*Quercus falcata* Michaux) in Louisiana. MS Thesis, Louisiana State Univerity, Baton Rouge, United States. https://doi.org/10.31390/gradschool_theses.1067

Gimmel ML, Ferro ML (2018) General overview of saproxylic Coleoptera. In: Ulyshen MD (Ed.) Saproxylic insects: Diversity, ecology, and conservation. Zoological Monographs, vol 1. Springer, Cham, 51–128. https://doi.org/10.1007/978-3-319-75937-1_2

Glen R (1950) Larvae of the elaterid beetles of the tribe Lepturoidini (Coleoptera: Elateridae). Smithsonian Miscellaneous Collections 111: 1–246. https://repository.si.edu/handle/10088/22856

Gomez DF, Rabaglia RJ, Fairbanks KEO, Hulcr J (2018) North American Xyleborini north of Mexico: a review and key to genera and species (Coleoptera, Curculionidae, Scolytinae). ZooKeys 768: 19–68. https://doi.org/10.3897/zookeys.768.24697

Goodrich MA, Springer CA (1999) The pleasing fungus beetles (Coleoptera: Erotylidae) of Nebraska. Transactions of the Nebraska Academy of Sciences and Affiliated Societies 25: 53–71. https://digitalcommons.unl.edu/tnas/62/

Gossner MM, Lachat T, Brunet J, Isacsson G, Bouget C, Brustel H, Brandl R, Weisser WW, Müller J (2013) Current near-to-nature forest management effects on functional trait composition of saproxylic beetles in beech forests. Conservation Biology 27: 605–614. https://doi.org/10.1111/cobi.12023

Gossner MM, Wende B, Levick S, Schall P, Floren A, Linsenmair KE, Steffan-Dewenter I, Schulze E-D, Weisser WW (2016) Deadwood enrichment in European forests – Which trees should be used to promote saproxylic beetle diversity? Biological Conservation 201: 92–102. https://doi.org/10.1016/j.biocon.2016.06.032

Graf M, Seibold S, Gossner MM, Hagge J, Weiß I, Bässler C, Müller J (2022) Coverage based diversity estimates of facultative saproxylic species highlight the importance of deadwood for biodiversity. Forest Ecology and Management 517: 120275. https://doi.org/10.1016/j.foreco.2022.120275

Graves RC (1960) Ecological observations on the insects and other inhabitants of woody shelf fungi (Basidiomycetes: Polyporaceae) in the Chicago area. Annals of the Entomological Society of America 53: 61–78. https://doi.org/10.1093/aesa/53.1.61

Gruber J (2008) Endomychid - *Clemmus minor*. https://bugguide.net/node/view/239002 (accessed 16 June 2023)

Haack RA (2020) Bark- and wood-infesting Coleoptera and associated parasitoids reared from shagbark hickory (*Carya ovata*) and slippery elm (*Ulmus rubra*) in Ingham County, Michigan. The Great Lakes Entomologist 53: 185–191. https://doi.org/10.22543/0090-0222.2384

Hagge J, Müller J, Birkemoe T, Buse J, Christensen RHB, Gossner MM, Gruppe A, Heibl C, Jarzabek-Müller A, Seibold S, Siitonen J, Soutinho JG, Sverdrup-Thygeson A, Thorn S, Drag L (2021) What does a threatened saproxylic beetle look like? Modelling extinction risk using a new morphological trait database. Journal of Animal Ecology 90: 1934–1947. https://doi.org/10.1111/1365-2656.13512

Halik S, Bergdahl DR (2006) Observations on the natural history, development, range, and future of *Eubulus parochus* (Herbst) (Coleoptera: Curculionidae). The Coleopterists Bulletin 60: 325–332. https://doi.org/10.1649/0010-065X(2006)60[325:OOTNHD]2.0.CO;2

Halstead DGH (1973) A revision of the genus *Silvanus* Latreille (s.l.) (Coleoptera: Silvanidae). Bulletin of the British Museum (Natural History) Entomology 29: 37–112. https://biostor.org/reference/113585

Hanula JL (1996) Relationship of wood-feeding insects and coarse woody debris. In: Biodiversity and Coarse Woody Debris in Southern Forests. General Technical Report SE-94. Proceedings of the Workshop on Coarse Woody Debris in Southern Forests: Effects on Biodiversity, Athens, Georgia (USA), October 1993. United States Department of Agriculture, Forest Service, Southern Research Station, Asheville, 55–81.

Harvey DJ, Gange AC, Hawes CJ, Rink M (2011) Bionomics and distribution of the stag beetle, *Lucanus cervus* (L.) across Europe. Insect Conservation and Diversity 4: 23–38. https://doi.org/10.1111/j.1752-4598.2010.00107.x

Hatch MH (1961) The Beetles of the Pacific Northwest. Part III: Pselaphidae and Diversicornia I. University of Washing Publications in Biology, Vol. 16. University of

Washington Press, Seattle, 503 pp. https://ir.library.oregonstate.edu/concern/technical_reports/w0892g23h

Hayes WP, Chu HF (1946) The larvae of the genus *Nosodendron* Latr. (Coleoptera, Nosodendridae). Annals of the Entomological Society of America 39: 69–79. https://doi.org/10.1093/aesa/39.1.69

Heikkala O, Martikainen P, Kouki J (2016) Decadal effects of emulating natural disturbances in forest management on saproxylic beetle assemblages. Biological Conservation 194: 39–47. https://doi.org/10.1016/j.biocon.2015.12.002

Helbig CE, Coyle DR, Klepzig KD, Nowak JT, Gandhi JK (2016) Colonization dynamics of subcortical insects on forest sites with relatively stressed and unstressed loblolly pine trees. Journal of Economic Entomology 109: 1729–1740. https://doi.org/10.1093/jee/tow083

Hendrix PF (1996) Earthworms, biodiversity, and coarse woody debris in forest ecosystems of the southeastern U.S.A. In: Biodiversity and Coarse Woody Debris in Southern Forests. General Technical Report SE-94. Proceedings of the Workshop on Coarse Woody Debris in Southern Forests: Effects on Biodiversity, Athens, Georgia (USA), October 1993. United States Department of Agriculture, Forest Service, Southern Research Station, Asheville, 43–48.

Hepting GH (1935) Decay following fire in young Mississippi Delta hardwoods. Technical Bulletin No. 494. United States Department of Agriculture, Washington D.C., 32 pp. https://doi.org/10.22004/ag.econ.164668

Hespenheide HA (2003a) A new *Eulechriops* for the United States (Coleoptera: Curculionidae: Conoderinae). The Coleopterists Bulletin 57: 95–98. https://doi.org/10.1649/0010-065X(2003)057[0095:ANEFTU]2.0.CO;2

Hespenheide HA (2003b) New *Lechriops* species for the United States (Coleoptera: Curculionidae: Conoderinae). The Coleopterists Bulletin 57: 345–352. https://doi.org/10.1649/580

Hespenheide HA (2019) A review of the genus *Laemosaccus* Schönherr, 1826 (Coleoptera: Curculionidae: Mesoptiliinae) from Baja California and America North of Mexico: diversity and mimicry. The Coleopterists Bulletin 73: 905–939. https://doi.org/10.1649/0010-065X-73.4.905

Hinson KR (2016) Rearing and bionomics of *Orchesia cultriformis* Laliberté (Coleoptera: Melandryidae). The Coleopterists Bulletin 70: 372–374. https://doi.org/10.1649/0010-065X-70.2.372

Hinson KR, Blinn RL (2018) Records and notes for two uncommon species of Coleoptera, *Trichodesma klagesi* (Fall) (Ptinidae) and *Oxylaemus americanus* LeConte (Teredidae), from North Carolina, USA. The Coleopterists Bulletin 72: 292–294. https://doi.org/10.1649/0010-065X-72.2.292

Hoffman RL (2006) The volvating scarabaeid beetles of Virginia (Coleoptera: Scarabaeidae: Ceratocanthinae). Banisteria 28: 49–52. https://biostor.org/reference/255860

Hoffmann CH (1937) Biological notes on *Pseudolucanus placidus* Say, *Platycerus quercus* Weber and *Ceruchus piceus* Weber (Lucanidae, Coleoptera). Entomological News 48: 281–284.

Hoffmann CH (1942) Annotated List of Elm Insects in the United States. United States Department of Agriculture Miscellaneous Publication, no. 466. United States Department of Agriculture, Washington D.C., 20 pp.

Holland JD (2009) Density of *Megacyllene caryae* (Gahan) (Coleoptera: Cerambycidae) larvae in hickory and notes on gallery mates. The Coleopterists Bulletin 63: 230–231. https://doi.org/10.1649/1153.1

Hopkins AD (1893) Catalogue of West Virginia forest and shade tree insects. West Virginia Agricultural and Forestry Experiment Station Bulletins 32: 171–251. https://doi.org/10.33915/agnic.32

Horák J, Zaitsev AA, Vávrová E (2011) Ecological requirements of a rare saproxylic beetle *Cucujus haematodes*- the beetles' stronghold on the edge of its distribution area. Insect Conservation and Diversity 4: 81–88. https://doi.org/10.1111/j.1752-4598.2010.00102.x

Horn GH (1886) A monograph of the species of the subfamilies Eucneminae, Cerophytinae and Peorthopinae inhabiting the United States. Transactions of the American Entomological Society 13: 5–58. https://doi.org/10.2307/25076466

Howden HF, Vogt GB (1951) Insect communities of standing dead pine (*Pinus virginia* Mill.). Annals of the Entomological Society of America 44: 581–595. https://doi.org/10.1093/aesa/44.4.581

Ivie MA (2002a) Nosodendridae Erichson 1846. In: Arnett RH, Thomas MC, Skelley PE, Frank JH (Eds) American Beetles. Polyphaga: Scarabaeoidea through Curculionoidea. CRC Press, Boca Raton, 224–227.

Ivie MA (2002b) Colydiidae Erichson 1845. In: Arnett RH, Thomas MC, Skelley PE, Frank JH (Eds) American Beetles. Polyphaga: Scarabaeoidea through Curculionoidea. CRC Press, Boca Raton, 445–462.

Jackman JA, Lu W (2002) Mordellidae Latreille 1802. In: Arnett RH, Thomas MC, Skelley PE, Frank JH (Eds) American Beetles. Polyphaga: Scarabaeoidea through Curculionoidea. CRC Press, Boca Raton, 423–430.

Janssen P, Cateau E, Fuhr M, Nusillard B, Brustel H, Bouget C (2016) Are biodiversity patterns of saproxylic beetles shaped by habitat fragmentation or dispersal limitation? A case study in unfragmented montane forests. Biodiversity and Conservation 25: 1167–1185. https://doi.org/10.1007/s10531-016-1116-8

Janssen P, Fuhr M, Cateau E, Nusillard B, Bouget C (2017) Forest continuity acts congruently with stand maturity in structuring the functional composition of saproxylic beetles. Biological Conservation 205: 1–10. https://doi.org/10.1016/j.biocon.2016.11.021

Jewett HH (1946) Identification of some larval Elateridae found in Kentucky. Kentucky Agricultural Experiment Station Bulletin 489: 1–40.

Johnson PJ (2015) A new species of *Drapetes* Megerle (Coleoptera: Elateridae), with taxonomic summaries and a key to the species of northern North America. Insecta Mundi 0445: 1–13. https://digitalcommons.unl.edu/insectamundi/950/

Johnston MA, Cortés Hernández KA (2021) Notes on Stenochiini Kirby, 1837 genera and species from western North America (Coleoptera: Tenebrionidae). Dugesiana 28: 81–87. https://doi.org/10.32870/dugesiana.v28i2.7144

Johnston JM, Crossley DA (1996) The significance of coarse woody debris for the diversity of soil mites. In: Biodiversity and Coarse Woody Debris in Southern Forests. General Technical Report SE-94. Proceedings of the Workshop on Coarse Woody Debris in Southern Forests: Effects on Biodiversity, Athens, Georgia (USA), October 1993. United States Department of Agriculture, Forest Service, Southern Research Station, Asheville, 82–87.

Jordal BH, Kirkendall LR (1998) Ecological relationships of a guild of tropical beetles breeding in *Cecropia* petioles in Costa Rica. Journal of Tropical Ecology 14: 153–176. https://doi.org/10.1017/S0266467498000133

Juzwik J, Banik MT, Reed ST, English JT, Ginzel MD (2015) *Geosmithia morbida* found on weevil species *Stenomimus pallidus* in Indiana. Plant Health Progress 16: 7–10. https://doi.org/10.1094/PHP-RS-14-0030

Kelly R (2011) *Ampedus militaris*. https://bugguide.net/node/view/501617/bgimage [accessed 26 June 2023]

Kim WG (2009) Lined flat bark beetle - *Charaphloeus adustus* - Female. https://bugguide.net/node/view/265524 [accessed 19 June 2023]

Kirk HB (1922) Biological notes on Elateridae and Melasidae (Col.). Entomological News 33: 236–240. https://biostor.org/reference/3708

Kissinger DG (1955) New distribution and habitat records of N.A. Coleoptera. The Coleopterists Bulletin 9: 13–15. https://doi.org/10.5962/p.372900

Kissinger DG (1963) Notes on the habits of some North America Curculionidae (Coleoptera). The Coleopterists Bulletin 17: 53–57. https://doi.org/10.5962/p.372300

Kissinger DG (1964) Curculionidae of America north of Mexico. A key to genera. Taxonomic Publications, South Lancaster, MA, 143 pp.

Klepzig KD, Ferro ML, Ulyshen MD, Gimmel ML, Mahfouz JB, Tiarks AE, Carlton CE (2012) Effects of small-scale dead wood additions on beetles in southeastern U.S. pine forests. Forests 3: 632–652. https://doi.org/10.3390/f3030632

Knull JN (1932) Notes on Coleoptera, No. 3. Entomological News 43: 42–45, 62–67. https://biostor.org/reference/70659

Knull JN (1946) A new species of *Dirhagus* with notes on other Eucnemidae (Coleoptera). Annals of the Entomological Society of America 39: 246–247. https://doi.org/10.1093/aesa/39.2.246

Knull JN (1947) New Elateridae with notes on Eucnemidae (Coleoptera). Entomological News 58: 177–181. https://biostor.org/reference/84620

Knull JN (1951) The checkered beetles of Ohio (Coleoptera: Cleridae). Ohio Biological Survey 42: 269–350.

Köhler F (2000) Totholzkäfer in Naturwaldzellen des nördlichen Rheinlandes. Vergleichende Studien zur Totholzkäferfauna Deutschlands und deutschen Naturwaldforschung. [Saproxylic beetles in the nature forests of the northern Rhineland. Comparative studies of the saproxylic beetles of Germany and contributions to German nature forest research]. Recklinghausen, Landesamt Agrarordnung NRW.

Kolibáč R (2013) Trogossitidae: a review of the beetle family, with a catalogue and keys. ZooKeys 366: 1–194. https://doi.org/10.3897/zookeys.366.6172

Kovarik PW, Caterino MS (2005) Histeridae. In: Beutel RG, Leschen RAB (Eds) Handbook of Zoology, Coleoptera, Vol. 1: Morphology and Systematics. Walter de Gruyter, Berlin, 190–222.

Lachat T, Wermelinger B, Gossner MM, Bussler H, Isacsson G, Müller J (2012) Saproxylic beetles as indicator species for dead-wood amount and temperature in European beech forests. Ecological Indicators 23: 323–331. https://doi.org/10.1016/j.ecolind.2012.04.013

Langor DW, Hammond HEJ, Spence JR, Jacobs J, Cobb TP (2008) Saproxylic insect assemblages in Canadian forests: diversity, ecology, and conservation. The Canadian Entomologist 140: 453–474. https://doi.org/10.4039/n07-LS02

Lassauce A, Paillet Y, Jactel H, Bouget C (2011) Deadwood as a surrogate for forest biodiversity: Meta-analysis of correlations between deadwood volume and species richness of saproxylic organisms. Ecological Indicators 11: 1027–1039. https://doi.org/10.1016/j.ecolind.2011.02.004

Lawrence JF (1973) Host preference in ciid beetles (Coleoptera: Ciidae) inhabiting the fruiting bodies of Basidiomycetes in North America. Bulletin of the Museum of Comparative Zoology 145: 163–212. https://biostor.org/reference/684

Lawrence JF (1977) Coleoptera associated with an *Hypoxylon* species (Ascomycetes: Xylariaceae) on oak. The Coleopterists Bulletin 31: 309–312. https://doi.org/10.5962/p.371939

Lawrence JF, de Viedma MG (1991) Anobiidae (Bostrichoidea). In: Stehr FW (Ed.) Immature Insects, Vol. 2. Kendall/Hunt Publishing Company, Dubuque, Iowa, 441–444.

Lawrence JF, Newton AF (1980) Coleoptera associated with the fruiting bodies of slime molds (Myxomycetes). The Coleopterists Bulletin 34: 129–143. https://www.jstor.org/stable/4000119

Lawrence JF, Stephan K (1975) The North American Cerylonidae (Coleoptera: Clavicornia). Psyche 82: 131–166. https://doi.org/10.1155/1975/16703

Leng CW, Davis WT (1924) List of the Coleoptera of Staten Island, New York. Proceedings of the Staten Island Institute of Arts and Sciences, vol. 2. Lancaster Press Inc., Lancaster, Pennsylvania, 82 pp.

Lettenmaier L, Seibold S, Bässler C, Brandl R, Gruppe A, Müller J, Hagge J (2022) Beetle diversity is higher in sunny forests due to higher microclimatic heterogeneity in deadwood. Oecologia 198: 825–834. https://doi.org/10.1007/s00442-022-05141-8

Liljeblad E (1945) Monograph of the Family Mordellidae (Coleoptera) of North America, North of Mexico. Miscellaneous publications, No. 62. Museum of Zoology, University of Michigan, Ann Arbor, Michigan, 229 pp. https://hdl.handle.net/2027.42/56307

Lindman L, Öckinger E, Ranius T (2023) Microclimate in hollow trees and how it affects an inhabiting beetle species, *Osmoderma eremita*. Ecological Entomology 48: 112–126. https://doi.org/10.1111/een.13206

Lingafelter SW (2007) Illustrated key to the longhorned woodboring beetles of the eastern United States. Special Publication No. 3, The Coleopterists Society, North Potomac, Maryland, 206 pp. https://doi.org/10.5962/t.208355

Lisberg AE, Young DK (2003) An annotated checklist of Wisconsin Mordellidae (Coleoptera). Insect Mundi 17: 195–202. https://digitalcommons.unl.edu/insectamundi/39/

Luk S (2007) Comb-clawed Beetle larva - *Androchirus erythropus*. https://bugguide.net/node/view/105394/bgimage [accessed 6 July 2023]

Luk S (2012) Beetle - *Microscapha clavicornis*. https://bugguide.net/node/view/620356 [accessed 29 June 2023]

Majka CG (2006) The checkered beetles (Coleoptera: Cleridae) of the Maritime Provinces of Canada. Zootaxa 1385: 31–46. https://doi.org/10.11646/zootaxa.1385.1.2

Majka CG (2007) The Eucnemidae (Coleoptera) of the Maritime Provinces of Canada: new records, observations on composition and zoogeography, and comments on the rarity of saproxylic beetles. Zootaxa 1636: 33–46. https://doi.org/10.11646/zootaxa.1636.1.2

Majka CG (2009) Recent research on forest beetles in the Maritime Provinces. In: Langor DW (Ed.) Arthropods of Canadian Forests, no. 4. Natural Resources Canada, Canadian Forest Service, Northern Forestry Centre, Edmonton, Alberta, and Biological Survey of Canada, University of Alberta, Edmonton, Alberta, 12–15.

Majka CG (2010) The Sphindidae (Coleoptera) of Nova Scotia, Canada. Journal of the Acadian Entomological Society 6: 30–33. https://acadianes.org/journal/papers/majka_sphindidae1007.pdf

Majka CG (2011) The Anthicidae and Ischaliidae (Coleoptera) of Atlantic Canada. Journal of the Acadian Entomological Society 7: 50–64. https://acadianes.org/journal/papers/anthicid_11-9.pdf

Majka CG, Johnson PJ (2008) The Elateridae (Coleoptera) of the Maritime Provinces of Canada: faunal composition, new records, and taxonomic changes. Zootaxa 1811: 1–33. https://doi.org/10.11646/zootaxa.1811.1.1

Majka CG, Pollock DA (2006) Understanding saproxylic beetles: new records of Tetratomidae, Melandryidae, Synchroidae, and Scraptiidae from the Maritime Provinces of Canada (Coleoptera: Tenebrionopidea). Zootaxa 1248: 45–68. https://doi.org/10.11646/zootaxa.1248.1.5

Majka CG, Bouchard P, Bousquet Y (2008) Tenebrionidae (Coleoptera) of the Maritime Provinces of Canada. The Canadian Entomologist 140: 690–713. https://doi.org/10.4039/n08-047

Majka CG, Langor D, Rücker WH (2009) Latridiidae (Coleoptera) of Atlantic Canada: new records, keys to identification, new synonyms, distribution, and zoogeography. The Canadian Entomologist 141: 317–370. https://doi.org/10.4039/n09-050

Martikainen P, Siitonen J, Punttila P, Kaila L, Rauh J (2000) Species richness of Coleoptera in mature managed and old-growth boreal forests in southern Finland. Biological Conservation 94: 199–209. https://doi.org/10.1016/S0006-3207(99)00175-5

Mathison BA (2021) Click beetles (Coleoptera: Elateridae) of the southeastern United States. Occasional Papers of the Florida State Collection of Arthropods 13: 1–414.

Matthewman WG, Pielou DP (1971) Arthropods inhabiting the sporophores of *Fomes fomentarius* (Polyporaceae) in Gatineau Park, Quebec. The Canadian Entomologist 103: 775–847. https://doi.org/10.4039/Ent103775-6

Mawdsley JR (2002) Ecological notes on species of Cleridae (Insecta: Coleoptera) associated with the prairie flora of central North America. The Great Lakes Entomologist 35: 15–22. https://doi.org/10.22543/0090-0222.2056

McClarin J (2005) Larvae from very dry wood - *Priobium sericeum*. https://bugguide.net/node/view/39078 [accessed 30 June 2023]

McClarin J (2007) Cross-grain eucnemid - *Melasis pectinicornis*. https://bugguide.net/node/view/96761 [accessed 25 June 2023]

McClarin J (2008a) Small, active larva, red oak bark - *Canifa pallipes*. https://bugguide.net/node/view/174587/bgimage [accessed 20 June 2023]

McClarin J (2008b) J larvae - *Mycetochara binotata*. https://bugguide.net/node/view/169704/bgimage [accessed 20 June 2023]

McElrath TC, McHugh JV (2018) Undocumented beetle diversity in the Southeastern United States: a case study of the minute clubbed beetles (Coleoptera: Monotomidae). Zootaxa 4472: 127–140. https://doi.org/10.11646/zootaxa.4472.1.6

Melvin JCE, Wong HR, McLeod BB (1967) The fauna of black knot of cherry, *Dibotryon morbosum* (Schw.) Theiss and Syd. (Ascomycetes: Dothideaceae) in Manitoba and Saskatchewan. Internal Report MS 58. Government of Canada, Department of Forestry and Rural Development, Forest Research Laboratory, Winnipeg, Manitoba., 7 pp. https://cfs.nrcan.gc.ca/pubwarehouse/pdfs/23296.pdf

Micó E (2018) Saproxylic insects in tree hollows. In: Ulyshen MD (Ed.) Saproxylic insects: Diversity, ecology, and conservation. Zoological Monographs, vol 1. Springer, Cham, 693–727. https://doi.org/10.1007/978-3-319-75937-1_21

Micó E, Ramilo P, Thorn S, Müller J, Galante E, Carmona CP (2020) Contrasting functional structure of saproxylic beetle assemblages associated to different microhabitats. Scientific Reports 10: 1520. https://doi.org/10.1038/s41598-020-58408-6

Minch EL (1952) Insect inhabitants of *Polyporus betulinus*. Journal of the New York Entomological Society 60: 31–35. https://www.jstor.org/stable/25005435

Moore M, Juzwik J, Miller F, Roberts L, Ginzel MD (2019) Detection of *Geosmithia morbida* on numerous insect species in four eastern states. Plant Health Progress 20: 133–139. https://doi.org/10.1094/PHP-02-19-0016-RS

Morimoto K (1961) On new Curculionidae from Japan (Coleoptera). Kontyû 29: 22–27.

Moser JC, Thatcher RS, Pickard LS (1971) Relative abundance of Southern Pine Beetle associates in East Texas. Annals of the Entomological Society of America 64: 72–77. https://doi.org/10.1093/aesa/64.1.72

Müller J, Bütler R (2010) A review of habitat thresholds for dead wood: a baseline for management recommendations in European forests. European Journal of Forest Research 129: 981–992. https://doi.org/10.1007/s10342-010-0400-5

Müller J, Brustel H, Brin A, Bussler H, Bouget C, Obermaier E, Heidinger IMM, Lachat T, Förster B, Horak J, Procházka J, Köhler F, Larrieu L, Bense U, Isacsson G, Zapponi L, Gossner MM (2015) Increasing temperature may compensate for lower amounts of deadwood in driving richness of saproxylic beetles. Ecography 38: 499–509. https://doi.org/10.1111/ecog.00908

Muona J (2000) A revision of the Nearctic Eucnemidae. Acta Zoologica Fennica 212: 1–106.

Nelson GH, Walters GC, Haines RD, Bellamy CL (2008) A catalog and bibliography of the Buprestoidea of America North of Mexico. Special Publication No. 4. The Coleopterists Society, North Potomac, Maryland, 274 pp. https://doi.org/10.5962/t.208313

Nikitsky NB, Pollock DA (2010) Melandryidae Leach, 1815. In: Leschen RAB, Beutel RG, Lawrence JF (Eds) Handbook of Zoology, Coleoptera, Vol. 2: Morphology and systematics. Walter de Gruyter, Berlin, 520–533. https://doi.org/10.1515/9783110911213.520

O’Brien CW (1997) A Catalog of the Coleoptera of America North of Mexico. Family: Curculionidae. Subfamilies: Acicnemidinae, Cossoninae, Rhytirrhininae, Molytinae, Petalochilinae, Trypetidinae, Dryophthorinae, Tachygoninae, Thecesterninae. Agricultural Handbook No. 529-143g. United States Department of Agriculture, Agricultural Research Service, Beltsville, Maryland, 48 pp.

Ollieu MM (1971) Damage to southern pines in Texas by *Pissodes nemorensis*. Journal of Economic Entomology 64: 1456–1459. https://doi.org/10.1093/jee/64.6.1456

Opitz W (2017) Classification, natural history, and evolution of the subfamily Peloniinae Opitz (Coleoptera: Cleroidea: Cleridae). Part VIII. Systematics of the checkered beetle genus *Chariessa* Perty. Insecta Mundi 0574: 1–42. https://digitalcommons.unl.edu/insectamundi/1063/

Opitz W (2019) Classification, natural history, and evolution of the subfamily Peloniinae Opitz (Coleoptera: Cleroidea: Cleridae). Part XV. Taxonomic revision of the new world genus *Cregya* LeConte. Faunitaxys 7: 1–126. https://doi.org/10.1649/0010-065X-73.1.45

Orledge GM, Reynolds SE (2005) Fungivore host-use groups from cluster analysis: patterns of utilisation of fungal fruiting bodies by ciid beetles. Ecological Entomology 30: 620–641. https://doi.org/10.1111/j.0307-6946.2005.00727.x

Osten Sacken BR (1862) Description of some larvae of North American Coleoptera. Proceedings of the Entomological Society of Philadelphia 1: 105–130. https://biostor.org/reference/70124

Ott J (2011a) Weevil - *Lechriops oculatus*. https://bugguide.net/node/view/491519/bgimage [accessed 23 June 2023]

Ott J (2011b) Handsome Fungus Beetle - *Stenotarsus hispidus*. https://bugguide.net/node/view/487355/bgimage [accessed 27 June 2023]

Otto RL (2012a) Eucnemid larvae of the Nearctic region. Part II: Description of the mature larva of *Deltometopus amoenicornis* (Say, 1836) (Coleoptera: Eucnemidae: Macraulacinae: Macralacini), with notes on its biology. The Coleopterists Bulletin 66: 285–288. https://doi.org/10.1649/072.066.0317

Otto RL (2012b) Eucnemid larvae of the Nearctic Region. Part I: Description of the larva of *Rhagomicrus bonvouloiri* (Horn, 1886) (Coleoptera: Eucnemidae: Melasinae:

Dirrhagini), with notes on its biology. The Coleopterists Bulletin 66: 219–223. https://doi.org/10.1649/072.066.0306

Otto RL (2014) Eucnemid larvae of the Nearctic region. Part IV: Description of the mature larva of *Entomophthalmus rufiolus* (LeConte, 1866) (Coleoptera: Eucnemidae: Melasinae: Dirhagini), with notes on its biology. The Coleopterists Bulletin 68: 331–335. https://doi.org/10.1649/0010-065X-68.2.331

Otto RL (2015) Eucnemid larvae of the Nearctic region. Part V: Fifth instar larval descriptions for eight species of *Microrhagus* Dejean, 1833 (Coleoptera: Eucnemidae: Melasinae: Dirhagini), with descriptions of four new species and notes on their biology. Insecta Mundi 0421: 1–46. https://journals.flvc.org/mundi/article/view/0421

Otto RL (2017) Eucnemid larvae of the Nearctic Region. Part VII: Description of the larvae of *Nematodes penetrans* (LeConte, 1852) (Coleoptera: Eucnemidae: Macraulacinae: Nematodini), with notes on its hypermetamorphic life cycle. Insecta Mundi 0545: 1–9. https://digitalcommons.unl.edu/insectamundi/1054/

Otto RL (2022) New state records for 33 species of Neactic false click beetles (Coleoptera: Eucnemidae). Insecta Mundi 0934: 1–13. https://digitalcommons.unl.edu/insectamundi/1436/

Otto RL, Karns KD (2017) New state records for Nearctic false click beetles (Coleoptera: Eucnemidae). Insecta Mundi 0582: 1–21. https://digitalcommons.unl.edu/insectamundi/1083/

Otto RE, Young DK (1998) Description of the larva of *Schizophilus subrufus* (Randall) (Coleoptera: Eucnemidae: Pseudomeninae), with notes on its natural history. The Coleopterists Bulletin 52: 306–312. https://www.jstor.org/stable/4009338

Palmer MW (2017) Aderidae? from rotting *Quercus velutina* wood - *Ganascus ventricosus*. https://bugguide.net/node/view/1351883/bgimage [accessed 16 June 2023]

Park O (1931) Studies in the ecology of forest Coleoptera. Ecology 12: 188–207. https://doi.org/10.2307/1932940

Payne NM (1931) Food requirements for the pupation of two coleopterous larvae, *Synchroa punctata* Newm. And *Dendroides canadensis* Lec. (Melandryidae, Pyrochroidae). Entomological News 42:13–15.

Peterson A (1960) Larvae of Insects. Part II: Coleoptera, Diptera, Neuroptera, Siphonaptera, Mecoptera, Trichoptera. Ohio State University, Columbus, Ohio, 416 pp.

Philips TK (2002) Anobiidae Fleming 1821. In: Arnett RH, Thomas MC, Skelley PE, Frank JH (Eds) American Beetles. Polyphaga: Scarabaeoidea through Curculionoidea. CRC Press, Boca Raton, 261–262. https://doi.org/10.1201/9781420041231.ch4

Philips TK, Young DK (2000) Micromalthidae Barber, 1913. In: Arnett RH, Thomas MC (Eds) American Beetles. Archestomata, Myxophaga, Adephaga, Polyphaga: Staphyliniformia. CRC Press, Boca Raton, 22–23.

Pierce WD (1930) Studies on the North American weevils belonging to the superfamily Platysomoidea. Proceedings of the United States National Museum 77: 1–34. https://doi.org/10.5479/si.00963801.77-2840.1

Pollock DA (2002) Scraptiidae Mulsant 1856. In: Arnett RH, Thomas MC, Skelley PE, Frank JH (Eds) American Beetles. Polyphaga: Scarabaeoidea through Curculionoidea. CRC Press, Boca Raton, 564–567.

Pollock DA (2012) Review of the Eustrophinae (Coleoptera, Tetratomidae) of America north of Mexico. ZooKeys 188: 1–153. https://doi.org/10.3897/zookeys.188.2976

Powell GS, Shukle JT, Richmond DS, Holland JD (2016) Saproxylic beetle biodiversity in golf course habitats. Crop, Forage & Turfgrass Management 2: 1–8. https://doi.org/10.2134/cftm2015.0194

Price MB, Young DK (2006) An annotated checklist of Wisconsin sap and short-winged flower beetle (Coleoptera: Nitidulidae, Kateretidae). Insecta Mundi 20: 69–84. https://digitalcommons.unl.edu/insectamundi/109/

Pulaski C (1979) Observations on the biology of *Phyllobaenus humeralis* (Say) (Coleoptera, Cleridae) with descriptions of its immature stages. Master's Thesis, Loyola University Chicago, Chicao, Illinois. https://ecommons.luc.edu/luc_theses/3044

Pushkin SV, Mykhailovych TB (2019) Ecologic and zoogeographic characteristics of the genus *Orphilus* Er. (Coleoptera: Dermestidae) in Palearctic zone. Entomology and Applied Science Letters 6: 27–32.

Ramberg FB (1979) A revision of the species of the genus *Ampedus* (Coleoptera, Elateridae) of America North of Mexico. PhD Dissertation, Cornell University, Ithaca, New York.

Reed SE, Juzwik J, English JT, Ginzel MD (2015) Colonization of artificially stressed black walnut trees by Ambrosia beetle, bark beetle, and other weevil species (Coleoptera: Curculionidae) in Indiana and Missouri. Environmental Entomology 44: 1455–1464. https://doi.org/10.1093/ee/nvv126

Ritcher PO (1958) Biology of Scarabaeidae. Annual Review of Entomology 3: 311–334. https://doi.org/10.1146/annurev.en.03.010158.001523

Ritcher PO (1966) White Grubs and Their Allies, a Study of North American Scarabaeoid Larvae. Oregon State University Monograph Series 4: 1–219.

Robinson W (1918) Beetles collected on a dead black oak in Virginia. Journal of the New York Entomological Society 26: 30–33. https://www.jstor.org/stable/25003794

Roth N, Doerfler I, Bässler C, Blaschke M, Bussler H, Gossner MM, Heideroth A, Thorn S, Weisser WW, Müller J (2019) Decadal effects of landscape-wide enrichment of dead wood on saproxylic organisms in beech forests of different historic management intensity. Diversity and Distributions 25: 430–441. https://doi.org/10.1111/ddi.12870

Rozen JG (1958) Biological notes on *Eucrada humeralis* (Melsheimer) (Anobiidae). The Coleopterists Bulletin 11: 53–54. https://doi.org/10.5962/p.372195

Savely HE (1939) Ecological relations of certain animals in dead pine and oak logs. Ecological Monographs 9: 321–385. https://doi.org/10.2307/1943233

Schmidl J, Bußler H (2004) Ökologische Gilden xylobionter Käfer Deutschlands und ihr Einsatz in der landschaftsökologischen Praxis–ein Bearbeitungsstan- dard. Naturschutz Landsch. 36: 202–218.

Schneider K (2017) Tiny orange beetle under log - Scraptiidae? - *Pentaria trifasciata*. https://bugguide.net/node/view/1390319/bgpage [accessed 20 June 2023]

Schnepp KE, Anderson RS (2021) *Phaenomerus foveipennis* (Morimoto) (Coleoptera: Curculionidae: Conoderinae) in the Southeastern USA. The Coleopterists Bulletin 75: 310–312. https://doi.org/10.1649/0010-065X-75.2.310

Seibold S, Thorn S (2018) The importance of dead-wood amount for saproxylic insects and how it interacts with dead-wood diversity and other habitat factors. In: Ulyshen MD (Ed.) Saproxylic insects: Diversity, ecology, and conservation. Zoological Monographs, vol 1. Springer, Cham, 607–637. https://doi.org/10.1007/978-3-319-75937-1_18

Seibold S, Brandl R, Buse J, Hothorn T, Schmidl J, Thorn S, Müller J (2015a) Association of extinction risk of saproxylic beetles with ecological degradation of forests in Europe. Conservation Biology 29: 382–390. https://doi.org/10.1111/cobi.12427

Seibold S, Bässler C, Brandl R, Gossner MM, Thorn S, Ulyshen MD, Müller J (2015b) Experimental studies of dead-wood biodiversity — a review identifying global gaps in knowledge. Biological Conservation 191: 139–149. https://doi.org/10.1016/j.biocon.2015.06.006

Seibold S, Bässler C, Brandl R, Büche B, Szallies A, Thorn S, Ulyshen MD, Müller J (2016) Microclimate and habitat heterogeneity as the major drivers of beetle diversity in dead wood. Journal of Applied Ecology 53: 934–943. https://doi.org/10.1111/1365-2664.12607

Seibold S, Bässler C, Brandl R, Fahrig L, Förster B, Heurich M, Hothorn T, Scheipl F, Thorn S, Müller J (2017) An experimental test of the habitat-amount hypothesis for saproxylic beetles in a forested region. Ecology 98: 1613–1622. https://doi.org/10.1002/ecy.1819

Seibold S, Hagge J, Müller J, Gruppe A, Brandl R, Bässler C, Thorn S (2018) Experiments with dead wood reveal the importance of dead branches in the canopy for saproxylic beetle conservation. Forest Ecology and Management 409: 564–570. https://doi.org/10.1016/j.foreco.2017.11.052

Shepherd WP, Goyer RA (2005) Impact of *Platysoma parallelum* and *Plegaderus transversus* (Coleoptera: Histeridae) predation on developing *Ips calligraphus* and *Ips grandicollis* (Coleoptera: Scolytidae) brood. Journal of Entomological Science 40: 80–87. https://doi.org/10.18474/0749-8004-40.1.80

Shockley FW, Ulyshen MD, Lord NP (2008) New distributional records and natural history notes for *Micropsephodes lundgreni* Leschen and Carlton (Coleoptera: Endomychidae). Coleopterists Bulletin 62: 350–352. https://doi.org/10.1649/1094.1

Shockley FW, Tomaszewska KW, McHugh JV (2009) Review of the natural history of the handsome fungus beetles (Coleoptera: Cucujoidea: Endomychidae). Insecta Mundi 0072: 1–24. https://doi.org/10.11646/zootaxa.1999.1.1

Siitonen J (2001) Forest management, coarse woody debris and saproxylic organisms: Fennoscandian forests as an example. Ecological Bulletins 49: 11–41.

Siitonen J, Saaristo L (2000) Habitat requirements and conservation of *Pytho kolwensis*, a beetle species of old-growth boreal forest. Biological Conservation 94: 211–220. https://doi.org/10.1016/S0006-3207(99)00174-3

Simeone JB (1960) Observations on *Hadrobregmus carinatus* (Say) and other wood-feeding Anobiidae (Coleoptera) in the northeastern United States. PhD Thesis, Cornell University, Ithaca, New York.

Skelley PE, Leschen RAB (2002) Endomychidae Leach 1815. In: Arnett RH, Thomas MC, Skelley PE, Frank JH (Eds) American Beetles. Polyphaga: Scarabaeoidea through Curculionoidea. CRC Press, Boca Raton, 366–370.

Skelley PE, Goodrich MA, Leschen RAB (1991) Fungal host records for the Erotylidae (Coleoptera: Cucujoidea) of America north of Mexico. Entomological News 102: 57–72.

Sleeper EL (1963) A study of the Zygopinae (Coleoptera: Curculionidae) of America North of Mexico. Bulletin of the Southern California Academy of Sciences 62: 209–220. https://biostor.org/reference/100004

Snider RJ (1996) Collembolans and coarse woody debris in southern forests: effects on biodiversity. In: Biodiversity and Coarse Woody Debris in Southern Forests. General Technical Report SE-94. Proceedings of the Workshop on Coarse Woody Debris in Southern Forests: Effects on Biodiversity, Athens, Georgia (USA), October 1993. United States Department of Agriculture, Forest Service, Southern Research Station, Asheville, 88–93.

Snow WE (1958) Stratification of arthropods in a wet stump cavity. Ecology 39: 83–88. https://doi.org/10.2307/1929969

Solomon JD (1995) Guide to insect borers of North American broadleaf trees and shrubs. Agricultural Handbook 706. United States Department of Agriculture, Forest Service, Washington D.C., 735 pp. https://www.fs.usda.gov/research/treesearch/22150

Speight MCD (1989) Saproxylic insects and their conservation. Strasbourg Council of Europe, France, 81 pp.

Staines CL (1984) An annotated checklist of the Scarabaeoidea (Coleoptera) of Maryland. The Maryland Entomologist 2: 79–89.

Staines CL, Staines SL (2021) An annotated checklist of the Coleoptera of the Smithsonian Environmental Research Center: The Tenebrionoidea. Banisteria 55: 32–49.

Steiner WE (1999) Flightless beetles in Appalachian "deserts:" Studies on the distribution and localized habitats of some species of Tenebrionidae (Coleoptera). In: Eckerlin RP (Ed.) Proceedings of the Appalachian Biogeography Symposium, Blacksburg, Virginia, June 1995. Virginia Museum of Natural History, Special Publication No. 7, 125–144.

Steiner WE (2008) A checklist of the Darkling Beetles (Insecta: Coleoptera: Tenebrionidae) of Maryland, with notes on the species recorded from Plummers Island through the 20th century. Bulletin of the Biological Society of Washington 15: 133–140. https://doi.org/10.2988/0097-0298(2008)15[133:ACOTDB]2.0.CO;2

Stenbacka F, Hjältén J, Hilszczański J, Dynesius M (2010) Saproxylic and non-saproxylic beetle assemblages in boreal spruce forests of different age and forestry intensity. Ecological Applications 20: 2310–2321. https://doi.org/10.1890/09-0815.1

Stephan KA (1989) The Bothrideridae and Colydiidae of America north of Mexico (Coleoptera: Clavicornia and Heteromera). Occasional Papers of the Florida State Collection of Arthropods, Vol 6, 65 pp.

Stephenson SL, Wheeler QD, McHugh JV, Fraissinet PR (1994) New North American associations of Coleoptera with Myxomycetes. Journal of Natural History 28: 921–936. https://doi.org/10.1080/00222939400770491

Steury BW, Paulsen MJ (2022) The Scarabaeoidea (Coleoptera) of the George Washington Memorial Parkway, Virginia, USA. The Maryland Entomologist 8: 58–79.

Stokland JN, Siitonen J, Jonsson BG (2012) Biodiversity in deadwood. Cambridge University Press, New York, 509 pp. https://doi.org/10.1017/CBO9781139025843

Thatcher RC (1960) Bark beetles affecting southern pines: A review of current knowledge. Occasional Paper of the Southern Forest Experiment Station 180, United States Department of Agriculture, Forest Service, Washington D.C., 25 pp.

Thayer MK, Lawrence JF (2002) Ciidae Leach in Samouelle 1819. In: Arnett RH, Thomas MC, Skelley PE, Frank JH (Eds) American Beetles. Polyphaga: Scarabaeoidea through Curculionoidea. CRC Press, Boca Raton, 403–412.

Thomas MC (1993) The Flat Bark Beetles of Florida (Coleoptera: Silvanidae: Passandridae: Laemophloeidae). Arthropods of Florida and Neighboring Land Areas. Vol 15. Florida Department of Agriculture & Consumer Sciences, Division of Plant Industry, Gainesville, Florida, 93 pp.

Thomas MC (2003) A revision of *Pediacus* Shuckard (Coleoptera: Cucujidae) for America north of Mexico, with notes on other species. Insecta Mundi 17: 157–177. https://digitalcommons.unl.edu/insectamundi/47/

Thomas MC (2009) A review of the genus *Dysmerus* Casey (Coleoptera: Laemophloeidae). Insecta Mundi 0074: 1–30. https://journals.flvc.org/mundi/article/view/0074

Thomas MC (2010) A review of *Lathropus* Erichson (Coleoptera: Laemophloeidae) in Florida and the Wast Indies, excluding the Lesser Antilles. Insecta Mundi 0120: 1–21. https://journals.flvc.org/mundi/article/view/0120

Thompson RT (1996) The species of *Phaenomerus* Schönherr (Coleoptera: Curculionidae: Zygopinae) of the Australian Region. Invertebrate Taxonomy 10: 937–993. https://doi.org/10.1071/IT9960937

Thorn S, Bässler C, Gottschalk T, Hothorn T, Bussler H, Raffa K, Müller J (2014) New insights into the consequences of post-windthrow salvage logging revealed by functional structure of saproxylic beetles assemblages. PLoS ONE 9: e101757. https://doi.org/10.1371/journal.pone.0101757

Tigreros G (2024) Deadwood dwellers: insects and fungi utilizing downed trees in a subtropical longleaf pine forest along the Georgia coastal plain. MS Thesis, University of Georgia, Athens, United States. https://esploro.libs.uga.edu/esploro/outputs/graduate/Deadwood-Dwellers-Insects-and-Fungi-Utilizing/9949666425502959

Traylor CR, Caterino MS, Ulyshen MD, Ferro ML, McHugh JV (2022a) Assessing the old-growth dependency of two saproxylic beetle species in the southern Appalachian Mountains. Insect Systematics and Diversity 6: 5. https://doi.org/10.1093/isd/ixac012

Traylor CR, Ulyshen MD, Wallace D, Loudermilk EL, Ross CW, Hawley C, Atchison RA, Williams JL, McHugh JV (2022b) Compositional attributes of invaded forests drive the diversity of insect functional groups. Global Ecology and Conservation 35: e02092. https://doi.org/10.1016/j.gecco.2022.e02092

Traylor CR, Ulyshen MD, McHugh JV (2023a) Forest age drives saproxylic beetle biodiversity in the southeastern United States. Biological Conservation 285: 110238. https://doi.org/10.1016/j.biocon.2023.110238

Traylor CR, Ulyshen MD, McHugh JV (2023b) Data from: Forest age drives saproxylic beetle biodiversity in the southeastern United States. Zenodo. https://zenodo.org/doi/10.5281/zenodo.8246614

Traylor CR, Ulyshen MD, McHugh JV (2023c) New host records and a review of deadwood associations for Mordellidae (Coleoptera) in North America. The Coleopterists Bulletin 77: 375–381. https://doi.org/10.1649/0010-065X-77.3.375

Traylor CR, Ulyshen MD, McHugh JV, Burner RC (2024) Forest age is a primary trait filter for saproxylic beetles in the southeastern United States. Forest Ecology and Management 553: 121545. https://doi.org/10.1016/j.foreco.2023.121545

Triplehorn CA (1965) Revision of the Diaperini of America north of Mexico with notes on extralimital species (Coleoptera: Tenebrionidae). Proceedings of the United States National Museum 117: 349–458. https://doi.org/10.5479/si.00963801.117-3515.349

Triplehorn CA, Spilman TJ (1973) A review of *Strongylium* of America north of Mexico, with descriptions of two new species (Coleoptera, Tenebrionidae). Transactions of the American Entomological Society 99: 1–27. https://www.jstor.org/stable/25078122

Uliana M (2003) *Lathropus sepicola* (Ph.W. Muller, 1821): osservazioni bio-etologiche e descrizione degli stadi preimmaginali (Coleoptera Cucujidae Laemophloeidae). Bollettino del Museo Civico di Storia Naturale di Venezia 54: 71–85.

Ulyshen MD (2014) Interacting effects of insects and flooding on wood decomposition. PLoS ONE 9: e101867. https://doi.org/10.1371/journal.pone.0101867

Ulyshen MD (2016) Wood decomposition as influenced by invertebrates. Biological Reviews 91: 70–85. https://doi.org/10.1111/brv.12158

Ulyshen MD (2018) Saproxylic insects: Diversity, ecology, and conservation. Zoological Monographs, vol 1. Springer, Cham, 904 pp. https://doi.org/10.1007/978-3-319-75937-1

Ulyshen MD, Hanula JL (2009a) Habitat associations of saproxylic beetles in the southeastern United States: A comparison of forest types, tree species and wood postures. Forest Ecology and Management 257: 653–664. https://doi.org/10.1016/j.foreco.2008.09.047

Ulyshen MD, Hanula JL (2009b) Responses of arthropods to large-scale manipulations of dead wood in loblolly pine stands of the southeastern United States. Environmental Entomology 38: 1005–1012. https://doi.org/10.1603/022.038.0407

Ulyshen MD, Hanula JL (2010) Patterns of saproxylic beetle succession in loblolly pine. Agricultural and Forest Entomology 12: 187–194. https://doi.org/10.1111/j.1461-9563.2009.00467.x

Ulyshen MD, Šobotník J (2018) An introduction to the diversity, ecology, and conservation of saproxylic insects. In: Ulyshen MD (Ed.) Saproxylic insects: Diversity, ecology, and conservation. Zoological Monographs, vol 1. Springer, Cham, 1–47. https://doi.org/10.1007/978-3-319-75937-1_1

Ulyshen MD, Horn S, Barnes B, Gandhi KJK (2010) Impacts of prescribed fire on saproxylic beetles in loblolly pine logs. Insect Conservation and Diversity 3: 247–251. https://doi.org/10.1111/j.1752-4598.2010.00095.x

Ulyshen MD, Barrington WT, Hoebeke ER, Herms DA (2012) Vertically stratified ash-limb beetle fauna in northern Ohio. Psyche 2012: 215891. https://doi.org/10.1155/2012/215891

Ulyshen MD, Pawson SM, Branco M, Horn S, Hoebeke ER, Gossner MM (2018) Utilization of non-native wood by saproxylic insects. In: Ulyshen MD (Ed.) Saproxylic Insects: Diversity, Ecology, and Conservation. Zoological Monographs vol. 1. Springer, Cham, 797–834. https://doi.org/10.1007/978-3-319-75937-1_23

Ulyshen MD, Lucky A, Work TT (2020) Effects of prescribed fire and social insects on saproxylic beetles in a subtropical forest. Scientific Reports 10: 9630. https://doi.org/10.1038/s41598-020-66752-w

Ulyshen MD, Urban-Mead KR, Dorey JB, Rivers JW (2023) Forests are critically important to global pollinator diversity and enhance pollination in adjacent crops. Biological Reviews 98: 1118–1141. https://doi.org/10.1111/brv.12947

Ulyshen MD, Horn S, Aubrey D, Hoebeke ER, Coyle DE (2024) Effects of Eucalyptus wood and leaf litter on saproxylic insects in the southeastern United States. Scientific Reports 14: 10641. https://doi.org/10.1038/s41598-024-61193-1

Valentine BD (1998) A review of Nearctic and some related Anthribidae (Coleoptera). Insecta Mundi 12: 251–296. https://digitalcommons.unl.edu/insectamundi/379/

Valentine BD (2007) Mutual grooming in cucujoid beetles (Coleoptera: Silvanidae). Insecta Mundi 0002: 1–3. https://digitalcommons.unl.edu/insectamundi/54/

Van Horn RW (1909) Notes on some of the Eucnemidae of the western states. (Coleoptera, Eucnemidae). Proceedings of the Entomological Society of Washington 11: 54–62.

Vogel S, Bussler H, Finnberg S, Müller J, Stengel E, Thorn S (2020) Diversity and conservation of saproxylic beetles in 42 European tree species: an experimental approach using early successional stages of branches. Insect Conservation and Diversity 14: 132–143. https://doi.org/10.1111/icad.12442

Waller DA, Moser JC (1990) Invertebrate enemies and nest associates of the leaf-cutting ant *Atta texana* (Buckley) (Formicidae, Attini). In: Vander Meer RK, Jaffe K, Cedano A (Eds) Applied Myrmecology: A World Perspective. Westview Press Studies in Insect Biology. Westview Press, Boulder, CO, 256-273.

Walter EV, Seaton L, Mathewson AA (1938) The Texas leaf-cutting ant and its control. Circular No. 494. United States Department of Agriculture, Washington D.C., 18 pp.

Warner RE (1966) A review of the *Hylobius* of North America, with a new species injurious to slash pine (Coleoptera: Curculionidae). The Coleopterists Bulletin 20: 65–81. https://doi.org/10.5962/p.383295

Webb D (2019) overwintering clicker - *Ampedus militaris*. https://bugguide.net/node/view/1765799/bgimage [accessed 26 June 2023]

Webster RP, Anderson RS, Sweeney JD, DeMerchant I (2012a) New Coleoptera records from New Brunswick, Canada: Anthribidae, Brentidae, Dryophthoridae, Brachyceridae, and Curculionidae, with additions to the fauna of Quebec, Nova Scotia and Prince Edward Island. ZooKeys 179: 349–406. https://doi.org/10.3897/zookeys.179.2626

Webster RP, Makepeace S, DeMerchant I, Sweeney JD (2012b) New Coleoptera records from New Brunswick, Canada: Histeridae. ZooKeys 179: 11–26. https://doi.org/10.3897/zookeys.179.2493

Webster RP, Sweeney JD, DeMerchant I (2012c) New Coleoptera records from New Brunswick, Canada: Mycetophagidae, Tetratomidae, and Melandryidae. ZooKeys 179: 215–242. https://doi.org/10.3897/zookeys.179.2598

Webster RP, Sweeney JD, DeMerchant I, Bouchard P, Bousquet Y (2012d) New Coleoptera records from New Brunswick, Canada: Tenebrionidae and Zopheridae. ZooKeys 179: 257–277. https://doi.org/10.3897/zookeys.179.2465

Weiss HB (1919) Notes on *Platydema ellipticum* Fab., and its fungus host. The Canadian Entomologist 51: 276–277. https://doi.org/10.4039/Ent51276-12

Weiss HB (1920) *Mordella marginata* Melsh., bred from fungus (Coleop.). Entomological News 31: 67–68.

Weiss HB, West E (1920) Fungous insects and their hosts. Proceedings of the Biological Society of Washington 33: 1–20. https://biostor.org/reference/12490

Weiss HB, West E (1922) Notes on fungous insects. The Canadian Entomologist 54: 198–199. https://doi.org/10.4039/Ent54198-9

Wheeler QD (1979) Slime mold beetles of the genus *Anisotoma* (Leiodidae): classification and evolution. Systematic Entomology 4: 251–309. https://doi.org/10.1111/j.1365-3113.1979.tb00642.x

Wheeler QD, Hoebeke ER (1984) A review of mycophagy in the Eucinetoidea (Coleoptera), with notes on an association of the eucinetid beetle, *Eucinetus oviformis*, with a Coniophoraceae fungus (Basidiomycetes: Aphyllophorales). Proceedings of the Entomological Society of Washington 86: 274–277. https://biostor.org/reference/55101

White RE (1963) A revision of the genus *Tricorynus* of North America (Coleoptera: Anobiidae). PhD Thesis, Ohio State University, Columbus, Ohio.

White RE (1982) A catalog of the Coleoptera of America north of Mexico. Family: Anobiidae. Agriculture Handbook Number 529-70. United States Department of Agriculture, Agricultural Research Service, Beltsville, Maryland, 58 pp.

White RE (1983) A Field Guide to the Beetles of North America. Peterson Field Guide Series. Houghton Mifflin Company, Boston, MA, 384 pp.

Wilson J (2012) Elateridae - *Drapetes exstriatus*. https://bugguide.net/node/view/681800/bgimage [accessed 26 June 2023]

Wolcott AB, Montgomery BE (1933) An ecological study of the Coleopterous fauna of a tamarack swamp. The American Midland Naturalist 14: 113–169. https://doi.org/10.2307/2420017

Wood SL (1982) The bark and ambrosia beetles of North and Central America (Coleoptera: Scolytidae), a taxonomic monograph. Great Basin Natural Memoirs 6: 1–1356. https://biostor.org/reference/239409

Wood SL, Bright DE (1992) A catalog of Scolytidae and Platypodidae (Coleoptera), Part 2. Taxonomic Index. Great Basin Natural Memoirs 13: 1–1553. https://biostor.org/reference/143868

Young DK (1985) Description of the larva of *Ischalia vancouverensis* Harrington (Coleoptera: Anthicidae: Ischaliinae), with observations on the systematic position of the genus. The Coleopterists Bulletin 39: 201–206. https://www.jstor.org/stable/4008271

Young DK (2002a) Lymexylidae Fleming 1821. In: Arnett RH, Thomas MC, Skelley PE, Frank JH (Eds) American Beetles. Polyphaga: Scarabaeoidea through Curculionoidea. CRC Press, Boca Raton, 261–262. https://doi.org/10.1201/9781420041231.ch4

Young DK (2002b) Pyrochroidae Latreille 1807. In: Arnett RH, Thomas MC, Skelley PE, Frank JH (Eds) American Beetles. Polyphaga: Scarabaeoidea through Curculionoidea. CRC Press, Boca Raton, 540–543.

Zanne AE, Flores-Moreno H, Powell JR, Cornwell WK, Dalling JW, Austin AT, Classen AT, Eggleton P, Okada K, Parr CL, Adair EC, Adu-Bredu S, Alam MA, Alvarez-Garzón C, Apgaua D, Aragón R, Ardon M, Arndt SK, Ashton LA, Barber NA, Beauchêne J, Berg MP, Beringer J, Boer MM, Bonet JA, Bunney K, Burkhardt TJ, Carvalho D, Castillo-Figueroa D, Cernusak LA, Cheesman AW, Cirne-Silva TM, Cleverly JR, Cornelissen JHC, Curran TJ, D'Angioli AM, Dallstream C, Eisenhauer N, Evouna Ondo F, Fajardo A, Fernandez RD, Ferrer A, Fontes MAL, Galatowitsch ML, González G, Gottschall F, Grace PR, Granda E, Griffiths HM, Guerra Lara M, Hasegawa M, Hefting MM, Hinko-Najera N, Hutley LB, Jones J, Kahl A, Karan M, Keuskamp JA, Lardner T, Liddell M, Macfarlane C, Macinnis-Ng C, Mariano RF, Méndez MS, Meyer WS, Mori AS, Moura AS, Northwood M, Ogaya R, Oliveira RS, Orgiazzi A, Pardo J, Peguero G, Penuelas J, Perez LI, Posada JM, Prada CM, Přívětivý T, Prober SM, Prunier J, Quansah GW, Resco de Dios V, Richter R, Robertson MP, Rocha LF, Rúa MA, Sarmiento C, Silberstein RP, Silva MC, Siqueira FF, Stillwagon MG, Stol J, Taylor MK, Teste FP, Tng DYP, Tucker D, Türke M, Ulyshen MD, Valverde-Barrantes OJ, van den Berg E, van Logtestijn RSP, Veen GF (Ciska), Vogel JG, Wardlaw TJ, Wiehl G, Wirth C, Woods MJ, Zalamea P-C (2022) Termite sensitivity to temperature affects global wood decay rates. Science 377: 1440–1444. https://doi.org/10.1126/science.abo3856

Supplementary material 1

List of beetle taxa with deadwood associations from experimental studies in the southeastern USA

Authors: Clayton R. Traylor, Michael D. Ulyshen, J. Winston Cornish, Gabriel Tigreros, Joseph V. McHugh

Data type: xlsx

Explanation note: Taxa were included if they were collected or emerged from deadwood, or if they were considered saproxylic (see Methods in main text). For taxa collected from deadwood, we provide tree type, collection types (emergent: E, hand-collected: H), and references for each record. For taxa considered saproxylic, we provide references for each study it occurred in. More information on the references can be found in Table 1 of the main text.

Link: https://doi.org/10.3897/zookeys.1232.143989.suppl1

ZooKeys 1232: 97–130 (2025)
DOI: 10.3897/zookeys.1232.142629

Research Article

Review of the spider genus *Solenysa* Simon, 1894 in Western Japan and Central Ryukyu with the description of three new species (Araneae, Linyphiidae)

Francesco Ballarin[1,2], Hauchuan Liao[3], Zento Touyama[4], Katsuyuki Eguchi[1]

1 Systematic Zoology Laboratory, Department of Biological Sciences, Tokyo Metropolitan University, 1-1 Minami-Osawa, Hachioji-shi, 192-0397, Tokyo, Japan
2 Department of Zoology, Museo di Storia Naturale of Verona, Lungadige Porta Vittoria, 9, I-37129 Verona, Italy
3 Department of Entomology, National Chung Hsing University, No.145 Xingda Rd., South Dist., Taichung City, 402202, Taiwan
4 Laboratory of Entomology, Department of Bioresource Development, Faculty of Agriculture, Tokyo University of Agriculture, 1737 Funako, Atsugi-shi, 243-0034, Kanagawa, Japan
Corresponding author: Francesco Ballarin (ballarin.francesco@gmail.com)

Abstract

Three new species of the genus *Solenysa* Simon, 1894 are recorded and described from Western Japan, all based on both sexes. Of these, two species are endemic to the Ryukyu Archipelago: *S. shimatchu* Ballarin & Eguchi, **sp. nov.** from Amami-Ōshima Island, and *S. yambaruensis* Ballarin & Eguchi, **sp. nov.** from Okinawa Honto and Kume-jima Islands. These species represent the first record of the genus *Solenysa* for the Central Ryukyus and belong to a newly defined species group. Another new species, *S. bilamellata* Ballarin & Eguchi, **sp. nov.** is recorded from eastern Kyushu in mainland Japan and belongs to the *mellotteei* group. The phylogenetic positions of the new species are discussed based on morphological and molecular data. New records, remarks, and photos of genitalia of other poorly known *Solenysa* species from surrounding areas (Taiwan, Kyushu, Shikoku, and western Honshu) are provided to facilitate future identifications.

Key words: Amami-Ōshima, endemic species, island biogeography, Kyushu, Okinawa, Ryukyu Archipelago, Yambaru National Park

Academic editor: Shuqiang Li
Received: 25 November 2024
Accepted: 20 January 2025
Published: 17 March 2025

ZooBank: https://zoobank.org/322DDAEF-972B-4D0A-A4F7-C94F029DC196

Citation: Ballarin F, Liao H, Touyama Z, Eguchi K (2025) Review of the spider genus *Solenysa* Simon, 1894 in Western Japan and Central Ryukyu with the description of three new species (Araneae, Linyphiidae). ZooKeys 1232: 97–130. https://doi.org/10.3897/zookeys.1232.142629

Introduction

Solenysa Simon, 1894 is a small genus of tiny, sheet-web weavers spiders belonging to the family Linyphiidae Blackwall, 1859. These spiders are easily recognizable from other linyphiid genera by having distinctive somatic features, such as a reddish-colored prosoma, a carapace with a microsculpture of rounded pits on the surface, and a raised cephalic area. Additionally, *Solenysa* species show uniquely shaped genitalia, including a mobile epigyne hanging from the distal end of a long solenoid (Tu and Hormiga 2011). *Solenysa* was originally erected by Simon (1894) based on the type species *Solenysa mellotteei* Simon, 1894 from Japan. The genus currently comprises 15 species divided into four species groups, all distributed in Eastern Asia, including mainland

China (six species), Taiwan (three species), Korea (one species), and mainland Japan (six species) (Wang et al. 2015; WSC 2024).

The taxonomy, phylogeny, and diversification of *Solenysa* have been studied in relatively good detail in previous research (Tu and Li 2006; Tu and Hormiga 2011; Wang et al. 2015; Tian et al. 2022). However, its systematic position within the subfamilies of Linyphiidae remains controversial (Wang et al. 2015). A recent study has proposed an ancient origin for this genus, suggesting *Solenysa* as a possible Cretaceous relict with an old evolutionary history and a late Cenozoic diversification (Tian et al. 2022). This, together with the possible need for specific microhabitats (e.g., humid forest leaf litter), may explain the relatively high level of endemism observed in this genus. Such a combination of features makes *Solenysa* a potentially interesting model taxon for future studies on the historical biogeography of Eastern Asia.

In Japan, six species of *Solenysa* are known to occur, all belonging to the *S. mellotteei* group sensu Tu and Hormiga (2011): *Solenysa macrodonta* Wang, Ono & Tu, 2015; *S. mellotteei* Simon, 1894; *S. ogatai* Ono, 2011; *S. partibilis* Tu, Ono & Li, 2007; *S. reflexilis* Tu, Ono & Li, 2007; and *S. trunciformis* Wang, Ono & Tu, 2015 (Tanikawa 2024; WSC 2024). The classification of the Japanese *Solenysa* species has been revised in detail by Tu et al. (2007) and Wang et al. (2015). However, the number of documented records remains relatively low and scattered across mainland Japan (Wang et al. 2015; Shinkai et al. 2024). Currently, no species of *Solenysa* have been recorded on the numerous islands forming the Ryukyu Archipelago except for a very recent finding of *S. reflexilis* on Yakushima (Shinkai and Tanikawa 2023), one of the archipelago's northernmost islands located approximately 70 km far from the southern coast of Kyushu. This absence of records in most of the Ryukyus is surprising given the archipelago's central position within the known distributional range of *Solenysa*, highlighting a significant gap in our geographic knowledge of the genus.

During recent field surveys in Taiwan, the Ryukyus, and western Japan, we conducted extensive forest leaf litter sifting, collecting numerous linyphiids species, including several individuals of *Solenysa*. A detailed morphological comparison of these specimens with other congeners revealed the presence of three undescribed species, two from the Ryukyus and one from mainland Kyushu, Japan.

In this study, we aim to report the new records for the Central Ryukyus and describe the new species based on both sexes. To aid future identifications, we provide detailed illustrations of their diagnostic characters, along with images and distribution notes for other poorly known *Solenysa* species endemic to the surrounding areas of the Ryukyus, including Taiwan, Kyushu, Shikoku, and western Honshu. Additionally, we use molecular data to support the validity of the new species and their phylogenetic relationships within *Solenysa*.

Material and methods

Specimens were collected by sieving forest leaf litter with an entomological litter reducer and immediately preserved in 99% ethanol for both morphological and molecular analyses. The molecular and morphological studies were conducted in the Laboratory of Systematic Zoology, Department of Biological Sciences, Tokyo Metropolitan University, Japan (**TMU**). Specimens were examined under a Nikon SMZ1270 stereo microscope and a Nikon Optiphot 2 biological microscope.

The left male palp and female epigyne were removed from the bodies using a sharp needle to facilitate the observation of diagnostic characters. Internal structures of epigynes were observed by dissecting the epigynes and macerating them in lactic acid for a few hours. Photos were taken using a Canon EOS Kiss X8 digital camera mounted on the same microscopes used for morphological examination. Final images were assembled with Helicon Focus v. 7 image stacking software (https://www.heliconsoft.com) and edited with Adobe Photoshop CC v. 20.0.6 (https://www.photoshop.com/). Lengths of leg segments were measured on the lateral side and are given as follows: total length (femur, patella, tibia, metatarsus, tarsus). All measurements are given in millimeters.

All vouchers used in this study are preserved in the following institutions and collections: the National Museum of Nature and Science, Tsukuba, Japan (**NSMT**); the Museum of Nature and Human Activities, Hyogo, Japan (**MNHAH**); the Museo Civico di Storia Naturale of Verona, Italy (**MSNVR**); the Taiwan Agricultural Research Institute, Taiwan (**TARI**); the Tokushima Prefectural Museum (**TKPM**); and in the personal collection of Francesco Ballarin (**FBPC**) and Zento Touyama (**ZTPC**).

The following abbreviations are used in the text and figures (after Tu and Hormiga 2011):

Male palp: **AP** anterior protrusion of MTA; **ATA** anterior terminal apophysis; **DSA** distal suprategular apophysis; **E** embolus; **LA** lamella; **LA1** anterior branch of LA; **LA2** median branch of LA; **LA3** posterior branch of LA; **MP** median protrusion of MTA; **MTA** median terminal apophysis; **P** paracymbium; **PBP** probasal cymbial apophysis; **PP** posterior protrusion of MTA; **PTA** posterior terminal apophysis; **PTP** proximal tibial apophysis; **R** radix; **RLP** cymbial retrolateral process; **STT** *Solenysa* tegular triangle; **T** tegulum; **VLP** ventral lobe of paracymbium.

Epigyne and vulva: **CD** copulatory duct; **CO** copulatory opening; **DP** dorsal plate; **EC** epigynal collar; **FD** fertilization duct; **LDP** lobe of the dorsal plate; **S** spermatheca; **SL** solenoid; **VP** ventral plate

Other: **TmI** position of trichobothrium on metatarsus I; **TmIV** trichobothrium on metatarsus IV.

Molecular analysis

Total genomic DNA was extracted using four legs of each sample using a Chelex-TE-ProK method. Protocols for DNA extraction and amplification follow Ballarin and Eguchi (2023). The standard DNA barcode (= the Folmer region) of the mitochondrial gene Cytochrome c oxidase subunit I (COI) was amplified using the universal primers pair LCO1490 and HCO2198 (Folmer et al. 1994). To ensure clear differences between the species groups and in particular the newly established *yambaruensis* group, we also amplified the nuclear gene Histone 3 (H3) using the primer pair H3aF and H3aR (Colgan et al. 1998). Additional *Solenysa* sequences for the genes COI and H3 were harvested from GenBank (https://www.ncbi.nlm.nih.gov/genbank/). The complete list of sequences used in this work is reported in Table 1.

Sequences were visually checked and aligned using the online version of MAFFT software v. 7 (https://mafft.cbrc.jp/alignment/server/) under the G-INS-I method and subsequently translated to proteins using MEGA X v. 10.0.5 (Kumar et al. 2018) to check for potential stopping codons. The species *Agyneta ramosa* Jackson, 1912, a basal Erigoninae Emerton, 1882, was

Table 1. List of the *Solenysa* species and related GenBank accession codes used in the phylogenetic analysis. Asterisks refer to newly amplified sequences.

Code	Species	COI	H3	Locality	Notes
	Agyneta ramosa	MZ610702	FJ838740		outgroup
Lin08	*S. bilamellata* sp. nov.	PQ872900*	na	Ōita Pref., Kyushu, Japan	
Lin38	*S. bilamellata* sp. nov.	PQ872906*	na	Ōita Pref., Kyushu, Japan	
	S. lanyuensis	OL693167	OL702838	Taiwan	
	S. longqiensis	KT002782	KT002883	Fujian Prov. PR China	
	S. macrodonta	OL693169	OL702840	Shimane Pref., Western Honshu, Japan	
	S. cf. *macrodonta*	KT002786	KT002887	Shimane Pref., Western Honshu, Japan	Reported as *S. reflexilis* A in GenBank, and as *S. reflexilis* in Tian et al. 2022, probably misidentification
Lin39	*S. macrodonta*	PQ872907*	na	Hiroshima Pref., Western Honshu, Japan	
	S. mellotteei	KT002781	KT002882	Kanagawa Pref., Central Honshu, Japan	
Lin64	*S. mellotteei*	PQ872910*	na	Tokyo Pref., Central Honshu, Japan	
	S. ogatai	OL693168	OL702839	Aichi Pref., Central Honshu, Japan	
	S. partibilis	KT002784	KT002885	Shiga Pref., Central Honshu, Japan	
	S. protrudens	KT002785	KT002886	Zhajiang Prov., PR China	
	S. cf. *protrudens*	GU338667	na	PR China	Reported as *Solenysa* sp. 14 IZCL110 in GenBank
	S. reflexilis	KT002787	KT002888	Kumamoto Pref., Kyushu, Japan	
Lin46	*S. reflexilis*	PQ872908*	na	Yakushima Is., Ryukyus, Japan	
	S. retractilis	KT002788	KT002889	Sichuan Prov., PR China	
	S. cf. *retractilis*	GU338658	na	PR China	Reported as *Solenysa* sp. 14 IZCL56 in GenBank
	S. tianmushana	KT002789	KT002890	Zhejinag Prov., PR China	
Lin18	*S. shimatchu* sp. nov.	PQ872901*	PQ879705*	Minami-Ōshima Is., Ryukyus, Japan	
Lin19	*S. shimatchu* sp. nov.	PQ872902*	PQ879706*	Minami-Ōshima Is., Ryukyus, Japan	
Lin20	*S. shimatchu* sp. nov.	PQ872903*	PQ879707*	Minami-Ōshima Is., Ryukyus, Japan	
Lin63	*S. trunciformis*	PQ872909*	na	Tokushima Pref., Shikoku, Japan	
	S. cf. *trunciformis*	KT002783	KT002884	Shikoku, Japan	Reported as *S. mellotteei* B in GenBank, probably misidentification
	S. wulingensis	KT002790	na	Hunan Prov., PR China	
Lin21	*S. yambaruensis* sp. nov.	PQ872904*	PQ879708*	Okinawa Is., Ryukyus, Japan	
Lin22	*S. yambaruensis* sp. nov.	PQ872905*	PQ879709*	Okinawa Is., Ryukyus, Japan	
	S. yangmingshana	OL693166	OL702837	Taiwan	

selected as outgroup due to the proximity of this genus with *Solenysa* [see for example Ballarin and Yamasaki (2021: fig. 5) or Tian et al. (2022)]. When both gene fragments were available for the same individual, COI and H3 sequences were concatenated in a single sequence.

We conducted two distinct phylogenetic analyses, one using a maximum likelihood (ML) analysis in RAxML-NG (Kozlov et al. 2019) and another with a Bayesian Inference (BI) analysis in MrBayes v. 3.2.7 (Ronquist et al. 2012). Both analyses were run remotely on CIPRES Science Gateway v. 3.3 (https://www.phylo.org/). Partition and model were tested under the corrected Akaike's Information Criterion (AICc). using the model selection option in the online version of IQtree Web Server (http://iqtree.cibiv.univie.ac.at/). Following the results the sequence dataset was partitioned by gene with the COI 3^{rd} codon considered separately.

ML analysis was performed under a rapid bootstrap of 1,000 replicates with a GTRGAMMAI model and the standard parameters suggested by the RAxML software. BI was performed running four Monte Carlo Markov chains (MCMCs) for one million generations with a 25% burning fraction using the substitution models suggested by IQtree: invgamma for both gene partitions and gamma for the COI 3rd codon. Trees were sampled every 1,000 generations. TRACER v. 1.7.1 (Rambaut et al. 2018) was used to check that the effective sample size and consequent chains convergence were properly reached (ESS > 200). The Figtree software v. 1.4.3 (http://tree.bio.ed.ac.uk/software/figtree/) was used to graphically represent the phylogenetic trees. Nodes with ML bootstrap value (BV) ≥ 75 or BI posterior probability (PP) ≥ 0.95 were considered highly supported, while BV ≥ 70 or PP ≥ 0.90 were considered middle supported.

An uncorrected pairwise-distance genetic divergence analysis was carried out in MEGA X to test the genetic variability among the species and within each species group. We created a reduced dataset by selecting a single sequence of the COI barcode for each species. Interspecific divergence was calculated under a bootstrap method with 1,000 replications and all the other options set as default.

Results

Taxonomic account

Family Linyphiidae Blackwall, 1859

Genus *Solenysa* Simon, 1894

Type species. *Solenysa mellotteei* Simon, 1894; type locality: Japan.

Distribution. East Asia: Eastern mainland China, Taiwan, Korea, Japan (mainland and Ryukyus, absent in Hokkaido).

Solenysa yambaruensis group sensu Ballarin & Eguchi

Composition. Two species, *S. yambaruensis* sp. nov.; *S. shimatchu* sp. nov.

Diagnosis. Males of the *S. yambaruensis* group can be separated from males of other species groups by the following combination of characters: a well-developed, protruding proximal tibial apophysis (PTP) bearing three robust spines (vs PTP reduced or bearing thinner setae); a cymbium with a massive probasal cymbial apophysis (PBP) strongly bent and concave to form a wide pocket, lacking any clear spurs (vs PBP less developed, or with a different shape, or bearing some spurs); a paracymbium (P) elongated dorsal-ventrally with a well-developed ventral lobe (vs P differently shaped, elongated antero-posteriorly or with a reduced ventral lobe); a protruding, lobated median terminal apophysis (MTA) longer than wide and lacking any clear protrusions (vs MTA wider than long, or with a different shape and having some protrusions); a lamella with three, uniquely shaped branches (LA1–3) all well-developed: LA1 ribbon-like and transparent, LA2 strongly sclerotized, needle-like, LA3 with a wide, ribbon-like basal part and ending with a sclerotized, needle-like tip (vs LA1–3 less sclerotized, or with a different shape).

Females of the *S. yambaruensis* group can be distinguished from females of other species groups by the following combination of characters: solenoid (SL) with a smooth surface folded into two transversal coils (vs SL differently shaped, with a wrinkled surface, lacking two clear wide folds); a dorsal plate (DP) with a short, undivided rectangular lobe (LDP) protruding posteriorly (vs LDP lacking, divided into two lobes, or differently shaped).

Description. Cephalic area distinctly elevated in both sexes. Carapace oval with conspicuous lateral lobes. Carapace, chelicera, mouth parts, and sternum uniformly brick-red. Chelicera with four promarginal and three retromarginal teeth. Legs uniformly red-yellowish. TmI = 0.54, TmIV absent. Leg Tibial spine formula = 1-1-1-1. Opisthosoma uniformly greyish with one or three white marks on dorsal side, one mark always on dorsal-posterior tip of opisthosoma. Other somatic features as in other *Solenysa* spp.

Palpal tibia elongated, ~ 2× longer than patella, bearing three long, thin setae on anterior-retrolateral side; proximal tibial apophysis (PTP) well-developed, bearing three robust spines. Cymbium with well-developed probasal cymbial apophysis (PBP), massive, folded to form a wide pocket strongly bent retrolaterally, hook-like when observed dorsally. Cymbial retrolateral process (CRP) thorn-like. Paracymbium (P) U-shaped, elongated dorsal-ventrally, ventral lobe (VLP) wide. Solenysa tegular triangle (STT) long and narrow. Lamella with three well-developed branches: anterior branch (LA1) ribbon-like, transparent; median branch (LA2) straight, strongly sclerotized, needle-like; posterior branch (LA3) with a more or less wide, ribbon-like basal part, ending with a sharp, sclerotized point, straight or bent anteriorly. Radix (R) strongly sclerotized. Distal suprategular apophysis (DSA) well-developed, strongly sclerotized. Median terminal apophysis (MTA) lobated, ~ 2× longer than wide, protruding antero-ventrally. Anterior terminal apophysis (ATA) ribbon-like, flattened, slightly twisted, and bent ventrally, ending with a more or less sharp tip, bearing a short median tooth (MT). Embolus (E) transparent, ribbon-like, and fringed.

Epigyne more or less protruding when observed laterally, Solenoid (S) with smooth surface lacking wrinkles, connected to the dorsal base of epigyne, folded anterodorsally with approximately two folds. Ventral plate (VP) V-shaped or trapezoidal; anterior border strongly concave, posterior border flat or slightly V-shaped. Dorsal plate (DP) undivided, bearing a more or less protruding lobe (LDP). Copulatory ducts (CD) thick, heading anteriorly then posteriorly before reaching spermathecae. Fertilization ducts (FD) thin, slightly twisted, bent anteriorly. Spermathecae (S) wide, oval.

Distribution. Ryukyu Archipelago

Remarks. The *Solenysa* species were grouped by Tu and Hormiga (2011) into four species groups based on the morphology of their genitalia: the *Solenysa longqiensis* group (*S. longqiensis*, *S. yangmingshana*, and *S. spiralis* (?) from Mainland China and Taiwan), the *S. wulingensis* group (*S. geumoensis*, *S. retractilis*, S. *wulingensis*, and *S. tianmushana* from Mainland China and Korea), the *S. protrudens* group (*S. protrudens* and *S. lanyuensis* from Mainland China and Taiwan), and the *S. mellotteei* group (*S. macrodonta*, *S. mellotteei*, *S. ogatai*, *S. partibilis*, *S. reflexilis*, and *S. trunciformis*, all from Japan) (Tu and Hormiga 2011; Tian and Tu 2018). Later molecular studies supported the monophyly of these groups. (Tian et al. 2022).

The two new species from the Central Ryukyus exhibit a unique combination of morphological characters that set them apart from the previously known species groups. Our molecular analysis further supports this distinction placing these species in a monophyletic clade, separated from the other existing species groups (Fig. 12). Based on these findings, we propose a new species group, the *Solenysa yambaruensis* group, to accommodate the two Ryukyuan species.

Solenysa shimatchu **Ballarin & Eguchi, sp. nov.**

https://zoobank.org/041CD89C-4412-40D9-A56B-A9382A71FDAD
Figs 1A–J, 4A–C, 5A, B
Japanese name: amamiarimanegumoアマミアリマネグモ

Material examined. ***Holotype*** ♂ **Japan:** • **Kagoshima Pref.**, Amami-Ōshima Is., Setouchi, Amurogama, 121 m, 28.22261°N, 129.31695°E, humid forest litter in a flat area near a creek, 10.Jul.2021, F. Ballarin leg. (NSMT-Ar26184). ***Paratypes*. Japan: Kagoshima Pref.**, Amami-Ōshima Is., • 3 ♀, Amami, Naze Oaza Asato, 176 m, 28.33066°N, 129.48115°E, forest litter, 8.Jul.2021, F. Ballarin leg. (NSMT-Ar26185) • 1 ♀, Sumiyocho Oaza Kawauchi, 54 m, 28.31219°N, 129.42390°E, forest litter on a steep cliff, 8.Jul.2021, F. Ballarin leg. (NSMT-Ar26186) • 1 ♂, Yamato, Ongachi, ~ 28.33111°N, 129.39436°E, 9.Mar.2014, T. Suguro leg. (TKPM-AR3243) • 1 ♂, 3 ♀, Yamato, Tsunagu, 196 m, 28.33224°N, 129.41763°E, humid forest litter with stones near a creek, 9.Jul.2021, F. Ballarin leg. (MSNVR-Ar032–035) • 2 ♀, Naze, Oaza Chinase, 63 m, 28.34896°N, 129.44969°E, broadleaf forest litter, 9.Jul.2021, F. Ballarin leg. (TKPM-AR3244) • 1 ♂, 5 ♀, Setouchi, Amurogama, 121 m, 28.22261°N, 129.31695°E, humid forest litter in a flat area near a creek, 10.Jul.2021, F. Ballarin leg. (MNHAH) • 1 ♂, 1 ♀, Tatsugo, Akina, 245 m, 28.42290°N, 129.54688°E, rather dry forest litter, F. Ballarin leg. (FBPC) • 2 ♀, Uken, Ashiken, 208 m, 28.30780°N, 129.27311°E, rather dry litter on a steep slope near a creek, 12.Jul.2021, F. Ballarin leg. (NSMT-Ar26187).

Other material examined. Japan: Kagoshima Pref., Amami-Ōshima Is., • 1 ♀, Naze, Oaza Chinase, same locality and date, 274 m, 28.35705°N, 129.45436°E, broadleaf forest litter, 9.Jul.2021, F. Ballarin leg. (FBPC) • 1 ♀, Tatsugo, Akina, 64 m, 28.42192°N, 129.55104°E, humid forest litter with stones, 11.Jul.2021, F. Ballarin leg. (FBPC) • Tokunoshima Is., 1 ♂, 1 ♀, Amagi-cho, Nishiagina, ~ 27.7639°N, 128.9398°E, 28.Mar.2018, T. Suguro leg. (NSMT)

Diagnosis. Species closely related to *S. yambaruensis* sp. nov. from which it can be easily separated by the dorsal color pattern of the opisthosoma, having a single white mark on the dorsal-posterior tip of the opisthosoma (vs three marks) (cf. Fig. 1A–E, F vs Fig. 2E, F). Males of *S. shimatchu* sp. nov. can be easily separated from males of *S. yambaruensis* sp. nov. by the different shape of the posterior branch of the lamella (LA3), thinner and ending with a long and straight single needle-like tip (vs LA3 wider, ribbon-like, and ending with a bent spine and two denticles) (cf. Fig. 4A–C vs Fig. 4D–F). Additionally, the paracymbium (P) has a less-developed and shorter ventral lobe (VLP), headed ventrally (vs VLP with a wider lobe headed antero-ventrally); the probasal cymbial apophysis (PBP) is less bent and headed retrolaterally when observed dorsally (vs PBP more bent and headed antero-retrolaterally); and the proximal tibial apophysis (PTP) is more developed and with thicker spines (vs PTP less developed and with thinner spines) (cf. Fig. 1A–D vs Figs 2A–D, 5A, B, C–F).

Females of *S. shimatchu* sp. nov. can be distinguished from females of *S. yambaruensis* sp. nov. by the different shape of the epigyne: more rounded and protruding when observed laterally (vs flatter and less protruding); having a more V-shaped ventral plate (VP) (vs VP more trapezoidal with flatter posterior borders); and a more protruding lobe of the dorsal plate (LDP) (vs LDP less protruding) (cf. Fig. 1G–J vs Fig. 2G–J).

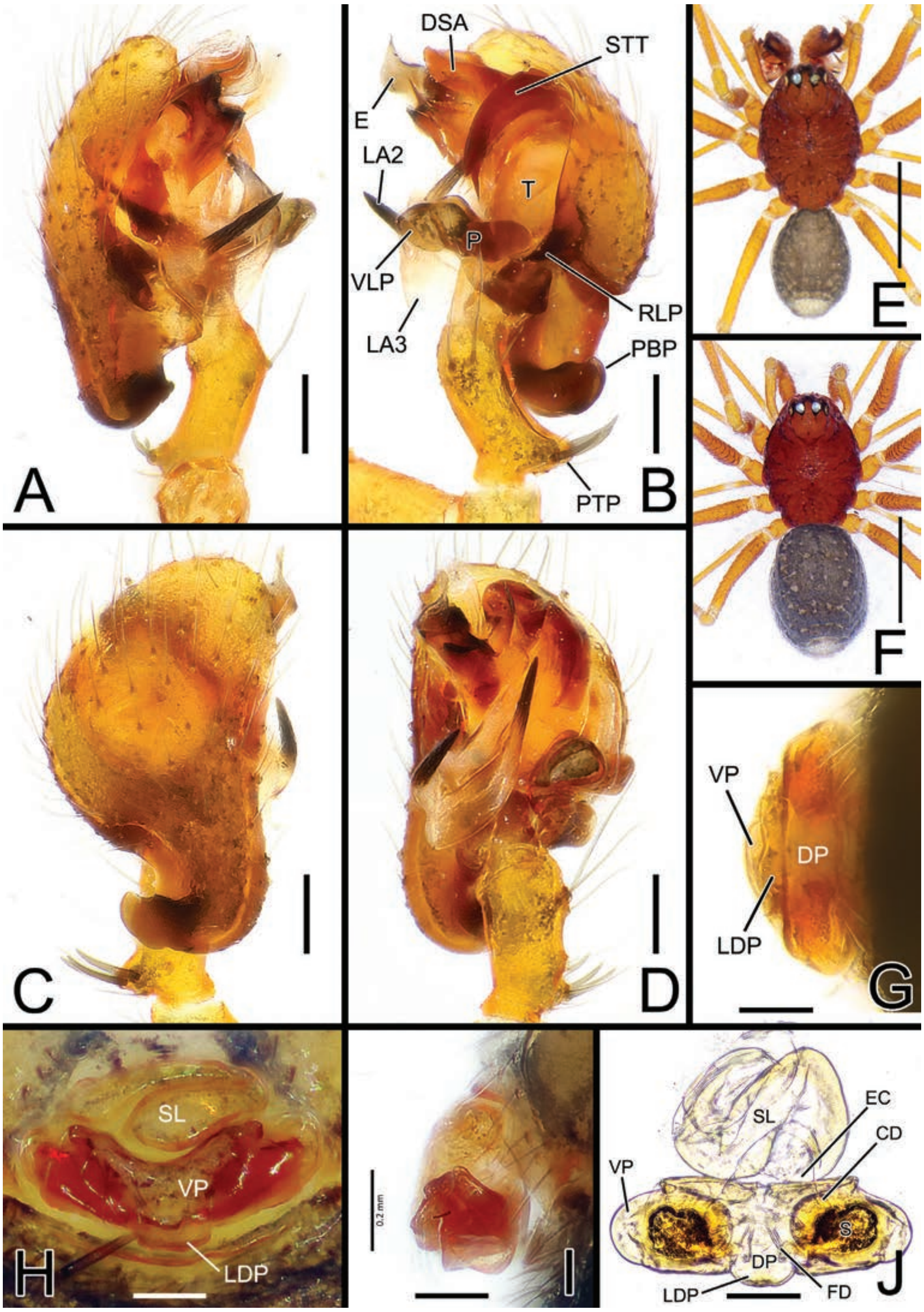

Figure 1. *Solenysa shimatchu* sp. nov. **A** male palp, prolateral **B** ditto, retrolateral **C** ditto, dorsal **D** ditto, ventral **E** habitus of male, dorsal **F** habitus of female, dorsal **G** epigyne, posterior **H** ditto, ventral **I** ditto, lateral **J** vulva, dorsal. Abbreviations: DP dorsal plate; DSA distal suprategular apophysis; E embolus; EC epigynal collar; LA2 median branch of lamella; LA3 posterior branch of lamella; LDP lobe of the dorsal plate; P paracymbium; PBP probasal cymbial apophysis; PTP proximal tibial apophysis; RLP cymbial retrolateral process; S spermatheca; SL solenoid; STT *Solenysa* tegular triangle; T tegulum; VLP ventral lobe of P; VP ventral plate. Scale bars: 0.05 mm (**A–D, G–J**); 0.5 mm (**E, F**).

For additional separation from other *Solenysa* spp. see the species group's diagnosis.

Description. Male (holotype). Total length: 1.21. Prosoma 0.71 long; 0.46 wide. Clypeus 0.24 long. Habitus as in Fig. 1E. Length of legs as follows: **I** 2.38 (0.62, 0.15, 0.63, 0.53, 0.45), **II** 2.02 (0.56, 0.14, 0.51, 0.43, 0.38), **III** 1.61

(0.43, 0.13, 0.37, 0.36, 0.33), IV 1.80 (0.50, 0.13, 0.44, 0.39, 0.34). Opisthosoma uniformly greyish with scattered small lighter dots, one wider, distinct dorsal whitish mark near posterior tip of opisthosoma. Other somatic characters as reported in species group.

Palp as in Figs 1A–D, 4A–C, 5A, B. Proximal tibial apophysis (PTP) strongly protruding antero-retrolaterally, bearing 3 thick spines. Probasal cymbial apophysis (PBP), massive, hook-like when observed dorsally, headed retrolaterally. Ventral lobe of paracymbium (VLP) headed ventrally. Lamella with 3 well-developed branches: LA1 wide, ribbon-like, transparent; LA2 and LA3 both sclerotized, strait, needle-like; LA2 shorter, headed antero-ventrally; LA3 longer, with a slightly wider, ribbon-like basal part, ending sharp and thin, headed antero-dorsally. Posterior terminal apophysis (PTA), thin and transparent, almost invisible. Median terminal apophysis (MTA) half-transparent, lobated, slightly twisted. Anterior terminal apophysis (ATA) ribbon-like, strongly sclerotized, flattened, slightly twisted, headed anteriorly, ending with a sharp tip. Median tooth (MT) of ATA small and stocky, headed anteriorly. Embolus (E) transparent, twisted, and fringed, partially hidden by ATA.

Female (one of the paratypes). Total length: 1.26. Prosoma 0.72 long; 0.46 wide. Clypeus 0.24 long. Habitus as in Fig. 1F. Length of legs as follows: I 2.22 (0.58, 0.16, 0.57, 0.50, 0.41), II 1.93 (0.53, 0.13, 0.47, 0.43, 0.37), III 1.61 (0.43, 0.14, 0.35, 0.36, 0.33), IV 1.95 (0.53, 0.14, 0.48, 0.43, 0.37). Color and other features as in male.

Epigyne and vulva as in Fig. 1G–J, strongly protruding when observed laterally. Solenoid (SL) folded anterodorsally with 2 wide transversal folds before reaching the dorsal base of epigyne. Ventral plate (VP) slightly V-shaped, anterior border strongly concave. Dorsal plate (DP) undivided, bearing a well-developed rectangular ventral lobe (LDP) protruding posteriorly. Copulatory ducts (CD) thick, heading antero-laterally then posteriorly before reaching posterior side of spermathecae. Fertilization ducts (FD) thin, Z-shaped, bent anteriorly. Spermathecae (S) wide, oval (Fig. 1J).

Etymology. The specific name is derived from the word “shimatchu” (島っちゅ) meaning “islander” in the Amami-Ōshima local language. The name refers to the insular origin of the species endemic to Amami-Ōshima and Tokunoshima islands. Name in apposition.

Distribution. Endemic to Amami-Ōshima and Tokunoshima islands, Central Ryukyus, Japan (Fig. 13).

Habitat. This species has been observed building simple sheet webs in open spaces in humid leaf litter on the floor of broadleaved forest.

Solenysa yambaruensis **Ballarin & Eguchi, sp. nov.**

https://zoobank.org/A990BEDD-90C6-47E4-B5AD-485D1899684B
Figs 2A–J, 4D–F, 5C–F
Japanese name: yanbaruarimanegumo ヤンバルアリマネグモ

Material examined. ***Holotype*** **♂. Japan: • Okinawa Pref.**, Okinawa Is., Kunigami Distr., Kunigami Vill., Yona, Yambaru National Park, 185 m, 26.74755°N, 128.22347°E, humid forest litter, 25.Feb.2021, F. Ballarin leg. (NSMT-Ar26188). ***Paratypes*****. Japan: Okinawa Pref.**, Okinawa Is., • 1 ♀, Kunigami Distr., Kunigami

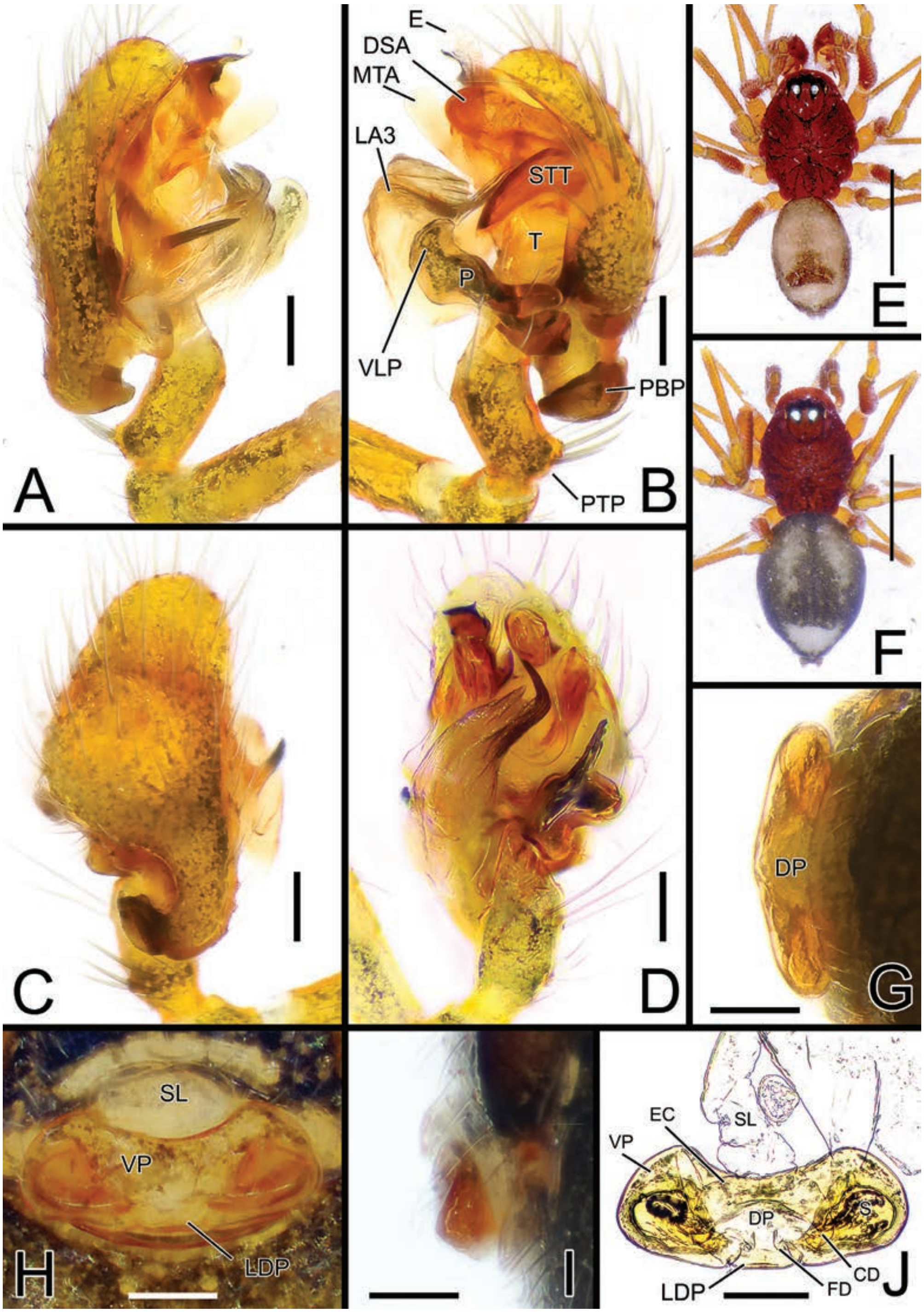

Figure 2. *Solenysa yambaruensis* sp. nov. **A** male palp, prolateral **B** ditto, retrolateral **C** ditto, dorsal **D** ditto, ventral **E** habitus of male, dorsal **F** habitus of female, dorsal **G** epigyne, posterior **H** ditto, ventral **I** ditto, lateral **J** vulva, dorsal. Abbreviations: CD copulatory duct; DP dorsal plate; DSA distal suprategular apophysis; E embolus; EC epigynal collar; FD fertilization duct; LA3 posterior branch of lamella; LDP lobe of the dorsal plate; MTA median terminal apophysis; P paracymbium; PBP probasal cymbial apophysis; PTP proximal tibial apophysis; S spermatheca; SL solenoid; STT *Solenysa* tegular triangle; T tegulum; VLP ventral lobe of P; VP ventral plate. Scale bars: 0.05 mm (**A–D, G–J**); 0.5 mm (**E, F**).

Vill., Yona, Yambaru National Park, 185 m, 26.74755°N, 128.22347°E, humid forest litter, 25.Feb.2021, F. Ballarin leg (NSMT-Ar26189) • 3 ♀, same locality, 46 m, 26.7601°N, 128.2190°E, 03.Sep.2023, humid forest leaf litter along the road, tullgren funnel, R. Itou, R. Kaneko, Y. Hiruma, and K. Watanabe leg. (MNHAH) • 2 ♀, same locality, 240 m, 26.74335°N, 128.22608°E, humid broadleaf litter near a small creek, 02.Sep.2024, F. Ballarin leg. (FBPC) • 1 ♂, Sate, 80 m, 26.78245°N, 128.22061°E, broadleaf forest litter on a slope with rocks, 13.May.2022, F. Ballarin leg. (FBPC) • 1 ♂, 3 ♀, same locality, 03.Sep.2023, F. Ballarin leg. (NSMT-Ar26190) • 1 ♂, 1 ♀, Ginama, 190 m, 26.82804°N, 128.25471°E, broadleaf forest litter, 04.Sep.2024, F. Ballarin leg. (TKPM-AR3245) • 1 ♂, 1 ♀, same locality, 210 m, 26.82743°N, 128.25885°E, pine forest litter, 04.Sep.2024, F. Ballarin leg. (MSNVR-Ar036–037) • 3 ♀, Oku, Ryukyu University Okuyamaso, 26.8365°N, 128.2715°E, 03.Sep.2023, forest leaf litter, sifter, R. Itou, R. Kaneko, Y. Hiruma, and K. Watanabe leg. (MNHAH) • 1 ♂, Nago, 10.Nov.2018, A. Tanikawa leg. (MNHAH)

Other material examined. Japan: Okinawa Pref., Okinawa Is., • 1 ♀, Nago, 13.Nov.2007, A. Tanikawa leg. (MNHAH); • 1 ♀, same locality, 6.Nov.2009, A. Tanikawa leg. (MNHAH) • 1 ♀, same locality, 8.Dec.2009, A. Tanikawa leg. (TKPM) • 1 ♀, same locality, 21.Oct.2010, A. Tanikawa leg. (TKPM) • 1 ♂, same locality, 15.Apr.2011, A. Tanikawa leg. (TKPM) • 1 ♂, 1 ♀, Onna, Tancha, near OIST campus, 140 m, 26.45947°N, 127.83674°E. mixed forest litter along the road, 30.Aug.2023, F. Ballarin leg. (FBPC) • 1 ♂, Kunigami Distr., Kunigami Vill., Hama, Near Nagao-Bashi Bridge, 26.70897°N, 128.19708°E, 2.Jan.2024, forest litter, Z. Touyama leg. (ZTPC) • 1 ♂, 1 ♀, same locality, 20.Mar.2024, Z. Touyama & R. Yamauchi leg. (ZTPC) • 1 ♀, Hama, 26.70130°N, 128.19685°E, 2.Jan.2024, Z. Touyama leg. (ZTPC) • Kumejima Is., 1 ♀, Shimajiri-gun, Maja, 95 m 26.34819°N, 126.80254°E, litter in a broadleaf forest, 18.May.2022, F. Ballarin leg. (FBPC).

Diagnosis. See the diagnosis of *S. shimatchu* sp. nov. above.

Description. Male (holotype). Total length: 1.24. Prosoma 0.68 long; 0.47 wide. Clypeus 0.24 long. Habitus as in Fig. 2E. Length of legs as follows: I 2.62 (0.69, 0.15, 0.70, 0.59, 0.49), II 2.31 (0.64, 0.15, 0.57, 0.50, 0.45), III 1.81 (0.51, 0.14, 0.41, 0.40, 0.36), IV 2.21 (0.64, 0.14, 0.53, 0.48, 0.42). Opisthosoma uniformly greyish with three distinct, white-greyish marks on dorsal side: two wide parallel, elongated marks in the central-anterior part of opisthosoma, one wide mark near posterior tip. Marks partially fused together in some individuals. Other somatic characters as in species group.

Palp as in Figs 2A–D, 4D–F, 5C–F. Proximal tibial apophysis (PTP) slightly protruding, bearing three spines. Probasal cymbial apophysis (PBP), massive, strongly bent, hook-like when observed dorsally, headed antero-retrolaterally. Ventral lobe of paracymbium (VLP) wide, laterally flattened, strongly protruding antero-ventrally. Lamella with three well-developed branches: LA1 transparent and wide, ribbon-like, half-twisted; LA2 and LA3 both sclerotized; LA2 thin, strait, needle-like, headed antero-ventrally; LA3 longer, basal part wide, ribbon-like, headed antero-retrolaterally, ending with two small denticles and one sharp needle-like tip bent with a 90° angle antero-dorsally. Posterior terminal apophysis (PTA), thin and transparent, headed anteriorly, clearly visible when the palp is observed ventrally. Median terminal apophysis (MTA) flattened, long and lobated, sightly sclerotized, strongly protruding antero-ventrally. Anterior terminal apophysis (ATA) ribbon-like, strongly sclerotized, flattened, slightly twisted, headed ventrally, ending with a blunt tip. Median tooth (MT) of ATA small, thorn-like with a sharp tip, headed posteriorly. Embolus (E) transparent, twisted, and fringed, partially hidden by ATA.

Female (one of the paratypes). Total length: 1.25. Prosoma 0.63 long; 0.44 wide. Clypeus 0.21 long. Habitus as in Fig. 2F. Length of legs as follows: I 2.42 (0.65, 0.15, 0.63, 0.52, 0.47), II 2.07 (0.52, 0.14, 0.51, 0.46, 0.44), III 1.73 (0.45, 0.12, 0.41, 0.37, 0.38), IV 2.06 (0.55, 0.14, 0.50, 0.45, 0.42). Color and other features as in male.

Epigyne and vulva as in Fig. 2G–J, flattened and only slightly protruding when observed laterally. Solenoid (SL) folded anterodorsally with 2 transversal folds before reaching the dorsal base of epigyne. Ventral plate (VP) trapezoidal with rounded lateral borders, anterior border concave, ventral border flattened. Dorsal plate (DP) undivided, bearing a short, rectangular ventral lobe (LDP) slightly protruding posteriorly. Copulatory ducts (CD) thick, heading anteriorly then posteriorly before reaching posterior side of spermathecae. Fertilization ducts (FD) thin, S-shaped, slightly twisted, bent anteriorly. Spermathecae (S) wide, oval (Fig. 2J).

Etymology. The specific name is derived from the type locality area where this species was initially found, the Yambaru National Park. This renowned protected area covers the Northern portion of Okinawa Island and has been included in the UNESCO World Heritage List since 2021.

Distribution. Endemic to Okinawa Honto and Kumejima islands, Central Ryukyus, Japan (Fig. 13).

Habitat. Humid leaf litter on the floor of broadleaved and mixed forests.

***Solenysa mellotteei* group sensu Tu & Hormiga (2011)**

Composition. Seven species: *Solenysa mellotteei* Simon, 1894; *S. macrodonta* Wang, Ono & Tu, 2015; S. *ogatai* Ono, 2011; *S. partibilis* Tu, Ono & Li, 2007; *S. reflexilis* Tu, Ono & Li, 2007; *S. trunciformis* Wang, Ono & Tu, 2015; *S. bilamellata* sp. nov.

Diagnosis. See Tu and Hormiga (2011) and Wang et al. (2015).

Description. See Tu and Hormiga (2011) and Wang et al. (2015).

Distribution. Mainland Japan (Honshu, Shikoku, Kyushu, absent in Hokkaido).

***Solenysa bilamellata* Ballarin & Eguchi, sp. nov.**

https://zoobank.org/4D81EE13-9BA8-4B82-AC37-75B93BAA8C8F
Figs 3A–J, 4G–I
Japanese name: ariakearimanegumoアリアケアリマネグモ

Material examined. ***Holotype*** ♂ **Japan: Kyushu Is., • Ōita Pref.:** Saiki City, Kitachi, Ono, 54 m, 32.92845°N, 131.94978°E, humid leaf litter in a mixed forest, 25.Mar.2019, F. Ballarin leg. (NSMT-Ar26191). ***Paratypes*****. Japan:** • **Kyushu Is., Saga Pref.:** 1 ♀, Saga City, Kinryumachi Kinryu, Kotohira Shrine (金刀比羅神社), 33.330°N, 130.299°E, 31.Jul.2005, A. Akihisa leg. (NSMT-Ar26192) • **Ōita Pref.:** 1 ♂, 1 ♀, Saiki City, Kamae Oaza Kamaeura, 159 m, 32.81950°N, 131.91222°E, leaf litter in a deciduous broadleaf forest on a steep hill, 21.Mar.2019, F. Ballarin leg. (MNHAH) • 2 ♀, Kitachi, Ono, 54 m, 32.92845°N, 131.94978°E, humid leaf litter in a mixed forest, 25.Mar.2019, F. Ballarin leg. (NSMT-Ar26193) • 2 ♀, Kunisaki Peninsula, Kunisaki City, Akimachi Yagawa, 203 m, 33.49561°N, 131.60430°E, leaf litter in a broadleaf forest on a slope, 02.Aug.2022, sifter, F. Ballarin leg. (TKPM-AR3246).

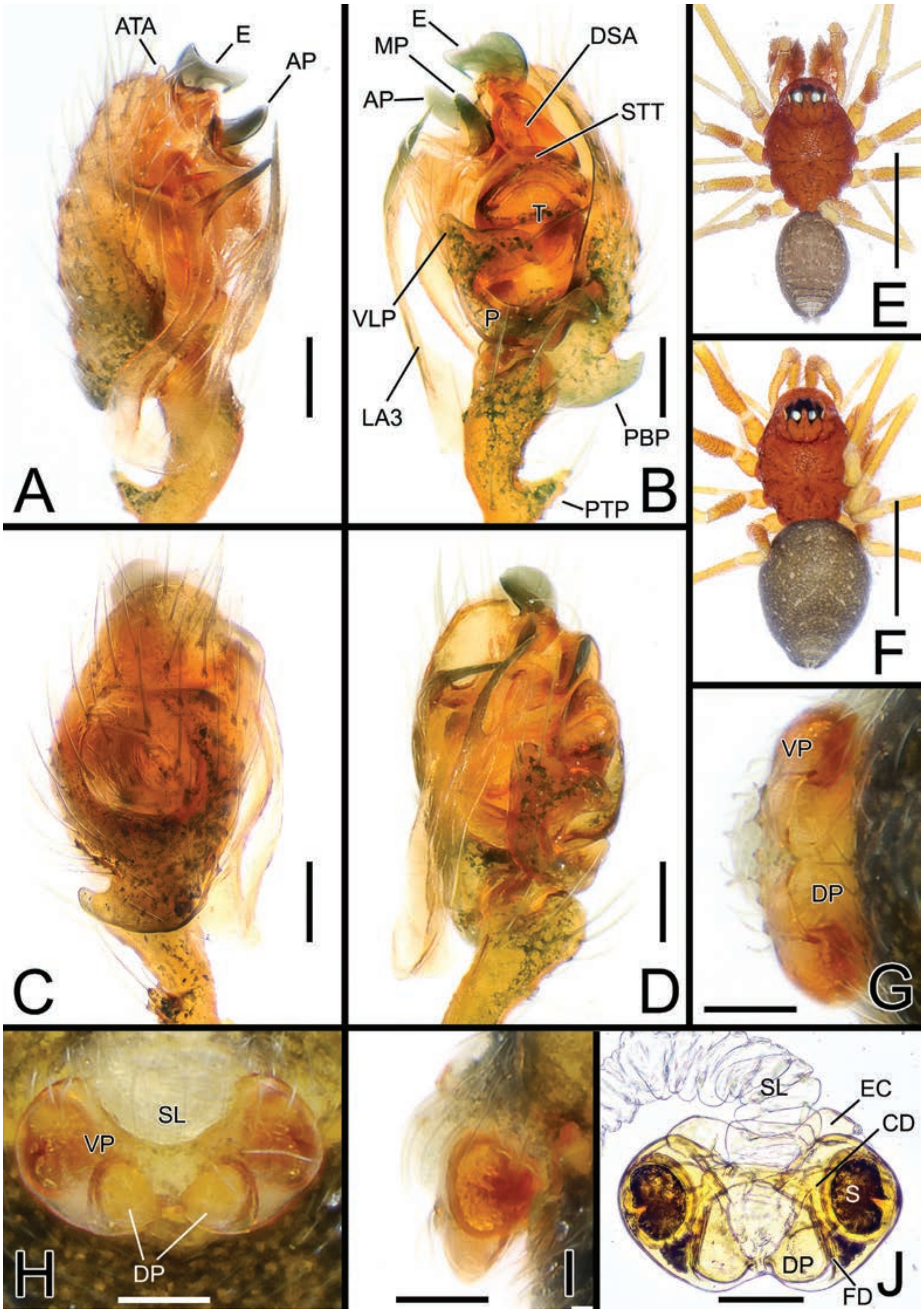

Figure 3. *Solenysa bilamellata* sp. nov. **A** male palp, prolateral **B** ditto, retrolateral **C** ditto, dorsal **D** ditto, ventral **E** habitus of male, dorsal **F** habitus of female, dorsal **G** epigyne, posterior **H** ditto, ventral **I** ditto, lateral **J** vulva, dorsal. Abbreviations: AP anterior protrusion of MTA; CD copulatory duct; DP dorsal plate; DSA distal suprategular apophysis; E embolus; EC epigynal collar; FD fertilization duct; LA3 posterior branch of lamella; MTA median terminal apophysis; P paracymbium; PBP probasal cymbial apophysis; PP posterior protrusion of MTA; PTP proximal tibial apophysis; S spermatheca; SL solenoid; STT *Solenysa* tegular triangle; T tegulum; VLP ventral lobe of P; VP ventral plate. Scale bars: 0.05 mm (**A–D, G–J**); 0.5 mm (**E, F**).

Diagnosis. Species closely related to other *Solenysa* species from western Japan. Males of *S. bilamellata* sp. nov. can be easily distinguished from males of *S. reflexilis*, *S. macrodonta*, and *S. trunciformis* by the presence of two large, lamellar-like protrusions of the median tegular apophysis (AP and MP) and having a rounded tip, both clearly visible when the palp is observed laterally (vs only AM visible and MP missing or reduced in *S. reflexilis*; or AM reduced and only MP clearly visible but with a pointed or truncated tip in the other three species). Additionally, *S. bilamellata* sp. nov. can be distinguished by the straight second branch of the lamella (LA2) (vs LA2 curved in *S. reflexilis* and *S. macrodonta*); by the smaller LA1 (LA1 longer in *S. reflexilis*); the sharper tip of the upper branch of LA3 (vs tip of LA3 wide and fringed in *S. macrodonta*), and by the shape of the lamellar-like anterior terminal hypophysis (ATA) (vs ATA with a different shape, wider in *S. reflexilis* or thinner in *S. macrodonta*, and *S. trunciformis*) (cf. Fig. 3A–D vs Figs 4G–I, 6A–D, 7A–D, 8A–D, 11A–F). Females of *S. bilamellata* sp. nov. can be distinguished from females of *S. reflexilis*, *S. macrodonta*, and *S. trunciformis* by the different shape of the epigyne, having a more transversely ovate ventral plate (VP) with short and pointed lateral borders headed internally and a dorsal plate (DP) with more rounded lobes (vs VP more trapezoidal with lateral borders headed externally and DP with more trapezoidal lobes in *S. reflexilis*; or VP more elongated posteriorly with longer lateral borders and DP with oval lobes in *S. macrodonta* and *S. trunciformis*) (cf. Fig. 3G–J vs Figs 6G–J, 7G–J, 8G–J).

Description. Male (holotype). Total length: 1.22. Prosoma 0.67 long; 0.48 wide. Clypeus 0.24 long. Habitus as in Fig. 3E. Cephalic area distinctly elevated. Carapace oval with conspicuous lateral lobes. Carapace, chelicera, mouth parts, and sternum uniformly brick-red. Chelicera with four promarginal and three retromarginal teeth. Legs uniformly red-yellowish. Length of legs as follows: I (0.64, 0.15, 0.63, 0.52, 0.42), II (0.60, 0.14, 0.55, 0.44, 0.40), III (0.47, 0.14, 0.38, 0.36, 0.33), IV (0.55, 0.13, 0.51, 0.44, 0.37). TmI = 0.54, Opisthosoma uniformly greyish with scattered small white marks on dorsal side, dorsal-posterior tip of opisthosoma lighter gray in some individuals.

Palp as in Figs 3A–D, 4G–I. Palpal tibia elongated, ~ 2× longer than patella, bearing four long, thin setae on anterior-retrolateral side; proximal tibial apophysis (PTP) well-developed, strongly protruding dorsally, bearing four–five long, thin setae. Cymbium with well-developed probasal cymbial apophysis (PBP), hook-like when observed laterally or dorsally, bent retrolaterally, with massive basal part, ending with thin, rounded tip. Cymbial retrolateral process (CRP) thorn-like. Paracymbium (P) U-shaped, elongated antero-posteriorly, ventral lobe (VLP) protruding anteriorly. *Solenysa* tegular triangle (STT) thick. Lamella with three well-developed branches: anterior branch (LA1) short and stocky; median branch (LA2) straight, strongly sclerotized, needle-like; posterior branch (LA3) with long, ribbon-like basal part, distal part forked into two needle-like branches headed antero-dorsally, ventral branch sclerotized, dorsal branch transparent ending blunt. Radix (R) strongly sclerotized. Distal suprategular apophysis (DSA) well-developed, strongly sclerotized. Median terminal apophysis (MTA) bearing two well-visible, sclerotized, lamellar protrusions protruding antero-ventrally: anterior protrusion (AP) lobated, longer than wide; median protrusion (MP) also longer than wide and lobated but slightly thinner and sharper than AP, ending with a rounded, serrated tip. Anterior terminal apophysis (ATA) stocky, lobated, lacking any median tooths. Embolus (E) sclerotized, ribbon-like, twisted, ending with a sharp tip.

Female (one of the paratypes). Total length: 1.25. Prosoma 0.63 long; 0.45 wide. Clypeus 0.21 long. Habitus as in Fig. 3F. Length of legs as follows: I (0.61, 0.14, 0.60, 0.47, 0.40), II (0.56, 0.14, 0.50, 0.43, 0.38), III (0.44, 0.14, 0.35, 0.29), IV (0.58, 0.14, 0.48, 0.42, 0.37). Color and other features as in male.

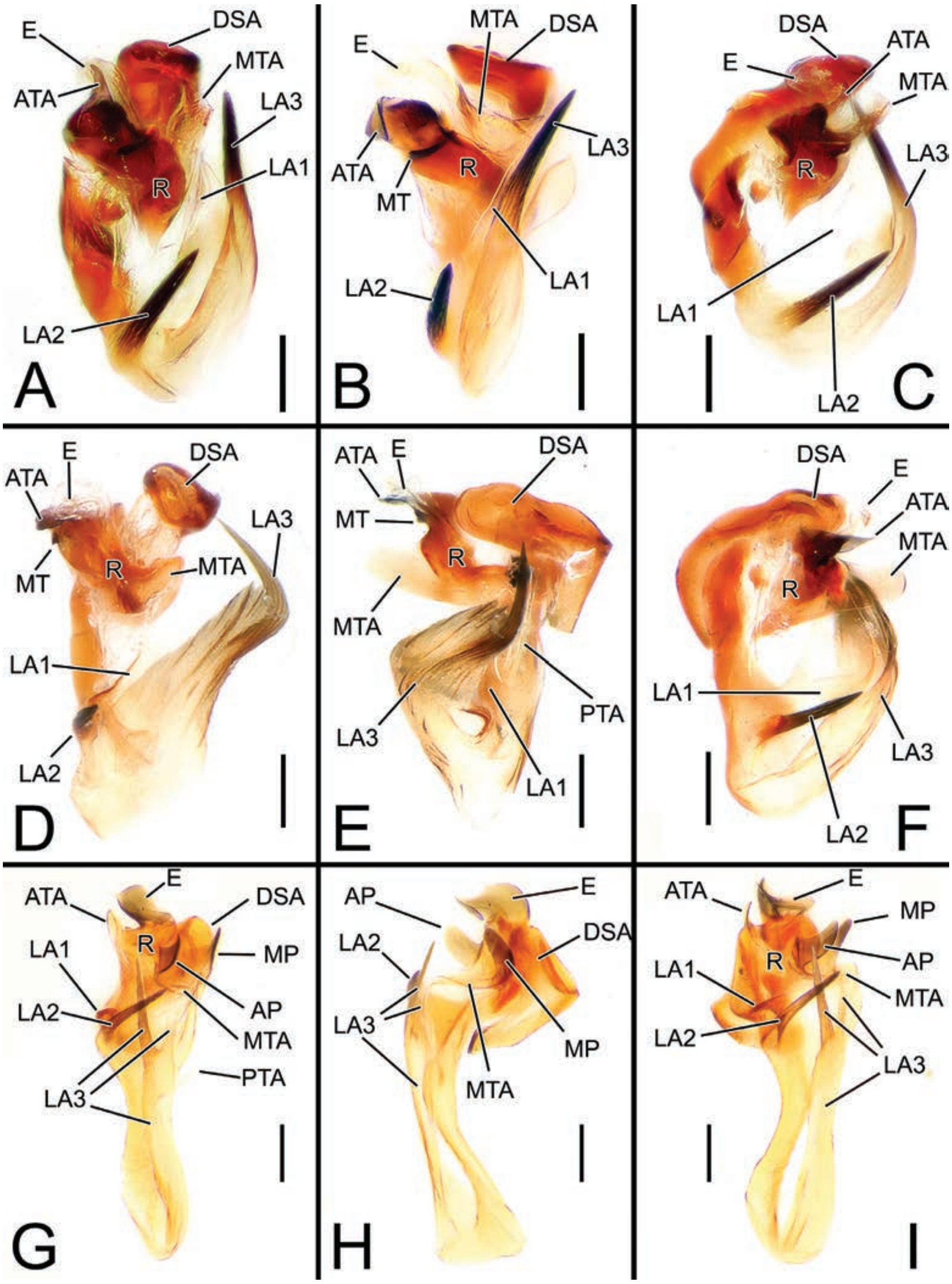

Figure 4. Embolic divisions of newly described *Solenysa* spp. **A** embolic division of *S. shimatchu* sp. nov., ventral **B** ditto, retrolateral **C** ditto, ventro-prolateral**D** embolic division of *S. yambaruensis* sp. nov., ventral **E** ditto, retrolateral **F** ditto, ventro-prolateral **G** embolic division of *Solenysa bilamellata* sp. nov., ventral **H** ditto, retrolateral **I** ditto, ventro-prolateral. Abbreviations: AP anterior protrusion of MTA; ATA anterior terminal apophysis; DSA distal supra-tegular apophysis; E embolus; LA1 anterior branch of lamella; LA2 median branch of lamella; LA3 posterior branch of lamella; MT median tooth on anterior terminal apophysis; MP median protrusion of MTA; MTA median terminal apophysis; PTA posterior terminal apophysis; R radix. Scale bars: 0.05 mm.

Epigyne and vulva as in Fig. 3G–J, protruding, ventral side flattened when observed laterally. Solenoid (SL) with numerous small coils give a wrinkled texture, lacking clear, wide folds. Ventral plate (VP) transversely ovate, with pointed lateral borders headed posteriorly; anterior border strongly concave, posterior border rounded. Dorsal plate (DP) divided into two rounded lobes separated

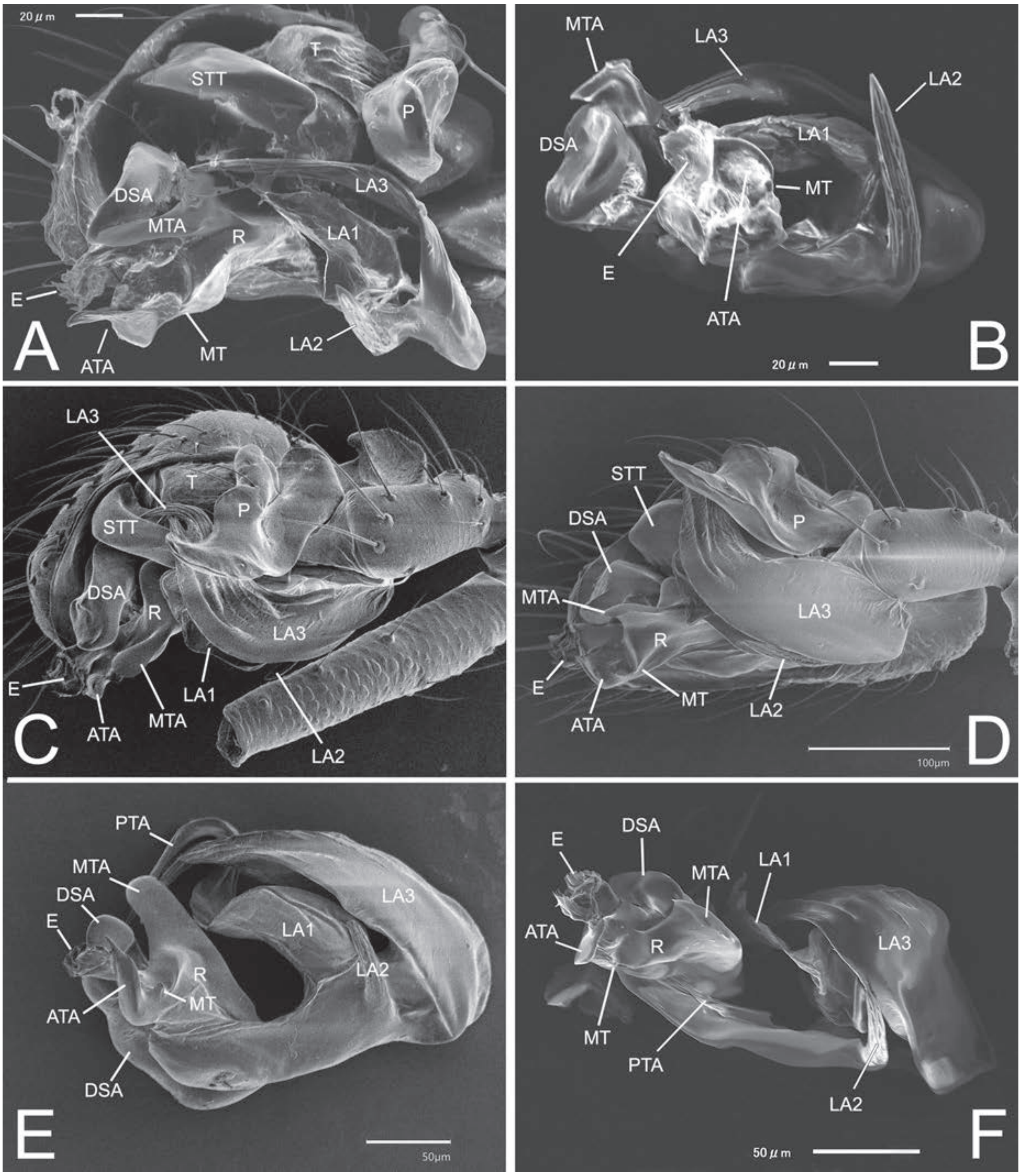

Figure 5. Palp and embolic division of *Solenysa* spp. under SEM microscope **A** palp of *S. shimatchu* sp. nov., ventro-retrolateral **B** ditto, embolic division, ventral **C** palp of *S. yambaruensis* sp. nov., ventro-retrolateral **D** ditto, ventral **E** ditto, embolic division, ventro-prolateral **F** ditto, ventral. Abbreviations: ATA anterior terminal apophysis; DSA distal supra-tegular apophysis; E embolus; LA1 anterior branch of lamella; LA2 median branch of lamella; LA3 posterior branch of lamella; MT median tooth on anterior terminal apophysis; MTA median terminal apophysis; P paracymbium; PTA posterior terminal apophysis; R radix; RLP cymbial retrolateral process; STT Solenysa tegular triangle; T tegulum.

from each other by ~ 1/3 of their width. Copulatory ducts (CD) headed anteriorly then posteriorly before reaching spermathecae. Fertilization ducts (FD) thin, bent anteriorly. Spermathecae (S) wide, kidney-shaped (Fig. 3J).

Etymology. The species name is derived from the Latin prefix *bi-* meaning “two,” and *lamellata* meaning “bearing lamellae.” It refers to the two flat, lamellar protrusions (AP and MP) of the median terminal apophysis that are diagnostic for this species. Adjective.

Distribution. Endemic to northern and eastern Kyushu, Western Japan (Fig. 13). See also remarks of *S. reflexilis*.

Habitat. Humid leaf litter on the floor of broadleaved forests.

Solenysa reflexilis Tu, Ono & Li, 2007

Figs 6A–J, 11A, B

Solenysa reflexilis Tu et al., 2007: 58, fig. 1A–H (♂♀); Ono et al. 2009: 332, figs 1100–1104 (♂♀);
Wang et al. 2015: 52, fig. 4E, F (♀).

Material examined. Japan: Kyushu Is., Kagoshima Pref., • 1 ♀, Kirishima City, Kirishima Taguchi, Kinkowan National Park, 746 m, 31.86888°N, 130.89015°E, humid broadleaf forest litter, 29.Sep.2021, F. Ballarin leg. (FBPC) • 1 ♀, Kagoshima City, Yoshino Town, near Ryugamizu train station, 32 m, 31.64580°N, 130.60283°E, broadleaf forest litter on a slope, 22.Sep.2021, F. Ballarin leg. (FBPC) • Yakushima Is., 1 ♂, Onoaida, near Onoaida onsen, 121 m, 30.24178°N, 130.54786°E, rather dry broadleaf forest litter with stones, 24.Sep.2021, F. Ballarin leg. (FBPC) • 1 ♀, Koseda, 190 m, 30.38286°N, 130.62455°E, broadleaf forest litter on a gentle slope, 24.Sep.2021, F. Ballarin leg. (FBPC) • 1 ♀, same locality, 30.37402°N, 130.62608°E, mixed forest litter, 23.Sep.2021, K. Eguchi leg. (NSMT) • 1 ♀, Anbo, 207 m, 30.28454°N, 130.61799°E, broadleaf forest litter on a gentle slope, 24.Nov.2021, F. Ballarin leg. (NSMT) • 1 ♀, Kurio, 185 m, 30.29394°N, 130.42351°E, broadleaf forest litter on a gentle slope 25.Sep.2021, F. Ballarin leg. (FBPC).

Diagnosis. See Tu et al. (2007).

Description. Habitus of male as in Fig. 6E, habitus of female as in Fig. 6F. Palp as in Fig. 6A–D, embolic division as in Fig. 11A, B; epigyne and vulva as in Fig. 6G–J. See Tu et al. (2007) for a detailed description.

Type locality. Shimo-kajiwara Itsuki-mura, Kuma-gun, Kumamoto Prefecture, Kyushu, Japan. (32.200°N, 130.500°E)

Remarks. The current known distribution of *S. reflexilis* covers Kyushu (Nagasaki, Kumamoto, Ōita, and Kagoshima Prefectures) with additional records from Shikoku (Tokushima and Ehime Prefectures), and the Chugoku area in Western Honshu (Shimane Prefecture), Japan (Shinkai et al. 2024, this work) (Fig. 13). Our new data confirm the presence of *S. reflexilis* in southern Kyushu, particularly in mainland Kagoshima Prefecture and on the island of Yakushima, where this species has been recently reported by Shinkai and Tanikawa (2023). Previous records of this species in northern and eastern Kyushu should be replaced by the closely related *S. bilamellata* sp. nov. The record from Ōita prefecture by Serita (2022) might refer to a misidentification of the similar *S. bilamellata* sp. nov. Records from Shimane Prefecture (Hayashi et al. 2013a, b) and Shikoku Island (Tsurusaki et al. 2011, 2012; Bando 2015, 2019), all except one, predate the revision of the Japanese *Solenysa* species by Wang et al. (2015) and the description of *S. macrodonta* and *S. trunciformis*.

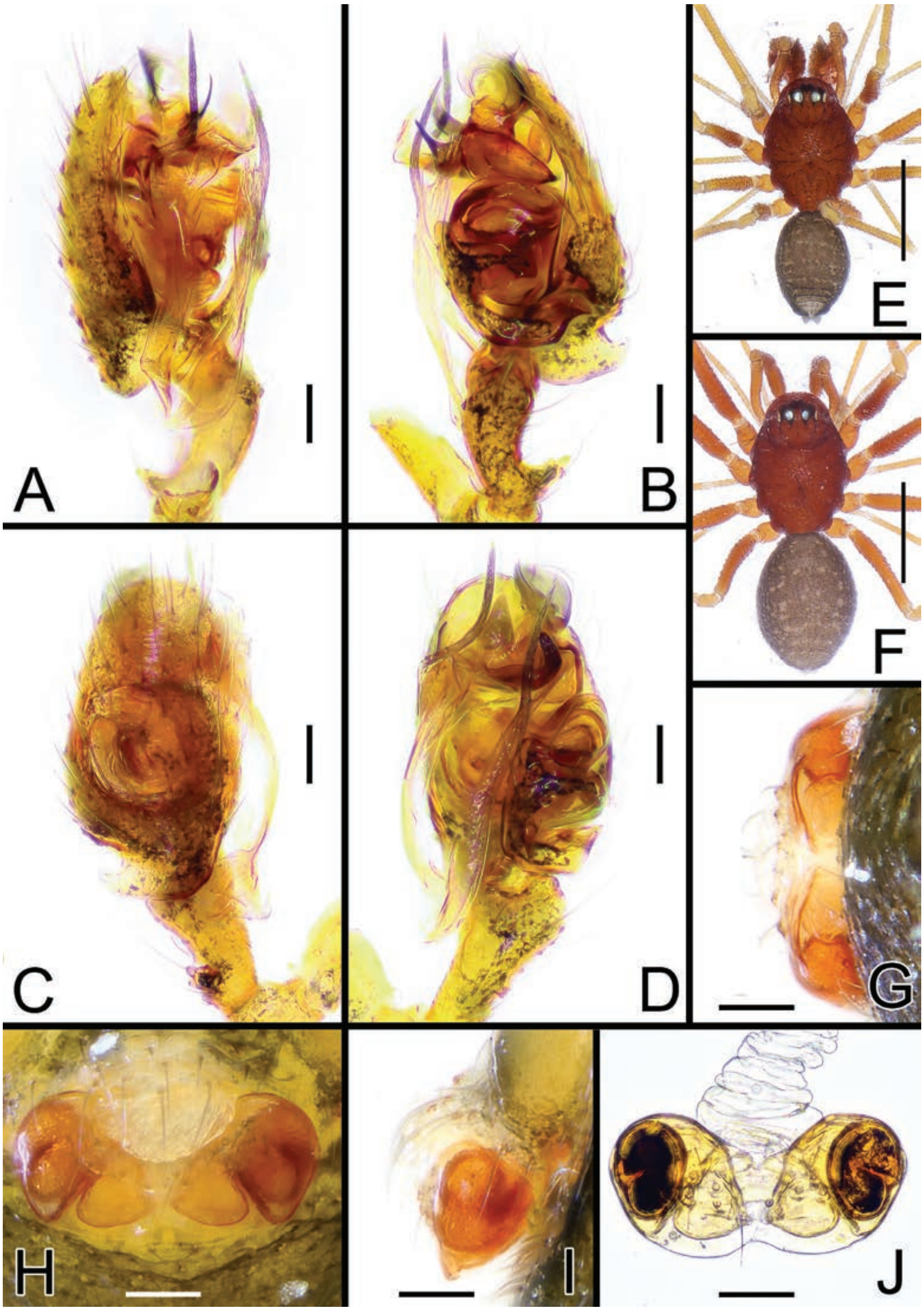

Figure 6. *Solenysa reflexilis* from Yakushima **A** male palp, prolateral **B** ditto, retrolateral **C** ditto, dorsal **D** ditto, ventral **E** habitus of male, dorsal **F** habitus of female, dorsal **G** epigyne, posterior **H** ditto, ventral **I** ditto, lateral **J** vulva, dorsal. Scale bars: 0.05 mm (**A–D, G–J**); 0.5 mm (**E, F**).

Samples published by Bando (2015) examined by us all refer to *S. trunciformis*. Due to the possibility of misidentifications with other closely related and morphologically similar species endemic to the same areas, the presence of *S. reflexilis* in Eastern Kyushu, Western Honshu, and Shikoku, remains unclear and should be properly validated based on more recent evidence. Similarly, the precise boundaries between the ranges of *S. reflexilis* and *S. bilamellata* sp. nov. in Kyushu are unknown and should be addressed in more detail.

Solenysa macrodonta **Wang, Ono & Tu, 2015**

Figs 7A–J, 11C, D

Solenysa macrodonta Wang et al., 2015: 48, figs 3A, 4C, D (♂♀).

Material examined. Japan: Hiroshima Pref., • 1 ♂, 6 ♀, Kure City, Yasuuracho Oaza Akozaka, 209 m, 34.31089°N, 132.72896°E, thick and rather dry broadleaf forest leaf litter on a steep slope, 04.Aug.2022, F. Ballarin leg. (FBPC).

Diagnosis. See Wang et al. (2015).

Description. Habitus of male as in Fig. 7E, habitus of female as in Fig. 7F. Palp as in Fig. 7A–D, embolic division as in Fig. 11C, D; epigyne and vulva as in Fig. 7G–J. See Wang et al. (2015) for a detailed description.

Type locality. Nishida, Yunotsu City, Shimane Prefecture, Honshu, Japan (35.084°N, 132.401°E).

Remarks. *Solenysa macrodonta* is distributed in the Chugoku area in Western Honshu with a few known records from Shimane and Okayama Prefectures (Shinkai et al. 2024). Here we report for the first time its presence in Hiroshima Prefecture (Fig. 13). Our male sample differs from the original description by having a shorter anterior protrusion (AP, central tooth in Wang et al. 2015) (cf. Fig. 11C, D vs Wang et al. 2015: fig. 6B). However, it shares the shape of the lamella with a transparent, upper branch of the LA2 ending with a wide, fringed tip. Additionally, we found no differences in the females' morphology and the barcode of our samples matches those available in GenBank for this species collected in the Shimane Prefecture, the type area of the species (Fig. 12). Accordingly, we consider the differences in the male palp as possibly part of the intraspecific diversity of the species. Future comparisons with a larger number of individuals of *S. macrodonta* from different localities will help to clarify this issue.

Solenysa trunciformis **Wang, Ono & Tu, 2015**

Figs 8A–J, 11E, F

Solenysa mellotteei: Tu and Li 2006: 91, figs 21–30 (♂♀, misidentified per Wang et al. 2015: 54); Tu and Hormiga 2011: 499, figs 7B, 11H (♂♀, misidentified per Wang et al. 2015: 54).
S. trunciformis Wang et al., 2015: 54, figs 1A–D, 3B, 5E, F (♂♀).

Material examined. Japan: Shikoku Is., Tokushima Pref., • 3 ♂, 7 ♀, Myozai District, Kamiyama Town, Ano, Nashinoki-Toge pass, 11.Oct.1999, 33.91391°N, 134.28702°E, H. Bando leg. (TKPM) • 2 ♂, 3 ♀, Mima City, Tsurugi Town, Ichu, Tachinomoto, 33.94936°N, 134.06863°E, 1.Jan.2010, H. Bando leg. (TKPM) • 1 ♂, 5 ♀ (identified as *S. reflexilis* in Bando 2015), Anan City, Kamo Town, Omatsu-daigongen, 33.91466°N, 134.55208°E, 29.Aug.2013, H. Bando leg. (TKPM) • 1 ♀ (identified as *S. reflexilis* in Bando 2015), Anan City, Tsubachi Town, Toyono, 33.82427°N, 134.64894°E, 23.Sep.2013, H. Bando leg. (TKPM) • 1 ♂, 1 ♀, Anan City, Asebi Town, Arita, along road n°28, 33.87834°N, 134.55234°E, in the litter in a forest of sugi trees (*Cryptomeria japonica*), 15.May.2019, F. Ballarin, T. and Yamasaki leg. (FBPC) • 1 ♂, 7 ♀, Tokushima City, Kamihachiman Town, Tatsumiyama, 34.01891°N, 134.51008°E, 18.Sep.2024, Y. Suzuki leg. (TKPM) • **Kochi Pref.,**

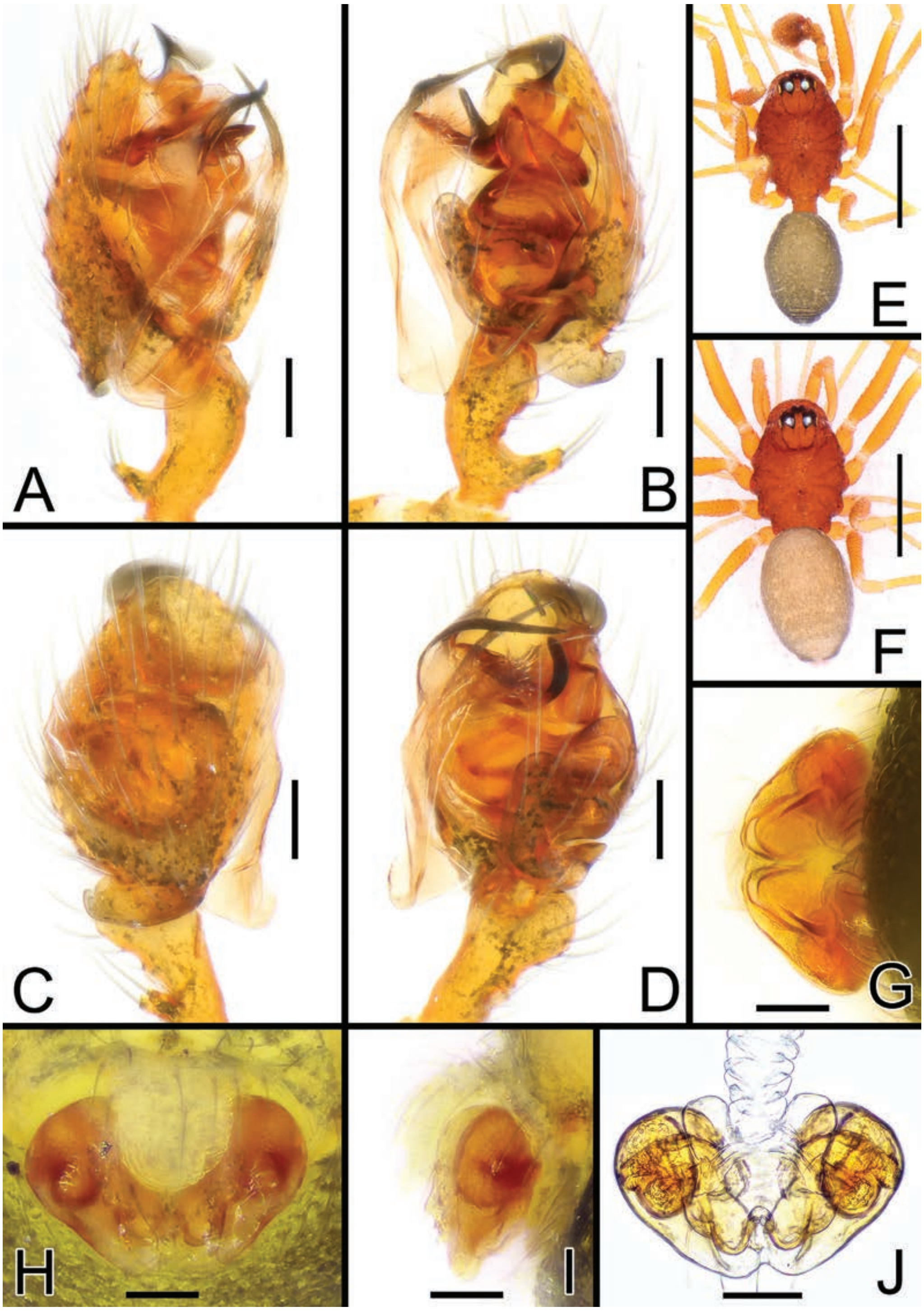

Figure 7. *Solenysa macrodonta* from Hiroshima **A** male palp, prolateral **B** ditto, retrolateral **C** ditto, dorsal **D** ditto, ventral **E** habitus of male, dorsal **F** habitus of female, dorsal **G** epigyne, posterior **H** ditto, ventral **I** ditto, lateral **J** vulva, dorsal. Scale bars: 0.05 mm (**A–D, G–J**); 0.5 mm (**E, F**).

1 ♀, Muroto Peninsula, Motootsu, 243 m, 33.31339°N, 134.12262°E, deciduous forest leaf litter, 01.Mar.2022, F. Ballarin leg. (FBPC) • 1 ♂, Tosa City, Usachoryu, 33.42255°N, 133.45036°E, 15.Sep.2023, Y. Tsuji leg. (TKPM) • 1 ♂, Shimanto City, Gudo, 32.99045°N, 132.91411°E, 12.Jul.2023, Y. Tsuji leg. (TKPM) • **Okayama Pref.,** 1 ♂, Maniwa City, Shimoazae, near the entrance of Suwa-do cave (諏訪洞), 183 m, 34.97021°N, 133.62441°E, in the leaf litter of a deciduous forest

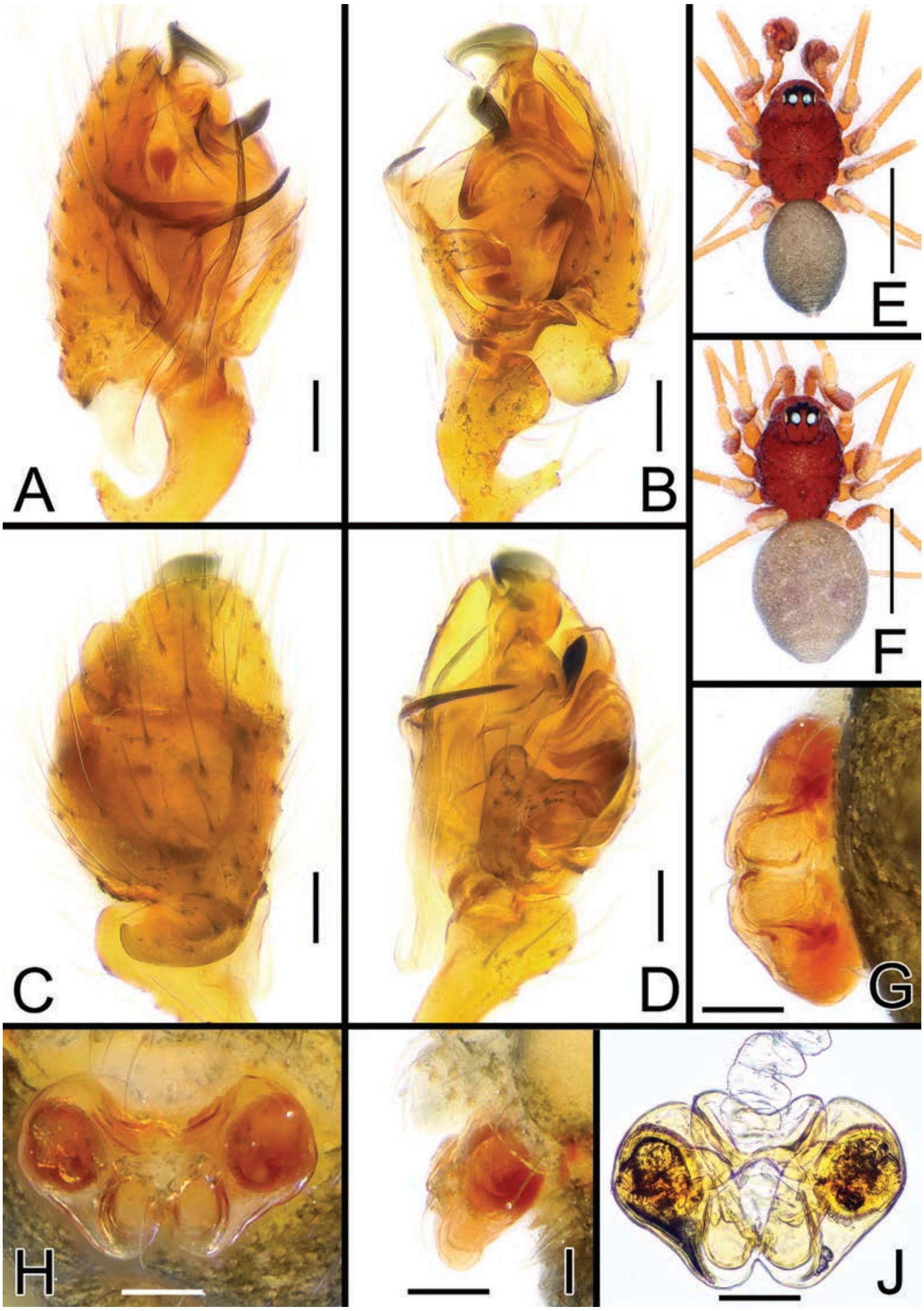

Figure 8. *Solenysa trunciformis* **A** male palp, prolateral, sample from Okayama **B** ditto, retrolateral **C** ditto, dorsal **D** ditto, ventral **E** habitus of male, dorsal **F** habitus of female, dorsal **G** epigyne, posterior, sample from Tokushima **H** ditto, ventral **I** ditto, lateral **J** vulva, dorsal. Scale bars: 0.05 mm (**A–D, G–J**); 0.5 mm (**E, F**).

20.Apr.2019, F. Ballarin and T. Yamasaki leg. (FBPC) • 1 ♂, 1 ♀, Niimi City, Toyonagauyama, Safushi river's valley (佐伏川), 254 m, 34.93934°N, 133.56580°E, in the litter of a deciduous forest on a very steep slope, 21.Apr.2019, F. Ballarin and T. Yamasaki leg. (MNHAH) • 1 ♀, Takahashi City, Kawakami Town, Kōyamaichi, Anatoyama Shrine (穴門山神社), 454 m, 34.74384°N, 133.39246°E, under stones near the shrine, 22.Apr.2019, F. Ballarin and T. Yamasaki leg. (FBPC).

Diagnosis. See Wang et al. (2015).

Description. Habitus of male as in Fig. 8E, habitus of female as in Fig. 8F. Palp as in Fig. 8A–D, embolic division as in Fig. 11E, F; epigyne and vulva as in Fig. 8G–J. See Wang et al. (2015) for a detailed description.

Type locality. Tondazaka, Shirahama City, Wakayama Prefecture, Honshu, Japan (33.625°N, 135.422°E).

Remarks. The current distribution of this species covers Shikoku (Tokushima, Kanagawa, and Kochi Pref.), eastern Chugoku (Okayama Pref.), and southern Kansai (Wakayama Pref.), Japan (Shinkai et al. 2024, this work; Fig. 13). The male specimens from Okayama collected by us exhibits a massive and more squared median protrusion (MP) of the MTA together with a much shorter and triangular posterior protrusion (PP) when compared with the holotype (cf. Fig. 11E, F vs Wang et al. 2015: fig. 6F). The male from eastern Shikoku examined by us exhibits both the median (MP) and posterior (PP) protrusions strongly reduced. In all cases, the shape of the lamella remains constant. Due to the lack of specimens examined from the type locality area we cannot confirm if this is part of the intraspecific variability of the species or if *S. trunciformis* is a potential complex of multiple morphologically similar species. Yet, our preliminary molecular results suggest little genetic difference among the individual from Tokushima Pref. with the putative *S. trunciformis* from Shikoku harvested from GenBank (Fig. 12). Further investigations involving a molecular analysis of a larger number of individuals from different localities may help shed light on this matter.

Solenysa longqiensis group sensu Tu & Hormiga (2011)

Solenysa longqiensis Li & Song, 1992

Figs 9A–J, 11G, H

Solenysa longqiensis Li & Song, 1992: 6, fig. 1A–G (♂♀); Song et al. 1993: 861, fig. 17A–G (♂♀); Li et al. 1994: 80, figs 18, 19 (♀); Song et al. 1999: 204, fig. 116J, K, Q, R (♂♀); Tu and Li 2006: 91, figs 12–20 (♂♀); Tu and Hormiga 2011: 503, figs 7A, 14A–H, 15A–H (♂♀).

Material examined. Taiwan: Nantou County, Ren’ai, • 1 ♀, Huisun Forest Area, 720 m, 24.09360°N, 121.03080°E, broadleaf forest litter, 09.July.2023, F. Ballarin leg. (TARI) • 1 ♂, same locality, 740 m, 24.08967°N, 121.03529°E, broadleaf forest litter along the trail, 12.July.2023, F. Ballarin leg. (TARI) • 1 ♂, 5 ♀, same locality, 685 m, 24.09295°N, 121.03247°E, broadleaf forest litter on a gentle slope, 13.July.2023, F. Ballarin leg. (NSMT) • 2 ♂, 4 ♀, same locality, 727 m, 24.09231°N, 121.03272°E, rather dry broadleaf forest litter, 14.July.2023, F. Ballarin leg. (FBPC) • 1 ♂, Menggu Waterfall, 910 m, 24.02824°N, 121.08067°E, broadleaf forest litter along the trail, 17.July.2023, F. Ballarin leg. (TARI).

Type locality. Mt. Longqi, Yujiaping Town, Jiangle County, Fujian Province, China (26.700°N, 117.400°E)

Diagnosis. See Tu and Li (2006) and Tu and Hormiga (2011).

Description. Habitus of male as in Fig. 9E, habitus of female as in Fig. 9F. Palp as in Fig. 9A–D, embolic division as in Fig. 11G, H; epigyne and vulva as in Fig. 9G–J. See Tu and Li (2006) for a detailed description.

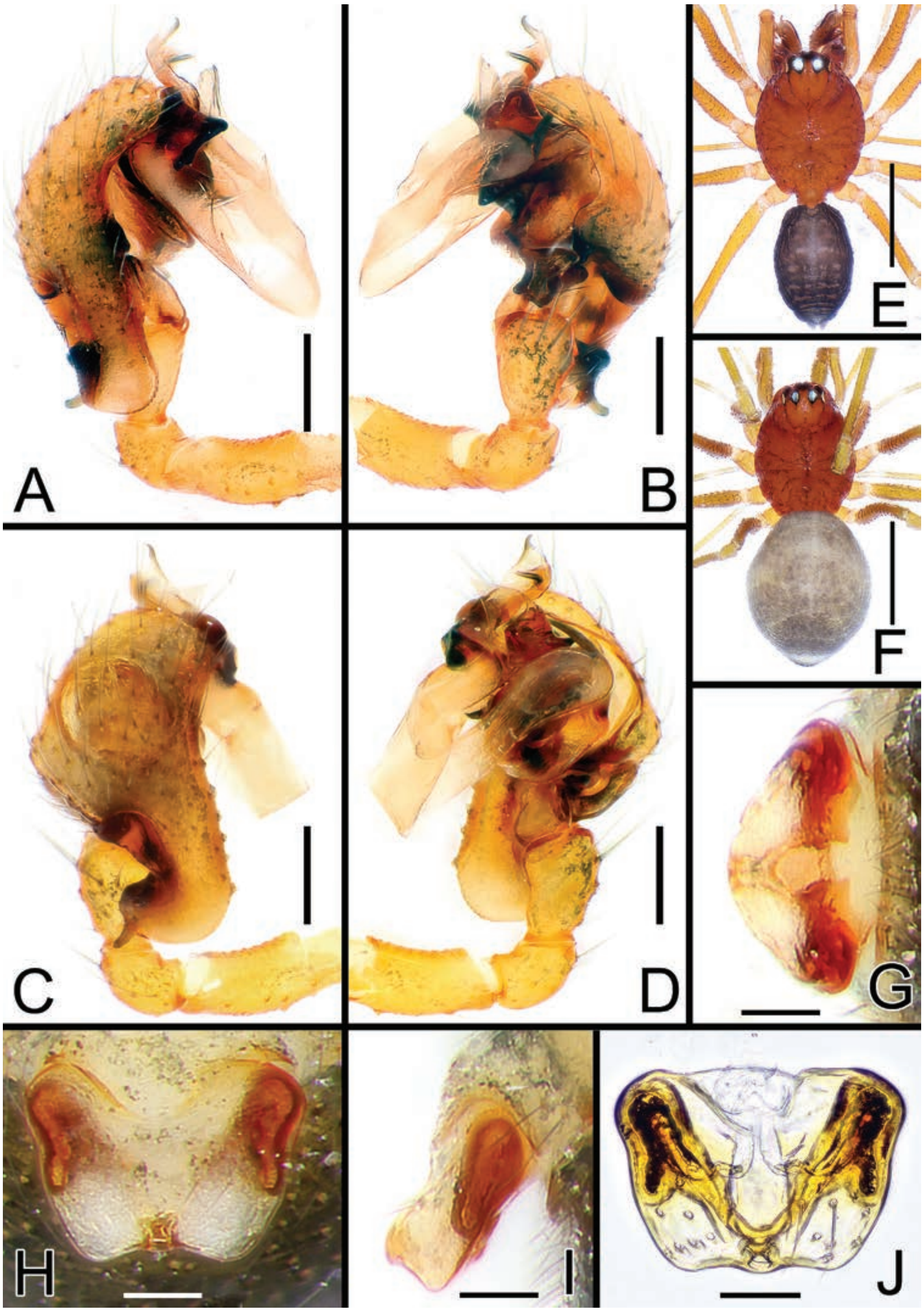

Figure 9. *Solenysa longqiensis* **A** male palp, prolateral **B** ditto, retrolateral **C** ditto, dorsal **D** ditto, ventral **E** habitus of male, dorsal **F** habitus of female, dorsal **G** epigyne, posterior **H** ditto, ventral **I** ditto, lateral **J** vulva, dorsal. Scale bars: 0.05 mm (**A–D, G–J**); 0.5 mm (**E, F**).

Remarks. This species was originally described from mainland China by Tu and Li (2006) and its presence in Taiwan was later confirmed by Tanasevitch (2011). Tian et al. (2022) in their map on *Solenysa* species distribution, report several records of the *S. longqiensis* group in Taiwan without specifying which species in particular they refer to. Our data from central Taiwan confirm that *S. longqiensis* is widespread across the island. Additionally, we report it as sympatric with the Taiwanese endemic and closely related *S. yangmingshana*, as we collected the two species together in the same habitat in more than one location (Fig. 13).

Solenysa yangmingshana **Tu, 2011**

Figs 10A–J, 11I, J

Solenysa yangmingshana Tu in Tu & Hormiga, 2011: 503, fig. 11A–G (♂♀).

Material examined. Taiwan: Nantou County, Ren'ai, • 2 ♀, Huisun Forest Area, 740 m, 24.08967°N, 121.03529°E, broadleaf forest litter along the trail, 12.July.2023 F. Ballarin leg. (FBPC) • 2 ♂, same locality, 930 m, 24.08421°N, 121.03438°E, rather humid broadleaf forest litter on a gentle slope, 14.July.2023, F. Ballarin leg. (FBPC) • 4 ♀, Menggu Waterfall, 910 m, 24.02824°N, 121.08067°E, broadleaf forest litter along the trail, 17.July.2023, F. Ballarin leg (NSMT) • **Taichung City Metropolitan Area,** 1 ♀, Dongshi District, Daxue Mountain, 860 m, 24.21595°N, 120.88943°E, broadleaf forest leaf litter along the trail, 18.July.2023, F. Ballarin leg. (TARI).

Type locality: Mt. Yangmingshan, Taipei City, Taiwan (~ 25.171°N, 121.553°E).

Diagnosis. See Tu and Hormiga (2011).

Description. Habitus of male as in Fig. 10E. Total length: 1.56. Prosoma 0.85 long; 0.60 wide. Clypeus 0.38 long. Cephalic area distinctly elevated in both sexes. Carapace oval, lacking lateral lobes. Carapace, chelicera, mouth parts, and sternum uniformly brick-red. Chelicera with four promarginal and three retromarginal teeth. Legs uniformly red-yellowish. TmI = 0.43. TmIV absent. Length of legs as follows: I 3.71 (1.01, 0.20, 1.04, 0.86, 0.60), II 3.21 (0.88, 0.18, 0.84, 0.75, 0.56), III 2.56 (0.78, 0.18, 0.60, 0.56, 0.44), IV 3.19 (0.92, 0.17, 0.83, 0.73, 0.54). Opisthosoma uniformly dark grey with some faint lighter dots on dorsal side. Some individuals with one light mark on dorsal-posterior part of opisthosoma. Palp as in Fig. 10A–D, embolic division as in Fig. 11I, J.

Habitus of female as in Fig. 10F. Total length: 1.55. Prosoma 0.79 long; 0.53 wide. Clypeus 0.28 long. Length of legs as follows: I 3.30 (0.95, 0.17, 0.89, 0.74, 0.55), II 2.91 (0.85, 0.16, 0.77, 0.62, 0.51), III 2.37 (0.68, 0.16, 0.55, 0.52, 0.46), IV 2.92 (0.89, 0.17, 0.75, 0.63, 0.48). Color and other features as in male. Epigyne and vulva as in Fig. 10G–J.

See Tu and Hormiga (2011) for a detailed description of genitalia.

Remarks. Species endemic to the island of Taiwan (Fig. 13). As far as we know, this species was previously recorded only from a few specimens collected in the north of the Island. Similarly to the previously mentioned *S. longqiensis*, *S. yangmingshana* is widespread across Taiwan and both species share the same habitat. In the original description by Tu and Hormiga (2011), the coordinates of the type locality are incorrectly reported and refer to the type locality of *S. longqiensis*. Additionally, in their distribution map, Tu and Hormiga (2011: 517) erroneously report the type locality as being in central Taiwan, while it is located in the north of the island. They also mention that the original male holotype was dried out and could not be properly measured thus limiting their description to the genitalia. Accordingly, here we redescribe the habitus of both male and female of this species reporting the related measurements.

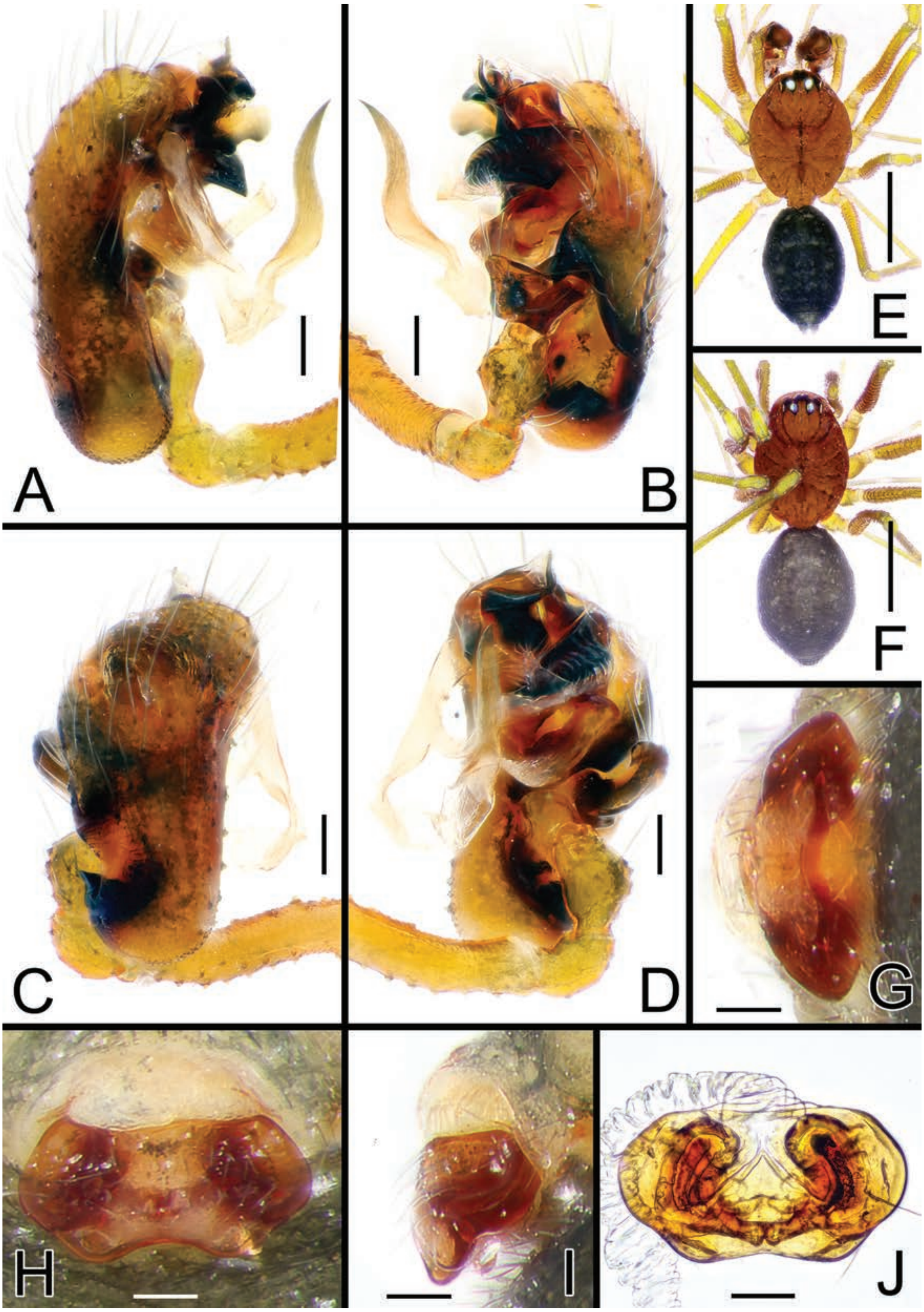

Figure 10. *Solenysa yangmingshana* **A** male palp, prolateral **B** ditto, retrolateral **C** ditto, dorsal **D** ditto, ventral **E** habitus of male, dorsal **F** habitus of female, dorsal **G** epigyne, posterior **H** ditto, ventral **I** ditto, lateral **J** vulva, dorsal. Scale bars: 0.05 mm (**A–D, G–J**); 0.5 mm (**E, F**).

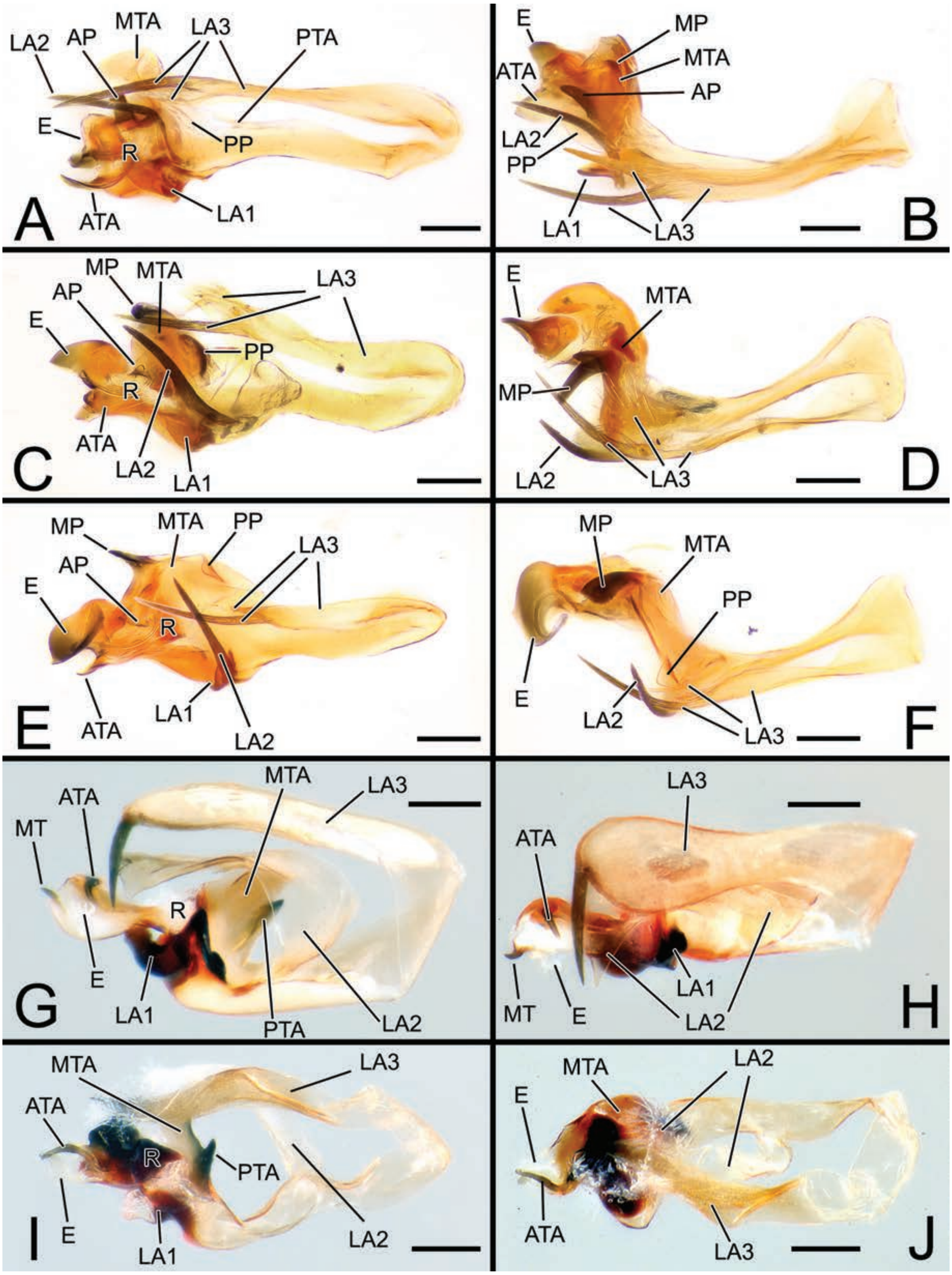

Figure 11. Embolic divisions of *Solenysa* species **A** *S. reflexilis* from Yakushima, ventral **B** ditto, retrolateral **C** *S. macrodonta* from Hiroshima, ventral **D** ditto, retrolateral **E** *S. trunciformis* from Okayama, ventral **F** ditto, retrolateral **G** *S.longqiensis*, ventral **H** ditto, retrolateral **I** *S. yangmingshana* **J** ditto, retrolateral. (N.B., in **A–D** embolus is broken). Abbreviations: AP anterior protrusion of MTA; ATA anterior terminal apophysis; E embolus; LA1 anterior branch of lamella; LA2 median branch of lamella; LA3 posterior branch of lamella; MP median protrusion of MTA; MT median tooth on anterior terminal apophysis; MTA median terminal apophysis; PP posterior protrusion of MTA; PTA posterior terminal apophysis; R radix. Scale bars: 0.05 mm.

***Solenysa lanyuensis* Tu, 2011**

Solenysa protrudens Tu in Tu and Li, 2006: 94, figs 31–39 (♂♀, misidentified).
S. lanyuensis: Tu and Hormiga 2011: 515, fig. 7C (♂♀).

Type locality. Lanyu Island (= Orchid Island), Taitung County, Taiwan (see remarks)

Diagnosis. See Tu and Li (2006)

Description. See Tu and Li (2006)

Remarks. The type series of *S. lanyuensis* (3 ♂ and 2 ♀) was originally misidentified as *S. protrudens* by Tu and Li (2006). Later, *S. lanyuensis* was recognized as a new species and described based on the same specimens by Tu and Hormiga (2011). The coordinates of the type locality reported by both Tu and Li (2006) and Tu and Hormiga (2011) refer to a coastal area in southeast Taiwan and are likely incorrect since the name of the locality, from which the species also takes its name, refer to Lanyu, a small volcanic island located ca. 75 km far from the Taiwanese coast. The exact collecting location of the type series on the island remains unknown. In 2019, we had the opportunity to conduct an extensive survey on Lanyu Island, which led to the discovery of several rare litter-dwelling spiders, including linyphiids (Ballarin et al. 2021). However, despite our extensive collecting effort, we failed to find any specimens of *Solenysa* on the island. As far as we know, this species remains recorded only from two localities, Lanyu Island from the original description and the location in central Taiwan reported by Tian et al. (2022, reported in the map but locality not specified). Additional collection in southwest Taiwan may help to clarify the distribution of this species.

Other comparative material examined

***Solenysa mellotteei* Simon, 1894: Japan: Tokyo Pref.,** 1 ♂, 1 ♀, Hachioji City, Naganumamachi, Naganuma Park (長沼公園), 150 m, 35.637°N, 139.368°E, forest leaf litter on a slope, 07.Aug.2019, F. Ballarin leg. (FBPC).

***Solenysa ogatai* Ono, 2011: Japan: Shizuoka Pref.,** 1 ♂, Fujinomiya City, Nukudo, Hoshiyama, Myojoyama Park (明星山公園), 17.Nov.2014, A. Tanikawa leg. (FBPC) • **Kanagawa Pref.,** 1 ♂, 1 ♀, Ashigarashimo-gun, Manazaru, Manatsuru cape, 90 m, 35.14409°N, 139.15556°E, thick leaf litter in a primary forest, 28.Jul.2021, F. Ballarin leg. (FBPC).

Molecular analysis

The final dataset used for the phylogenetic analysis included 27 ingroup terminals and 16 *Solenysa* species. The concatenated sequences had a total of 1047 bp (COI = 696 bp, H3 = 351 bp). Both the ML and BI analyses produced the same tree topology, with similar support for the wide majority of the nodes. The resulting tree is shown in Fig. 12.

In the tree, the separation of the *Solenysa* species identified by morphology is endorsed by strongly supported nodes. The new species from Kyushu, *S. bilamellata* sp. nov., is reconstructed with strong support as monophyletic and closely related to the other species of the *S. mellotteei* group distributed in mainland Japan. The two new species from the Ryukyus, *S. shimatchu* sp. nov. and *S. yambaruensis* sp. nov., are both strongly supported. Together they form a distinct monophyletic

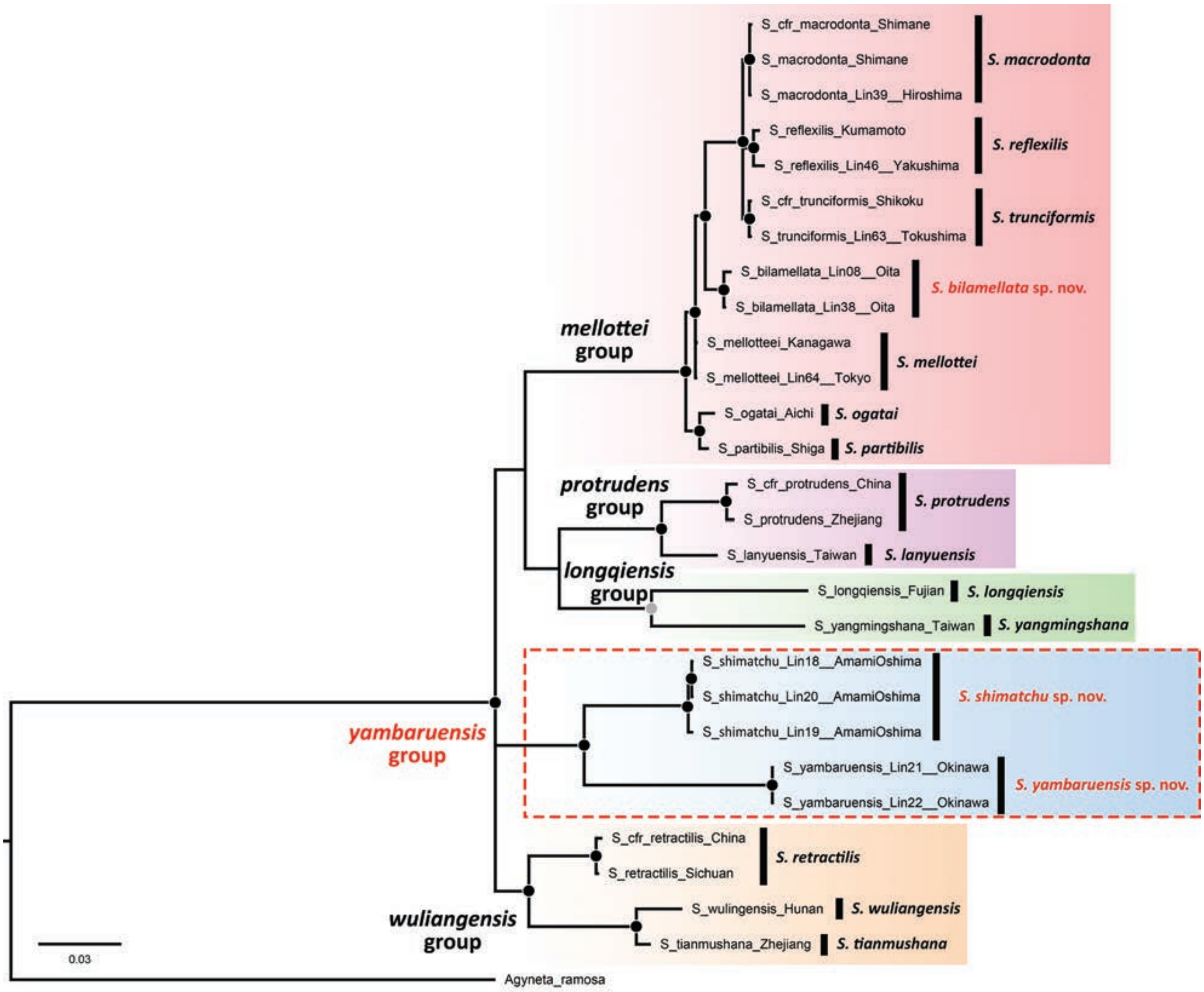

Figure 12. Phylogenetic tree based on combined COI and H3 gene fragments reconstructed using maximum likelihood (ML) on RAxML and Bayesian inference (BI) on MrBayes. Support at each node denotes the ML bootstrap value (BV) and BI posterior probability (PP). Nodes highly supported by at least one method (BV ≥ 75 or PP ≥ 0.95) are highlighted by a black dot, nodes with medium support (BV ≥ 70 or PP ≥ 0.90) are reported in grey, low supported nodes lack a dot. Branch lengths were scaled to the number of substitutions per site. *Solenysa* species groups are highlighted with different colors. New taxa discussed in this work are reported in red.

lineage with a long basal branch and well separated from all the other known species groups. This further supports the establishment of a new species group, the *S. yambaruensis* group, to accommodate them. All four previously known *Solenysa* species groups, although generally poorly supported at the basal node, are reconstructed as distinct lineages, separated to each other by long basal branches. These results are consistent with the morphological analysis and previous studies.

The interspecific genetic diversity of *Solenysa* species is reported in Table 2, ranging from 0.4% to 13.5%, with an average of 9%. Genetic diversity between species groups ranges from 7.7% to 13.5% (average 10.6%). The average genetic diversity within the species groups is as follows: *S. yambaruensis* group = 11%, *S. longqiensis* group = 9.7%, *S. wulingensis* group = 5.3%, *S. protrudens* group = 4.2%, *S. mellotteei* group = 2.6%. The *S. mellotteei* group shows the lowest interspecific ranging spanning from 0.4% to 4.4%. *Solenysa bilamellata* sp. nov. shares a genet-

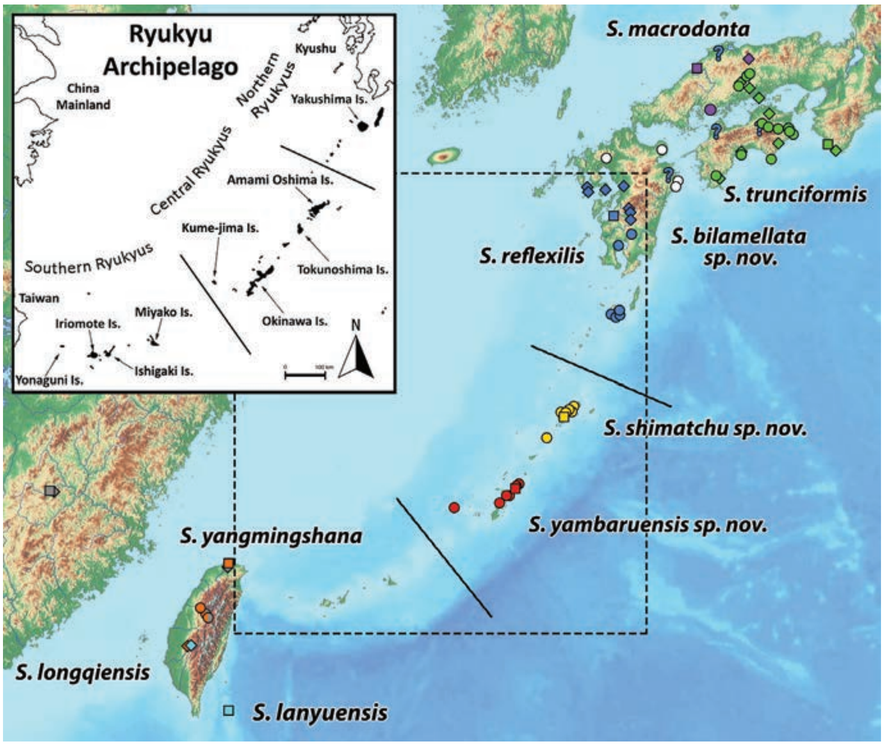

Figure 13. Distribution of *Solenysa* species in the Ryukyu Archipelago and surrounding areas. The Ryukyu Archipelago is marked with a dashed line. Diamonds refer to records of *Solenysa* spp. from the literature (Shinkai et al. 2024; WSC 2024), dots refer to new records, squares indicate the species type locality, and question marks indicate uncertain records of *S. reflexilis*.

ic distance with other species of the *S. mellotteei* group ranging from 1.2% to 4.4% (average 3%). The lowest genetic distance in the group is calculated between *S. mellotteei* and *S. partibilis*, revealing a surprisingly low value of only 0.4%. Fresh samples of *S. partibilis* were not available for our pairwise analysis, thus for this species we relied on sequences harvested from GenBank. Given the well-known problem of misidentifications in online genetic databases, we cannot exclude that the COI barcode attributed to *S. partibilis* and used by us for the pairwise analysis may actually belong to another misidentified species in the *S. mellotteei* group.

Discussion and conclusions

Despite being a relatively well-studied linyphiid genus, the diversity of *Solenysa* still seems far to be completely defined. Our study increases the number of species from Japan from six to nine, and the total number of known *Solenysa* species from 15 to 18. The *S. mellotteei* group is confirmed as the most speciose within the genus, consisting solely of species distributed in mainland Japan. Nevertheless, this group also exhibits the lowest interspecific diversity among the species groups, suggesting a recent diversification, as previously proposed by other studies (Tian et al. 2022). The discovery of *Solenysa bilamellata* sp. nov. from Kyushu, along with the morphological differences observed among allopatric populations in other species of the same group, suggests that the true magnitude of the diversity of the S. *mellotteei* group may still be underestimated and that additional species may remain undetected in Japan.

Table 2. Uncorrected Pairwise-distance between the species and species groups of *Solenysa* based on the barcode COI partial sequences.

Species		***S. bilamellata* sp. nov.**	***S. lanyuensis***	***S. longqiensis***	***S. macrodonta***	***S. mellotteei***	***S. ogatai***	***S. partibilis***	***S. protrudens***	***S. reflexilis***	***S. retractilis***	***S. tianmushana***	***S. shimatchu***	***S. trunciformis***	***S. wulingensis***	***S. yambaruensis***
	Species group	mellotteei gr.	protrudens gr.	longqiensis gr.	mellotteei gr.	mellotteei gr.	mellotteei gr.	mellotteei gr.	protrudens gr.	mellotteei gr.	wulingensis gr.	wulingensis gr.	yambaruensis gr.	mellotteei gr.	wulingensis gr.	yambaruensis gr.
***S. bilamellata* sp. nov.**	mellotteei gr.															
S .lanyuensis	protrudens gr.	0.108														
S. longqiensis	longqiensis gr.	0.115	0.088													
S. macrodonta	mellotteei gr.	0.029	0.104	0.108												
S. mellotteei	mellotteei gr.	0.015	0.108	0.110	0.026											
S. ogatai	mellotteei gr.	0.031	0.115	0.117	0.040	0.009										
S. partibilis	mellotteei gr.	0.022	0.108	0.110	0.035	0.004	0.013									
S.protrudens	protrudens gr.	0.115	0.042	0.088	0.102	0.106	0.113	0.106								
S. reflexilis	mellotteei gr.	0.034	0.104	0.104	0.013	0.029	0.044	0.035	0.102							
S. retractilis	wulingensis gr.	0.102	0.077	0.086	0.099	0.097	0.104	0.097	0.084	0.095						
S. tianmushana	wulingensis gr.	0.097	0.079	0.095	0.095	0.097	0.104	0.097	0.088	0.091	0.060					
S. shimatchu	yambaruensis gr.	0.112	0.095	0.117	0.111	0.115	0.115	0.108	0.102	0.113	0.097	0.097				
S. trunciformis	mellotteei gr.	0.035	0.102	0.106	0.007	0.029	0.038	0.033	0.099	0.015	0.095	0.091	0.110			
S. wulingensis	wulingensis gr.	0.108	0.093	0.097	0.095	0.104	0.106	0.108	0.095	0.095	0.071	0.029	0.097	0.091		
S. yambaruensis	yambaruensis gr.	0.114	0.132	0.130	0.120	0.118	0.132	0.130	0.135	0.117	0.113	0.117	0.109	0.128	0.121	
S. yangmingshana	longqiensis gr.	0.117	0.093	0.097	0.110	0.115	0.121	0.115	0.115	0.106	0.102	0.106	0.113	0.106	0.106	0.130

Recent taxonomic studies on spiders in the Ryukyus have highlighted high levels of heterogeny and endemism at small geographic scales, proposing the role of the archipelago as a hotspot of spider diversity (Xu et al. 2019; Ihara et al. 2021; Suzuki et al. 2022; Ballarin and Eguchi 2022, 2023). The discovery of two undescribed *Solenysa* species in the Ryukyus, belonging to a new and distinct species group, further supports this hypothesis and fills a gap that was present in the distribution of the genus. However, the position of this species group within the genus remains poorly defined in our phylogenetic study and requires further comprehensive analyses. Linyphiidae are well-known to perform ballooning (Duffey 1998) and thus allowing them to potentially disperse in distant lands and islands. Yet, our study supports a strong level of endemism in *Solenysa* in both the Ryukyus and mainland Japan, possibly linked to the specific microhabitat conditions needed by these spiders. This trait, combined with the genus' putative old origin and high local diversification in mainland Japan, suggest that *Solenysa* may represent a valuable model subject for future biogeographic studies. Further research on this genus my offer new opportunities to shed light on the origin, adaptive radiation, and potential ancient routes of colonization of terrestrial arthropods in the Ryukyus and mainland Japan.

Acknowledgments

We are particularly thankful to the students of the TMU summer field course - Ryoku Itou, Rena Kaneko, Yusei Hiruma, and Kotone Watanabe - for their assistance in collecting part of the material used in this study and particularly to Rena Kaneko for defining the Japanese names of the new species. We also thank Takeshi Yamasaki, Mamoru Araki, and Takahiro Yoshida respectively for their help in the surveys in mainland Japan and Taiwan. We are equally thankful to Akio Tanikawa and Tatsumi Suguro for kindly providing additional *Solenysa* samples from their personal collections and to Yuya Suzuki for lending samples from the Tokushima Prefectural Museum. The survey in the Yambaru National Park was conducted with permission issued from the Ministry of the Environment, Japan (環九地沖許第n°2308189). We thank Atsushi Takashima (Yona Field, Faculty of Agriculture, University of the Ryukyus) for his assistance during our field survey in Yambaru. The survey in Taiwan was conducted with permission issued from the National Chung Hsing University (文號1121702204, 1121701242), and from the National Taiwan University (興農字第1121702205號). The manuscript has benefited from the comments and suggestions of Shuqiang Li, Andrei Tanasevitch, and an anonymous reviewer.

Additional information

Conflict of interest

The authors have declared that no competing interests exist.

Ethical statement

No ethical statement was reported.

Funding

This study was supported by the following funds: the Fund for the Promotion of Joint International Research (Fostering Joint Inter-national Research (B), JSPS KAKENHI, no. 22KK0087, leader: Katsuyuki Eguchi, FY2022–2025), Grant-in-Aid for Scientific Research

(C) (JSPS KAKENHI, no 23K05299, Leader: Emiko Oguri, FY2023–2026), the Tokyo Metropolitan University Fund for TMU Strategic Research (leader: Noriaki Murakami, FY2020–FY2022), and the Asahi Glass Foundation (leader: Katsuyuki Eguchi, FY2017–FY2023).

Author contributions

FB designed the study, conducted fieldwork, performed the taxonomic and molecular analyses, prepared illustrations and photographs, and wrote the initial draft of the manuscript. HL and KE helped obtain the collecting permissions, assisted with fieldwork, and provided valuable suggestions and corrections during the study. ZT revised part of the material used in the study, provided new specimens, distributional data, and SEM illustrations. All authors have equally contributed to revising and finalizing the manuscript.

Author ORCIDs

Francesco Ballarin https://orcid.org/0000-0003-1417-2519
Katsuyuki Eguchi https://orcid.org/0000-0002-1054-1295

Data availability

All of the data that support the findings of this study are available in the main text.

References

Ballarin F, Eguchi K (2022) Taxonomic notes on leptonetid spiders from the Ryukyu Archipelago with the description of two new species and the first record of the genus *Longileptoneta* from Japan (Araneae: Leptonetidae). Zootaxa 5213(4): 371–387. https://doi.org/10.11646/zootaxa.5213.4.3

Ballarin F, Eguchi K (2023) Integrative taxonomic revision of the genera *Nesticella* and *Howaia* in Japan with the description of five new species (Araneae, Nesticidae, Nesticellini). ZooKeys 1174: 219–272. https://doi.org/10.3897/zookeys.1174.101251

Ballarin F, Yamasaki T (2021) *Nihonella* gen. nov., a new troglophilic genus of dwarf spiders from Japan with a discussion on its phylogenetic position within the subfamily Erigoninae (Araneae, Linyphiidae). European Journal of Taxonomy 733: 1–18. https://doi.org/10.5852/ejt.2021.733.1215

Ballarin F, Yamasaki T, Su YC (2021) A survey on poorly known rainforest litter-dwelling spiders of Orchid Island (Lanyu, Taiwan) with the description of a new species (Araneae: Linyphiidae, Tetrablemmidae, and Theridiosomatidae). Zootaxa 4927(2): 197–208. https://doi.org/10.11646/zootaxa.4927.2.2

Bando H (2015) Spiders found in Anan City. Awa Society Bulletin, 60: 67–78. [In Japanese].Bando H (2019) Spiders found in the Nishi-Iyayama area of Miyoshi City. Awa Society Bulletin, 62: 45–55. [In Japanese].

Colgan DJ, McLauchlan A, Wilson GDF, Livingston SP, Edgecombe GD, Macaranas J, Cassis G, Gray MR (1998) Histone H3 and U2 snRNA DNA sequences and arthropod molecular evolution. Australian Journal of Zoology 46: 419–437. https://doi.org/10.1071/ZO98048

Duffey E (1998) Aerial dispersal in spiders. Proceedings of the 17th European Colloquium of Arachnology, Edinburgh 1997 (ed. P.A. Selden), British Arachnological Society, Burnham Beeches, UK, 189–191.

Folmer O, Black M, Hoeh W, Lutz R, Vrijenhoek R (1994) DNA primers for amplification of mitochondrial cytochrome c oxidase subunit I from diverse metazoan invertebrates. Molecular Marine Biology and Biotechnology 3: 294–299.

Hayashi N, Nojima K, Kataoka D (2013a) Spider habitat survey at Furusato Sawanouchi Park, Kijicho, Unnan City, Shimane Prefecture (2011–2012). Hoshizaki Green Foundation Research Report 16: 103–120. [In Japanese]

Hayashi N, Nojima K, Kataoka D (2013b) Spider habitat survey at Furusato Sawanouchi Park, Kijicho, Unnan City, Shimane Prefecture (2013). Hoshizaki Green Foundation Research Report 17: 129–134. [In Japanese]

Ihara Y, Koike N, Nakano T (2021) Integrative taxonomy reveals multiple lineages of the spider genus *Cybaeus* endemic to the Ryukyu Islands, Japan (Arachnida: Araneae: Cybaeidae). Invertebrate Systematics 35(2): 216–254. https://doi.org/10.1071/IS20070

Kozlov AM, Darriba D, Flouri T, Morel B, Stamatakis A (2019) RAxML-NG: a fast, scalable and user-friendly tool for maximum likelihood phylogenetic inference, Bioinformatics, 35(21): 4453–4455. https://doi.org/10.1093/bioinformatics/btz305

Kumar S, Stecher G, Li M, Knyaz C, Tamura K (2018) MEGA X: molecular evolutionary genetics analysis across computing platforms. Molecular Biology and Evolution 35(6): 1547–1549. https://doi.org/10.1093/molbev/msy096

Li SQ, Song DX (1992) On two new species of soil linyphiid spiders from China (Araneae: Linyphiidae: Erigoninae). Acta Arachnologica Sinica 1(1): 6–9.

Li SQ, Song DX, Zhu CD (1994) On the classification of spiders of subfamily Linyphiinae, Linyphiidae. Sinozoologia 11: 77–82.

Ono H, Matsuda M, Saito H (2009) Linyphiidae, Pimoidae. In: Ono H (Ed.) The spiders of Japan with keys to the families and genera and illustrations of the species. Tokai University Press, Kanagawa, 253–344.

Rambaut A, Drummond AJ, Xie D, Baele G, Suchard MA (2018) Posterior summarization in Bayesian phylogenetics using Tracer 1.7. Systematic Biology 67 (5): 901–904. https://doi.org/10.1093/sysbio/syy032

Ronquist F, Teslenko M, Van Der Mark P, Ayres DL, Darling A, Höhna S, Huelsenbeck JP (2012) MrBayes 3.2: efficient Bayesian phylogenetic inference and model choice across a large model space. Systematic Biology 61(3): 539–542. https://doi.org/10.1093/sysbio/sys029

Serita R (2022) Spiders collected in Kyushu. Kishidaia 121: 113–118.

Shinkai A, Tanikawa A (2023) Collection information. Yuushi, newsletter of the Japanese Society of Arachnology 52: 2–4. [In Japanese]

Shinkai A, Andoh A, Tanikawa A, Ikeda H, Kuwata T (2024) Japanese Spiders ver.2024. Self-published CD by the authors. https://kakureobi.sakura.ne.jp/CD2/mainindex.htm [In Japanese] [last accessed on Sep. 2024]

Simon E (1894) Histoire Naturelle des Araignées, seconde édition. Tome 1, Fascicule 3. Libraire encyclopédique de Roret, Paris, 489–760.

Song DX, Zhu MS, Li SQ (1993). Arachnida: Araneae. In: Huang, C. M. (ed.) Animals of Longqi Mountain. China Forestry Publishing House, Beijing, 852–890

Song DX, Zhu MS, Chen J (1999) The spiders of China. Hebei Science and Technology Publishing House, Shijiazhuang, 640 pp.

Suzuki Y, Hiramatsu T, Tatsuta H (2022) Two new species and a new genus of ray spiders (Araneae, Theridiosomatidae) from the Ryukyu Islands, southwest Japan, with notes on their natural history. ZooKeys 1109: 76–101. https://doi.org/10.3897/zookeys.1109.83807

Tanasevitch AV (2011) On some linyphiid spiders from Taiwan (Araneae: Linyphiidae). Zootaxa 3114: 31–39. https://doi.org/10.11646/zootaxa.3114.1.3

Tanikawa A (2024) A Check List of Japanese Spiders ver. 2024 R2. https://www.asahi-net.or.jp/~dp7a-tnkw/japan.pdf [accessed Sep. 2024]

Tian JH, Tu LH (2018) A new species of the spider genus *Solenysa* from China (Araneae, Linyphiidae). Zootaxa 4531(1): 142–146. https://doi.org/10.11646/zootaxa.4531.1.10

Tian J, Zhan Y, Shi C, Ono H, Tu L (2022) *Solenysa*, a Cretaceous relict spider group in East Asia. Diversity 14(2): 120. https://doi.org/10.3390/d14020120

Tsurusaki T, Ishikawa H, Ihara T (2011) Spiders of Ehime Prefecture. Research Report of the Ehime Prefectural Museum of Nature and Science 16: 33–57. [In Japanese]

Tsurusaki T, Ishikawa H, Takasuka K (2012) Catalog of true spiders found in Matsuyama City (2nd edn.). Catalog of wild fauna and flora in Matsuyama City 2012, 253–264. [In Japanese]

Tu LH, Hormiga G (2011) Phylogenetic analysis and revision of the linyphiid spider genus *Solenysa* (Araneae: Linyphiidae: Erigoninae). Zoological Journal of the Linnean Society 161(3): 484–530. https://doi.org/10.1111/j.1096-3642.2010.00640.x

Tu LH, Li SQ (2006) A review of the linyphiid spider genus *Solenysa* (Araneae, Linyphiidae). Journal of Arachnology 34(1): 87–97. https://doi.org/10.1636/H03-26.1

Tu LH, Ono H, Li SQ (2007) Two new species of *Solenysa* Simon, 1894 (Araneae: Linyphiidae) from Japan. Zootaxa 1426: 57–62. https://doi.org/10.11646/zootaxa.1426.1.4

Wang F, Ono H, Tu LH (2015) A review of *Solenysa* spiders from Japan (Araneae, Linyphiidae), with a comment on the type species *S. mellotteei* Simon, 1894. ZooKeys 481: 39–56. https://doi.org/10.3897/zookeys.481.8545

World Spider Catalog (2024) World Spider Catalog. Version 25.0. Natural History Museum Bern (http://wsc.nmbe.ch [last accessed on Sep. 2024). https://doi.org/10.24436/2

Xu X, Ono H, Kuntner M, Liu FX, Li DQ (2019). A taxonomic monograph of the liphistiid spider genus *Heptathela*, endemic to Japanese islands. ZooKeys 888: 1–50. https://doi.org/10.3897/zookeys.888.34494

ZooKeys 1232: 131–172 (2025)
DOI: 10.3897/zookeys.1232.141693

Research Article

The ant genus *Nesomyrmex* Wheeler (Formicidae, Myrmicinae) from the threatened Colombian tropical dry forest: three new species, a new synonymy, and new distributional data

Brandon S. Arredondo[1], Roberto J. Guerrero[1]

1 *Universidad del Magdalena, Santa Marta, Colombia*
Corresponding author: Roberto J. Guerrero (rguerrero@unimagdalena.edu.co)

Abstract

The species of the ant genus *Nesomyrmex* inhabiting the tropical dry forest (TDF) of Colombia are reviewed. Three new species of this genus, *Nesomyrmex iku* **sp. nov.**, *Nesomyrmex konina* **sp. nov.**, and *Nesomyrmex xerophilus* **sp. nov.**, are described based on worker caste. *Nesomyrmex vargasi* Longino, 2006 is recorded for the first time in South America, and *Nesomyrmex antoniensis* (Forel, 1912) is proposed as a junior synonym of *Nesomyrmex asper* (Mayr, 1887). A worker-based taxonomic identification key for the Colombian species is provided. High-resolution images and illustrations, and a distribution map for the species present in the Colombian TDF are provided.

Key words: Biodiversity, conservation, morphology, Neotropical region, taxonomy, threatened ecosystems

Academic editor: Jeffrey Sosa-Calvo
Received: 13 November 2024
Accepted: 30 January 2025
Published: 17 March 2025

ZooBank: https://zoobank.org/0AA099A2-EA57-4E27-937A-0976B9F8A4B5

Citation: Arredondo BS, Guerrero RJ (2025) The ant genus *Nesomyrmex* Wheeler (Formicidae, Myrmicinae) from the threatened Colombian tropical dry forest: three new species, a new synonymy, and new distributional data. ZooKeys 1232: 131–172. https://doi.org/10.3897/zookeys.1232.141693

Introduction

Nesomyrmex Wheeler (Formicidae: Myrmicinae) is a monophyletic genus in the tribe Crematogastrini Forel, 1893 (Ward et al. 2015). These ants are monomorphic and differentiated from any other ant genera of the subfamily Myrmicinae by the combination of the following characters (Bolton 2003; Fernández and Serna 2019): mandibles with 3–5 teeth; median portion of the clypeus with anterior projection, forming a prominent lobe projecting over the dorsum of the mandibles; antenna of 11 or 12 antennomeres with distinct 3-segmented club; rounded or angled propodeal lobe; propodeum armed with a pair of spines of variable lengths.

Nesomyrmex ants are small and live mostly on dead or living branches of trees. Currently, 85 species and one subspecies (*Nesomyrmex angulatus lybica* (Menozzi, 1934)) of *Nesomyrmex* are recognized (Bolton 2024) including two extinct species from Dominican amber (De Andrade et al. 1999), with higher species richness concentrated in the tropics and subtropics (Janicki et al. 2016). The genus *Nesomyrmex* occurs in the Afrotropical (30 species; Mbanyana and Robertson 2008; Hita Garcia et al. 2017), Malagasy (32 species; Csősz and Fisher 2015, 2016a, b, c, d), Nearctic (2 species; Smith 1943; Dáttilo et al. 2020), Neotropical (23 species; Kempf 1959; Diniz 1975; Brandão 1991; Bolton 1995;

Longino 2006), and Palearctic region (4 species; Collingwood 1985; Collingwood and Agosti 1996; Sharaf et al. 2017, 2020). For Colombia seven species are recorded (Kempf 1959; Fernández et al. 1996; Fernández and Serna 2019), several of which occur in different forest types, including the tropical dry forest (TDF).

The tropical dry forest in Colombia is one of the most threatened terrestrial ecosystems, with a substantial reduction in its extension of approximately 82%, with forest fragments that amount to only 720,000 hectares (Pizano et al. 2014). Agricultural and livestock expansion, the exploitation of non-renewable resources (e.g., mineral coal in the north of the country), urban expansion and tourism are the main factors causing the drastic reduction of TDF in Colombia (Pizano et al. 2016). Despite the ecological importance and imminent systematic reduction, only 5% of the TDF is covered by the national protected areas program, thus increasing concern about the loss of its biodiversity and ecosystem services. Given this panorama, several initiatives have focused on collecting information from different biological models, including ants (Ramos and Guerrero 2023), to develop comprehensive TDF management plans (Pizano et al. 2016).

Since 2020, the research project "Patterns of historical and ecological diversity of ants in the socio-ecosystem of the tropical dry forest of Colombia and its implications for conservation" has been under development. This project integrates multiple approaches such as taxonomy, evolution, and ecology of ants, to understand the conservation status of the TDF in Colombia. In line with this research project, we seek to generate information about the diversity of the different genera of ants in the Colombian TDF. Interestingly, new ant species in the genera *Forelius* (Guerrero and Fernández 2008), *Dorymyrmex* (Cuezzo and Guerrero 2012), and *Pheidole* (Camargo-Vanegas and Guerrero 2020) have been described from the Colombian TDF. Here we review the *Nesomyrmex* ants that inhabit the Colombian TDF, describing three new species, two known so far from the TDF fragments in the Colombian Caribbean. Also, we propose *Nesomyrmex antoniensis* (Forel, 1912) as a junior synonym of *Nesomyrmex asper* (Mayr, 1887), considering the wide morphological variation of the latter's workers. New distributional data are also provided for each species discussed here, and an illustrated worker-based taxonomic key for the species in Colombia is provided.

Materials and methods

Specimen processing

Specimens were observed using a Nikon SMZ 745 stereomicroscope. All of them were identified based on taxonomic keys (Kempf 1959), comparison with high-resolution photographs of type material provided by AntWeb (2024) and MZSP. For specimens found that did not correspond to any currently recognized species, the criterion of morphological discontinuity in a comparative framework (Bolton 2000; Longino 2003; Branstetter 2013; Fernández and Serna 2019) was used to support hypotheses of new species. Morphological terminology follows Bolton (2000) and Serna and Mackay (2010). Additionally, head, mesosoma and metasoma regions are illustrated and defined (Figs 1, 2). Sculptural terminology follows Harris (1979). Measurements mainly follow those proposed by Hita Garcia et al. (2017) and Sharaf et al. (2017). Measurements were made with a dual-axis micrometer stage with output in increments of 0.001 mm. However, variation in specimen orientation, alignment of crosshairs with edges of structures, and interpretation of structure boundaries resulted in measurement accuracy to the nearest 0.01 mm. All measurements (Fig. 3) are presented in mm:

HL	Head length: in full-face view, maximum distance from the midpoint of the anterior margin of the clypeus to the midpoint of the posterior cephalic margin.
HW	Head width: in full-face view, width of the head immediately posterior to the eyes.
PW	Pronotal width: in dorsal view, maximum width of pronotum.
PTW	Petiole width: in dorsal view, maximum width of petiole (if the petiole presents lateral tubercles, this measurement should be taken at the maximum petiole width excluding the tubercles).
PPW	Postpetiole width: in dorsal view, maximum width of postpetiole (if the postpetiole presents lateral tubercles, this measurement should be taken at the maximum postpetiole width excluding the tubercles).
PH	Pronotal height: in lateral view, maximum height of the pronotum measured from the lower margin to the upper margin of the pronotum.
PTH	Petiole height: in lateral view, maximum height of petiolar node.
PPH	Postpetiole height: in lateral view, maximum height of postpetiole.
SL	Scape length: in full-face view, maximum length of the scape excluding the neck that occurs just distal of the condylar bulb. Where the scapes were not aligned with the frontal view of the head, it was necessary to place the cephalic capsule obliquely to take a correct measurement of the scape.
GL	Gaster length: in lateral view, maximum length from the point of insertion with the postpetiole to the most distal part of the gaster, excluding the stinger (this measurement is affected by the degree to which the sternites are retracted or protracted).
PTL	Petiole length: in lateral view, maximum length of the petiole from the anterior corner of subpetiolar process to the insertion with the postpetiole.
PPL	Postpetiole length: in lateral view, maximum length from the most anterior point of insertion with the petiole to the insertion of the gaster.
WL	Weber's length: in lateral view, diagonal length of the mesosoma from the most anterior point of the pronotal slope (excluding the pronotal projection), to the posterior margin of the propodeal lobe.
EL	Eye length: in lateral view, maximum diameter of the compound eye.

Indices

CI	Cephalic index: (HW/HL) *100.
SI	Scape index: (SL/HW) *100.

Specimen drawing, imaging, and distribution maps

The drawings of the different *Nesomyrmex* species recorded here were created using Sketchbook Pro v. 9.0. Stacked color images of the species were generated at Laboratorio de equipos ópticos del Departamento de Biología (Universidad Nacional de Colombia, Sede Bogotá) and Laboratorio de Entomología de la Universidad de la Amazonia (LEUA), using a Leica M205A Auto-Montage with

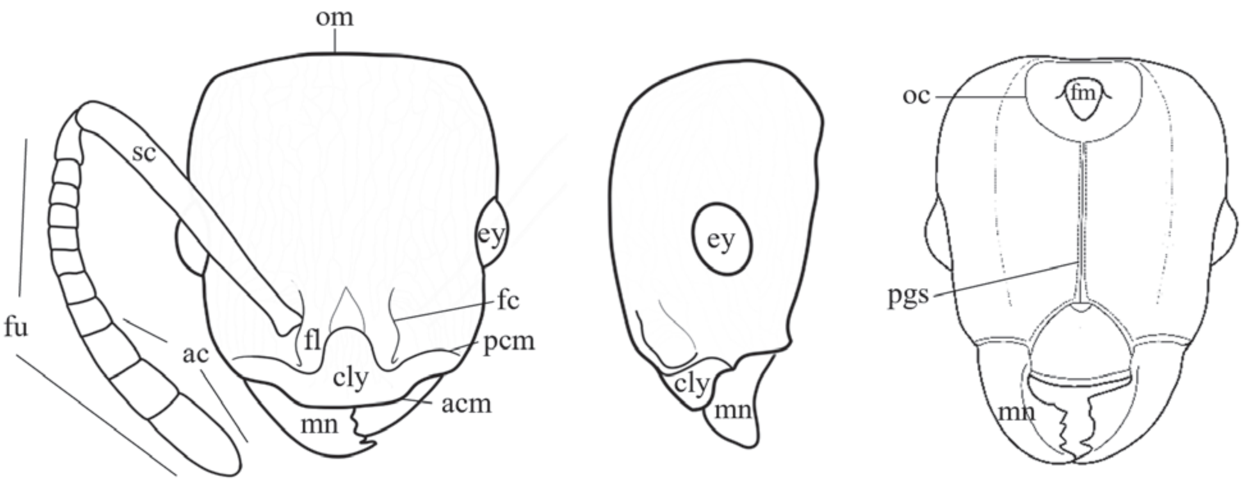

Figure 1. *Nesomyrmex* worker head morphology. Abbreviations: ac (antenal club), acm (anterior clypeal margin), cly (clypeus), ey (eye), fc (frontal carina), fl (frontal lobe), fm (*foramen magnun*), fu (funiculus), gn (gena), mn (mandible), oc (occipital carina), om (occipital margin), pcm (posterior clypeal margin), pgs (postgenal suture), sc (scape).

integrated camera (DFC450) and LAS v. 4.6 software. Images were edited and organized (Adobe Photoshop v. 25.3.1) to improve image characteristics such as brightness and contrast. The species distribution maps were made using the information obtained from the different labels of the specimens; this information was processed with the Quantum Gis v. 3.36 software (QGIS 2024).

Repositories

We examined specimens deposited in the following collections. Those marked with an asterisk (*) are not registered in Evenhuis (2024).

CASC	California Academy of Sciences, USA
CBUMAG	Centro de Colecciones Biológicas de la Universidad del Magdalena, Santa Marta, Magdalena, Colombia
CTNI	Colección Taxonómica Nacional de Insectos Luis María Murillo, Corporación Colombiana de Investigación Agropecuaria-AGROSAVIA, Tibaitatá, Mosquera, Cundinamarca, Colombia. CELM in Evenhuis (2024)
IAvH	Colección de Entomología del Instituto de Investigaciones de recursos biológicos Alexander von Humboldt, Villa de Leyva, Boyacá, Colombia
ICN	Colección de Entomología del Instituto de Ciencias Naturales, Universidad Nacional de Colombia, Bogotá D. C., Colombia
MEFLG	Museo Entomológico Francisco Luis Gallego, Universidad Nacional de Colombia, Medellín. Medellín, Antioquia, Colombia
MHNG	Muséum d'Histoire Naturelle, Geneva, Switzerland
MPUJ	Colección de Artrópodos del Museo de Historia Natural de la Pontificia Universidad Javeriana. Bogotá D. C., Colombia
MSNG	Museo di Storia Naturale Giacomo Doria, Genova, Italy

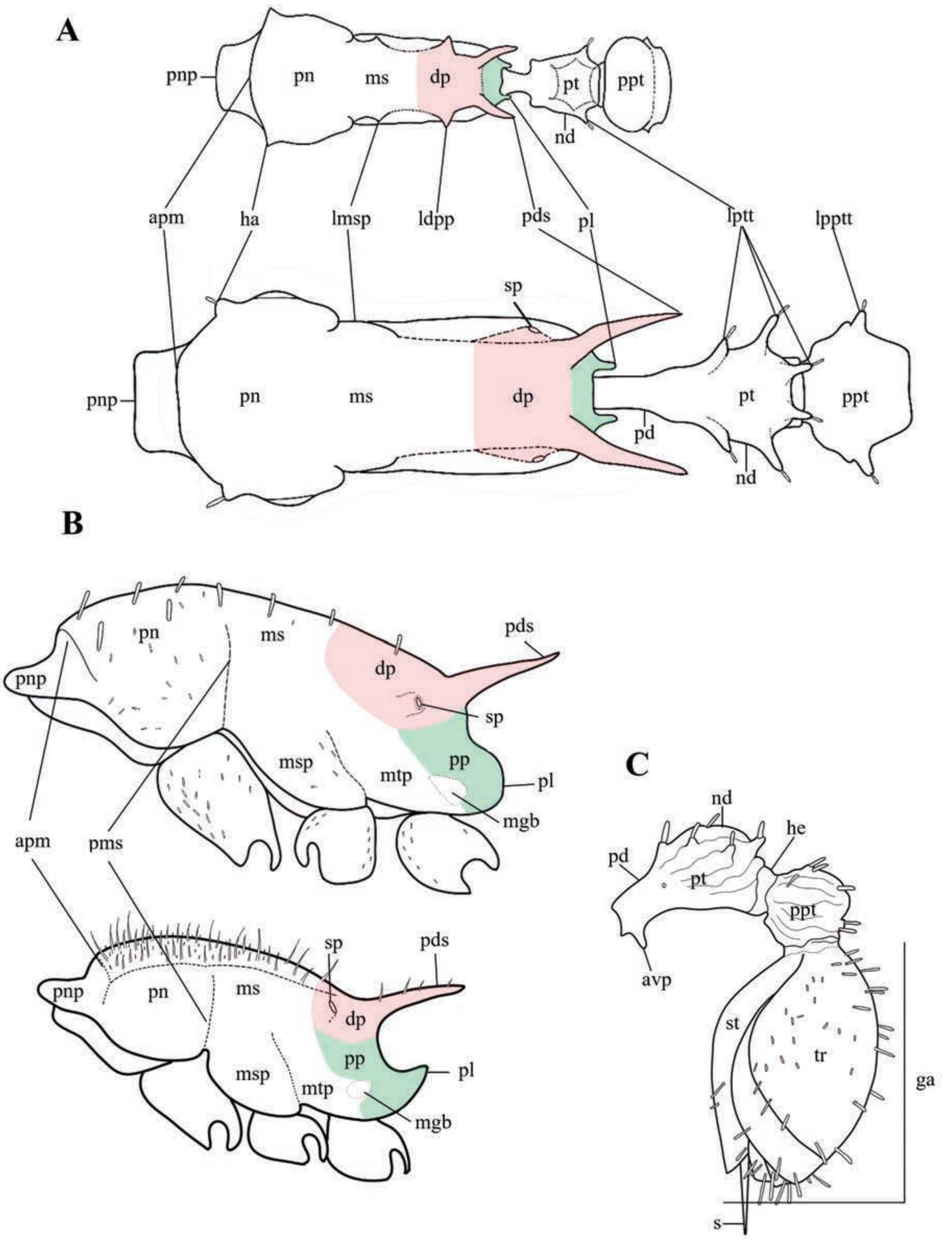

Figure 2. *Nesomyrmex* worker mesosoma and metasoma morphology **A** body in dorsal view **B** mesosoma in lateral view **C** metasoma in lateral view. The red area delimits the dorsopropodeum, while the green area delimits the posteropropodeum. Abbreviations: amp (anterior pronotal margin), avp (anteroventral process), dp (dorsopropodeum), ga (gaster), ha (humeral angles), he (helcium), ldpp (lateral dorsopropodeal process), lmsp (lateral mesonotal process), lpptt (lateral postpetiolar tubercle), lptt (lateral petiolar tubercle), mgb (metapleural gland bulla), ms (mesonotum), msp (mesopleura), mtp (metapleura), nd (node of petiole), pd (peduncle of petiole), pds (propodeal spine), pl (propodeal lobe), pms (promesontal suture), pn (pronotum), pnp (pronotal projection), pp (posteropropodeum), ppt (postpetiole), pt (petiole), sp (spiracle), st (sternite) tr (tergite).

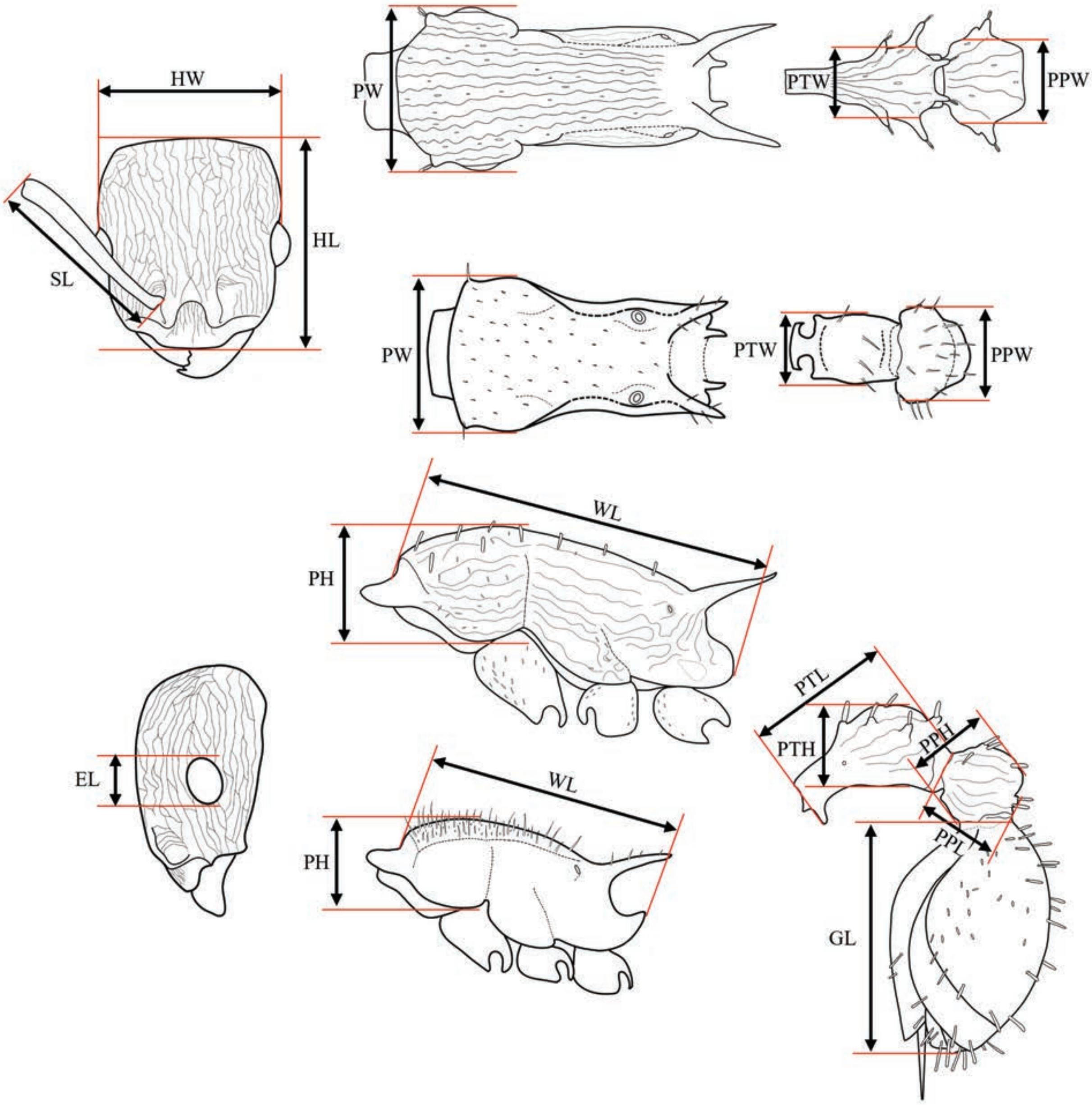

Figure 3. Measurements recorded in the habitus of *Nesomyrmex* worker. Definitions of the acronyms are described in Materials and methods.

MUSENUV	Museo de Entomología de la Universidad del Valle, Valle del Cauca, Santiago de Cali, Colombia
MZSP	Museo de Zoologia da Universidade de São Paulo, São Paulo, Brazil
NHMW	Naturhistorisches Museum, Vienna, Austria
UCDC	R.M. Bohart Museum of Entomology, Davis, CA, USA
UNAB	Museo Entomológico Universidad Nacional de Colombia, Facultad de Ciencias Agrarias, Bogotá. D. C., Colombia

Results

Synoptic list of *Nesomyrmex* species from the tropical dry forest in Colombia

Nesomyrmex asper (Mayr, 1887)
= *Nesomyrmex antoniensis* (Forel, 1912), syn. nov.
Nesomyrmex echinatinodis (Forel, 1886)
Nesomyrmex iku sp. nov.
Nesomyrmex konina sp. nov.
Nesomyrmex pittieri (Forel, 1899)
Nesomyrmex pleuriticus (Kempf, 1959)
Nesomyrmex spininodis (Mayr, 1887)
Nesomyrmex vargasi Longino, 2006
Nesomyrmex xerophilus sp. nov.

Key to Colombian *Nesomyrmex* species based on workers

(adapted and modified from Kempf (1959), * species probably present in Colombia)

1 Antenna with 12 antennomeres **2**
– Antenna with 11 antennomeres **9**
2 Antennal scape in repose reaching or surpassing the occipital margin (SI > 82) (Fig. 4A). In dorsal view, humerus (ha) distinctly dentate (Fig. 5A). Mesosoma length (= WL) greater than or equal 1.4 mm **3**
– Antennal scape in repose failing to reach the occipital margin (SI < 81) (Fig. 4B). In dorsal view, humerus (ha) distinctly angled (Fig. 5B), Slightly angled (Fig. 5C) or rounded (Fig. 5D). Mesosoma length (= WL) less than or equal 1.3 mm **4**

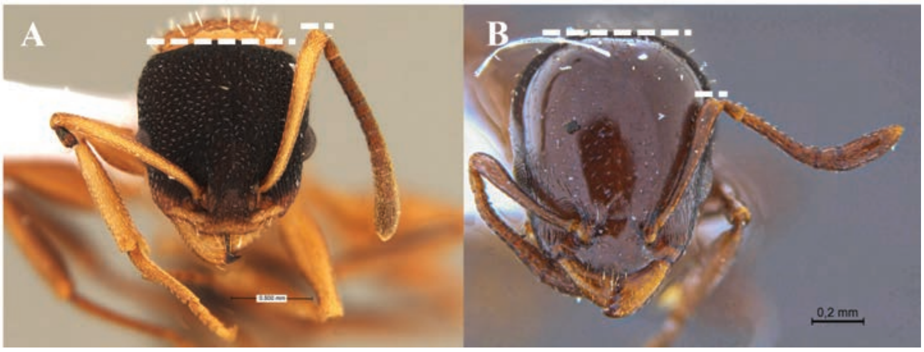

Figure 4. Relative length of antennal scapes **A** scape in repose reaching or surpassing the occipital margin **B** scape in repose failing to reach the occipital margin.

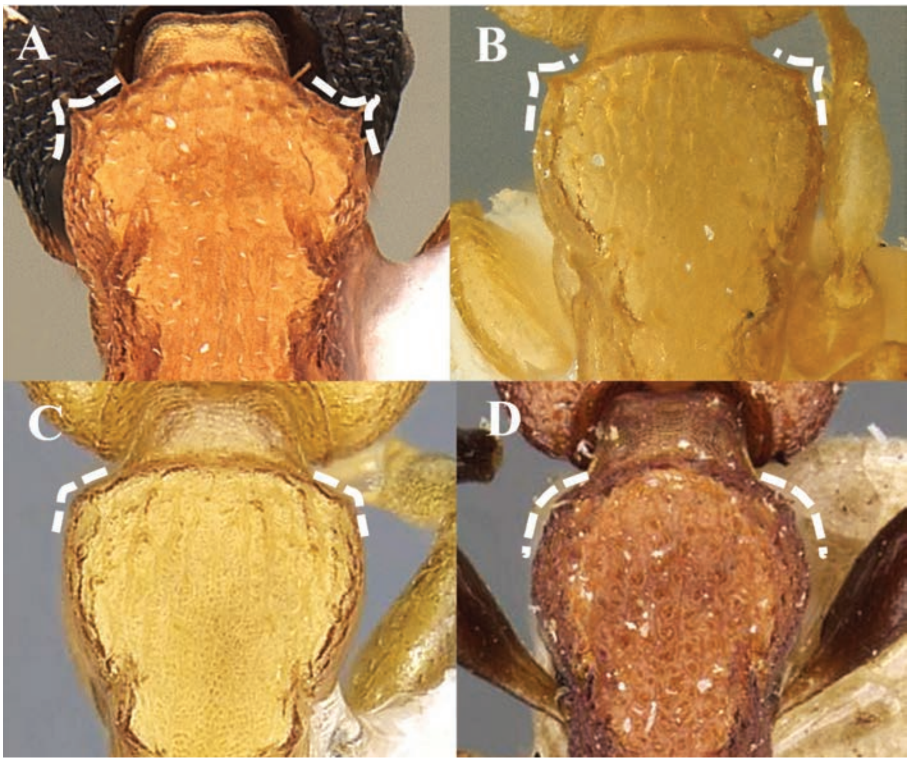

Figure 5. Humerus shape (dorsal view) **A** dentate **B** strongly angled **C** slightly angled **D** rounded.

3 In dorsal view, lateral mesonotum process (lmsp) dentate (Fig. 6A). Lateral margins of the mesosoma constricted anteriorly and posteriorly to the mesonotal projection .... ***N. pulcher* (Emery)***

– In dorsal view, mesonotum lacking lateral projections, sometimes rounded or slightly rounded margins (Fig. 6B). Lateral margins of mesonotum weakly constricted anteriorly and posteriorly to mesonotum .... ***N. anduzei* (Weber)**

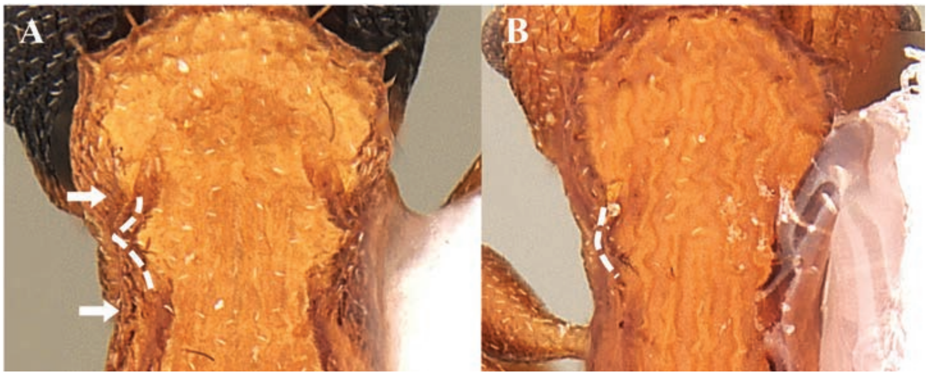

Figure 6. Mesonotal lateral projection **A** triangular lobe-shaped **B** rounded or slightly rounded lobe-shaped. White arrows indicate anterior and posterior constrictions to the lateral projection of the mesonotum.

4 Dorsal surface of the head longitudinally costate (Fig. 7A) or rugose (Fig. 7B).. **5**

– Dorsal surface of the head foveate (Fig. 7C), or smooth and shiny (Fig. 7D).. **7**

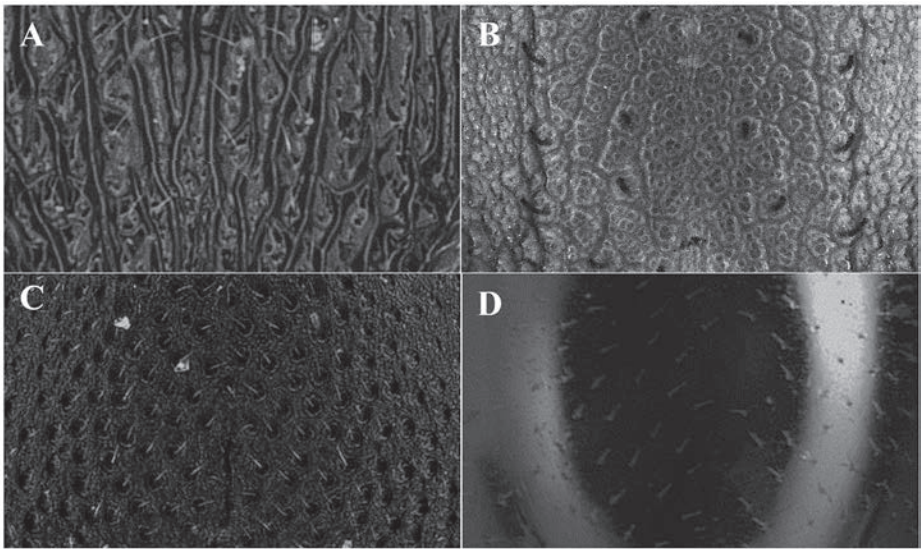

Figure 7. Types of sculpture **A** costate **B** rugose **C** foveate **D** smooth.

5 Frontal lobe projected laterally (widest posterior to torulus) (Fig. 8A), covering the antennal insertions. In dorsal view, lateral projection of the mesonotum dentate (lmsp) (Fig. 9A). Lateral dorsopropodeal processes (ldpp) long, covering propodeal spiracle in dorsal view (Fig. 9A). Dorsal surface of mesosoma and postpetiole with longitudinal costae strongly elevated..***N. xerophilus* sp. nov.**

– Frontal lobes without lateral projection, antennal insertions partially exposed (Fig. 8B). In dorsal view, lateral projection of the mesonotum blunt (lmsp) (Fig. 9B). Lateral dorsopropodeal processes (ldpp) short, not covering spiracle in dorsal view (Fig. 9B). Dorsal surface of mesosoma and postpetiole with weakly elevated longitudinal roughness..........................**6**

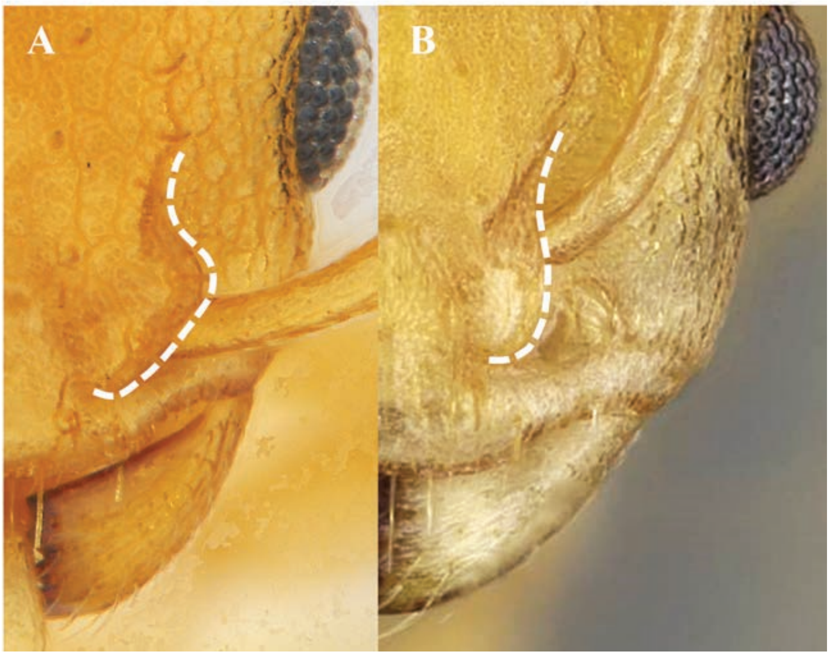

Figure 8. Frontal lobes **A** with lateral expansion **B** without lateral projection.

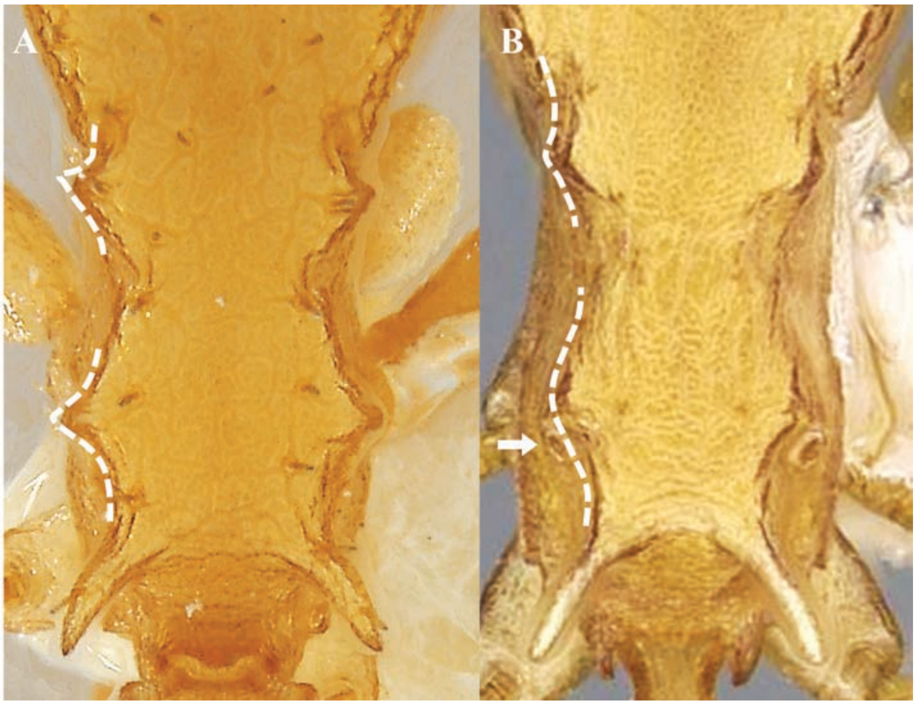

Figure 9. Mesosomal dorsum, in dorsal view **A** lateral projection of the mesonotum dentate, dorsopropodeum projected laterally over the spiracle **B** lateral projection of the mesonotum angled, dorsopropodeum without lateral projection over the spiracle. White arrows indicate the propodeal spiracle.

6 In lateral view, mesosomal profile straight (Fig. 10A). In dorsal view, humerus (ha) strongly angled (Fig. 5B)...................................... ***N. iku* sp. nov.**

– In lateral view, mesosomal profile convex (Fig. 10B). In dorsal view, humerus (ha) slightly angulated (Fig. 5C) ....***N. itinerans* (Kempf)**

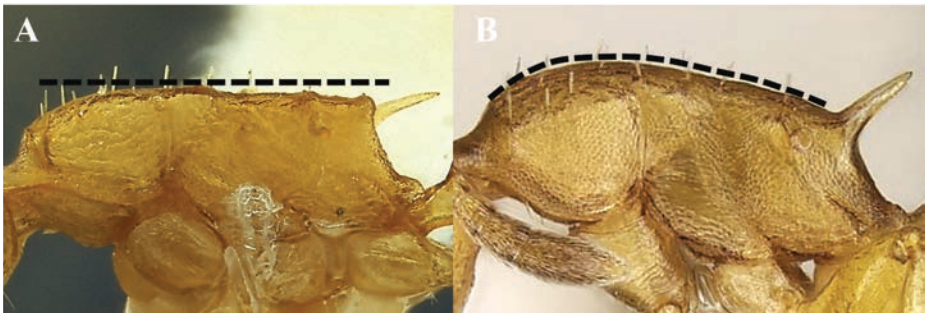

Figure 10. Mesosomal dorsal profile **A** straight **B** convex.

7 Dorsal surface of the head smooth and shiny (Fig. 7D). Head length > 1.1 ×mesosoma length. Anterior margin of pronotum without carina (Fig. 11A). Postpetiolar node smooth and shiny..... ***N. tonsuratus* (Kempf)**

– Dorsal surface of the head foveate, or weakly foveated (Fig. 7C). Head length smaller than mesosoma length. Anterior margin of pronotum carinate (Fig. 11B). Postpetiolar node sculpted and matte..............................**8**

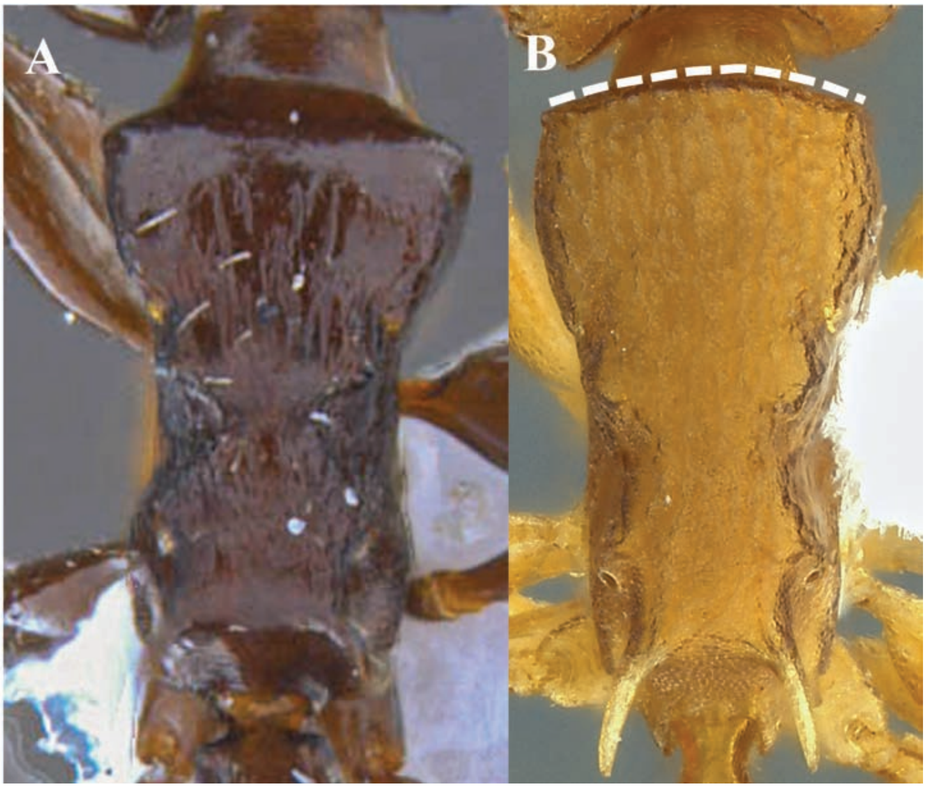

Figure 11. Anterior margin of pronotum **A** without carina **B** carinate.

8 Dorsal surface of the head foveate. Antennal scape curved at its base. Propodeal spines as long as the distance between their apices .... ***N. pittieri* (Forel)**

– Dorsal surface of the head weakly foveated. Antennal scape straight at its base. Propodeal spines short and subconical, much shorter than the distance between their apices................................***N. brasiliensis* (Kempf)***

9 Antennal scape in repose reaching or surpassing the occipital margin (S > 82) (Fig. 4A). Propodeal lobe (pl) angulate, apex blunt (Fig. 12A)...........**10**

– Antennal scape barely reaching the occipital margin by a distance equal to its greatest width (SI < 81) (Fig. 4B). Propodeal lobe (pl) short and uniformly rounded (Fig. 12B)..**13**

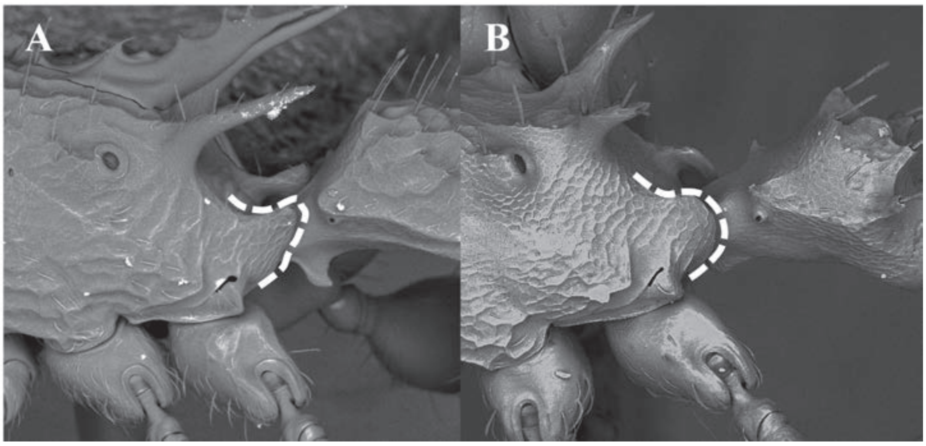

Figure 12. Propodeal lobe shape **A** angulate, apex blunt **B** short, uniformly rounded.

10 Inner area of the dorsal surface of the mandibles finely imbricate and subopaque (Fig. 13A). Sides of the mesosoma roughly sculptured ....***N. asper* (Mayr)**

– Inner area of the dorsal surface of the mandible smooth and shiny (Fig. 13B). Sides of the mesosoma smooth, with little or no roughness **11**

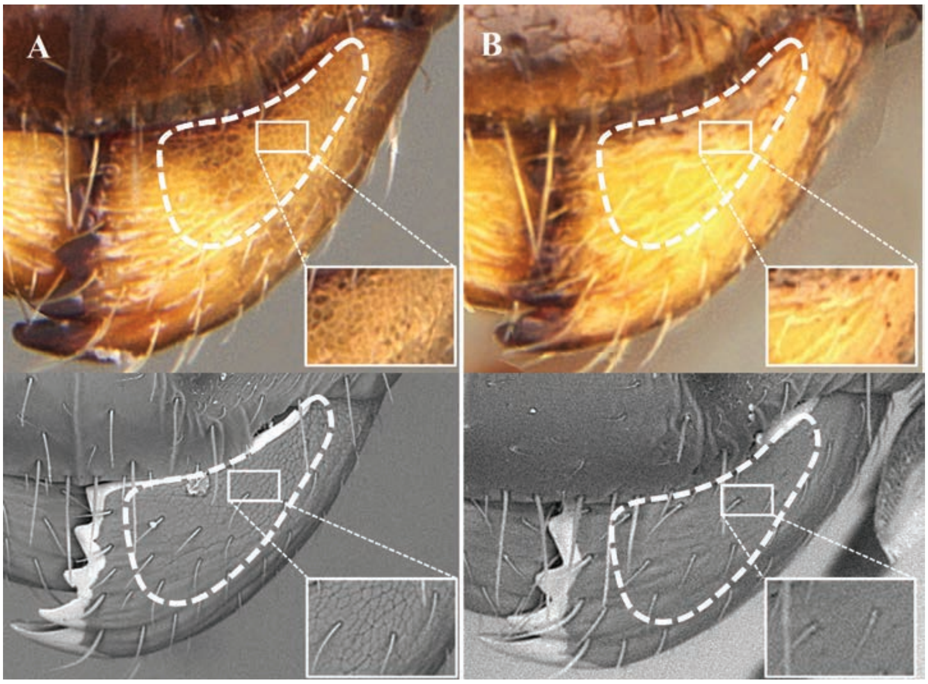

Figure 13. Medial area of the dorsal surface of the mandible, photomicrography and electron micrography **A** reticulated and opaque **B** smooth and shiny. White box is a close-up to observe the detail of the sculpture in question.

11 Dorsal surface of the head rugose (Fig. 7B), matte sculpture. Legs lacking erect hairs (Fig. 14A)..***N. brimodus* (Bolton)***

– Dorsal surface of the head smooth and shiny (Fig. 7D). Legs with long erect hairs (Fig. 14B)...**12**

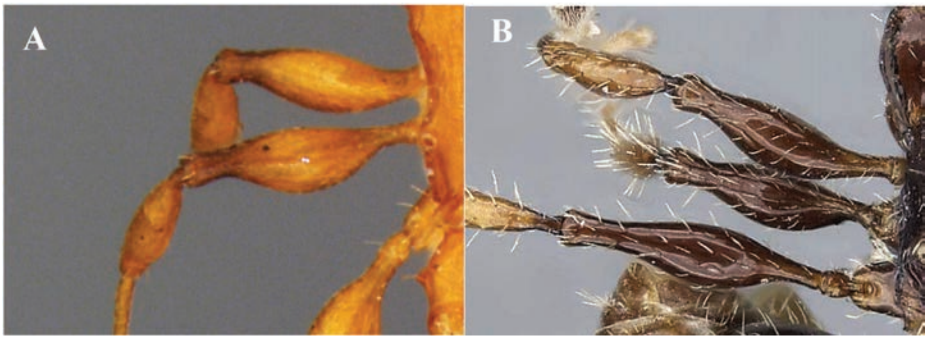

Figure 14. Leg pilosity **A** without presence of pilosity **B** with long erect or suberect hairs.

12 Anterior margin of pronotum straight (Fig. 15A). Sculpture of mesosoma dorsum opaque and strongly marked, with reticulate microsculpture. Sides of mesosoma with variable sculpture, but never longitudinally striate..***N. pleuriticus*** **(Kempf)**

– Anterior margin of pronotum convex (Fig. 15B). Sculpture of dorsum of mesosoma partially smooth and shiny, with weakly marked longitudinal striae. Sides of mesosoma with longitudinal striations .... ***N. vargasi*** **Longino**

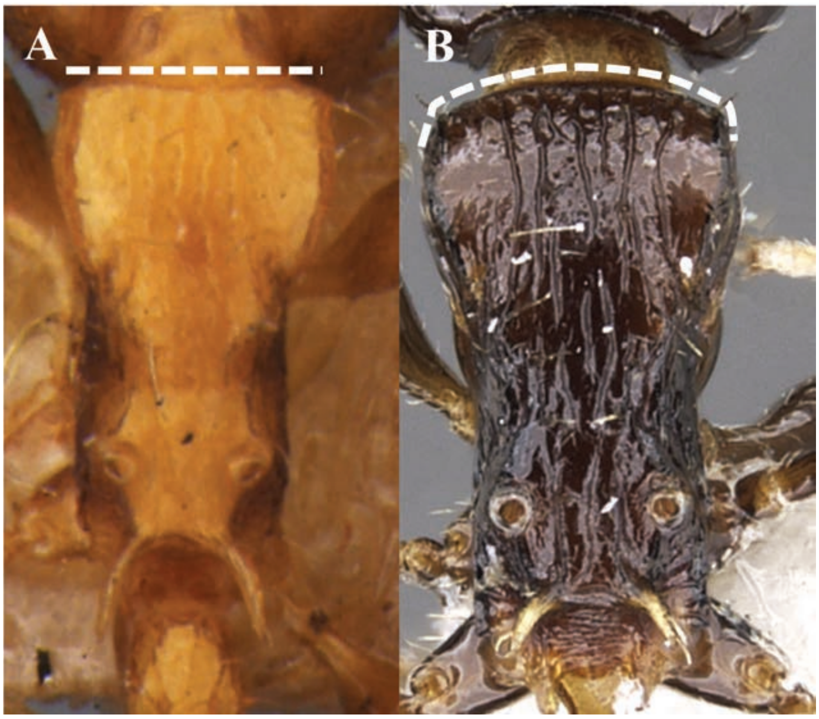

Figure 15. Anterior margin of pronotum **A** straight **B** convex.

13 Dorsal surface of the head smooth and shiny. Mesosoma with weakly marked longitudinal striation. First tergite gastral without sculpture, completely smooth and shining (Fig. 16A). Coloration uniformly pale yellow ... .***N. konina*** **sp. nov.**

– Dorsal surface of the head with sculpture, partly or completely rugose. Mesosoma with marked longitudinal striation. First gastral tergite with variable sculpture (Fig. 16B). Testaceous or yellowish brown to dark brown coloration...**14**

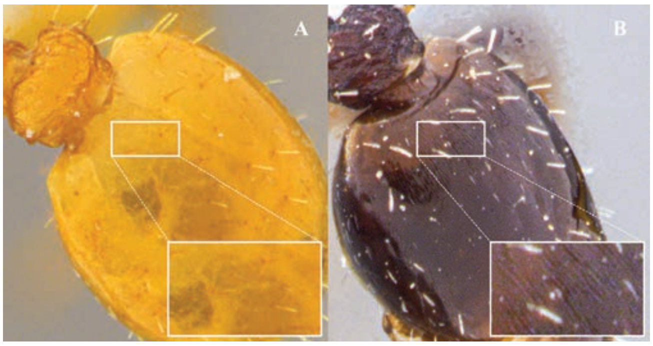

Figure 16. Sculpting of the first gastral tergite **A** smooth **B** sculpted. The inset square corresponds to an enlargement of the dorsal surface of the first gastral tergum.

14 In full-face view, front and vertex opaque, finely reticule-punctate and longitudinally rugose, without shining areas (Fig. 17A). Coloration concolor, testaceous or yellowish-brown. First gastric tergite usually more sharply aciculate-striate on the anterior half gastric tergite....***N. spininodis* (Mayr)**

– In full-face view, front and vertex partly or completely smooth and shiny (Fig. 17B). Color always darker, at least head and gaster brown to black. First gastric tergite very lightly sculptured ....***N. echinatiodis* (Forel)**

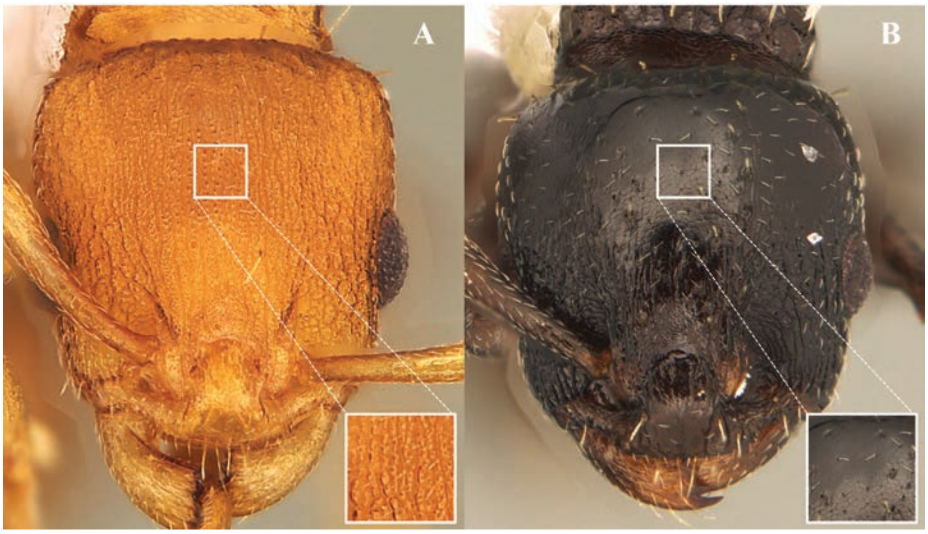

Figure 17. Sculpting of front and vertex (full-face view) **A** finely reticulate-punctate and longitudinally rugose, without shining areas **B** partly or completely smooth and shining. White box is a close-up to observe the detail of the sculpture in question.

Species accounts

***Nesomyrmex asper* (Mayr, 1887)**

Figs 18–20, 29

Leptothorax asper Mayr, 1887: 618. Syntype series (worker, queen, male): Brazil, Santa Catarina. [NHMW] (AntWeb image examined, CASENT0901801).

Combination in *Leptothorax* (*Goniothorax*): Emery 1896: 59.

Leptothorax (*Goniothorax*) *asper* var. *rufa* Emery, 1896: 61. Syntype series (queen, worker): Brazil, Pará. [MSNG]. (AntWeb image examined, CASENT0904722). Synonymy by Kempf 1959: 414.

Leptothorax (*Goniothorax*) *tristani* Emery, 1896: 61. Syntype series (queen, worker): Costa Rica. [MSNG]. (AntWeb image examined, CASENT0904724). Synonymy by Longino 2006: 136.

Leptothorax asper var. *antoniensis* Forel, 1912: 18. Syntype series. (worker): Colombia, Sierra Nevada de Santa Marta, San Antonio. [MHNG]. (AntWeb image examined, CASENT0909002). syn. nov.

Leptothorax asper var. *sulfurea* Forel, 1912: 18. Syntype series (worker): Brazil. [MHNG]. (AntWeb image examined, CASENT0909003). Synonymy by Kempf (1959: 414).

Combination in *Leptothorax* (*Nesomyrmex*): Kempf 1959: 414.

Combination in *Nesomyrmex*: Bolton 2003: 272.

Figure 18. Variation of lateral petiole tubercles in *Nesomyrmex asper*. White arrows indicate the tubercles.

Worker measurements. (*n* = 8) HL 0.86–1.08, HW 0.78–0.99, SL 0.68–0.84, ML 0.41–0.53, EL 0.19–0.24, PW 0.51–0.66, PTW 0.21–0.31, PPW 0.31–0.44, WL 1.05–1.38, PH 0.29–0.34, PTL 0.37–0.46, PTH 0.23–0.29, PPL 0.24–0.34, PPH 0.26–0.32, GL 0.88–1.01. CI 90–92, SI 84–87.

Geographic range. Argentina, Bolivia, Colombia, Ecuador, French Guaina, Nicaragua, Panama, Paraguay, Trinidad and Tobago, Venezuela

Examined material. Colombia • 1 worker; Atlántico, Usicurí, Vda. Luriza, CIALU; 10.75198°N, 75,03075°W; 155 m a.s.l.; 28–30 Mar. 2023; J. Camargo, H. Sierra, S. De la Hoz legs.; Winkler; CBUMAG:ENT:54657 • 1 worker; Bolívar, Turbaco, Finca el Huerto; 10.371944°N, 75.349667°W; 102 m a.s.l.; 05 Jul. 2015; A. Sagoval, C. Cantor legs.; secondary forest; ICN 106553. • 1 worker; Cesar, La Jagua de Ibirico; 9.561111°N, 73.336389°W; 150 m a.s.l.; 2007; F. Fernández leg.; pitfall; ICN 019802. • 1 worker; Huila, Aipe, Cuenca Río Aipe,

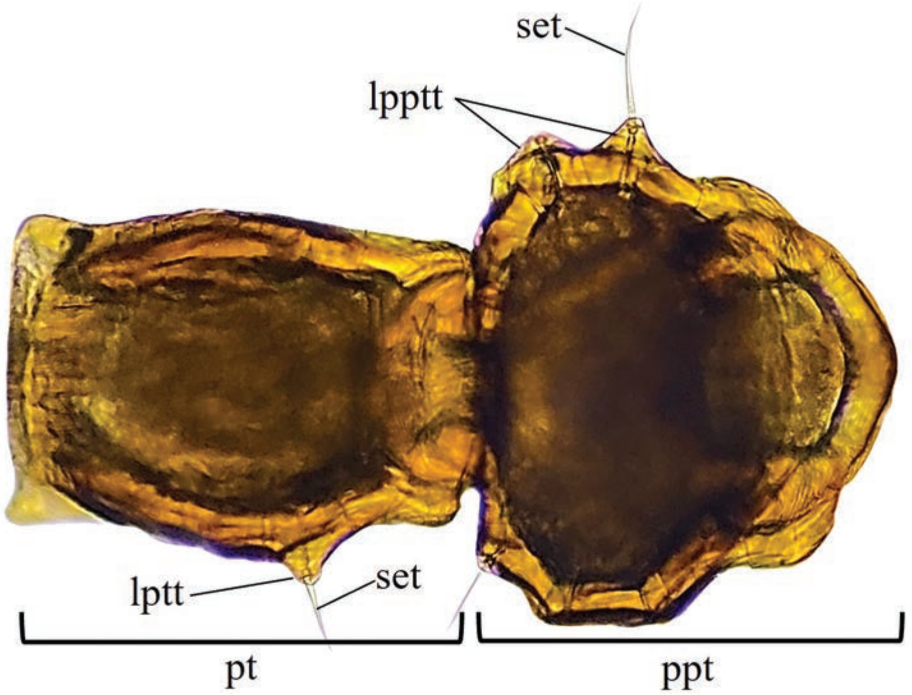

Figure 19. Lateral petiole and postpetiole tubercles (Setigerous tubercles). Abbreviations: lpptt (lateral postpetiolar tubercles), lptt (lateral petiolar tubercles), pt (petiole), ppt (postpetiole), set (seta).

Vda. San Isidro; 3.3453561°N, 75.3057781°W; 841 m a.s.l.; 25 Nov. 2017; L. Arcila leg.; Winkler; IAvH. • 1 worker; Valle del Cauca, Dagua, Cuenca Río Dagua, Vda. Limonar; 3.6238689°N, 75.6945069°W; 1071 m a.s.l.; 17 Aug. 2021; L. Arcila leg.; Pitfall; IAvH. • 2 workers; Cauca, Santander de Quilichao, Las Chatas; 3.1096°N, 76.5265°W; 909 m a.s.l.; 17 Aug. 2021; M. A. Bautista-Giraldo; I. Armbrecht legs.; meadow; CBUMAG:ENT:40121, CBUMAG:ENT:40122.

Natural history. Some workers were collected foraging during the day on vegetation in TDF fragments in the Valle del Cauca. Additionally, one worker was collected foraging on the grassland soil using pitfall traps.

Comments. This species is recognized by the set of the following characters: 11 antennomeres, clypeus sculpture ranges from smooth and shiny to longitudinally costate or reticulate, inner area of dorsal surface of mandibles finely reticulate and opaque, propodeal lobe angulate, apex blunt. *Nesomyrmex asper* presents intraspecific morphological variation in some traits throughout its distribution in the Colombian TDF. The lateral tubercles of the petiole and postpetiole are variable characteristics, both in quantity and size, between populations of the species (Fig. 18). For example, workers from populations in the Valle del Cauca (western Colombia) have no lateral tubercles on the petiole and postpetiole (Fig. 18A) while in more northern populations such as those from La Guajira and Magdalena there are between one and three tubercles distributed asymmetrically on the sides of the petiole (Fig. 18D, E). Analysis of *N. asper* specimens across the Colombian TDF suggests that populations of this species are morphologically cohesive in terms of the diagnostic characteristics that define it, but traits such as lateral tubercles on the petiole/postpetiole show extensive phenotypic plasticity.

Our novel observations of variability in number and shape of lateral petiole and postpetiole tubercles in *N. asper* contrasts with the use of presence and

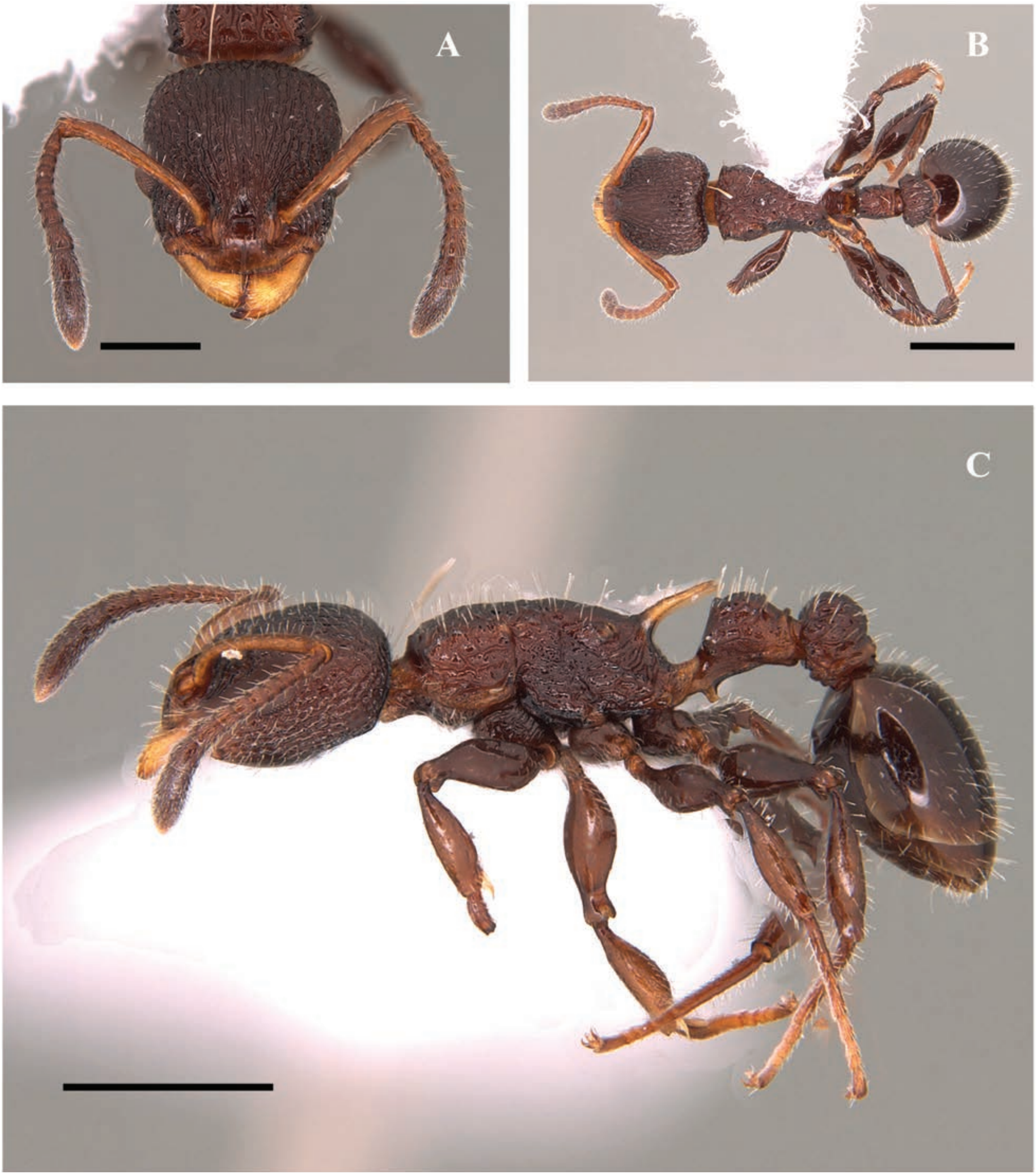

Figure 20. *Nesomyrmex asper* worker (ICN 106553) **A** full-face view **B** lateral view **C** dorsal view. Scale bars: 0.5 mm (**A**); 1.0 mm (**B**).

absence of tubercles as a diagnostic trait for some nomenclatural changes in *N. asper* (Kempf 1958, 1959, 1975; Longino 2006). Longino (2006) proposed *Nesomyrmex tristani* (Emery, 1896) as a junior synonym of *Nesomyrmex asper* considering the similarity of the lateral processes (i.e., lateral tubercles) of the petiole between the workers of both taxa. The same author used the differentiation of the lateral processes of the postpetiole (described there as "acuminate teeth": p. 136) observed between the workers of *Nesomyrmex asper* var. *antoniensis* (Forel, 1912) and *N. asper* s. str, to recognize *N. antoniensis* (Forel, 1912) as a valid species. Considering the intraspecific morphological variation in the lateral tubercles of *N. asper* workers, we compared this trait with the type worker of *N. antoniensis* (CASENT0909002), finding that the latter falls within the high intraspecific variability of *N. asper*. Likewise, the type specimens of both *N. antoniensis* (CASENT0909002) and *N. asper* (CASENT0901801), and the workers of *N. asper* present in Colombia and the Sierra Nevada de Santa Marta (type locality of *N. antoniensis*) were measured, finding that the type of *N. antoniensis* (HL 0.89, HW 0.83, SL 0.72, ML 0.43) matches the morphometric range of *N. asper* (HL 0.86–1.08, HW 0.78–0.99, SL 0.68–0.84, ML 0.41–0.53). Based on the evidence, we found that the morphological variation between *N. antoniensis* and *N. asper* is not distinct, with the form referred to as *N. antoniensis* falling within the variability observed in *N. asper*. Therefore, we propose *N. antoniensis* as a junior synonym of *Nesomyrmex asper*. The highly variable number and shape of tubercles on lateral petiole and postpetiole in *N. asper* should not be used to separate taxonomic units in these species groups. Interestingly, the lateral processes of the petiole and postpetiolar node described as "acuminate teeth" by Longino (2006: 136) are setigerous tubercles (Fig. 19; also see Kempf 1959) and their variation in shape is due to projection and orientation relative to the body.

***Nesomyrmex echinatinodis* (Forel, 1886)**

Figs 21, 29

Leptothorax echinatinodis Forel, 1886: 48. Holotype (worker): Brazil, Rio de Janeiro. [NHMW] (AntWeb image examined, CASENT0909004).
Combination in *Leptothorax* (*Goniothorax*): Emery 1896: 59.
Leptothorax (*Goniothorax*) *aculeatinodis* Emery, 1896: 60. Holotype (worker): Costa Rica, Jiménez. [MSNG]. (AntWeb image examined, CASENT090475). Synonymy by Kempf 1959: 425.
Leptothorax (*Goniothorax*) *pungentinodis* Emery, 1896: 2. Holotype (queen): Panama, Gulf of Darien. [MSNG]. (AntWeb image examined, CASENT0904726) Synonymy by Kempf 1959: 425.
Leptothorax echinatinodis r. *dalmasi* Forel, 1899: 55. Syntype (worker): Colombia, Sierra Nevada de Santa Marta, San Antonio [MHNG]. (AntWeb image examined, CASENT0909005). Synonymy by Kempf 1959: 425.
Combination in *Leptothorax* (*Caulomyrma*): Forel 1914: 233.
Leptothorax (*Goniothorax*) *echinatinodis* subsp. *schmidti* Menozzi, 1927: 275 Syntype series (male, queen, worker): Costa Rica, San José. [DEIB]. (AntWeb image examined, FOCOL0198-1). Synonymy by Kempf 1959: 426.
Leptothorax (*Goniothorax*) *echinatinodis* subsp. *cordincola* Wheeler, 1942: 205. Syntype (worker): Panama, Canal zone, Chivachiva Trail. [MCZC]. (AntWeb image examined, CASENT0912925). Synonymy by Kempf 1959: 426.
Combination in *Leptothorax* (*Nesomyrmex*): Smith 1950: 30.
Combination in *Nesomyrmex*: Bolton 2003: 272.

Worker measurements. (*n* = 15) HL 0.55–0.7, HW 0.49–0.65, SL 0.38–0.54, ML 0.28–0.35, EL 0.11–0.19, PW 0.30–0.45, PTW 0. 15–0.26, PPW 0.19–0.31, WL 0.63–0.91, PH 0.17–0.28, PTL 0. 20–0.34, PTH 0.16–0.25, PPL 0.19–0.35, PPH 0.17–0.25, GL 0.67–0.93. CI 89–92, SI 77–83.

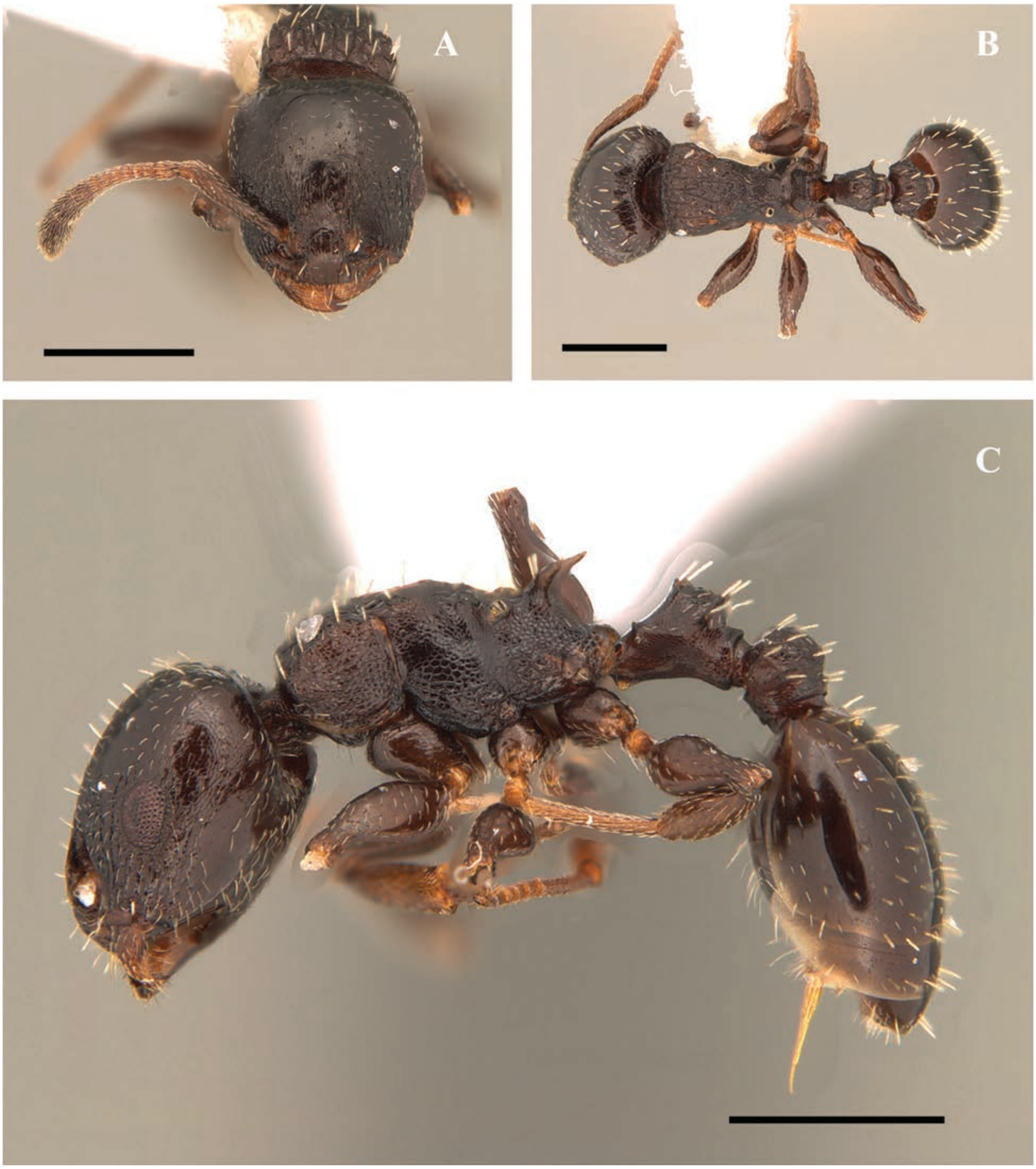

Figure 21. *Nesomyrmex echinatinodis* worker (MEFLG-NC 53153) **A** full-face view **B** lateral view **C** dorsal view. Scale bars: 0.5 mm.

Geographic range. Argentina, Brazil, Colombia, Costa Rica, Ecuador, French Guiana, Guatemala, Guyana, Honduras, Mexico, Nicaragua, Panama, Paraguay, Peru, Suriname, Venezuela

Examined material. COLOMBIA • 1 worker; Antioquia, Santa Fe de Antioquia, Vda. El Espinal, Estación Agraria Cotové, Universidad Nacional de Colombia Sede Medellín; 6.5613889°N, 75.83166667°W; 600 m a.s.l.; 06 Oct. 2000; E. Vergara, F. Serna legs.; manual coll; UNAB. • 1 worker; Antioquia, Santa Fé de Antioquia, Vda. El Espinal, Estación Agraria Cotové, Universidad Nacional de

Colombia Sede Medellín; 6.5358333°N, 75.82972222°W; 515 m a.s.l.; 02 Apr. 2020; B. Arredondo leg.; MEFLG-NC 53153. • 2 workers; Arauca, Tame, La Casirba; 6.360678°N, 71.894257°W; 675 m a.s.l.; 20 Mar. 2024; H. Sierra y S. De La Hoz legs.; Manual coll; CBUMAG:ENT:41658. • 1 worker; Arauca, Tame, La Casirba; 6.360678°N, 71.894257°W; 675 m a.s.l.; 19 -21 Mar. 2024; H. Sierra y S. De La Hoz legs.; Winkler; CBUMAG:ENT:41659. • 1 worker; Bolívar, San Jacinto, SFF los Colorados, La Yaya; 9.899947°N, 75.116645°W; 280 m a.s.l.; 06 -21 Apr. 2001; E. Deulefe leg.; Malaise trap; IAvH-E-251264. • 9 workers; Cundinamarca, Anapoima; 4.566113°N, 74.529935°W; 25 Mar. 1981; I. Zenner leg.; CTNI-NC 8245-1, 8245-2, 8245-3, 8245-4, 8245-5, 8245-6, 8245-7, 8245-8, 8245-9. • 1 worker; Cesar, Codazzi, Cgto. Casacará, Vda. Villa Matilde, RNSC Altahona-Castro; 9.793531°N, 73.190414°W; 403 m a.s.l.; 22 -24 Sep. 2023; H. Sierra, L. Ramos, R.J. Guerrero, S. De La Hoz legs.; Pitfall.; CBUMAG:ENT:41660. • 1 worker; La Guajira, Barranca, Cgto. San Pedro; 10.878276°N, 72.704619°W; 422 m a.s.l.; 10 -11 Sep. 2023; H. Sierra, S. De la Hoz, R.J. Guerrero, L. Ramos legs.; Manual coll.; CBUMAG:ENT:41662. • 1 worker; La Guajira, Barranca, Cgto. San Pedro; 10.876713°N, 72.704164°W; 404 m a.s.l.; 10 -11 Sep. 2023; H. Sierra, S. De la Hoz, R.J. Guerrero, L. Ramos legs.; Manual coll.; CBUMAG:ENT:41663. • 1 worker; La Guajira, Barranca, Cgto. San Pedro; 10.913786°N, 72.733971°W; 221 m a.s.l.; 09 -11 Sep. 2023; H. Sierra, L. Ramos, R. Guerrero, S. De La Hoz legs.; Winkler.; CBUMAG:ENT:41661. • 1 worker; Magdalena, Santa Marta, Parque Nacional Natural Tayrona, sector Zaino, sendero 9 Piedras; 11.2833333°N, 74.18333333°W; 600 m a.s.l.; C. Martínez leg.; manual coll.; ICN 106594. • 1 worker; Sucre, Ovejas; 9.53°N 75.23361111°W; 277 m. a.s.l.; 05 Apr. 2016; H. Cadena leg.; manual coll.; MEFLG-NC 48120. • 1 worker; Sucre, Ovejas; 9.5346111°N, 75.22086111°W; 277m. a.s.l.; 05 Apr. 2016; H. Cadena leg.; manual coll.; MEFLG-NC 48121. • 3 workers; Valle del Cauca, Santander de Quilichao, Las Chatas; 3.1096°N, 76.5265°W; 909 m a.s.l.; 17 Aug. 2021; M. A. Bautista-Giraldo; I. Armbrecht legs.; meadow; CBUMAG:ENT:40123, CBUMAG:ENT:40124, CBUMAG:ENT:40125.

Natural history. Workers were collected in dry forest fragments associated with mango (*Mangifera indica* L.) and Uvito (*Cordia dentata* Poir.) trees. Several workers were collected foraging on the ground on secondary TDF fragments in Arauca. A single record comes from the Malaise trap inside the mature TDF in SFF Los Colorados, to the northwest of Colombia. These ants are distributed from sea level up to 909m altitude.

Comments. *Nesomyrmex echinatinodis* populations throughout its distribution in Colombia (unpublished data), including those from TDF, show wide morphological variability as noted by Kempf (1959) in his discussion of this species. For example, the sculpture on the head and mesosoma may present intra and intercolonial variability, but all the ants studied here share the diagnostic traits proposed by Kempf (1959) for this species, i.e., 11 antennomeres, mesosoma at least partly dark-colored, head with frontal and vertex area partially smooth and shiny, clypeus smooth and shiny, propodeal lobe short and uniformly rounded, basal third of the first gastral tergum slightly striate, were determined as *N. echinatinodis* s. str.

Nesomyrmex echinatinodis, *N. spininodis*, and *N. konina* sp. nov. share several traits, thus form the *echinatinodis* group, which can be recognized by short scapes which in repose do not reach the occipital margin, laterally serrated mesonotum, long and curved propodeal spines, propodeal lobe short and uniformly rounded., petiolar and postpetiolar node with lateral tubercles, scapes and legs lacking erect hairs.

Nesomyrmex echinatinodis has been previously recorded for the departments of Cundinamarca and La Guajira (Kempf 1959), Huila (Fernández et al. 1996), Magdalena (Fernández and Serna 2019), and Valle del Cauca (Armbrecht et al. 2001, Chacón de Ulloa et al. 2012). *Nesomyrmex echinatinodis* is one of two species previously recorded for the tropical dry forest in Colombia (Valle del Cauca), extending its distribution to TDF fragments in the departments of Antioquia, Bolívar, Cundinamarca, and Sucre.

***Nesomyrmex iku* sp. nov.**

https://zoobank.org/44B9782F-3DBC-467D-A3F8-58CFB3F6A0E4
Figs 22, 29

Type material. *Holotype*. Colombia • 1 worker; Magdalena, Santa Marta, Sierra Nevada de Santa Marta; 10.816667°N, 73.650000°W; IAvH-E-75014 [IAvH]. ***Paratype*** (*n* = 1). 1 worker; same data as holotype; IAvH-E-75007 (CBUMAG).

Geographic range. Colombia.

Holotype worker measurements. HL 0.86, HW 0.73, SL 0.63, ML 0.34, EL 0.18, PW 0.48, PTW 0.25, PPW 0.28, WL 1.13, PH 0.34, PTL 0.47, PTH 0.30, PPL 0.3, PPH 0.29, GL 0.91. CI 85, SI 86.

Paratype worker measurements. (*n* = 1) HL 0.89, HW 0.74, SL 0.63, ML 0.35, EL 0.18, PW 0.48, PTW 0.26, PPW 0.30, WL 1.18, PH 0.35, PTL 0.48, PTH 0.30, PPL 0.32, PPH 0.29, GL 0.96. CI 85, SI 86.

Diagnosis. Mesosomal dorsum straight. Lateral margins of pronotum rounded, converging towards mesonotum. Lateral margins of mesonotum and dorsopropodeum with slightly angled lateral projections. Lateral dorsopropodeal processes short, not covering spiracle in dorsal view.

Description. Worker. In full-face view, head longer than wide (CI 84–85), lateral margins straight, slightly curved posterior to the eyes, continuing into occipital margin, weakly convex mesally; mandible triangular, masticatory margin of mandible with five teeth, separated from basal margin by fifth tooth; anterior clypeal margin convex, projecting above the mandibles; lateral eyes protruding, below half the length of the head, with 11 ommatidia at their greatest diameter; full-face view, frontal lobes not prominent and weakly rounded, partially covering antennal insertions; frontal carina extending to anterior margin of eye; antenna with 12 antennomeres, 3-segmented club; scape curved at base, relatively long (SI 85–86) but not reaching the occipital margin by a distance almost twice its apical width; pedicel longer than wide, almost as long as the next three antennomeres together.

Mesosoma. In lateral view, mesosomal profile straight; in dorsal view, pronotum wider than long, maximum width towards anterior margin, the latter slightly convex; humeral angles angulate; lateral margins of pronotum curved posteriorly; in lateral view, promesonotal suture marked; in dorsal view, lateral mesonotal and dorsopropodeal projections slightly angulated; propodeal spines divergent, longer than half the distance between their apices; propodeal spiracle small, circular, projecting posterodorsally; propodeal lobe short and uniformly rounded.

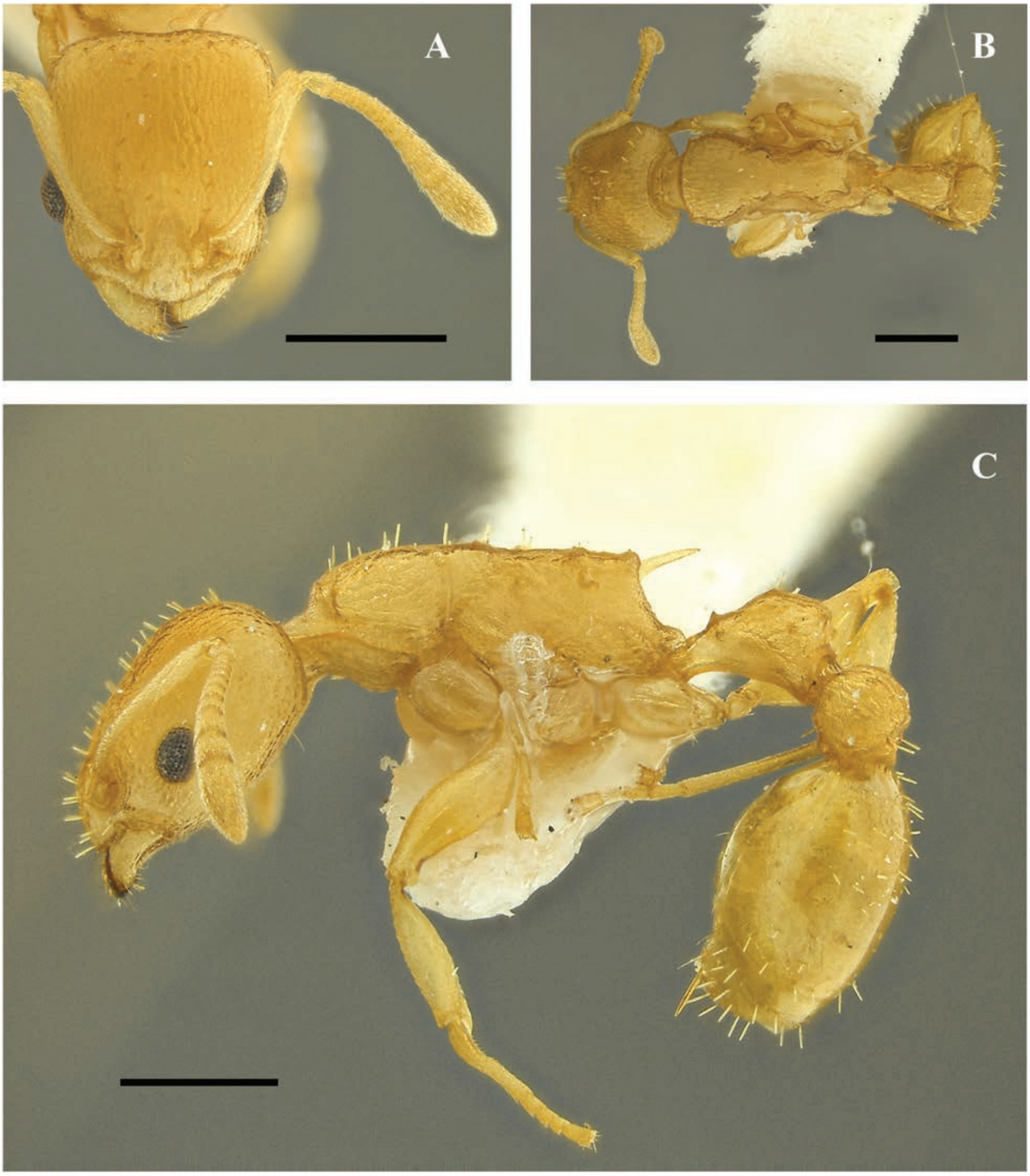

Figure 22. *Nesomyrmex iku* sp. nov. Holotype worker (IAvH-E-75014) **A** full-face view **B** lateral view **C** dorsal view. Scale bars: 0.5 mm.

Metasoma. In dorsal view, petiole trapezoidal with anterior portion narrower than posterior portion, lateral margins diverging posteriorly; in lateral view, peduncle and petiole node without apparent differentiation, forming a continuous outline, extending to dorsal face of petiole node; anterior face of petiole with anteromedial petiolar spine above petiolar spiracle; dorsal surface weakly rounded and short, continuing with a straight posterior face; anteroventral process of petiole pyramidal; in dorsal view, postpetiole oval, slightly wider than long, in lateral view postpetiole globose, taller than long.

Sculpture. Body generally opaque; body surface rugose-reticulate, excluding smooth, shiny gaster; clypeus with medial longitudinal costae; dorsal surface of mandible, scapes, and legs weakly punctate and shiny.

Pilosity and color. Dorsal surface of body with flattened erect hairs, mostly separated by a distance equal to or greater than their length, hairs as long as base of propodeal spines; in full-face view, scapes partly covered with short decumbent hairs, no erect hairs present; legs devoid of erect hairs, with sparse simple decumbent hairs restricted to apex of femur; gaster with sparse erect hairs, separated from each other by a distance twice their length. Body concolorous yellow.

Queen and male. Unknown.

Natural history. No related information.

Etymology. The name of this species refers to the Arhuaco people with ancestral lands close to the type locality of the species. The Arhuaco people self-identify as Iku, which translates as “people” in the Ika language (Tracy 1997). Iku (Arhuacos) - Guardians of life, defenders of the peaceful coexistence of men among themselves and with the forces of nature. This is a name in apposition and thus invariable.

Comments. This species is only known from the type material. *Nesomyrmex iku* sp. nov. is easily recognized by the shape of the straight mesosomal profile and by the lateral dorsopropodeal processes short, not covering spiracle in dorsal view. Morphologically, the closest species is *Nesomyrmex xerophilus* sp. nov., but they can be differentiated mainly by the lateral projection of the frontal lobes, the latter being wider posterior to the torulus, whereas *N. iku* does not have such a projection on the frontal lobes. On the other hand, in *N. xerophilus* the propodeal spiracles are not visible in dorsal view, since the lateral portion of the dorsopropodeal projects above them, whereas in *N. iku* the propodeal spiracles are visible in dorsal view.

Another species with similar morphology is *N. brasiliensis*. When comparing the type workers of *N. iku* (IAvH-E-75014, IAvH-E-75007) with the type ones of *N. brasiliensis* (MZSP87370, MZSP87374) we found that both species share a straight mesosomal profile, petioles and postpetioles lacking tubercles and body concolorous yellow. However, they differ in several features: The antennal flagellum of *N. iku* has 12 antennomeres, while *N. brasiliensis* has 11; additionally, the sculpture of the frontal area in N. brasiliensis is foveated in contrast to the frontal area striated in *N. iku*. Other distinguishing characteristics include the length of the propodeal spines, and the size and shape of the antennal scapes. A more extensive discussion on the similarity of *N. brasiliensis*, *N. iku*, and *N. xerophilus* will be possible when more material can be analyzed.

Nesomyrmex konina **sp. nov.**

https://zoobank.org/BD83D862-28F6-41A7-B3D2-AB18EBB2371E
Figs 23, 29

Type material. ***Holotype***. Colombia • 1 worker; Arauca, Tame, Parcela del Humboldt; 6.359289°N, 71.894258°W; 675 m a.s.l.; 19 Mar. 2024–21 Mar. 2024; H. Sierra, S. de La Hoz legs.; Winkler; CBUMAG:ENT:35951 [CBUMAG]. ***Paratypes*** (*n* = 4). Colombia • 3 workers; same data as holotype; CBUMAG:ENT:40035,

CBUMAG:ENT:40036, CBUMAG:ENT:41654 (CBUMAG). • 1 worker; Cundinamarca, Medina, Vda. Periquito; 4.512722°N, 73.426833°W; 1043 m a.s.l.; 07–21 Feb. 2019; MPUJ_ENT0064660 (MPUJ).

Holotype worker measurements. HL 0.66. HW 0.57, SL 0.44, ML 0.26, EL 0.16, PW 0.4, PTW 0.19, PPW 0.25, WL 0.76, PH 0.24, PTL 0.23, PTH 0.2, PPL 0.21, PPH 0.21, GL 0.66. CI 86, SI 77.

Paratype worker measurements. (*n* = 3). HL 0.66–0.67, HW 0.57–0.58, SL 0.44–0.46, ML 0.25–0.28, EL 0.15–016, PW 0.39–0.4, PTW 0.17–0.19, PPW 0.24– 0.25, WL 0.75–0.77, PH 0.21–0.26, PTL 0.21–0.24, PTH 0.19–0.2, PPL 0.18–0.21, PPH 0.20–0.21, GL 0.66–0.69. CI 86, SI 77–79.

Geographic range. Colombia.

Diagnosis. Dorsal surface of head and clypeus smooth and shiny. Clypeus without longitudinal median carina. Mesosome with slightly impressed longitudinal striation. Dorsal surface of mesosoma, petiole and postpetiole opaques. Legs and antennal scapes smooth and shiny. Basal third of first gastral tergum smooth and shiny.

Description. Worker. In full-face view, head slightly longer than wide (CI 86), slightly narrow anterior to the eyes, posterolateral corners rounded, occipital margin weakly convex to straight; mandible triangular, inner mandibular margin with five teeth; anterior margin of clypeus weakly convex, projecting over mandibles; lateral eyes, with 10 ommatidia at greatest diameter, Posterior margin barely reaching midline of head length; frontal lobes straight, slightly expanded laterally, antennal insertions slightly exposed; front carina extending to anterior margin of eye; antenna of 11 antennomeres; scapes relatively short (SI 77), not extending past occipital margin, curved from base to mid-length; pedicel longer than wide, and nearly as long as next two antennomeres together; antennal club of three antennomeres.

Mesosoma. In lateral view, mesosomal profile convex; in dorsal view, pronotum broader than long, greater width medially, anterior margin of pronotum slightly convex, humeral angle slightly angulated; in lateral view, promesonotal suture present, absent dorsally; lateral mesonotal projection rounded; lateral dorsopropodeal processes long, covering propodeal spiracle in dorsal; propodeal spines sharped divergent, as long as half the distance between their apices; in lateral view, propodeal spines forming an acute angle; propodeal spiracle small, circular, projecting posterodorsally; propodeal lobe short and uniformly rounded.

Metasoma. In dorsal view, petiole subrectangular, anterior and posterior margins of petiole of equal width, lateral margins forming a rhombus, with their sides meeting towards the middle of their length; anterior and posterior margin of node with two tubercles of equal length located laterally; lateral margin of petiole node with a posterolateral tubercle; in lateral view, petiole trapezoidal, peduncle and petiole node without apparent differentiation, forming a continuous line, which extends to the dorsal face of the petiole node; anterior face of petiole with anteromedial petiolar spine on each side, above the petiole spiracle; dorsal face weakly rounded and short; anteroventral process of petiole developed, triangular in shape; in dorsal view, postpetiole hexagonal, twice as wide as long, with two lateral tubercles towards its middle length; in lateral view, postpetiole globose, taller than long.

Sculpture. Dorsal surface of head mostly smooth and shiny, with reticulated area restricted to anterior area of eyes, continuing into frontal lobes and malar area; dorsal surface of mandibles partly smooth and shiny, with slight striation

Figure 23. *Nesomyrmex konina* sp. nov. Holotype worker (CBUMAG:ENT:35951) **A** full-face view **B** lateral view **C** dorsal view. Scale bars: 0.2 mm (**A**); 0.5 mm (**B, C**).

restricted to inner margin; clypeus smooth and shiny; scapes smooth and shiny; dorsum of mesosoma rugose-reticulate; lateral surface of mesosoma finely reticulate; petiole and postpetiole dull and rough-reticulate; gaster smooth and shiny.

Pilosity and color. Dorsal surface of body, except head, with erect flattened hairs mostly separated by a distance equal to or greater than its length; hairs as long as base of propodeal spines; in full-face view, head capsule with simple, erect to suberect hairs; erect hairs restricted to vertex area; scapes covered with short decumbent hairs; propodeal spines with sparse erect hairs; legs with simple, appressed hairs, sparse and restricted to apex of femur; gaster with abundant erect hairs, separated by a distance equal to its length. Body yellowish brown, except for dark brown masticatory margin of mandible and antennomeres posterior to pedicel, varying from pale yellow to dark brown on antennal club.

Natural history. Several of the type workers were extracted from the leaf litter in a fragment of tropical dry forest that has been recovering for more than 20 years in eastern Colombia.

Queen and male. Unknown.

Etymology. The word *konina* means smooth and shiny in the Sikuani aboriginal language, the language of the indigenous population that has shared the habitat where this species lives. The word is used to refer to the smooth and shiny sculpture of the cephalic dorsum of the ants of this species. This is a name in apposition and thus invariable.

Comments. *Nesomyrmex konina* is included in the group of echinatinodis species due to its morphological similarity (see comments in *N. echinatinodis*). It is distinguished from the other species in the group by its coloration and the smooth, shiny sculpture of the first gastral tergite.

***Nesomyrmex pittieri* (Forel, 1899)**

Figs 24, 29

Leptothorax pittieri Forel, 1899: 56. Holotype (worker): Costa Rica. [MHNG] (AntWeb image examined, CASENT0908997).
Combination in *Leptothorax* (*Goniothorax*): Emery 1924: 250.
Combination in *Leptothorax* (*Nesomyrmex*): Kempf 1958: 93.
Combination in *Nesomyrmex*: Bolton 2003: 272.

Worker measurements. (*n* = 1) HL 0.81, HW 0.68, SL 0.53, ML 0.33, EL 0.21, PW 0.51, PTW 0.24, PPW 0.36, WL 0.98, PH 0.3, PTL 0.35, PTH 0.26, PPL 0.24, PPH 0.24, GL 0.78. CI 83, SI 78.

Geographic range. Colombia, Costa Rica, Guatemala, Honduras, Mexico, Nicaragua, Panama, Trinidad and Tobago.

Examined material. Colombia • 1 worker; Valle del Cauca, Jamundí, Vda. San Isidro, Colindres; 3.33931°N, 76.5413°W; 979 m a.s.l.; 30 Jul. 2021; M.A. Bautista-Giraldo, I. Armbrecht legs.; CBUMAG:ENT:41664.

Natural history. Species collected by manual sampling on vegetation in Parque Nacional Natural Tuparro.

Comments. This species is recognized by the following characters: wide and deep foveae on the dorsal surface of the head, antennal scapes curved at their base, and propodeal spines as long as the distance between their tips.

The only specimen examined shows variation in coloration with respect to specimens from other forest types in Colombia (unpublished data). Populations found in premontane forest show bicoloration, with variations between reddish brown to dark. The sculpture of the frontal area is consistent in all populations (Fig. 24).

Figure 24. *Nesomyrmex pittieri* worker (CBUMAG:ENT:41664) **A** full-face view **B** lateral view **C** dorsal view. Scale bars: 0.2 mm (**A**); 0.5 mm (**B, C**).

Nesomyrmex pleuriticus **(Kempf, 1959)**

Figs 25, 29

Leptothorax (*Nesomyrmex*) *pleuriticus* Kempf, 1959: 414. Syntype series (male, queen, worker): Guyana, Kartabo. [MCZC, MZSP]. (image examined, MZSP87353, MZSP87354).

Combination in *Nesomyrmex*: Bolton 2003: 272.

Figure 25. *Nesomyrmex pleuriticus* worker (IAvH-E-79866) **A** full-face view **B** lateral view **C** dorsal view. Scale bars: 0.2 mm.

Worker measurements. (*n* = 1) HL 0.61, HW 0.58, SL 0.50, ML 0.25, EL 0.15, PW 0.36, PTW 0.16, PPW 0.22, WL 0.77, PH 0.21, PTL 0.242, PTH 0.16, PPL 0.18, PPH 0.19, GL 0.64.

Geographic range. Bolivia, Brazil, Colombia, Costa Rica, Ecuador, French Guyana, Guatemala, Guyana, Honduras, Mexico, Panama, Surinam, Venezuela

Examined material. Colombia • 1 worker; Vichada, Cumaribo, Cgto. Santa Rita, Parque Nacional Natural el Tuparro; 5.331667°N, 67.890833°W; 135 m a.s.l.; 08 Feb. 2004–10 Feb. 2004; I. Quintero; E. González legs.; Winkler; IAvH-E-79866.

Natural history. Foragers were collected on vegetation.

Comments. This species can be distinguished from other ones by having a straight anterior margin of the pronotum, an opaque mesosoma with striate sculpture and imbricate microsculpture, a dorsum of the postpetiole with longitudinal striations, scapes and legs covered with long, erect hairs, and a smooth, shiny clypeus.

The previous records of *N. pleuriticus* for the tropical dry forest in Colombia are based on information recorded for the departments of Cauca (Chacón de Ulloa et al. 2014) and Valle del Cauca (Armbrecht et al. 2001, Chacón de Ulloa et al. 2012) but we were unable to analyze these specimens to confirm the taxonomic identity of these ants (see comments on *N. vargasi*).

Nesomyrmex spininodis **(Mayr, 1887)**

Figs 26, 29

Leptothorax spininodis Mayr, 1887: 617. Lectotype worker: Brazil, Rio de Janeiro or Chile, Valparaiso. [NHMW]. (AntWeb image examined, CASENT0919734).

Combination in *Leptothorax* (*Goniothorax*): Emery 1896: 59.

Leptothorax (*Goniothorax*) *umbratilis* Wheeler, 1921: 160. Syntype (queen, worker): Guyana, Bartica, Penal Settlement. [MCZC, MZSP]. (Image examined, MZSP78366). Synonymy by Kempf 1959: 427.

Leptothorax (*Goniothorax*) *genualia* Santschi, 1922: 252. Holotype (worker): Paraguay, Asuncion. [NHMB]. (AntWeb image examined, CASENT0913001). Synonymy by Kempf 1959: 427.

Combination in *Leptothorax* (*Nesomyrmex*): Kempf 1959: 427

Combination in *Nesomyrmex*: Bolton 2003: 272.

Worker measurements. (n = 1) HL 0.68, HW 0.62, SL 0.48, ML 0.29, EL 0.15, PW 0.44, PTW 0.21, PPW 0.28, WL 0.82, PH 0.25, PTL 0.32, PTH 0.22, PPL 0.22, PPH 0.22, GL 0.79, CI 91, SI 77.

Geographic range. Argentina, Bolivia, Brazil, Colombia, Costa Rica, Ecuador, French Guiana, Paraguay, Suriname, Venezuela.

Examined material. Colombia • 1 worker; Vichada, Cumaribo, Parque Nacional Natural Tuparro; 5.350278°N, 67.876667°W; 100 m a.s.l.; 12 Apr. 1995; J. Muñoz leg.; Manual coll.; IAvH-E-251254.

Natural history. Species collected by manual sampling on vegetation in Parque Nacional Natural Tuparro.

Comments. This species can be recognized by 11 antennomeres, uniformly testaceous or yellowish-brown coloration, dorsal surface of head finely reticulate-punctate and longitudinally rugose, without presence of shiny areas, and basal third of first gastral tergite generally aciculate-striate in its sculpture.

Kempf (1959) synonymized all previously described species and subspecies within the *echinatinodis* complex under the nominal species, except for *N. spininodis*. A potential revision of the *N. echinatinodis* complex could either result in the synonymization of certain species or the division of the complex into multiple forms. It is common to find *N. echinatinodis* exhibiting sculpture similar to that of *N. spininodis*, particularly in populations from Colombia different from those living in the TDF (Unpublished data). Additionally, coloration is highly variable within the *echinatinodis* complex. For this reason, using coloration as the primary criterion for distinguishing between different forms is not recommended. Thus, the separation of both species should not rely solely on coloration; instead, the sculpture of the frontal area of the head and the first gastral tergum should also be compared.

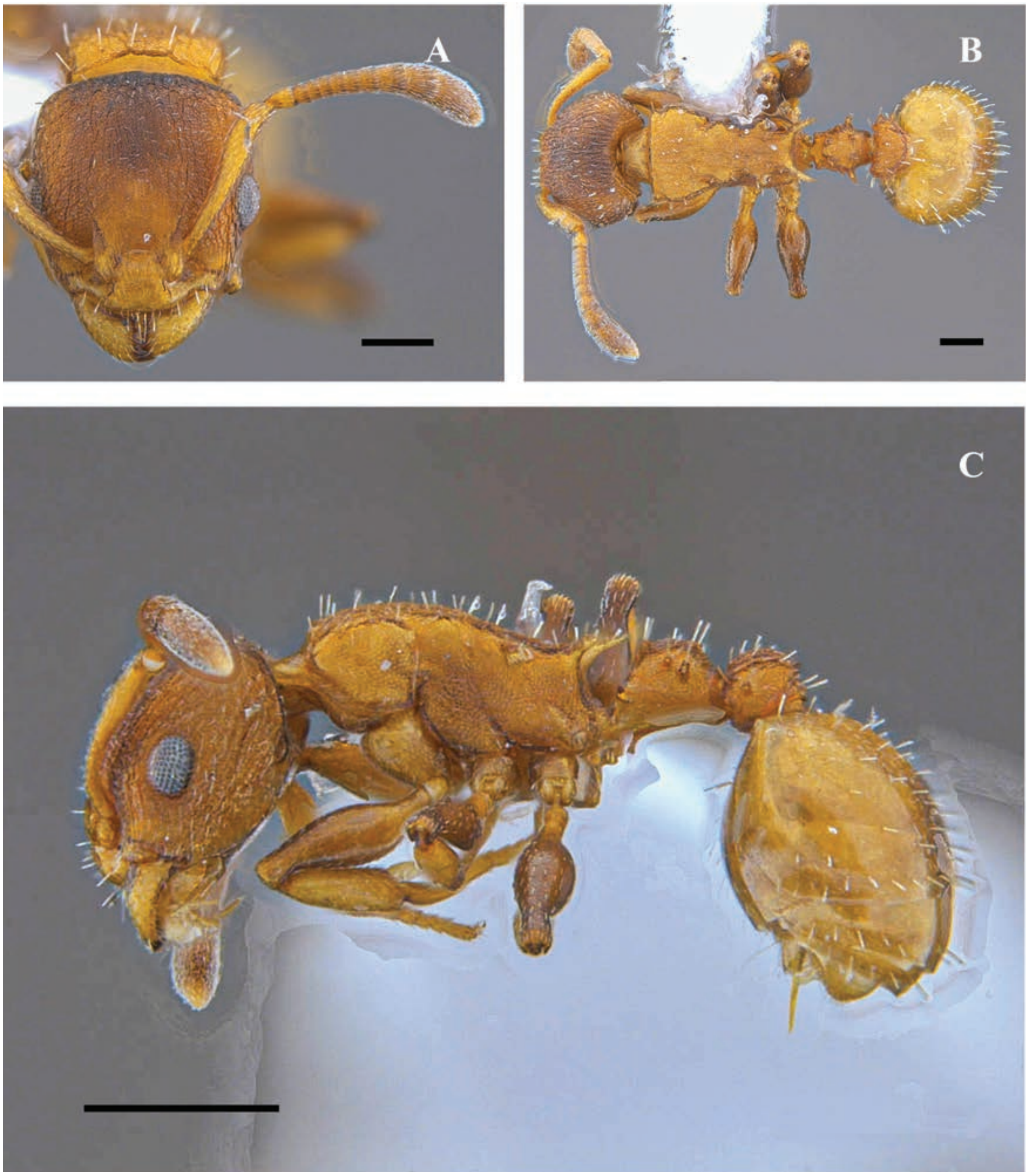

Figure 26. *Nesomyrmex spininodis* worker (IAvH-E-251254) **A** full-face view **B** lateral view **C** dorsal view. Scale bars: 0.2 mm (**A, B**); 0.5 mm (**C**).

Nesomyrmex vargasi Longino, 2006

Figs 27, 29

Nesomyrmex vargasi Longino, 2006: 136. Holotype worker: Costa Rica, Heredia Prov. [INBC]. (AntWeb image examined, JTLC000008517, JTLC000008518, LACMENT144699).

Worker measurements. (*n* = 5) HL 0.70–0.76, HW 0.64–0.68, SL 0.54–0.61, ML 0.28–0.33, EL 0.15–0.16, PW 0.42–0.46, PTW 0.14–0.18, PPW 0.25–0.27, WL 0.88–0.96, PH 0.24–0.30, PTL 0.33–0.38, PTH 0.19–0.21, PPL 0.18–21, PPH 0.21–0.23, GL 0.79–0.91. CI 89–91, SI 84–89.

Geographic range. Colombia, Costa Rica.

Examined material. Colombia • 1 worker; Bolivar, Zambrano; 9.744721°N, 74.82421°W; 1993–1994; Pitfall; IAvH-E-251258 • 1 worker; Cesar, Valledupar, Vda. Tierras nuevas; 10.241965°N, 73.761216°W; 881 m a.s.l.; 31 Mar. 2016; R. Achury leg.; Pitfall; CBUMAG:ENT:41665. • 1 worker; Vichada, Cumaribo, Cgto. Santa Rita, Parque Nacional Natural el Tuparro; 5.331667°N, 67.890833°W; 135 m a.s.l.; 08–10 Feb. 2004; I. Quintero; E. González legs.; Winkler; IAvH-E-79867.

Note. Longino (2006) presents the diagnosis for *N. vargasi* but does not fully describe the species. To address the possible variability of this taxon, we offer a redescription of the worker caste based on specimens from Colombia.

Diagnosis. Anterior margin of pronotum convex; mesosoma with marked longitudinal striations, space between the striae smooth and shiny; dorsum of postpetiole smooth and shiny; clypeus smooth and shiny; body surface smooth and shiny; antennal scape and legs with erect hairs (Longino, 2006).

Description. Worker. In full-face view, head subquadrate, slightly longer than wide (CI: 89), slightly narrowing behind the eyes; occipital margin slightly straight; occipital angles rounded; lateral margins slightly convex, converging posteriorly; anterior margin of clypeus rounded, projecting over mandibles; mandible triangular; inner margin with five teeth, separated from basal margin by fifth tooth; lateral eyes, with 12 ommatidia at greatest diameter, situated toward mid-length of head; frontal lobes slightly expanded, antennal insertions partly exposed; front carina extending to anterior margin of eye; antenna with 11 antennomeres; scapes of moderate size (SI: 84), at rest reaching occipital margin; pedicel longer than wide, as long as next two antennomeres; antennal club with three antennomeres.

Mesosoma. In lateral view, mesosomal profile convex; in dorsal view, pronotum wider than long, with its greatest width towards anterior margin, anterior margin of pronotum slightly convex; humeral angles slightly angulated; lateral margins of pronotum curved; in lateral view, pronotal suture marked; lateral dorsopropodeal processes (ldpp) long, covering propodeal spiracle in dorsal; propodeal spines of moderate size, slightly longer than the distance between their apices, in dorsal view propodeal spines diverge; in lateral view, propodeal spines curved; propodeal spiracle large, circular, projecting posterodorsally, diameter (0.071 mm) approximately equal to length of third and fourth antennomere; propodeal lobe angulate, apex blunt.

Metasoma. In dorsal view, petiole rectangular, anterior and posterior margins of petiole of equal length; lateral margins of petiole parallel, twice the size of anterior margin; lateral margins of petiole node with 1 posterolateral tubercle on each side; in lateral view, petiole trapezoidal, peduncle and petiole node without apparent differentiation forming a continuous outline, extending to dorsal surface of petiole node; anterior surface of petiole with anteromedial petiolar spine on each side, superior to petiole spiracle; dorsal surface weakly rounded and short; anteroventral process of petiole broad, triangular in shape; in dorsal view, postpetiole cup-shaped, twice as wide as long; in lateral view postpetiole globose, taller than long.

Sculpture. Dorsal surface of head mostly smooth and shiny, with a striate area restricted to the lower part of the frontal area, between the antennal insertions and the eyes; dorsal surface of mandibles smooth and shiny, with slight striation restricted to inner margin; clypeus smooth and shiny; scapes smooth and shiny; dorsum of mesosoma with longitudinal striations extending over entire surface; lateral surface of mesosoma smooth and shiny, with longitudinal

Figure 27. *Nesomyrmex vargasi* worker (CBUMAG:ENT:41665) **A** full-face view **B** lateral view **C** dorsal view. Scale bars: 0.5 mm.

striation restricted to lower margin; dorsum of petiole and postpetiole smooth and shiny; gaster smooth and shiny.

Pilosity and color. Dorsal surface of body with erect hairs, separated by a distance less than the length; erect hairs as long as the length of propodeal spines; in full-face view, head capsule with simple, erect to suberect hairs; scapes covered with erect hairs as long as the maximum width of the scape; antennae and mandibles pale brown; propodeal spines and legs with erect hairs equal to the length of propodeal spines; gaster with abundant erect hairs, separated by a distance less than its length.

Natural history. Ants were collected in lowlands, foraging on the ground and in leaf litter.

Comments. According to Longino (2006), *N. vargasi* and *N. pleuriticus* are parapatric species differentiated by the sculpture of the body surface, much smoother and shinier in *N. vargasi*. The latter is distributed in humid forests at medium elevations of ~ 1100 m, while *N. pleuriticus* lives in lowlands, below 500 m. In Colombia, the populations of *N. vargasi* and *N. pleuriticus* present a sympatric distribution since workers of both species were collected as foragers on the vegetation in the same fragment of TDF in the Tuparro National Natural Park (Vichada). This record increases the distribution range of *N. vargasi* from 135 m in the tropical dry forest to 1100 m in humid forest.

The examined workers of *N. vargasi* fit the definition of Longino (2006), with a smooth and shiny body, although they are slightly paler in color. Sympatric populations of *N. pleuriticus* and *N. vargasi* show variation in size, sculpture, coloration and shape of the petiole and postpetiole, exhibiting contrasting characteristics between both species, reaffirming the description of *N. vargasi* by Longino (2006). This record expands the distribution of *N. vargasi*, being the first report for South America.

Nesomyrmex xerophilus **Arredondo-H & Guerrero, sp. nov.**

https://zoobank.org/93376D41-ADB1-4AE0-AD39-E550F07516C7
Figs 28, 29

Type material. ***Holotype***. Colombia • 1 worker; Magdalena, Santa Marta, Vda. Puerto Mosquito, Reserva la Iguana Verde; 11.176972°N, 74.185167°W; 02 Nov. 2019; M. Escárraga leg.; Manual capture; CBUMAG:ENT:12440 [CBUMAG]. ***Paratypes*** (*n* = 14). Colombia • 8 workers; same data as holotype; CBUMAG:ENT:12441 (ICN), CBUMAG:ENT:41656 (CBUMAG), CBUMAG:ENT:42097 (CBUMAG), CBUMAG:ENT:42098 (CBUMAG), CBUMAG:ENT:42099 (CBUMAG), CBUMAG:ENT:42100 (CBUMAG), CBUMAG:ENT:42101 (CBUMAG), CBUMAG:ENT:42102 (MEFLG). • 1 worker; Cesar, Valledupar, Cgto. Los Corazones, PNR Los Besotes; 10.572165°N, 73.271218°W; 584 m a.s.l.; 14 16 Sep. 2023; H. Sierra, L. Ramos, R. Guerrero y S. De La Hoz legs.; Winkler; CBUMAG:ENT:41655 (CBUMAG). • 2 workers; Magdalena, Santa Marta, Reserva Caoba; 11.213139°N, 74.101667°W; 27 Nov. 2018; M. Escárraga leg.; CBUMAG:ENT:12164, CBUMAG:ENT:12165 (CBUMAG). • 1 worker; Magdalena, Santa Marta, Cerro Taganga; 11.259111°N, 74.180139°W; 117.3 m a.s.l.; 03 Mar. 2007; D. Ramírez y D. Olivero-G legs.; Pitfall; CBUMAG:ENT:12163 (IAvH). • 2 workers. Magdalena, Santa Marta, Ciénaga, 5 km SE, Río Frío; 10.883306°N, 74.133333W; 100 m a.s.l.; 16 ago. 1985; P. Ward leg.; ICN 019704 (ICN).

Geographic range. Colombia.

Holotype worker measurements. HL 0.69, HW 0.6, SL 0.44, ML 0.29, EL 0.15, PW 0.43, PTW 0.28, PPW 0.37, WL 0.88, PH 0.23, PTL 0.23, PTH 0.25, PPL 0.22, PPH 0.23, GL 0.66 CI 86, SI 0.73.

Paratype worker measurements. (*n* = 4) HL 0.69–0.7, HW 0.59–0.6, SL 0.43–0.44, ML 0.29, EL 0.15–0.16, PW 0.43–0.44, PTW 0.28–0.29, PPW 0.36–0.37, WL 0.9–0.91, PH 0.22–0.23, PTL 0.23–0.27, PTH 0.24–0.25, PPL 0.22–0.23, PPH 0.23–0.24, GL 0.66–0.68, CI 85–86, SI 72–73.

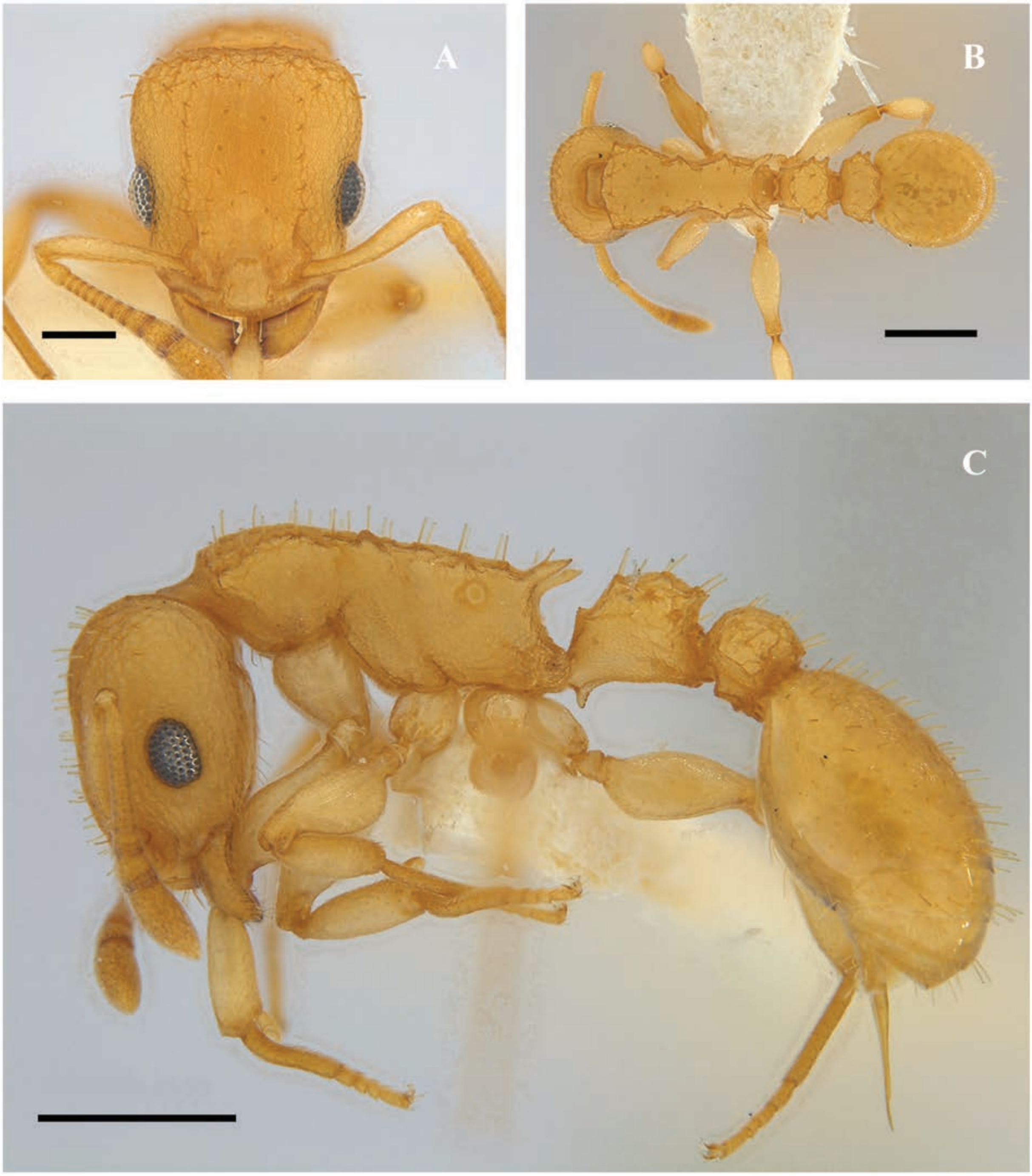

Figure 28. *Nesomyrmex xerophilus* sp. nov. Holotype worker (CBUMAG: ENT 12440) **A** full-face view **B** lateral view **C** dorsal view. Scale bars: 0.2 mm (**A**); 0.5 mm (**B, C**).

Diagnosis. Frontal lobe projected laterally, covering the antennal insertions. Frontal carina extending to posterior cephalic vertex, forming a weak scrobus. Dorsum of mesosoma straight and flattened. Lateral margin of pronotum straight, converging towards mesonotum. Lateral projection of the mesonotum dentate. Lateral dorsopropodeal processes long, covering propodeal spiracle in dorsal view.

Description. Worker. In full-face view, head longer than wide (CI 85–86), slightly narrowing behind the eyes; occipital margin weakly convex; occipital angles rounded; lateral margins slightly curved posteriorly; anterior margin of clypeus weakly convex, projecting over mandibles; eyes lateral, with 10 ommatidia at greatest diameter; frontal lobes laterally expanded, antennal insertions completely hidden by frontal lobes; frontal carina extending to posterior cephalic vertex, as if forming a weak scrobus; antenna with 12 antennomeres; mandible triangular; inner margin with five teeth, separated from basal margin by fifth tooth; scapes short (SI 72–73) barely reaching posterior margin of eye, curved towards mid-length; pedicel longer than wide, and almost as long as next three antennomeres together; antennal club with three antennomeres.

Mesosoma. In lateral view, mesosomal profile straight; in dorsal view, pronotum wider than long, with its maximum width towards anterior margin, the latter slightly convex, humeral angle angulated, lateral margins of pronotum curved; in lateral view, promesonotal suture present, in dorsal view, absent; in dorsal view, mesosomal lateral projection angulate; dorsopropodeal lateral projection angulate, projecting over propodeal spiracles; propodeal spines short, less than half the distance between their apices in length, and divergent; in lateral view, propodeal spiracle small (diameter = 0.057 mm), approximately equal to the length of the 10th antennomere, circular, projected posterolaterally; propodeal lobe short and uniformly rounded.

Metasoma. In dorsal view, petiole trapezoidal, anterior margin shorter than posterior margin; posterior margin with two mesial tubercles of equal length; lateral margins diverging from anterior to posterior margin; lateral margin with two posterolaterals tubercles; in anteroposterior direction, first tubercle poorly developed, length less than half the total length of the following tubercle; in lateral view, petiole subquadrate, peduncle and petiolar node without apparent differentiation, forming a continuous outline, which extends to the dorsal surface of the petiolar node; anterior surface of petiole with anteromedial petiolar spine on each side, superior to the petiolar spiracle; dorsal surface weakly rounded and short; anteroventral process of petiole acute; in dorsal view, postpetiole hexagonal, twice as wide as long; in lateral view postpetiole globose, taller than long.

Sculpture. Body generally opaque, with smooth, shiny areas restricted to gaster; dorsal surface of body rugose-reticulate, excluding gaster; lateral surface of mesosoma reticulate; clypeus smooth and shiny, with medial longitudinal carina; dorsal surface of mandibles shiny, with weakly marked striation; scape and legs shiny with superficial sculpture; gaster weakly imbricate.

Pilosity and color. Dorsal surface of body with flattened erect hairs, mostly separated by a distance equal to or greater than its length; hairs as long as the base of the propodeal spines; in full-face view, head capsule with erect hairs restricted to the clypeus, area between the frontal carinae and vertex; scapes covered with short decumbent hairs, without erect hairs; propodeal spines with erect hairs; legs with simple, appressed, sparse hairs restricted to the apex of the femora; gaster with abundant erect hairs, separated by a distance equal to its length. Body pale yellow, legs slightly paler, base and apex of femur and tibia darker.

Queen and male. Unknown.

Natural history. This species lives within dead branches of shrub vegetation. Populations are distributed in fragments ~ 100 m altitude. In all cases, the ants were found within dry forest with dense vegetation.

Etymology. The epithet *xerophilus* is a word composed of the prefix *xero-* (from ancient Greek *ξηρο-* meaning dry) and the suffix *-philo* or *-philus* (from ancient Greek *φίλος* meaning attraction towards). The species epithet refers to the dry habitat where these ants live, that is, the tropical dry forest, a life zone

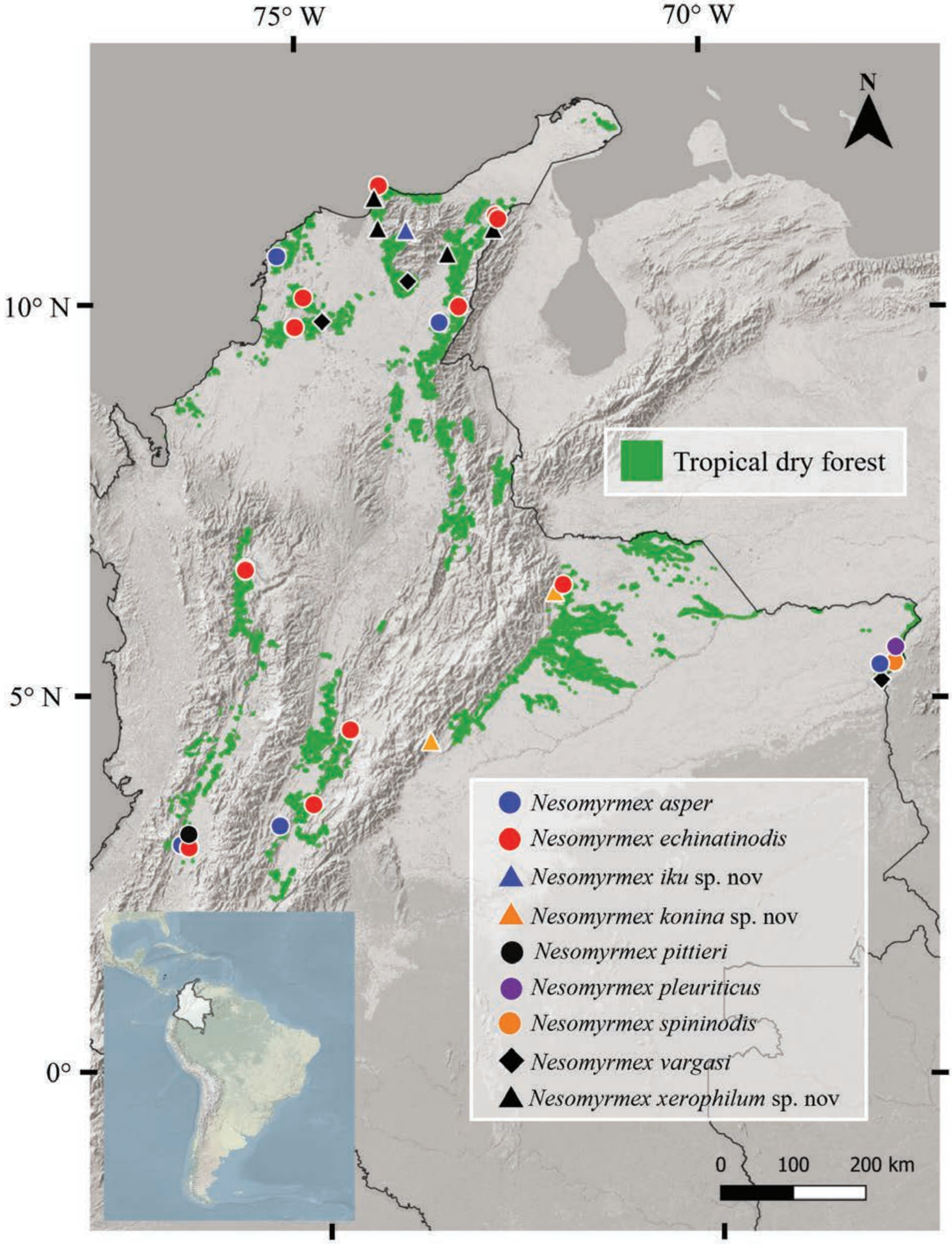

Figure 29. Distributional map of *Nesomyrmex* species from the tropical dry forest in Colombia.

highly threatened by the high rate of deforestation in Colombia. It is a noun in apposition and thus invariant.

Comments. Species easily recognizable by the lateral expansion of the frontal lobes and the lateral projection of the mesosoma and dorsopropodeum in the form of an angled lobe. Morphologically, the closest species to *N. xerophilus* is *N.* iku (see comments on *Nesomyrmex iku* sp. nov.). *N. xerophilus* is morphologically similar to *N. wilda*, with both species exhibiting a lateral projection of the mesonotum dentate, long lateral dorsopropodeal processes covering of the propodeal spiracle in dorsal view. Additionally, they share the shape of the propodeal lobes, coloration, and sculpture. Despite these similarities, *N. xerophilus* differs from *N. wilda* in the number of antennomeres, as well as in the shape of the frontal lobes, petiole, and postpetiole.

Unlike *N. asper*, the position and number of petiolar and postpetiolar tubercles in *N. xerophilous* remain consistent across its populations, with no variation observed in this characteristic. This stability may be attributed to its limited distribution in the tropical dry forest of the Colombian Caribbean region. In contrast, the variation in the position and number of petiolar and postpetiolar tubercles in *N. asper* appears to be linked to its altitudinal distribution and geographic location (see comments on *N. asper*).

General comments

The taxonomy of neotropical *Nesomyrmex* has been neglected, which has substantially limited the understanding of the morphological limits of the species and, therefore, their diversity, natural history, and distribution. This work is not a taxonomic revision of the genus *Nesomyrmex*, but it does seek to lay the foundations for future taxonomic approaches based on morphological characters aimed at solving nomenclatural problems and descriptions of new species within this genus. In this sense, we evaluate the taxonomic utility of the morphological traits used by Kempf (1959) and propose new characters for the delimitation of the species. Kempf (1959) used the presence or absence of petiole tubercles to argue the taxonomic limits of some species (e.g., *Nesomyrmex asper*), however, the analysis of that characteristic throughout the distribution of *N. asper* in the Colombian dry forest shows that petiolar tubercles can be phenotypically variable. In contrast to the variability in petiolar tubercles, we were able to determine that the sculpture of the dorsum of the clypeus together with the shape of the propodeal lobe are useful traits in the identification of this species. Body surface sculpture, mainly on the head, was also widely used by Kempf (1959) to define taxonomic boundaries of some species; for example, that same author defined *Nesomyrmex echinatinodis* as having head with frontal and vertex area partially smooth and shiny, however, when exploring in detail the head sculpture in workers of that species variability is observed, since the sculpture on the head of *N. echinatinodis* can range from smooth and shiny, finely reticulate-punctate to longitudinally rugose, the latter similar to that found in *Nesomyrmex spininodis*. This phenotypic convergence between some workers of *N. echinatinodis* and the workers of *N. spininodis* can generate confusion in the identification between both species, however, the sculpture in the first gastral tergite separates them from each other (see comments on *N. spininodis*).

Although head sculpture generated uncertainty in the identification between a pair of species, body sculpture was consistent and useful for identifying between *Nesomyrmex pleuriticus* and *Nesomyrmex vargasi* in the Colombian TDF. In both dry forest and other regions of Colombia (unpublished data), *Nesomyrmex pleuriticus* workers have anastomosing longitudinal striations on the dorsum of the mesosoma and marked reticule-punctate sculpture on the mesopleura, in broad contrast to the parallel longitudinal striations without microsculpture (smooth, shiny surface appearance) in *N. vargasi*. The sculpture of the dorsum of both the mandible and the clypeus, the shape and expansion of the frontal lobes, the length of the scape, as well as the sculpture of the first gastral tergum were shown to be taxonomically useful and should be used for a broader taxonomic approach.

Six ant species have been recorded in Colombia (Fernández and Serna 2019). Our study, conducted in a little-explored ecosystem, adds three new species and one new record, expands the known distribution of others, and includes a morphological analysis. Based on these findings, we propose nomenclatural changes, suggest new species, and provide additional biological data. Also, we identified the regions that concentrate the highest number of *Nesomyrmex* species in their TDF fragments. Both the Caribbean and the Eastern regions have five species of the nine recorded here. Interestingly, new species are recorded from each of these regions, two for the Caribbean region and one for the Eastern region. Likewise, our results show that *N. asper* and *N. echinatinodis* are the most widely distributed species in the Colombian TDF.

Acknowledgments

We sincerely thank the curators and support staff of the Colombian Entomological Collections and Natural History Museums for allowing us to study the specimens deposited in each of them. Many thanks to Yennifer Carreño, Dr. Jean Gamboa and Laboratorio de Entomología de la Universidad de la Amazonia (LEUA) for all the multifocus images and SEM micrographs. Many thanks to Dr. Francisco Serna and Dr. Fernando Fernández for their valuable discussions on ant morphology, which resulted in a better understanding of the traits of *Nesomyrmex*. We also thank Dr. Gabriela Camacho and Dr. Mônica Ulysséa for the images of the Kempf collection´s type material. We deeply thank Sebastian Salata, Jeffrey Sossa-Calvo, and an anonymous reviewer, who thoroughly reviewed this manuscript, providing comments and suggestions that improved its scientific quality. This contribution is a result of the research project “Patrones de diversidad histórica y ecológica de las hormigas en el socioecosistema bosque seco tropical de Colombia y sus implicaciones para la conservación” supported by Minciencias with contract 2021–2029 (Universidad del Magdalena and Icetex).

Additional information

Conflict of interest

The authors have declared that no competing interests exist.

Ethical statement

No ethical statement was reported.

Funding

This work was supported by Ministerio de Ciencia, Tecnología e Innovación-Minciencias (Colombia).

Author contributions

BSA and RJG contributed equally to the conceptualization and development of this work. The taxonomic identification of the ants was carried out by BSA, while the validation, data curation, and analysis of the information were carried out by BSA and RJG. BSA prepared the first draft of the manuscript. BSA and RJG reviewed and edited the final version of the manuscript. RJG oversaw obtaining funds for this research. All authors have read and agreed to the published version of the manuscript.

Author ORCIDs

Brandon S. Arredondo https://orcid.org/0000-0003-2777-5909
Roberto J. Guerrero https://orcid.org/0000-0003-3244-2754

Data availability

All of the data that support the findings of this study are available in the main text.

References

AntWeb (2024) AntWeb Version 8.112. California Academy of Science. https://www.antweb.org [accessed 13 October 2024]

Armbrecht I, Tischer I, Chacón P (2001) Nested subsets and partition patterns in ant assemblages (Hymenoptera, Formicidae) of Colombian dry forest fragments. Pan-Pacific Entomologist 77(3): 196–209.

Bolton B (1995) A new general catalogue of the ants of the world. Harvard University Press, Cambridge, MA, 504 pp.

Bolton B (2000) The ant tribe Dacetini. Memoirs of the American Entomological Institute 65: 1–1028.

Bolton B (2003) Synopsis and classification of Formicidae. Memoirs of the American Entomological Society 71: 1–370.

Bolton B (2024) An online catalog of the ants of the world. https://antcat.org [accessed 20 Feb. 2024]

Brandão CRF (1991) Adendos ao catálogo abreviado das formigas da região Neotropical (Hymenoptera: Formicidae). Revista Brasileira de Entomologia 35: 319–412.

Branstetter MG (2013) Revision of the Middle American clade of the ant genus *Stenamma* Westwood (Hymenoptera, Formicidae, Myrmicinae). ZooKeys 295: 1–277. https://doi.org/10.3897/zookeys.295.4905

Camargo-Vanegas JJ, Guerrero RJ (2020) Las hormigas *Pheidole* (Formicidae: Myrmicinae) en el bosque seco tropical de Santa Marta, Colombia. Revista Colombiana de Entomología 46: e8433. https://doi.org/10.25100/socolen.v46i2.8433

Chacón de Ulloa PA, Osorio-García M, Achury R, Bermúdez-Rivas C (2012) Hormigas (Hymenoptera: Formicidae) del Bosque seco tropical (Bs-T) de la cuenca alta del Rio Cauca, Colombia. Biota Colombiana 13(2): 165–181.

Chacón de Ulloa P, Valdes-Rodriguez S, Hurtado-Giraldo A, Cleopatra Pimienta M (2014) Arboreal ants of Gorgona National Park (Pacific of Colombia). Revista de Biología Tropical 62(1): 277–287. https://doi.org/10.15517/rbt.v62i0.16341

Collingwood CA (1985) Hymenoptera: Fam. Formicidae of Saudi Arabia. Fauna of Saudi Arabia 7: 230–302.

Collingwood CA, Agosti D (1996) Formicidae (Insecta: Hymenoptera) of Saudi Arabia (part 2). Fauna of Saudi Arabia 15: 300–385.

Csősz S, Fisher BL (2015) Diagnostic survey of Malagasy Nesomyrmex species-groups and revision of *hafahafa* group species via morphology-based cluster delimitation protocol. ZooKeys 526: 19–59. https://doi.org/10.3897/zookeys.526.6037

Csősz S, Fisher BL (2016a) Taxonomic revision of the Malagasy members of the *Nesomyrmex angulatus* species group using the automated morphological species delineation protocol NC-PART-clustering. PeerJ 4: e1796. https://doi.org/10.7717/peerj.1796

Csősz S, Fisher BL (2016b) Toward objective, morphology-based taxonomy: a case study on the Malagasy *Nesomyrmex sikorai* species group (Hymenoptera: Formicidae). PLOS ONE 11(4): e0152454. https://doi.org/10.1371/journal.pone.0152454

Csősz S, Fisher BL (2016c) Taxonomic revision of the Malagasy *Nesomyrmex madecassus* species-group using a quantitative morphometric approach. ZooKeys 603: 105–130. https://doi.org/10.3897/zookeys.603.8271

Csősz S, Fisher BL (2016d) Taxonomy of Malagasy *Nesomyrmex brevicornis* species-group using conventional morphology-based approach. ZooKeys 616: 125–159. https://doi.org/10.3897/zookeys.616.9532

Cuezzo F, Guerrero, RJ (2012) The ant genus *Dorymyrmex* Mayr (Hymenoptera: Formicidae: Dolichoderinae) in Colombia. Psyche 516058. 1–24. https://doi.org/10.1155/2012/516058

Dáttilo W, Vásquez-Bolaños M, Ahuatzin DA, Antoniazzi R, Chávez-González E, Corro E, Luna P, Guevara R, Villalobos F, Madrigal-Chavero R, de Faria Falcão JC, Bonilla-Ramírez A, García Romero AR, de la Mora A, Ramírez-Hernández A, Escalante-Jiménez AL, Martínez-Falcón AP, Villarreal AI, García Colón Sandoval A, Aponte B, Juárez-Juárez B, Castillo-Guevara C, Moreno CE, Albor C, Martínez-Tlapa DL, Huber-Sannwald E, Escobar F, Montiel-Reyes FJ, Varela-Hernández F, Castaño-Meneses G, Pérez-Lachaud G, Pérez-Toledo GR, Alcalá-Martínez I, Rivera-Salinas IS, Chairez-Hernández I, Chamorro-Florescano, IA, Hernández-Flores J, Martínez Toledo J, Lachaud J, Reyes-Muñoz JL, Valenzuela-González JL, Horta-Vega JV, Cruz-Labana JD, Reynoso-Campos JJ, Navarrete-Heredia JL, Rodríguez-Garza, JA, Pérez-Domínguez JF, Benítez-Malvido J, Ennis KK, Sáenz L, Díaz-Montiel LA, Tarango-Arámbula JA, Quiroz-Robedo LM, Rosas-Mejía M, Villalvazo-Palacios M, Gómez-Lazaga M, Cuautle M, Aguilar-Méndez MJ, Baena ML, Madora-Astudillo M, Rocha-Ortega M, Pale M, García-Martínez MA, Soto-Cárdenas MA, Correa-Ramírez MM, Janda M, Rojas P, Torres-Ricario R, Jones RW, Coates R, Gómez-Acevedo RL, Ugalde-Lezama R, Philpott SM, Joaqui T, Marques T, Zamora-Gutierrez V, Martínez Mandujano V, Hajian-Forooshani Z, MacGregor-Fors I (2020) Mexico ants: incidence and abundance along the Nearctic-Neotropical interface. Ecology 101(4): e02944. https://doi.org/10.1002/ecy.2944

De Andrade ML, Baroni Urbani C, Brandão CR, Wagensberg J (1999) Two new species of *Leptothorax* "*Nesomyrmex*" fossils in Dominican amber (Hymenoptera: Formicidae). Beiträge zur Entomologie 49: 133–140. https://doi.org/10.21248/contrib.entomol.49.1.133-140

Diniz JLM (1975) *Leptothorax* (*Nesomyrmex*) *mirassolis*, nova espécie de formiga da região norte-ocidental do estado de São Paulo, Brasil (Hymenoptera, Formicidae). Revista Brasileira de Entomologia 19: 79–83.

Emery C (1896) Studi sulle formiche della fauna neotropica. XVII-XXV. Bullettino della Società Entomologica Italiana 28: 33–107.

Evenhuis NL (2024) The insect and spider collections of the world website, Bernice P. Bishop Museum, Honolulu, Hawaii, USA. http://hbs.bishopmuseum.org/codens/ [accessed 22 Dec 2024]

Fernández F, Serna FJ (2019) Subfamilia Myrmicinae. In: Fernández F, Guerrero RJ, Delsinne T (Eds) Hormigas de Colombia. Editorial Universidad Nacional, Bogotá, 791–888.

Fernández F, Palacio EE, MacKay WP, MacKay ES (1996) Introducción al estudio de las hormigas (Hymenoptera: Formicidae) de Colombia. In: Andrade MG, Amat García G, Fernández F (Eds) Insectos de Colombia. Estudios escogidos. Bogotá: Academia Colombiana de Ciencias Exactas, Físicas y Naturales, 349–412.

Forel A (1886) Espèces nouvelles de fourmis américaines. Annales de la Société Entomologique de Belgique 30: 38–49.

Forel A (1893) Sur la classification de la famille des Formicides, avec remarques synonymiques. Annales de la Société Entomologique de Belgique 37: 161–167.

Forel A (1899) Formicidae. [part]. Biologia Centrali-Americana Hymenoptera 3: 25–56.

Forel A (1912) Formicides néotropiques. Part IV. 3eme sous-famille Myrmicinae Lep. (suite). Mémoires de la Société Entomologique de Belgique 20: 1–32. https://doi.org/10.5962/bhl.part.19251

Forel A (1914) Formicides d'Afrique et d'Amérique nouveaux ou peu connus. Bulletin de la Société Vaudoise des Sciences Naturelles 50: 211–288.

Guerrero RJ, Fernández F (2008) A new species of the ant genus *Forelius* (Formicidae: Dolichoderinae) from the dry forest of Colombia. Zootaxa 1958: 51–60. https://doi.org/10.11646/zootaxa.1958.1.5

Harris RA (1979) A glossary of surface sculpturing. Occasional Papers in Entomology, State of California Department of Food and Agriculture 28: 1–31. https://doi.org/10.5281/zenodo.26215

Hita Garcia F, Mbanyana N, Audisio TL, Alpert GD (2017) Taxonomy of the ant genus *Nesomyrmex* Wheeler (Formicidae, Myrmicinae) in the Afrotropical region, with a review of current species groups and description of a new species of the *N. angulatus* group from Mozambique. European Taxation Journal 258: 1–31. https://doi.org/10.5852/ejt.2017.258

Janicki J, Narula N, Ziegler M, Guénard B, Economo EP (2016) Visualizing and interacting with large-volume biodiversity data using client-server web-mapping applications: The design and implementation of antmaps.org. Ecological Informatics 32: 185–193. https://doi.org/10.1016/j.ecoinf.2016.02.006

Kempf WW (1958) Sôbre algumas formigas neotrópicas do gênero *Leptothorax* Mayr (Hymenoptera: Formicidae). Anais da Academia Brasileira de Ciencias 30: 91–102.

Kempf WW (1959) A synopsis of the New World species belonging to the *Nesomyrmex*-group of the ant genus *Leptothorax* Mayr (Hymenoptera: Formicidae). Studia Entomologica 2: 391–432.

Kempf WW (1975) Miscellaneous studies on neotropical ants. VI. (Hymenoptera, Formicidae). Studia Entomologica 18: 341–380.

Longino JT (2003) The *Crematogaster* (Hymenoptera, Formicidae, Myrmicinae) of Costa Rica. Zootaxa 151: 1–150. https://doi.org/10.11646/zootaxa.151.1.1

Longino JT (2006) New species and nomenclatural changes for the Costa Rican ant fauna (Hymenoptera: Formicidae). Myrmecological News 8: 131–143.

Mayr G (1887) Südamerikanische Formiciden. Verhandlungen der Kaiserlich-Königlichen Zoologisch-Botanischen Gesellschaft in Wien 37: 511–632.

Mbanyana N, Robertson HG (2008) Review of the ant genus *Nesomyrmex* (Hymenoptera: Formicidae: Myrmicinae) in southern Africa. African Natural History 4: 35–55.

Menozzi C (1927) Formiche raccolte dal Sig. H. Schmidt nei dintorni di San José di Costa Rica. Entomologische Mitteilungen. Berlin-Dahlem 16: 266–277.

Menozzi C (1934) Reperti mirmecofaunistici raccolti dal Prof. L. di Caporiacco nelle oasi di Cufra e in altre località del deserto Libico. Atti della Società dei Naturalisti e Matematici di Modena 65(6): 153–166.

Pizano C, Cabrera M, García H (2014) Bosque seco tropical en Colombia; generalidades y contexto. In: Pizano C, García H (Eds) El Bosque seco Tropical en Colombia. Instituto de Investigación de Recursos Biológicos Alexander von Humboldt, Bogotá, D. C., 37–47.

Pizano C, González-M R, López R, Jurado RD, Cuadros H, Castaño-Naranjo A, Rojas A, Pérez K, Vergara-Varela H, Idárraga A, Isaacs P, García H (2016). El Bosque Seco Tropical en Colombia. In: Gómez MF, Moreno LA, Andrade GI, Rueda C (Eds) Biodiversidad 2015. Estado y Tendencias de la Biodiversidad Continental de Colombia. Instituto de Investigación de Recursos Biológicos Alexander von Humboldt, Bogotá, D. C., 36–37. https://doi.org/10.21068/B001.2015.202

QGIS (2024) QGIS Geographic Information System. Project of the Open-Source Geospatial Foundation. http://qgis.osgeo.org

Ramos Ortega LM, Guerrero RJ (2023) Spatial turnover and functional redundancy in the ants of urban fragments of tropical dry forest. Diversity 15(7): 880. https://doi.org/10.3390/d15070880

Santschi F (1922) Description de nouvelles fourmis de l'Argentine et pays limitrophes. Anales de la Sociedad Cientifica Argentina 94: 241–262.

Serna F, Mackay W (2010) A descriptive morphology of the ant genus *Procryptocerus* (Hymenoptera: Formicidae). Journal of Insect Science 10: 1–36. https://doi.org/10.1673/031.010.11101

Sharaf MR, Akbar SA, Aldawood AS, Hita Garcia F (2017) Review of the ant genus *Nesomyrmex* Wheeler, 1910 (Hymenoptera, Formicidae, Myrmicinae) from the Arabian Peninsula. African Invertebrates 58: 21–37. https://doi.org/10.3897/AafrInvertebr.58.12782.

Sharaf MR, Mohamed AA, Al Dhafer HM, Aldawood AS (2020) *Nesomyrmex micheleae*, a new ant species (Hymenoptera: Formicidae) from the Dhofar Governorate, Oman, with a synoptic list, distribution map and key to the Arabian Nesomyrmex. Journal of Natural History 54: 351–365. https://doi.org/10.1080/00222933.2020.1762013

Smith MR (1943) The first record of *Leptothorax*, subgenus *Goniothorax* Emery, in the United States, with the description of a new species. Proceedings of the Entomological Society of Washington 45: 154–156.

Smith MR (1950) On the status of *Leptothorax* Mayr and some of its subgenera. Psyche (Cambridge) 57: 29–30. https://doi.org/10.1155/1950/80458

Tracy H (1997) Ka'gɨmmɨri nivizaku ni (La tierra es nuestra madre: La importancia de la tierra para la sobrevivencia del grupo étnico Ika: Otro punto de vista sobre la cuestión de las tierras en Bogotá: Instituto Lingüístico de Verano. http://www.sil.org/americas/colombia/pubs/38351.pdf

Ward PS, Brady SG, Fisher BL, Schultz TR (2015) The evolution of myrmicine ants: phylogeny and biogeography of a hyperdiverse ant clade (Hymenoptera: Formicidae). Systematic Entomology 40: 61–81. https://doi.org/10.1111/syen.12090

Wheeler WM (1910) Three new genera of myrmicine ants from tropical America. Bulletin of the American Museum of Natural History 28: 259–265.

Wheeler WM (1921) The *Tachigalia* ants. Zoologica (New York) 3: 137–168. https://doi.org/10.5962/p.184627

Wheeler WM (1942) Studies of Neotropical ant-plants and their ants. Bulletin of the Museum of Comparative Zoology 90: 1–262.

ZooKeys 1232: 173–186 (2025)
DOI: 10.3897/zookeys.1232.141880

Research Article

Revised diagnoses of the gudgeons *Belobranchus belobranchus* and *B. segura* (Actinopterygii, Gobiiformes, Eleotridae)

Muhammad Afrisal[1,2], Nurjirana Nurjirana[1], Haryono Haryono[1], Daniel Frikli Mokodongan[1], Kunto Wibowo[1], Abigail Mary Moore[3], Nicolas Hubert[4]

1 *Museum Zoologicum Bogoriense, Research Center for Biosystematics and Evolution, National Research and Innovation Agency, Cibinong 16911, Indonesia*
2 *Capture Fisheries Department, Indonesia Defense University, Belu 85752, Indonesia*
3 *Graduate School, Hasanuddin University, Makassar 90245, Indonesia*
4 *ISEM, Université de Montpellier, CNRS, IRD, Montpellier, France*
Corresponding author: Kunto Wibowo (kuntowe@gmail.com)

Abstract

Diagnostic characters distinguishing the gudgeons *Belobranchus belobranchus* and *Belobranchus segura* were reassessed and found to be inconsistent, making it difficult to accurately identify them. Numerous specimens of both species were examined combining genetic (mitochondrial COI gene) and morpho-meristic analyses. Our findings demonstrate that *B. belobranchus* and *B. segura* can be reliably distinguished from each other based on revised diagnostic characters, including several morphometric features (interorbital width, jaw length, and caudal-peduncle depth) as well as distinct head, body, and fin coloration.

Key words: COI, coloration, distribution, Indonesia, morphology, morphometrics

Academic editor: Tihomir Stefanov
Received: 15 November 2024
Accepted: 12 February 2025
Published: 17 March 2025

ZooBank: https://zoobank.org/2A45A273-DBF9-47CB-85D9-ACC5C21CA7FA

Citation: Afrisal M, Nurjirana N, Haryono H, Mokodongan DF, Wibowo K, Moore AM, Hubert N (2025) Revised diagnoses of the gudgeons *Belobranchus belobranchus* and *B. segura* (Actinopterygii, Gobiiformes, Eleotridae). ZooKeys 1232: 173–186. https://doi.org/10.3897/zookeys.1232.141880

Introduction

The eleotrid genus *Belobranchus* Bleeker, 1856 is distinguishable from all other genera in the family Eleotridae by a unique combination of morphological characteristics (Kottelat et al. 1993; Larson and Murdy 2001). Members of this genus have a scaleless head covered with sensory papillae arranged in a longitudinal pattern. The head lacks elongated papillae or branched barbels, and there is no distinct ridge above the eye or on the dorsal surface of the snout. Additionally, the first branchiostegal ray, or sometimes the first and second rays, bears an anteriorly directed spine. The genus comprises two species, *Belobranchus belobranchus* (Valenciennes, 1837) and *Belobranchus segura* Keith, Hadiaty & Lord, 2012, which have overlapping distributions in the eastern Indian Ocean and western Pacific. *Belobranchus belobranchus* was originally described as *Eleotris belobrancha* based on five syntypes from Manado Island, Sulawesi, Indonesia, while the latter species was described from 13 specimens from several rivers of West Papua and Halmahera, Indonesia.

In the original description of *B. segura*, Keith et al. (2012) distinguished the new species from *B. belobranchus* based on meristic counts (number of scales in the transverse forward, transverse back, and pre-dorsal series) and coloration of the body and fins (including dorsal, anal, pectoral, and caudal fins). However, molecular and morphological examinations of both type and numerous non-type specimens of *B. segura* and *B. belobranchus* in this study revealed variability in most of the diagnostic characters provided by Keith et al. (2012).

Although this genus consists of only two species, the unclear diagnostic characters make it difficult to accurately identify them. This study provides a revised morphological diagnosis, including morphometric characters and coloration patterns of the head and body, to precisely distinguish the two species.

Material and methods

All counts and measurements were taken from the left side of the body, unless the left side was damaged. Counts and measurements generally followed Watson (1995) and Nakabo (2002), with the following modifications: head width and head depth were measured at the posterior margin of the preopercle, snout width was defined as the distance between the nostrils, and body width was measured at the origin of the pectoral fin. Measurements were taken point-to-point with digital calipers to the nearest 0.01 mm. Meristic counts were determined through observation under a stereomicroscope (Nikon SMZ460). Standard length is abbreviated as SL. Sex was determined by confirming the shape of the urogenital papilla (in males, the urogenital papilla long or triangular with pointed distal tip, whereas in females, the urogenital papilla somewhat bulbous in appearance with a fimbriate distal tip). Observations of fresh coloration were based on photographs deposited on the Barcode of Life Data System website (BOLD, www.barcodinglife.org) and the newly collected specimens in this study. All specimens of the genus *Belobranchus* examined in this study are deposited at the Museum Zoologicum Bogoriense, Indonesia (**MZB**; Bogor).

Phylogenetic analysis was performed in MEGA 11 (Tamura et al. 2021) to visualize the evolutionary divergence between *Belobranchus* species, and the final tree was edited in the Inkscape 1.2.2. The 38 sequences of the cytochrome c oxidase I (COI) mitochondrial gene of the species of *Belobranchus*, accession numbers KU692344.1–KU692375.1 and KU692379.1 (Dahruddin et al. 2016); MT706791.1, MT706722.1, MT706726.1, MN045250.1, MN069306.1, and MN069308.1 (Sahami and Habibie 2021), and a sequence of *Eleotris fusca* MN045250.1 (Mennesson et al. 2019), used for phylogenetic reconstruction in this study are currently available in the NCBI GenBank database (www.ncbi.nlm.nih.gov/). Additionally, a sequence of *Eleotris fusca* (Bloch & Schneider, 1801) (KU692479.1) was included as an outgroup. The sequences were aligned using CLUSTALW 1.6 (Higgins et al. 1996) and trimmed to produce 652 bp homologous fragments of the COI gene. Phylogenetic relationships among sequences were inferred using the Neighbor-Joining algorithm (Saitou and Nei 1987) based on the Kimura 2-Parameter (K2P) model (Kimura 1980). Genetic distances (number of base substitutions per site) were computed using the Maximum Composite Likelihood method (Tamura et al. 2004) with 1,000 bootstrap replications (Felsenstein 1985). Graphs of morphometric relationships were generated using Microsoft Excel.

Results

***Belobranchus belobranchus* (Valenciennes, 1837)**
Figs 1, 2, 3A–D, 5A, 6, Tables 1, 2
English name: Throat-spine Gudgeon

Eleotris belobrancha Valenciennes in Cuvier and Valenciennes 1837: 243 (type locality: Manado Island, Sulawesi, Indonesia)
Belobranchus quoyi Bleeker, 1856: 300 (type locality: Manado Island, Sulawesi, Indonesia)
Belobranchus taeniopterus Bleeker, 1856: 301 (type locality: Boleling, Bali, Indonesia)

Material examined. ***Non-type specimens*.** 94 specimens, all specimens from Indonesia. **Java:** • MZB.16307, 84.6 mm SL, male, Cibareno, Pasir Baru, Cisolok, Sukabumi, Jawa Barat, S. Sauri et al., 23 Jun. 2002 • MZB.16328, 63.1 mm SL, female, Cilumajan, Pasir Baru, Cisolok, Sukabumi, Jawa Barat, S. Sauri et al., 24 May 2002 • MZB.26872 [ex BIF.01651], 71.7 mm SL, male, Cibareno, Lebak, Banten, 6°57'48.0"S, 105°23'42.0"E, N. Hubert et al., 10 Dec. 2013 • MZB.26873 [ex BIF.1696], 77.5, female, MZB.26906 [ex BIF01694], 58.7 mm SL, male, Citiis, Sukabumi, Jawa Barat, 6°56'46.0"S, 106°26'45.6"E, N. Hubert et al., 11 Dec. 2013 • MZB.23934, 33.9 mm SL, male, Purworejo, Jawa Tengah, R. Hadiaty, 10 Sep. 2017. **Bali:** • MZB.26874 [ex BIF.2385], 74.8 mm SL, male, MZB.26907 [ex BIF.2384], 65.0 mm SL, female, Nbang, Jembrana, Bali, 8°22'01.2"S, 114°45'07.2"E, N. Hubert et al., 15 Apr. 2014. **Sulawesi:** • MZB.4795, 67.4–106.9 mm SL, 2 specimens, male and female, Watu Songu, Ulubongka, Poso, Sulawesi Tengah, Suyanto, 10 Nov. 1982 • MZB.11665, 70.1–108.6 mm SL, 3, 1 male, 2 females, MZB.11676, Lambuno, Wana Mukti, Mountong, Donggala, Sulawesi Tengah, Agus, 3 May 2002 • MZB.11715, 45.4–52.1 mm SL, 6 specimens, 2 males, 4 females, Haryono and A. Munim, 8 Aug. 2001 • MZB.11731, 66.1–100.2 mm SL, 8 specimens, 2 males, 6 females, Wapo river, Lombongo, Suwawa, Gorontalo, Haryono and A. Munim, 7 Aug. 2001 • MZB.11735, 57.3–65.2 mm SL, 4 specimens, 3 males, 1 female, Tolumolu, Kota Selatan, Sulawesi Utara, 8 Aug. 2001 • MZB.11964, 109.5 mm SL, female, MZB.11975, 113.0 mm SL, female, MZB.12048, 62.3 mm SL, female, Bolaang Mongondow, Sulawesi Utara, Haryono and Hesron, 21–26 May 2002 • MZB.20004, 58.6–77.1 mm SL, 3 specimens, 1 male, 2 females, Masembo, Mekongga, Tinukari, Wawo, Kolaka Utara, Sulawesi Tenggara, Jumaring, 30 Nov. 2010 • MZB.20352, 36.4–115.4 mm SL, 17 specimens, 11 males, 6 females, MZB.20381, 52.9–96.2 mm SL, 9 specimens, 5 males, 4 females, MZB.20391, 78.9 mm SL, female, MZB.20398, 107.0–129.5 mm SL, 3 specimens, 2 males, 1 female, MZB.20406, 58.5–63.8 mm SL, 3 specimens, 1 male, 2 females, MZB.20415, 51.0–100.3 mm SL, 3 males, Tinukari, Wawo, Kolaka Utara, Sulawesi Tenggara, R. Hadiaty et al., 28 Jun.–3 Jul. 2011 • MZB.22703, 84.1 mm SL, male, Bonepuso, Bulagi Selatan, Banggai Kepulauan, S. Sauri, 20 Sep. 2014 • MZB.24579, 101.4 mm SL, male, Marinding, Luwu, Sulawesi Selatan, 3°21'43.5"S, 120°15'54.3"E, seine net, D. Lumbantobing, 12 Aug. 2016. **Alor:** • MZB.5346, 115.3 mm SL, male, Alor, Nusa Tenggara Timur, Sudarmanu, Apr. 1984. **Halmahera:** • MZB.18812, 85.3 mm SL, male, MZB.18830, 61.3–79.7 mm SL, 3 males, MZB.21174, 32.8 mm SL, male, MZB.21184, 93.4 mm SL, female, MZB.21209, 71.8–98.4 mm SL, 5 specimens, 1 male, 4 females,

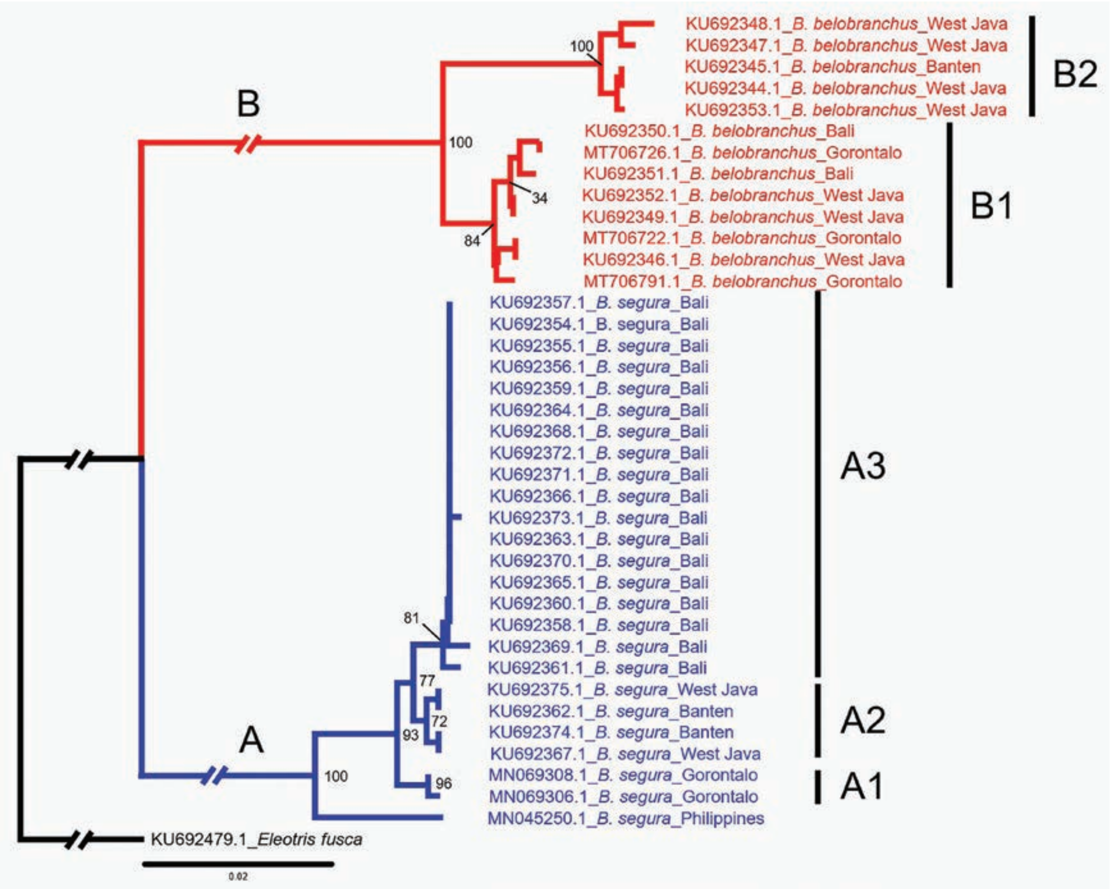

Figure 1. Neighbor-join phylogenetic tree of COI GenBank accessions for the genus *Belobranchus* [Kimura 2-Parameter model (K2P); 1000 bootstrap replications; *Eleotris fusca* as outgroup].

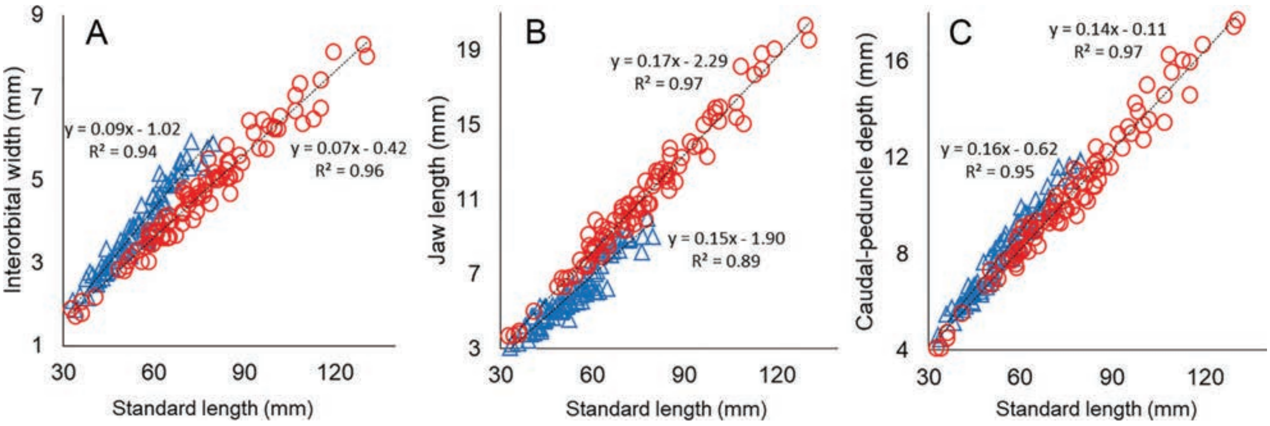

Figure 2. Morphometric relationships in *Belobranchus belobranchus* (circles) and *B. segura* (triangles) **A** interorbital width **B** jaw length **C** caudal-peduncle depth.

MZB.21219, 58.2 mm SL, female, MZB.26661 [ex MZB.18747], 63.3–130.7 mm SL, 7 specimens, 1 male, 6 females, MZB.26662 [ex MZB.18820], 71.8 mm SL, female, Ake Jira, Weda Tengah, R. Hadiaty et al., 4 Feb. 2010–16 Jul. 2011. **Papua:** • MZB.15631, 95.2 mm SL, female, Waigeo, Raja Ampat, Papua, R. Hadiaty et al., 4 Jun. 2007 • MZB.17098, 65.3–97.6 mm SL, 2 males, MZB.17118, 59.7–61.0 mm SL, male and female, MZB.17140, 91.9 mm SL, male, Batanta, Raja Ampat, Papua Barat, R. Hadiaty et al., 30 July–5 May 2008.

Table 1. Counts and measurements (expressed as percentages of standard length) of *B. belobranchus* and *B. segura*.

	B. belobranchus		***B. segura***			
	Non-type specimens		**Holotype**	**Paratypes**	**Non-type specimens**	
	n = 94		**MZB.20786**	**n = 9**	**n = 78**	
Standard length (SL, mm)	32.8–130.7	mode	72.1	41.0–72.5	33.4–79.8	mode
Counts						
Pored lateral-line scales	51–62	56 or 57	59	53–58	50–62	54 or 56
Caudal-fin rays	13	13	13	13	13	13
Pectoral-fin rays	20–23	20	21	20–22	20–22	20
Transverse backward scales	17–23	19	19	19–21	16–21	19
Transverse forward scales	18–34	22	26	22–27	18–28	22
Pre-dorsal scales	20–39	26	20	16–23	16–32	24
Zigzag series	17–21	19	19	17–19	17–21	19
Measurements (% SL)		**mean**				**mean**
Head length	26.6–33.1	30.4	29.5	28.3–31.4	23.9–30.9	28.6
Head width	17.6–29.2	24.7	23.3	20.2–24.6	16.8–26.4	21.8
Head depth	12.1–20.0	16.5	16.7	13.9–18.3	13.0–19.8	16.0
Mouth width	8.7–21.7	16.1	13.0	9.7–15.0	8.5–16.4	12.0
Eye diameter	3.7–5.9	4.9	6.2	5.5–7.0	4.4–7.0	5.7
Snout width	4.9–7.1	6.1	7.4	6.2–8.2	5.6–8.4	7.0
Interorbital width	4.8–8.0	6.0	11.6	7.4–11.0	6.4–11.2	8.2
Distance snout to isthmus	9.1–14.6	11.2	10.8	10.5–12.9	8.7–15.2	11.7
Postocular length	13.7–21.3	17.4	16.2	13.3–17.7	12.6–17.5	15.6
Jaw length	10.3–16.7	14.1	12.3	10.1–12.9	8.7–13.5	11.1
Body depth	15.2–21.8	18.6	21.1	18.3–22.0	15.7–20.9	18.9
Body width	10.7–19.9	15.5	16.2	13.6–17.5	10.5–17.9	14.5
Pre-dorsal-fin length	38.3–44.8	41.5	41.1	38.1–41.5	36.8–42.6	40.2
Snout to second dorsal-fin origin length	55.6–65.6	60.6	61.9	59.4–62.3	54.8–63.1	59.7
Second dorsal-fin length	18.8–23.8	21.6	25.0	21.3–24.1	19.8–25.7	22.9
Length of first dorsal-fin base	9.8–14.1	11.9	12.9	11.7–14.8	10.4–15.6	12.8
Length of second dorsal-fin base	10.2–13.3	11.3	11.4	10.1–12.1	10.3–13.5	11.6
First dorsal-fin origin to second dorsal-fin origin	17.2–22.8	19.6	21.2	19.8–22.6	17.7–22.9	20.2
First dorsal-fin origin to pelvic-fin origin	15.8–24.8	21.3	22.3	18.7–22.2	16.0–23.5	20.4
First dorsal-fin origin to anal-fin origin	25.7–32.0	29.0	31.2	28.1–30.4	25.8–31.9	29.1
Second dorsal-fin origin to anal-fin origin	14.2–21.0	18.1	20.8	16.6–20.7	15.8–20.7	18.2
Interval between first and second dorsal-fin bases	5.2–9.8	7.7	8.5	7.4–9.3	4.2–10.3	7.3
Pelvic-fin origin to anal-fin origin	30.0–41.2	34.8	35.5	33.6–35.3	29.1–38.8	33.9
Pelvic-fin origin to second dorsal-fin origin	31.4–40.9	36.2	37.3	33.0–37.7	32.2–39.7	36.1
Anal-fin length	18.5–23.5	21.4	23.7	21.4–23.5	20.1–24.1	22.2
Pre-anal-fin length	62.2–70.6	65.9	64.9	63.7–66.4	60.7–68.3	64.8
Length of anal-fin base	8.4–11.9	9.8	10.6	8.7–10.2	8.5–12.5	10.2
Caudal-peduncle depth	11.9–15.0	13.6	15.5	13.5–16.0	13.2–16.6	14.7
Caudal-peduncle length	19.6–29.0	22.4	27.2	26.0–27.6	20.0–31.7	24.4
Caudal-fin length	19.7–25.1	22.4	23.8	20.1–23.9	18.8–24.1	21.4

Diagnosis. A species of *Belobranchus* with the following combination of characters: head relatively depressed; interorbital width 4.8–8.0% (mean 6.0%) of SL; jaw length 10.3–16.7% (14.1%) of SL; caudal-peduncle depth 11.9–15.0% (13.6%) of SL; body with 3 dark-brown bands seaparated by pale bands, with many dark horizontal lines (one per scale row) along lateral surface; dorsal and lateral surfaces of head with many small whitish spots; 1 or 2 distinct oblique brown lines extending from eye to posterior edge of operculum (not always visible); first dorsal fin typically uniformly mottled dark brown or with thin yellowish distal edge; largest recorded specimen 130.7 mm SL.

Distribution and habitat. *Belobranchus belobranchus* has been recorded from the South China Sea (Randall and Lim 2000), Indonesia: Java, Bali, Lombok, Flores, Alor, Timor, Buton, Sulawesi, and Halmahera islands, and West Papua (Roberts 1993; Tjakrawidjaja 2002; Larson and Pidgeon 2004; Larson et al. 2007; Keith et al. 2012; Tweedley et al. 2013; Dahruddin et al. 2016; Miesen et al. 2016; this study); the Philippines (Jamandre 2023); Japan (Sakai et al. 2001; Nakabo 2002); Papua New Guinea (Fricke et al. 2014; Amick and Toko 2021) (Fig. 6). *Belobranchus belobranchus* is an amphidromous species, characterized by migration between freshwater and coastal environments (Keith et al. 2012; Sahami et al. 2019); its habitat predominantly encompasses the lower regions of rivers, typically at altitudes to 5 m, and it has been observed in muddy to clear river systems featuring sandy to rocky or gravel bottoms (Parenti 2021). Like most eleotrids, this fish is carnivorous (Kiruba-Sankar et al. 2018).

Belobranchus segura Keith, Hadiaty & Lord, 2012
Figs 1, 2, 3E–H, 4, 5B, 6, Tables 1, 2
New English name: Segura Gudgeon

Belobranchus segura Keith, Hadiaty & Lord, 2012: 480, figs 1, 2, 3A, 3C (type locality: Ake Jira, Leililef Waibulen, Halmahera, Indonesia)

Material examined. *Holotype*. MZB.20786, 72.1 mm SL, male, Ake Jira, Leililef Waibulen, Halmahera, Indonesia, R. Hadiaty et al., 26 Jan. 2010.

***Paratypes*.** 9 specimens, 40–72 mm SL, all specimens collected from Maluku Island, Indonesia. • MZB.18658, 61–66 mm SL, 2 males, Ake Kobe, Halmahera, R. Hadiaty et al., 23 Jan. 2010 • MZB.18684, 64–72 mm SL, 3 males, same data as holotype • MZB.18747, 55 mm SL, female, MZB.18751, 40–44 mm SL, 2 females, MZB.18820, 44 mm SL, female, Ake Jira, Weda Tengah, Halmahera, R. Hadiaty et al., 4–7 Feb. 2010.

Non-type materials. 78 specimens, 33.4–79.8 mm SL, all specimens collected from Indonesia. **Java:** • MZB.23934, 33.9 mm SL, male, Purworejo, Jawa Tengah, R. Hadiaty, 10 Sep. 2017 • MZB.26667 (ex BIF.1483), 42.1 mm SL, male, MZB.26890 [ex BIF.1482], 39.1 mm SL, male, Cibeber, Pandeglang, Banten, 6°35'29.0"S, 105°37'48.0"E, N. Hubert et al., 7 Dec. 2013. **Bali:** • MZB.26668 (ex BIF.2389), 56.3 mm SL, female, MZB.26891 (ex BIF.2386), 50.2 mm SL, female, MZB.26892 (ex BIF.2374), 55.1 mm SL, male, MZB.26893 (ex BIF.2375), 61.5 mm SL, male, MZB.26894 (ex BIF.2387), 52.6 mm SL, female, MZB.26895 (ex BIF.2373), 59.0 mm SL, male, MZB.26896 (ex BIF.2376), 60.8 mm SL, male, MZB.26897 (ex BIF.2388), 35.9 mm SL, female, Nbang, Jembrana, Bali, 8°22'01.2"S, 114°45'07.2"E, N. Hubert et al., 15 Apr. 2014 • MZB.26670 (ex BIF.2460), 52.0 mm SL, female, MZB.26898 (ex BIF.2457), 60.3 mm SL, male, MZB.26899 (ex BIF.2456), 65.1 mm SL, male, MZB.26900 (ex BIF.2459), 55.3 mm SL, male, MZB.26901 (ex BIF.2454), 69.2 mm SL, male, MZB.26902 (ex BIF.2455), 68.9 mm SL, male, Yeh Sumbul, Jembrana, Bali, 8°21'36.0"S, 114°47'02.4"E, N. Hubert et al., 16 Apr. 2014. **Sulawesi:** • MZB.11715, 41.3–52.1 mm SL, 6 specimens, 2 males, 4 females, MZB.11717, 46.1–68.0 mm SL, 6 specimens, 3 males, 3 females, MZB.11727, 37.8–62.2 mm SL, 6 specimens,

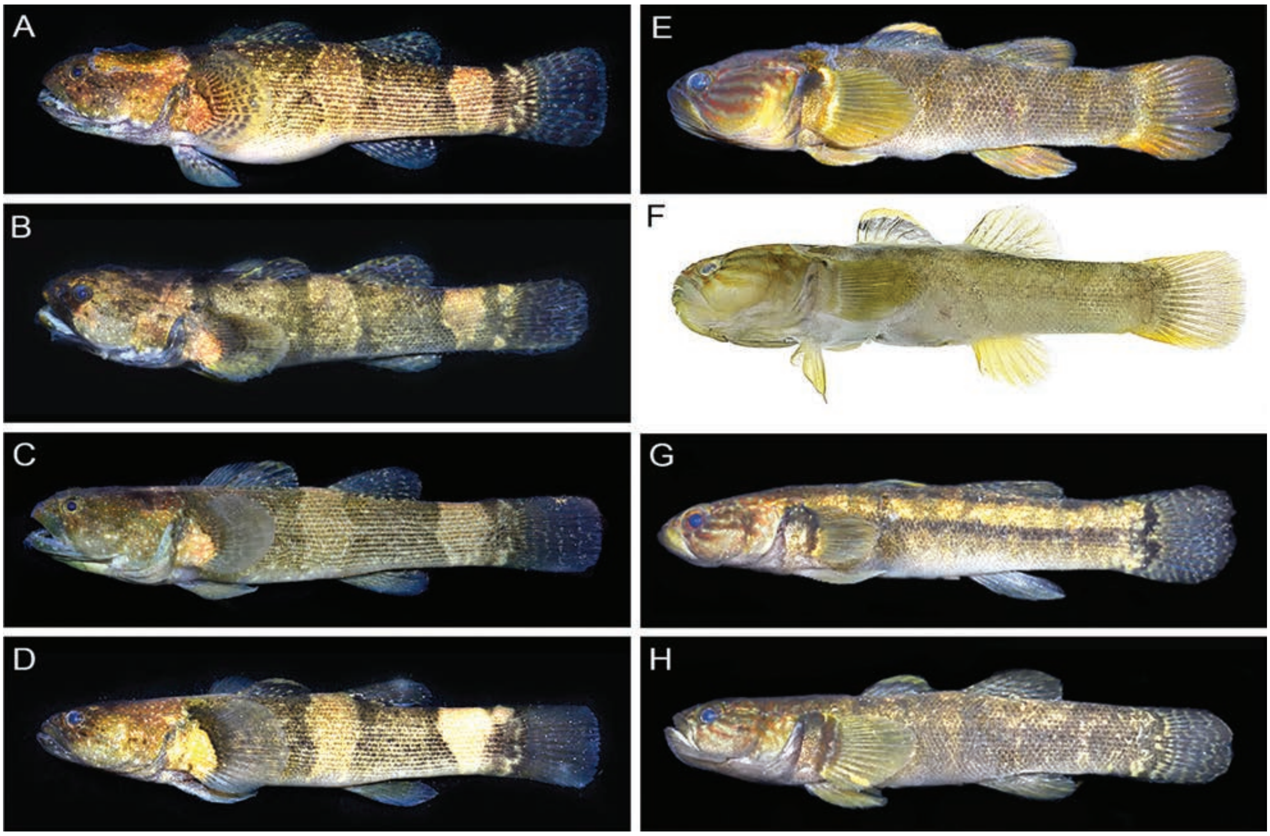

Figure 3. Fresh specimens of *Belobranchus* species **A–D** *B. belobranchus* **A** MZB.26873, 77.5 mm SL **B** MZB.26907, 74.8 mm SL **C** MZB.26872, 71.7 mm SL **D** MZB.26906, 58.7 mm SL) **E–H** *B. segura* **E** MZB.26902, 68.9 mm SL **F** MZB.26687, 59.6 mm SL **G** MZB.26668, 56.3 mm SL **H** MZB.26894, 52.6 mm SL.

4 males, 2 females, Baliohuto, Lombongo, Suwawa, Gorontalo, Haryono and A. Munim, 6–8 Aug. 2001 • MZB.12048, 62.3 mm SL, female, Molong, Pusian Dumoga, Bolaang Mongondow, Sulawesi Utara, Haryono and Hesron, 26 May 2002 • MZB.26663 (ex MZB.11676), 47.3–69.4 mm SL, 11 specimens, 6 males, 5 females, Mountong, Donggala, Sulawesi Tengah, Agus, 2 May 2002 • MZB.26664 (ex MZB.1197), 61.2–76.1 mm SL, male and female, Bolaang Mongondow, Sulawesi Utara, Haryono and Hesron, 22 May 2002 • MZB.26669 (ex MZB.22703), 49.1–50,4 mm SL, male and female, Bonepuso, Bulagi Selatan, Banggai Kepulauan, S. Sauri, 20 Sep 2014. **Lombok:** • MZB.22933, 42.0–50.5 mm SL, 3 females, Ormori, Kawinda Toi, Tambora, Sumbawa, Nusa Tenggara Barat, Mulyadi, 24 Apr. 2015. **Flores:** • MZB.6359, 43.4–53.5 mm SL, 4 specimens, 2 males, 2 females, Wae Laku, Ruteng, Flores, Nusa Tenggara Timur, Agus and Munir, 26 May 1994. **Timor:** • MZB.26903, 59.6 mm SL, male, MZB.26904, 59.6 mm SL, male, MZB.26905, 57.8 mm SL, male, MZB.26906, 44.4 mm SL, male, MZB.26908, 66.1 mm SL, male, Jenilu, Kakuluk Mesak, Belu, Nusa Tenggara Timur, 9°00'41.8"S, 124°52'52.2"E, M. Afrisal et al., 23 Jan. 2023. **Halmahera:** • MZB.18700, 67.2 mm SL, male, MZB.18706, 76.4–79.8 mm SL, 3 males, MZB.18711, 56.7 mm SL, female, MZB.26909 (ex MZB.18820), 59.0–58.1 mm SL, 2 females, Ake Jira, Weda Tengah, R. Hadiaty et al., 27 Jan.–7 Feb. 2010 • MZB.21219, 58.2 mm SL, female, Ake Kobe, Weda Tengah, R. Hadiaty et al., 7 Jul. 2011 • MZB.26665 (ex MZB.18747), 38.4–43.8 mm SL, 2 females, MZB.26666 (ex MZB.18751), 33.4–43.0 mm SL, 4 females, Ake Saki, Weda Tengah, R. Hadiaty et al., 7 Feb. 2010.

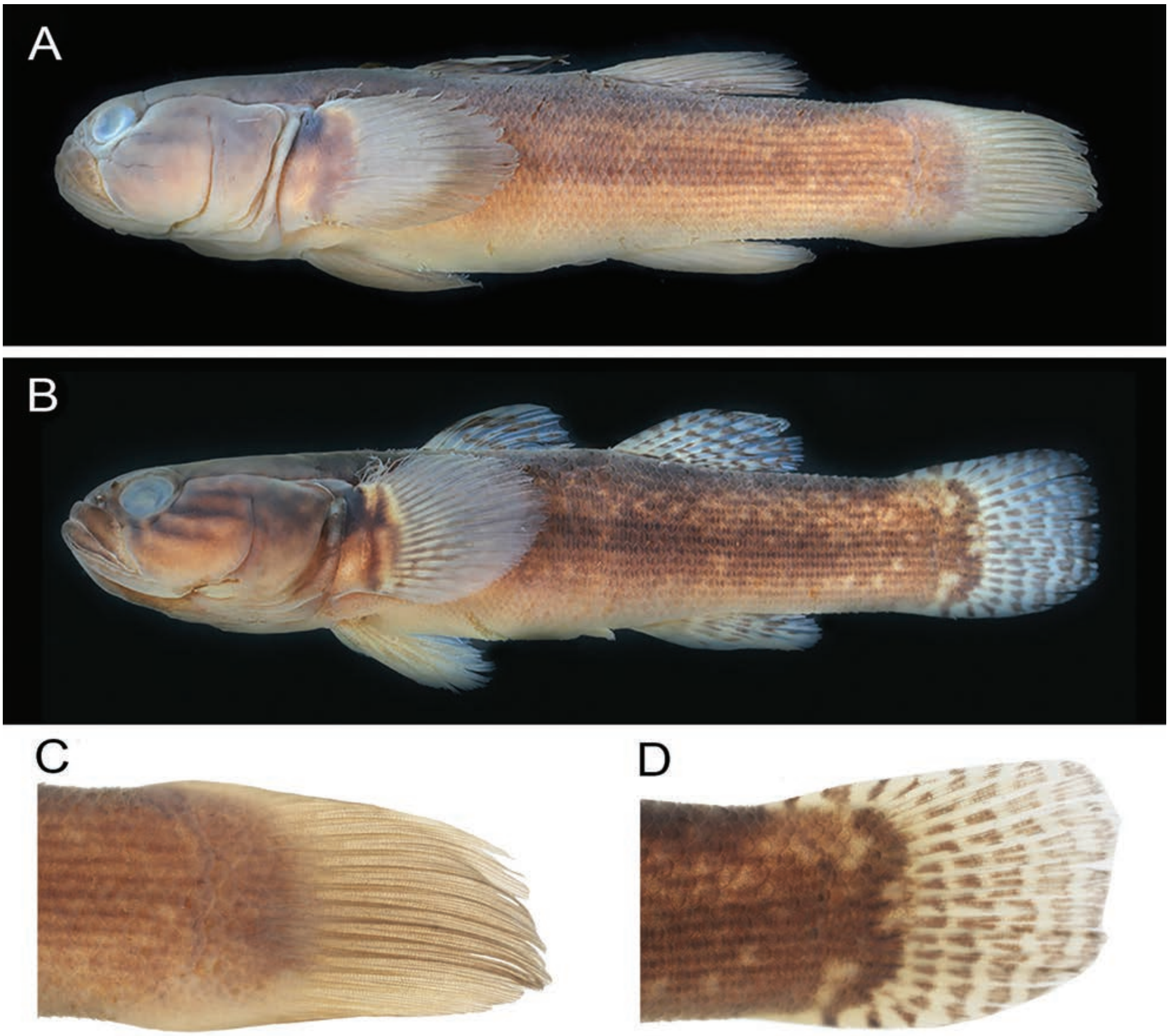

Figure 4. Preserved specimens of *B. segura* **A** MZB.20786, holotype, 72.1 mm SL **B** MZB.18747, paratype, 55.9 mm SL **C, D** caudal fins of the holotype and the paratype, respectively.

Diagnosis. A species of *Belobranchus* with the following combination of characters: head somewhat convex; interorbital width 6.4–11.6% (mean 8.2%) of SL; jaw length 8.7–13.5% (11.1%) of SL; caudal-peduncle depth 13.2–16.6% (14.7%) of SL; body with 4 or 5 dark-brown bands separated by narrow pale bars, lacking dark horizontal lines; dorsal and lateral surfaces of head without small whitish spots; 3 or 4 oblique brown lines extending from eye to posterior edge of operculum; upper margin of first dorsal fin yellowish to orange; largest recorded specimen 79.8 mm SL.

Distribution and habitat. *Belobranchus segura* has been recorded from Indonesia: Sumatra, Java, Bali, Lombok, Sulawesi, Halmahera, Sumbawa, Flores, Timor, Papua Barat (Kottelat et al. 1993; Keith et al. 2012; Dahruddin et al. 2016; Miesen et al. 2016; Sahami and Habibie 2021; Hasan et al. 2023; this study), the Philippines (Vedra et al. 2013), Japan (Suzuki et al. 1995), Papua New Guinea (Amick and Toko 2021: fig. 2P,Q), Solomon Islands and Vanuatu (Keith et al. 2012), and Philippines (Gonzalez et al. 2023) (Fig. 6). This species

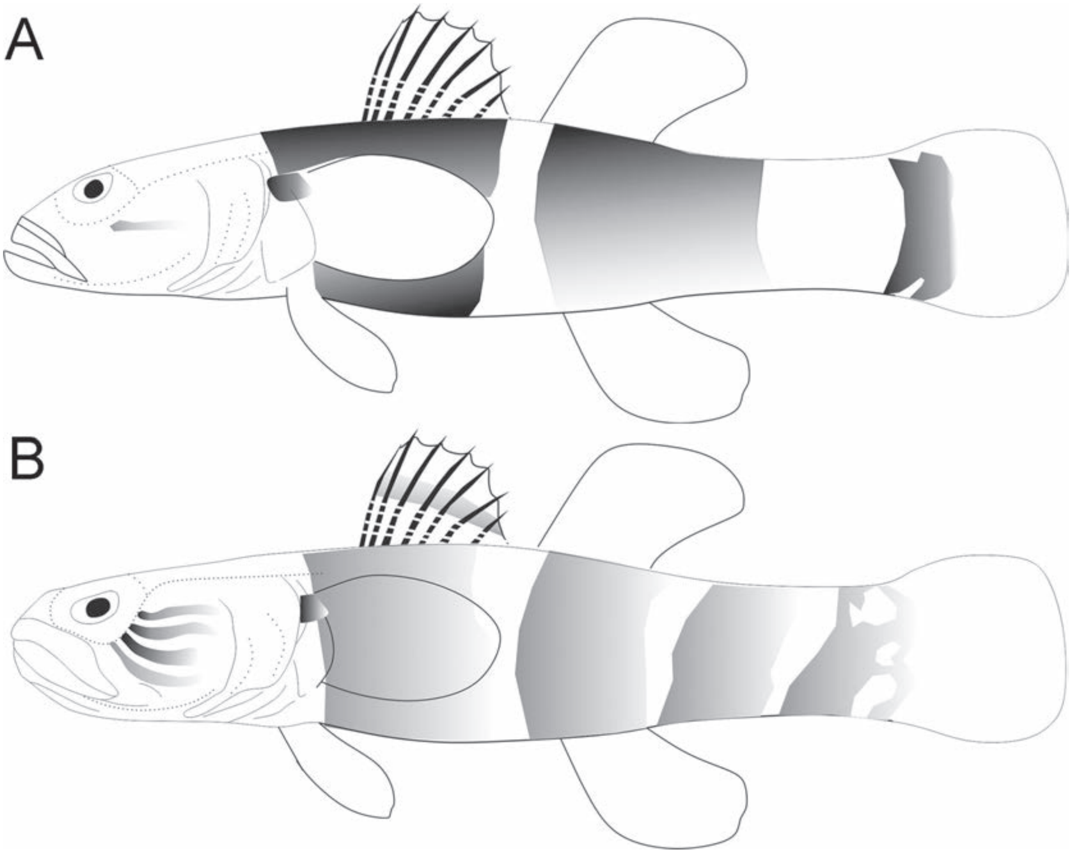

Figure 5. Schematic illustration of the number and patterns of lines on the cheek and lateral bands on the body of *Belobranchus* species **A** *B. belobranchus* **B** *B. segura*.

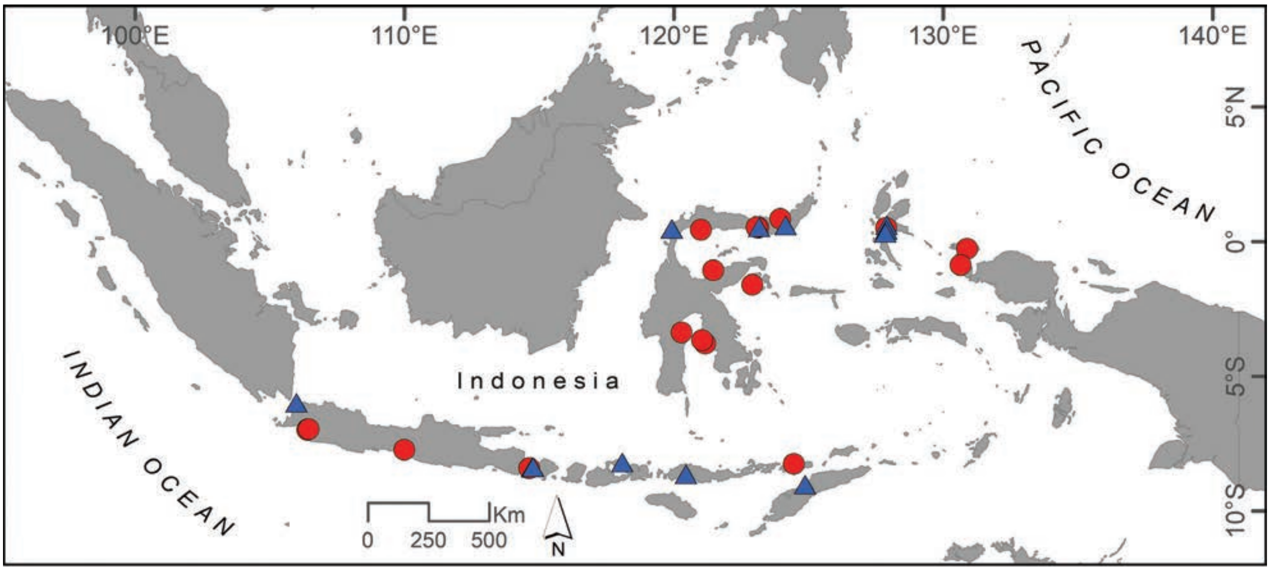

Figure 6. Distributional records of *B. belobranchus* (circles) and *B. segura* (triangles) based on collected specimens examined in this study.

is considered amphidromous (Keith et al. 2012; Sahami and Habibie 2021) and has been found in the lower reaches of muddy to clear rivers with sandy to gravel substrate, to 5 m in altitude, close to estuaries. Like most eleotrids, this fish is considered carnivorous (Kiruba-Sankar et al. 2018).

Table 2. Frequency distributions of selected counts of *B. belobranchus* and *B. segura*.

	n	Pored lateral–line scales															n	Transverse backward series							
		50	51	52	53	54	55	56	57	58	59	60	61	62	63			16	17	18	19	20	21	22	23
B. belobranchus (Keith et al. 2012)	13	–	–	–	–	–	–	1	1	3	2	3	1	1	1		14	–	–	–	–	4	4	4	2
B. segura (Keith et al. 2012)	13	–	–	–	–	–	2	3	1	2	2	3	–	–	–		14	–	–	3	6	4	1	–	–
B. belobranchus (this study)	94	1	–	–	2	13	9	16	16	16	13	7	2	1	–		94	–	2	3	53	24	11	2	1
B. segura (this study)	88	2	1	6	8	18	8	18	13	6	5	1	1	1	–		88	1	3	9	58	12	5	–	–

	n	Transverse forward series																	
		18	19	20	21	22	23	24	25	26	27	28	29	30	31	32	33	34	35
B. belobranchus (Keith et al. 2012)	13	–	–	–	1	–	1	3	3	3	2	–	–	–	–	–	–	–	–
B. segura (Keith et al. 2012)	13	–	–	–	–	–	–	–	–	–	2	2	2	2	2	–	1	1	1
B. belobranchus (this study)	94	1	–	2	–	30	1	22	–	17	2	10	1	4	–	3	–	3	–
B. segura (this study)	88	2	1	16	3	32	2	19	2	8	1	2	–	–	–	–	–	–	–

	n	Pre–dorsal midline series																							
		16	17	18	19	20	21	22	23	24	25	26	27	28	29	30	31	32	33	34	35	36	37	38	39
B. belobranchus (Keith et al. 2012)	14	–	–	–	–	–	2	1	1	–	3	1	1	1	1	–	–	–	–	1	–	–	–	–	–
B. segura (Keith et al. 2012)	9	1	1	1	–	1	1	1	3	–	–	–	–	–	–	–	–	–	–	–	–	–	–	–	–
B. belobranchus (this study)	94	–	–	–	–	4	1	5	2	7	6	14	7	8	13	6	3	8	3	2	1	2	–	1	3
B. segura (this study)	88	3	2	5	6	4	6	10	4	16	5	7	4	8	4	2	1	1	–	–	–	–	–	–	–

Discussion

The *Belobranchus* phylogenetic tree based on partial COI (652 bp) sequences reveals two main clades with a 14.4% mean pairwise genetic distance (Fig. 1). The monophyletic group of *B. segura* in Clade A includes one sequence from the Philippines (previously identified as *B. belobranchus*; see Mennesson et al. 2019) along with all other *B. segura* sequences, while clade B, containing all *B. belobranchus* sequences, also forms a monophyletic group. This clade is supported by a bootstrap proportion of 90%. Clade A corresponds to the geographic areas as follows: A1 from Tomini Bay, Gorontalo, Sulawesi; A2 from Java (West Java and Banten); and A3 from West Bali. Clade B is divided into two clusters, B1 containing sequences from various origins and B2 comprised entirely of sequences from West Java. The pairwise genetic distances among the *B. segura* clusters (A1, A2 and A3) were ca 1.0% on average, while the mean pairwise genetic distance was 3.4% between the two *B. belobranchus* clusters (B1 and B2). However, morphological examinations based on the diagnostic characters given by Keith et al. (2012), including meristic and color characters, did not correspond well with the results of the phylogenetic analysis.

In the paper by Keith et al. (2012), there were also inconsistencies in the stated number of specimens between the material examined and results section. The number of *B. belobranchus* specimens was stated as 13 in the material examined, but data were provided for 14 specimens in the results (see Keith et al. (2012): table 1: transverse backward series). There was a similar discrepancy for *B. segura*, with a total of 13 specimens described in the material examined, but data from 14 specimens included in the results.

The meristic data presented in Keith et al. (2012: table 1), including the transverse backward scale, transverse forward scale, and pre-dorsal scale counts, initially appeared sufficient to distinguish between *B. segura* and *B. belobranchus*. However, upon examining numerous specimens of both species, the range of values for each character expanded, resulting in significant overlap, suggesting that these characters may not be reliable for distinguishing between the two species (Table 2).

Keith et al. (2012: table 1) also differentiated the two species based on morphometric characters, such as head and predorsal lengths. However, after examining numerous specimens of both species, it became apparent that these characters also overlapped too much, making them unreliable for differentiation (Table 1). In this study, we identified several morphometric characters that help distinguish *B. segura* from *B. belobranchus*, although the proportional length measurements for these characters overlap between the two species: interorbital width 6.4–11.6% (mean 8.2%) of SL in *B. segura* [vs 4.8–8.0% (mean 6.0%) of SL in *B. belobranchus*]; jaw length 8.7–13.5% (mean 11.1%) of SL [vs 10.3–16.7% (mean 14.1%) of SL]; and caudal-peduncle depth 13.2–16.6% (mean 14.7%) of SL [vs 11.9–15.0% (mean 13.6%) of SL] (Fig. 2).

With respect to coloration, Keith et al. (2012) distinguished *B. segura* from *B. belobranchus* by the upper first dorsal fin being yellowish to orange and the middle and lower parts mottled greyish (vs first dorsal fin uniformly dark brown in *B. belobranchus*). Although our examination of multiple *B. segura* specimens indicates that this character seemed to be consistent, the first dorsal fin of *B. belobranchus* specimens was not always uniformly dark brown, and a thin yellowish hue was observed on the upper first dorsal fin of many individuals (Fig. 3). Keith et al. (2012) also distinguished *B. segura* from *B. belobranchus* based on the color of the second dorsal, anal, and pectoral fins, described as yellowish to orange in *B. segura*. However, our examination indicated that these characters are not consistent (Fig. 3). Moreover, Keith et al. (2012) mentioned one character that seemed relatively consistent for distinguishing between the two species: the caudal fin of *B. segura* was described as never having spots, while the caudal fin of *B. belobranchus* always had spots. Our examination also revealed significant variability in this character, as four of nine *B. segura* paratypes, and many non-type specimens of the species we examined had clearly visible spots on the caudal fin (Fig. 4). However, among the many coloration characters given by Keith et al. (2012) to distinguish these two species, two appear to be reliable: the fresh coloration of the first dorsal fin and the lateral surface of the body (Fig. 3). In *B. belobranchus*, the first dorsal fin is typically uniformly mottled dark brown or exhibits a narrow yellowish distal edge, while the lateral surface of body with many dark horizontal lines (one per scale row). In contrast, *B. segura* consistently has a yellowish to orange upper margin on the first dorsal fin, and the body lacks dark horizontal lines.

The fresh and preserved coloration of the two species, including lines, dots, and bands on the lateral surfaces of the head and body, greatly aid in their identification. For example, *B. segura* has three or four oblique brown lines extending from the eye to the posterior edge of the operculum, compared to one or two in *B. belobranchus*. Additionally, the dorsal and lateral surfaces of the head in *B. segura* lack small whitish spots, whereas *B. belobranchus* has many small whitish spots in these areas. The number of dark-brown bands on the body also differs, with *B. segura* having four or five indistinct bands, compared to 3 distinct bands in *B. belobranchus* (Figs 3–5).

In terms of morphology, *B. segura* exhibits a somewhat different head shape compared to *B. belobranchus*. The dorsal profile of the head in *B. segura* is relatively convex, whereas in *B. belobranchus* the dorsal profile is flatter. In addition, *B. segura* apparently attains a smaller adult maximum size than *B. belobranchus*, the maximum recorded length being 79.8 mm SL (vs 130.7 mm SL in the latter species).

Belobranchus belobranchus and *B. segura* both have distributions ranging from western Indonesia to Vanuatu and as far north as Japan (see Distribution and habitat). The *B. belobranchus* specimens previously reported by Kottelat et al. (1993: pl. 62), Suzuki et al. (1995: fig. 6), Keith et al. (2012: fig. 3B), and Vedra et al. (2013: fig. 2A) from Indonesia, Japan, Vanuatu, and the Philippines, respectively, were identified in this study as *B. segura*, having four oblique brown lines extending from the eye to the posterior edge of the operculum and the absence of small whitish spots on the dorsal and lateral surfaces of the head.

Acknowledgements

We extend our gratitude to Mr Sopian Sauri and Mr Yayat Supriatna (MZB) for their assistance with specimen collection. We would like to express our sincere thanks to anonymous reviewers and editors for their constructive comments, which greatly improved an early draft. MA gratefully acknowledges a postdoctoral program provided by Management Talenta of the National Research and Innovation Agency (BRIN).

Additional information

Conflict of interest

The authors have declared that no competing interests exist.

Ethical statement

No ethical statement was reported.

Funding

MA acknowledges financial support from the "Manajemen Talenta" postdoctoral program of the National Research and Innovation Agency (BRIN).

Author contributions

Conceptualization: HH, DFM, KW, AMM; Data curation: MA, NN; Formal analysis: MA, DFM, KW, AMM; Funding acquisition: MA; Supervision: HH, KW, NH; Methodology: MA, NN, KW; Visualization: MA, DFM, KW, AMM; Software: MA, DFM, AMM, NH; Writing - original draft: MA, NN; Writing - review and editing: MA, NN, HH, DFM, KW, AMM, NH; Validation: HH, DFM, KW, AMM, NH.

Author ORCIDs

Muhammad Afrisal https://orcid.org/0000-0002-4809-999X
Nurjirana Nurjirana https://orcid.org/0000-0003-4801-1481
Haryono Haryono https://orcid.org/0000-0002-5143-6790
Daniel Frikli Mokodongan https://orcid.org/0000-0003-4052-0783
Kunto Wibowo https://orcid.org/0000-0003-4465-3022
Abigail Mary Moore https://orcid.org/0000-0002-4122-3740
Nicolas Hubert https://orcid.org/0000-0001-9248-3377

Data availability

All of the data that support the findings of this study are available in the main text.

References

Amick PK, Toko PS (2021) Notes on the ichthyofauna of inland streams of the Whiteman Range, New Britain Island, Papua New Guinea. FishTaxa 20(12): 1–13.

Cuvier G, Valenciennes A (1837) Histoire naturelle des poissons. Tome douzième. Suite du livre quatorzième. Gobioïdes. Livre quinzième. Acanthoptérygiens à pectorales pédiculées 12(1): 344–368.

Dahruddin H, Hutama A, Busson F, Sauri S, Hanner R, Keith P, Hadiaty R, Hubert N (2016) Revisiting the ichthyodiversity of Java and Bali through DNA barcodes: taxonomic coverage, identification accuracy, cryptic diversity and identification of exotic species. Molecular Ecology Resources 17(2): 1–12. https://doi.org/10.1111/1755-0998.12528

Felsenstein J (1985) Confidence limits on phylogenies: an approach using the bootstrap. Evolution 39(4): 783–791. https://doi.org/10.2307/2408678

Fricke R, Allen GR, Andréfouët S, Chen W, Hamel MA, Laboute P, Mana R, Tan HH (2014) Checklist of the marine and estuarine fishes of Madang District, Papua New Guinea, western Pacific Ocean, with 820 new records. Zootaxa 3832(1): 1–247. https://doi.org/10.11646/zootaxa.3832.1.1

Gonzalez JB, Gado VJH, Mantes BG (2023) Freshwater ichthyofauna of wetlands in Tablas Island, Romblon, The Philippines. Academia Journal of Biology 45(1): 121–138. https://doi.org/10.15625/2615-9023/17521

Hasan V, Baptista Y, Mamat NB, Vieira LO, Ottoni FP, South J (2023). Ichthyological note first records of Segura's throatspine gudgeon *Belobranchus segura* Keith, Hadiaty & Lord 2012 (Gobiiformes: Eleotridae) in Sumatra, Indonesia. Cybium 47(4): 473–475.

Higgins DG, Thompson JD, Gibson TJ (1996) Using Clustal for multiple sequence alignments. Methods in Enzymology 266: 383–402. https://doi.org/10.1016/S0076-6879(96)66024-8

Jamandre BW (2023) Freshwater fishes of the Philippines: a provisional checklist. Zootaxa 5301(2): 151–181. https://doi.org/10.11646/zootaxa.5301.2.1

Keith P, Hadiaty RK, Lord C (2012) A new species of *Belobranchus* (Teleostei: Gobioidei: Eleotridae) from Indonesia. Cybium 36(3): 479–484.

Kimura M (1980) A simple method for estimating evolutionary rates of base substitutions through comparative studies of nucleotide sequences. Journal of Molecular Evolution 16(2): 111–120. https://doi.org/10.1007/BF01731581

Kiruba-Sankar R, Raj JP, Saravanan K, Kumar KL, Angel JRJ, Velmurugan A, Roy SD (2018) Invasive species in freshwater ecosystems-threats to ecosystem services. Biodiversity and Climate Change Adaptation in Tropical Islands 9: 257–296. https://doi.org/10.1016/B978-0-12-813064-3.00009-0

Kottelat M, Whitten AJ, Kartikasari SN, Wirjoatmodjo S (1993) Freshwater Fishes of Western Indonesia and Sulawesi. Periplus, Hong Kong, 221 pp.

Larson HK, Murdy EO (2001) Families Eleotridae, Gobiidae. In: Carpenter KE, Niem VH (Eds) FAO Species Identification Guide for Fishery Purposes. The Living Marine Resources of the Western Central Pacific. Vol. 6. Bony Fishes Part 4 (Labridae to Latimeriidae), Estuarine Crocodiles, Sea Turtles, Sea Snakes and Marine Mammals. FAO, Rome, 3574–3603.

Larson HK, Pidgeon B (2004) New records of freshwater fishes from East Timor. The Beagle: Records of the Museums and Art Galleries of the Northern Territory 20: 195–198. https://doi.org/10.5962/p.286327

Larson HK, Buckle D, Lynas J, Story A, Humphrey C (2007) Additional records of fresh water fishes from Timor-Leste, with notes on the fish fauna of the unique land-locked

Irasiquero River system. The Beagle: Records of the Museums and Art Galleries of the Northern Territory 23: 131–135. https://doi.org/10.5962/p.320166

Mennesson MI, Maeda K, Keith P (2019) Evolutionary aspects of cephalic sensory papillae of the Indo-Pacific species of *Eleotris* (Teleostei: Eleotridae). Zoologica Scripta 48(5): 1–13. https://doi.org/10.1111/zsc.12366

Miesen FW, Hüllen S, Hadiaty K, Herder F (2016) An annotated checklist of the inland fishes of Sulawesi. Bonn Zoological Bulletin 64(2): 77–106.

Nakabo (2002) Fishes of Japan with Pictorial Keys to the Species. English Edition. Tokai University Press, Tokyo, 1748 pp.

Parenti P (2021) A checklist of the gobioid fishes of the world (Percomorpha: Gobiiformes). Iranian Journal of Ichthyology 8: 1–480.

Randall JE, Lim KKP (2000) A checklist of the fishes of the South China Sea. Raffles Bulletin of Zoology 8: 569–667.

Roberts TR (1993) The freshwater fishes of Java, as observed by Kuhl and van Hasselt in 1820–1823. Zoologische Verhandelingen 285(1): 1–92.

Sahami FM, Habibie SA (2021) Diversity of species in making up Nike fish schools and a new record of *Eleotris melanosoma* in Tomini Paguyaman Bay, Gorontalo, Indonesia. Biodiversitas: Journal of Biological Diversity 22(12): 5459–5467. https://doi.org/10.13057/biodiv/d221229

Sahami FM, Kepel RC, Olii AH, Pratasik SB (2019) What species make up the Nike fish assemblages at the macrotidal estuary in Gorontalo Bay, Indonesia? F1000Research 8: 1–6. https://doi.org/10.12688/f1000research.19501.1

Saitou N, Nei M (1987) The neighbor-joining method: a new method for reconstructing phylogenetic trees. Molecular Biology and Evolution 4(4): 406–425.

Sakai H, Sato M, Nakamura M (2001) Annotated checklist of the fishes collected from the rivers in the Ryukyu Archipelago. Bulletin of Natural Science Museum, Series A (Zoology) 27(2): 81–139.

Suzuki T, Senou H, Yoshino T, Hosokawa M, Yoshigou H (1995) First record of a gobiid fish *Belobranchus belobranchus* from Japan. IOP Diving News 6(2): 4–6 [in Japanese].

Tamura K, Nei M, Kumar S (2004) Prospects for inferring very large phylogenies by using the neighbor-joining method. Proceedings of the National Academy of Sciences of the United States of America 101(30): 11030–11035. https://doi.org/10.1073/pnas.0404206101

Tamura K, Stecher G, Kumar S (2021) MEGA11: Molecular evolutionary genetics analysis version 11. Molecular Biology and Evolution 38(7): 3022–3027. https://doi.org/10.1093/molbev/msab120

Tjakrawidjaja AH (2002) Freshwater fishes of Manggarai Flores, with the various limnology aspect. Jurnal Ikhtiologi Indonesia 2(2): 15–22.

Tweedley JR, Bird DJ, Potter IC, Gill HS, Miller PJ, O'Donovan G, Tjakrawidjaja AH (2013) Species compositions and ecology of the riverine ichthyofaunas in two Sulawesian islands in the biodiversity hotspot of Wallacea. Journal of Fish Biology 82(6): 1916–1950. https://doi.org/10.1111/jfb.12121

Vedra SA, Ocampo P, de Lara A, Rebancos C, Pacardo E, Briones ND (2013) Indigenous goby population in Mandulog River System and its conservation by communities in Iligan City, Philippines. Journal of Environmental Science and Management 16(2): 11–18. https://doi.org/10.47125/jesam/2013_2/02

Watson RE (1995) Gobies of the genus *Stiphodon* from French Polynesia, with descriptions of two new species (Teleostei: Gobiodei: Sicydiinae). Ichthyological Exploration of Freshwaters 6: 33–48.

ZooKeys 1232: 187–203 (2025)
DOI: 10.3897/zookeys.1232.143944

Research Article

Paucibranchia glemareci sp. nov. (Annelida, Eunicidae), a new species from the French Atlantic continental shelf

Lucas Pinsivy[1,2], Nicolas Lavesque[3], Guillemine Daffe[4], Flore Daramy[3], Pat Hutchings[5,6]

1 *UAR 3113, Observatoire Marin, Université de Brest, 29280 Plouzané, France*
2 *Laboratoire des Sciences de l'Environnement Marin (LEMAR), UMR6539 CNRS/UBO/IRD/IFREMER, Plouzané, France*
3 *Université de Bordeaux, CNRS, Bordeaux INP, EPOC, UMR 5805, Arcachon, France*
4 *CNRS, Université de Bordeaux – Observatoire Aquitain des Sciences de l'Univers, UAR 2567, POREA, Pessac, France*
5 *Australian Museum Research Institute, Australian Museum, NSW 2010, Sydney, Australia*
6 *Marine Ecology Group, School of Natural Sciences, Faculty of Science and Engineering, Wallumattagal Campus, Macquarie University, NSW 2109, Australia*
Corresponding author: Lucas Pinsivy (pinsivy.lucas@orange.fr)

Abstract

In this study, we describe a new species belonging to the genus *Paucibranchia* Molina-Acevedo, 2018 found in the area "La Grande Vasière" on the French Atlantic continental shelf (Bay of Biscay). *Paucibranchia glemareci* **sp. nov.** lives between 100 and 130 m depth on muddy sands. It is easily distinguished from most other European species of the genus by the absence of compound spinigerous chaetae. A key to the European species of the genus *Paucibranchia* is given.

Key words: Bay of Biscay, COI, morphology, taxonomic key

Academic editor: Alexei Tchesunov
Received: 9 December 2024
Accepted: 14 February 2025
Published: 18 March 2025

ZooBank: https://zoobank.org/0A9637CB-31D1-4D68-8B9B-DDFBB6319C71

Citation: Pinsivy L, Lavesque N, Daffe G, Daramy F, Hutchings P (2025) *Paucibranchia glemareci* sp. nov. (Annelida, Eunicidae), a new species from the French Atlantic continental shelf. ZooKeys 1232: 187–203. https://doi.org/10.3897/zookeys.1232.143944

Introduction

The genus *Paucibranchia* was erected to include species of the genus *Marphysa* Quatrefages, 1865, which is characterized by branchiae restricted to a short anterior region of the body (Molina-Acevedo 2018). This group of species was already recognized as a subgroup of *Marphysa* by Fauchald in his study of the order Eunicida (Fauchald 1970) and by Orensanz in his study of the Antarctic and Subantarctic "Eunicemorph" polychaetes (Orensanz 1990).

Worldwide, the genus *Paucibranchia* includes 19 accepted species (Read and Fauchald 2025), with the type species, *Paucibranchia bellii* (Audouin & Milne Edwards, 1833), described from the Chausey Islands in the English Channel. Among them, eight species possess only compound falcigers, whereas all other species have compound spinigers or both falcigers and spinigers.

Several species have been reported from European waters including *P. adenensis* (Gravier, 1900) (type locality: Gulf of Aden, Yemen, Indian Ocean), *P. bellii* (type locality: Chausey Islands, France, English Channel), *P. cinari* (Kurt-Sahin, 2014) (type locality: Sea of Marmara, Turkey, Mediterranean Sea), *P. fallax* (Marion & Bobretzky, 1875) (type locality: Gulf of Marseille, France, Mediterranean Sea), *P. kinbergi* (McIntosh, 1910) (type locality: off Cap

Finisterre, Spain, Atlantic Ocean), and *P. totospinata* (Lu & Fauchald, 1998) (type locality: near Blacksod Bay, Ireland, Atlantic Ocean). *Paucibranchia adenensis* is the only species characterised by having only compound falcigers in European waters. This species, was originally described from the Gulf of Aden and has since been recorded (questionably) within the Mediterranean Sea, from Levantine Sea to the Tyrrhenian Sea (Katsiaras et al. 2014; Katsiaras 2021; Rousou et al. 2023; Langeneck et al. 2024).

In this study, we describe a second European species of the genus *Paucibranchia* having only compound falcigers. It is the first species known from the North-East Atlantic.

Materials and methods

Sampling and morphological analyses

Specimens of the new species where collected from the northern Bay of Biscay (Fig. 1) during the oceanographic cruises APPEAL ATL 19-1 (https://doi.org/10.17600/18001040), APPEAL ATL 19-2 (https://doi.org/10.17600/18001062), and EVHOE 2022 (https://doi.org/10.17600/18001822) in May 2019, September 2019 and October 2022, respectively, using grabs and Rallier du Baty dredges. Samples were fixed in 4% formaldehyde–seawater solution and later transferred to 70% ethanol or directly sieved and frozen onboard for molecular analyses. Specimens of *Paucibranchia bellii* matching well the redescription of this species by Molina-Acevedo (2018) were collected on Brittany's shore for molecular analyses (Table 1, Fig. 1). These specimens were sampled using grabs or hand corer in 2022 or 2023 and fixed in 70% ethanol.

Preserved specimens were examined under a Nikon SMZ25 stereomicroscope and a Nikon Eclipse E400 microscope and photographed with a Nikon DS-Ri 2 camera. Measurements were made with the NIS-Elements Analysis software. Map was made using R v. 4.4.1 statistical software (R Core Team 2024) and the "maps" v. 3.4.2 package (Becker et al. 2023). Information on bathymetry was provided by EMODnet Digital Bathymetry (DTM 2022). Drawings of parapodia were made using Inkscape software. For SEM pictures, selected parapodia along the body were removed from a paratype (AM W.55323), dehydrated in ethanol, critical-point dried, covered with 20 nm of gold, examined under the scanning electron microscope (JEOL JSM 6480LA) and imaged with a secondary detector at Macquarie University, Sydney, Australia.

The terminology used to describe jaws morphology follows Molina-Acevedo and Carrera-Parra (2015) and the terminology of pectinate chaetae follows Carrera-Parra and Salazar-Vallejo (1998) for the relative length of external and internal teeth, Zanol et al. (2014, 2016) for the thickness of the shaft, Molina-Acevedo and Carrera-Parra (2015) for the thickness of the blade, and Glasby et al. (2019) for the size of internal teeth.

Repositories

The studied material is deposited at the Australian Museum, Sydney, Australia (**AM**), the Muséum national d'Histoire naturelle, Paris, France (**MNHN**), and the Station Marine d'Arcachon, Arcachon, France (**SMA**).

Table 1. Terminal taxa used in molecular part of the study (COI gene), with type localities, collection localities, GenBank accession numbers and references.

Species	Type locality	Collection locality	GenBank accession no.	Reference
Eunice cf. *violaceomaculata*	Tortugas, Caribbean	Carrie Bow Cay, Belize	GQ497542	Zanol et al. 2010
Palola viridis	Samoa, Pacific Ocean	Kosrae, Micronesia	GQ497556	Zanol et al. 2010
Leodice rubra	Saint Thomas, Caribbean	Ceara, Brazil	GQ497528	Zanol et al. 2010
M. aegypti	Suez Canal, Egypt	Suez Canal, Egypt	MF196969	Elgetany et al. 2018
M. bifurcata	WA, Australia	Qld, Australia	KX172177	Zanol et al. 2016
M. bifurcata	WA, Australia	Qld, Australia	KX172178	Zanol et al. 2016
M. brevitentaculata	Tobago	Quintana Roo, Mexico	GQ497548	Zanol et al. 2010
M. californica	California, USA	California, USA	GQ497552	Zanol et al. 2010
M. chirigota	Bay of Cadiz, Spain	Bay of Cadiz, Spain	MN816442	Martin et al. 2020
M. chirigota	Bay of Cadiz, Spain	Bay of Cadiz, Spain	MN816443	Martin et al. 2020
M. chirigota	Bay of Cadiz, Spain	Bay of Cadiz, Spain	MN816444	Martin et al. 2020
M. davidattenboroughi	Bass Strait, Australia	Bass Strait, Australia	OQ622195	Lavesque et al. 2023
M. davidattenboroughi	Bass Strait, Australia	Bass Strait, Australia	OQ622196	Lavesque et al. 2023
M. davidattenboroughi	Bass Strait, Australia	Bass Strait, Australia	OQ622197	Lavesque et al. 2023
M. davidattenboroughi	Bass Strait, Australia	Bass Strait, Australia	OQ622198	Lavesque et al. 2023
M. davidattenboroughi	Bass Strait, Australia	Bass Strait, Australia	OQ622199	Lavesque et al. 2023
M. fauchaldi	NT, Australia	NT, Australia	KX172165	Zanol et al. 2016
M. gaditana	Bay of Cadiz, Spain	Bay of Cadiz, Spain	MN816441	Martin et al. 2020
M. hongkongensa	Hong Kong	Hong Kong	MH598525	Wang et al. 2018
M. hongkongensa	Hong Kong	Hong Kong	MH598526	Wang et al. 2018
M. iloiloensis	Iloilo, Philippines	Tigbauan, Philippines	MN106279	Glasby et al. 2019
M. iloiloensis	Iloilo, Philippines	Tigbauan, Philippines	MN106280	Glasby et al. 2019
M. iloiloensis	Iloilo, Philippines	Tigbauan, Philippines	MN106281	Glasby et al. 2019
M. kristiani	NSW, Australia	NSW, Australia	KX172160	Zanol et al. 2016
M. kristiani	NSW, Australia	NSW, Australia	KX172161	Zanol et al. 2016
M. kristiani	NSW, Australia	NSW, Australia	KX172162	Zanol et al. 2016
M. kristiani	NSW, Australia	NSW, Australia	KX172158	Zanol et al. 2016
M. madrasi	Chennai, India	Chennai, India	MT813506	Hutchings et al. 2020
M. madrasi	Chennai, India	Chennai, India	MT813507	Hutchings et al. 2020
M. mossambica	Mozambique	Iloilo, Philippines	KX172164	Zanol et al. 2016
M. mullawa	Qld, Australia	NSW, Australia	KX172166	Zanol et al. 2016
M. mullawa	Qld, Australia	NSW, Australia	KX172167	Zanol et al. 2016
M. mullawa	Qld, Australia	NSW, Australia	KX172168	Zanol et al. 2016
M. mullawa	Qld, Australia	NSW, Australia	KX172176	Zanol et al. 2016
M. papuaensis	Papua New Guinea	Papua New Guinea	OP184050	Lavesque et al. 2022
M. pseudosessiloa	NSW, Australia	NSW, Australia	KY605405	Zanol et al. 2010
M. pseudosessiloa	NSW, Australia	NSW, Australia	KY605406	Zanol et al. 2010
M. regalis	Bermuda	Ceara, Brazil	GQ497562	Zanol et al. 2010
M. sanguinea	Devon, UK	Callot Island, France	GQ497547	Zanol et al. 2010
M. sanguinea	Devon, UK	Cornwall, UK	MK541904	Lavesque et al. 2019
M. sanguinea	Devon, UK	Arcachon Bay, France	MK950853	Lavesque et al. 2019
M. sanguinea	Devon, UK	Brest, France	MK967470	Lavesque et al. 2019
M. sherlockae	Durban, South Africa	Strand, South Africa	MT840349	Kara et al. 2020
M. sherlockae	Durban, South Africa	Strand, South Africa	MT840350	Kara et al. 2020
M. sherlockae	Durban, South Africa	Strand, South Africa	MT840351	Kara et al. 2020
M. tripectinata	Beihai, China	Beihai, China	MN106271	Glasby et al. 2019
M. tripectinata	Beihai, China	Beihai, China	MN106272	Glasby et al. 2019
M. tripectinata	Beihai, China	Beihai, China	MN106273	Glasby et al. 2019

Species	Type locality	Collection locality	GenBank accession no.	Reference
M. tripectinata	Beihai, China	Beihai, China	MN106274	Glasby et al. 2019
M. tripectinata	Beihai, China	Beihai, China	MN106275	Glasby et al. 2019
M. tripectinata	Beihai, China	Beihai, China	MN106276	Glasby et al. 2019
M. tripectinata	Beihai, China	Beihai, China	MN106277	Glasby et al. 2019
M. tripectinata	Beihai, China	Beihai, China	MN106278	Glasby et al. 2019
M. victori	Arcachon Bay, France	Arcachon Bay, France	MG384996	Lavesque et al. 2017
M. victori	Arcachon Bay, France	Arcachon Bay, France	MG384997	Lavesque et al. 2017
M. victori	Arcachon Bay, France	Arcachon Bay, France	MG384998	Lavesque et al. 2017
M. victori	Arcachon Bay, France	Arcachon Bay, France	MG384999	Lavesque et al. 2017
M. victori	Arcachon Bay, France	Mangoku-ura Inlet, Japan	LC467767	Abe et al. 2019
M. victori	Arcachon Bay, France	Sendai Bay, Japan	LC467769	Abe et al. 2019
M. victori	Arcachon Bay, France	Ena Bay, Japan	LC467772	Abe et al. 2019
M. victori	Arcachon Bay, France	China	MT012514	Lavesque et al. 2020
M. viridis	Florida, USA	Ceara, Brazil	GQ497553	Zanol et al. 2010
M. zanolae	Papua New Guinea	Papua New Guinea	OP184049	Lavesque et al. 2022
P. bellii	France	France, Brittany	PV019092	This study
P. bellii	France	France, Brittany	PV019093	This study
P. bellii	France	France, Brittany	PV019094	This study
P. bellii	France	France, Brittany	PV019095	This study
P. disjuncta	California, USA	California, USA	GQ497549	Zanol et al. 2010
P. glemareci sp. nov.	France, Brittany	France, Brittany	PV021094	This study
P. triantennata	Korean Peninsula	Korean Peninsula	OM158712	Kim et al. 2022
P. triantennata	Korean Peninsula	Korean Peninsula	OM158713	Kim et al. 2022

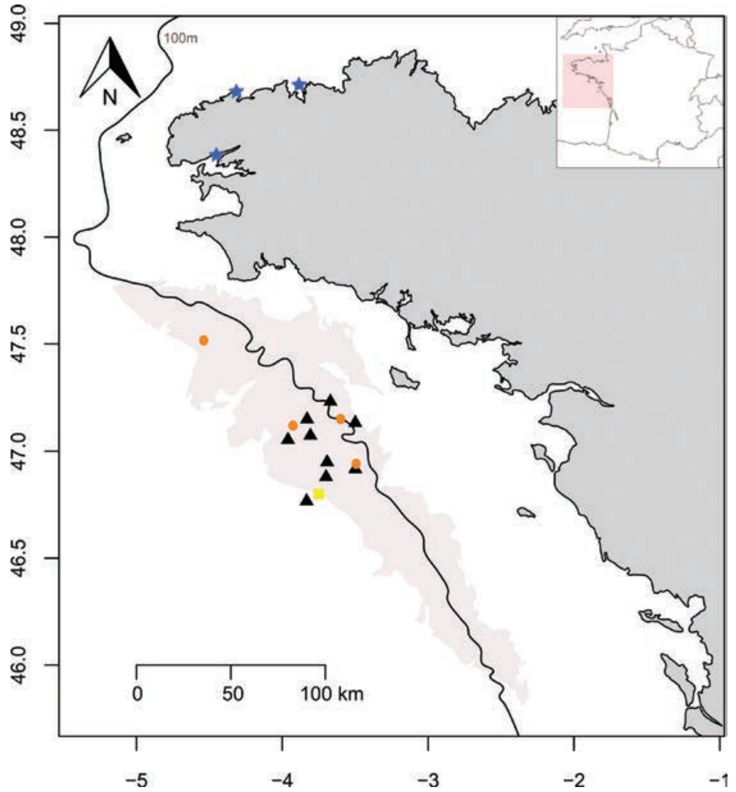

Figure 1. Sampling localities of *Paucibranchia glemareci* sp. nov. on the area of the "Grande Vasière" (in grey on the map). Yellow squares: holotype, orange circles: paratypes, black triangles: additional material collected. The blue stars indicate the sampling localities of the *Paucibranchia bellii* specimens analysed in this study.

Molecular analyses

Extraction of DNA was done with Maxwell (Promega), an automated DNA/RNA isolation, with Maxwell® RSC Blood DNA kit, following protocol supplied by the manufacturers. Approximately 600 bp of the COI (cytochrome c oxidase subunit I) gene were amplified, using the primers polyLCO and polyHCO (Carr et al. 2011). Polymerase Chain Reaction (PCR) was performed with GoTaq® G2 Flexi DNA Polymerase Kit in 20 µL mixtures containing: 4 µL of 5× Green GoTaq® Flexi Reaction Buffer (final concentration of 1×), 1.2 µL of MgCl2 (25 Mm) solution, 0.4 µL of PCR nucleotide mix (final concentration of 0.2 mM each dNTP), 0.2 µl of each primer (final concentration of 1 µM), 0.1 µl of Taq DNA Polymerase (5U/µl), 1 µl template DNA and 12.9 µL of nuclease-free water. The temperature profile was as follows 94 °C / 300 s – (94 °C / 40 s–45 °C / 40 s–72 °C / 1 min)*5 cycles – (94 °C / 40 s–51 °C/ 40 s–72 °C / 1 min)*35 cycles – 72 °C / 300 s – 4 °C. Amplified products were sent to Eurofins Genomics Company to complete double strain sequencing, using same set of primers as used for PCR. Forward and reverse sequence fragments were merged into consensus sequences.

A total of 65 COI sequences were downloaded from GenBank and five sequences obtained during this study, with 67 sequences belonging to *Marphysa* or *Paucibranchia* species, whilst the remaining three were of closely related genera within the Eunicidae and used as outgroups (Table 1). All COI sequences were aligned in Geneious Prime 2025.0.2 using the MUSCLE plugin and default settings. The maximum-likelihood analysis was performed in IQ-TREE 2.2.0 (Trifinopoulos et al. 2016) with the best fitting evolutionary model TIM2+F+I+G4 selected. Bootstrap support was estimated using an ultrafast bootstrap algorithm (UFBoot) (Minh et al. 2013) for 1000 replicates. Pair-wise Kimura 2-parameter (K2P) genetic distance was performed using MEGA v. 7.0.26.

Taxonomic account

Family Eunicidae Berthold, 1827

Genus *Paucibranchia* Molina-Acevedo, 2018

Type species. *Paucibranchia bellii* (Audouin & Milne Edwards, 1833) (type by original designation).

Paucibranchia glemareci sp. nov.

https://zoobank.org/5D00BBF5-7D2A-4821-A913-92864E2394ED
Figs 2–4

Material examined. ***Holotype*****.** France – **Bay of Biscay** • “Grande Vasière”; 46.800, −3.750; depth 128 m; Sep. 2019; APPEAL ATL 19-2 Campaign; station FLLD2; Hamon grab; MNHN-IA 2000-2112 ***Paratypes*****.** France – **Bay of Biscay** • 3 specimens; same collection data as for the holotype; MNHN-IA 2000-2113 and MNHN-IA 2000-2114, AM W.55320 • 1 spec.; “Grande Vasière”; 47.116, −3.910; depth 116 m; Sep. 2019; APPEAL ATL 19-2 Campaign; stn FLLC3; Hamon grab; MNHN-IA 2000-2115 • 1 spec.; “Grande Vasière”; 46.940, −3.480; depth 109 m; Sep. 2019;

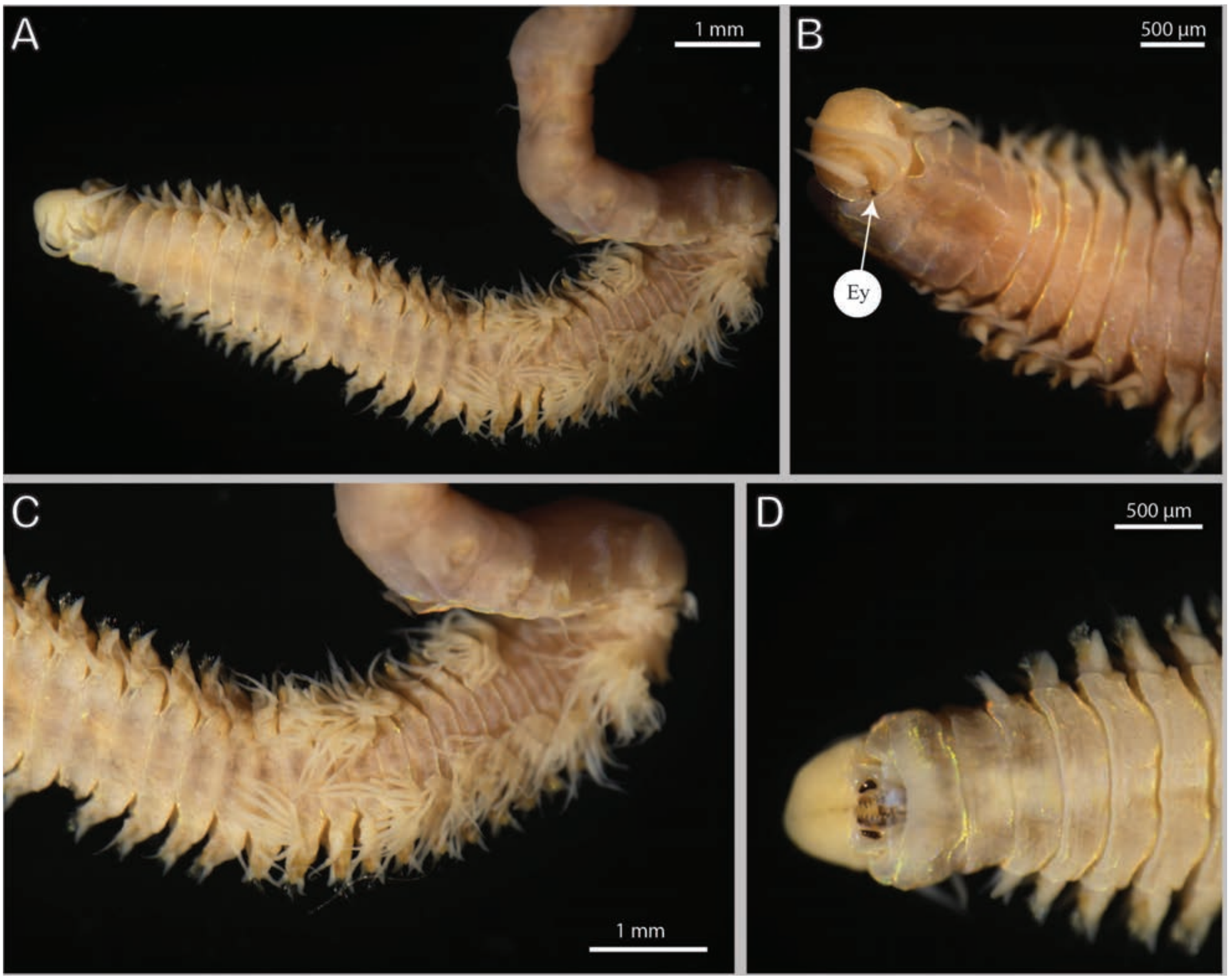

Figure 2. *Paucibranchia glemareci* sp. nov. paratype MNHN-IA 2000-2113 (**A, C, D**), holotype MNHN-IA 2000-2112 (**B**) **A** anterior end, dorsal view **B** anterior end, dorsal view **C** branchial chaetigers, dorsal view **D** anterior end, ventral view. Abbreviations: Ey, eyes.

APPEAL ATL 19-2 Campaign; stn FLLBB1; Hamon grab; MNHN-IA 2000-2116 • 1 spec.; "Grande Vasière"; 47.150, −3.587; depth 101 m; May 2019; APPEAL ATL 19-1 Campaign; stn 5880; Rallier du Baty dredge; MNHN-IA 2000-2117 • 1 spec. (mounted for SEM); same data as for MNHN-IA 2000-2117; AM W.55323.

Additional material for molecular analyses. *Paucibranchia glemareci* sp. nov. France – **Bay of Biscay** • 1 spec.; "Grande Vasière"; 47.514, −4.540; depth 112 m; Oct. 2022; EVHOE 2022 Campaign; stn A1470; Rallier du Baty dredge; GenBank no: PV021094 (COI); SMA-NL298 *Paucibranchia bellii*. France – **Brittany** • 1 spec.; Morlaix Bay, Pierre Noire; 48.708, −3.866; depth 17 m; Feb. 2023; Céline Houbin leg.; Van Veen grab; GenBank no: PV019095 (COI); SMA-NL194 • 2 specs; Brignogan; 48.673, −4.321; Intertidal; Mar. 2023; Jacques Grall leg.; Hand corer; GenBank no: PV019094, PV019092 (COI); SMA-NL192 and SMA-NL183 • 1 spec.; Brest, "du Château" harbour; 48.378, −4.488; depth 5 m; Jul. 2022; Vincent Le Garrec leg.; Day grab; GenBank no: PV019093 (COI); SMA-NL185.

Diagnosis. Prostomium anteriorly rounded with ventral sulcus. Five prostomial appendages arranged in an arc on posterior margin of prostomium. Eyes present, round and dark. Maxillary formula: 1+1, 8+9(8), 9+0, 5(6)+10, 1+1. Branchiae pectinate, present from chaetiger 14–16 to 31–33 with 8–13 long filaments. Dorsal cirri always well developed, slightly longer but thinner in postbranchial chaetigers. Ventral cirri shorter than dorsal cirri, bluntly triangular in pre-branchial region, becoming bluntly conical and thinner through the body. Postchaetal lobes well developed in anterior part of body, becoming inconspicuous from about chaetiger 45 onwards. Three or four light brown aciculae in prebranchial chaetigers, decreasing to two in anterior part of branchial region and to one thereafter. Subacicular hooks light brown, bidentate, commencing from chaetiger 33–37 and present in all following chaetigers; most often one per chaetiger but sometimes two in posterior part of body. Compound chaetae all bidentate falcigers, with two sizes of blades, short ones about 50 µm, long ones about 90 µm. One type of pectinate chaetae identified: narrow, isodont with 2–5 long and slender internal teeth. Posterior pectinate chaetae, if different, unknown. Pygidium unknown.

Description (based on holotype, with variation in parentheses for paratypes). Specimens fixed in alcohol whitish, specimens fixed in formalin pinkish with reddish spots on prostomium, ventrum, parapodia, dorsal cirri, and lateral parts of dorsum (Fig. 2B, C). All specimens incomplete, holotype with 60 chaetigers (longest paratype with about 90 chaetigers), about 26 mm (13.3–47.5 mm) long, 1.9 mm (1.0–2.5 mm) wide at chaetiger 10, including parapodia. Body round in cross section anteriorly (about chaetiger 7–8), dorsoventrally flattened thereafter.

Prostomium anteriorly rounded (slightly conical), without dorsal median sulcus, ventral sulcus deep (Figs 2A–D, 4A, B). Palps and antennae arranged in an arc on posterior margin of prostomium. Median antenna isolated by gap from lateral antennae and palps. Median antenna longer than lateral ones, lateral antennae longer than palps, antennae much longer and palps slightly longer (same size) than prostomium (Figs 2B, 4A). Median antenna reaching chaetiger 3 (2), lateral antennae end of chaetiger 1 (end of second peristomial ring) and palps second peristomial ring (end of first peristomial ring) (Figs 2B, 4A). Ceratostyles and palpostyles slender and tapering, with indistinct cylindrical articulations. Ceratophores and palpophores indistinct. Eyes present, one pair, rounded, black, situated at posterior base of palps and lateral to lateral antennae (Fig. 2B). Separation between both peristomial rings distinct on all sides. First peristomial ring as long as second one dorsally (1½ × as long as second one), twice as long laterally (Figs 2B, 4A). Anterior dorsal margin of first peristomial ring forming convoluting collar on holotype and most paratypes (Fig. 2B). Some small specimens (non-type), less than 1 mm wide, lacking palps.

Maxillary formula as follows: MF = 1+1, 8+9(8), 9+0, 5(6)+10, 1+1, MVI absent (Fig. 3E). Maxillary carrier approximately 2× shorter than MI, rectangular anteriorly, triangular posteriorly, with a pair of rounded wings situated at posterolateral margins. MI forceps-like, without attachment lamellae, with falcal arch developed, rounded; with outer edge of base straight and with curvature in basal inner edge where base of maxillae II is supported. Closing system approximately 5× shorter than MI. MII without attachment lamella but with small basal ligament, teeth triangular, distributed on half of plate length. MIII, single, longer than left MIV, slightly curved, with equal-sized triangular teeth, without attachment lamella but with small basal ligament. Left MIV short (less than half length of right MIV), attachment lamella dark, 2× shorter than corresponding MIV, subtriangular. Right MIV long, with teeth triangular, decreasing in size posteriorly; attachment lamella oval, 3× shorter than corresponding MIV, dark.

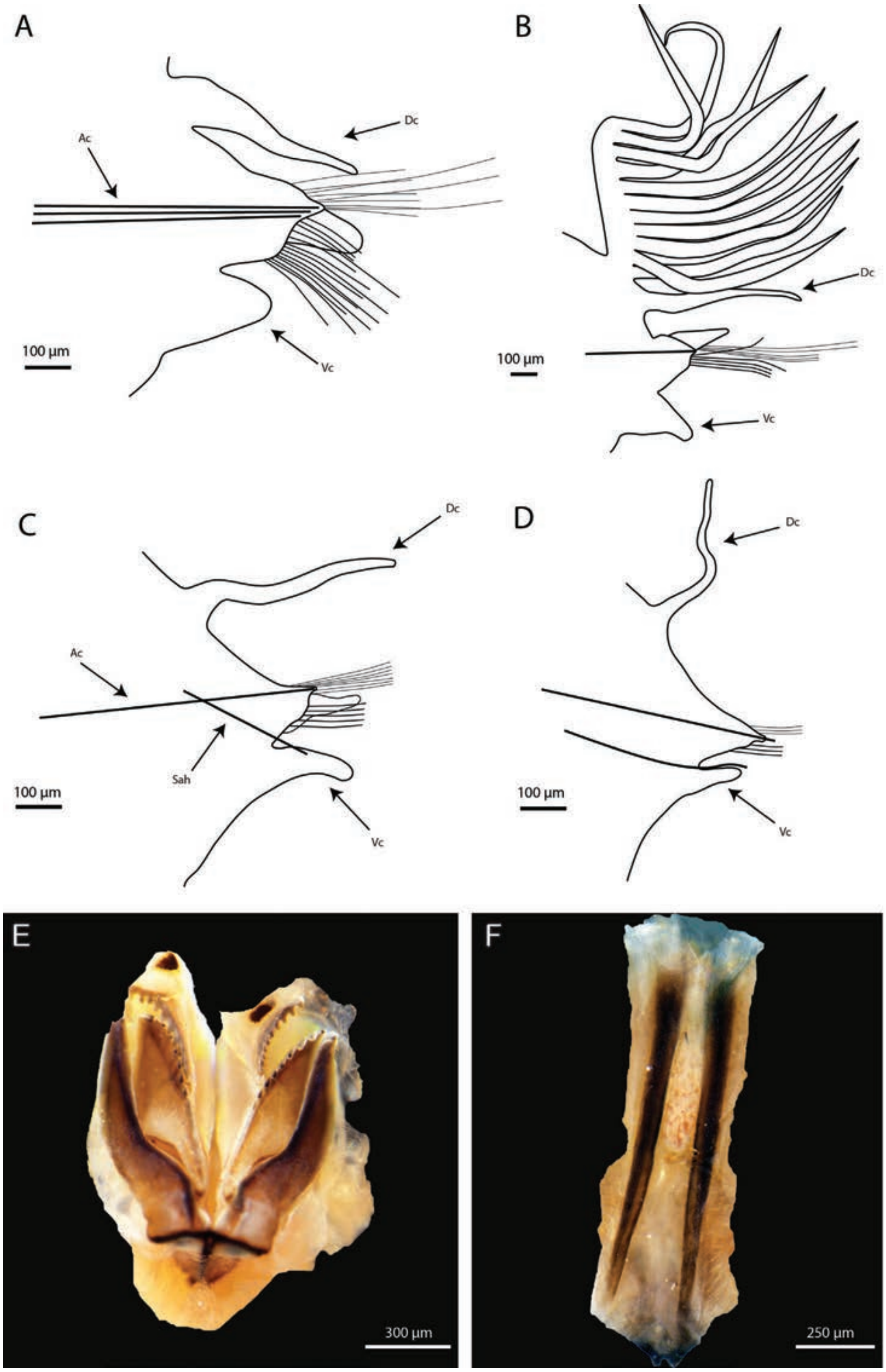

Figure 3. *Paucibranchia glemareci* sp. nov. paratype MNHN-IA 2000-2116 (**A, D**), paratype MNHN-IA 2000-2114 (**B, C, E, F**) **A** parapodia from chaetiger 10 **B** parapodia from chaetiger 22 **C** parapodia from chaetiger 40 **D** parapodia from chaetiger 87 **E** maxilla, dorsal view **F** mandibles, dorsal view. Abbreviations: Ac, acicula; Dc, dorsal cirri; Sah, sub-acicular hook; Vc, ventral cirri.

MV, paired, longer than high, whitish (Fig. 3E). Mandibles light brown, with concentric stripes; longer than MI; cutting plates whitish (Fig. 3F).

First three parapodia smallest; most developed from chaetiger 4 to end of branchial chaetigers, following ones becoming gradually smaller (Fig. 3A–D). Prechaetal lobes as transverse fold in all chaetigers. Postchaetal lobes well developed until end of branchial chaetigers, bluntly triangular in first 9–10 chaetigers, becoming conical, longer and thinner through branchial region, then decreasing in size, becoming inconspicuous from about chaetiger 45. Dorsal cirri conical, tapering, becoming slender and longer from first chaetiger to end of branchial region, then filiform until end of body. Dorsal cirri slightly longer in post-branchial region than in pre-branchial chaetigers. Ventral cirri shorter than dorsal cirri, bluntly triangular in pre-branchial region, becoming bluntly conical and thinner throughout body (Fig. 3A–D).

Branchiae pectinate, commencing from chaetiger 16 (14–15) continuing for a limited number of segments, until chaetiger 32 (31–33); with 8–13 long filaments; branchial filament about 1.5× longer than dorsal cirri where best developed (Figs 2C, 3B). Smaller specimens (non-type) have branchiae starting earlier and less numerous (from chaetiger 11 to 20 for a specimen 0.8 mm wide).

Aciculae light brown with paler blunt tips, three or four aciculae on pre-branchial chaetigers, two on anterior part of branchial region, and one from mid part of branchial region and following chaetigers; some posterior chaetigers with two aciculae. Supra-acicular chaetae with limbate capillaries and pectinates; capillaries present from first chaetiger to posterior ones, numbering up to 15 in anterior chaetigers and up to five in posteriormost chaetigers (Fig. 4C, D). One type of pectinate chaetae identified: narrow, isodont with 2–5 long and slender internal teeth; inner teeth with terminal filaments; outer teeth longer, but of different length (Fig. 4E, F), anterior body with two or three pectinate chaetae by parapodium, mid-body chaetigers with one chaeta, not seen posteriorly (but longest paratype with most of posterior chaetae broken). Subacicular chaetae including compound falcigers and subacicular hooks, compound spinigers absent (Fig. 4C, D). Compound falcigers bidentate, with two sizes of blades, short ones about 50 µm, long ones about 90 µm, commencing from first chaetiger to posterior part, with more than 30 chaetae within parapodium in anterior part, with about seven chaetae in mid-body and four or five on last chaetigers (Fig. 4C, D). Subacicular hooks (SAH) light brown, bidentate, commencing from chaetiger 35 (33–37) and present in all chaetigers thereafter, ventral to bundle of falcigers, generally one per parapodium; few posterior chaetigers with two hooks (Fig. 4D). Smaller specimens (non-type) have SAH starting earlier (at 19th chaetiger for a specimen of 0.6 mm wide and at 29th for a specimen 0.8 mm wide).

Pygidium unknown.

Etymology. This species is named after Michel Glemarec for his major contribution to the ecology of the Grande Vasière and the taxonomy of polychaetes.

Type locality. Northeastern Atlantic Ocean, Bay of Biscay, “Grande Vasière”, Station FLLD2 (46.800, −3.750, 128 m depth).

Distribution. Known from the “Grande Vasière” area.

Habitat. Fine sands to muddy sands, between 100 and 130 m depth.

Remarks. *Paucibranchia glemareci* sp. nov. is easily distinguished from other species described from Europe by the presence of compound falcigers and the absence of compound spinigers. It is, however, very close to *P. adenensis* (Gravier, 1900), described from Yemen and (questionably) later reported from the Mediterranean Sea (Katsiaras et al. 2014; Katsiaras 2021; Rousou et al. 2023; Langeneck et al. 2024). These two species share the presence of rounded eyes, only falcigerous compound chaetae, same branchial distribution and similar looking bidentate sub-acicular hooks. They can however be separated

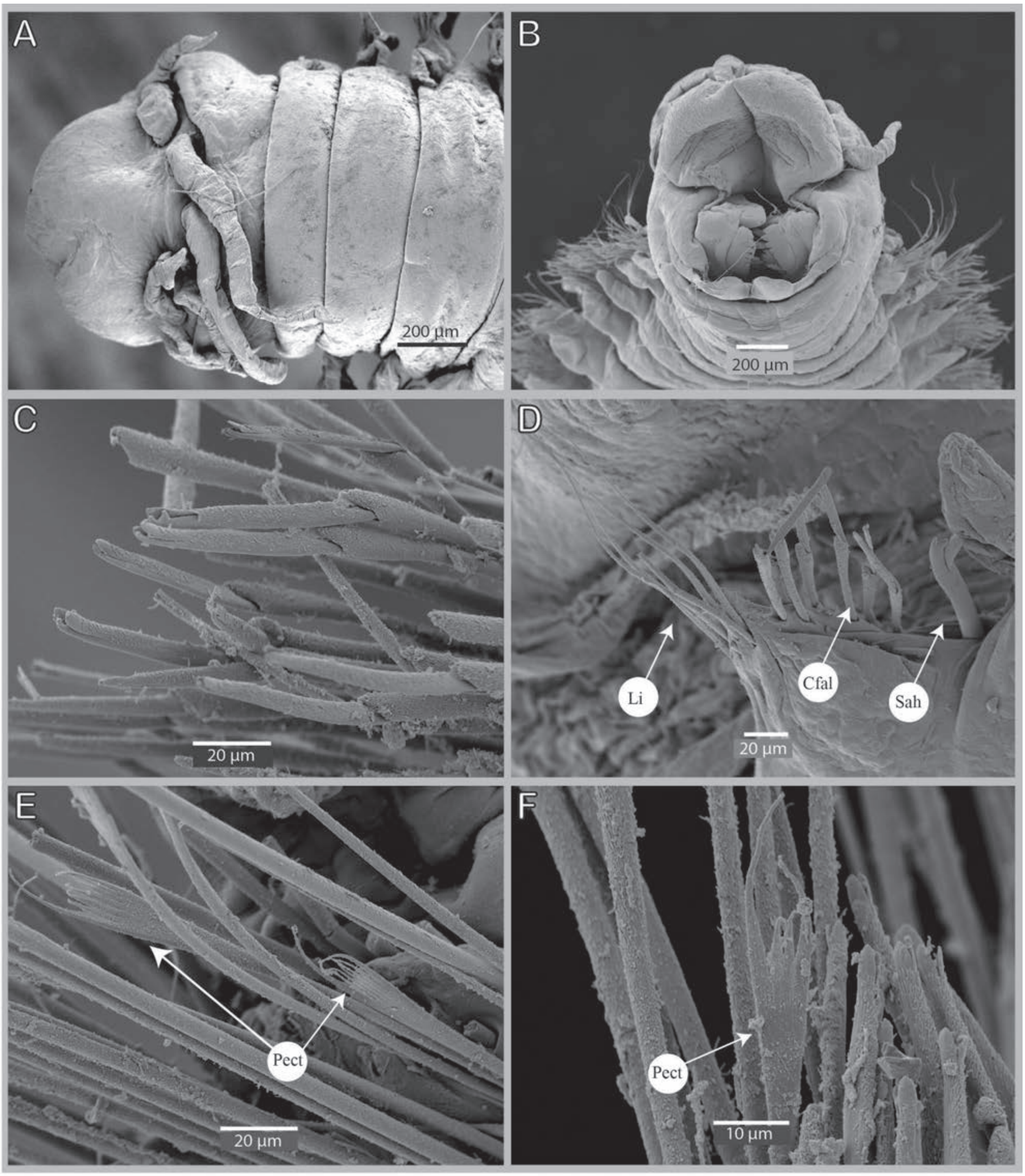

Figure 4. *Paucibranchia glemareci* sp. nov. paratype AM W.55323, SEM **A** anterior end, dorsal view **B** anterior end, ventral view **C** compound falcigers, chaetiger 9 **D** parapodia, chaetiger 47 **E** pectinate chaetae, chaetiger 6 **F** pectinate chaetae, chaetiger 2. Abbreviations: Cfal, compound falciger; Li, limbate chaetae; Pect, pectinate chaetae; Sah, Sub-acicular hook.

based on morphological characters. According to the redescription of *P. adenensis* by Molina-Acevedo (2018), *P. glemareci* sp. nov. differs by its maxillary formula (1+1, 8+9(8), 9+0, 5(6)+10, 1+1) versus (1+1, 7(8)+7(8), 6(7)+0, 4(5)+7(8-9), 1+1) for *P. adenensis*, the number of aciculae on prebranchial chaetigers (up to four for *P. glemareci* sp. nov. versus up to two for *P. adenensis*) and shorter blades on anterior compound falcigers (50 and 90 µm for *P. glemareci* sp. nov. versus 90 and 105 µm for *P. adenensis*). Moreover, both species appear to have a different colouration after fixation; *P. glemareci* sp. nov. presents reddish spots on most specimens, but never brown colouration as observed on some non-type specimens of *P. adenensis* by Molina-Acevedo (2018).

Worldwide, *P. glemareci* sp. nov. shares the absence of compound spinigers with *P. conferta* (Moore, 1911), *P. gathofi* Molina-Acevedo, 2018, *P. gemmata* (Mohammad, 1973), *P. miroi* Molina-Acevedo, 2018, *P. patriciae* Molina-Acevedo, 2018, *P. purcellana* (Willey, 1904), *P. triantennata* Kim, Soh & Jeong, 2022 and with an undescribed species (*Paucibranchia* sp. 2 of Molina-Acevedo 2018). However, it differs from *P. conferta*, *P. gemmata*, *P. miroi*, *P. patriciae*, *P. purcellana*, and *P.* sp. 2 by the chaetiger on which the branchiae start (chaetiger 14–16 for *P. glemareci* sp. nov. versus chaetiger 22 for *P. gemmata*, chaetiger 10–12 for *P. triantennata* and chaetiger 7 or 8 for the other five species) and from *P. gathofi* by the chaetiger where subacicular hooks start (chaetiger 33–37 for *P. glemareci* sp. nov. versus chaetiger 17–30 for *P. gathofi*).

Paucibranchia glemareci sp. nov. may have been mistaken in the past for *P. bellii* (as *Marphysa bellii*), the only name for specimens with pectinate branchiae restricted to the anterior part of the body in the early literature (e.g. Fauvel 1923). Thus, old records of *P. bellii* from offshore area in the Bay of Biscay should be regarded as doubtful.

Molecular analyses

COI gene was successfully sequenced and published at NCBI GenBank for one specimen of the new species *Paucibranchia glemareci* sp. nov. and for four specimens of *Paucibranchia bellii* collected from the same geographical area (Table 1, Figs 1, 5). The new species *P. glemareci* sp. nov. is clearly different from other species of the *Marphysa*-*Paucibranchia* group for which molecular data are available. With an interspecific distance (K2P) of 19.2%, *P. glemareci* sp. nov. is relatively close to *Marphysa regalis* Verrill, 1900 described from Bermuda. *Paucibranchia glemareci* sp. nov. lives in the same geographical area as *P. bellii*, and their interspecific distance is 20.6% (standard error: 0.15%) (Fig. 5). *Paucibranchia glemareci* sp. nov. is separated from the main *Marphysa* clade by a mean intraspecific distance of 22.3% (standard error: 0.2%) (Fig. 5).

Based on our molecular analysis, the status of the genera *Marphysa* and *Paucibranchia* is still not clear. Indeed, *Paucibranchia* species seem to be separated from the main *Marphysa* clade, but *M. regalis* is a sister species of *P. glemareci* sp. nov., and *Marphysa papuaensis* Lavesque, Daffe, Glasby, Hourdez & Hutchings, 2022 is isolated. When they described *M. papuaensis*, Lavesque et al. (2022) hesitated as to which genus it should be assigned to as this species has a limited number of branchial segments. However, the maxillae I (Lavesque et al. 2022: fig. 6D) are more similar to those of *Marphysa* (the base arch lacking a curvature in the basal inner edge) than those of *Paucibranchia* (the base straight with a curvature in the basal inner edge) (Molina-Acevedo 2018). A phylogenetic study based on molecular data of the genera *Marphysa*, *Paucibranchia*, and closely related *Treadwellphysa* Molina-Acevedo & Carrera-Parra, 2017 is really necessary to test their monophyly and placement within Eunicidae (Zanol, pers. comm.).

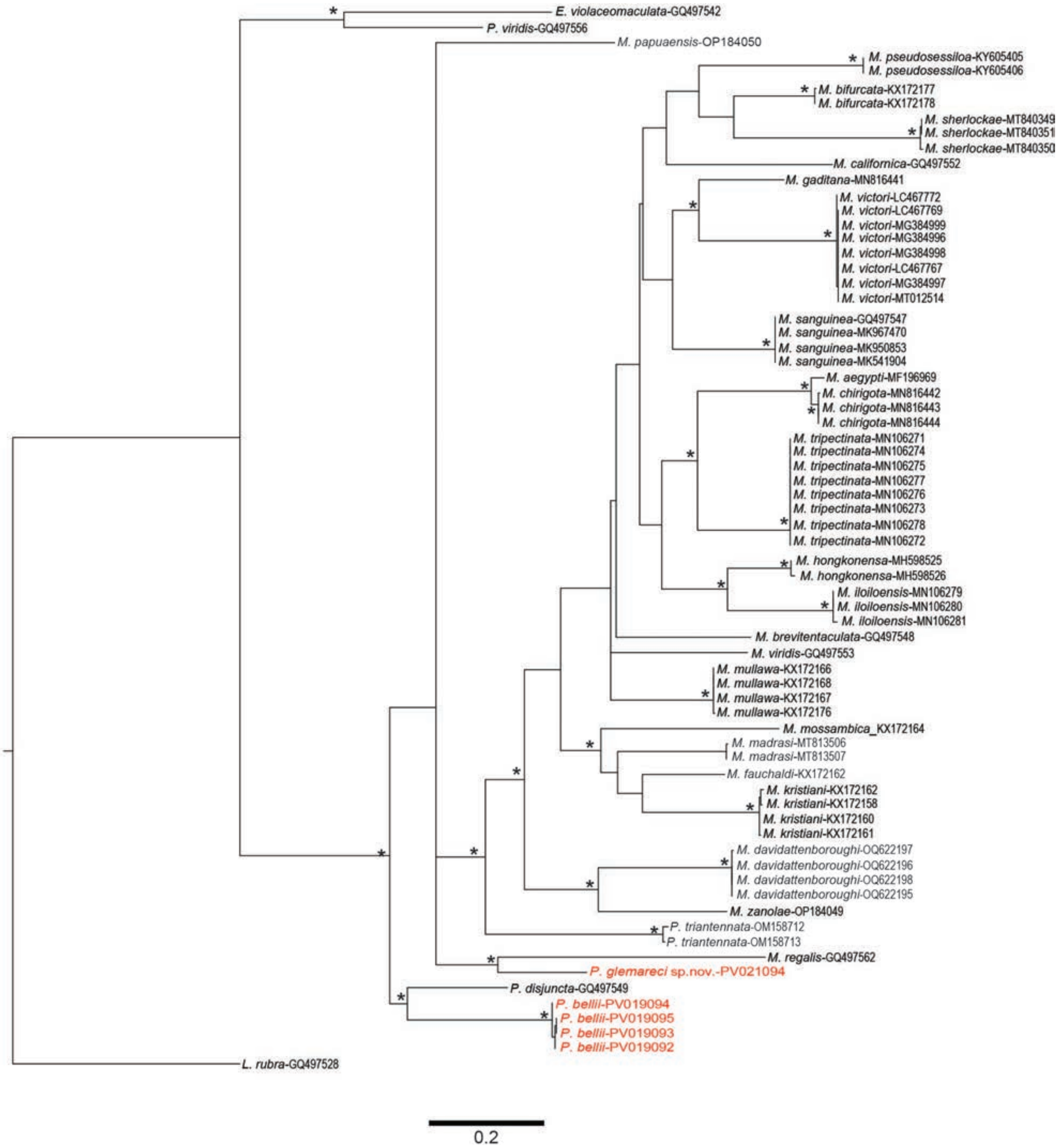

Figure 5. Maximum-likelihood tree of *Marphysa* and *Paucibranchia* species based on COI sequences. Asterisks indicate the bootstrap support values of the ML analysis > 70%. Text in red indicates specimens analysed in this study.

Key to the European species of *Paucibranchia*

1 Branchiae present over most of the body, prostomium anteriorly bilobed.. ....***Marphysa* Quatrefages, 1865**

– Branchiae limited to anterior part of the body, prostomium anteriorly rounded ***Paucibranchia* Molina-Acevedo, 2018**...**2**

2 Composed chaetae only spinigers................. ***P. kinbergi* (McIntosh, 1910)**

– Composed chaetae only falcigers...**3**

– Composed chaetae both spinigers and falcigers **4**

3 Up to four aciculae on pre-branchial chaetigers, presence of reddish spots in preserved specimens..***P. glemareci* sp. nov.**

– Up to two (three in Mediterranean questionably identified specimens) aciculae on pre-branchial chaetigers. With or without brown colouration .. ..***P. adenensis* (Gravier, 1900)**

4 Branchiae with up to two filaments... ***P. fallax* (Marion & Bobretzky, 1875)**

– Branchiae with six or more filaments...**5**

5 Falcigerous composed chaetae on posterior chaetigers only .... ***P. cinari* (Kurt-Sahin, 2014)**

– Falcigerous composed chaetae along body..**6**

6 Spinigerous composed chaetae on anterior body only (up to chaetiger 53 max) ....***P. bellii* (Audouin & Milne-Edwards, 1833)**

– Spinigerous composed chaetae all along body ....***P. totospinata* (Lu & Fauchald, 1998)**

Acknowledgements

The authors thank the crew member of the R/V Côtes de la Manche and Thalassa, François Le Loc'h, responsible of the scientific project APPEAL, and all people involved in the field sampling and samples processing. We also thank Céline Houbin, Jacques Grall, and Vincent Le Garrec for providing additional material for molecular analyses, Sue Lindsay (Macquarie University, Sydney) for taking SEM pictures, and João Gil (University of Algarve) for sharing bibliography and valuable information. Finally, we would like to thank the two anonymous reviewers for their pertinent comments that improve the manuscript.

Additional information

Conflict of interest

The authors have declared that no competing interests exist.

Ethical statement

No ethical statement was reported.

Funding

No funding was reported.

Author contributions

LP: sampling, conceptualization, formal analysis, investigation, methodology, writing original draft. NL and PH: supervision, validation, writing (review & editing). GD & FD: molecular analysis, methodology, writing (review & editing).

Author ORCIDs

Lucas Pinsivy https://orcid.org/0009-0006-6854-1374
Nicolas Lavesque https://orcid.org/0000-0001-5701-2393
Guillemine Daffe https://orcid.org/0000-0002-7085-3151
Flore Daramy https://orcid.org/0000-0002-1141-4554
Pat Hutchings https://orcid.org/0000-0001-7521-3930

Data availability

All of the data that support the findings of this study are available in the main text or Supplementary Information.

References

Abe H, Tanaka M, Taru M, Abe S, Nishigaki A (2019) Molecular evidence for the existence of five cryptic species within the Japanese species of *Marphysa* (Annelida: Eunicidae) known as "Iwa-mushi." Plankton and Benthos Research 14(4): 303–314. https://doi.org/10.3800/pbr.14.303

Audouin JV, Milne Edwards H (1833) Classification des annélides, et description de celles qui habitent les côtes de la France. Annales des Sciences Naturelles 1(28): 187–247. https://doi.org/10.5962/bhl.part.8010

Becker RA, Minka TP, Deckmyn A (2023) maps: draw geographical maps. R package version 3.4.2. https://CRAN.R-project.org/package=maps

Berthold AA (1827) Naturliche Familien des Thierreichs aus dem Franzosischen. Mit Anmerkungen und Zusätzen. Landes-Industrie Comptoirs, Weimar, 606 pp. https://doi.org/10.5962/bhl.title.11652

Carr CM, Hardy SM, Brown TM, Macdonald TA, Hebert PDN (2011) A tri-oceanic perspective: DNA barcoding reveals geographic structure and cryptic diversity in Canadian Polychaetes. PLoS ONE 6(7): e22232. https://doi.org/10.1371/journal.pone.0022232

Carrera-Parra LF, Salazar-Vallejo SI (1998) A new genus and 12 new species of Eunicidae (Polychaeta) from the Caribbean Sea. Journal of the Marine Biological Association of the United Kingdom 78(1): 145–182. https://doi.org/10.1017/S0025315400040005

Elgetany AH, El-Ghobashy AE, Ghoneim AM, Struck TH (2018) Description of a new species of the genus *Marphysa* (Eunicidae), *Marphysa aegypti* sp. n., based on molecular and morphological evidence. Invertebrate Zoology 15(1): 71–84. https://doi.org/10.15298/invertzool.15.1.05

EMODnet Bathymetry Consortium (2022) EMODnet Digital Bathymetry (DTM 2022). https://doi.org/10.12770/ff3aff8a-cff1-44a3-a2c8-1910bf109f85

Fauchald K (1970) Polychaetous annelids of the families Eunicidae, Lumbrineridae, Iphitimidae, Arabellidae, Lysaretidae and Dorvilleidae from western Mexico. Allan Hancock Monographs in Marine Biology 5: 1–335. https://repository.si.edu/handle/10088/3457

Fauvel P (1923) Polychètes errantes. Faune de France 5. Librairie de la Faculté des Sciences, Paris, 488 pp. https://archive.org/details/FauneDeFrance5

Glasby CJ, Mandario MAE, Burghardt I, Kupriyanova E, Gunton LM, Hutchings PA (2019) A new species of the *sanguinea*-group Quatrefages, 1866 (Annelida: Eunicidae: *Marphysa*) from the Philippines. Zootaxa 4674(2): 264–282. https://doi.org/10.11646/zootaxa.4674.2.7

Gravier C (1900) Contribution à l'étude des annélides polychètes de la mer Rouge. Première partie. Nouvelles Archives du Muséum d'Histoire Naturelle, Paris, Series 4(2): 137–282. https://biodiversitylibrary.org/page/36872698

Hutchings P, Lavesque N, Priscilla L, Daffe G, Malathi E, Glasby CJ (2020) A new species of *Marphysa* (Annelida: Eunicida: Eunicidae) from India, with notes on previously described or reported species from the region. Zootaxa 4852(3): 285–308. https://doi.org/10.11646/zootaxa.4852.3.2

Kara J, Molina-Acevedo IC, Zanol J, Simon C, Idris I (2020) Morphological and molecular systematic review of *Marphysa* Quatrefages, 1865 (Annelida: Eunicidae) species from South Africa. PeerJ 8: e10076. https://doi.org/10.7717/peerj.10076

Katsiaras N (2021) Biodiversity of benthic communities on coastal ecosystems, with a focus on biogenic habitats. PhD Thesis, University of the Aegean, Mytilene, Lesvos Island, Greece. https://doi.org/10.12681/eadd/50831

Katsiaras N, Simboura N, Koutsoubas D (2014) The rare subgroup C1 of *Marphysa* (Polychaeta, Eunicidae): re-description of species and first records in the Mediterranean Sea. Zootaxa 3873(3): 201–217. https://doi.org/10.11646/zootaxa.3873.3.1

Kim DH, Soh HY, Jeong M-K (2022) First Report of a *Paucibranchia* (Polychaeta, Eunicidae) species without lateral palps in Korean subtidal waters, with genetic evidence for its taxonomic position. Diversity 14(12): 1131. https://doi.org/10.3390/d14121131

Kurt Sahin G (2014) *Marphysa cinari*, a new species of Eunicidae (Polychaeta) from the coasts of Turkey (eastern Mediterranean) and re-descriptions of *Marphysa kinbergi* McIntosh, 1910 and *Marphysa disjuncta* Hartman, 1961. Journal of Natural History 48(33–34): 1989–2006. https://doi.org/10.1080/00222933.2014.905125

Langeneck J, Bertasi F, Grossi L, Lefons F, Vani D, Verni S, Musco L, Castelli A (2024) New records of one cryptogenic and two questionable alien species of polychaetes (Annelida) in Italian waters. Acta Adriatica 65(2): 153–168. https://doi.org/10.32582/aa.65.2.3

Lavesque N, Daffe G, Bonifácio P, Hutchings P (2017) A new species of the *Marphysa sanguinea* complex from French waters (Bay of Biscay, NE Atlantic) (Annelida, Eunicidae). ZooKeys 716: 1–17. https://doi.org/10.3897/zookeys.716.14070

Lavesque N, Daffe G, Grall J, Zanol J, Gouillieux B, Hutchings P (2019) Guess who? On the importance of using appropriate name: case study of *Marphysa sanguinea* (Montagu, 1813). ZooKeys 859: 1–15. https://doi.org/10.3897/zookeys.859.34117

Lavesque N, Hutchings P, Abe H, Daffe G, Gunton L, Glasby C (2020) Confirmation of the exotic status of *Marphysa victori* Lavesque, Daffe, Bonifácio & Hutchings, 2017 (Annelida) in French waters and synonymy of *Marphysa bulla* Liu, Hutchings & Kupriyanova, 2018. Aquatic Invasions 15(3): 355–366. https://doi.org/10.3391/ai.2020.15.3.01

Lavesque N, Daffe G, Glasby C, Hourdez S, Hutchings P (2022) Three new deep-sea species of *Marphysa* (Annelida, Eunicida, Eunicidae) from Papua New Guinea (Bismarck and Solomon seas). ZooKeys 1122: 81–105. https://doi.org/10.3897/zookeys.1122.89990

Lavesque N, Zanol J, Daffe G, Flaxman B, Hutchings P (2023) Two new species of *Marphysa* (Annelida, Eunicidae) from southern Australia. Zootaxa 5277(1): 113–130. https://doi.org/10.11646/zootaxa.5277.1.5

Lu H, Fauchald K (1998) *Marphysa belli* (Polychaeta: Eunicidae) and two related species, *Marphysa oculata* and *M. totospinata*, a new species, with notes on size-dependent features. Proceedings of the Biological Society of Washington 111(4): 829–842. https://repository.si.edu/handle/10088/3449

Marion AF, Bobretzky N (1875) Étude des annélides du golfe de Marseille. Annales des Sciences Naturelles, Paris 6(2): 1–106. http://www.biodiversitylibrary.org/page/33155516

Martin D, Gil J, Zanol J, Meca MA, Pérez Portela R (2020) Digging the diversity of Iberian bait worms *Marphysa* (Annelida, Eunicidae). PLoS ONE 15(1): e0226749. https://doi.org/10.1371/journal.pone.0226749

McIntosh WC (1910) A monograph of the British annelids. Polychaeta. Syllidae to Ariciidae. Ray Society of London 2(2): 233–524. https://doi.org/10.5962/bhl.title.54725

Minh BQ, Nguyen MAT, Von Haeseler A (2013) Ultrafast approximation for phylogenetic bootstrap. Molecular Biology and Evolution 30(5): 1188–1195. https://doi.org/10.1093/molbev/mst024

Mohammad M-BM (1973) New species and records of polychaete annelids from Kuwait, Arabian Gulf. Zoological Journal of the Linnean Society 52(1): 23–44. https://doi.org/10.1111/j.1096-3642.1973.tb01876.x

Molina-Acevedo IC (2018) Morphological revision of the subgroup 1 Fauchald, 1970 of *Marphysa* de Quatrefages, 1865 (Eunicidae: Polychaeta). Zootaxa 4480(1): 1–125. https://doi.org/10.11646/zootaxa.4480.1.1

Molina-Acevedo IC, Carrera-Parra LF (2015) Reinstatement of three species of the *Marphysa sanguinea* complex (Polychaeta: Eunicidae) from the Grand Caribbean Region. Zootaxa 3925(1): 37–55. https://doi.org/10.11646/zootaxa.3925.1.3

Molina-Acevedo IC, Carrera-Parra LF (2017) Revision of *Marphysa* de Quatrefages, 1865 and some species of *Nicidion* Kinberg, 1865 with the erection of a new genus (Polychaeta: Eunicidae) from the Grand Caribbean. Zootaxa 4241(1): 1–62. https://doi.org/10.11646/zootaxa.4241.1.1

Moore JP (1911) The polychaetous annelids dredged by the U.S.S. "Albatross" off the coast of Southern California in 1904. III. Euphrosynidae to Goniadidae. Proceedings of the Academy of Natural Sciences of Philadelphia 63: 234–318. https://www.biodiversitylibrary.org/page/26283655

Orensanz JM (1990) The eunicemorph polychaete annelids from Antarctic and Subantarctic seas: with addenda to the Eunicemorpha of Argentina, Chile, New Zealand, Australia, and the southern Indian Ocean. Antarctic Research Series 52: 1–183. https://doi.org/10.1029/AR052p0001

Quatrefages A (1865) Histoire naturelle des annelés marins et d'eau douce. Annélides et géphyriens. Tome premier. Librairie Encyclopédique de Roret, Paris, 588 pp. https://doi.org/10.5962/bhl.title.122818

R Core Team (2024) R: a language and environment for statistical computing. R Foundation for Statistical Computing, Vienna, Austria. https://www.R-project.org/

Read G, Fauchald K (Ed.) (2025) World Polychaeta Database. *Paucibranchia* Molina-Acevedo, 2018. World Register of Marine Species. https://www.marinespecies.org/aphia.php?p=taxdetails&id=1297882 [Accessed on 2025–01–27]

Rousou M, Langeneck J, Apserou C, Arvanitidis C, Charalambous S, Chrysanthou K, Constantinides G, Dimitriou PD, García Gómez SC, Hadjieftychiou SI, Katsiaras N, Kleitou P, Kletou D, Küpper FC, Louizidou P, Martins R, Moraitis ML, Papageorgiou N, Papatheodoulou M, Petrou A, Xevgenos D, Vasiliades L, Voultsiadou E, Chintiroglou CC, Castelli A (2023) Polychaetes (Annelida) of Cyprus (Eastern Mediterranean Sea): an updated and annotated checklist including new distribution records. Diversity 15(8): 941. https://doi.org/10.3390/d15080941

Trifinopoulos J, Nguyen L-T, von Haeseler A, Minh BQ (2016) W-IQ-TREE: a fast online phylogenetic tool for maximum likelihood analysis. Nucleic Acids Research 44(W1): W232–W235. https://doi.org/10.1093/nar/gkw256

Verrill AE (1900) Additions to the Turbellaria, Nemertina, and Annelida of the Bermudas, with revisions of some New England genera and species. Transactions of the Connecticut Academy of Arts and Sciences 10(2): 595–671. https://doi.org/10.5962/bhl.part.7035

Wang Z, Zhang Y, Qiu JW (2018) A new species in the *Marphysa sanguinea* Complex (Annelida, Eunicidae) from Hong Kong. Zoological Studies 57(48): 1–13. https://doi.org/10.6620/ZS.2018.57-48

Willey A (1904) Littoral Polychaeta from the Cape of Good Hope. Transactions of the Linnean Society of London, Series 2, Zoology 9(6): 255–268. https://doi.org/10.1111/j.1096-3642.1904.tb00450.x

Zanol J, Halanych KM, Struck TH, Fauchald K (2010) Phylogeny of the bristle worm family Eunicidae (Eunicida, Annelida) and the phylogenetic utility of noncongruent 16S, COI and 18S in combined analyses. Molecular Phylogenetics and Evolution 55(2): 660–676. https://doi.org/10.1016/j.ympev.2009.12.024

Zanol J, Halanych KM, Fauchald K (2014) Reconciling taxonomy and phylogeny in the bristleworm family Eunicidae (Polychaeta, Annelida). Zoologica Scripta 43(1): 79–100. https://doi.org/10.1111/zsc.12034

Zanol J, Da Silva TDSC, Hutchings P (2016) *Marphysa* (Eunicidae, Polychaeta, Annelida) species of the *sanguinea* group from Australia, with comments on pseudo-cryptic species. Invertebrate Biology 135(4): 328–344. https://doi.org/10.1111/ivb.12146

Supplementary material 1

Metadata of specimens examined in the study

Authors: Lucas Pinsivy

Data type: csv

Explanation note: Metadata of specimens examined in the study with specimens registration numbers, type status, associated COI sequences in genbank, taxon name, geolocation and depth.

Link: https://doi.org/10.3897/zookeys.1232.143944.suppl1

ZooKeys 1232: 205–236 (2025)
DOI: 10.3897/zookeys.1232.142699

Research Article

Water mite diversity from southwestern Türkiye through the lens of the DNA barcodes, with the description of one new species (Acari, Hydrachnidia)

Vladimir Pešić[1], Andrzej Zawal[2], Pınar Gülle[3], İskender Gülle[3], Milica Jovanović[1], Aleksandra Bańkowska[4], Stanisław Musielak[2], Harry Smit[5,6]

1 Department of Biology, University of Montenegro, Džordža Vašingtona b.b., 81000 Podgorica, Montenegro
2 Institute of Marine and Environmental Sciences, Center of Molecular Biology and Biotechnology, University of Szczecin, Wąska 13, 71–415 Szczecin, Poland
3 Faculty of Science and Arts, Burdur Mehmet Akif Ersoy University, Burdur, Turkiye
4 Institute of Biology, University of Szczecin, Wąska 13, 71-415 Szczecin, Poland
5 Naturalis Biodiversity Center, P.O. Box 9517, 2300 RA Leiden, Netherlands
6 Museums Victoria Research Institute, Museums Victoria, GPO Box 666, Melbourne, VIC 3001, Australia
Corresponding author: Vladimir Pešić (vladopesic@gmail.com)

Academic editor: Fernando Jacinavicius
Received: 25 November 2024
Accepted: 13 February 2025
Published: 18 March 2025

ZooBank: https://zoobank.org/B7DFF2E2-C37B-4283-969B-A7648C555734

Citation: Pešić V, Zawal A, Gülle P, Gülle İ, Jovanović M, Bańkowska A, Musielak S, Smit H (2025) Water mite diversity from southwestern Türkiye through the lens of the DNA barcodes, with the description of one new species (Acari, Hydrachnidia). ZooKeys 1232: 205–236. https://doi.org/10.3897/zookeys.1232.142699

Abstract

This study presents the molecular and morphological results from an analysis of water mites collected in southwestern Türkiye. 83 COI barcodes are provided, clustered into 40 BINs, with 23 BINs being unique and deposited for the first time in the Barcode of Life Data Systems (BOLD). The first DNA barcodes for eight water mite species are uploaded into the BOLD database. In total, 34 water mite species were identified and one of them, *Iranothyas marismortui* (Gerecke, 1999) is newly reported from Türkiye. *Iranothyas alhajarica* Pešić, Gerecke & Smit, 2009 is excluded from the fauna of Türkiye. *Sperchon fundamentalis* Bader & Sepasgozarian, 1980, a species previously synonymized with *S. glandulosus* Koenike, 1886 is resurrected as a valid species. One species, *Atractides turani* Pešić, Zawal, Gülle & Smit, **sp. nov**. (Hygrobatidae), is described as new to science.

Key words: Cytochrome c oxidase subunit I (COI), new records, new species, running waters, springs, taxonomy, water mites

Introduction

The knowledge of water mites from Türkiye is still insufficient. The checklist published by Erman et al. (2010, 2019) listed 335 species in 62 genera and 25 families and summarized all previous research on water mites in Türkiye. In recent years, an increased number of regional and/or international DNA barcoding initiatives resulted in the formation and curation of water mites DNA barcode libraries (e.g., Montenegro, Pešić et al. 2021a; Norway, Gerecke et al. 2022; Corsica, Pešić and Smit 2022; Portugal, Pešić et al. 2024). The public dataset of barcodes of water mites of Iran and Türkiye (available at https://doi.org/10.5883/DS-TRIRHYD; Pešić et al. 2021b, 2022, 2023a) is still modest and includes 249 public sequences (including the sequences of this study), 188 of these are from Türkiye. As emphasized by Pešić et al. (2023d, 2024) formation of such barcode libraries and their further continuous improvement by expanding their taxonomic and geographical coverage provides is on one hand a basis for a deeper understanding of the diversity of water mites in particular areas. On the other hand, it is a valuable contribution to the integrative taxonomic research of challenging groups of species, especially for detecting cryptic or pseudocryptic species.

This paper is based on material collected in southwestern Anatolia (mainly Burdur and Isparta provinces) in 2024. As a result of this investigation, we describe one species new to science.

Materials and methods

Water mites were collected by hand netting and immediately preserved in 96% ethanol for the purpose of molecular analyses. The specimens used for molecular study are listed in Table 1. After non-destructive DNA extraction, the specimen vouchers were stored in 96% ethanol and morphologically examined. Some of these vouchers were dissected and slide mounted in Faure's medium, while the rest was transferred to Koenike's fluid.

Morphological nomenclature follows Gerecke et al. (2016). The holotype of the new species is deposited in Naturalis Biodiversity Center in Leiden (**RMNH**). In the section 'Material examined', collecting site abbreviations are derived from the geographical database of the first and second authors.

All measurements are given in µm. The photographs of selected structures were made using a camera on Samsung Galaxy smartphone. The following abbreviations are used:

Ac-1-3	first to third acetabula;	**P-1-P-5**	palp segment 1-5;
Cx-I-IV	first to fourth coxae;	**S-1**	proximal large ventral seta at I-L-5;
Dgl-4	dorsoglandularia 4;	**S-2**	distal large ventral seta at I-L-5;
dL	dorsal length;	**Vgl-1**	ventroglandulare 1;
H	height;	**Vgl-2**	ventroglandulare 2;
I-L-4-6	fourth-sixth segments of first leg;	**vL**	ventral length;
L	length;	**W**	width.
lL	lateral length;		
mL	medial length;		

Molecular and DNA barcode analyses

Molecular analyses were conducted at the Canadian Centre for DNA Barcoding, Guelph, Canada (CCDB; http://ccdb.ca/). In the later institution, the specimens were sequenced for the barcode region of COI using standard invertebrate DNA extraction, amplification, and sequencing protocols (see for details: Ivanova et al. 2007; Ivanova and Grainger 2007a, b).

Consensus sequences were made available in the Barcode of Life Data Systems (BOLD) (Ratnasingham and Hebert 2007). The Barcode Index Numbers (BIN), grouping DNA sequences based on the Refined Single Linkage (RESL) analysis performed in BOLD (Ratnasingham and Hebert 2013), were obtained.

Table 1. Details on DNA barcoded specimens, including localities and coordinates of sampling sites, sample codes and the barcode index number codes (^{N} indicates a new BIN that contains only sequences from this study). BOLD data presented here was last accessed on 10 May 2024.

Locality	Coordinates	Sample ID	Process ID	BIN
Hydrachnidae Leach, 1815				
***Hydrachna globosa* (De Geer, 1778)**				
Burdur, Gölhisar Lake	37.1227°N, 29.599937°E	CCDB-48501-A04	HYDCG099-24	BOLD:ACI2447
		CCDB-48501-A05	HYDCG100-24	
Hydrodromidae Viets, 1936				
***Hydrodroma torrenticola* (Walter, 1908)**				
Antalya, pond	36.87547°N, 30.8454°E	CCDB-48498-C04	HYDCG028-24	^{N}BOLD:AGG7908
		CCDB-48498-C05	HYDCG029-24	
		CCDB-48498-C08	HYDCG032-24	BOLD:AFC2822
Hydryphantidae Piersig, 1896				
***Protzia longiacetabulata* Gülle & Boyaci, 2014**				
Burdur, Karacaören, stream	37.327335°N, 30.869408°E	CCDB-48498-F01	HYDCG061-24	BOLD:AEH8558
Isparta, Yazılıkanyon Tabiat Parkı, stream	37.46882°N, 30.919449°E	CCDB-48498-G10	HYDCG082-24	
		CCDB-48498-G05	HYDCG077-24	
Burdur, waterfall	37.33291°N, 30.879221°E	CCDB-48498-E01	HYDCG049-24	
***Protzia vietsi* Özkan, 1982**				
Burdur, Söbüce, stream	37.287872°N, 30.067743°E	CCDB-48498-A05	HYDCG005-24	^{N}BOLD:AGG3760
Söbüce, rheocrenic spring	37.295727°N, 30.089523°E	CCDB-48498-A06	HYDCG006-24	
Burdur, Kemer, helocrenic spring	37.301468°N, 30.097061°E	CCDB-48498-B02	HYDCG014-24	
		CCDB-48498-B03	HYDCG015-24	
Isparta, Yazılıkanyon Tabiat Parkı, stream	37.46882°N, 30.919449°E	CCDB-48498-G04	HYDCG076-24	
***Trichothyas petrophila* (Michael, 1895)**				
Burdur, waterfall	37.33291°N, 30.879221°E	CCDB-48498-D12	HYDCG048-24	^{N}BOLD:AGG3771
***Iranothyas marismortui* (Gerecke, 1999)**				
Burdur, helocrenic spring near Burdur lkae	37.733643°N, 30.112862°E	CCDB-48498-D05	HYDCG041-24	^{N}BOLD:AGG3782
		CCDB-48498-D06	HYDCG042-24	
		CCDB-48498-D07	HYDCG043-24	
Lebertiidae Thor, 1900				
***Lebertia glabra* Thor, 1897**				
Burdur, Söbüce, first order stream	37.295727°N, 30.089523°E	CCDB-48498-A10	HYDCG010-24	BOLD:ACS0595
		CCDB-48498-A11	HYDCG011-24	
Burdur, waterfall and outflow	37.33291°N, 30.879221°E	CCDB-48498-E06	HYDCG054-24	
Burdur, Akyayla, spring	37.482956°N, 30.326647°E	CCDB-48498-F12	HYDCG072-24	
Burdur, Söbüce, stream	37.287872°N, 30.067743°E	CCDB-48498-H06	HYDCG090-24	
***Lebertia rivulorum* K. Viets, 1933**				
Burdur, Sazak, spring	37.544933°N, 29.94381°E	CCDB-48498-B06	HYDCG018-24	^{N}BOLD:AGG5208
Burdur, Kestel, canal	37.429718°N, 30.399193°E	CCDB-48498-H11	HYDCG095-24	
Burdur, Çavdir, spring	37.14478°N, 29.656534°E	CCDB-48498-E12	HYDCG060-24	
Sperchontidae Thor, 1900				
***Sperchon beneckei* Bader & Sepasgosarian, 1982**				
Isparta, Yazılıkanyon Tabiat Parkı, stream	37.46882°N, 30.919449°E	CCDB-48498-G01	HYDCG073-24	BOLD:AED2730
***Sperchon compactilis* Koenike, 1911**				
Burdur, Söbüce, stream	37.287872°N, 30.067743°E	CCDB-48498-H05	HYDCG089-24	BOLD:ACS1036
Burdur, canal	37.429718°N, 30.399193°E	CCDB-48498-H10	HYDCG094-24	

Locality	Coordinates	Sample ID	Process ID	BIN
***Sperchon thienemanni* Koenike, 1907**				
Burdur, Söbüce, stream	37.287872°N, 30.067743°E	CCDB-48498-A07	HYDCG007-24	BOLD:AES4247
		CCDB-48498-A03	HYDCG003-24	
Burdur, Akyayla, spring	37.482956 °N, 30.326647 °E	CCDB-48498-F09	HYDCG069-24	^{N}BOLD:AGG3777
***Sperchon papillosus* Thor, 1901**				
Isparta, Çukurköy, stream	37.651257°N, 30.81791°E	CCDB-48498-D03	HYDCG039-24	^{N}BOLD:AGH7685
Isparta, Kışlaköy	37.66509°N, 30.725111°E	CCDB-48501-A12	HYDCG107-24	
***Sperchon serapae* Boyaci, Gülle & Özkan, 2012**				
Burdur, Akyayla, spring	37.482956°N, 30.326647°E	CCDB-48498-F10	HYDCG070-24	^{N}BOLD:AGG3776
***Sperchon setiger* Thor, 1898**				
Burdur, Çavdir, spring	37.14478°N, 29.656534°E	CCDB-48498-E11	HYDCG059-24	^{N}BOLD:AGH7686
Burdur, Kestel, canal	37.429718°N, 30.399193°E	CCDB-48498-H09	HYDCG093-24	^{N}BOLD:AGG3936
Family Torrenticolidae Piersig, 1902				
***Torrenticola baueri* Bader & Sepasgozarian, 1987**				
Burdur, Karacaören, stream	37.327335°N, 30.869408°E	CCDB-48498-F04	HYDCG064-24	BOLD:AFG4655
		CCDB-48498-F06	HYDCG066-24	
***Monatractides stadleri* (Walter, 1924)**				
Burdur, waterfall and outflow	37.33291°N, 30.879221°E	CCDB-48498-E03	HYDCG051-24	BOLD:AGC6044
Limnesiidae Thor, 1900				
***Limnesia fulgida* Koch, 1836**				
Antalya, limnocrene spring	37.09568°N, 30.58095°E	CCDB-48498-E07	HYDCG055-24	^{N}BOLD:AGG4400
		CCDB-48498-E09	HYDCG057-24	
Hygrobatidae Koch, 1842				
***Atractides fonticola* K. Viets, 1920**				
Isparta, Kışlaköy	37.66509°N, 30.725111°E	CCDB-48501-A08	HYDCG103-24	^{N}BOLD:AGG3788
Burdur, Akyayla, spring	37.515774°N, 30.35459°E	CCDB-48498-B11	HYDCG023-24	
***Atractides graecus* K. Viets, 1950**				
Burdur, Karacaören, stream	37.327335°N, 30.869408°E	CCDB-48498-F07	HYDCG067-24	^{N}BOLD:AGG3781
***Atractides inflatipalpis* K. Viets, 1950**				
Burdur, Akyayla, spring	37.515774°N, 30.35459°E	CCDB-48498-B12	HYDCG024-24	^{N}BOLD:AGG3787
		CCDB-48498-C02	HYDCG026-24	
***Atractides lunipes* Lundblad, 1956**				
Burdur, Karacaören, stream	37.327335°N, 30.869408°E	CCDB-48498-F08	HYDCG068-24	^{N}BOLD:AGG3780
***Atractides nikooae* Pesic, 2004**				
Burdur, Karamusa stream	37.186405°N, 29.75374°E	CCDB-48498-D10	HYDCG046-24	^{N}BOLD:AGG3766
		CCDB-48498-D11	HYDCG047-24	
Burdur, Çavdir, spring	37.14478°N, 29.656534°E	CCDB-48498-E10	HYDCG058-24	
***Atractides robustus* (Sokolow, 1940)**				
Isparta, Yazılıkanyon Tabiat Parkı, stream	37.46882°N, 30.919449°E	CCDB-48498-G02	HYDCG074-24	BOLD:AEK3669
Isparta, Çukurköy, stream	37.651257°N, 30.81791°E	CCDB-48498-D04	HYDCG040-24	^{N}BOLD:AGH5609
***Atractides subasper* Koenike, 1902**				
Burdur, Söbüce, stream	37.287872°N, 30.067743°E	CCDB-48498-H02	HYDCG086-24	^{N}BOLD:AGG3778
***Atractides turani* sp. nov.**				
Burdur, Söbüce, stream	37.287872°N, 30.067743°E	CCDB-48498-A09	HYDCG009-24	^{N}BOLD:AGG3768
Burdur, Akyayla, spring	37.482956°N, 30.326647°E	CCDB-48498-F11	HYDCG071-24	^{N}BOLD:AGG3774
***Hygrobates longipalpis* (Hermann, 1804)**				
Burdur, Sazak, spring	37.544933°N, 29.94381°E	CCDB-48498-B05	HYDCG017-24	BOLD:AES0232
		CCDB-48498-B07	HYDCG019-24	
Burdur, Dereköy, spring	37.42846°N, 29.809637°E	CCDB-48498-B10	HYDCG022-24	
Antalya, limnocrene spring	37.09568°N, 30.58095°E	CCDB-48498-E08	HYDCG056-24	
Burdur, Kayali, limnocrene	37.306606°N, 29.931082°E	CCDB-48501-A09	HYDCG104-24	
Isparta, Kışlaköy	37.66509°N, 30.725111°E	CCDB-48501-A11	HYDCG106-24	

Locality	Coordinates	Sample ID	Process ID	BIN
Hygrobates persicus **Pešić & Asadi, 2017**				
Antalya, Düden river	36.959763°N, 30.731194°E	CCDB-48498-C09	HYDCG033-24	BOLD:ACB5533
		CCDB-48498-C10	HYDCG034-24	
		CCDB-48498-C11	HYDCG035-24	
		CCDB-48498-C12	HYDCG036-24	
Isparta, Kışlaköy	37.66509°N, 30.725111°E	CCDB-48501-A06	HYDCG101-24	
		CCDB-48501-A07	HYDCG102-24	
Hygrobates quanaticola **Schwoerbel & Sepasgozarian, 1976**				
Burdur, Kuzköy, spring	37.55402°N, 30.440313°E	CCDB-48498-A02	HYDCG002-24	BOLD:AEM9575
		CCDB-48501-A10	HYDCG105-24	
		CCDB-48498-A01	HYDCG001-24	^{N}BOLD:AGG3789
Burdur, Dereköy, spring	37.42846°N, 29.809637°E	CCDB-48498-B09	HYDCG021-24	
Burdur, canal	37.429718°N, 30.399193°E	CCDB-48498-H08	HYDCG092-24	
Unionicolidae Oudemans, 1909				
Neumania imitata **Koenike, 1908**				
Antalya, pond	36.87547°N, 30.8454°E	CCDB-48498-C06	HYDCG030-24	^{N}BOLD:AGG4333
		CCDB-48498-C07	HYDCG031-24	
Neumania limosa **(Koch, 1836)**				
Burdur, Duger, limnocrene spring	37.574345°N, 30.021276°E	CCDB-48501-C04	HYDCG123-24	BOLD:AEF5902
Pionidae Thor, 1900				
Piona alpicola **(Neuman, 1880)**				
Uylupinar, limnocrene spring	37.10993°N, 29.613293°E	CCDB-48501-A03	HYDCG098-24	BOLD:ACR9570
Arrenuridae Thor, 1900				
Arrenurus compactus **Piersig, 1894**				
Uylupinar, limnocrene spring	37.10993 °N, 29.613293 °E	CCDB-48501-A01	HYDCG096-24	BOLD:AEJ6492
Arrenurus fontinalis **K. Viets, 1920**				
Burdur, Kemer, helocrenic spring	37.301468°N, 30.097061°E	CCDB-48498-A12	HYDCG012-24	^{N}BOLD:AGH5781
		CCDB-48498-B01	HYDCG013-24	
		CCDB-48498-B04	HYDCG016-24	
Burdur, Akyayla, spring	37.515774°N, 30.35459°E	CCDB-48498-C03	HYDCG027-24	
Arrenurus suecicus **Lundblad, 1917**				
Burdur, limnocrene spring	37.10993°N, 29.613293°E	CCDB-48501-A02	HYDCG097-24	BOLD:AAV9863

Relevant voucher information, photos, and newly generated DNA barcodes are publicly accessible through https://doi.org/10.5883/DS-TRIRHYD in BOLD. Data related to each BIN, which are often considered proxies for species, including the minimum *p*-distance to the nearest neighboring BIN, was estimated using BOLD tools. In this study DNA was extracted from 83 specimens from Türkiye listed in Table 1. For all other species, COI sequence data were downloaded from the respective sequence data archives.

Sequence alignments were performed using MUSCLE (Edgar 2004). Intra- and interspecific genetic distances were calculated based on the Kimura 2-parameter model (K2P; Kimura 1980), using MEGA 11 software (Tamura et al. 2021). The latter software was used to calculate Neighbor-Joining (NJ) trees based on K2P distances (standard for barcoding studies) using pairwise deletion for missing data. Branch support was calculated using nonparametric bootstrap (Felsenstein 1985) with 1000 replicates and shown next to the branches.

Additionally, the sequence data were analyzed using the Assemble Species by Automatic Partitioning (ASAP) method (Puillandre et al. 2012). We used the online ASAP version (https://bioinfo.mnhn.fr/abi/public/asap/asapweb.html) with default settings and K2P distance model.

Results and discussion

We generated 83 DNA barcodes from 34 water mite species collected in southwestern Türkiye during our collecting trip in April 2024. The collected water mites represent 11 families and 15 genera. The most sequence-rich family was Hygrobatidae with 31 sequences (14 BINs), followed by Hydryphantidae with 13 sequences (4 BINs), and Sperchontidae with 11 sequences (8 BINs). Some families were rare, such as Hydrachnidae, Hydrodromidae, and Pionidae, represented by a single BIN each.

The resulting sequences clustered into 40 BINs, with 23 BINs (57.5%) being unique and deposited for the first time in BOLD. Two BINs were detected for six species, i.e., *Hydrodroma torrenticola* (Walter, 1908) (BOLD:AFC2822, BOLD:AGG7908), *Sperchon thienemanni* Koenike, 1907 (BOLD:AES4247, BOLD:AGG3777), *S. setiger* Thor, 1898 (BOLD:AGG3936, BOLD:AGH7686), *Atractides robustus* (Sokolow, 1940) (BOLD:AGH5609, BOLD:AEK3669), *A. turani* sp. nov. (BOLD:AGG3768, BOLD:AGG3768) and *Hygrobates quanaticola* Schwoerbel & Sepasgozarian, 1976 (BOLD:AGG3789, BOLD:AEM9575). Our study provided the first DNA barcodes for *Protzia vietsi* Özkan, 1982 (BOLD:AGG3760), *Iranothyas marismortui* (Gerecke, 1999) (BOLD:AGG3782), *Trichothyas petrophila* (Michael, 1895) (BOLD:AGG3771), *Sperchon serapae* Boyaci, Gülle & Özkan, 2012 (BOLD:AGG3776), *Atractides graecus* K. Viets, 1950 (BOLD:AGG3781), *A. inflatipalpis* K. Viets, 1950 (BOLD:AGG3787), *A. lunipes* Lundblad, 1956 (BOLD:AGG3780), and *A. nikooae* Pesic, 2004 (BOLD:AGG3766).

Our findings added the first record of *Iranothyas marismortui* (Gerecke, 1999) for Türkiye. One species of the genus *Atractides* (*A. turani* sp. nov.) is described as new to science.

In summary, even though sampling was conducted in a short period (22–27 April 2024), this study exemplifies the high molecular diversity of water mites of southwestern Türkiye and at the same time highlights the need to intensify further studies with the aim of the generation and curation of DNA barcode reference libraries at the regional level.

Systematics

Famıly Hydrachnidae Leach, 1815
Genus *Hydrachna* Müller, 1776

Hydrachna globosa (De Geer, 1778)

Material examined. Burdur • TR21-2024, Gölhisar Lake, 37.1227°N, 29.599937°E, 26 Apr. 2024, leg. Pešić, Zawal, Saboori, Gülle & Gülle, 2♀ (sequenced).

Remarks. The sequences obtained from the specimens from Türkiye fall into BOLD:ACI2447, which, in addition to the specimens used in this study for molecular analysis, includes specimens of *H. globosa* from the Netherlands and Norway, available in the BOLD database.

Distribution. Palaearctic.

Family Hydrodromidae Viets, 1936
Genus *Hydrodroma* Koch, 1837

Hydrodroma torrenticola (Walter, 1908)

Material examined. Antalya • TR29-2024 Aksu, pond near Antalya city, 36.87547°N, 30.8454°E, 27 Apr. 2024 leg. Pešić, Zawal, Gülle & Gülle, 3♀ (sequenced).

Remarks. The sequences obtained from the three females collected in a pond near Antalya cluster within two BINs. One specimen falls within BOLD:AFC2822, which in addition to the specimen from this study, includes one specimen of *H. torrenticola* from Norway, with the nearest neighboring BIN being BOLD:ACI2515, which includes specimens of *H. torrenticola* from Montenegro from which it differs by 3.24% *p*-distance. Two specimens of *H. torrenticola* from the same locality, form the unique BOLD:AGG7908, with the nearest neighboring BIN being BOLD:AFC2822, from which it differs by 3.86% *p*-distance.

Distribution. Central, Western, and Southern Europe, Türkiye.

Family Hydryphantidae Piersig, 1896
Genus *Protzia* Piersig, 1896

Protzia longiacetabulata Gülle & Boyaci, 2014

Material examined. Isparta • TR18-2024, Yazılıkanyon Tabiat Parkı, stream from cave (moss), 37.46882°N, 30.919449°E, 25 Apr. 2024, leg. Pešić, Zawal, Gülle & Gülle, 1♂, 1♀ (sequenced). **Burdur** • TR19-2024 waterfall and outflow, 37.33291°N, 30.879221°E, 25 Apr. 2024, leg. Pešić, Zawal, Gülle & Gülle, 1♀ (sequenced) • TR20-2024, Karacaören, stream, 37.327335°N, 30.869408°E, 25 Apr. 2024, Pešić, Zawal, Gülle & Gülle, 1♀ (sequenced).

Remarks. The sequenced specimens from this study cluster together with specimens, collected from the Sütçüler stream in Isparta Province, morphologically assigned by Pešić et al. (2021c) to *P. longiacetabulata*. The latter rhitrobiontic species was originally described by Gülle and Boyaci (2014) from the Dim stream in Alanya province. The examined specimens of *P. longiacetabulata* belongs to BIN (BOLD:AEH8558), with a *p*-distance of 3.85% to the nearest BIN being BOLD:AEH8557 which groups two sequences of the latter species from Isparta Province.

Distribution. Türkiye.

Protzia vietsi Özkan, 1982

Material examined. Burdur • TR9 Kemer, helocrenic spring 37.301468°N, 30.097061°E, 22 Apr. 2024, leg. Pešić, Zawal, Gülle & Gülle, 2♀ (sequenced) • TR10-2024 Söbüce, rheocrenic spring, 37.295727°N, 30.089523°E, 24 Apr.

2024, leg. Pešić, Zawal, Gülle & Gülle, 1♀ (sequenced) • TR11-2024, Söbüce, first order stream, 37.287872°N, 30.067743°E, 24 Apr. 2024, leg. Pešić, Zawal, Gülle & Gülle, 1♀ (sequenced). **Isparta** • TR18-2024, Yazılıkanyon Tabiat Parkı, stream from cave (mosses), 37.46882°N, 30.919449°E, 25 Apr. 2024, leg. Pešić, Zawal, Gülle & Gülle, 1♀ (sequenced).

Remarks. The examined specimens from southwestern Türkiye used in this study for molecular analysis match the description of *P. vietsi*. The latter species, originally described by Oezkan (1982) from Erzurum province belongs to the *eximia* species group (see Gerecke 1996 for discussion on diagnostic features of *P. vietsi*). The molecularly studied specimens from Burdur and Isparta forms a unique BIN (BOLD:AGG3760).

Distribution. Türkiye.

Genus *Iranothyas* Bader, 1984

Iranothyas marismortui (Gerecke, 1999)

Material examined. Burdur • TR4-2024 helocrenic spring near Burdur Lake, 37.733643°N, 30.112862°E, 23 Apr. 2024, leg. Pešić, Zawal, Gülle & Gülle 3♀ (sequenced).

Remarks. The genus *Iranothyas* includes three species, *Iranothyas circularis* (Schwoerbel & Sepasgozarian, 1976), known from a single female from the type locality in western Iran (Schwoerbel and Sepasgozarian 1976), *Iranothyas alhajarica* Pešić, Gerecke & Smit, 2009, a species originally described from Oman (Pešić et al. 2009), and *I. marismortui* (Gerecke, 1999), a species so far known only from Israel (Gerecke 1999).

In regard to the shape of the frontal shield (in agreement with *Iranothyas circularis*, nearly circular, outline equally rounded, without a posteromedial extension as in *I. alhajarica*) and position of Ac-2 (in agreement with *I. alhajarica*, halfway between Ac-1 and Ac-3, not close to Ac-3 as in *I. circularis*) the examined specimens from a helocrenic spring located on the west coast of the Burdur Lake matches the description of *I. marismortui* (Gerecke, 1999). Genetic data indicate that these specimens form a unique BIN (BOLD:AGG3782).

Gülle et al. (2017) reported the presence of *Iranothyas alhajarica* Pešić, Gerecke & Smit, 2009 from the same spring located on the west coast of the Burdur Lake (Fig. 6C) where we found an *Iranothyas* population of here assigned to *I. marismortui*. Therefore, we assume that the record of *I. alhajarica* in Gülle et al. (2017) refers to *I. marismortui*, indicating that *I. alhajarica* should be excluded for Turkish fauna. Gülle et al. (2017) mentioned that the larvae of the *Iranothyas* population on the aforementioned locality were found as parasites on the hydrophilic beetle *Laccobius gracilis* Motschulsky, 1855.

Distribution. Israel, Türkiye.

Genus *Trichothyas* K. Viets, 1926

Trichothyas (*Lundbladia*) *petrophila* (Michael, 1895)

Material examined. Burdur • TR19-2024 waterfall and outflow, 37.33291°N, 30.879221°E, 25 Apr. 2024, leg. Pešić, Zawal, Gülle & Gülle, 1♀ (sequenced).

Remarks. The single specimen from southwestern Türkiye, molecularly analyzed in this study, matches the description of *T. petrophila*. This specimen forms a unique BIN (BOLD:AGG3771).

Distribution. Southern and Western Europe, Great Britain, Balkan, Türkiye.

Family Lebertiidae Thor, 1900
Genus *Lebertia* Neuman, 1880

Lebertia (*Lebertia*) *glabra* Thor, 1897

Material examined. Burdur • TR2-2024 Akyayla, rheocrenic spring, 37.482956°N, 30.326647°E, 22 Apr. 2024, leg. Pešić, Zawal, Gülle & Gülle, 1♂ (sequenced); **Burdur** • TR10-2024 Söbüce, first order stream, 37.295727°N, 30.089523°E, 24 Apr. 2024, leg. Pešić, Zawal, Gülle & Gülle, 2♀ (sequenced) • TR11-2024, Söbüce, stream, 37.287872°N, 30.067743°E, 24 Apr. 2024, leg. Pešić, Zawal, Gülle & Gülle, 1♂ (sequenced) • TR19-2024 waterfall and outflow, 37.33291°N, 30.879221°E, 25 Apr. 2024 leg. Pešić, Zawal, Gülle & Gülle, 1♀ (sequenced).

Remarks. The specimens from Burdur match the description of *L. glabra*, a species widely distributed in the Western Palaearctic (Di Sabatino et al. 2010). The Turkish specimens were clustered in BOLD:ACS0595, which includes specimens of *L. glabra* from the Netherlands, Bulgaria, Norh Macedonia, Montenegro, Italy, Poland, Slovakia, Romania, Germany, Austria, Serbia, Norway, Bosnia and Herzegovina, and Türkiye.

Distribution. Western Palaearctic.

Lebertia (*Lebertia*) *rivulorum* K. Viets, 1933

Material examined. Burdur • TR6-2024 Sazak, rheocrenic spring, 37.544933°N, 29.94381°E, 23 Apr. 2024, leg. Pešić, Zawal, Gülle & Gülle, 1♀ (sequenced) • TR23-2024, Çavdir, spring, 37.14478°N, 29.656534°E, 26 Apr. 2024, leg. Pešić, Zawal, Gülle & Gülle, 1♀ (sequenced) • TR26-2024 Kestel, canal with fast-flowing water, 37.429718°N, 30.399193°E, 27 Apr. 2024, leg. Pešić, Zawal, Gülle & Gülle, 1♀ (sequenced).

Remarks. The examined specimens from Burdur, molecularly analyzed in this study, matches the description of *L. rivulorum*. These specimens form a unique BIN (BOLD:AGG5208). The *p*-distance to its nearest neighboring BIN (BOLD:AED9196), which includes specimens of *L. rivulorum* from North Macedonia, was estimated at 6.31%.

Distribution. Central, Western, and Southern Europe, Türkiye.

Family Sperchontidae Thor, 1900
Genus *Sperchon* Kramer, 1877

Sperchon beneckei Bader & Sepasgosarian, 1982

Material examined. Isparta • TR18-2024, Yazılıkanyon Tabiat Parkı, stream from cave (moss), 37.46882°N, 30.919449°E, 25 Apr. 2024, leg. Pešić, Zawal, Gülle & Gülle, 1♀ (sequenced).

Remarks. The sequence obtained from one specimen from Isparta fell into BIN BOLD:AED2730, which besides the specimen from this study, includes one specimen from Iran morphologically assigned to *S. beneckei*. The latter species was originally described from Iran. Asadi et al. (2010) synonymized the species with *S. algeriensis* Lundblad, 1942, a species described from northern Africa (Lundblad 1942) and subsequently recorded from many sites in the central and western Mediterranean area (Di Sabatino et al. 2010). Recently, Pešić et al. (2024) emphasized that high genetic distance of 15.4% between Iberian populations of *S. algeriensis* and the specimen from Iran, suggests that *S. beneckei* is a distinct species and its synonymization with *S. algeriensis* should be rejected. The new findings of *S. beneckei* from southeastern Türkiye show that this species is widespread, and therefore, the known populations of *S. algeriensis* from Türkiye (e.g., Esen et al. 2013b) should be checked using molecular methods to see if they can be assigned to *S. beneckei*.

Distribution. Iran, Türkiye.

Sperchon (*Hispidosperchon*) *compactilis* Koenike, 1911

Material examined. Burdur • TR11-2024, Söbüce, first order stream, 37.287872°N, 30.067743°E, 24 Apr. 2024 leg. leg. Pešić, Zawal, Gülle & Gülle, 1♂ (sequenced) • TR26-2024 Kestel, canal with fast-flowing water, 37.429718°N, 30.399193°E, 27 Apr. 2024, leg. Pešić, Zawal, Gülle & Gülle, 1♀ (sequenced).

Remarks. The sequences obtained from specimens collected in Burdur, keyed out to *S. compactilis* following Di Sabatino et al. (2010), clustered in BOLD:ACS1036, which, in addition to specimens used in this study, includes specimens of *S. compactilis* from the Netherlands, Germany, and Türkiye.

Distribution. Central and SW Europe, Türkiye, Iran.

Sperchon (*Sperchon*) *thienemanni* Koenike, 1907

Fig. 1

Material examined. Burdur • TR2-2024 Akyayla, rheocrenic spring, 37.482956°N, 30.326647°E, 22 Apr. 2024, leg. Pešić, Zawal, Gülle & Gülle, 1♀ (sequenced) • TR10-2024, Söbüce, first order stream, 37.287872°N, 30.067743°E, 24 Apr. 2024 leg. leg. Pešić, Zawal, Gülle & Gülle, 2♂ (sequenced).

Compared material. *Sperchon thienemanni*: The Netherlands • Overijssel, De Lutte, 52.329°N, 6.987°E, 19 May 2012 leg. Smit 2♂, 1♀, 1♂ (NLACA054-15/RMNH.ACA.1072), 1♀ (NLACA055-15/RMNH.ACA.1073) sequenced, dissected, and slide mounted (RMNH) • Limburg, Schin op Geul: Genhoes, 50.854°N, 5.858 °E, 27 Apr. 2012 leg. Smit 3♀ (sequenced; NLACA426-15/RMNH.ACA.851, NLACA427-15/RMNH.ACA.852, NLACA428-15/RMNH.ACA.853), dissected and slide mounted (RMNH) • Limburg, Epen: Terziet, 50.755°N, 5.904°E, 27 Apr. 2012 leg. Smit 1♂ (NLACA422-15/RMNH.ACA.847), 1♀ (NLACA421-15/RMNH.ACA.846), sequenced, dissected and slide mounted (RMNH).

Remarks. The specimens sequenced from this study were clustered within two BINs. The first one, BOLD:AES4247, in addition to two specimens from this study, includes four specimens from Austria. The second BIN, BOLD:AGG3777,

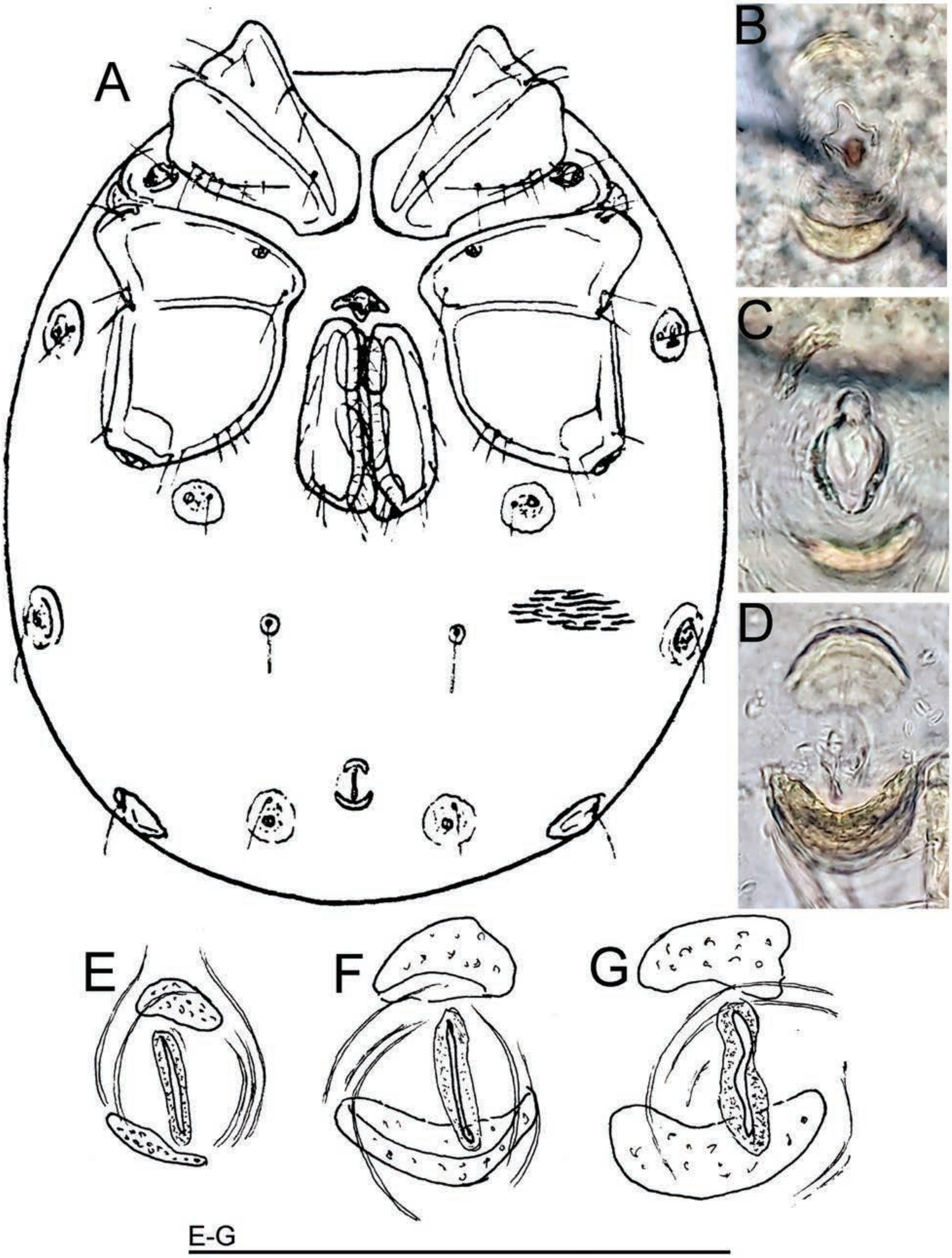

Figure 1. *Sperchon thienemanni*: **A** idiosoma, ventral view (from K. Viets 1936: fig. 146b) **B–G** excretory pore **B** RMNH.ACA.851, Netherlands **C** RMNH.ACA.852, Netherlands **D** RMNH.ACA.1073, Netherlands **E** ♂, CCDB-48498-A03, Türkiye **F** ♂, CCDB-48498-A07, Türkiye **G** ♀, CCDB-48498-F09, Türkiye. Scale bar: 100 µm.

is unique and includes one specimen collected in a rheocrenic spring in this study. The *p*-distance between these two BINs was estimated at 2.73%. In the phylogenetic tree, the two above-mentioned BINs of *S. thienemanni* from Türkiye forms a highly supported clade which is placed (albeit with a low support) as sister to clade grouping specimens of *S. thienemanni* from the Netherlands. The latter specimens belong to BOLD:ACS0087.

In all barcoded specimens from southwestern Türkiye as well in examined specimens of *S. thienemanni* from the Netherlands belonging to BOLD:ACS0087 and BOLD:ACR9585, respectively, the excretory pore sclerotized ring was not complete, and was reduced to a separate sclerotized platelets located anterior and posterior of excretory pore, respectively (as illustrated in Fig. 1B–G). The excretory pore, not completely surrounded by a sclerite ring is well visible in K. Viets' figure (1936: fig. 146b), but in recent water mite literature it has not been recognized as an important diagnostic character of the latter species. For example, in a key to Central European water mites (Di Sabatino et al. 2010), the excretory pore of *S. thienemanni* is described as unsclerotized without mentioning the presence of separate sclerites located anteriorly and posteriorly to the excretory pore which may lead to confusion in the identification of this species

Sperchon thienemanni was considered to be synonymous with *S. glandulosus* Koenike, 1886 for a long time and was only distinguished as a separate species by Szalay (1941, 1956). Following Bader (1974), and later accepted by Gerecke (1991) and Di Sabatino et al. (2010), the excretory pore in *S. glandulosus* is completely surrounded by a sclerotized ring.

The applied ASAP procedure (see Fig. 2) grouped together the COI sequences of *S. thienemanni*-like mites belonging to the following BINs: BOLD:ADV4077 (specimens from Austria, Switzerland, and Poland available in BOLD database), BOLD:AEO5165 (specimens from Corsica), BOLD:AER8061 (specimens from Austria), BOLD:ACR9585 (specimens from Netherlands), BOLD:AEI8945 (specimens from Bosnia and Herzegovina), BOLD:ACS0087 (specimens from Netherlands), BOLD:AGG3777 (specimen from Türkiye), and BOLD:AES4247 (specimens from Türkiye and Austria).

The two lineages of *S. glandulosus*-like mites from Europe were identified as separate MOTUs (hypothetical species). The first MOTU includes Norwegian specimens of two BINs, BOLD:ACQ0530 (shared with Romania and Belgium) and BOLD:ACR5909 (shared with Canada), indicating a rather wide, and possible a circumpolar, distribution of this species. The second MOTU represented by BOLD:ADC0986 includes two specimens from Norway, with a *p*-distance of 4.99% to the closest BIN being BOLD:AEZ0976, which includes one non-identified specimen from Canada. In the phylogenetic tree, the latter BIN is placed as a sister (albeit with a low support) of clades grouping sequences of *S. brevirostris* Koenike, 1895, indicating that likely this species is phylogenetically closer to the *S. brevirostris* complex than to the *S. glandulosus* complex.

Recently, Gerecke et al. (2022) showed that DNA barcodes attributed to Norwegian *S. glandulosus* grouped into two distinct lineages, suggesting that further revision of Norwegian *glandulosus*-like mites will result in a revival of the junior synonym *S. multiplicatus* Thor, 1902, a species described from northern and eastern Norway. However, for a more sound taxonomic

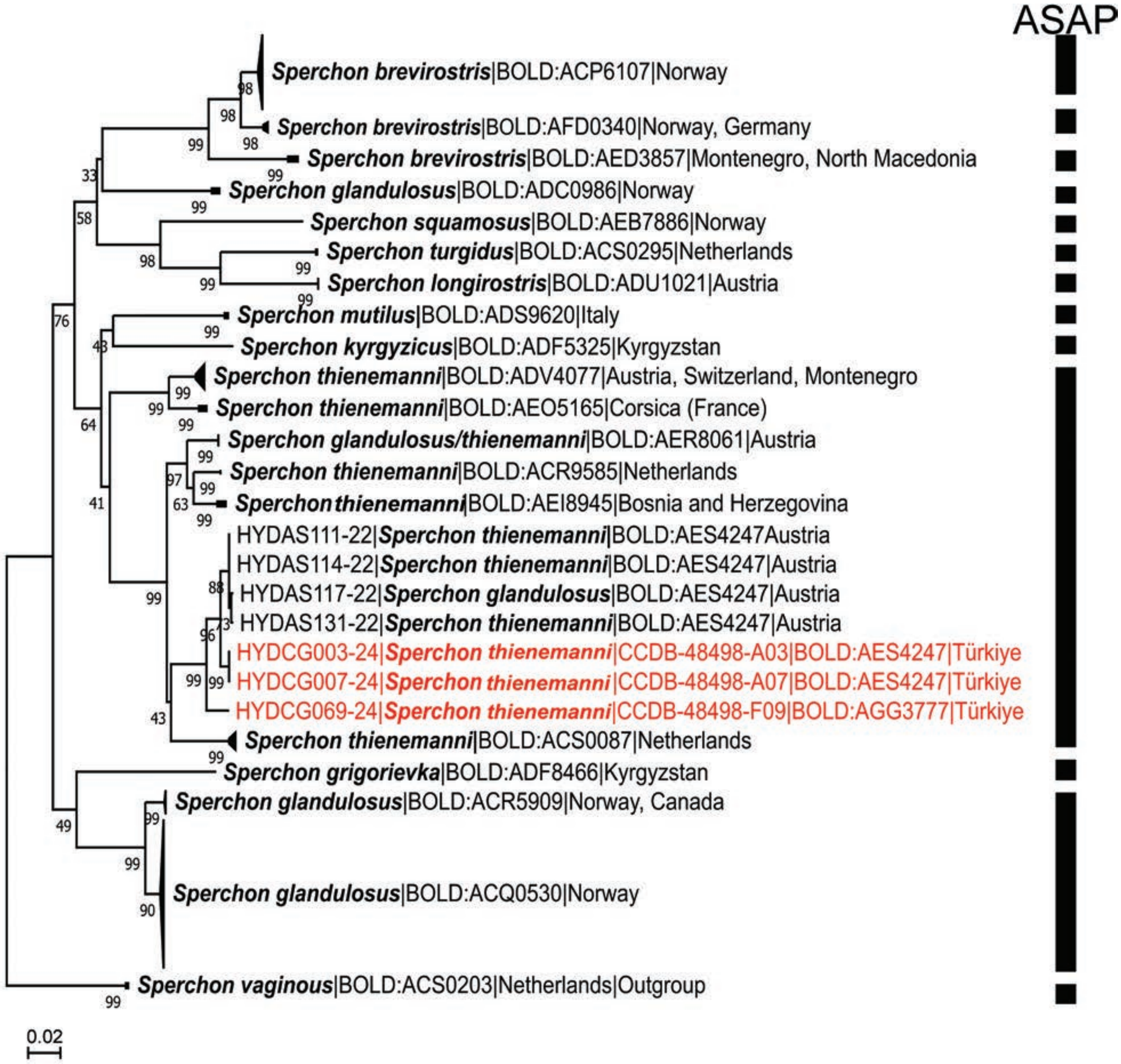

Figure 2. Neighbor-Joining tree of the subgenus *Sperchon* s. str. obtained from 161 nucleotide COI sequences listed in Suppl. material 1. *Sperchon vaginosus* Thor, 1902 from the subgenus *Hispidosperchon* was used to root the tree. The results of species delimitation by ASAP procedure are indicated by vertical bars. BINs are based on the barcode analysis from 4 November 2024. New sequences from this study are marked in red.

revision of *S. glandulosus*-like mites it is necessary to analyze molecularly more samples from a wider geographical area, preferably by including an additional genetic marker.

Sperchon fundamentalis Bader & Sepasgozarian, 1980, a species originally described from Iran (Bader and Sepasgozarian 1980), but later proposed to be a synonym of *S. glandulosus* by Esen et al. (2010), differs in the presence of muscle attachment plates on the dorsal and ventral sides of idiosoma (see Bader and Sepasgozarian 1980 for details). Therefore, synonymization of the latter species with *S. glandulosus* needs to be rejected and *S. fundamentalis* should be resurrected as a valid species.

Distribution. Europe (except Scandinavia), Türkiye.

Sperchon (*Hispidosperchon*) *papillosus* Thor, 1901

Material examined. Isparta • TR15a-2024 Kışlaköy, spring, 37.66509°N, 30.725111°E, 25 Apr. 2024 leg. leg. Pešić, Zawal, Gülle & Gülle, 1♀ (sequenced) • TR17-2024 Çukurköy, stream, 37.651257°N, 30.81791°E, 25 Apr. 2024, leg. 1♀ (sequenced).

Remarks. The sequences obtained from specimens collected in Burdur, keyed to *S. papillosus* following Di Sabatino et al. (2010), forms a unique BOLD:AGH7685. The *p*-distance to its nearest neighboring BIN (BOLD:AED2135), which includes specimens from Iran morphologically assigned to *S. papillosus*, was estimated at only 1.53%.

Distribution. Europe, Türkiye, Iran.

Sperchon (*Hispidosperchon*) *serapae* Boyaci, Gülle & Özkan, 2012

Material examined. Burdur • TR2-2024 Akyayla, rheocrenic spring, 37.482956°N, 30.326647°E, 22 Apr. 2024, leg. Pešić, Zawal, Gülle & Gülle, 1♀ (sequenced), one palp dissected and slide mounted.

Remarks. The single examined female in this study matches the description of *Sperchon serapae*, a species originally described by Boyaci et al. (2012) from Taurus Mountains in southern Turkey. This specimen forms a unique BIN (BOLD:AGG3776). The *p*-distance to its nearest neighboring BIN (BOLD:AAN0076), which includes specimens of *S. violaceus*, was estimated at 11.44%.

Distribution. Türkiye.

Sperchon (*Hispidosperchon*) *setiger* Thor, 1898

Material examined. Burdur • TR23-2024, Çavdır, spring, 37.14478°N, 29.656534°E, 26 Apr. 2024, leg. 1♀ (sequenced) • TR26-2024 Kestel, canal with fast-flowing water, 37.429718°N, 30.399193°E, 27 Apr. 2024, leg. leg. Pešić, Zawal, Gülle & Gülle, 1♀ (sequenced).

Remarks. The sequenced specimens from this study, keyed to *S. setiger* following Di Sabatino et al. (2010), clustered within two unique BINs, i.e. BOLD:AGG3936 and BOLD:AGH7686. The *p*-distance between these two BINs was estimated at 5.97%.

Distribution. Western Palaearctic.

Family Torrenticolidae Piersig, 1902
Genus *Torrenticola* Piersig, 1896

Torrenticola (*Torrenticola*) *baueri* Bader & Sepasgozarian, 1987

Material examined. Burdur • TR20-2024, Karacaören, stream, 37.327335°N, 30.869408°E, 25 Apr. 2024, Pešić, Zawal, Gülle & Gülle, 2♂ (sequenced).

Remarks. The sequenced specimens from southwestern Türkiye were clustered within BOLD:AFG4655, which includes specimens from northern Iran and western Türkiye morphologically assigned to *T. baueri*.

Distribution. Iran, Türkiye.

Genus *Monatractides* K. Viets, 1926

Monatractides (*Monatractides*) *stadleri* (Walter, 1924)

Material examined. Burdur • TR19-2024 waterfall and outflow, 37.33291°N, 30.879221°E, 25 Apr. 2024, leg. Pešić, Zawal, Gülle & Gülle, 1♂ (sequenced), dissected and slide mounted (RMNH).

Remarks. The single male from southwestern Türkiye, molecularly analyzed in this study, matches the description of *M. stadleri*, a species widely distributed in the Mediterranean region, often very frequent in lowland running waters (Di Sabatino et al. 2010). The sequenced specimen was clustered within BOLD:AGC6044 which, in addition to the specimen from this study, includes one specimen from Greece. The *p*-distance to the nearest BIN BOLD:AEN9161, which includes specimens of *M. corsicus* from Corsica and Sardinia, was estimated at 8.14%.

In the phylogenetic tree, the sequence obtained from the specimen from Türkiye was nested within clades of *M. stadleri* complex, as a sister clade (albeit with a low support) to *M. corsicus* Pešić & Smit, 2023, a species described from Corsica (Pešić and Smit 2023) and later reported from Sardinia by Pešić and Goldschmidt (2023). The status of the newly detected clade from Türkiye and Greece (BOLD:AGC6044) as well the status of the previously detected clade from Balkans (Montenegro and Greece; BOLD:AEN9161) should be left unnamed until the sequences of *M. stadleri* from its type locality are available.

Distribution. Central, Western, and Southern Europe, Türkiye.

Family Limnesiidae Thor, 1900
Genus *Limnesia* Koch, 1836

Limnesia (*Limnesia*) *fulgida* Koch, 1836

Material examined. Antalya • TR27-2024 limnocrene spring, 37.09568°N, 30.58095°E, 27 Apr. 2024, leg. Pešić, Zawal, Gülle & Gülle, 1♂, 2♀ (2♀ sequenced), 1♂ dissected and slide mounted (RMNH).

Remarks. The sequenced specimens from this study identified as *L. fulgida* following Di Sabatino et al. (2010), forms a unique BIN (BOLD:AGG4400). The *p*-distance to its nearest neighboring BIN (BOLD:ACR9738), which includes specimens of *L. fulgida* from the Netherlands and Norway, was estimated at 7.22% suggesting phylogeographic break between European and Turkish populations of this species.

Distribution. Holarctic.

Family Hygrobatidae Koch, 1842
Genus *Atractides* Koch, 1837

Atractides (*Atractides*) *fonticola* K. Viets, 1920

Material examined. Burdur • TR3-2024 Akyayla, rheohelocrenic spring, 37.515774°N, 30.35459°E, 22 Apr. 2024, leg. Pešić, Zawal, Gülle & Gülle, 1♂, 1♀ (sequenced), one palp and I-leg of ♀ dissected and slide mounted. **Isparta** • TR15a-2024 Kışlaköy, spring, 37.66509°N, 30.725111°E, 25 Apr. 2024, leg. Pešić, Zawal, Gülle & Gülle, 1♀ (sequenced).

Remarks. The examined females in our study identified as *A. fonticola* following Gerecke (2003), form a unique BIN (BOLD:AGG3788). The *p*-distance between the latter BIN and its nearest neighbor, BOLD:ADS3489, which includes specimens of *A. fonticola* from Germany, Italy and Montenegro, was estimated at 9.56% suggesting phylogeographic break between European and Turkish populations of this species.

Distribution. Europe, except British Isles and Sweden, Türkiye.

Atractides (*Atractides*) *graecus* K. Viets, 1950

Material examined. Burdur • TR20-2024, Karacaören, stream, 37.327335°N, 30.869408°E, 25 Apr. 2024, Pešić, Zawal, Gülle & Gülle, 1♀ (sequenced), palp and I-leg on one side dissected and slide mounted (RMNH).

Remarks. The single female from Burdur used in this study for molecular analysis matches the description of *A. graecus*. Genetic data indicate that this specimen forms a unique BIN (BOLD:AGG3781).

Distribution. Mediterranean; Türkiye.

Atractides (*Atractides*) *inflatipalpis* K. Viets, 1950
Fig. 3

Material examined. Burdur • TR3-2024 Akyayla, rheohelocrenic spring, 37.515774°N, 30.35459°E, 22 Apr. 2024, leg. Pešić, Zawal, Gülle & Gülle, 1♂, 2♀ (sequenced), 1♂, 1♀ dissected and slide mounted (RMNH).

Remarks. In regard to the lineated integument and the shape of I-leg and palp, the examined specimens match the description of *Atractides inflatipalpis*. These specimens forms a unique BIN (BOLD:AGG3787), with the nearest neighboring BIN being BOLD:AEF1145, which include one female from Montenegro morphologically assigned by the first author to *A. inflatipalpis*. The *p*-distance between these two BINs was estimated at 3.66%. In the phylogenetic tree, the BIN is positioned as a sister clade of *A. fonticolus*. From the latter species, *A. inflatipalpis* differs in more distant S-1 and S-2 setae on I-L-5, a weakly enlarged S-2, a slenderer I-L-6 (Fig. 3A, B) and the strongly protruding finger-like extension of the male P-2 (Fig. 3D).

Distribution. Mediterranean (Greece, Bulgaria, Italy, France, Italy). In Türkiye previously reported from Erzurum Province (Erman et al. 2010).

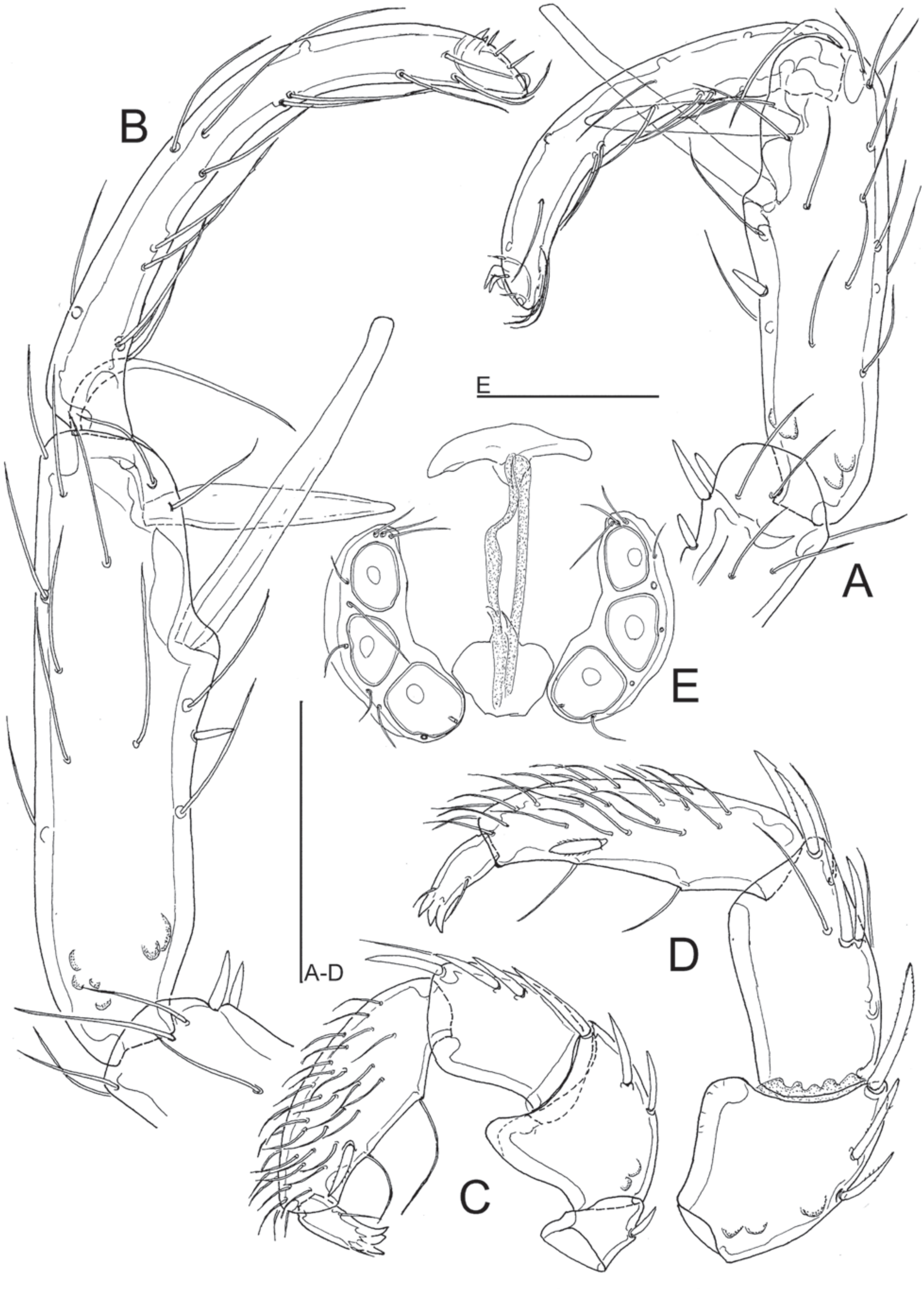

Figure 3. *Atractides inflatipalpis* K. Viets, 1950 (**A, C** male **B, D–E** female [CCDB-48498-C02], Burdur, Akyayla, rheohelocrenic spring: **A, B** I-L-5 and I-L-6 **C, D** palp, medial view **E** genital field. Scale bars: 100 μm.

Atractides **(*Atractides*)** ***lunipes*** **Lundblad, 1956**

Material examined. Burdur • TR20-2024, Karacaören, stream, 37.327335°N, 30.869408°E, 25 Apr. 2024, Pešić, Zawal, Gülle & Gülle, 1♀ (sequenced), dissected and slide mounted (RMNH).

Remarks. Genetic data indicate that the examined specimen from Turkey forms a unique BIN (BOLD:AGG3780). The single female from Burdur used in this study for molecular analysis is in good agreement with the redescription of *Atractides lunipes* given by Gerecke (2021) based on populations from Calabria and Sicily. In the phylogenetic tree, the specimen from Türkiye, morphologically assigned to *A. lunipes*, was placed as a sister to *A. zagrosensis* Pesic, Saboori & Asadi, 2016 and *A. corsicus* E. Angelier, 1954, the latter known only from Corsica and Sardinia and considered by Gerecke (2021) as an insular sister species of *A. lunipes*. *Atractides zagrosensis* was originally described by Pesic et al. (2004) as *A.* cf. *lunipes* Lundblad, 1956, based on specimens collected in Chahar Mahal and Bakhtiari Province, Iran. Later, this taxon was raised to the status of a separate species (Pešić et al. 2016) and recently barcoded on basis of specimens collected in Iran and Turkey's Aegean Region (Aydin province, see Pešić et al. 2023a for details). From *Atractides zagrosensis*, *A. lunipes* differs in relatively shorter I-L-5 (I-L-5/6 L ratio 1.15–1.2), more slender setae S-1 and S-2 (L/W S-1 > 17.0, S-2, > 7.0), and slenderer I-L-6 (see Pešić et al. 2016 for details).

Distribution. Western and Southwestern Europe, Türkiye.

Atractides **(*Atractides*)** ***nikooae*** **Pesic, 2004**

Material examined. Burdur • TR25-2024 Karamusa stream, 37.186405°N, 29.75374°E, 26 Apr. 2024, leg. Pešić, Zawal, Gülle & Gülle, 2♀ (sequenced) • TR23-2024, Çavdır, spring, 37.14478°N, 29.656534°E, 26 Apr. 2024, leg. Pešić, Zawal, Gülle & Gülle, 1♂ (sequenced), one palp and one I-leg dissected and slide mounted (RMNH).

Remarks. The specimens from southwestern Türkiye match the description of *Atractides nikooae*, a species originally described from the Markazi Province, West Iran (Pesic et al. 2004), and later reported from Siirt Province in Turkey (Esen et al. 2013a). The specimens from Türkiye form a unique BIN (BOLD:AGG3766), with the nearest neighboring BIN being BOLD:ACS0163, which includes specimens of *A. distans* from the Netherlands, Poland, and Italy. The *p*-distance between these two BINs is estimated at 14.63%.

Distribution. Iran, Türkiye.

Atractides **(*Atractides*)** ***robustus*** **(Sokolow, 1940)**

Material examined. Isparta • TR17-2024 Çukurköy, stream, 37.651257°N, 30.81791°E, 25 Apr. 2024, leg. 1♂ (sequenced) • TR18-2024, Yazılıkanyon Tabiat Parkı, stream from cave (moss), 37.46882°N, 30.919449°E, 25 Apr. 2024, leg. Pešić, Zawal, Gülle & Gülle, 1deutonymph (sequenced).

Remarks. The sequenced specimens from southwestern Türkiye were clustered within two BINs, i.e. BOLD:AGH5609 which include one specimen from this study and BOLD:AEK3669, which in addition to a single deutonymph from our study includes one specimen of *A. robustus* from eastern Türkiye (Bingöl province). The *p*-distance between these two BINs was estimated at 2.89%.

For a long time, *A. robustus*, a species originally described from the Caucasus (the affluents of the Kuban River) has been considered as a common species in Europe (Gerecke 2003). However, recent genetic data revealed that this species consists of several distinct lineages (Pešić et al. 2023b). The results of the applied ASAP procedure revealed that both BINs from southwestern Türkiye belong to a single MOTU (hypothetical species), which grouped also sequences of *A. robustus* like mites from eastern Türkiye and northern Iran. On the other hand, the second MOTU, which includes European populations of *robustus*-like mites belonging to BOLD:ADZ9348 and BOLD:AFF2463, possible represent a cryptic species new to science.

Distribution. Europe, Türkiye, Caucasus, Iran.

***Atractides* (*Atractides*) *subasper* Koenike, 1902**

Material examined. Burdur • TR11-2024, Söbüce, first order stream, 37.287872°N, 30.067743°E, 24 Apr. 2024, leg. Pešić, Zawal, Gülle & Gülle, 1♀ (sequenced), dissected and slide mounted (RMNH).

Remarks. The female from Burdur used in this study for molecular analysis, matches the description of *A. subasper*, a species easily identified by a pointed and protruding gnathosomal rostrum, three pairs of acetabula arranged in a weakly curved line and a rather homomorphic S-1 and S-2 setae on I-L-5 (see Gerecke 2003). The specimen from Türkiye forms a unique BIN (BOLD:AGG3778) with the nearest neighboring BIN being BOLD:AEX4044, which includes specimens from Serbia, Italy, Bulgaria, Albania, and Switzerland. The *p*-distance between these two BINs is estimated at 8.67%. The only public sequence in BOLD:AEX4044 belongs to a female specimen from Serbia morphologically assigned by Jovanović et al. (2024) to *A. glandulosus* (Walter, 1918), a species with certainty known from the Alps, southern Germany, and the Pyrenees (Gerecke 2003). Re-examination of the female from Serbia revealed good agreement with *A. subasper*, except in the shape of the gnathosoma, which is with a short rostrum, not pointed and protruding as in typical *subasper* specimens. The results of the applied ASAP procedure grouped the sequences of these two BINS into the same MOTU (hypothetical species). The BIN BOLD:AES6460 which groups the sequence of *A. subasper* from Sardinia forms a separate MOTU with a high genetic distance (10.91% *p*-distance) to the next closest BIN of *A. subasper* (BOLD:AEX4044) indicating that the populations from Sardinia probably represent a species new to science.

Distribution. Central and southern Europe, Türkiye, Caucasus.

***Atractides* (*Atractides*) *turani* Pešić, Zawal, Gülle & Smit, sp. nov.**

https://zoobank.org/260B41B7-7CE4-429A-BBD3-CD585188C062

Fig. 4

Type material. *Holotype* • ♂, sequenced (Voucher Id: CCDB-48498-A09), dissected and slide mounted (RMNH), Burdur, TR11-2024, Söbüce, stream, 37.287872°N, 30.067743°E, 24 Apr. 2024, leg. Pešić, Zawal, Gülle & Gülle.

Other material. • 1♂, sequenced (Voucher Id: CCDB-48498-F11), one palp and one I-leg dissected and conserved in Koenike's fluid, **Burdur**, TR2-2024 Akyayla, rheocrenic spring, 37.482956°N, 30.326647°E, 22 Apr. 2024, leg. Pešić, Zawal, Gülle & Gülle.

Diagnosis. (female unknown) Integument lineated, P-2 with a weakly developed protrusion, P-4 sword seta slightly posterior to distoventral seta, the latter closely approaching the distoventral edge of the segment, I-L-5 elongate, with setae S-1/-2 close to each other, interspace 9 µm, I-L-6 shortened and distally narrowed, L I-L-5/6 ratio > 1.6.

Description. Male (holotype). Integument lineated; dorsal and ventrocaudal idiosoma without sclerotized muscle insertions. Genital plate with nearly straight anterior margin, posterior margin medially indented in an obtuse angle. Gonopore long, flanked by ~ 10 pairs of fine setae. Acetabula subtriangular, arranged in an obtuse triangle. Excretory pore smooth, Vgl-1/2 separate.

Gnathosoma without particularly projecting rostrum, palp with a rounded distoventral projection at P-2, P-4 slightly protruding near proximoventral seta, sword seta long and curved, inserting slightly posterior to distoventral seta, distoventral seta closely approaching the distoventral edge of the segment (Fig. 4C), ventral margin divided in sectors 3: 5: 1.

I-L-5 elongate, dorsal and ventral margin diverging only towards distal segment end; setae S-1 and S-2 bluntly pointed and close to each other (separation < 10 µm), S-1 slightly shorter and more slender than S-2; I-L-6 shortened and curved, equally narrowed from base to tip (Fig. 4B).

Measurements (holotype [CCDB-48498-A09], in parentheses some measurements of specimen from Akyayla [CCDB-48498-F11] — Idiosoma L 590 (603), W (456); maximum diameter Dgl-4, 24 (25). Coxal shield L 303; Cx-III W 344; Cx-I+II mL 94, Cx-I+II lL 211. Genital field L/W 116 (127)/125 (132), ratio 0.93 (0.96), L Ac-1-3: 44 (45–48), 39–42 (48–56), 38–39 (42).

Palp — Total L 288 (307); dL/H: P-1, 30/30 (33/30); P-2, 66/48 (69/53); P-3, 64/42 (66/42); P-4, 97/37 (105/35); P-5, 31/12 (34/12); L ratio P-2/P-4, 0.68 (0.63). Chelicera total L 197, capitulum vL 121.

Legs — I-L-5 dL 170 (183), vL 134 (138), dL/vL ratio 1.28 (1.33), maximum H 50 (58), dL/maximum H ratio 3.4 (3.16), S-1 L 77 (88), L/W ratio 9.2 (10.4), S-2 L 65 (73), L/W ratio 5.5 (6.7), distance S-1-2, 9 (11), dL ratio S-1/2, 1.19 (1.14); I-L-6 dL 95 (113), central H 22 (23), dL/central H ratio 4.27 (4.9); L I-L-5/6 ratio 1.79 (1.62).

Female. Unknown.

Etymology. The new species is named after Prof. Davut Turan (Recep Tayyip Erdoğan University, Rize, Türkiye) in appreciation of his comprehensive work on Turkish ichthyofauna.

Species delimitation using DNA barcodes. The final alignment for species delimitation using COI sequence data comprised 681 nucleotide positions

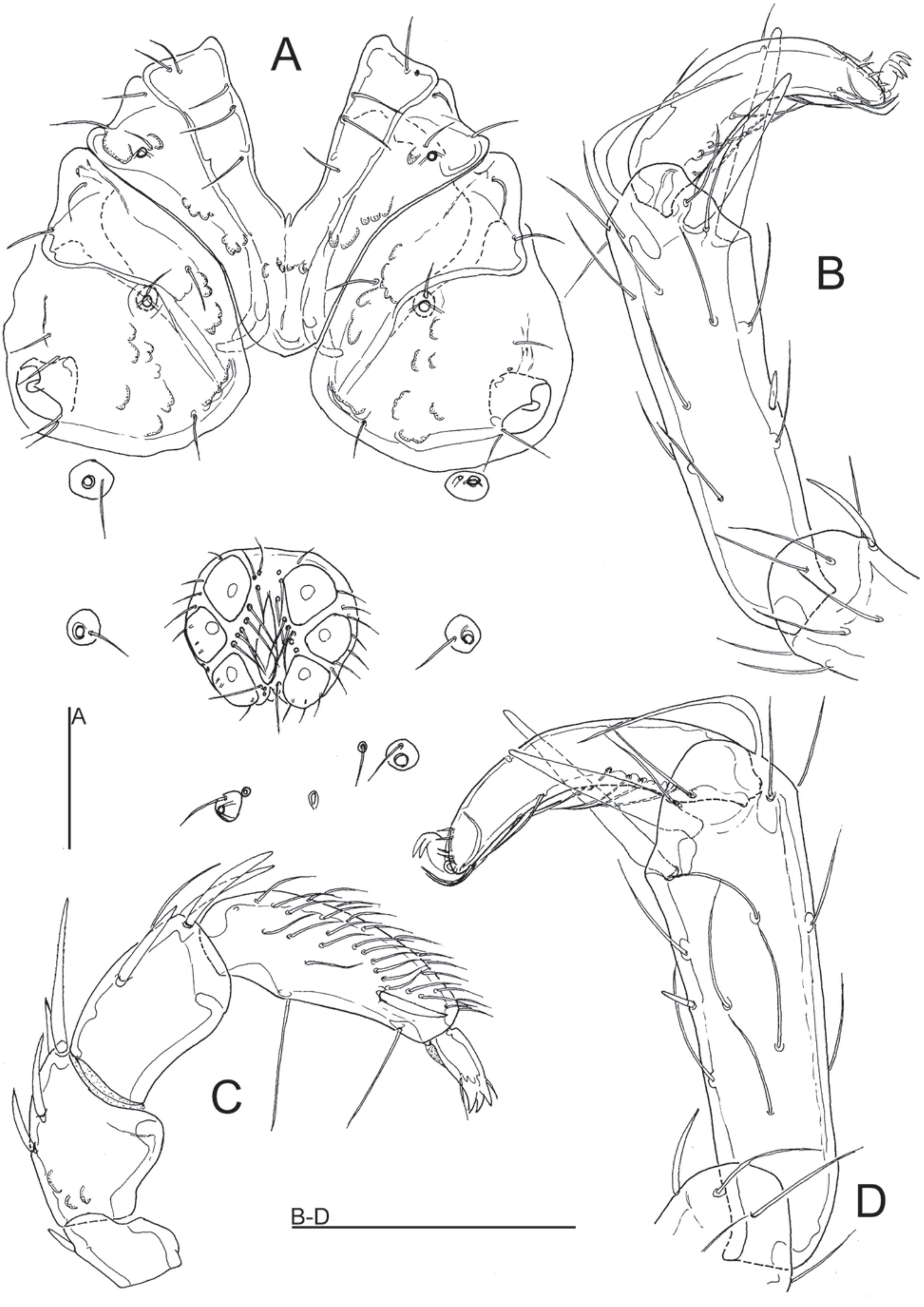

Figure 4. *Atractides turani* sp. nov., ♂ (**A–C** holotype [CCDB-48498-A09] **D** specimen from Akyayla [CCDB-48498-F11], Burdur, Söbüce, stream: **A** coxal and genital field **B, D** I-L-5 and I-L-6 **C** palp, medial view. Scale bars: 100 µm.

(nps) of the 353 *Atractides* specimens listed in Suppl. material 1. *Atractides acutirostris* from the subgenus *Tympanomegapus* was used to root the tree. The NJ tree is presented in Fig. 5. The COI tree sequences retrieved from two specimens collected in southeastern Türkiye reveals the presence of two maximally supported clades corresponding to each of sequenced individuals. These two clades were placed, albeit with a low support, as a sister group to the cluster of sequences belonging to *A. fissus* (Walter, 1927).

Differential diagnosis. In the Western Palaearctic fauna, the most similar species (combining a lineated integument with a weakly developed protrusion of P-2 in males) are *A. panniculatus* (K. Viets, 1925), *A. fissus* (Walter, 1927), *A. rivalis* Lundblad, 1956, and *A. elazigensis* Esen & Pešić, 2024. From all these species (in parentheses data from Gerecke 2003 and Esen and Pešić 2024), the new species can be distinguished by having a narrower separation of setae S-1/2, < 10 µm (> 20 µm), a rather high I-L-5/6 ratio of 1.7 (L ratio I-L-5/6 < 1.5) and I-L-6 basally thickened and distally narrowed (I-L-6 longer, not narrowed in distal part).

Further European species with a rather high I-L-5/6 ratio (for details see Gerecke 2003) are *Atractides fonticolus* (K. Viets, 1920), *A. pennatus* (K. Viets, 1920), and *A. legeri* (Motaș, 1927). These three species form a distinctive species group, differing from the new species in the shape of P-2 with a ventral projection in males and the shape of I-L-6 (with dorsal and ventral margins parallel up to the base of the claw furrow, distally not continuously narrowed, see Gerecke 2003 for details).

The single sequenced male collected in spring near Akyayla differs from the type specimen in longer and consequently more slender I-L-6 (compare Fig. 4B with Fig. 4C). Genetic data indicate that this specimen forms a unique BIN (BOLD:AGG3774). The *p*-distance between this BIN and BOLD:AGG3768, which include type specimen of *A. turani* sp. nov., was estimated at 6.26%. The results of the applied ASAP procedure grouped the sequences of these two BINS into the same MOTU (hypothetical species).

Distribution. Türkiye.

Genus *Hygrobates* Koch, 1837

Hygrobates (*Hygrobates*) *persicus* Pešić & Asadi, 2017

Material examined. Antalya • TR28-2024 Düden river, 36.959763°N, 30.731194°E, 27 Apr. 2024, leg. leg. Pešić, Zawal, Gülle & Gülle, 1♂, 3♀ (sequenced). **Isparta** • TR15a-2024 Kışlaköy, spring, 37.66509°N, 30.725111°E, 25 Apr. 2024, leg. Pešić, Zawal, Gülle & Gülle, 2♂ (sequenced).

Remarks. The specimens from southwestern Türkiye morphologically match the description of *Hygrobates persicus*. This species is widely distributed in Iran, while in Türkiye it is known only from the Çoruh River in northeast Anatolia (Bayburt province, Pešić et al. 2017). The sequenced specimens from Antalya and Isparta provinces cluster within BOLD:ACB5533, which, in addition to the specimens used in this study, includes specimens morphologically assigned to *H. persicus*.

Distribution. Iran, Türkiye.

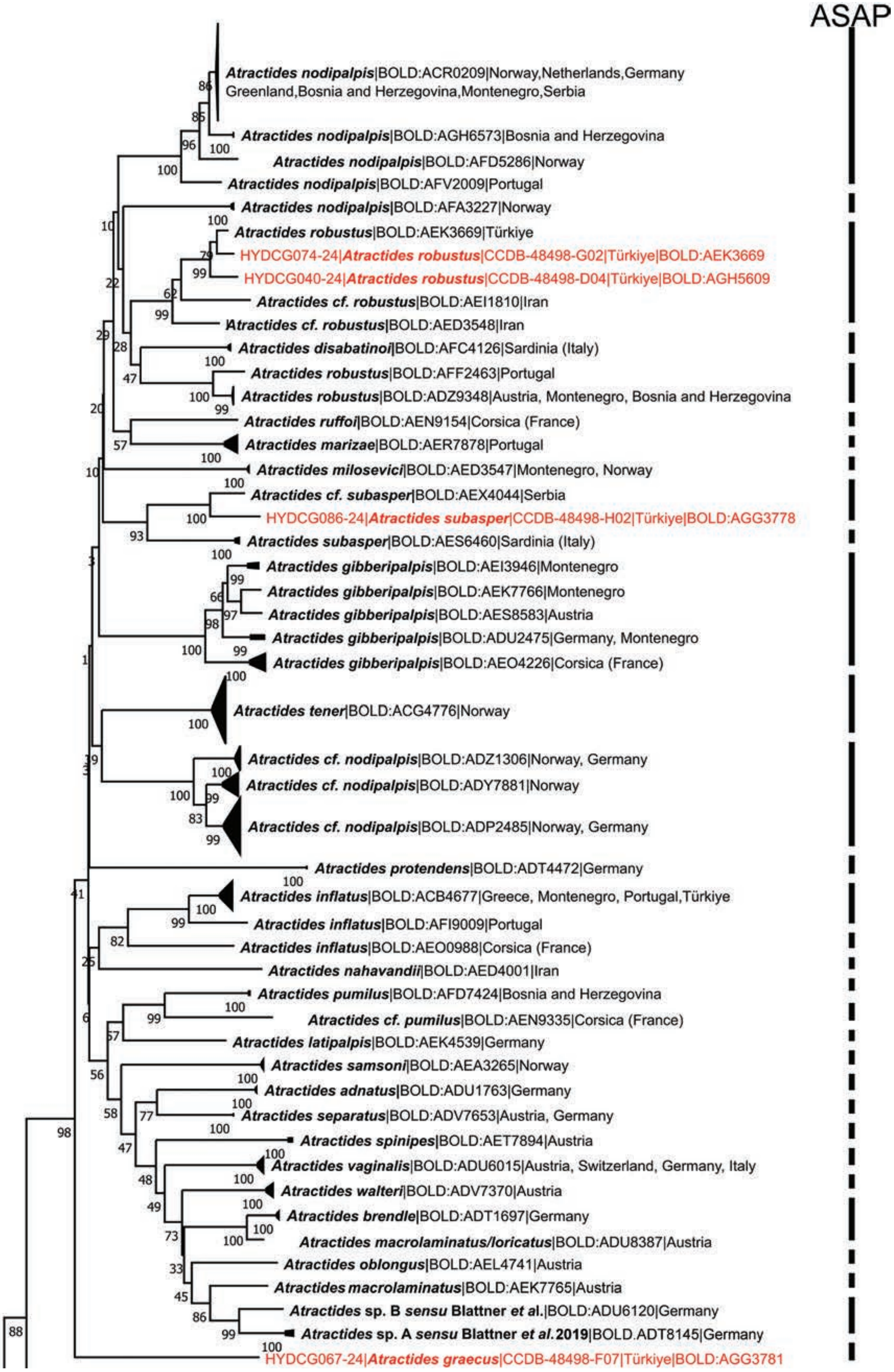

Figure 5. Neighbor-Joining tree of the subggenus *Atractides* s. str. obtained from 353 nucleotide COI sequences listed in Suppl. material 1. *Atractides acutirostris* (Motas & Angelier, 1927) from the subgenus *Tympanomegapus* was used to root the tree. The results of species delimitation by ASAP procedure are indicated by vertical bars. BINs are based on the barcode analysis from 4 November 2024. New sequences from this study are marked in red.

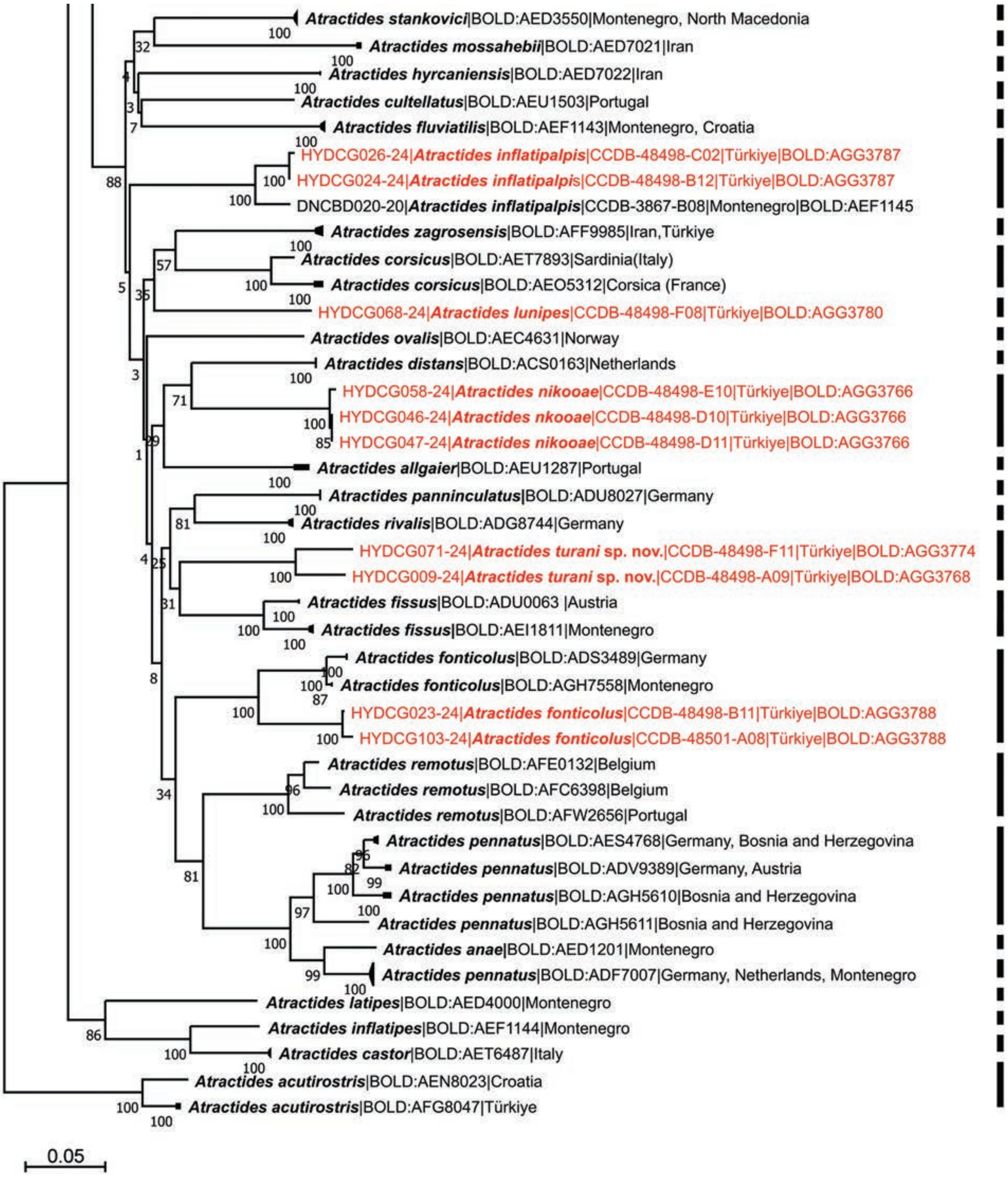

Figure 5. Continued.

Hygrobates (*Hygrobates*) *longipalpis* (Hermann, 1804)

Material examined. Burdur • TR6-2024 Sazak, rheocrenic spring, 37.544933°N, 29.94381°E, 23 Apr. 2024, leg. 1♂, 1♀ (sequenced) • TR12-2024, Burdur, Kayalı, limnocrene spring, 37.306606°N, 29.931082°E, 24 Apr. 2024, leg. Pešić, Zawal, Gülle & Gülle, 1♂ (sequenced) • TR14-2024 Dereköy, spring, 37.42846°N, 29.809637°E, 24 Apr. 2024, leg. Pešić, Zawal, Gülle & Gülle, 1♀ (sequenced). **Isparta** • TR15-2024, Kışlaköy, river, 37.66509°N, 30.725111°E, 25 Apr. 2024, leg. Pešić, Zawal, Gülle

& Gülle, 1♂ (sequenced). **Antalya** • TR27-2024 limnocrene spring, 37.09568°N, 30.58095°E, 27 Apr. 2024, leg. Pešić, Zawal, Gülle & Gülle, 1♂ (sequenced).

Remarks. The sequenced specimens from this study are clustered in BOLD:AES0232, which, in addition to the specimens from this study, includes specimens from North Macedonia and Montenegro as well as specimens from Burdur province identified as *H. longipalpis* in Pešić et al. (2023c).

Distribution. Western Palaearctic.

***Hygrobates* (*Rivobates*) *quanaticola* Schwoerbel & Sepasgozarian, 1976**

Material examined. Burdur • TR1-2024 Kuzköy, spring, 37.55402°N, 30.440313°E, 22 Apr. 2024, leg. Pešić, Zawal, Gülle & Gülle 3♀ (sequenced) • TR14-2024 Dereköy, rheocrenic spring, 37.42846°N, 29.809637°E, 24 Apr. 2024, leg. Pešić, Zawal, Gülle & Gülle, 1♀ (sequenced) • TR26-2024 Kestel, canal with fast-flowing water, 37.429718°N, 30.399193°E, 27 Apr. 2024, leg. Pešić, Zawal, Gülle & Gülle, 1♀ (sequenced).

Remarks. The sequences obtained from the specimens assigned morphologically to *H. quanaticola* are clustered within two BINs, i.e. BOLD:AGG3789, which includes three specimens from this study, and BOLD:AEM9575, which in addition to two specimens from this study, includes three specimens from Burdur published in Pešić et al. (2023c). The *p*-distance between these two BINs was estimated at 2.57%.

Distribution. Iran, Türkiye.

Family Unionicolidae Oudemans, 1909
Subfamily Pionatacinae K. Viets, 1916
Genus *Neumania* Lebert, 1879

***Neumania* (*Neumania*) *imitata* Koenike, 1908**

Material examined. Antalya • TR29-2024 Aksu, pond near Antalya city, 36.87547°N, 30.8454°E, 27 Apr. 2024 leg. Pešić, Zawal, Gülle & Gülle, 2♀ (sequenced).

Other material examined. *Neumania imitata*, the Netherlands, Merkske • Halsche Beemden, 51.422°N, 4.826°E, 13 Jun. 2016 leg. Smit 3♂ (sequenced; NLACA976-17/RMNH.5070734, NLACA977-17/ RMNH.5070735, NLACA978-17/ RMNH.5070736), dissected and slide mounted (RMNH).

Remarks. The examined male in our study, identified as *Neumania imitata* following Gerecke et al. (2016), forms a unique BIN (BOLD:AGG4333). The *p*-distance between this BIN and its nearest neighbor, BOLD:ADF7924, which includes specimens of *N. imitata* from the Netherlands, is estimated at 2.25%.

Distribution. Europe; rare, reported from France, Italy, Germany, the Netherlands, Poland, Montenegro, and Portugal (Pešić et al. 2024).

***Neumania* (*Neumania*) *limosa* (Koch, 1836)**

Material examined. Burdur • TR5-2024 Düger, limnocrene spring, 37.574345°N, 30.021276°E, 23 Apr. 2024, leg. Pešić, Zawal, Gülle & Gülle, ♀ (sequenced).

Remarks. The sequenced specimens from this study cluster in BOLD:AEF5902, which includes specimens of *N. limosa* from Montenegro. The *p*-distance between this BIN and its nearest neighbor BOLD:ACS0551, which includes specimens from the Netherlands and Portugal assigned to *N. limosa*, is estimated at 3.21%.

Distribution. Palaearctic.

Family Pionidae Thor, 1900
Genus *Piona* Koch, 1842

Piona alpicola (Neuman, 1880)

Material examined. Burdur • TR22-2024 Uylupınar, limnocrene spring, 37.10993°N, 29.613293°E, 26 Apr. 2024, leg. Pešić, Zawal, Gülle & Gülle, 1♀ (sequenced).

Remarks. The single female from Burdur, molecularly analyzed in this study, clusters in BOLD:ACR9570, which includes specimens from the Netherlands.

Distribution. Holarctic.

Family Arrenuridae Thor, 1900
Genus *Arrenurus* Dugès, 1834

Arrenurus (*Arrenurus*) *compactus* Piersig, 1894

Material examined. Burdur • TR22-2024 Uylupınar, limnocrene spring, 37.10993°N, 29.613293°E, 26 Apr. 2024, leg. Pešić, Zawal, Gülle & Gülle, 1♀ (sequenced).

Remarks. The examined female from Burdur clusters in BOLD:AEJ6492, which includes a single specimen from Norway assigned to *Arrenurus compactus*.

Distribution. Palaearctic.

Arrenurus (*Arrenurus*) *suecicus* Lundblad, 1917

Material examined. Burdur • Uylupinar, limnocrene spring, 37.10993°N, 29.613293°E, 26 Apr. 2024, leg. Pešić, Zawal, Gülle & Gülle, 1♀ (sequenced).

Remarks. The examined female from Burdur clusters in BOLD:AAV9863, which includes a specimen of *Arrenurus suecicus* from Sweden. The *p*-distance from the nearest neighboring BIN BOLD:ADF6369, which includes a single specimen of *A. suecicus* from the Netherlands, was estimated at 2.24%.

Distribution. Western Palaearctic.

Arrenurus (*Truncaturus*) *fontinalis* K. Viets, 1920

Material examined. Burdur • TR3-2024 Akyayla, rheohelocrenic spring, 37.515774°N, 30.35459°E, 22 Apr. 2024, leg. Pešić, Zawal, Gülle & Gülle, 2♀ (sequenced) • TR9 Kemer, helocrenic spring 37.301468°N, 30.097061°E, 22 Apr. 2024, leg. Pešić, Zawal, Gülle & Gülle, 1♂, 2♀ (sequenced).

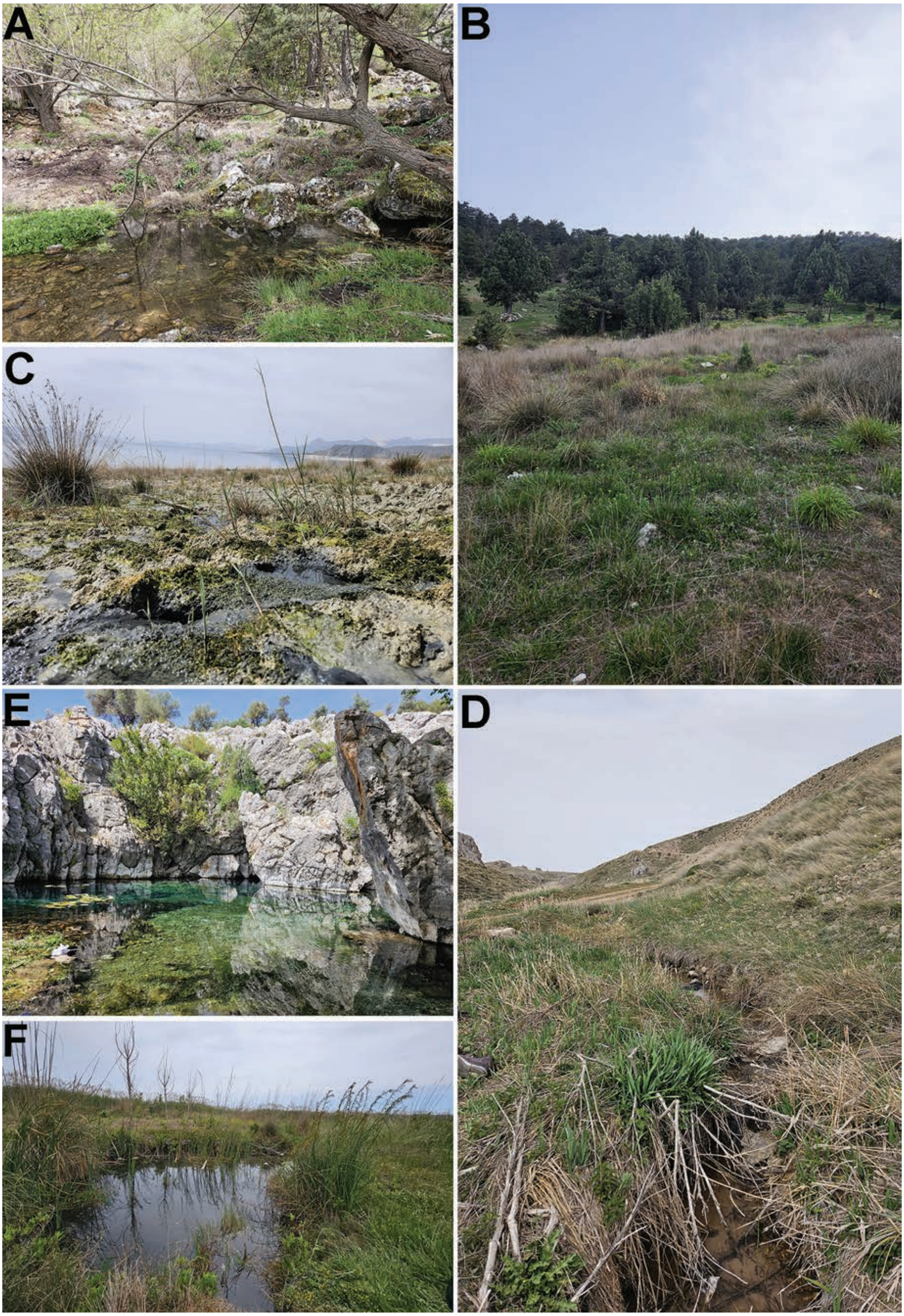

Figure 6. Photographs of selected sampling sites **A** Burdur, TR2-2024 Akyayla, spring **B** Burdur, TR3-2024 Akyayla, rheohelocrenic spring **C** Burdur, TR4-2024 helocrenic spring near Burdur Lake **D** Burdur, TR11-2024, Söbüce, first order stream **E** Antalya, TR27-2024 limnocrene spring **F** Antalya, TR29-2024 Aksu, pond. Photographs by VP.

Remarks. The sequenced specimens from southwestern Türkiye form a unique BIN (BOLD:AGH5781) with the nearest neighboring BIN being BOLD:ADS8719, which includes two specimens of *A. fontinalis*, one from the Germany and one from an unknown locality. The *p*-distance between these two BINs was estimated at 11.78%, indicating the need for taxonomic revision of *A. fontinalis* complex to identify possible undescribed cryptic species.

Distribution. Western Palaearctic.

Conclusions

This study provides the first insight into the molecular diversity of water mites in southwestern Türkiye. The formation of a DNA barcode reference library, one of the key results of this study, is a continuation of our ongoing work on the molecular characterization of water mites that inhabit Türkiye. BOLD contains a relatively small number of barcodes of Turkish water mites, with approximately 44% of the barcodes added by this study. Despite the short collection period and the limited number of individuals included in the molecular analyses, our study provided 40 BINs, 23 of which were new to BOLD. Broader sampling during different seasons and more comprehensive efforts through various ongoing barcode initiatives at the regional and international level would certainly result in higher estimates of the molecular richness of water mites in the study area.

Acknowledgements

We thank three anonymous reviewers, whose constructive comments greatly improved this work.

Additional information

Conflict of interest

The authors have declared that no competing interests exist.

Ethical statement

No ethical statement was reported.

Funding

The project was partly supported by the Minister of Science under the “Regional Excellence Initiative” Program for 2024-2027 (RID/SP/0045/2024/01).

Author contributions

All authors have contributed equally.

Author ORCIDs

Vladimir Pešić https://orcid.org/0000-0002-9724-345X
Andrzej Zawal https://orcid.org/0000-0002-5838-6060
Milica Jovanović https://orcid.org/0000-0003-1836-1210
Aleksandra Bańkowska https://orcid.org/0000-0003-1037-0550
Stanisław Musielak https://orcid.org/0000-0002-4770-1432
Harry Smit https://orcid.org/0000-0002-0376-6808

Data availability

All of the data that support the findings of this study are available in the main text or Supplementary Information.

References

Asadi M, Pešić V, Etemadi I (2010) A revised survey of water mites (Acari: Hydrachnidia) from Iran: new synonyms and descriptions of three new species. Zootaxa 2628: 43–55. https://doi.org/10.11646/zootaxa.2628.1.3

Bader C (1974) Die Sperchoniden der glandulosus-Gruppe (Acari, Prostigmata). Archiv für Hydrobiologie 73(4): 470–491. https://doi.org/10.1127/archiv-hydrobiol/73/1974/470

Bader C, Sepasgozarian H (1980) Wassermilben (Acari, Prostigmata, Hydrachnellae) aus dem Iran. 3. Mitteilung. Entomologische Mitteilungen aus dem Zoologischen Museum Hamburg 6(110): 381–392. https://doi.org/10.1080/01647958008683211

Boyaci YÖ, Gülle P, Özkan M (2012) Water mites of the genus *Sperchon* Kramer (Acari: Hydrachnidia: Sperchontidae) from Turkey, with description of a new species from Taurus Mountains (southern Turkey). Aquatic Insects 34(1): 85–92. https://doi.org/10.1080/01650424.2012.718080

Di Sabatino A, Gerecke R, Gledhill T, Smit H (2010) Acari: Hydrachnidia II. In: Gerecke R (Ed.) Chelicerata: Acari II. Süßwasserfauna von Mitteleuropa, Vol. 7, 2–2, Elsevier Spektrum Akademischer Verlag, Heidelberg, 1–234. https://doi.org/10.1007/978-3-8274-2266-8_1

Edgar RC (2004) MUSCLE: multiple sequence alignment with high accuracy and high 679 throughput. Nucleic acids research 32(5): 1792–1797. https://doi.org/10.1093/nar/gkh340

Erman O, Pešić V, Esen Y, Özkan M (2010) A checklist of the water mites of Turkey (Acari: Hydrachnidia) with description of two new species. Zootaxa 2624: 1–48. https://doi.org/10.11646/zootaxa.2624.1.1

Erman O, Gülle P, Özkan M, Candoğan H, Boyacı YÖ (2019) Checklist of the water mites (Acari: Hydrachnidia) of Turkey: First supplement. Zootaxa 4686(3): 376–396. https://doi.org/10.11646/zootaxa.4686.3.4

Esen Y, Pešić V (2024) Contributions to the knowledge of the water mite fauna (Acariformes, Hydrachnidia) of Türkiye with descriptions of two new species. Acarological Studies 6(1): 24–33. https://doi.org/10.47121/acarolstud.1387311

Esen Y, Pešić V, Erman O (2010) Water mites of the genus *Sperchon* Kramer (Acari: Hydrachnidia: Sperchontidae) from Turkey, with description of two new species. Zootaxa 2514: 35–46. https://doi.org/10.11646/zootaxa.2514.1.3

Esen Y, Pešić V, Erman O, Kaya Y (2013a) New water mites of the family Hygrobatidae (Acari, Hydrachnidia) from Turkey. ZooKeys 361: 15–25. https://doi.org/10.3897/zookeys.361.6389

Esen Y, Dilkaraoğlu S, Erman O (2013b) A systematic study on water mites (Acari, Hydrachnidia) of Kemaliye district (Erzincan Province). Turkish Journal of Entomology 37(3): 263–276.

Felsenstein J (1985) Confidence limits on phylogenies: An approach using the bootstrap. Evolution 39: 783–791. https://doi.org/10.2307/2408678

Gerecke R (1991) Taxonomische, faunistische und ökologische Untersuchungen an Wassermilben (Acari, Actinedida) aus Sizilien unter Berücksichtigung anderer aquatischer Invertebraten. Lauterbornia 7: 1–304.

Gerecke R (1996) Untersuchungen über die Wassermilben der Familie Hydryphantidae (Acari, Actinedida) in der Westpalaearktis I.: Beitrag zur Kenntnis der westpalaearktischen Arten der Gattung Protzia. Archiv für Hydrobiologie, Supplement 77(3/4): 271–336.

Gerecke R (1999) Further studies on hydryphantoid water mites in the W Palaearctic region (Acari, Actinedida). Archiv für Hydrobiologie, Supplement 121: 119–158.

Gerecke R (2003) Water mites of the genus *Atractides* Koch, 1837 (Acari: Parasitengona: Hygrobatidae) in the western Palaearctic region: a revision. Zoological Journal of the Linnean Society 138: 141–378. https://doi.org/10.1046/j.1096-3642.06-0.00051.x

Gerecke R (2021) The water mites of the family Hygrobatidae (Acari, Hydrachnidia) in Italy. Zootaxa 5009(1): 1–85. https://doi.org/10.11646/zootaxa.5009.1.1

Gerecke R, Gledhill T, Pešić V, Smit H (2016) Chelicerata: Acari III. In: Gerecke R (Ed.) Süßwasserfauna von Mitteleuropa, Bd. 7/2–3. Springer-Verlag Berlin, Heidelberg, 1–429. https://doi.org/10.1007/978-3-8274-2689-5

Gerecke R, Kjærstad G, Ekrem T, Stur E (2022) A faunistic study of water mites (Hydrachnidia and Halacaridae) from southern Norway. Norwegian Journal of Entomology 69: 243–268.

Gülle P, Boyaci YO (2014) A new *Protzia* species and the first description of the female of *Atractides* (*Polymegapus*) *persicus* Pesic & Asadi, 2010 from Turkey. Zootaxa 3852(5): 585–590. https://doi.org/10.11646/zootaxa.3852.5.7

Gülle İ, Gülle P, Boyacı YÖ (2017) Iranothyas alhajarica Pesic, Gerecke & Smit, 2009 (Acari; Hydrachnidia; Hydryphantidae)' nın Bazı Biyo-ekolojik Özellikleri. Mehmet Akif Ersoy Üniversitesi Fen Bilimleri Enstitüsü Dergisi, 8 (Ek (Suppl.) 1): 202–205. https://doi.org/10.29048/makufebed.329206

Ivanova NV, Grainger CM (2007a) CCDB protocols, COI amplification. http://ccdb.ca/site/wp-content/uploads/2016/09/CCDB_Amplification.pdf [Accessed on: 2024-12-20]

Ivanova NV, Grainger CM (2007b) CCDB protocols, sequencing. http://ccdb.ca/site/wp-content/uploads/2016/09/CCDB_Sequencing.pdf [Accessed on: 2024-12-20]

Ivanova NV, de Waard JR, Hebert PDN (2007) CCDB protocols, glass fiber plate DNA extraction. http://ccdb.ca/site/wp-content/uploads/2016/09/CCDB_DNA_Extraction.pdf [Accessed on 20 Dec 2024]

Jovanović M, Manović A, Pešić V (2024) An updated checklist of water mites (Acari, Hydrachnidia) of Serbia with new records revealed by DNA barcodes. Ecologica Montenegrina 74: 9–20. https://doi.org/10.37828/em.2024.74.2

Kimura M (1980) A simple method for estimating evolutionary rate of base substitutions through comparative studies of nucleotide sequences. Journal of Molecular Evolution 16: 111–120. https://doi.org/10.1007/BF01731581

Lundblad O (1942) Afrikanische Hydracarinen. Entomologisk Tidskrift 63: 155–209.

Oezkan M (1982) Wassermilben (Acari, Actinedida) aus der Türkei. Entomologica Basiliensia 7: 29–60.

Pešić V, Goldschmidt T (2023) New DNA-assisted records of water mites from Sardinia, with the description of a new species (Acari, Hydrachnidia). Ecologica Montenegrina 69: 24–44. https://doi.org/10.37828/em.2023.69.4

Pešić V, Smit H (2022) Water mites of Corsica: DNA barcode and morphological evidences. International Journal of Acarology 48: 418–428. https://doi.org/10.1080/01647954.2022.2086619

Pešić V, Smit H (2023) Integrative taxonomy reveals a new species of the water mite genus *Monatractides* K. Viets, 1926 from Corsica (Acari, Hydrachnidia: Torrenticolidae). International Journal of Acarology 49(2): 87–94. https://doi.org/10.1080/01647954.2023.2194885

Pesic V, Saboori A, Asadi M, Vafaei R (2004) Studies on water mites of the family Hygrobatidae (Acari, Hydrachnidia) from Iran, I. The water mite genus *Atractides* Koch, with the description of five new species. Zootaxa 495(1): 24–28. https://doi.org/10.11646/zootaxa.495.1.1

Pešić V, Gerecke R, Smit H (2009) A redefinition of *Iranothyas* Bader, 1984 with the description of a new species from Oman. Zootaxa 2290: 59–64. https://doi.org/10.11646/zootaxa.2290.1.6

Pešić V, Saboori A, Asadi M (2016) New species of the genus *Atractides* Koch, 1837 (Acari: Hydrachnidia: Hygrobatidae) from Iran. Systematic and Applied Acarology 21(9): 1250–1266. https://doi.org/10.11646/zootaxa.3911.3.2

Pešić V, Asadi M, Cimpean M, Dabert M, Esen Y, Gerecke R, Martin P, Savić A, Smit H, Stur E (2017) Six species in one: Evidence of cryptic speciation in the *Hygrobates fluviatilis* complex (Acariformes, Hydrachnidia, Hygrobatidae). Systematic & Applied Acarology 22: 1327–1377. https://doi.org/10.11158/saa.22.9.4

Pešić V, Zawal A, Manović A, Bańkowska A, Jovanović M (2021a) A DNA barcode library for the water mites of Montenegro. Biodiversity Data Journal 9: e78311. https://doi.org/10.3897/BDJ.9.e78311

Pešić V, Zawal A, Saboori A, Smit H (2021b) New records of water mites (Acari, Hydrachnidia) from Iran with the description of one new species based on morphology and DNA barcodes. Zootaxa 5082: 425–440. https://doi.org/10.11646/zootaxa.5082.5.2

Pešić V, Smit, H, Gülle P, Dabert M (2021c) Molecular DNA barcoding of the water mite genus *Protzia* Persig, 1896 with a description of three new species and the unknown male of *P. longiacetabulata* (Acari, Hydrachnidia). Systematic & Applied Acarology 26(7): 1213–1228. https://doi.org/10.11158/saa.26.7.3

Pešić V, Esen Y, Gülle P, Zawal A, Saboori A, Jovanović M, Bańkowska A, Smit H (2022) New records of water mites from Turkey and Iran revealed by DNA barcoding, with the description of a new species (Acari, Hydrachnidia). Systematic & Applied Acarology 27(7): 1393–1407. https://doi.org/10.11158/saa.27.7.7

Pešić V, Zawal A, Saboori A, Bańkowska A, Cakmak I, Smit H (2023a) New records of water mites (Acari, Hydrachnidia) from Iran and Türkiye based on morphology and DNA barcodes with description of one new species. Ecologica Montenegrina 66: 11–29. https://doi.org/10.37828/em.2023.66.2

Pešić V, Smit H, Zawal A (2023b) A new species of the genus *Atractides* Koch, 1837 from Montenegro (Acari: Hydrachnidia: Hygrobatidae), separated from *A. nodipalpis* (Thor, 1899), one of the most common water mite species in running waters in Europe. Systematic & Applied Acarology 28(5): 852–863. https://doi.org/10.11158/saa.28.5.7

Pešić V, Esen E, Gülle P, Zawal A, Jovanović M, Rewicz T, Smit H (2023c) An appraisal of the water mite genus *Hygrobates* Koch, 1837 from Türkiye, based on morphological and molecular data (Acariformes, Hydrachnidia, Hygrobatidae). Systematic & Applied Acarology 28(4): 742–754. https://doi.org/10.11158/saa.28.4.10

Pešić V, Zawal A, Saboori A, Bańkowska A, Cakmak I, Smit H (2023d) New records of water mites (Acari, Hydrachnidia) from Iran and Türkiye based on morphology and DNA barcodes with description of one new species. Ecologica Montenegrina 66: 11–29. https://doi.org/10.37828/em.2023.66.2

Pešić V, Zawal A, Ferreira S, Benitez-Bosco L, Cruz-Oliveira A, Girão D, Padilha A, Turaccio P, Rossini S, Ballini L, Staffoni G, Fratini S, Ciofi C, Iannucci A, Ekrem T, Stur E (2024) DNA barcode library of Portuguese water mites, with the descriptions of two new species (Acari, Hydrachnidia). ZooKeys 1217: 119–171. https://doi.org/10.3897/zookeys.1217.131730

Puillandre N, Lambert A, Brouillet S, Achaz G (2012) ABGD, Automatic Barcode Gap Discovery for primary species delimitation. Molecular Ecology 21(8): 1864–1877. https://doi.org/10.1111/j.1365-294X.2011.05239.x

Ratnasingham S, Hebert PDN (2007) BOLD: The barcode of life data system. Molecular Ecology Notes 7: 355–364. https://doi.org/10.1111/j.1471-8286.2007.01678.x

Ratnasingham S, Hebert PDN (2013) A DNA-based registry for all animal species: The Barcode Index Number (BIN) system. PloS ONE 8: e66213. https://doi.org/10.1371/journal.pone.0066213

Schwoerbel J, Sepasgozarian H (1976) Wassermilben (Acari, Prostigmata, Hydrachnellae) aus dem Iran. 1. Mitteilung. Acta Ecologica Iranica 1: 9–18.

Szalay L (1941) Grundlagen zur Kenntnis der Hydracarinen-Fauna des Komitates Bars in Ungarn. Annales Musei Nationalis Hungarici, pars Zoologica 34: 192–216.

Szalay L (1956) Beiträge zur Hydrachnellen-Fauna aus der Karpato-Ukraine. Acta Zoologica Academiae Scientiarum Hungaricae 2(4): 421–431.

Tamura K, Stecher G, Kumar S (2021) MEGA 11: Molecular Evolutionary Genetics Analysis Version 11. Molecular Biology and Evolution 38(7): 3022–3027. https://doi.org/10.1093/molbev/msab120

Viets K (1936) Wassermilben oder Hydracarina (Hydrachnellae und Halacaridae). In: Dahl F (Ed.) Tierwelt Deutschlands, Jena (G. Fischer) 31: 10 + 1–288.

Supplementary material 1

List of *Atractides* and *Sperchon* specimens

Authors: Vladimir Pešić, Andrzej Zawal, Pınar Gülle, İskender Gülle, Milica Jovanović, Aleksandra Bańkowska, Stanisław Musielak, Harry Smit

Data type: docx

Explanation note: List of specimens of genera *Sperchon* and *Atractides*, respectively, used for building the Neighbor-Joining (NJ) tree (Figs 2, 5).

Link: https://doi.org/10.3897/zookeys.1232.142699.suppl1

ZooKeys 1232: 237–248 (2025)
DOI: 10.3897/zookeys.1232.144830

Short Communication

A new species of *Monstrilla* (Copepoda, Monstrilloida) in coastal waters of northern South China Sea

Zhiqian Zhou[1,2], Xiping Lian[1], Yehui Tan[1,2]

1 *Marine Biodiversity Collections of South China Sea, Key Laboratory of Tropical Marine Bio-resources and Ecology, South China Sea Institute of Oceanology, Chinese Academy of Sciences, Guangzhou, 510301, China*
2 *University of Chinese Academy of Sciences, Beijing, 100049, China*
Corresponding author: Xiping Lian (xplian@scsio.ac.cn)

Abstract

A new monstrilloid copepod species, *Monstrilla pseudograndis* **sp. nov.**, from coastal waters in the northern South China Sea is described and illustrated. The diagnostic characters of this new species include the presence of small setae and sensilla on the forehead and four pairs of nipple-like scars on the ventral surface of the cephalothorax. Although the new species closely resembles *Monstrilla grandis* Giesbrecht, 1891 in overall morphology, it can be distinguished by the shorter antennule, the thumb-like process on the fifth leg, and the distinctive shape of the oral papilla. This represents the eighth record of this genus from China seas.

Key words: copepods, *Monstrilla*, zooplankton, taxonomy, China seas

Academic editor: Maria Cristina Bruno
Received: 19 December 2024
Accepted: 26 February 2025
Published: 18 March 2025

ZooBank: https://zoobank.org/4FA13ABA-0D63-4648-B4D4-8C0522F7BBDE

Citation: Zhou Z, Lian X, Tan Y (2025) A new species of *Monstrilla* (Copepoda, Monstrilloida) in coastal waters of northern South China Sea. ZooKeys 1232: 237–248. https://doi.org/10.3897/zookeys.1232.144830

Introduction

The order Monstrilloida Sars, 1901 is renowned for its unique and enigmatic copepods that exhibit a fascinating life cycle transitioning from endoparasitic juveniles to free-living, non-feeding adults (Huys and Boxshall 1991; Suárez-Morales 2011, 2018). Monstrilloids are known to parasitize various marine benthic invertebrates, including polychaetes and molluscs, during their preadult stages (Huys et al. 2007; Suárez-Morales 2011; Suárez-Morales et al. 2014). Adults are characterized by their non-feeding, free-swimming nature, and lack of mouthparts; they are typically encountered in plankton samples from coastal and estuarine environments (Sale et al. 1976; Suárez-Morales 2011; Lee et al. 2016).

In recent decades, the records of monstrilloids have increased rapidly, with seven valid genera, about 183 accepted species, recognized within the single family Monstrillidae Dana, 1849 (Grygier and Ohtsuka 2008; Suárez-Morales 2011, 2018, 2019; Suárez-Morales and Mckinnon 2014; Jeon et al. 2018; Walter and Boxshall 2024). Currently, research on the taxonomy and diversity of Monstrilloida continues to expand globally, with studies covering marine regions of Australia (Suárez-Morales and Mckinnon 2014), Korea (Lee and Chang 2016; Lee et al. 2016; Jeon et al. 2018), China (Lian and Tan 2019), the Philippines (Suárez-Morales 2021), Brazil (Da Cruz Lopes da Rosa et al. 2021), Canada

(Delaforge et al. 2017), Mexico (Suárez-Morales 2024; Suárez-Morales and Velazquez-Ornelas 2024), and the Mediterranean Sea (Suárez-Morales et al. 2017). In addition to diversity studies, research has focused on the biology and ecology of monstrilloids, particularly their parasitic behavior, host interactions, and effects on host health, especially on mussels (Suárez-Morales et al. 2010, 2014; Carneiro-Schaefer et al. 2017).

Monstrilla Dana, 1849–1852, is one of the most diverse genera within Monstrillidae (Suárez-Morales 2011, 2018; Jeon et al. 2024), and the proportion of antennule and the shape of fifth leg are important identification criteria in the morphological identification of females of this genus (Lee and Chang 2016; Suárez-Morales 2024). *Monstrilla* has a global distribution comprising 53 species to date and includes about 29% of all recorded monstrilloids (Walter and Boxshall 2024). Despite its extensive contribution to marine biodiversity, taxonomic studies on monstrilloid copepods in China are limited (Suárez-Morales 2018), with only seven species of *Monstrilla* having been recorded in the seas of China (Chen and Li 2008; Chen and Huang 2012; Walter and Boxshall 2024). The absence of data on Chinese species may lead to an underappreciation of the diversity of monstrilloids and hinder adequate risk assessments for mussels and other benthic marine invertebrate aquaculture industries.

During a recent re-examination of zooplankton deposited in the South China Sea marine biodiversity collections of the Chinese Academy of Sciences (SCSMBC), an adult female specimen of *Monstrilla* was discovered. This specimen, after taxonomic analysis and comparison with known congeners, was identified as a new species, *M. pseudograndis* sp. nov. This discovery not only contributes to the growing knowledge of monstrilloid diversity but also expands our understanding of the distribution of the genus *Monstrilla*.

Material and methods

Zooplankton was collected in the coast near Fangchenggang (21°22'53"N, 108°19'38"E), Guangxi Province, China on 7 June 2023 by vertical tow net (0.505 mm mesh, 0.8 m diameter at towing speed of 0.5 m/s) from the surface to a depth of 15 m (Fig. 1). The material was immediately preserved in 5% formaldehyde. Observation and measurements were carried out under a microscope (SMZ18, Nikon, Japan), and drawings were made with the aid of a camera lucida (Leica MC 190HD). Morphologic terminology follows Huys and Boxshall (1991). The nomenclature for the female monstrilloid antennulary armature proposed by Grygier and Ohtsuka (1995) is adopted. The type specimen is deposited in the South China Sea marine biodiversity collections, Chinese Academy of Sciences (**SCSMBC**).

Taxonomy

Subclass Copepoda Milne Edwards, 1840
Order Monstrilloida Sars, 1901
Family Monstrillidae Dana, 1849
Genus *Monstrilla* Dana, 1849–1852

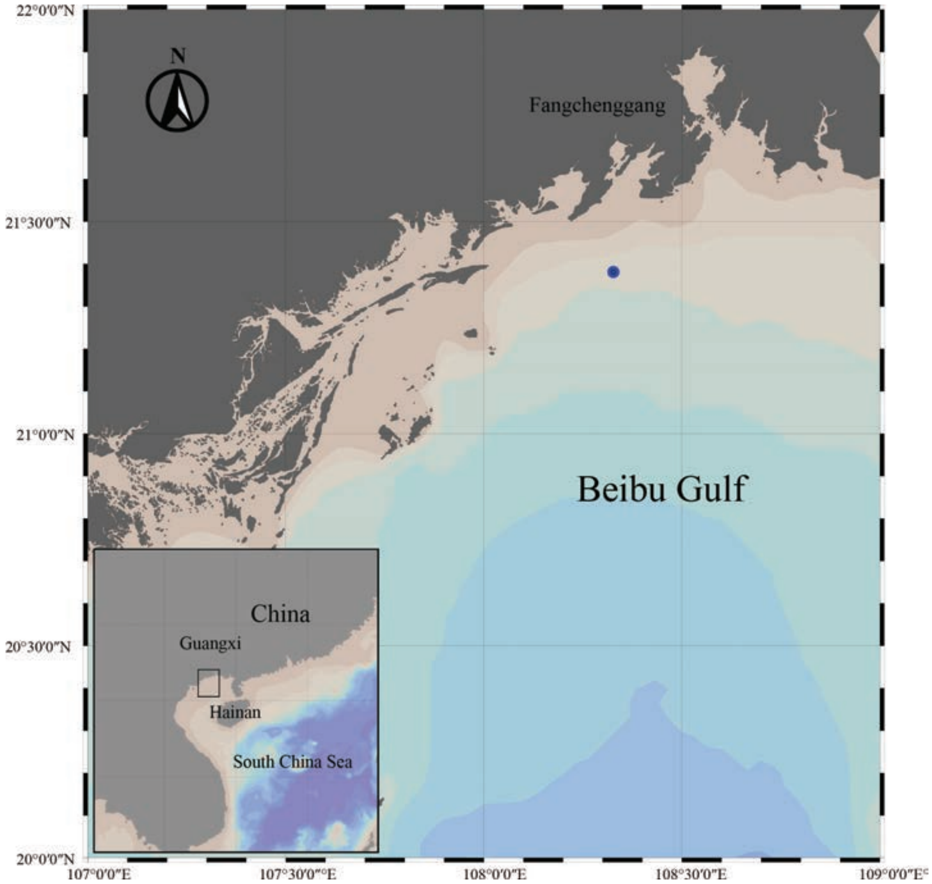

Figure 1. Sampling site of *Monstrilla pseudograndis* sp. nov. near Fangchenggang, Guangxi Province, China.

Monstrilla pseudograndis **sp. nov.**

https://zoobank.org/D8D11F64-1FCB-482D-BE80-7DF0CF40076B
Figs 2–4, Tables 1, 2

Type material. ***Holotype*****:** • adult female (SCSMBC 240185); Zhiqian Zhou leg.; 7 June 2023; partially dissected, formaldehyde preserved.

Type locality. China • Guangxi Province; coast near Fangchenggang. 21°22'53"N, 108°19'38"E; salinity 29.42, temperature 31 °C; depth 17 m.

Etymology. The species name is derived from the Greek word *pseudo*, meaning "false", and the name of the closely similar *M. grandis* Giesbrecht, 1891.

Diagnosis. Female *Monstrilla* with smooth cuticle on cephalothorax; forehead medially concave, bearing a pair of short sensilla and small setae bilaterally near antennule bases. Cephalothorax ventrally marked by four pairs of small, nipple-like scars, arranged symmetrically anterior to oral papilla. Oral papilla located at approximately midlength of cephalothorax, ventrally posteriorly-bent. Antennule two-segmented, segments fused distally, reaching 37.8% of total body length. Legs 1–4 with relatively short outer exopodal spines. Fifth legs bilobed, outer lobe elongate, with three plumose setae; inner lobe shorter, bearing two plumose setae and a basal protuberance on inner margin. Caudal rami 2.1 times as long as wide, divergent posteriorly, each armed with six well-developed caudal setae.

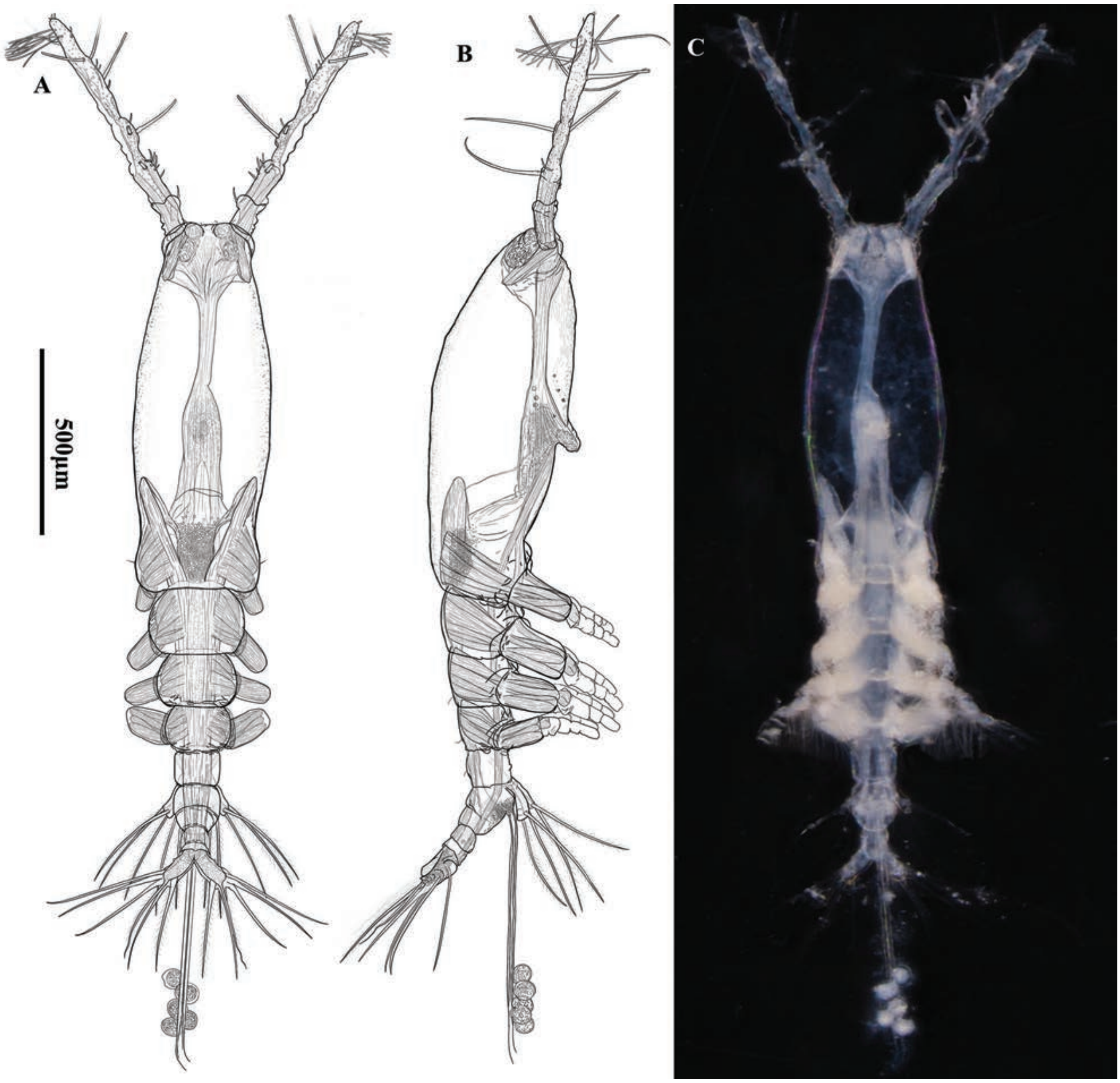

Figure 2. *Monstrilla pseudograndis* sp. nov., female holotype **A** habitus, dorsal **B** habitus, lateral **C** habitus, ventral. **A–C** share the same scale bar.

Description of adult female holotype. Body moderately elongate (Fig. 2A–C), about 1.68 mm, measured from anterior end of cephalothorax to posterior margin of caudal rami, excluding antennules and caudal setae. Cephalothorax rather large and relatively long, accounting for about 57.7% of total body length, transparent, dorsal surface smooth; anterior 2/5 slightly swollen laterally and ventrally. Nauplius eye present, weakly developed, elliptical, ocelli unpigmented with separate oval hyaline bodies, separated by 1½ eye diameter (Fig. 2A). Anteriormost part of cephalothorax with ventral, rounded convex protuberance with irregular margin in lateral view (Fig. 2B); cuticular ornamentation observed on the surface of cephalothorax in lateral and ventral view. Forehead slightly concave medially between antennulary bases in dorsal view, without rostral protrusion, bearing a pair of short, slender sensilla in the middle and a pair of setae near first antennule (Fig. 3B at arrow); weak, fine, longitudinal and transverse

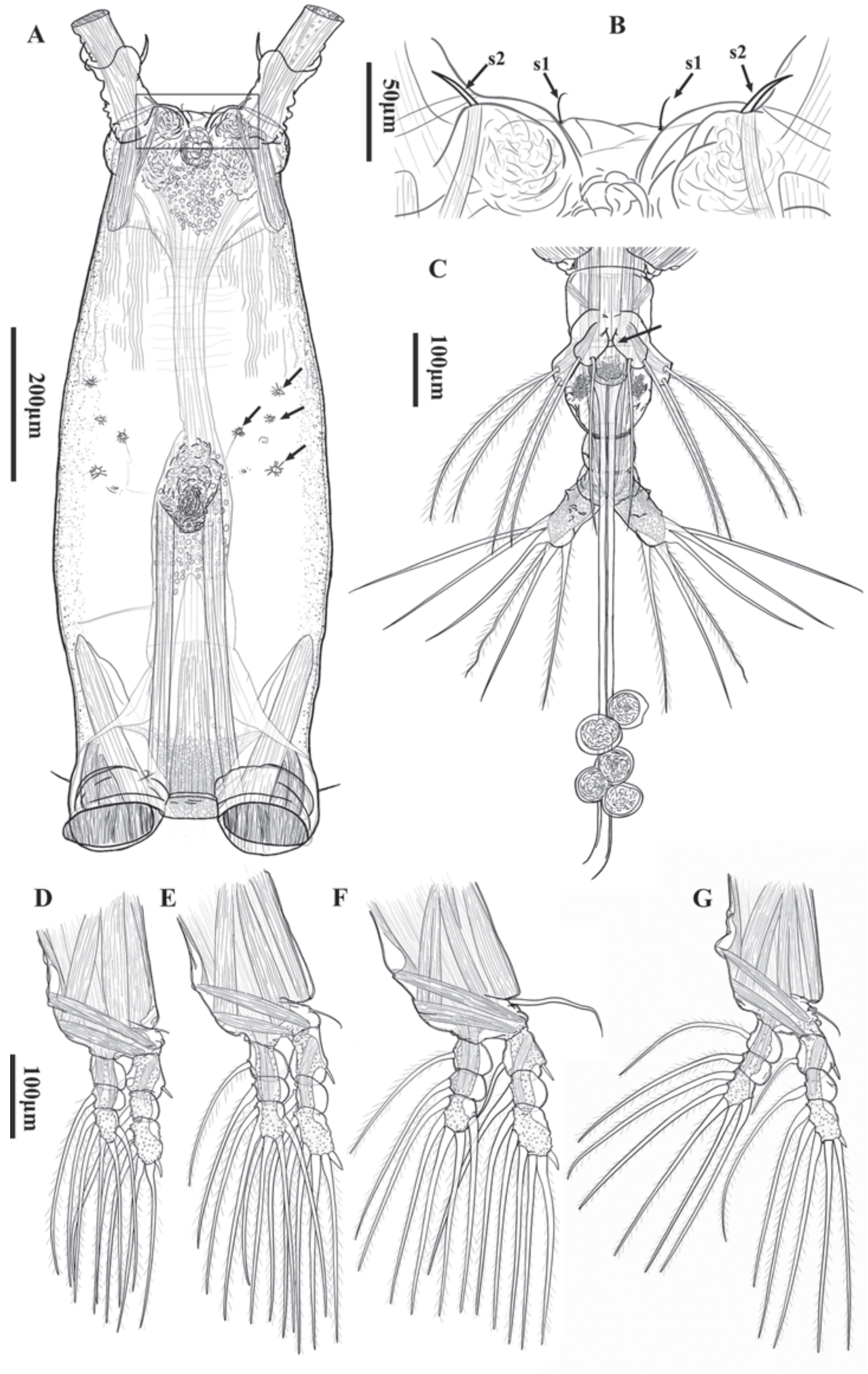

Figure 3. *Monstrilla pseudograndis* sp. nov., female holotype **A** cephalosome view, ventral (arrow indicates nipple-like processes) **B** anterior part of cephalothorax, ventral (s1 = sensilla; s2 = setae) **C** postgenital urosomites and caudal rami, ventral **D–G** leg 1–4. **D–G** share the same scale bar.

wrinkles running behind antennular bases on each side of lateroventral surfaces, flanked by four pairs of small nipple-like scars ahead of oral papilla (Fig. 3A at arrow), without sensory pore. Oral papilla situated slightly posterior to mid-length of cephalothorax, accounting for about 52.9%, protruding ventrally, with distal half posteriorly-bent (Fig. 3A).

Antennule long (Fig. 4A, B), about 37.8% of total body length, about 65.5% of the cephalothorax; antennule two-segmented, only first segment distinctly separate, remaining segments fused, with constrictions along antennular body representing places of intersegmental divisions (purported 2–5), length ratio of antennule segments, from basal to distal one: 14.0:86.0 (= 100). In terms of the pattern described by Grygier and Ohtsuka (1995) for female monstrilloid antennulary armature, setae (Roman numerals) and spines (Arabic numerals), short, slender element 1 present on first segment; purported segment two with elements $2d_1$, $2d_2$, $2v_1$, $2v_2$, $2v_3$, IId; purported segment three with elements 3, IIId and IIIv; purported segment four with elements $4v_{1-2}$, $4d_1$, IVd and IVv as well as 4aes (aesthetasc); purported segment five with elements 5, Vd, Vv and Vm; setae b_{1-3}, b_5 all dichotomously branched from proximal half or third, setae b_4 simple, without b_6. Apical elements 6_1, 6_2, and 6aes present, but 6aes absent on right antennule in dorsal view.

Legs 1–4 (Fig. 3D–G) all with both endopod and exopod three-segmented. Coxa without setae and lacking marginal rows of setae or spines. Basis not fully divided medially from coxa; all outer basal setae on legs 1–4 slender, naked; seta on leg 3 much longer. First and second exopodal segments of legs 1–4 slightly swollen, third exopodal segement undulate along outer distal margin; outer margins of all endopodal segments swollen and smooth. Outer distal spines on first and third exopodal segments of legs 1–4 feeble, much shorter than segments bearing them. Seta/spine armature of swimming legs 1–4 as in Table 1.

Table 1. Armature of legs 1–4 including basis, exopods, and endopods in *Monstrilla pseudograndis* sp. nov. Roman numerals indicate numbers of spines, and Arabic numerals indicate numbers of setae.

	Coxa	Basis	Endopod	Exopod
Leg 1	0-0	1-0	0-0; 0-1; 1,2,2	I-1;0-1;I,1,3
Leg 2–4	0-0	1-0	0-1; 0-1; 1,2,2	I-1;0-1;I,2,3

Leg 5 bilobed, both lobes confluent basally and divided distally. Outer lobe elongate, armed with three long, plumose setae apically or subapically, of subequal lengths. Inner lobe relatively short, with a basal protuberance on inner margin (arrowed in Fig. 3C), its tip exceeding the half of the outer lobe, armed with two plumose setae apically or subapically.

Urosome consisting of four urosomites: fifth pedigerous somite, genital double-somite, free postgenital somite and anal somite, accounting for 17.9% of total body length, excluding caudal setae; ratio of lengths 30.3:44.0:15.4:10.3 (=100). Genital double-somite representing almost half-length of urosome (44.0%), somewhat swollen laterally, partial suture visible; about 1.7 times longer than the combined length of the next two segments. Genital double-somite bearing pair of long ovigerous spines, these being inserted on middle of ventral surface, basally separated, with pointed tips extending far beyond tips of caudal setae, in total equal to about 38.2% of total body length. Anal somite trapezoidal; lateral margin nearly smooth in dorsal but with apparent notch in ventral; lacking wrinkles or striae both on dorsal and ventral surfaces.

Caudal rami long (Fig. 3C), about 2.1 times as long as wide; divergent outward; with small cuticular protuberance at basal part of outer face and slightly swollen at

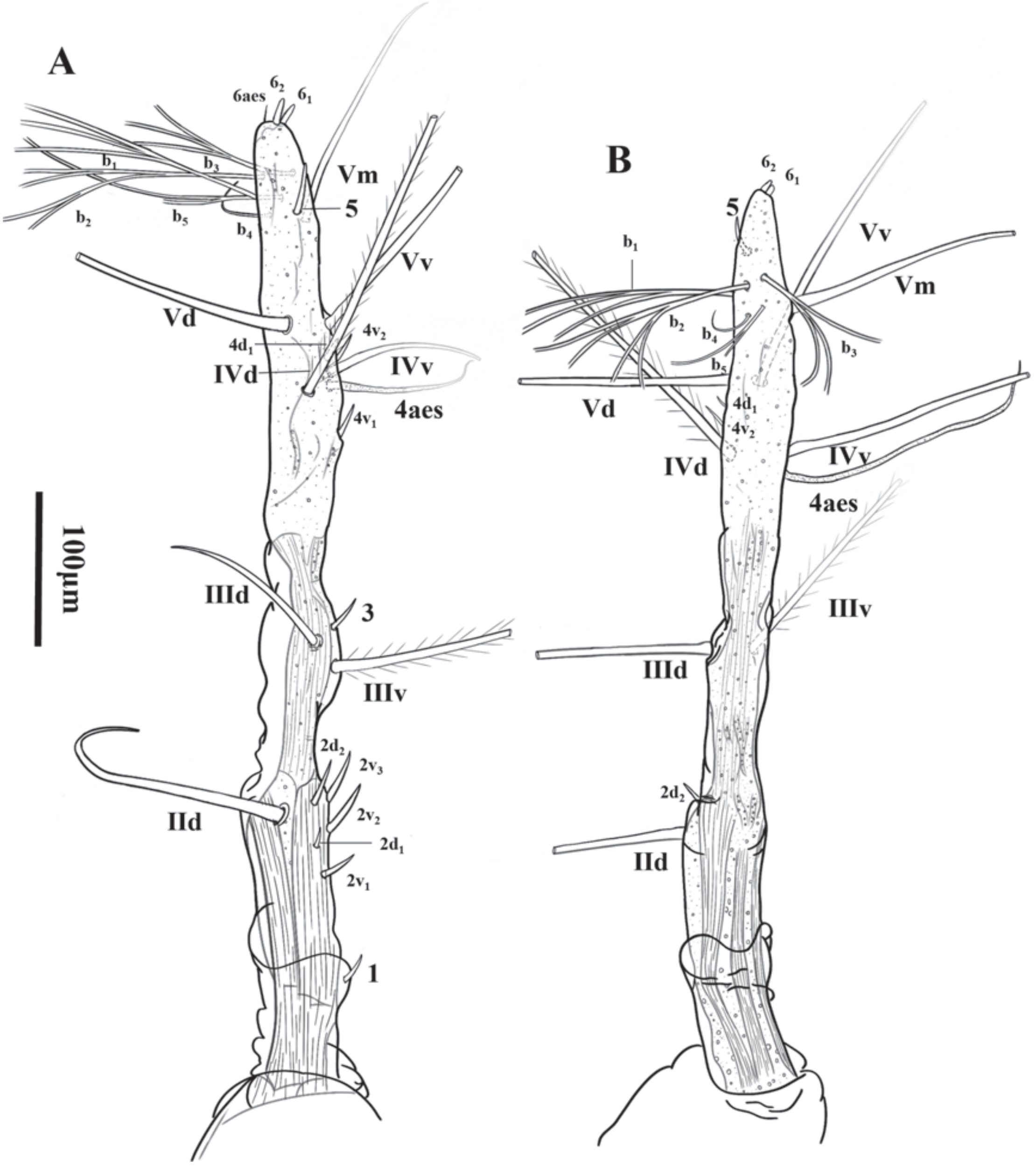

Figure 4. *Monstrilla pseudograndis* sp. nov., female holotype **A** left antennule, in dorsal view but tilted little from the medial side **B** right antennule, lateral. **A, B** share the same scale bar.

distal part of inner face; each ramus armed with six well-developed caudal setae, consisting of two distal, two lateral, one inner distal, and one dorsomedial setae.

Remarks. The new species is assigned to the genus *Monstrilla* based on the presence of one free postgenital somite and anal somite in the female, six caudal setae, and the oral papilla located ventrally at nearly midlength of the cephalothorax (Isaac 1975; Huys and Boxshall 1991; Suárez-Morales 2011). Among the females of *Monstrilla*, there are two main types of fifth leg, one of which is formed by a single lobe, such as *M. mariaeugeniae* Suarez-Morales & Islas-Landeros, 1993 (Suárez-Morales and Islas-Landeros 1993). The type II fifth leg is bilobed. Six species, *M. annulata* Suárez-Morales, 2024, *M. cymbula* A. Scott, 1909, *M. gibbosa* Suárez-Morales & Palomares-García, 1995, *M. grandis*, *M. grygieri* Suárez-Morales, 2000, and *M. investigatoris* Sewell, 1949, are similar to the new species in having the type II fifth leg and the antennule that exceeds ½ the length of the cephalothorax (Table 2) (Giesbrecht 1891; Scott 1909; Sewell 1949; Suárez-Morales and Palomares-García 1995; Suárez-Morales 2000b, 2000a, 2024; Chang 2014). Notably, only two species, *M. cymbula* and *M. grandis*, share similar features with *M. pseudograndis* sp. nov., including six well-developed caudal setae on the caudal rami and five setae on the bilobed fifth leg. These three species exhibit the same setation pattern in the fifth leg, a plesiomorphic character state with three exopodal and two endopodal setae, largest number of setae found on the fifth leg in monstrilloids (Huys and Boxshall 1991; Suárez-Morales 2024).

The forehead between the antennular bases exhibits different cuticular dorsal ornamentations in various species. This area may appear concave with a pair of small setae (Lee and Chang 2016), they may form a protrusion (Suárez-Morales et al. 2013, 2017; Suárez-Morales and Castellanos-Osorio 2019; Suárez-Morales 2024), or they present a flat surface lacking both sensilla and setae (Suárez-Morales and Gasca 2003; Suárez-Morales et al. 2020; Suárez-Morales 2021). Notably, setae and sensilla are either present singly or absent in other species. The new species possesses two distinctive features that render it readily distinguishable among its congeners and support its status as a new member of *Monstrilla*. First, *M. pseudograndis* sp. nov. bears a pair of bilateral setae on the forehead and a pair of medial sensilla (Fig. 3B), marking a unique combination that has not been previously reported in *Monstrilla*. Second, the new species has four pairs of small, nipple-like scars on the cephalothorax, flanked in ventral view, which are commonly recorded as 1–3 pairs in *Monstrilla* (Suárez-Morales 2011, 2018; Jeon et al. 2024).

Table 2. Comparison of main characters of females in seven similar *Monstrilla* species (elongate cephalothorax and fifth leg with bilobed). Sequence from A to G: *Monstrilla*, *Monstrilla*, *Monstrilla* sp. nov.

Item	*M. annulata*	*M. cymbula*	*M. gibbosa*	*M. grandis*	*M. grygieri*	*M. investigatoris*	*M. pseudograndis* sp. nov.
Antennule length >½ cephalothorax	Yes	Yes	–	Yes	Yes	Yes	Yes
Number of segments of antennule	4	2	3	3	2	2	2
Nauplius eye with pigmented	No	–	No	No	No	Yes	No
Nauplius eye elliptical	–	–	Yes	No	Yes	–	Yes
Oral papilla with posteriorly-bent distal half	Yes	Yes	Yes	No	Yes	–	Yes
Oral papilla near midlength of cephalothorax	No	Yes	No	Yes	Yes	–	Yes
Sensory pores on ventral cephalothorax	No	No	No	Yes	No	No	No
Fifth leg bilobed	Yes	Yes	Yes	Yes	Yes	Yes	Yes
Basal protuberance on inner margin of inner lobe	No	No	No	No	No	No	Yes
Distal thumb-like process on inner margin of outer lobe	No	No	No	Yes	No	No	No
Number of setae on fifth leg	2	5	4	5	4	3	5
Number of setae on caudal rami	5	6	5	6	6	6	6

Among all known species of *Monstrilla*, the new species is most closely related to *M. grandis*, which was reported by Giesbrecht (1891) in the southeastern Atlantic Ocean from southern Patagonia. As a widespread species, *M. grandis* has been extensively redescribed by researchers worldwide (Huys and Boxshall 1991; Suárez-Morales 2000b; Chang 2014). *Monstrilla grandis* and the new species share similar body proportions, including total body length, the position of the oral papilla, and the relative lengths of the cephalothorax and ovigerous spines. In addition to the two distinctive features above mentioned, several significant differences also exist: 1) the relative length of the antennule and the number of segments, which is 37.8% and two in *M. pseudograndis* sp. nov., compared to 48% of the total body length and three in *M. grandis*; 2) the ventral sensory pores of cephalothorax are absent in *M. pseudograndis* sp. nov., whereas they are present in *M. grandis*; 3) *M. pseudograndis* sp. nov. bears a protruding ventral oral papilla, with the distal half posteriorly-bent, in contrast to the slightly protruding, unbent midventral papilla in *M. grandis*.; 4) the setae on the first segment of endopod of leg 2 present in *M. pseudograndis* sp. nov., whereas absent in *M. grandis*; 5) a thumb-like process is absent on the distal part of the inner margin of the outer lobe in *M. pseudograndis* sp. nov., and it is present in *M. grandis*; 6) the inner margin of the inner lobe bears a basal protuberance in *M. pseudograndis* sp. nov., which is absent in *M. grandis*.

Acknowledgements

We thank the two anonymous reviewers for their valuable taxonomic insights. Special gratitude is extended to the editors for their meticulous editorial review and constructive feedback during the revision process. We acknowledge Jun Wang for his skilled assistance in specimen illustration and Haochen Huang for his critical advice on manuscript submission.

Additional information

Conflict of interest

The authors have declared that no competing interests exist.

Ethical statement

No ethical statement was reported.

Funding

This work was supported by Funding Biological Resources Program, Chinese Academy of Sciences (CAS-TAX-24-042); National Animal Collection Resource Center, China; Tropical Ocean Environment in Western Coastal Waters Observation and Research Station of Guangdong Province (2024B1212040008); the Program for Capacity Building for Strategic Biological Resources, Chinese Academy of Sciences (KFJ-BRP-017-48).

Author contributions

Conceptualization: ZZ, XL. Funding acquisition: XL. Investigation: ZZ. Methodology: ZZ, XL. Visualization: ZZ. Supervision: YT, XL. Project administration: YT, XL. Writing – original draft: ZZ. Writing – review & editing: ZZ, XL.

Author ORCIDs

Zhiqian Zhou https://orcid.org/0009-0006-8587-586X
Xiping Lian https://orcid.org/0009-0002-3301-1999
Yehui Tan https://orcid.org/0000-0002-6378-2156

Data availability

All of the data that support the findings of this study are available in the main text.

References

Carneiro-Schaefer AL, Sühnel S, Dias CDO, Melo CMRD, Magalhães ARM (2017) Ocorrência de *Monstrilla* sp. em Perna perna cultivado no Brasil. Boletim do Instituto de Pesca 43: 437–445. https://doi.org/10.20950/1678-2305.2017v43n3p437

Chang CY (2014) Two new records of monstrilloid copepods (Crustacea) from Korea. Animal Systematics, Evolution and Diversity 30: 206–214. https://doi.org/10.5635/ASED.2014.30.3.206

Chen QC, Huang ZG (2012) Family Monstrillidae Dana, 1849. In: Huang ZG, Lin M (Eds) The Living Species in China's Seas. China Ocean Press, Beijing, 722 pp.

Chen QC, Li KZ (2008) Family Monstrillidae Dana, 1849. In: Liu RY (Ed.) Checklist of Marine Biota of Chinese Seas. Science Press, Beijing, 632 pp.

Da Cruz Lopes da Rosa J, Dias CDO, Suárez-Morales E, Weber LI, Fischer LG (2021) Record of *Caromiobenella* (Copepoda, Monstrilloida) in Brazil and Discovery of the male of *C. brasiliensis*: morphological and molecular evidence. Diversity 13: 241. https://doi.org/10.3390/d13060241

Delaforge A, Suárez-Morales E, Walkusz W, Campbell K, Mundy CJ (2017) A new species of *Monstrillopsis* (Crustacea, Copepoda, Monstrilloida) from the lower Northwest Passage of the Canadian Arctic. ZooKeys 709: 1–16. https://doi.org/10.3897/zookeys.709.20181

Giesbrecht W (1891) Elenco dei copepodi: pescati dalla R. Corvetta "Vettor Pisani", secondo la loro distribuzione geografica. Atti della Accademia Nazionale dei Lincei, Classe di Scienze Fisiche Matematiche e Naturali Rendiconti (4)7 sem. 2: 63–68, 276–282.

Grygier MJ, Ohtsuka S (1995) Sem observation of the nauplius of *Monstrilla hamatapex*, new species, from Japan and an example of upgraded descriptive standards for monstrilloid copepods. Journal of Crustacean Biology 15: 703. https://doi.org/10.2307/1548820

Grygier MJ, Ohtsuka S (2008) A new genus of monstrilloid copepods (Crustacea) with anteriorly pointing ovigerous spines and related adaptations for subthoracic brooding. Zoological Journal of the Linnean Society 152: 459–506. https://doi.org/10.1111/j.1096-3642.2007.00381.x

Huys R, Boxshall GA (1991) Copepod Evolution. The Ray Society, London, 468 pp.

Huys R, Llewellyn-Hughes J, Conroy-Dalton S, Olson PD, Spinks JN, Johnston DA (2007) Extraordinary host switching in siphonostomatoid copepods and the demise of the Monstrilloida: integrating molecular data, ontogeny and antennulary morphology. Molecular Phylogenetics and Evolution 43: 368–378. https://doi.org/10.1016/j.ympev.2007.02.004

Isaac MJ (1975) Copepoda, sub-order: Monstrilloida. Fiches d'Identification du Zooplancton 144/145: 1–10.

Jeon D, Lee W, Soh HY (2018) A new genus and two new species of monstrilloid copepods (Copepoda: Monstrillidae): integrating morphological, molecular phylogenetic, and ecological evidence. Journal of Crustacean Biology 38: 45–65. https://doi.org/10.1093/jcbiol/rux095

Jeon D, Song C, Jeong HG, Ohtsuka S, Lee W, Soh HY, Eyun S (2024) An integrated phylogenomic approach for potential host-associated evolution of monstrilloid copepods. In: Todd PA, Russell BD (Eds) Oceanography and Marine Biology, an Annual Review, Volume 62. Taylor & Francis, 350–375. https://doi.org/10.1201/9781003477518-9

Lee J, Chang CY (2016) A new species of *Monstrilla* Dana, 1849 (Copepoda: Monstrilloida: Monstrillidae) from Korea, including a key to species from the north-west Pacific. Zootaxa 4174: 396–409. https://doi.org/10.11646/zootaxa.4174.1.24

Lee J, Kim D, Chang CY (2016) Two new species of the genus *Monstrillopsis* Sars, 1921 (Copepoda: Monstrilloida: Monstrillidae) from South Korea. Zootaxa 4174: 410–423. https://doi.org/10.11646/zootaxa.4174.1.25

Lian X, Tan Y (2019) A new species of *Cymbasoma* Thompson, 1888 (Copepoda: Monstrilloida) from the Fujian coast, China. Journal of Oceanology and Limnology 37: 1708–1713. https://doi.org/10.1007/s00343-019-8219-5

Sale PF, McWilliam PS, Anderson DT (1976) Composition of the near-reef zooplankton at Heron Reef, Great Barrier Reef. Marine Biology 34: 59–66. https://doi.org/10.1007/BF00390788

Scott A (1909) The Copepoda of the Siboga Expedition, Part I. Free swimming, littoral and semi-parasitic Copepoda. Siboga Expeditie 29a: 1–323. https://doi.org/10.5962/bhl.title.58653

Sewell RBS (1949) The littoral and semi-parasitic Cyclopoida, Monstrilloida and Notodelphyoida. John Murray Expedition 1933–34 Scientific Reports 9: 17–199.

Suárez-Morales E (2000a) A new species and new geographic records of *Monstrilla* (Copepoda: Monstrilloida) from the Philippines. Journal of Crustacean Biology 20: 680–686. https://doi.org/10.1163/20021975-99990092

Suárez-Morales E (2000b) Taxonomic report on some monstrilloids (Copepoda, Monstrilloida) from Toulon Bay, France. Bulletin de l’Institut Royal des Sciences Naturelles de Belgique, Biologie 70: 107–118.

Suárez-Morales E (2011) Diversity of the Monstrilloida (Crustacea: Copepoda). PLoS ONE 6: e22915. https://doi.org/10.1371/journal.pone.0022915

Suárez-Morales E (2018) Monstrilloid copepods: the best of three worlds. Bulletin, Southern California Academy of Sciences 117: 92–103. https://doi.org/10.3160/3646.1

Suárez-Morales E (2019) A new genus of the Monstrilloida (Copepoda) with large rostral process and metasomal spines, and redescription of *Monstrilla spinosa* Park, 1967. Crustaceana 92: 1099–1112. https://doi.org/10.1163/15685403-00003925

Suárez-Morales E (2021) A new species of *Monstrilla* (Crustacea: Copepoda: Monstrilloida: Monstrillidae) collected by the R/V albatross (1908) from the Sulu Sea, philippines. Journal of Natural History 55: 3041–3052. https://doi.org/10.1080/00222933.2022.2032444

Suárez-Morales E (2024) Two new species of *Monstrilla* (Copepoda: Monstrilloida: Monstrillidae) from a protected reef system of the Mexican Caribbean. European Journal of Taxonomy 917: 152–169. https://doi.org/10.5852/ejt.2024.917.2395

Suárez-Morales E, Castellanos-Osorio IA (2019) A new species of *Monstrilla* (Copepoda, Monstrilloida) from the plankton of a large coastal system of the northwestern Caribbean with a key to species. ZooKeys 876: 111–123. https://doi.org/10.3897/zookeys.876.38400

Suárez-Morales E, Gasca R (2003) On the invalidity of *Strilloma* Isaac (Copepoda: Monstrilloida): observations from the type species. Zoological Studies 43: 292–299.

Suárez-Morales E, Islas-Landeros ME (1993) A new species of *Monstrilla* (Copepoda: Monstrilloida) from a reef lagoon off the Mexican coast of the Caribbean Sea. Hydrobiologia 271: 45–48. https://doi.org/10.1007/BF00005694

Suárez-Morales E, Mckinnon AD (2014) The Australian Monstrilloida (Crustacea: Copepoda) I. *Monstrillopsis* Sars, *Maemonstrilla* Grygier & Ohtsuka, and *Australomonstrillopsis* gen. nov. Zootaxa 3779: 301–340. https://doi.org/10.11646/zootaxa.3779.3.1

Suárez-Morales E, Palomares-García R (1995) A new species of *Monstrilla* (Copepoda: Monstrilloida) from a coastal system of the Baja California Peninsula, Mexico. Journal of Plankton Research 17: 745–752. https://doi.org/10.1093/plankt/17.4.745

Suárez-Morales E, Velazquez-Ornelas K (2024) A new species of the genus *Monstrilla* (Copepoda: Monstrilloida: Monstrillidae) from the Gulf of California, Mexico. Revista Mexicana de Biodiversidad 95: e955361. https://doi.org/10.22201/ib.20078706e.2024.95.5361

Suárez-Morales E, Scardua MP, Da Silva PM (2010) Occurrence and histopathological effects of *Monstrilla* sp. (Copepoda: Monstrilloida) and other parasites in the brown mussel *Perna perna* from Brazil. Journal of the Marine Biological Association of the United Kingdom 90: 953–958. https://doi.org/10.1017/S0025315409991391

Suárez-Morales E, Carrillo A, Morales-Ramírez A (2013) Report on some monstrilloids (Crustacea: Copepoda) from a reef area off the Caribbean coast of Costa Rica, Central America with description of two new species. Journal of Natural History 47: 619–638. https://doi.org/10.1080/00222933.2012.742933

Suárez-Morales E, Harris LH, Ferrari FD, Gasca R (2014) Late postnaupliar development of *Monstrilla* sp. (Copepoda: Monstrilloida), a protelean endoparasite of benthic polychaetes. Invertebrate Reproduction & Development 58: 60–73. https://doi.org/10.1080/07924259.2013.816787

Suárez-Morales E, Goruppi A, De Olazabal A, Tirelli V (2017) Monstrilloids (Crustacea: Copepoda) from the Mediterranean Sea (northern Adriatic Sea), with a description of six new species. Journal of Natural History 51: 1795–1834. https://doi.org/10.1080/00222933.2017.1359698

Suárez-Morales E, Vásquez-Yeomans L, Santoya L (2020) A new species of the *Cymbasoma longispinosum* species-group (Copepoda: Monstrilloida) from Belize, western Caribbean. Revista Mexicana de Biodiversidad 91: 913176. https://doi.org/10.22201/ib.20078706e.2020.91.3176

Walter TC, Boxshall G (2024) World of Copepods Database. *Monstrilla* Dana, 1849–1852. https://www.marinespecies.org/aphia.php?p=taxdetails&id=119780 [Accessed on 2024-10-29]

ZooKeys 1232: 249–266 (2025)
DOI: 10.3897/zookeys.1232.139844

Research Article

Complete mitochondrial genomes of *Sinonovacula rivularis* and *Novaculina chinensis* and their phylogenetic relationships within family Pharidae

Yiping Meng[1,2], Liyuan Lv[3], Zhihua Lin[2], Demin Zhang[1], Yinghui Dong[2,3]

1 *School of Marine Sciences, Ningbo University, Ningbo 315010, China*
2 *College of Advanced Agricultural Sciences, Zhejiang Wanli University, Ningbo 315101, China*
3 *Ninghai Institute of Mariculture Breeding and Seed Industry, Zhejiang Wanli University, Ninghai 315604, China*
Corresponding author: Yinghui Dong (dongyinghui118@126.com)

Academic editor: Ruiqi Li
Received: 21 October 2024
Accepted: 26 January 2025
Published: 19 March 2025

ZooBank: https://zoobank.org/84C0DFB1-2719-454A-AFD7-5C6753B3FADD

Citation: Meng Y, Lv L, Lin Z, Zhang D, Dong Y (2025) Complete mitochondrial genomes of *Sinonovacula rivularis* and *Novaculina chinensis* and their phylogenetic relationships within family Pharidae. ZooKeys 1232: 249–266. https://doi.org/10.3897/zookeys.1232.139844

Abstract

Pharidae is one of the most ecologically and commercially significant families of marine Bivalvia; however, the taxonomy and phylogeny of Pharidae has been ongoing for quite some time and remains a contentious issue. Here, to resolve some problematical relationships among this family, the complete mitochondrial genomes (mitogenomes) of *Sinonovacula rivularis* (17,159 bp) and *Novaculina chinensis* (15,957 bp) were assembled, and a comparative mitochondrial genomic analysis was conducted. Both mitogenomes contain 12 protein-coding genes, 22 transfer RNA genes, and two ribosomal RNA genes. Among the published Pharidae mitogenomes, *N. chinensis* exhibited the smallest genome size but the highest AT content. The results of the phylogenetic trees confirmed the monophyly of the family Solenoidea, and indicated that *N. chinensis* and *Sinonovacula* (*S. constricta* and *S. rivularis*) were closely related in the family Pharidae. From the CREx analysis, we found that transposition and tandem duplication random losses (TDRLs) might have occurred between Pharidae and Solenidae. Moreover, positive selection was detected in nad5 of the foreground *N. chinensis*, and divergent evolution occurred at site 144 in the freshwater and marine lineages. Overall, our findings provide new molecular data on the phylogenetic and evolutionary relationships of Pharidae, and contribute to unraveling the salinity adaptations of Pharidae.

Key words: Gene arrangement, mitogenome, Pharidae, phylogeny, positive selection

Introduction

Pharidae belongs to Solenoidea which is one of the most ecologically and commercially significant superfamilies of marine Bivalvia, and the North-West and Indo-West Pacific regions exhibit the highest levels of species diversity, encompassing approximately 85% of all species, predominantly distributed in intertidal zones (Lin 2009; Saeedi et al. 2016; Costello and Saeedi 2019). According to the China Fisheries Statistics Yearbook (2024), the annual output of razor clams is 850,000 tons, accounting for 5.16% of the total output of mollusks. This Pharidae family has an extensive fossil record, dating back to approximately 103 million years ago (Mya) in the middle Cretaceous (Bolotov et al. 2018b). Although Pharidae is well-established as a clade, the internal taxonomic research has been ongoing and remains a contentious problem. Cosel (1993) promoted Solenidae to Solenoidea in 1993 and divided the superfamily into Solenidae and Pharidae according to the number of main teeth. Among them, the genus *Sinonovacula* was once classified by Graham into the family Solecurtidae, which belongs to the superfamily Tellinoidea (Graham 1935). However, an increasing number research findings contradict this, where the genus *Sinonovacula* should be categorized into the family Pharidae (Taylor et al. 2007; Guoquan et al. 2010; Yuan et al. 2012c; Yu et al. 2016). For example, the comparison of mitogenomes of six heterodont bivalves indicated that *S. constricta* (Lamarck, 1818) was more closely related to *Solen grandis* (Dunker, 1862), which belonged to Solenidae (Yuan et al. 2012c). The phylogenetic tree and molecular clock of tandem mitochondrial gene and nuclear gene (*COI*, *16S*, *28S*) revealed that *Siliqua*, *Sinonovacula*, *Cultellus*, and *Novaculina* belonged to Pharellinae, and *Pharella javanica* (Lamarck, 1818) was classified under the *Sinonovacula* subclade (Bolotov et al. 2018b). Moreover, Pharidae were divided into four subfamilies which were composed of 14 existing genera, including Pharinae (*Nasopharus*, *Pharus*, *Sinupharus*), Cultellinae (*Afrophaxas*, *Cultellus*, *Ensis*, *Ensiculus*, *Phaxas*, *Sinucultellus*), Siliquinae (*Siliqua*), and Pharellinae (*Novaculina*, *Orbicularia*, *Pharella*, *Sinonovacula*), and Bolotov et al. (2018b) argued that Novaculininae was considered to be a junior synonym of Pharellinae (Appeltans et al. 2012; Signorelli et al. 2021). Nevertheless, since the above studies are only based on a limited number of taxa, the phylogenetic relationship of Pharidae has not been fully studied.

Mitochondrial DNA (mtDNA) is a genetic material independent of the nucleus DNA. Owing to their small size, rapid evolution, maternal inheritance, and simple structure, mitogenomes have become an attractive candidate tool for resolving phylogenetic relationships across a wide spectrum of metazoans (Boore 1999; Curole and Kocher 1999; Saccone et al. 1999; Miya et al. 2001; Gissi et al. 2008; Osigus et al. 2013; Cameron 2014). Mitogenomes of metazoan are usually circular double-stranded molecules, and range in size from 14 kb to 42 kb (Okimoto et al. 1992; Wolstenholme 1992; Smith and Snyder 2007). The typical mitogenome is composed of 37 genes compactly organized in a near-invariant arrangement, including 13 protein-coding genes of the oxidative phosphorylation (OXPHOS) system (*cox1–3*, *cob*, *nad1–6*, *nad4L*, *atp6*, *atp8*), 22 transfer RNAs (tRNAs) and two ribosomal RNAs homologous to the 16s and 23s of *Escherichia coli* (*rrnS* and *rrnL*) (Wolstenholme 1992; Shadel and Clayton 1997; Andrews et al. 1999; Boore 1999). In general, metazoan mtDNA molecules have few or no nucleotides between genes except for a single non-coding region that contains signals for regulating replication and transcription (designated as the control region) (Clayton 1984; Wolstenholme 1992; Shadel and Clayton 1997). However, the phylum Mollusca has generated a vast array of unexpected deviations from the ‘textbook description’, including exceptional variation in size, frequent genome rearrangements, the integration of novel genes, and a complex inheritance system dubbed ‘doubly uniparental inheritance’ (Wu et al. 2012; Williams et al. 2017; Wu et al. 2019; Malkócs et al. 2022).

In mollusks, with the development of DNA sequencing technology, a large number of mitogenomes have been determined during the last thirty years (Yokobori et al. 2004; Yuan et al. 2012d; Kong et al. 2020; Ma et al. 2023; Taite et al. 2023). For instance, through comparing the complete mtDNA sequences of three scallop species from the subfamily Chlamydinae, it was found that the three genomes exhibited high variation in non-coding regions and different tRNA gene sets (Wu et al. 2009). Besides, the results of the phylogenetic analysis based on concatenated 12 protein-coding genes (PCGs) and two rRNA genes validated the monophyly of the family Mactridae and indicated that genera *Mactrinula*, *Spisula*, *Rangia*, and *Mulinia* should not be placed under subfamily Mactrinae (Ma et al. 2023). Nevertheless, to date, only four mitogenomes of Pharidae, which are ecologically and economically important deep-burrowing bivalves, are available (Zheng et al. 2010; Feng et al. 2021; Li et al. 2022).

Sinonovacula rivularis (R. Huang & Y.-F. Zhang, 2007), the member of the genus *Sinonovacula*, is similar to *S. constricta* in reproduction and morphology (Huang and Zhang 2007). In contrast to *S. constricta*, which exhibits tolerance to wide salinity (5–40 ppt), *S. rivularis* is capable of thriving in low salt aquatic environments (4–20 ppt), and can even endure in freshwater conditions for over four days (Huang and Zhang 2007; Wang et al. 2009; Peng et al. 2019; Wang et al. 2024). In addition, a typical freshwater genus *Novaculina* is found in the family Pharidae (Schram 2010; Bolotov et al. 2018b). As a species of *Novaculina*, *N. chinensis* (Y.-Y. Liu & W.-Z. Zhang, 1979) was first discovered in Taihu Lake and Gaoyou Lake in China (Liu 1979). However, due to the pollution of water and the lack of protection awareness, they have been in danger of extinction (Liu 1979; Rao et al. 2003). In this study, we assembled the complete mitogenome of *S. rivularis* and *N. chinensis*, and analyzed their basic genome characteristics, nucleotide composition and relative synonymous codon usage (RSCU). The phylogenetic tree of Solenoidea was constructed and gene arrangement events between Pharidae and Solenidae were predicted. Furthermore, selective pressure analysis was conducted to explore the evolutionary adaptation of freshwater and marine species. Briefly, our findings will enrich the basis for the taxonomic study of Pharidae and contribute to deepening the understanding of the phylogenetic relationship between Solenoidea and its related groups.

Materials and methods

Sample collection

The samples for whole-genome sequencing of *S. rivularis* and *N. chinensis* were collected from the coastal area of Quanzhou in Fujian Province and the Qiantang River in Zhejiang Province, respectively, following the relevant guidelines and regulations. A total of ten individuals each of *S. rivularis* and *N. chinensis* were sampled, with average shell length of 55.98 ± 3.47 mm and 45.41 ± 2.74 mm, respectively. All specimens were preserved in 85% ethanol as voucher specimens. These specimens were deposited at Zhejiang Key Laboratory of Aquatic Germplasm Resource, Zhejiang Wanli University, Ningbo, China.

Mitogenome assembly and annotation

Raw genome reads were acquired through both Illumina HiSeq sequencing and PacBio Sequel IIe third-generation sequencing (unpublished), and assembled for the mitogenomes of these two species. Initially, a de novo mitogenome assembly was carried out with SPAdes v3.9.0 after filtering the unqualified reads by Trimmomatic v. 0.39 (Bankevich et al. 2012; Bolger et al. 2014). The scaffold sequences were then obtained by extending the contigs using SSPACE. The assembly quality was evaluated by GetOrganelle software (Jin et al. 2020). Finally, the MitoZ program was used to annotate the protein-coding genes (PCGs), two ribosomal RNAs (rRNAs) and transfer RNAs (tRNAs) (Meng et al. 2019).

Mitogenome characteristics analysis

The content and proportion of nucleotide bases were analyzed by MEGA 11. The base skew values were calculated according to the formulae: AT-skew = (A − T) / (A + T) and GC-skew = (G − C) / (G + C). The RSCU of the two mitogenomes was counted using PhyloSuite v1.2.3.

Phylogenetic analysis and gene arrangement analysis

To explore the evolutionary relationship of *S. rivularis* and *N. chinensis*, the published mitogenome sequences of Solenoidea and Hiatelloidea were retrieved from GenBank, and *Solecurtus divaricatus* was selected as the outgroup (Table 1). The phylogenetic analysis was performed using PhyloSuite software (Zhang et al. 2020). First, using an invertebrate mitochondrial code table, MAFFT was used to independently align 12 protein-coding genes. The *ATP8* gene was excluded due to its deletion in the majority of mollusks. Poorly aligned regions of the sequences were pruned by Gblocks under default parameters. The resulting alignments were then concatenated and transferred to ModelFinder for the best model prediction. Phylogenetic trees were estimated through maximum likelihood (ML) and Bayesian inference (BI) methods. The ML phylogenetic tree was generated using IQ-Tree with 1000 bootstrap replicates. The BI analyses were performed by MrBayes 3.2.6 with Markov Chain Monte Carlo (MCMC) for 5000,000 generations. The first 25% of trees were discarded as burn-in and the sampling was terminated when the convergence value was less than 0.01. The iTOL tool was exploited to visualize the phylogenetic tree (https://itol.embl.de/).

In addition, the most plausible gene order rearrangement events that might have occurred between Pharidae and Solenidae were reconstructed by pairwise comparisons of mitogenomes through the Common Interval Rearrangement Explorer (CREx) (Bernt et al. 2007).

Selective pressure analysis

The branch-site model was used to analyze the selection pressure on 12 PCGs of razor clams in the PAML package. In this model, *N. chinensis* was marked as the foreground branch to investigate the evolutionary adaptation between freshwater and marine species. The null model (model = 2, Nssites = 2, fix_omega = 1, omega = 1) and alternative model (model = 2, Nssites = 2, fix_omega = 0, omega = 2) were compared by likelihood ratio test (LRT). Subsequently, *P*-values were calculated through the chi-square distribution. Then, the posterior probability of the amino acid sites under positive selection was calculated according to the Bayesian empirical Bayes (BEB) method. The inference of positively selected sites was based on a posterior probability of greater than 95%.

Table 1. List of species used for phylogenetic analysis in this study and their GenBank accession numbers.

Order	Superfamily	Family	Species	Length (bp)	Accession number	Percent of AT (%)
Adapedonta	Solenoidea	Pharidae	*Novaculina chinensis*	15,957	PP874232	71.50
			Sinonovacula rivularis	17,159	PP874231	66.80
			Sinonovacula constricta	17,224	JN398366.1	67.00
			Ensis leei	16,926	MW727513.1	65.50
			Cultellus attenuatus	16,888	MW653805.1	66.46
			Siliqua minima	17,064	MT375556.1	66.41
		Solenidae	*Solen strictus*	16,535	NC_017616.1	62.70
			Solen grandis	16,784	NC_016665.1	64.84
	Hiatelloidea	Hiatellidae	*Panopea abrupta*	15,381	NC_033538.1	64.40
			Panopea globosa	15,469	NC_025636.1	63.70
			Panopea generosa	15,585	NC_025635.1	63.70
			Panopea japonica	16,128	NC_072278.1	63.80
			Hiatella sp.	19,507	OR420023.1	64.00
			Hiatella arctica	18,244	DQ632742.1	66.40
Cardiida	Tellinoidea	Solecurtidae	*Solecurtus divaricatus*	16,749	JN398367.1	60.10

Results

General features of *S. rivularis* and *N. chinensis* mitogenomes

The lengths of *S. rivularis* and *N. chinensis* mitogenomes were 17,159 bp and 15,957 bp, respectively (Fig. 1A). Both mitogenomes contain 12 PCGs, 22 tRNAs, and 2 rRNAs, all of which were located on the heavy chain. The *ATP8* gene was missing in this two mitogenomes. Their composition was similar to that of other species in Pharidae, indicating a certain degree of conservation in this family. The detailed genes information was shown in Table 2. The base composition of *S. rivularis* and *N. chinensis* mitogenomes was displayed in Table 3 with AT contents of 66.80% and 71.50%, respectively, both of which exhibited an obvious AT bias. The AT content of *N. chinensis* was the highest among the published Adapedonta mitogenomes. In addition, the two mitogenomes all exhibited negative AT-skew and positive GC-skew, reflecting that the base composition ratios were A biased to T, and G biased to C. There were some differences in the types of start and termination codons of 12 PCGs between the two species (Table 2). Specifically, the start codons of 12 genes in *S. rivularis* were found to be ATN, TTG and GTG types, whereas in *N. chinensis*, all genes began with the codon ATN, with the exception of the *ND4* gene, which used TTG as the start codon. Concerning termination codons, six genes in *S. rivularis* (*cytb*, *atp6*, *cox3*, *nad4*, *nad3*, *nad1*) and seven genes in *N. chinensis* (*cytb*, *nad6*, *atp6*, *cox3*, *nad4l*, *nad3*, *nad1*) were detected TAA or TAG at the sequence end. The remaining genes featured an incomplete termination codon consisting of a T that might be complemented into a complete stop codon by polyadenylation following transcription to the resultant mRNA (Ojala et al. 1981). Furthermore, the non-coding regions of the mitochondrial genomes of *N. chinensis* and *S. rivularis* account for 11.92% and 19.33%, respectively. The longest non-coding region (NCR) of *N. chinensis* and *S. rivularis* was both located between nad2 and trnK, with lengths of 443 bp and 1,639 bp respectively, which was identified as a putative control region (CR).

As illustrated in Fig. 1B, the preferred codons for 22 amino acids of two species ended in A or U, consisting with the result of AT bias of the mitogenome

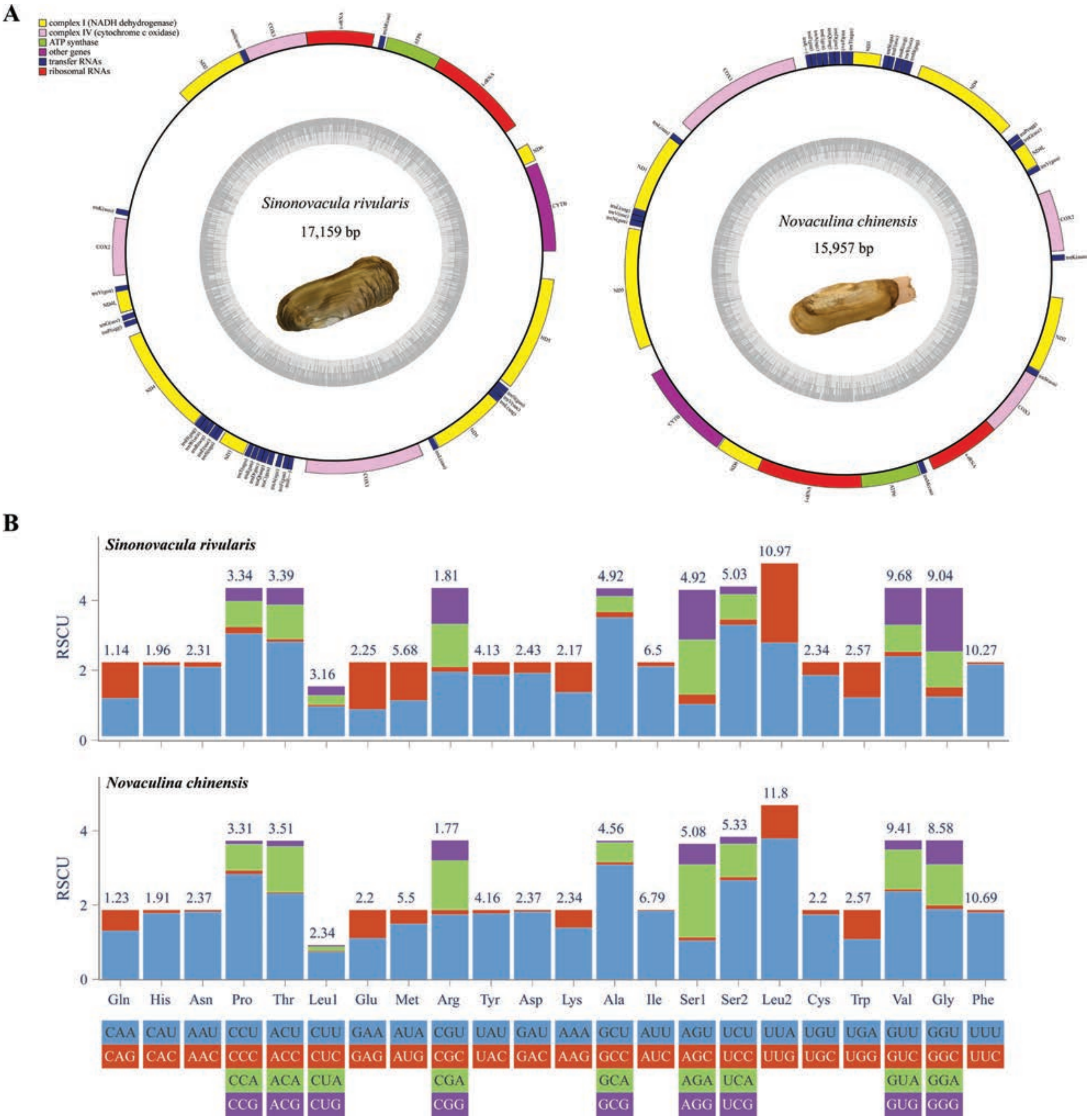

Figure 1. Maps of **A** the mitogenomes of *S. rivularis* and *N. chinensis* and their **B** RSCU.

sequence. As a consequence of the duplication of tRNA-Leu and tRNA-Ser, Leu and Ser were each encoded by six and eight codons, respectively. The most frequently used codons were UUA (Leu2), UCU (Ser2), GCU (Ala) and CCU (Pro). Compared to *S. rivularis*, CUG (Leu1), AUC (Ile), AAC(Asn) were utilized to a lesser extent in *N. chinensis*.

Phylogenetic analysis

The 12 protein-coding genes from 15 taxa were concatenated to generate a sequence matrix of 10,806 bp. The tree topologies derived from the ML and BI analyses were largely congruent exhibiting high posterior probabilities (PP) and bootstrap support values (BS) in most nodes (Fig. 2). Phylogenetic analyses

Table 2. Mitochondrial genome organization of *Sinonovacula rivularis* and *Novaculina chinensis*.

Gene	***Sinonovacula rivularis***					***Novaculina chinensis***				
	Size (bp)	**Start**	**End**	**Codon start/stop**	**Intergenic nucleotide (bp)**	**Size (bp)**	**Start**	**End**	**Codon start/stop**	**Intergenic nucleotide (bp)**
CYTB	1120	13	1132	TTG/TAG	36	1146	9247	10392	ATG/TAA	12
ND6	227	1169	1395	TTG/T--	265	531	10405	10935	ATG/TAG	-30
l-rRNA		1661	2957		-35		10906	12201		
ATP6	700	2923	3622	ATG/TAA	23	699	12164	12862	ATG/TAA	15
trnM		3646	3713		76		12878	12943		77
s-rRNA		3790	4637		-2		13021	13869		-2
COX3	790	4636	5425	ATG/TAG	-2	789	13868	14656	ATG/TAG	-1
trnS		5424	5491		5		14656	14722		6
ND2	899	5497	6395	GTG/T--	1639	898	14729	15626	ATT/T--	443
trnK		8035	8102		48		113	179		45
COX2	725	8151	8875	ATG/T--	132	726	225	950	ATG/T--	256
trnY		9008	9072		-20		1207	1270		7
ND4L	287	9053	9339	ATT/T--	33	288	1278	1565	ATG/TAA	1
trnG		9373	9439		20		1567	1632		10
trnP		9460	9525		122		1643	1707		122
ND4	1354	9648	11001	TTG/TAG	8	1254	1830	3083	TTG/T--	103
trnH		11010	11076		-1		3187	3250		2
trnW		11076	11144		2		3253	3319		3
trnR		11147	11213		13		3323	3387		18
trnE		11227	11294		-7		3406	3472		-6
trnS		11288	11351		30		3467	3529		33
ND3	337	11382	11718	ATA/TAA	15	333	3563	3895	ATT/TAG	-1
trnT		11734	11800		9		3895	3960		3
trnI		11810	11876		8		3964	4029		15
trnD		11885	11951		-1		4045	4110		0
trnQ		11951	12018		5		4111	4178		10
trnC		12024	12092		42		4189	4253		2
trnA		12135	12200		23		4256	4320		5
trnF		12224	12288		223		4326	4389		200
COX1	1488	12512	13999	CGA/**T--**	142	1512	4590	6101	ATT/T--	154
trnL		14142	14209		8		6256	6320		0
ND1	919	14218	15136	GTG/TAA	2	927	6321	7247	ATG/TAA	4
trnL		15139	15207		1		7252	7319		0
trnV		15209	15274		2		7320	7383		0
trnN		15277	15343		35		7384	7449		36
ND5	1443	15379	16821	ATT/T--	350	1441	7486	8926	ATT/**T--**	320

Table 3. Nucleotide composition and skewness of the mitogenomes of *S. constricta*, *S. rivularis*, and *N. chinensis*.

Species	AT (%)	GC (%)	AT skew	GC skew
S. constricta	67.00%	32.90	-0.22687	0.367781
S. rivularis	66.80%	28.50	-0.21958	0.319298
N. chinensis	71.50%	33.20	-0.23653	0.379518

revealed that the genus *Hiatella* from Hiatelloidea was closely related to the superfamily Solenoidea, indicating a close evolutionary relationship between them. Additionally, both analyses strongly confirmed the monophyly of Solenoidea, which was divided into two major branches, Solenoidae and Pharidae.

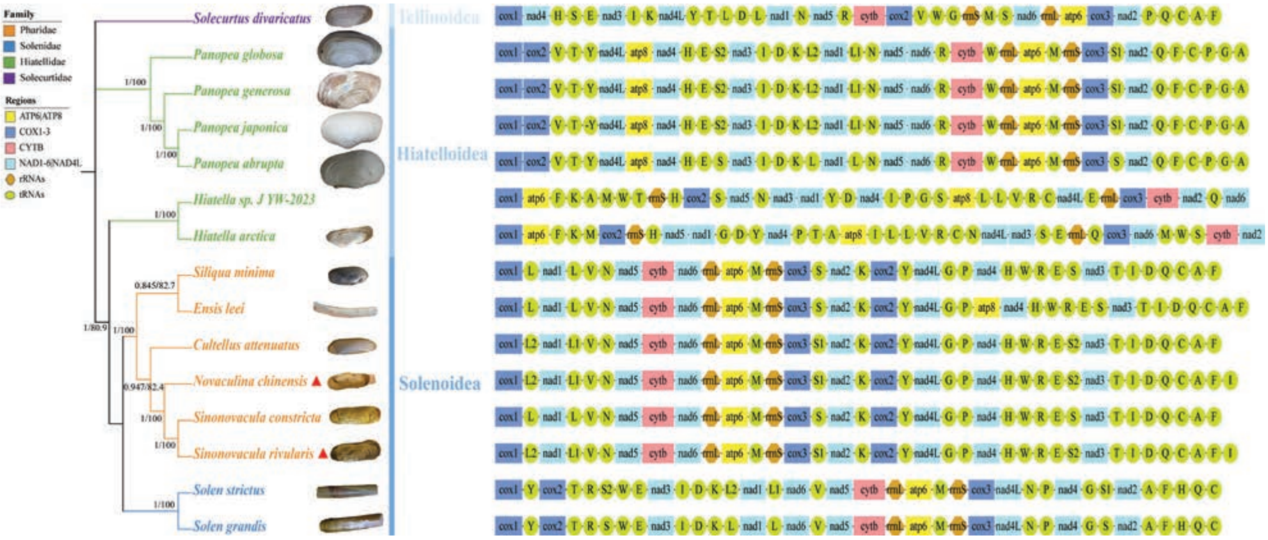

Figure 2. The phylogenetic trees based on concatenated 12 mitochondrial PCGs, and the gene orders of Adapedonta species. Values shown next to nodes are posterior probabilities (left) and ML bootstrap support values (right). Newly assembly mitogenomes are marked with triangles. Except for *Panopea abrupta* (https://inverts.wallawalla.edu) and *Panopea globose* (Góngora-Gómez et al. 2016), the images of the other species are all from https://www.inaturalist.org.

In the family Pharidae, the genus *Sinonovacula* (including *S. rivularis* and *S. constricta*) was clustered alongside *N. chinensis*, with *Cultellus attenuatus* emerging as a sister group. *Siliqua minima* and *Ensis leei* were clustered in a separate cluster.

Gene arrangement

The mitogenomes of Solenoidea all exhibited the identical composition of 12 PCGs, 22 tRNAs, and 2 rRNAs, except for *Ensis leei*, which contained an additional *ATP8* gene (Fig. 3). The gene arrangement was consistent within each family, and there was a certain level of conservation in gene arrangement between Solenidae and Pharidae. A large block, rrnL-ATP6-M-rrnS-cox3, and five small blocks, L2-nad1-L1, S-nad2, nad5-cytb, I-D, Q-C were shared by both families, providing further evidence of the close lineage relationship observed in the phylogenetic analysis of this study. The CREx analysis suggested that three transposition and four tandem duplication random losses (TDRLs) might have occurred between Pharidae and Solenidae.

Select pressure analysis

The species of Solenoidea were selected for molecular evolution analysis, with *N. chinensis* designated as the foreground branch (Fig. 4). The branch-site model (BSM) in the PAML package was employed to detect positively selected genes (PSGs). As illustrated in Table 4, the substitution model A was significantly better than the neutral selection model null in *nad5*, indicating that this gene underwent positive selection in the foreground branch ($P < 0.05$). According to the BEB analysis, there were five positive selection sites in the nad5 amino acid sequences (140 A 0.509, 143 F 0.547, 144 L 0.865, 442 A 0.700, 446 F 0.620). Moreover, discrepancies were observed in the 144th site between freshwater *N. chinensis* (Ala) and marine razor clams (Leu) (Fig. 5). However, the evidence for each site was somewhat inconclusive. These findings suggest that the *nad5* gene may have played a pivotal role in the adaptive evolution of freshwater environments.

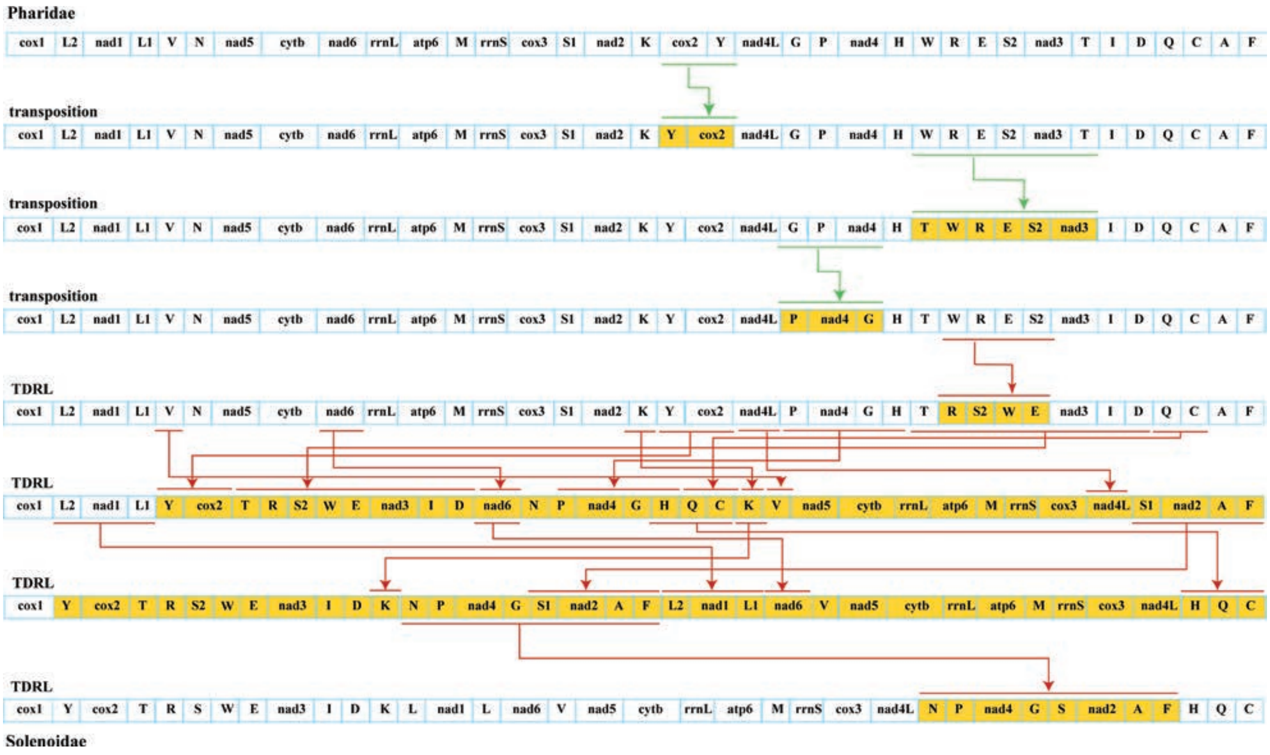

Figure 3. Putative gene rearrangement events between Pharidae and Solenidae. Green and red lines represent transposition and TDRL events, respectively, which were step by step identified by CREx.

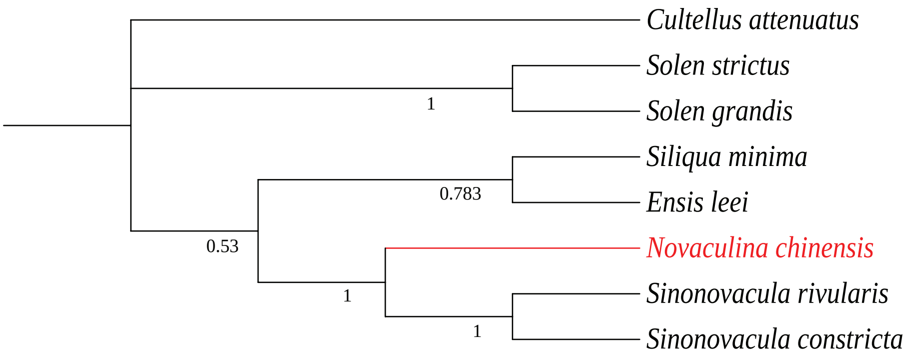

Figure 4. Phylogenetic tree of Solenoidea for selective stress analysis. The branch marked in red is the foreground branch.

Table 4. The results of positively selected gene sites for 12 PCGs.

Gene	lnL0	lnL1	Np0	Np1	Omega	P value	Positively selected sites (PSGs)
nad3	-1552.22	-1552.22	17	18	2.52856	1	
nad1	-4134.56	-4134.56	17	18	2.35774	1	
cytb	-4826.79	-4826.79	17	18	2.62875	1	
nad4L	-1236.77	-1236.78	17	18	3.31711	0.895254	
nad5	-6913.41	-6842.58	17	18	3.34388	0	140 A 0.509, 143 F 0.547, 144 L 0.865, 442 A 0.700, 446 F 0.620
cox1	-5205.94	-5205.94	17	18	2.64645	0.998872	
nad2	-4693.2	-4693.2	17	18	3.07094	1	
nad6	-877.007	-877.007	17	18	2.68959	1	
nad4	-6088.71	-6088.71	17	18	3.25046	1	
cox3	-3173.94	-3173.94	17	18	2.39696	1	
cox2	-2763.71	-2763.71	17	18	1.96195	1	
atp6	-2882.5	-2884.28	17	18	3.30394	0.058789	

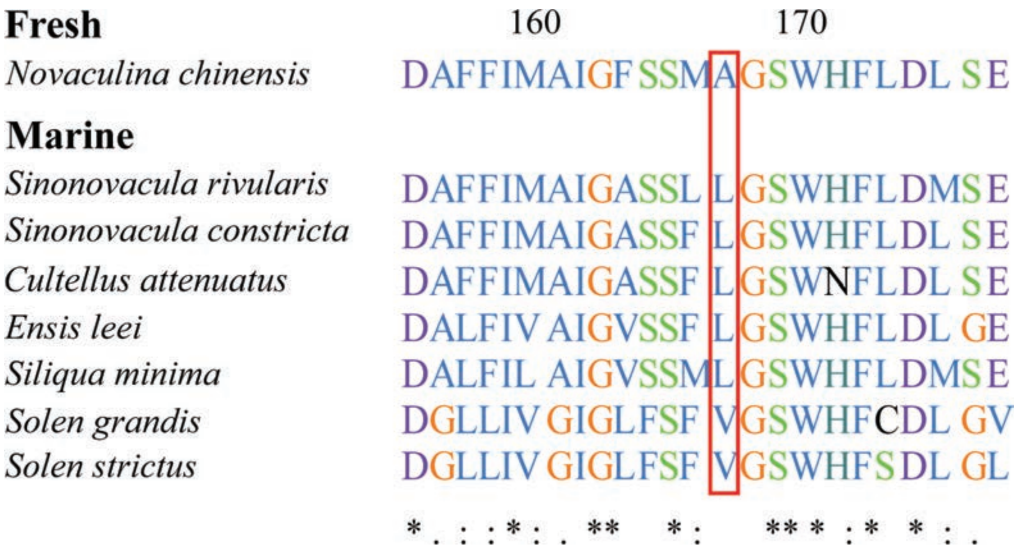

Figure 5. The difference of the 144th positive selected amino acid site in NAD5 of eight Solenoidea species. The 144th site is indicated by a red frame.

Discussion

General features of Pharidae mitogenomes

The mitogenomes of *S. rivularis* and *N. chinensis* were newly assembled, with lengths of 17,159 and 15,957 bp, respectively. In compared with the previously sequenced Adapedonta mtDNA size (ranged from 15,381 bp to 19,507 bp), their mitogenome sizes were within the normal range (Zheng et al. 2010; Yuan et al. 2012b; Feng et al. 2021; Li et al. 2022). Notably, the genome size of *N. chinensis* was the smallest in the family Pharidae, which was associated with the variation in length of the control region. The CR is the region with the largest sequence and length variation in the mitogenome, and has the fastest evolution, which is crucial for the regulation of mitochondrial DNA replication and transcription (Wolstenholme 1992; Boore 1999). The substantial differences in the content and structure of the control region within the mollusk lineage provide valuable insights for population genetic analysis (Sasuga et al. 1999; Tomita et al. 2002; Kawashima et al. 2013). Among the published mitogenomes of Pharidae, there is a large control region between *nad2* and *trnK*, such as *S. constricta* (1,492 bp), *S. minima* (1,371 bp), *C. attenuatus* (1,173 bp) and *E. leei* (1,101 bp) (Zheng et al. 2010; Feng et al. 2021; Li et al. 2022). In this study, *S. rivularis* displayed a moderately larger control region size of 1,639 bp, whereas it was only 441 bp in *N. chinensis*, making it a different mitogenome size in the family Pharidae. Intriguingly, a similar control region was not observed in the species of Solenidae (Yuan et al. 2012a, b). This distinction provides evidence for the taxonomic division of the subfamily of Solenoidea.

Molecular phylogeny and gene arrangement of the family Pharidae

The topological tree constructed from the 12 mitochondrial PCGs sequence based on the BI and ML methods yielded consistent results, demonstrating that Solenoidea is clearly divided into Solenoidae and Pharidae, which is consistent with the prior research results (Yuan et al. 2012d; Feng et al. 2021). Previously, *S. rivularis* was identified as a new species of *Sinonovacula* distinct from *S. constricta* based on morphological studies and a comparative analysis of COI and 16SrRNA fragments (Huang and Zhang 2007; Weng et al. 2013). In this research, this classification view was supported at the level of mitogenomes, and *Sinonovacula* belonged to the family Pharidae (Adapedonta: Solenoidea). In addition, *N. chinensis* was previously classified into Solecurtidae, whereas the results of this study demonstrated that *N. chinensis* and *Sinonovacula* are clustered together, forming a novel branch in the family Pharidae, which was consistent with the taxa in WoRMS (Liu 1979; Appeltans et al. 2012). Recently, the phylogenetic tree and molecular clock of tandem mitochondrial gene and nuclear gene (*COI*, *16S*, *28S*) revealed that *Siliqua*, *Sinonovacula*, *Cultellus*, and *Novaculina* belonged to Pharellinae (Bolotov et al. 2018b). However, *Cultellus* and *Siliqua* were categorized into the subfamily Cultellinae and Siliquinae, respectively, by Ahyong (Appeltans et al. 2012). Previously, Pharidae were divided into four subfamilies: Pharinae (*Nasopharus*, *Pharus*, *Sinupharus*), Cultellinae (*Afrophaxas*, *Cultellus*, *Ensis*, *Ensiculus*, *Phaxas*, *Sinucultellus*), Siliquinae (*Siliqua*), and Pharellinae (*Novaculina*, *Orbicularia*, *Pharella*, *Sinonovacula*). However, the present results indicate that Pharidae are divided into two clades, in which *Cultellus* is clustered alongside the *Sinonovacula* and *Novaculina*, while *Siliqua* and *Ensis* clustered together. These observations reflect that the current categorization of the subfamily Pharidae requires further research and refinement, particularly in combination with more species information.

Unlike stable gene arrangements of Vertebrata and Arthropoda, the gene orders of all genes within mtDNA exhibit considerable variability in every major molluscan lineage, including Cephalopoda, Bivalvia, Scaphopoda, and Monoplacophora (Rawlings et al. 2001; Dreyer and Steiner 2004; Yuan et al. 2012c; Stöger et al. 2016; Ma et al. 2023). Gene rearrangements may be caused by reverse transpositions, transpositions, inversions, and TDRL, which can provide important clues about the evolutionary history of species (Boore and Brown 1998; Serb and Lydeard 2003; Wang et al. 2021). In this paper, CREx analysis predicted that three transpositions and four TDRLs might have occurred between Pharidae and Solenidae, implying that dramatic mitogenome changes occurred during species differentiation. Moreover, the gene order illustration of Adapedonta revealed that species with a closer genetic relationship tended to share a similar gene arrangement, indicating that there is a potential relationship between evolution and gene rearrangement (Fig. 2). However, in this study, three distinct gene arrangement types were observed in the family Hiatellidae, especially in the genus *Hiatella* with nad3 and nad1 transpositions in terms of 12 PCGs arrangement (Fig. 2). The similar case that different gene arrangements in the same genus has also been reported in the genera *Dendropoma* and *Crassostrea* (Rawlings et al. 2010; Ren et al. 2010). Therefore, the taxonomic evolution of species cannot be substantiated exclusively through the examination of gene sequences; it also necessitates the integration of phylogenetic reconstruction.

Adaptive evolution of Pharidae mitochondrial genes to freshwater environment

Pharidae is a major marine family, with the exception of *Novaculina*, that is a relict marine-derived freshwater lineage (Annandale 1922; Bolotov et al. 2018a). The branch-site model study was used to determine whether positive selection occurs at a few places in freshwater razor clam. The results suggested that the *nad5* gene underwent positive selection. NADH dehydrogenase is the initial and most substantial enzyme complex in the respiratory chain, functioning as a proton pump (da Fonseca et al. 2008). *Nad2*, *nad4*, and *nad5* are considered to be the actual proton pumping devices because of their sequence homology with a class of Na^+/H^+ antiporters (Brandt 2006). The efficiency of the proton transfer process may be interfered by the mutation of the complex, which could be a crucial factor in adaptive evolution (Hassanin et al. 2009; Yu et al. 2011). For instance, the outcomes of positive selection sites in mussels from disparate habitats reflected that the p-value of *nad4* was significant in freshwater branches and six sites were identified as positive sites with BEB analysis (> 95%), which implies that *nad4* may contribute to the adaptation of *Limnoperna fortunei* in freshwater (Zhao et al. 2022). Significant non-synonymous changes were detected in the *cytb* and *nad5* genes by comparing mitogenomes of panpulmonate gastropods that are distributed from marine to intertidal and terrestrial habitats (Romero et al. 2016). Therefore, the positive selection of *nad5* gene in *N. chinensis* may be the result of the adaptive evolution of freshwater environment. Moreover, divergent selection occurred at site 144 of *nad5*, where the amino acids Ala and Leu were identified in the freshwater *Novaculina chinensis* and seven marine lineages, respectively, indicating divergent evolution exists the family Pharidae. Divergent evolution is the process by which separate species with common ancestors evolve distinct features to adapt to their unique living environment, which is one of the important mechanisms for the formation of biodiversity (Gautam 2020). However, the evidence supporting the positive selection of individual nad5 sites is insufficient. To provide more robust statistical support for the differences in evolutionary adaptation between freshwater and seawater species, it is necessary to include more freshwater razor clam sequences.

Conclusions

In summary, the mitogenomes of *S. rivularis* and *N. chinensis* were assembled using next-generation sequencing data, with the genomes measuring 17,159 bp and 15,957 bp, respectively. Both genomes consist of 12 protein-coding genes, 22 transfer RNA genes, and two ribosomal RNA genes. Among the published Pharidae mitogenomes, *N. chinensis* exhibits the smallest genome size but the highest AT content. The results of the phylogenetic analysis showed that *N. chinensis* and *Sinonovacula* (*S. constricta* + *S. rivularis*) were closely related and belonged to the family Pharidae. The gene order rearrangements in Solenoidea can be attributed to transposition and TDRL events. Moreover, the *nad5* genes carry a signal of positive selections in the foreground *N. chinensis*, which promotes the adaptation to freshwater environments. We also show that divergent evolution occurred at site 144 in the freshwater and marine lineages. Overall, this study provides further theoretical support for the phylogenetic relationship of Pharidae, and contributes to deepening the understanding of the mitogenomic adaptations of Pharidae.

Acknowledgements

This work was supported financially by Zhejiang Major Program of Science and Technology (2021C02069-7), Ningbo Major Project of Science and Technology (2021Z114) and National Marine Genetic Resource Center Program.

Additional information

Conflict of interest

The authors have declared that no competing interests exist.

Ethical statement

No ethical statement was reported.

Funding

This work was supported by Zhejiang Major Program of Science and Technology (2021C02069-7), Ningbo Major Project of Science and Technology (2021Z114) and National Marine Genetic Resource Center Program.

Author contributions

Yinghui Dong and Demin Zhang conceived and designed the experiments. Yiping Meng performed the experiments and drafted the manuscript. All authors reviewed the paper.

Data availability

All of the data that support the findings of this study are available in the main text.

References

Andrews RM, Kubacka I, Chinnery PF, Lightowlers RN, Turnbull DM, Howell N (1999) Reanalysis and revision of the Cambridge reference sequence for human mitochondrial DNA. Nature Genetics 23(2): 147–147. https://doi.org/10.1038/13779

Annandale N (1922) The Marine Element in the Fauna of the Ganges. Bijdr Dierk Amsterdam, 143–154. https://doi.org/10.1163/26660644-02201020

Appeltans W, Ahyong S, Anderson G, Angel M, Artois T, Bailly N, Bamber R, Barber A, Bartsch I, Berta A, Błażewicz-Paszkowycz M, Bock P, Boxshall G, Boyko C, Brandão S, Bray R, Bruce N, Cairns S, Chan TY, Cheng L, Collins A, Cribb T, Curini-Galletti M, Dahdouh-Guebas F, Davie P, Dawson M, De Clerck O, Decock W, De Grave S, De Voogd N, Domning D, Emig C, Erséus C, Eschmeyer W, Fauchald K, Fautin D, Feist S, Fransen C, Furuya H, Garcia-Alvarez O, Gerken S, Gibson D, Gittenberger A, Gofas S, Gómez-Daglio L, Gordon D, Guiry M, Hernandez F, Hoeksema B, Hopcroft R, Jaume D, Kirk P, Koedam N, Koenemann S, Kolb J, Kristensen R, Kroh A, Lambert G, Lazarus D, Lemaitre R, Longshaw M, Lowry J, Macpherson E, Madin L, Mah C, Mapstone G, McLaughlin P, Mees J, Meland K, Messing C, Mills C, Molodtsova T, Mooi R, Neuhaus B, Ng P, Nielsen C, Norenburg J, Opresko D, Osawa M, Paulay G, Perrin W, Pilger J, Poore G, Pugh P, Read G, Reimer J, Rius M, Rocha R, Saiz-Salinas J, Scarabino V, Schierwater B, Schmidt-Rhaesa A, Schnabel K, Schotte M, Schuchert P, Schwabe E, Segers H, Self-Sullivan C, Shenkar N, Siegel V, Sterrer W, Stöhr S, Swalla B, Tasker M, Thuesen E, Timm T, Todaro M, Turon X, Tyler S, Uetz P, Van der Land J, Vanhoorne B, Van Ofwegen L, Van Soest R, Vanaverbeke J, Walker-Smith G, Walter T, Warren A, Williams G, Wilson S, Costello M (2012) The magnitude of global marine species diversity. Current Biology 22(23): 2189–2202. https://doi.org/10.1016/j.cub.2012.09.036

Bankevich A, Nurk S, Antipov D, Gurevich AA, Dvorkin M, Kulikov AS, Lesin VM, Nikolenko SI, Son P, Prjibelski AD, Pyshkin AV, Sirotkin AV, Vyahhi N, Tesler G, Alekseyev MA, Pevzner PA (2012) SPAdes: a new genome assembly algorithm and its applications to single-cell sequencing. Journal of Computational Biology 19(5): 455–477. https://doi.org/10.1089/cmb.2012.0021

Bernt M, Merkle D, Ramsch K, Fritzsch G, Perseke M, Bernhard D, Schlegel M, Stadler PF, Middendorf M (2007) CREx: inferring genomic rearrangements based on common intervals. Bioinformatics 23(21): 2957–2958. https://doi.org/10.1093/bioinformatics/btm468

Bolger AM, Lohse M, Usadel B (2014) Trimmomatic: a flexible trimmer for Illumina sequence data. Bioinformatics 30(15): 2114–2120. https://doi.org/10.1093/bioinformatics/btu170

Bolotov IN, Aksenova OV, Bakken T, Glasby CJ, Gofarov MY, Kondakov AV, Konopleva ES, Lopes-Lima M, Lyubas AA, Wang Y, Bychkov AY, Sokolova AM, Tanmuangpak K, Tumpeesuwan S, Vikhrev IV, Shyu JBH, Win T, Pokrovsky OS (2018a) Discovery of a silicate rock-boring organism and macrobioerosion in fresh water. Nature Communications 9(1): 2882–2892. https://doi.org/10.1038/s41467-018-05133-4

Bolotov IN, Vikhrev IV, Lopes-Lima M, Lunn Z, Chan N, Win T, Aksenova OV, Gofarov MY, Kondakov AV, Konopleva ES, Tumpeesuwan S (2018b) Discovery of *Novaculina myanmarensis* sp nov (Bivalvia: Pharidae: Pharellinae) closes the freshwater razor clams range disjunction in Southeast Asia. Scientific Reports 8(1): 16325–16336. https://doi.org/10.1038/s41598-018-34491-8

Boore JL (1999) Animal mitochondrial genomes. Nucleic Acids Research 27(8): 1767–1780. https://doi.org/10.1093/nar/27.8.1767

Boore JL, Brown WM (1998) Big trees from little genomes: mitochondrial gene order as a phylogenetic tool. Current Opinion in Genetics & Development 8(6): 668–674. https://doi.org/10.1016/S0959-437X(98)80035-X

Brandt U (2006) Energy converting NADH:quinone oxidoreductase (complex I). Annual Review of Biochemistry 75: 69–92. https://doi.org/10.1146/annurev.biochem.75.103004.142539

Cameron SL (2014) Insect mitochondrial genomics: implications for evolution and phylogeny. Annual Review of Entomology 59: 95–117. https://doi.org/10.1146/annurev-ento-011613-162007

Clayton DA (1984) Transcription of the mammalian mitochondrial genome. Annual Review of Biochemistry 53: 573–594. https://doi.org/10.1146/annurev.bi.53.070184.003041

Cosel RV (1993) The razor shells of the eastern Atlantic. Part 1: Solenidae and Pharidae I (Bivalvia: Solenacea). Archiv für Molluskenkunde 122: 207–321. https://doi.org/10.1127/arch.moll/122/1993/207

Costello M, Saeedi H (2019) The Biology, Ecology, Importance Razor Clams. In: Encyclopedia of the World's Biomes. Elsevier, Oxford, 494–498. https://doi.org/10.1016/B978-0-12-409548-9.11681-1

Curole JP, Kocher TD (1999) Mitogenomics: digging deeper with complete mitochondrial genomes. Trends in Ecology & Evolution 14(10): 394–398. https://doi.org/10.1016/S0169-5347(99)01660-2

da Fonseca RR, Johnson WE, O'Brien SJ, Ramos MJ, Antunes A (2008) The adaptive evolution of the mammalian mitochondrial genome. BMC Genomics 9: 119–140. https://doi.org/10.1186/1471-2164-9-119

Dreyer H, Steiner G (2004) The complete sequence and gene organization of the mitochondrial genome of the gadilid scaphopod *Siphonondentalium lobatum* (Mollusca). Molecular Phylogenetics and Evolution 31(2): 605–617. https://doi.org/10.1016/j.ympev.2003.08.007

Feng J, Guo Y, Yan C, Ye Y, Yan X, Li J, Xu K, Guo B, Lu Z (2021) Novel gene rearrangement in the mitochondrial genome of *Siliqua minima* (Bivalvia, Adapedonta) and phylogenetic implications for Imparidentia. PLoS ONE 16(4): 1–21. https://doi.org/10.1371/journal.pone.0249446

Gautam P (2020) Divergent Evolution. In: Vonk J, Shackelford T (Eds) Encyclopedia of Animal Cognition and Behavior. Springer, Cham, 8 pp. https://doi.org/10.1007/978-3-319-47829-6_501-1

Gissi C, Iannelli F, Pesole G (2008) Evolution of the mitochondrial genome of Metazoa as exemplified by comparison of congeneric species. Heredity 101(4): 301–320. https://doi.org/10.1038/hdy.2008.62

Góngora-Gómez AM, Sotelo-Gonzalez MI, Hernández-Sepúlveda JA, Domínguez-Orozco AL, García-Ulloa Gómez M (2016) Nuevo registro de la almeja generosa *Panopea globosa* (Dall, 1898) (Bivalvia: Hiatellidae) en el estado de Sinaloa, México. Latin American Journal of Aquatic Research 44: 411–415. https://doi.org/10.3856/vol44-issue2-fulltext-22

Graham A (1935) The structure and relationships of lamellibranchs possessing a cruciform muscle. Proceedings of the Royal Society of Edinburgh 54: 158–187. https://doi.org/10.1017/S0370164600016138

Guoquan Z, Jun F, Shouju J, Yongpu Z, Chen C, Yaoyao Z, Junqi Y (2010) Biochemical genetic analysis of eight isozymes in intra-populations of razor clam *Cultellus attenuatus*. Fisheries Science 29: 669–673. https://doi.org/10.0000/1003-1111-15350

Hassanin A, Ropiquet A, Couloux A, Cruaud C (2009) Evolution of the mitochondrial genome in mammals living at high altitude: new insights from a study of the tribe Caprini (Bovidae, Antilopinae). Journal of Molecular Evolution 68(4): 293–310. https://doi.org/10.1007/s00239-009-9208-7

Huang R, Zhang Y (2007) A new species of the genus *Sinonovacula*. Journal of oceanography In Taiwan Strait 26(1): 115–120.

Jin J, Yu W, Yang J, Song Y, dePamphilis CW, Yi T, Li D (2020) GetOrganelle: a fast and versatile toolkit for accurate de novo assembly of organelle genomes. Genome Biology 21(1): 1–31. https://doi.org/10.1186/s13059-020-02154-5

Kawashima Y, Nishihara H, Akasaki T, Nikaido M, Tsuchiya K, Segawa S, Okada N (2013) The complete mitochondrial genomes of deep-sea squid (*Bathyteuthis abyssicola*), bob-tail squid (*Semirossia patagonica*) and four giant cuttlefish (*Sepia apama*, *S. latimanus*, *S. lycidas* and *S. pharaonis*), and their application to the phylogenetic analysis of Decapodiformes. Molecular Phylogenetics and Evolution 69(3): 980–993. https://doi.org/10.1016/j.ympev.2013.06.007

Kong L, Li Y, Kocot KM, Yang Y, Qi L, Li Q, Halanych KM (2020) Mitogenomics reveals phylogenetic relationships of Arcoida (Mollusca, Bivalvia) and multiple independent expansions and contractions in mitochondrial genome size. Molecular Phylogenetics and Evolution 150: 1–11. https://doi.org/10.1016/j.ympev.2020.106857

Li H, Yu R, Ma P, Li C (2022) Complete mitochondrial genome of *Cultellus attenuatus* and its phylogenetic implications. Molecular Biology Reports 49(8): 8163–8168. https://doi.org/10.1007/s11033-022-07276-6

Lin Z (2009) The genetic structure and diversity analysis of three species of razor clam using AFLP markers. Marine Sciences 33(10): 26–30.

Liu Y (1979) A new species of freshwater razor clam, *Novaculina chinensis*, from jiangsu province, China. Acta Zootaxonomica Sinica 4: 356–358.

Ma P, Liu Y, Wang J, Chen Y, Zhang Z, Zhang T, Wang H (2023) Comparative analysis of the mitochondrial genomes of the family Mactridae (Mollusca: Venerida) and their phylogenetic implications. International Journal of Biological Macromolecules 249: 1–9. https://doi.org/10.1016/j.ijbiomac.2023.126081

Malkócs T, Viricel A, Becquet V, Evin L, Dubillot E, Pante E (2022) Complex mitogenomic rearrangements within the Pectinidae (Mollusca: Bivalvia). BMC Ecology and Evolution 22(1): 29–49. https://doi.org/10.1186/s12862-022-01976-0

Meng G, Li Y, Yang C, Liu S (2019) MitoZ: a toolkit for animal mitochondrial genome assembly, annotation and visualization. Nucleic Acids Research 47(11): 63–69. https://doi.org/10.1093/nar/gkz173

Ministry of Agriculture and Rural Affairs of the People's Republic of China (2024) China Fisheries Statistical Yearbook. China Agriculture Press, Beijing, 23.

Miya M, Kawaguchi A, Nishida M (2001) Mitogenomic exploration of higher teleostean phylogenies: a case study for moderate-scale evolutionary genomics with 38 newly determined complete mitochondrial DNA sequences. Molecular Biology and Evolution 18(11): 1993–2009. https://doi.org/10.1093/oxfordjournals.molbev.a003741

Ojala D, Montoya J, Attardi G (1981) tRNA punctuation model of RNA processing in human mitochondria. Nature 290(5806): 470–474. https://doi.org/10.1038/290470a0

Okimoto R, Macfarlane JL, Clary DO, Wolstenholme DR (1992) The mitochondrial genomes of two nematodes, *Caenorhabditis elegans* and *Ascaris suum*. Genetics 130(3): 471–498. https://doi.org/10.1093/genetics/130.3.471

Osigus H-J, Eitel M, Bernt M, Donath A, Schierwater B (2013) Mitogenomics at the base of Metazoa. Molecular Phylogenetics and Evolution 69(2): 339–351. https://doi.org/10.1016/j.ympev.2013.07.016

Peng M, Liu X, Niu D, Ye B, Lan T, Dong Z, Li J (2019) Survival, growth and physiology of marine bivalve (*Sinonovacula constricta*) in long-term low-salt culture. Scientific Reports 9(1): 1–9. https://doi.org/10.1038/s41598-019-39205-2

Rao X, Xu Y, Chen Y, Lin G (2003) A study on induced spawning of *Novaculina chinensis*. Journal of Fujian Normal University 19(3): 78–81.

Rawlings TA, Collins TM, Bieler R (2001) A major mitochondrial gene rearrangement among closely related species. Molecular Biology and Evolution 18(8): 1604–1609. https://doi.org/10.1093/oxfordjournals.molbev.a003949

Rawlings TA, MacInnis MJ, Bieler R, Boore JL, Collins TM (2010) Sessile snails, dynamic genomes: gene rearrangements within the mitochondrial genome of a family of caenogastropod molluscs. BMC Genomics 11(1): 440–463. https://doi.org/10.1186/1471-2164-11-440

Ren J, Liu X, Jiang F, Guo X, Liu B (2010) Unusual conservation of mitochondrial gene order in *Crassostrea oysters*: evidence for recent speciation in Asia. BMC Evolutionary Biology 10(1): 394–407. https://doi.org/10.1186/1471-2148-10-394

Romero PE, Weigand AM, Pfenninger M (2016) Positive selection on panpulmonate mitogenomes provide new clues on adaptations to terrestrial life. BMC Evolutionary Biology 16(1): 164–176. https://doi.org/10.1186/s12862-016-0735-8

Saccone C, De Giorgi C, Gissi C, Pesole G, Reyes A (1999) Evolutionary genomics in Metazoa: the mitochondrial DNA as a model system. Gene 238(1): 195–209. https://doi.org/10.1016/S0378-1119(99)00270-X

Saeedi H, Basher Z, Costello MJ (2016) Modelling present and future global distributions of razor clams (Bivalvia: Solenidae). Helgoland marine research 70(1): 23–34. https://doi.org/10.1186/s10152-016-0477-4

Sasuga J, Yokobori S, Kaifu M, Ueda T, Nishikawa K, Watanabe K (1999) Gene contents and organization of a mitochondrial DNA segment of the squid *Loligo bleekeri*. Journal of Molecular Evolution 48(6): 692–702. https://doi.org/10.1007/PL00006513

Schram FR (2010) Checklist of Marine Biota of China Seas. Journal of Crustacean Biology 30(2): 339-339. https://doi.org/10.1651/09-3228.1

Serb JM, Lydeard C (2003) Complete mtDNA sequence of the north American freshwater mussel, *Lampsilis ornata* (Unionidae): an examination of the evolution and phylogenetic utility of mitochondrial genome organization in bivalvia (Mollusca). Molecular Biology and Evolution 20(11): 1854–1866. https://doi.org/10.1093/molbev/msg218

Shadel GS, Clayton DA (1997) Mitochondrial DNA maintenance in vertebrates. Annual Review of Biochemistry 66: 409–435. https://doi.org/10.1146/annurev.biochem.66.1.409

Signorelli JH, Trovant B, Marquez F (2021) A cryptic species of *Ensis* (Bivalvia: Pharidae) from the southeastern Pacific coast revealed by geometric morphometric methods. Scientia Marina 86(2): 1–9. https://doi.org/10.3989/scimar.05241.032

Smith DR, Snyder M (2007) Complete mitochondrial DNA sequence of the scallop *Placopecten magellanicus*: evidence of transposition leading to an uncharacteristically large mitochondrial genome. Journal of Molecular Evolution 65(4): 380–391. https://doi.org/10.1007/s00239-007-9016-x

Stöger I, Kocot KM, Poustka AJ, Wilson NG, Ivanov D, Halanych KM, Schrödl M (2016) Monoplacophoran mitochondrial genomes: convergent gene arrangements and little phylogenetic signal. BMC Evolutionary Biology 16(1): 274–291. https://doi.org/10.1186/s12862-016-0829-3

Taite M, Fernandez-Alvarez FA, Braid HE, Bush SL, Bolstad K, Drewery J, Mills S, Strugnell JM, Vecchione M, Villanueva R, Voight JR, Allcock AL (2023) Genome skimming elucidates the evolutionary history of Octopoda. Molecular Phylogenetics and Evolution 182: 1–11. https://doi.org/10.1016/j.ympev.2023.107729

Taylor JD, Williams ST, Glover EA, Dyal P (2007) A molecular phylogeny of heterodont bivalves (Mollusca: Bivalvia: Heterodonta): new analyses of 18S and 28S rRNA genes. Zoologica Scripta 36(6): 587–606. https://doi.org/10.1111/j.1463-6409.2007.00299.x

Tomita K, Yokobori S, Oshima T, Ueda T, Watanabe K (2002) The cephalopod *Loligo bleekeri* mitochondrial genome: multiplied noncoding regions and transposition of tRNA genes. Journal of Molecular Evolution 54(4): 486–500. https://doi.org/10.1007/s00239-001-0039-4

Wang Y, Sun T, Wu J, Cui D, Wang A, Wang X (2009) Influence of salinity on the survival and growth of *Sinonovacula rivularis*. Shandong Fisheries 26(12): 6–7.

Wang Y, Yang Y, Liu H, Kong L, Yu H, Liu S, Li Q (2021) Phylogeny of Veneridae (Bivalvia) based on mitochondrial genomes. Zoologica Scripta 50(1): 58–70. https://doi.org/10.1111/zsc.12454

Wang S, Shi Y, Dong Y, Meng Y, Yao H, He L (2024) Molecular identification of *Sinonovacula constricta*, *Sinonovacula rivularis* and their interspecific hybrids using microsatellite markers. Frontiers in Marine Science 11: 1–9. https://doi.org/10.3389/fmars.2024.1360596

Weng Z, Xie Y, Xiao Z, Ren P, Wang Z, Jianfang G (2013) Molecular identification of the taxonomic status of *Sinonovacula rivularis* and genus *Sinonovacula* using mitochondrial COI and 16S rRNA fragments. Acta Hydrobiologica Sinica 37(4): 684–690.

Williams ST, Foster PG, Hughes C, Harper EM, Taylor JD, Littlewood DTJ, Dyal P, Hopkins KP, Briscoe AG (2017) Curious bivalves: Systematic utility and unusual properties of anomalodesmatan mitochondrial genomes. Molecular Phylogenetics and Evolution 110: 60–72. https://doi.org/10.1016/j.ympev.2017.03.004

Wolstenholme DR (1992) Animal mitochondrial DNA: structure and evolution. International Review of Cytology 141: 173–216. https://doi.org/10.1016/S0074-7696(08)62066-5

Wu X, Xu X, Yu Z, Kong X (2009) Comparative mitogenomic analyses of three scallops (Bivalvia: Pectinidae) reveal high level variation of genomic organization and a diversity of transfer RNA gene sets. BMC Research Notes 2: 69–69. https://doi.org/10.1186/1756-0500-2-69

Wu X, Li X, Li L, Xu X, Xia J, Yu Z (2012) New features of Asian *Crassostrea oyster* mitochondrial genomes: A novel alloacceptor tRNA gene recruitment and two novel ORFs. Gene 507(2): 112–118. https://doi.org/10.1016/j.gene.2012.07.032

Wu R, Liu X, Wang S, Roe KJ, Ouyang S, Wu X (2019) Analysis of mitochondrial genomes resolves the phylogenetic position of Chinese freshwater mussels (Bivalvia, Unionidae). ZooKeys 812: 23–46. https://doi.org/10.3897/zookeys.812.29908

Yokobori S, Fukuda N, Nakamura M, Aoyama T (2004) Long-term conservation of six duplicated structural genes in cephalopod mitochondrial genomes. Molecular Biology and Evolution 21(11): 2034–2046. https://doi.org/10.1093/molbev/msh227

Yu L, Wang X, Ting N, Zhang Y (2011) Mitogenomic analysis of Chinese snub-nosed monkeys: evidence of positive selection in NADH dehydrogenase genes in high-altitude adaptation. Mitochondrion 11(3): 497–503. https://doi.org/10.1016/j.mito.2011.01.004

Yu Z, Li Q, Kong L (2016) New insight into the phylogeny of *Sinonovacula* (Bivalvia: Solecurtidae) revealed by comprehensive DNA barcoding analyses of two mitochondrial genes. Mitochondrial DNA Part A 27(2): 1554–1557. https://doi.org/10.3109/19401736.2014.953135

Yuan Y, Li Q, Kong L, Yu H (2012a) The complete mitochondrial genome of *Solen strictus* (Bivalvia: Solenidae). Mitochondrial DNA 23(2): 112–114. https://doi.org/10.3109/19401736.2011.653802

Yuan Y, Li Q, Kong L, Yu H (2012b) The complete mitochondrial genome of the grand jackknife clam, *Solen grandis* (Bivalvia: Solenidae): a novel gene order and unusual non-coding region. Molecular Biology Reports 39(2): 1287–1292. https://doi.org/10.1007/s11033-011-0861-8

Yuan Y, Li Q, Yu H, Kong L (2012c) The complete mitochondrial genomes of six heterodont bivalves (Tellinoidea and Solenoidea): variable gene arrangements and phylogenetic implications. PLoS ONE 7(2): 1–12. https://doi.org/10.1371/journal.pone.0032353

Yuan Y, Li Q, Yu H, Kong L (2012d) The complete mitochondrial genomes of six Heterodont bivalves (Tellinoidea and Solenoidea): variable gene arrangements and phylogenetic implications. PLoS ONE 7(2): 1–9. https://doi.org/10.1371/journal.pone.0032353

Zhang D, Gao F, Jakovlic I, Zou H, Zhang J, Li WX, Wang GT (2020) PhyloSuite: an integrated and scalable desktop platform for streamlined molecular sequence data management and evolutionary phylogenetics studies. Molecular Ecology Resources 20(1): 348–355. https://doi.org/10.1111/1755-0998.13096

Zhao B, Gao S, Zhao M, Lv H, Song J, Wang H, Zeng Q, Liu J (2022) Mitochondrial genomic analyses provide new insights into the “missing” atp8 and adaptive evolution of Mytilidae. BMC Genomics 23(1): 738–752. https://doi.org/10.1186/s12864-022-08940-8

Zheng R, Li J, Niu D (2010) The complete DNA sequence of the mitochondrial genome of *Sinonovacula constricta* (Bivalvia: Solecurtidae). Acta Oceanologica Sinica 29(2): 88–92. https://doi.org/10.1007/s13131-010-0026-y

ZooKeys 1232: 267–284 (2025)
DOI: 10.3897/zookeys.1232.136907

Research Article

Three new species of the cockroach genus *Nocticola* Bolívar, 1892 (Blattodea, Corydioidea, Nocticolidae) from China

Ting-Ting Li[1], De-Xing Liu[1], Jian Chen[1], Xiao-Ya Wei[1], Qiao-Yun Yue[2], De-yi Qiu[1]

1 *State Key Laboratory of Medical Vector Surveillance (Guangdong), Technology Center of Zhongshan Customs, Zhongshan, Guangdong 528400, China*
2 *Zhongshan Torch Polytechnic, Zhongshan, Guangdong 528400, China*
Corresponding author: De-yi Qiu (1610097453@qq.com)

Abstract

Three new species of *Nocticola* Bolívar, 1982 from Guangxi Province, China are described: *Nocticola baiguensis* **sp. nov.**, *Nocticola cordiformis* **sp. nov.**, and *Nocticola appendiculata* **sp. nov.** Morphological features associated with the wings, the specialized abdominal tergum, and genitalia of these new species are described and illustrated in detail. A key to the recorded *Nocticola* species from China is provided in this paper.

Key words: Cave cockroach, epigean, identification key, new species, *Nocticola*, taxonomy

Introduction

The genus *Nocticola*, with the type species *Nocticola simoni* Bolívar, was established by Bolívar (1892), who also described *N. caeca* Bolívar, 1892 in the same year; the first family-group name based on *Nocticola* is Nocticolinae (Bolívar 1892). Nocticolidae was first used by Bruner (1915) for two species described by Silvestri (1946), *N. sinensis* Silvestri and *N. termitopila* Silvestri, with *N. sinensis* being the earliest recorded *Nocticola* in China. Currently 29 known *Nocticola* species have been described all over the world (Beccaloni 2014; Trotter et al. 2017; Liu et al. 2017). They are very small and delicate, with reduced male wing veins. Among them, 17 species are cavernicolous, eight epigean, and four termitophilous (Fernando 1957; Roth 1988, 1991, 1995, 2003a; Roth and McGavin 1994; Andersen and Kjaerandsen 1995; Lucañas and Lit 2016; Lucañas et al. 2021; Lucañas and Maosheng 2023; Liu et al. 2017; Trotter et al. 2017). Handlirsch (1925) once classified *Nocticola* as Blattoidea based on the characteristics of the ovipositor valves in the seventh abdominal plate of *Nocticola* females, and subsequently, Princis (1966) listed Nocticolidae as a branch of Blattoidea. Roth (1988) suggested that Nocticolidae could be placed between Polyphagidae and Blattoidea. In recent years, molecular analysis has recovered Nocticolidae as sister to Corydiidae, particularly Latindiinae (Inward et al. 2007, Murienne 2009; Djernæs et al. 2012), supporting the position of Nocticolidae and Latindiinae as sister groups, and infer that Nocticolidae may be a specialized form of Latindiinae (Djernæs et al. 2015; Legendre et al. 2015; Li and Huang 2020). Subsequently, Han et al.

Academic editor: Fred Legendre
Received: 12 September 2024
Accepted: 6 February 2025
Published: 19 March 2025

ZooBank: https://zoobank.org/6FE030C5-C8F3-4BD3-9176-3101800B791B

Citation: Li T-T, Liu D-X, Chen J, Wei X-Y, Yue Q-Y, Qiu D-y (2025) Three new species of the cockroach genus *Nocticola* Bolívar, 1892 (Blattodea, Corydioidea, Nocticolidae) from China. ZooKeys 1232: 267–284. https://doi.org/10.3897/zookeys.1232.136907

(2023) assess the phylogenetic relationships of 35 Corydioidea species with mitochondrial genomes and two nuclear gene fragments, and they infer that the Latindiinae belong to the family Nocticolidae.

Materials and methods

Morphological study

Specimens were collected in Guangxi Province from 2023–2024. The examined material of *N. xiai* Liu, Zhu, Dai & Wang, 2017 (Fig. 1A–C) is deposited in the Institute of Entomology of the Shanghai Entomological Museum, Chinese Academy of Sciences, Shanghai (**SHEM**). The type specimens of the three new species and the examined specimens of *N. sinensis* Silvestri, 1946 (Fig. 2A–L) were deposited in the Zhongshan Customs Technology Center (**ZSCTC**).

The lateral tergum behind the seventh abdominal tergum (T7) of the male specimen was cut off, placed into a 1.5 ml centrifuge tube with 10% NaOH and digested at 70 °C for 30–45 min. After digestion, the NaOH was removed from the centrifuge tube, and the specimen was rinsed thrice with water before examination. The specimens were dissected and observed under a ZEISS Discovery V12 stereo microscope. Photographs were taken with a ZEISS/Smart Zoom5 and Canon EOS 5D Mark III, and illustrated with Adobe Photoshop 2022 software. After illustration, the genitalia were stored in 0.5 ml centrifuge tubes containing

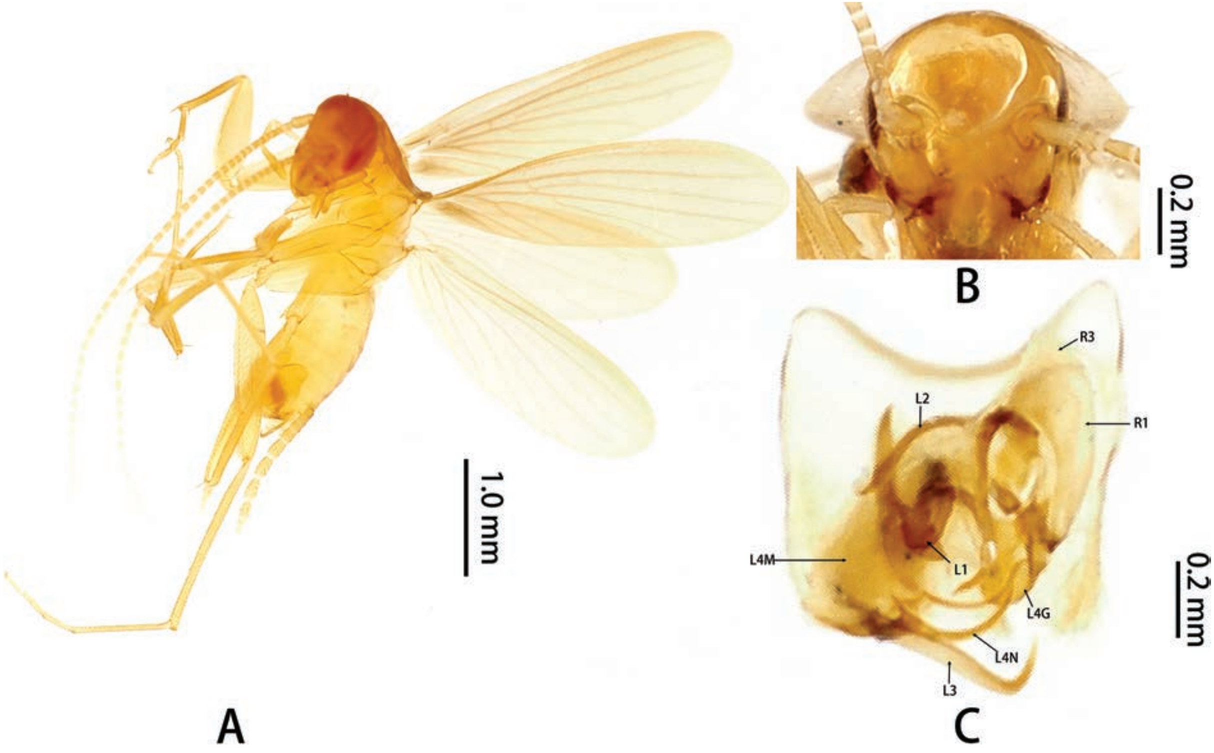

Figure 1. *Nocticola xiai* Liu, Zhu, Dai & Wang, 2017: **A** holotype male, lateral **B** head **C** phallomeres (photographs provided by Han-Qiang Wang, SHEM). Abbreviations: L1, L2, L3, L4G, L4N, L4M: sclerites of the left phallomere (L1 situated in the central dorsal wall; L2 arch-shaped sclerite situated in the ventral to L1; L3 situated in the left wall protrudes a large hook-process; L4G situated in the posterior ventral wall of the ventral lobe; L4N accessory hook-like phallomere; L4M situated in the ventral wall); R1, R3: sclerites of the left phallomere (R1 situated in the dorsal or ventral walls, or in the posterior part of dorsal and ventral wall; R3 plate-like situated in the anteriormost ventral wall).

50% glycerol, and preserved with the remainder of the specimen, which was stored in ethyl alcohol. Terminologies used for male genitalia follow Klass (1997) and for other characters follow Roth (2003b).

Molecular biology study

DNA was obtained from hind tarsus of adult and nymph cockroaches using TIANamp Genomic DNA Kit produced by Tiangen. The primers used for PCR amplification were the universal primers for cytochrome C oxidase subunit I (COI) gene: LOC1490 5'-GGTCAACAAATCATAAAGATATTGG-3', HCO2198 5'-TAAACTTCAGGGTGACCAAAAAATCA-3' (Folmer et al. 1994). The reagents for primers synthesized, EX-Taq DNA polymerase and dNTP were purchased from Takara Biotechnology (Dalian) Co., Ltd. The amplification conditions were denaturation at 95 °C for 5 min; 95 °C for 30 s, 50 °C for 30 s, 72 °C for 60 s, 35 cycles; final extension at 72 °C for 10 min, then held at 4 °C. The amplified samples with bands in Gel imaging System were sequenced by Tianyi Huiyuan Gene Technology Co., Ltd. (Guangzhou).

A total of 20 COI sequences were analyzed, of which 15 sequences were obtained in this study and Five sequences were downloaded from GenBank (Yanagisawa et al. 2021; Han et al. 2023; Li et al. 2022). *Latindia* sp. 1, *Latindia* sp. 2, and *Eucorydia dasytoides* were selected as outgroups (Table 1). Unfortunately, molecular data for *N. xiai* were not obtained, so could not be included in this study. All 15 sequences have been submitted to GenBank (https://www.ncbi.nlm.nih.gov/nuccore) with accession numbers PQ601347–PQ601361. The COI fragments were processed using the MUSCLE algorithm within MEGA 6.0 (Tamura et al. 2013), and a phylogenetic tree was constructed using Maximum Likelihood (ML) tree (Kimura 1980) and visualized using FigTree v. 1.4.4 (http://tree.bio.ed.ac.uk/software/figtree/). Nucleotide sites differences, genetic distances, both interspecific and intraspecific were calculated using the Kimura-2-paramaters (K2P) with 1,000 ultrafast bootstrap replicates (Hoang et al. 2018).

Table 1. Samples used in the phylogenetic analysis.

Species	Voucher number	Location	GenBank number
N. baiguensis sp. nov.	LI49-1	Yanshan District, Guilin City, Guangxi Province	PQ601347
	LI49-2		PQ601348
	LI69-1	Xiangshan District, Guilin City, Guangxi Province,	PQ601353
	LI69-2		PQ601354
	LI70	Diecai District, Guilin City, Guangxi Province,	PQ601355
	LI71-1		PQ601356
	LI71-2		PQ601357
N. cordiformis sp. nov.	LI51	Lingui District, Guilin City, Guangxi Province	PQ601349
	LI85		PQ601352
	LI86		PQ601358
	LI95		PQ601359
	LI96		PQ601360
N. appendiculata sp. nov.	LI81	Lingchuan County, Guilin City, Guangxi Province,	PQ601350
	LI82	Lingui District, Guilin City, Guangxi Province	PQ601351
N. sinensis	LII16	Jiangyong County, Yongzhou City, Hunan Province	PQ601361
Nocticola sp. 3 ZQW-2023c	/	/China	OR478956
Nocticola sp. 2 ZQW-2023c	/	/China	OR478955
Latindia sp. 1	B467	French Guiana	OL740656
Latindia sp. 2	B481	French Guiana	OL810009
Eucorydia dasytoides	/	Taiwan, China	LC480880

Results

Taxonomy

Family Nocticolidae Bolívar, 1892

Genus *Nocticola* Bolívar, 1892

Nocticola Bolívar, 1892: 29.

Type species. *Nocticola simoni*. First used as Nocticolidae Brunner 1915. Roth (1988) diagnosed and discussed Nocticolidae.

Diagnosis. The following description is in accordance with the traits proposed by Roth (1988) and the diagnosis of Andersen and Kjaerandsen (1995). Habitus small and delicate. Eyes well developed, variably reduced or absent; ocelli present or absent. Male wings are either reduced or well developed; front and hind wings are similar if well developed, membranous hyaline with minute pubescence and with few, essentially straight veins. Anteroventral margin of front femur with a row of piliform setae only, terminating at one or more large spines (= Type C); arolia and pulvilli absent; tarsal claws very small, simple, and symmetrical. Left and right phallomeres of the male genitalia are complex, always with a hook. Modification of the male abdomen tergal gland divides *Nocticola* into two groups: the *simoni* species group (male terga unspecialized) and the *uenoi* species group (male fourth abdominal terga specialized).

Differential diagnosis. Gravely (1910) compared the wing veins of *Alluaudellina himalayensis* and *Cardacus willeyi*, and concluded that the wing veins cannot be an important feature to distinguish these two genera. He distinguished the two genera by the presence or absence of ocelli, and whether the head is exposed or covered by the pronotum. Karny (1924) distinguished *Cardacopsis*, *Alluaudellina* and *Cardacus* by the degree of eye development, wing venation, and the presence or absence of ocelli, but he did not include *Nocticola* in the discussion. Roth (1988) considered that Chopard (1946) established the genus *Typhloblattodes* using a nymph specimen, questioning the validity of this genus. Chopard (1932, 1946, 1966) believed that there was polymorphism in the wing veins of *Alluaudellina himalayensis*, and, in *Nocticola*, polymorphism in wings and eyes development, making these features of questionable value in generic diagnosis. Consequently, he was unable to distinguish *Nocticola* from *Alluaudellina* and believed that they may be synonyms. The genus *Nocticola* can be distinguished from *Typhloblatta* and *Pholeosilpha* by the following characteristics: anteroventral margin of front femur Type C, in contrast forefemoral spination type B2 in *Typhloblatta* and *Pholeosilpha*. The genus *Nocticola* can be distinguished from *Spelaeoblatta* by the following characteristics: 1) anteroventral margin of front femur Type C, in contrast fore femoral spination type B1 in *Spelaeoblatta*; 2) abdominal terga are unspecialized or have a gland on the fourth segment, while in *Spelaeoblatta* tergal glands on the second and third abdominal tergum; 3) female apterous, whereas female of *Spelaeoblatta* lack hind wings but have reduced lateral tegminal pads; 4) male tegmina membranous, with distinctive venation, while in *Spelaeoblatta* tegmina corneous, with poorly defined veins. The genus *Nocticola* can be distinguished from *Helmablatta* by the following characteristics: 1) anteroventral margin of front femur Type C, in contrast fore femoral spination type intermediate between A1 and B1 in *Helmablatta*; 2) abdominal terga are unspecialized or have a gland on the fourth segment, while in *Helmablatta* third to fifth abdominal tergum form a composite gland, and eighth abdominal tergum is specialized. The genus *Nocticola* can be distinguished from *Metanocticola* by the following characteristics: abdominal terga are unspecialized or have a gland on the fourth segment, while in *Metanocticola* male has a sex gland on the metanotum. According to current molecular analysis research, it has been shown that *Nocticola* is polyphyletic (Kovacs et al. 2024). The three new species are placed in the genus *Nocticola* based on features of the eyes, male wings, anteroventral margin of front femur type, arolia, pulvilli, abdomen tergal, and male genitalia.

Key to species of *Nocticola* from China (males)

1 Fourth abdominal tergum specialized, with dense setae on median area .. .. ***N. appendiculata*** **sp. nov.**

– Fourth abdominal tergum not specialized **2**

2 Tegmina not extending beyond the end of abdomen .... ***N. sinensis*** **Silvestri, 1946**

– Tegmina extending beyond the end of abdomen **3**

3 Tegmina and wings almost equal in length **4**

– Tegmina developed; hind wings reduced.................. ***N. baiguensis*** **sp. nov.**

4 Subgenital plate weakly asymmetrical; accessory hook-like phallomere (L4N) parabola-like .... ***N. xiai*** **Liu, Zhu, Dai & Wang, 2017**

– Subgenital plate symmetrical; accessory hook-like phallomere (L4N) fin-shaped... ***N. cordiformis*** **sp. nov.**

Nocticola sinensis **Silvestri, 1946**
Fig. 2A–L

Nocticola sinensis Silvestri, 1946: 329; Silvestri 1947: 15; Princis 1952: 43; Princis 1966: 603; Roth 1988: 299; Liu et al. 2017.

Material examined. CHINA • 1 ♂ (deposited in SHEM); Hong Kong • 1 ♂, (deposited in ZSCTC), Hunan Province, Yongzhou City, Jiangyong County; 25°20.51'N, 111°20.34'E; 330 m; 14 July 2024, Hao-fei Fan leg.

Description. Small size, adult yellowish. Male. (Fig. 2A, B). ***Head:*** vertex of head exposed (Fig. 2C); eyes reduced to a few ommatidia narrowly grouped near antennal sockets (Fig. 2D); ocelli absent. Pronotum suboval, middle of posterior margin with weak invagination, anterior margin, and lateral margin with 12 setae (Fig. 2C). ***Tegmina and hind wings:*** tegmina not extending beyond the end of abdomen (Fig. 2A), veins reduced in number, densely pubescent (Fig. 2F). Hind wings reduced, veins reduced in number (Fig. 2G). ***Legs:*** legs long and slender. Anteroventral margin of front femur Type C1 (Fig. 2E); the first tarsus of the hind leg longer than the sum of the remaining tarsi; tarsal claws symmetrical and unspecialized (Fig. 2H), arolium and pulvillus absent (Fig. 2I). ***Abdomen and genitalia:*** abdominal tergal gland unspecialized. Supra-anal plate symmetrical, middle of the hind margin triangular concave. Cerci 10 segments; ventral surface of segments not spinous setae (Fig. 2J). Subgenital symmetri-

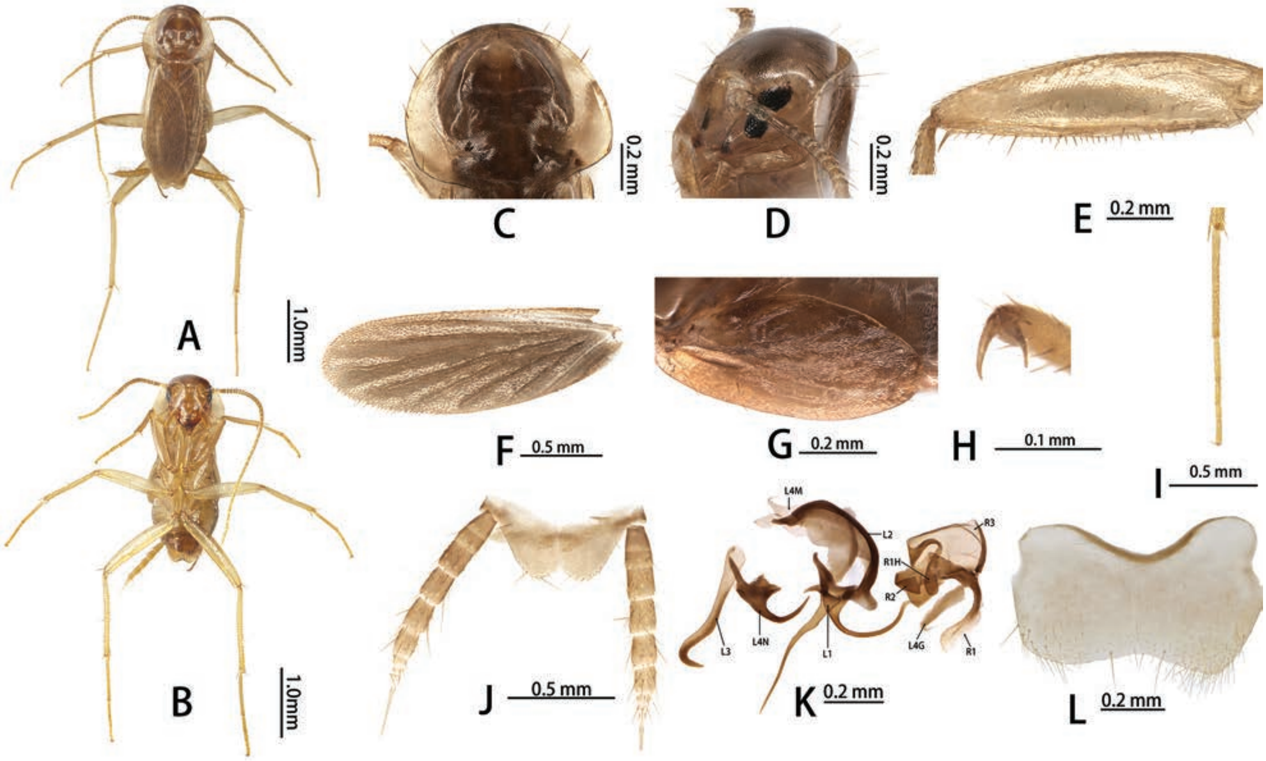

Figure 2. *Nocticola sinensis* Silvestri, 1946: **A** male, dorsal view **B** male, ventral view **C** pronotum **D** head **E** fore femur **F** tegmen **G** hind wings **H** tarsal claw **I** hind tarsus **J** supra-anal plate, dorsal view; male genitalia **K** phallomeres **L** subgenital plate, ventral view. Abbreviations: L1, L2, L3, L4G, L4N, L4M sclerites of the left phallomere (L1 situated in the central dorsal wall; L2 arch-shaped sclerite situated in the ventral to L1; L3 situated in the left wall protrudes a large hook-process; L4G situated in the posterior ventral wall of the ventral lobe; L4N accessory hook-like phallomere; L4M situated in the ventral wall); R1, R2, R3, R1H sclerites of the left phallomere (R1 situated in the dorsal or ventral walls, or in the posterior part of dorsal and ventral wall; R2 a ridge on the ventral margin; R3 plate-like situated in the anteriormost ventral wall; R1H a larger lobed situated in the dorsal wall, with extensions into the ventral wall).

cal, middle of the hind margin concave (Fig. 2L). Style absent. Male genitalia: genital hook (L3) elongate, ventral to hook with approximately 14 strong setae; accessory hook-like phallomere (L4N), curved inward to approach a right angle, heavily sclerotized; L2 narrow; left process of L1 extends downward, and the right process curved inward; R1 membranous; R2 surface with scale-like tubercles; R3 membranous; R1H reduced, rounded margin (Fig. 2K).

Measurements (mm). Male, pronotum: length × width: 0.76–0.90 × 0.98–1.20, tegmen: 1.73–2.00, body length (the length from the tip of vertex up to the tip of abdomen): 2.70–3.00;

Distribution. China (Hong Kong, Hunan Prov.).

Nocticola baiguensis **sp. nov.**

https://zoobank.org/63BC7718-864D-4327-84F6-9433E063A45D

Figs 3A–M, 4A–F

Type material. ***Holotype***: China • 1 ♂; Guangxi Province, Guilin City, Yanshan District, Wangjia Village, Baigu Cave; 25°13.85'N, 110°20.52'E; 162 m; 1 November 2023, Hao-fei Fan leg; ZSCTC-LI0001. ***Paratype***: China • 9 ♂; same data as for holotype; 14 March 2024, Ting-Ting Li leg; ZSCTC-LI-0002- LI-00010

• 8 ♀; same collection data as for preceding; 14 March 2024, De-Xing Liu leg; ZSCTC-LI-00011- LI-00018 • 6 nymphs; same collection data as for preceding; 14 March 2024, Ting-Ting Li leg; ZSCTC-LI-00019- LI-00024 • 1 ♂; Guangxi Province, Guilin City, Xiangshan District, Guilin National Forest Park in Guanxi; 25°13.93'N, 110°13.92'E; 148 m; 18 March 2024, Hao-fei Fan leg; ZSCTC-LI-0025 • 1 ♂; Guangxi Province, Guilin City, Diecai District, Baiyun Temple, 25°18.75'N, 110°22.38'E; 526 m; 28 March 2024, Hao-fei Fan leg; ZSCTC-LI-0026 • 1 ♀; same collection data as for preceding; 28 March 2024, Hao-fei Fan leg; ZSCTC-LI-0027

Diagnosis. The absence of a specialized abdominal tergal gland places the new species into the *simoni* species group. This species is similar to *N. baumi* Lucañas, Blaha, Rahmadi & Patoka, 2021, *N. bolivari* Chopard, 1950, *N. brooksi* Roth, 1995, *N. cockingi* Trotter, McRae, Main & Finston, 2017, *N. gonzalezi* Lucañas & Lit, 2016, *N. leleupi* Chopard, 1966, *N. quartermaieni* Trotter, McRae, Main & Finston, 2017, and *N. termitophila* Silvestri, 1946 as all these species are apterous. It can be distinguished by its eyes reduced to a few ommatidia narrowly grouped near antennal sockets (Fig. 3D), while in *N. baumi*, *N. bolivari*, and *N. cockingi* eyes are absent. In addition, the tegmina of this species are distinctly longer than the end of the abdomen, while in *N. brooksi*, *N. gonzalezi*, *N. leleupi*, *N. quartermaieni*, and *N. termitophila* tegmina do not extend beyond the end of abdomen.

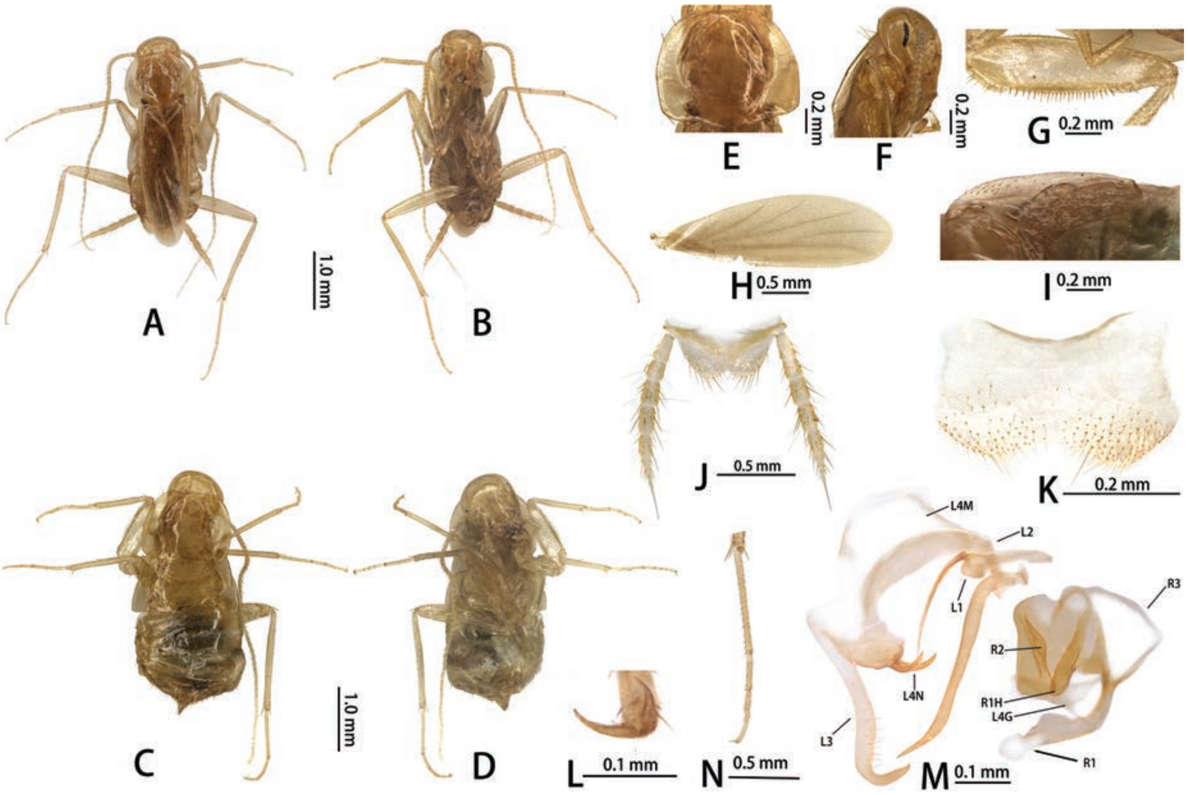

Figure 3. *Nocticola baiguensis* sp. nov.: adult male **A** dorsal view **B** ventral view; adult female **C** dorsal view **D** ventral view **E** male pronotum **F** male head **G** forefemur **H** tegmen **I** hindwings **J** supra-anal plate, ventral view **K** subgenital plate, ventral view **L** tarsal claw **N** hind tarsus; male genitalia **M** phallomeres. Abbreviations: L1, L2, L3, L4G, L4N, L4M: sclerites of the left phallomere (L1 situated in the central dorsal wall; L2 arch-shaped sclerite situated in the ventral to L1; L3 situated in the left wall protrudes a large hook-process; L4G situated in the posterior ventral wall of the ventral lobe; L4N accessory hook-like phallomere; L4M situated in the ventral wall); R1, R2, R3, R1H: sclerites of the left phallomere (R1 situated in the dorsal or ventral walls, or in the posterior part of dorsal and ventral wall; R2 a ridge on the ventral margin; R3 plate-like situated in the anteriormost ventral wall; R1H a larger lobed situated in the dorsal wall, with extensions into the ventral wall).

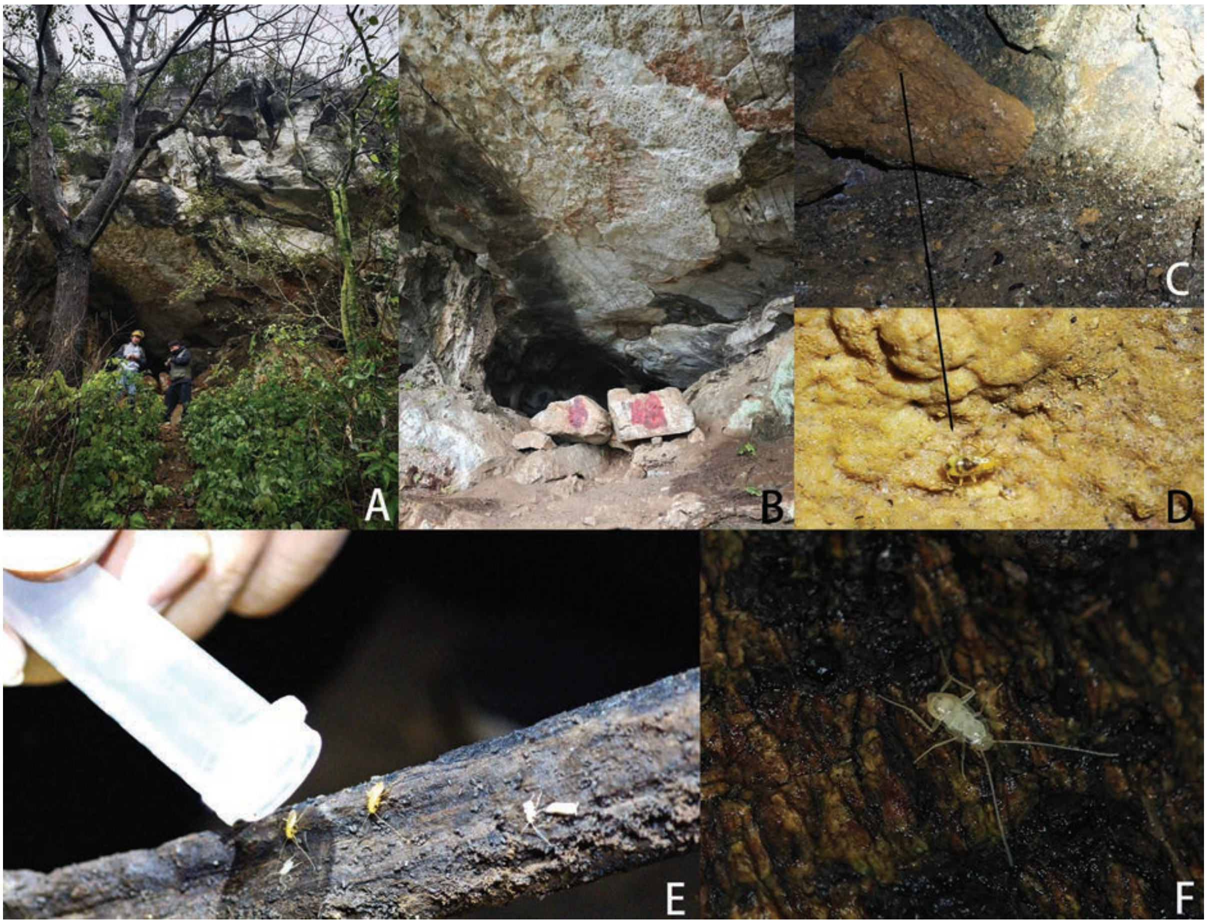

Figure 4. Habitats of *Nocticola baiguensis* sp. nov. from China **A, B** external environment of the Baigu Cave **C, D** *N. baiguensis* sp. nov. found on stone, surrounded by some animal feces **E** *N. baiguensis* sp. nov. found on rotting branch **F** nymphs of *Nocticola baiguensis* sp. nov.

Measurements (mm). Male, pronotum: length × width: 0.80–1.01 × 1.09–1.30, tegmen: 2.29–2.32, overall length (including tegmen): 2.99–3.02, body length (the length from the tip of vertex up to the tip of abdomen): 2.85–3.35. Female, pronotum: length × width: 0.96–1.15 × 1.30–1.51, body length (the length from the tip of vertex up to the tip of abdomen): 3.16–3.67.

Description. Small size. Nymphs whitish (Fig. 4F), adult yellowish. Male. (Figs 3A, B, 4E). ***Head:*** vertex of head exposed; eyes reduced to a few ommatidia narrowly grouped near antennal sockets (Fig. 3F); ocelli absent (Fig. 3F). Pronotum suboval, both sides of posterior margin with weak invagination, anterior margin and lateral margin with 12 setae (Fig. 3E). ***Tegmina and hind wings:*** tegmina extending beyond the end of abdomen (Fig. 3A, B), veins reduced in number, densely pubescent (Fig. 3H). Lateral portions of metanotum pubescent, somewhat produced, suggesting a wing surface, but this region not separated from metanotum. ***Legs:*** legs long and slender (Fig. 3I). Anteroventral margin of front femur Type C1 (Fig. 3G); the first tarsus of the hind leg longer than the sum of the remaining tarsi; tarsal claws symmetrical and unspecialized (Fig. 3L), arolium and pulvillus absent (Fig. 3N). ***Abdomen and genitalia:*** abdominal tergal gland unspecialized. Supra-anal plate symmetrical, middle of the hind margin triangular concave. Cerci with 11 segments; ventral surface of segments without spinous setae (Fig. 3J). Subgenital symmetrical, middle of the hind margin concave (Fig. 3K). Style absent. Male genitalia: genital hook (L3) elongate, ventral to hook with approximately 17 strong setae; accessory hook-like phallomere (L4N), apex short and with double-hook, heavily sclerotized; L2 narrow, L1 elongate, process long spine-like; R1 membranous, distal capitate-like; R2 sinuate protrusion of central part, surface with scale-like tubercles; R3 membranous; R1H reduced, rounded margin (Fig. 3M).

Female: Apterous (Fig. 4C, D). Supra-anal plate triangular, transverse of hind margin, middle with U-shaped invagination. Subgenital lobate (Fig. 3C, D). Cerci with 11 segments; ventral surface of segments without spinous setae.

Etymology. The specific name *baiguensis* is derived from the cave called Baigu Cave (Fig. 4A, B), which is the first collection site of this species.

Distribution. China (Guangxi).

Nocticola cordiformis sp. nov.

https://zoobank.org/867C3F19-3F52-4B41-80D9-8ECE341029E7

Figs 5A–M, 6A–C

Type material. ***Holotype***: China • 1 ♂; Guangxi Province, Guilin City, Lingui District, Huixian Town, Edi Village, Yanzi Cave; 25°3.30'N, 110°11.27'E; 195 m; 13 December 2023; Hao-Fei Fan leg; ZSCTC-LI-0028**.** ***Paratype***: China • 1 ♂; Guangxi Province, Guilin City, Lingui District, Lingjiaodi Village; 25°13.58'N, 110°14.50'E; 148 m; 30 December 2023; Hao-Fei Fan leg; ZSCTC-LI-0029 • 1 ♀; same collection data as for preceding; 30 December 2023; Hao-Fei Fan leg; ZSCTC-LI-0030 • 2 ♂; Guangxi Province, Guilin City, Lingui District, Huixian Town, Edi Village, 25°3.07'N, 110°10.25'E; 176 m; 29 April 2024; Hao-Fei Fan leg; ZSCTC-LI-0031 to 0032.

Diagnosis. The absence of a specialized abdominal tergal gland places the new species into the *simoni*-species group. This species is similar to *N. adebratti* Roth, 1994, *N. babindaensis* Roth, 1994, *N. clavate* Andersen & Kjaerandsen, 1995, *N. gerlachi* Roth, 2003, *N. pheromosa* Lucañas & Maosheng, 2023, *N. scytale* Andersen & Kjaerandsen, 1995, *N. wliensis* Andersen & Kjaerandsen, 1995, and *N. xiai* Liu, Zhu, Dai & Wang, 2017, with tegmina and wings developed. It differs from *N. adebratti* and *N. gerlachi* by its ocelli absent (Fig. 5F), while in *N. adebratti* and *N. gerlachi* ocelli are present. The subgenital plate of the newly described species is symmetrical (Fig. 5L), while in *N. adebratti*, *N. babindaensis*, *N. clavate*, *N. gerlachi*, *N. pheromosa*, *N. scytale*, and *N. wliensis*, the subgenital plate is asymmetrical. It differs from *N. xiai* as follows: 1) tegmina and wings extending beyond the end of abdomen, body length is about half of the wing length, while in *N. xiai* tegmina and wings slightly extend beyond the end of abdomen, but not exceeding half of the body length (Fig. 1A); 2) eyes well developed, while in *N. xiai* eyes reduced (Fig. 1B); and 3) accessory hook-like phallomere (L4N) fin-shaped, whereas L4N is parabola-like in *N. xiai* (Fig. 1C).

Measurements (mm). Male, pronotum: length × width: 0.81–1.02 × 0.99–1.21, tegmen: 4.04–4.25, overall length (including tegmen): 4.83–5.24, body length (the length from the tip of vertex up to the tip of abdomen): 3.19–3.27. Female, pronotum: length × width: 1.13–1.22 × 1.35–1.42, body length (the length from the tip of vertex up to the tip of abdomen): 3.45–3.66.

Description. Small size. Body tawny. **Male.** (Figs 5A, B, 6C). ***Head:*** vertex of head exposed; Eyes well developed, with heptagon concave; ocelli absent (Fig. 5F). Pronotum subtrapezoidal, densely pubescent, anterior margin and lateral margin

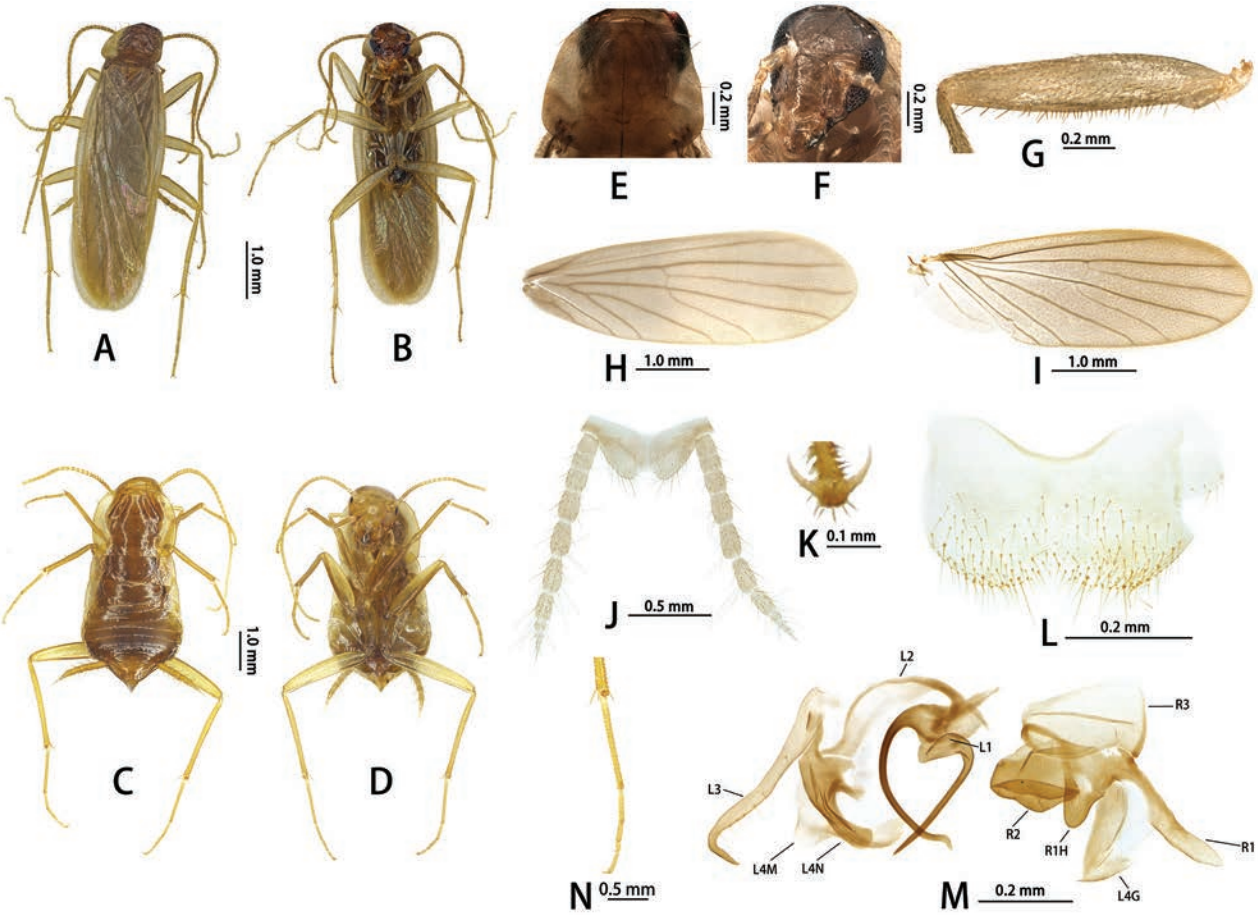

Figure 5. *Nocticola cordiformis* sp. nov.: **A** male, dorsal view **B** male, ventral view **C** female, dorsal view **D** female, ventral view **E** pronotum **F** head **G** front femur **H** tegmen **I** wings **J** supra-anal plate, ventral view **K** tarsal claw **L** subgenital plate, ventral view **N** hind tarsus; male genitalia, **M** phallomeres. Abbreviations: L1, L2, L3, L4G, L4N, L4M sclerites of the left phallomere (L1 situated in the central dorsal wall; L2 arch-shaped sclerite situated in the ventral to L1; L3 situated in the left wall protrudes a large hook-process; L4G situated in the posterior ventral wall of the ventral lobe; L4N accessory hook-like phallomere; L4M situated in the ventral wall); R1, R2, R3, R1H sclerites of the left phallomere (R1 situated in the dorsal or ventral walls, or in the posterior part of dorsal and ventral wall; R2 a ridge on the ventral margin; R3 plate-like situated in the anteriormost ventral wall; R1H a larger lobed situated in the dorsal wall, with extensions into the ventral wall).

with 12 setae (Fig. 5E). ***Tegmina and hind wings:*** tegmina and wings well developed, extending beyond the end of abdomen, body length is about half of the wing length (Fig. 5A, B), veins reduced in number, densely pubescent (Fig. 5H, I). ***Legs:*** legs long and slender. Anteroventral margin of front femur Type C1 (Fig. 5G); the first tarsus of the hind leg longer than the sum of the remaining tarsi; tarsal claws symmetrical and unspecialized (Fig. 5K), arolium and pulvillus absent (Fig. 5N). ***Abdomen and genitalia:*** abdominal tergal gland unspecialized. Supra-anal plate symmetrical, middle of the hind margin concave (Fig. 5J). Subgenital plate symmetrical, middle of the hind margin weakly concave (Fig. 5L). Style absent. Male genitalia: L3 elongate, ventral to hook with 7 strong setae; L4N fin-shaped; L2 narrow; left and right process of L1 towards curved, heart-shape; R1 long handle-like, covered with some setae; R2 sinuate protrusion, with scale-like tubercles; R3 membranous; R1H reduced, rounded margin, with scale-like tubercles (Fig. 5M).

Female: Apterous. Supra-anal plate triangular, transverse of hind margin, middle with triangular invagination. Subgenital lobate (Fig. 5C, D). Cerci 11 segments; ventral surface of segments not spinous setae.

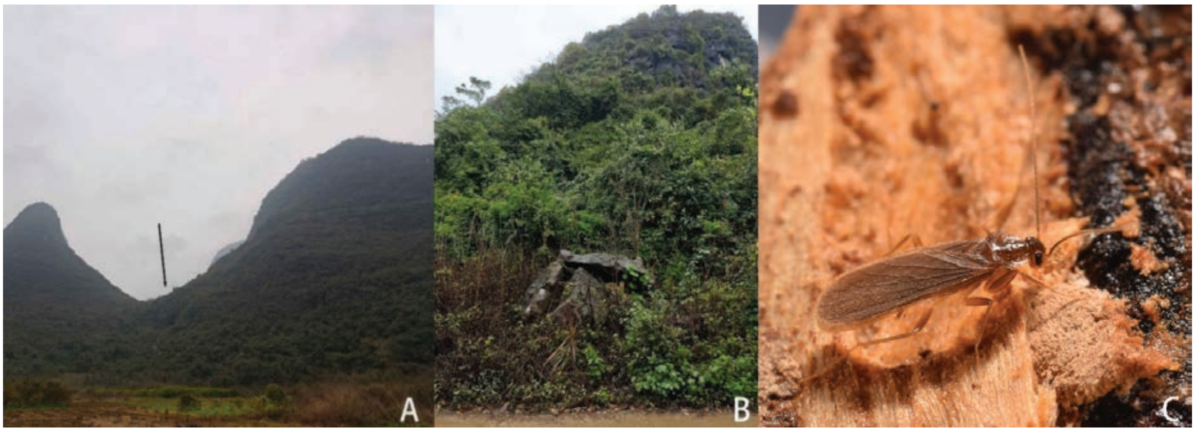

Figure 6. Habitats of *Nocticola cordiformis* sp. nov. from China **A, B** habitats of holotype specimen of *N. cordiformis* sp. nov. **C** adult of *N. cordiformis* sp. nov. on wood.

Etymology. The specific name is derived from the Latin word *cordiformis*, in reference to the L1 heart-shaped structure of left aedeagus.

Distribution. China (Guangxi).

Nocticola appendiculata sp. nov.

https://zoobank.org/C49BF683-1E94-4EFF-8E5A-E49684049B8C
Figs 7A–P, 8A–D

Type material. ***Holotype***: China • 1 ♂; Guangxi Province, Guilin City, Lingchuan County, Haiyang Town, Xiaofu Village, 25°15.17'N, 110°35.33'E; 329 m; 26 April 2024; Hao-Fei Fan leg; ZSCTC-LI-0033. ***Paratype***: China • 1 ♂, 1 ♀; same data as for holotype; Hao-Fei Fan leg; ZSCTC-LI-0034 to 0035 • 2 ♂; Guangxi Province, Guilin City, Lingui District, Huixian Town, Edi Village, 25°3.67'N, 110°10.25'E; 176 m; 29 April 2024; Hao-Fei Fan leg; ZSCTC-LI-0036 to 0037.

Diagnosis. The fourth abdominal tergum specialized tergal gland places the new species into the *uenoi*-species group. It closely resembles *Nocticola currani* Trotter, McRae, Main & Finston, 2017 in terms of the well-developed tegmina and fourth abdominal tergum specialized. It differs from *N. currani* as follows: 1) wings curved, longer than tegmina and extending beyond the end of abdomen, while in *N. currani* wings reduced, not extending beyond the first abdomen; 2) ventral of L3 hook with ~ 10 strong setae scattered, while in *N. currani* with 11 long and strong setae clustered on distal end below the curve of L3 hook; and 3) accessory hook-like phallomere (L4N) inner margin curved and smooth at distal end, whereas L4N is spear-shaped, with longitudinal ribbing of distal end in *N. currani*. In addition, the tegmina of this species are distinctly longer than the end of the abdomen, with a small appendicular field, while the tegmina of *N. australiensis* Roth, 1988, *N. uenoi kikaiensis* Asahina, 1974, *N. uenoi miyakoensis* Asahina, 1974, *N. uenoi uenoi* Asahina, 1974 and *N. rohini* (Fernando, 1962) are shorter than the end of the abdomen, and without appendicular field.

Measurements (mm). Male, pronotum: length × width: 1.01–1.21 × 1.08–1.29, tegmen: 2.66–2.87, wings: 3.05–3.26, overall length (including tegmen): 4.08, body length (the length from the tip of vertex up to the tip of abdomen): 2.48–2.65. Female, pronotum: length × width: 1.10 × 1.33; body length (the length from the tip of vertex up to the tip of abdomen): 3.50.

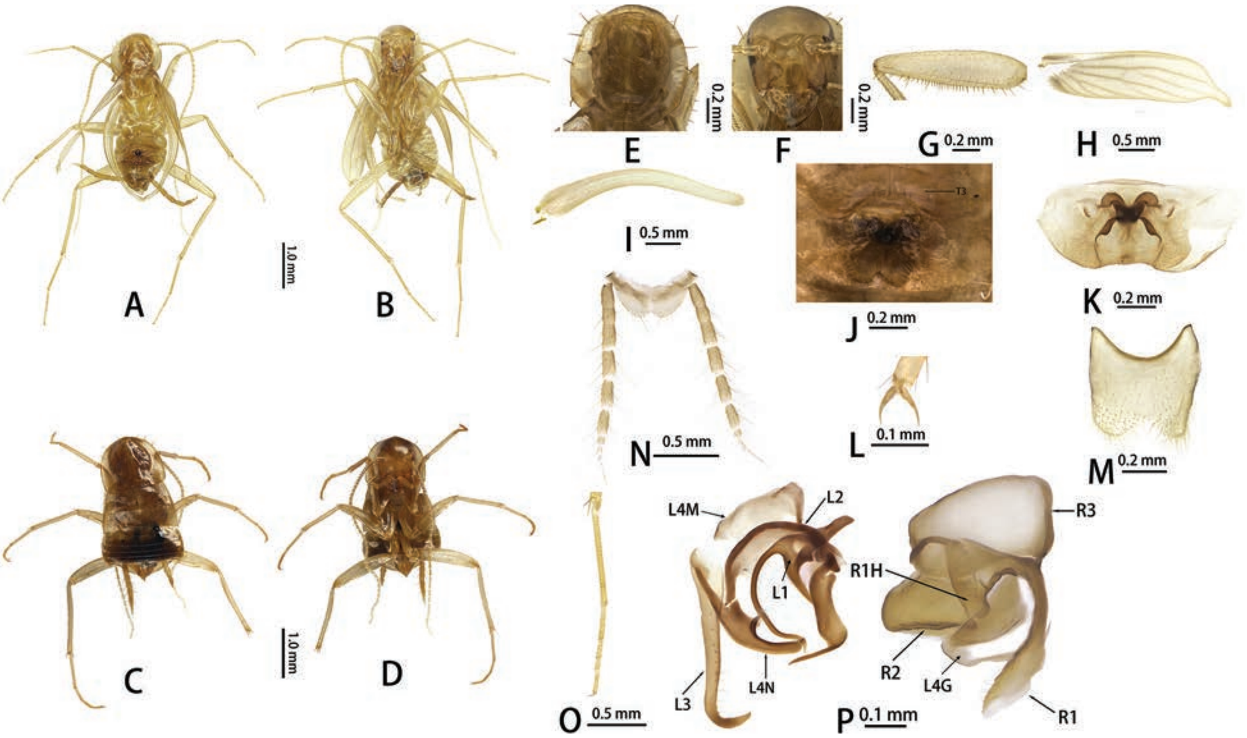

Figure 7. *Nocticola appendiculata* sp. nov. **A** male, dorsal view **B** male, ventral view **C** female, dorsal view **D** female, ventral view **E** pronotum **F** head **G** front femur **H** tegmen **I** wings **J, K** male T4, dorsal view **L** tarsal claw **N** supra-anal plate, ventral view **M** subgenital plate, dorsal view **O** hind tarsus, male genitalia **P** phallomeres. Abbreviations: L1, L2, L3, L4G, L4N, L4M: sclerites of the left phallomere (L1 situated in the central dorsal wall; L2 arch-shaped sclerite situated in the ventral to L1; L3 situated in the left wall protrudes a large hook-process; L4G situated in the posterior ventral wall of the ventral lobe; L4N accessory hook-like phallomere; L4M situated in the ventral wall); R1, R2, R3, R1H: sclerites of the left phallomere (R1 situated in the dorsal or ventral walls, or in the posterior part of dorsal and ventral wall; R2 a ridge on the ventral margin; R3 plate-like situated in the anteriormost ventral wall; R1H a larger lobed situated in the dorsal wall, with extensions into the ventral wall).

Description. Small size. Nymphs whitish (Fig. 8B). Body yellowish. **Male** (Figs 7A, B, 8B, C, D). ***Head:*** vertex of head exposed; eyes reduced; ocelli absent (Fig. 7D). Pronotum ovoid, densely pubescent, hind margin weakly concave, anterior and lateral margins with 12 setae (Fig. 7B). ***Tegmina and hind wings:*** tegmina extending beyond the end of abdomen, with a small appendicular at the apical (Fig. 7H). Wings inflexion, longer than tegmina and extending beyond the end of abdomen, veins indistinct, with some setae. Hind wings are placed on both sides of the abdomen and not covered by the tegmina (Fig. 7A, B, I). **Legs:** legs long and slender. Anteroventral margin of front femur Type C1 (Fig. 7G); the first tarsus of the hind leg longer than the sum of the remaining tarsi; tarsal claws symmetrical and unspecialized (Fig. 7L), arolium and pulvillus absent (Fig. 7O). ***Abdomen and genitalia:*** second and third abdominal tergum deeply concave on hind margin, exposing the gland of the fourth abdominal tergum. Fourth abdominal tergum specialized, median area has dense setae convex and a large and deep invagination; Posterior margin has three convexities, with the middle one being smaller than the two sides (Fig. 7J, K). Supra-anal plate symmetrical, middle of the hind margin concave (Fig. 7N). Subgenital plate symmetrical, middle of the hind margin weakly concave (Fig. 7M). Style absent. Male genitalia of left phallomere: L3 elongate, ventral to hook with ~ 10 strong setae scattered; L4N inner margin smooth; L2 narrow; L1 long, apex of left process slightly curved towards L4N. Male genitalia of right phallomere: R1 medial border with several

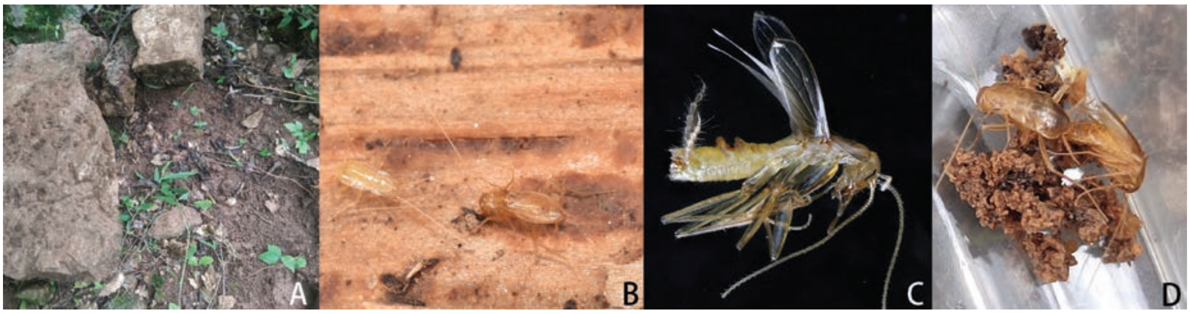

Figure 8. Habitats of *Nocticola appendiculata* sp. nov. from China **A** habitats of *N. appendiculata* sp. nov. **B** nymphs and an adult of *N. appendiculata* sp. nov. on wood **C** *N. appendiculata* sp. nov., side view **D** female and male of *N. appendiculata* sp. nov. mating.

long setae; R2 sinuate protrusion, with scale-like tubercles; R3 membranous; R1H reduced, rounded margin, with scale-like tubercles (Fig. 7P).

Female: Apterous (Fig. 8D). Supra-anal plate triangular, transverse of hind margin, U-shaped invagination slightly to the right in the middle of hind margin. Subgenital lobate (Fig. 7C, D). Cerci with 11 segments; ventral surface of segments without spinous setae.

Etymology. The specific name is derived from the Latin word *appendiculatus*, in reference to the extended appendicular field of tegmina.

Distribution. China (Guangxi).

Molecular analysis based on COI

We collected the 14 COI sequences of the three new species and blasted them on GenBank. The resulting sequence alignment comprised 658 nucleotides. Sequence comparisons reveal sequence differences in nucleotide numbers (Table 2, above diagonal), as well as intra- and interspecific genetic distances (Table 2, below diagonal). The intraspecific genetic distance of these three new species is 0. The interspecific genetic distance between *N. baiguensis* sp. nov. and *N. cordiformis* sp. nov. is 19.40%, while that between *N. baiguensis* sp. nov. and *N. appendiculata* sp. nov. is 21.05%; The genetic distance between *N. appendiculata* sp. nov. and *N. cordiformis* sp. nov. is 4.26%. The COI sequence of these two species differ in 27 nucleotide sites.

The phylogenetic tree of the 20 COI sequences, derived from Table 1, is depicted in Fig. 9. The maximum likelihood (ML) tree shows that samples with the same morphology exhibit high bootstrap values in forming monophyletic groups, although most of the other nodes did not have high bootstrap values.

Discussion

In this study, we used morphological differential diagnosis to conclude that *N. baiguensis*, *N. cordiformis*, and *N. appendiculata* are new species of the genus *Nocticola*. The three species have significant differences in male genitalia. Molecular comparison of these three species show that the maximum genetic distance between them was 21.05% (*N. baiguensis* and *N. cordiformis*), while the minimum interspecies genetic distance was 4.26% (*N. cordiformis*, and *N. appendiculata*).

Nocticola is mainly distributed in Africa, Asia, and Australasia (Beccaloni 2014), with two species *N. xiai* Liu, Zhu, Dai & Wang, 2017 and *N. sinensis* Silvestri, 1946 recorded in China, both of which are termitophilous (Silvestri 1946; Liu et al. 2017); the other two termitophilous species are *N. termitophila* Silvestri, 1946 and *N. jodarlingtonae* Roth, 2003 (Silvestri 1946; Roth 2003a). The four species of *Nocticola* were found in termite nests, but at that time, there were no research records of a relationship between *Nocticola* and termites. In March 2023, we discovered a female *Nocticola* sp. with reduced eyes in Jiangjunshan Park, Zhuhai City, Guangdong Province. It was found in a relatively dry, mud-built, ant nest at the bottom of some decaying wood; the ant species was identified as *Camponotus nicobarensis* Mayr, 1865. Unfortunately, we only found one female *Nocticola* sp.

Table 2. Genetic distances (below diagonal) and nucleotide sites differences (above diagonal) of three new species based on COI sequences.

Specimen	LI49-1	LI49-2	LI69-1	LI69-2	LI70	LI70-1	LI70-2	LI51	LI85	LI86	LI95	LI96	LI81	LI82
LI49-1*N. baiguensis* sp. nov.		0	0	0	0	0	0	112	112	112	112	112	120	120
LI49-2 *N. baiguensis* sp. nov.	0.0000		0	0	0	0	0	112	112	112	112	112	120	120
LI69-1 *N. baiguensis* sp. nov.	0.0000	0.0000		0	0	0	0	112	112	112	112	112	120	120
LI69-2 *N. baiguensis* sp. nov.	0.0000	0.0000	0.0000		0	0	0	112	112	112	112	112	120	120
LI70 *N. baiguensis* sp. nov.	0.0000	0.0000	0.0000	0.0000		0	0	112	112	112	112	112	120	120
LI70-1 *N. baiguensis* sp. nov.	0.0000	0.0000	0.0000	0.0000	0.0000		0	112	112	112	112	112	120	120
LI70-2 *N. baiguensis* sp. nov.	0.0000	0.0000	0.0000	0.0000	0.0000	0.0000		112	112	112	112	112	120	120
LI51 *N. cordiformis* sp. nov.	0.1940	0.1940	0.1940	0.1940	0.1940	0.1940	0.1940		0	0	0	0	27	27
LI85 *N. cordiformis* sp. nov.	0.1940	0.1940	0.1940	0.1940	0.1940	0.1940	0.1940	0.0000		0	0	0	27	27
LI86 *N. cordiformis* sp. nov.	0.1940	0.1940	0.1940	0.1940	0.1940	0.1940	0.1940	0.0000	0.0000		0	0	27	27
LI95 *N. cordiformis* sp. nov.	0.1940	0.1940	0.1940	0.1940	0.1940	0.1940	0.1940	0.0000	0.0000	0.0000		0	27	27
LI96 *N. cordiformis* sp. nov.	0.1940	0.1940	0.1940	0.1940	0.1940	0.1940	0.1940	0.0000	0.0000	0.0000	0.0000		27	27
LI81 *N. appendiculata* sp. nov.	0.2105	0.2105	0.2105	0.2105	0.2105	0.2105	0.2105	0.0426	0.0426	0.0426	0.0426	0.0426		0
LI82 *N. appendiculata* sp. nov.	0.2105	0.2105	0.2105	0.2105	0.2105	0.2105	0.2105	0.0426	0.0426	0.0426	0.0426	0.0426	0.0000	

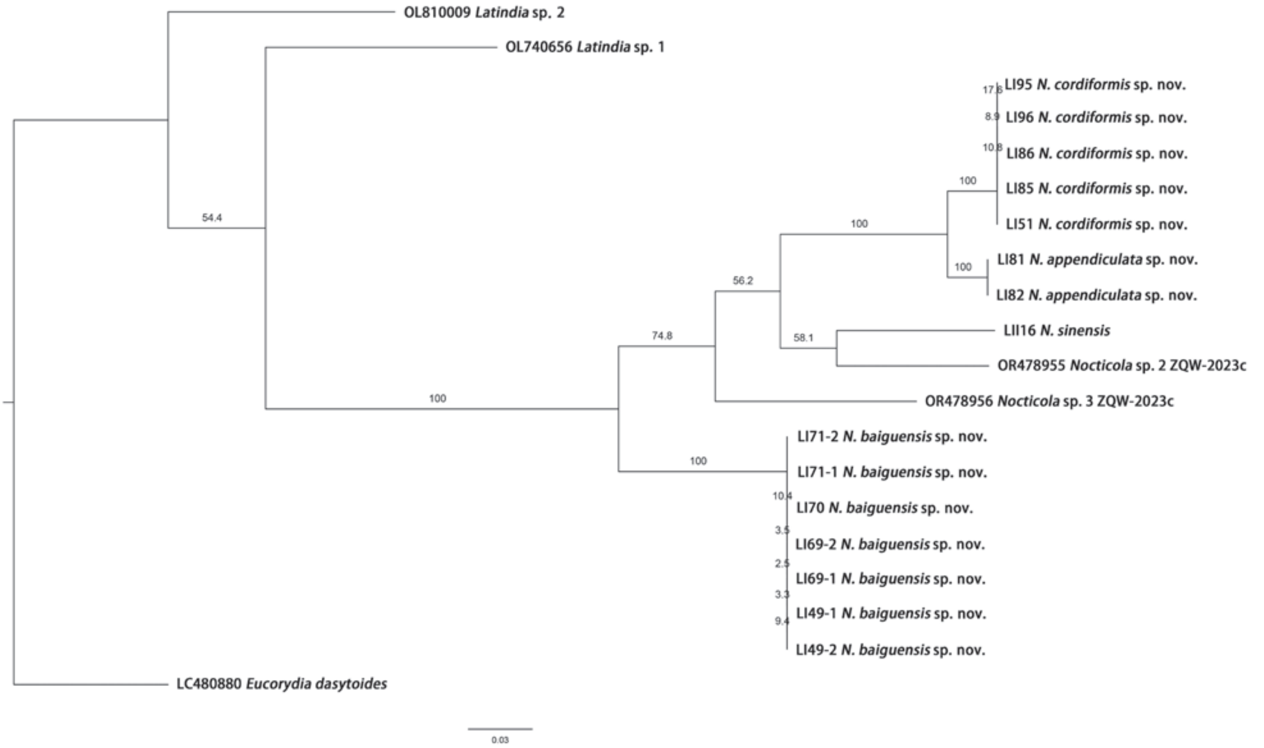

Figure 9. Maximum likelihood (ML) tree of *N. baiguensis* sp. nov., *N. cordiformis* sp. nov. and *N. appendiculata* sp. nov. based on a portion of the COI sequence. Bootstrap values are reported above each branch.

Due to the scarcity of evidence, we cannot determine whether this *Nocticola* sp. accidentally entered the nest or had a relationship with *C. nicobarensis*.

This article describes three new species: *N. baiguensis* sp. nov., *N. cordiformis* sp. nov., and *N. appendiculata* sp. nov. Among them, *N. baiguensis* sp. nov. was first discovered in the Baigu Cave, which is a natural karst cave. We found them on some decaying branches and stones next to the bat feces. We collected four pairs of *N. baiguensis* sp. nov. in the cave, and one of them was surrounded by many small nymphs. We brought them back to the laboratory for breeding. Kept under observation, we found that they feed on mycelium on wood at a slow rate. They prefer to hide under the bottom of wood and wet tissues and did not seem to be very active. We also found some ants identified as *C. nicobarensis* living together with *N. baiguensis* sp. nov.

China is a country with the largest area of karst caves, a total of approximately 3.4 million square kilometers and approximately 500,000 karst caves (Zhang et al. 2021). Most of the karst caves have constant temperature and humidity inside because of the underground space with dark environments and complex terrain (Ran 2013). Due to some social and historical reasons, the exploration of cave-dwelling organisms started relatively late in China (Zhang 1992), resulting in few reports on cave insects and the present research on cave cockroaches. *Nocticola cordiformis* sp. nov. and *N. appendiculata* sp. nov. were found under rocks at the roadside. The eyes and wings of *N. cordiformis* sp. nov. are well developed, while the eyes of *N. baiguensis* sp. nov. and *N. appendiculata* sp. nov. were smaller. *Nocticola appendiculata* sp. nov. has well-developed front and hind wings, whereas tegmina are well developed and hind wings reduced in *N. baiguensis* sp. nov. During the sample collection process, it was common to find *N. cordiformis* sp. nov. and *N. appendiculata* sp. nov. living under the same stone, with overlapping areas, although they have certain differences in morphology and COI sequences. Further research on the living habits of *Nocticola* and exploration of their relationship with ants should be carried out in the future.

Acknowledgments

We are very grateful to Mr Hao-Fei Fan for efforts collecting specimens. We thank Mr Han-Qiang Wang (SHEM) for kindly loaning the specimen of *N. xiai* Liu, Zhu, Dai & Wang, 2017. We are also very grateful to Dr Christopher Glasby for revising the manuscript.

Additional information

Conflict of interest

The authors have declared that no competing interests exist.

Ethical statement

No ethical statement was reported.

Funding

This project was funded by the Gongbei Customs Research Project (2023GK002, 2023GK004, 2025GK002); General customs administration Research Project (2024HK219, 2022HK100).

Author contributions

Tingting Li: Data curation (equal); methodology (lead); visualization (lead); writing – original draft (lead); writing – review and editing (equal); investigation (equal); funding acquisition (equal). Dexing Liu: Data curation (equal); visualization (supporting); investigation (equal); writing – review and editing (supporting). Jian Chen: Data curation (equal); supervision (equal); resources (equal). Xiaoya Wei: Data curation (equal); project administration (equal). Qiaoyun Yue: Resources (equal). Deyi Qiu: Funding acquisition (equal); project administration (equal); supervision (equal); writing – review and editing (equal).

Author ORCIDs

Ting-Ting Li https://orcid.org/0000-0001-5127-5344
De-Xing Liu https://orcid.org/0009-0009-9946-9864
Jian Chen https://orcid.org/0000-0002-2025-7079
Xiao-Ya Wei https://orcid.org/0009-0007-3297-8109

Data availability

All of the data that support the findings of this study are available in the main text.

References

Andersen T, Kjaerandsen J (1995) Three new species of *Nocticola* Bolívar from Ghana, West Africa (Blattaria: Nocticolidae). Journal of African Zoology 109(4): 377–385.

Beccaloni GW (2014) Cockroach Species File Online. Version 5.0/5.0.World Wide Web Electronic Publication. http://Cockroach.SpeciesFile.org [Accessed 1 April 2024]

Bolívar I (1892) Voyage de M. E. Simon aux l’île Philippines (Mars et Avril 1890). Études sur les Arthropodes cavernicoles de l’île de Luzon. Annales de la Société Entomologique de France 61: 29–34. https://doi.org/10.1080/21686351.1892.12279282

Bruner L (1915) Preliminary catalogue of the Orthopteroid insects of the Philippine Islands. University Studies of the University of Nebraska 15: 195–281.

Chopard L (1932) Un cas de microphtalmie liée à l’atrophie des ailes chez une blatte cavernicole. In: Société Entomologique de France (Ed.) Livre du Centenaire. Société Entomologique de France, Paris, 485–496.

Chopard L (1946) Note sur quelques Orthoptères cavernicoles de Madagascar. Revue Francaise d’Entomologie 13: 146–155.

Chopard L (1950) Les blattes cavernicoles du genre *Nocticola* Bol. Eos, Revista Española de Entomología 29: 301–310. http://hdl.handle.net/10261/153622

Chopard L (1966) Une espèce nouvelle de *Nocticola* provenant d’une grotte du Transvaa (Dictyoptères, Nocticolidae). In: Bulletin de la Société entomologique de France 71: 307–310. https://doi.org/10.3406/bsef.1966.20908

Djernæs M, Klass KD, Picker MD, Damgaard J (2012) Phylogeny of cockroaches (Insecta, Dictyoptera, Blattodea), with placement of aberrant taxa and exploration of outgroup sampling. Systematic Entomology 37(1): 65–83. https://doi.org/10.1111/j.1365-3113.2011.00598.x

Djernæs M, Klass KD, Eggleton P (2015) Identifying possible sister groups of Cryptocercidae + Isoptera: A combined molecular and morphological phylogeny of Dictyoptera. Molecular Phylogenetics and Evolution 84: 284–303. https://doi.org/10.1016/j.ympev.2014.08.019

Fernando W (1957) New species of Insects from Ceylon (I). Ceylon Journal of Science (Biological Sciences) 1(1): 7–18. https://dl.nsf.gov.lk/handle/1/7778

Fernando W (1962) The Gastric Caeca and Proventriculus in the Blattidae. Ceylon journal of science (Biological Sciences) 4(2): 87–95.

Folmer O, Black M, Hoeh W, Lutz R, Vrijenhoek R (1994) DNA primers for amplification of mitochondrial cytochrome c oxidase subunit I from diverse metazoan invertebrates. Molecular Marine Biology and biotechnology 3(5): 294.

Gravely FH (1910) *Alluaudella himalayensis*, a new species of degenerate (♂) cockroach. With an account of the venation found in the genera *Cardax* and *Alluaudella*. Records of the Indian Museum 5: 307–311. https://doi.org/10.5962/bhl.part.10504

Han W, Qiu L, Zhang JW, Wang ZQ, Che YL (2023) Phylogenetic reconstruction of Corydioidea (Dictyoptera: Blattodea) provides new insights on the placement of Latindiinae and supports the proposal of the new subfamily Ctenoneurinae. Systematic Entomology 49(1): 156–172. https://doi.org/10.1111/syen.12610

Handlirsch A (1925) Geschichte, Literatur, Technik, Paläontologie, Phylogenie und Systematik der Insekten. In: Schröder C (Ed.) Handbuch der Entomologie. Band III. Gustav Fischer, Jena pp 1201.

Hoang DT, Chernomor O, von Haeseler A, Minh BQ, Vinh LS (2018) UFBoot2: Improving the ultrafast bootstrap approximation. Molecular Biology and Evolution 35(2): 518–522. https://doi.org/10.1093/molbev/msx281

Inward D, Beccaloni G, Eggleton P (2007) Death of an order: a comprehensive molecular phylogenetic study confirms that termites are eusocial cockroaches. Biology Letters 3: 331–335. https://doi.org/10.1098/rsbl.2007.0102

Karny HH (1924) Beiträge zur Malayischen Orthopterenfauna. Treubia 5: 1–234. https://doi.org/10.14203/treubia.v5i1-3.1681

Kimura M (1980) A simple method for estimating evolutionary rates of base substitutions through comparative studies of nucleotide sequences. Journal of Molecular Evolution 16(2): 111–120. https://doi.org/10.1007/BF01731581

Klass KD (1997) The external male genitalia and the phylogeny of Blattaria and Mantodea. Bonner Zoologische Monographien 42: 1–340.

Kovacs TGL, Walker J, Hellemans S, Bourguignon T, Tatarnic NJ, McRae JM, Ho SYW, Lo N (2024) Dating in the Dark: Elevated Substitution Rates in Cave Cockroaches (Blattodea: Nocticolidae) Have Negative Impacts on Molecular Date Estimates. Systematic Biology 73(3): 532–545. https://doi.org/10.1093/sysbio/syae002

Legendre F, Nel A, Svenson GJ, Robillard T, Pellens R, Grandcolas P (2015) Phylogeny of Dictyoptera: Dating the Origin of Cockroaches, Praying Mantises and Termites with Molecular Data and Controlled Fossil Evidence. Plos One 10: 1–27. https://doi.org/10.1371/journal.pone.0130127

Li XR, Huang DY (2020) A new mid-Cretaceous cockroach of stem Nocticolidae and reestimating the age of Corydioidea (Dictyoptera: Blattodea). Cretaceous Research 106: 1–39. https://doi.org/10.1016/j.cretres.2019.104202

Li TT, Liu DX, Chen J, Wei XY, Qiu DY, Ke MJ, Yue QY (2022) Morphological identification of two non-recorded cockroach species (Latindiinae: *Latindia*) firstly intercepted in China. Chinese Journal of Vector Biology and Control 33(5): 742–747. https://doi.org/10.11853/j.issn.1003.8280.2022.05.024

Liu XW, Zhu WB, Dai L, Wang HQ (2017) Cockroaches of southeastern China. Henan Science and Technology Press, Zhengzhou, 15–19. [in Chinese]

Lucañas CC, Lit IL (2016) Cockroaches (Insecta, Blattodea) from caves of Polillo Island (Philippines), with description of a new species. Subterranean Biology 19(1): 51–64. https://doi.org/10.3897/subtbiol.19.9804

Lucañas CC, Maosheng F (2023) A new macropterous *Nocticola* Bolívar, 1892 (Blattodea: Nocticolidae) from Singapore. Journal of Asia-Pacific Entomology 26(2): 1–5. https://doi.org/10.1016/j.aspen.2023.102062

Lucañas CC, Blaha M, Rahmadi C, Patoka J (2021) The first *Nocticola* Bolívar, 1892 (Blattodea: Nocticolidae) from New Guinea. Zootaxa 5082(3): 294–300. https://doi.org/10.11646/zootaxa.5082.3.7

Murienne J (2009) Molecular data confirm family status for the *Tryonicus*-*Lauraesilpha* group (Insecta: Blattodea: Tryonicidae). Organisms, Diversity and Evolution 9: 44–51. https://doi.org/10.1016/j.ode.2008.10.005

Princis K (1952) Blattarien aus Venezuela, gesammelt von Herrn G. Marcuzzi. Annuario Dell'Istituto e Museo di Zoologia della Universita di Napoli 6(12), 1–11.

Princis K (1966) Blattariae: Subordo Blaberoidea. Fam.: Blattidae, Nocticolidae. In: Beier M (Ed.) Orthopterorum Catalogus Pars 8. Uitgeverij Dr. W. Junk, 's-Gravenhage, 402–614.

Ran JC (2013) The Biological World of Karst Caves in the Dark World. Forests and Humans 7: 120–125.

Roth LM (1988) Some cavernicolous and epigean cockroaches with six new species, and a discussion of the Nocticolidae (Dictyoptera: Blattaria). Revue Suisse de Zoologie 95: 297–321. https://doi.org/10.5962/bhl.part.79654

Roth LM (1991) A new cave-dwelling cockroach from Western Australia (Blattaria: Nocticolidae). Records of the Western Australian Museum 15(1): 17–21.

Roth LM (1995) New species and records of cockroaches from Western Australia (Blattaria). Records of the Western Australian Museum 17: 153–161.

Roth LM (2003a) Some Cockroaches from Africa and Islands of the Indian Ocean, with Descriptions of Three New Species (Blattaria). Transactions of the American Entomological Society 129(1): 167–186. https://doi.org/10.2307/25078802

Roth LM (2003b) Systematics and phylogeny of cockroaches (Dictyoptera: Blattaria). Oriental Insects 37: 1–186. https://doi.org/10.1080/00305316.2003.10417344

Roth LM, Mcgavin GC (1994) Two new species of Nocticolidae (Dictyoptera: Blattaria) and a rediagnosis of the cavernicolous genus *Spelaeoblatta* Bolívar. Journal of Natural History 28(6): 1319–1326. https://doi.org/10.1080/00222939400770671

Silvestri F (1946) Prima nota su alcuni termitofili dell'Indocina. Bollettino del Laboratorio di Entomologia Agraria di Portici 6: 313–330.

Silvestri F (1947) Seconda nota su alcuni termitofili dell'Indocina con una appendices ul Macrotermes barneyi Light. Bollettino del Laboratorio di Entomologia Agraria di Portici 7: 13–40.

Tamura K, Stecher G, Peterson D, Peterson D, Filipski A, Kumar S (2013) MEGA6: molecular evolutionary genetics analysis version 6.0. Molecular biology and evolution 30(12): 2725–2729. https://doi.org/10.1093/molbev/mst197

Trotter AJ, McRae JM, Main DC, Finston TL (2017) Speciation in fractured rock landforms: towards the understanding of subterranean cockroaches (Dictyoptera: Nocticolidae) in Western Australia. Zootaxa 4250(2): 143–170. https://doi.org/10.11646/zootaxa.4250.2.2.

Yanagisawa S, Hiruta SF, Sakamaki Y, Liao JR, Shimano S (2021) Two new species of the genus *Eucorydia* (Blattodea: Corydiidae) from the Nansei Islands in Southwest Japan. Zoological Science 38(1): 90–102. https://doi.org/10.2108/zs200048

Zhang F (1992) Review and prospect of cave biology research in China. Yunnan Geographical Environment Research 4(1): 87–91.

Zhang YH, Zhu DH, Shui XJ (2021) The Mysterious World of 500000 Chinese Karst Caves. Forests and Humanity 8: 1–30.

ZooKeys 1232: 285–310 (2025)
DOI: 10.3897/zookeys.1232.145622

Research Article

Filling a zoogeographical gap in China: Taxonomic descriptions of six new spider species of the *Pholcus phungiformes* species group (Araneae, Pholcidae)

Jinglin Li[1], Qiaoqiao He[1], Shuqiang Li[2], Zhiyuan Yao[1]

1 *College of Life Science, Shenyang Normal University, Shenyang 110034, Liaoning, China*
2 *Institute of Zoology, Chinese Academy of Sciences, Beijing 100101, China*
Corresponding author: Zhiyuan Yao (yaozy@synu.edu.cn)

Abstract

The spiders of the *Pholcus phungiformes* species group in China are distributed across the Lüliang Mountains and the Yanshan-Taihang Mountains in northern China, and the Changbai Mountains, which border northeastern China and North Korea. This study presents the first collection of the *P. phungiformes* species group from mountainous regions situated between the Yanshan-Taihang and Changbai Mountains, revealing six new species: *Pholcus chaoyang* S. Li & Yao, **sp. nov.**, *P. hebei* S. Li & Yao, **sp. nov.**, *P. huludao* S. Li & Yao, **sp. nov.**, *P. jinzhou* S. Li & Yao, **sp. nov.**, *P. liaoning* S. Li & Yao, **sp. nov.**, and *P. qin* S. Li & Yao, **sp. nov.** Detailed diagnoses, descriptions, photomicroscopy images, and DNA barcodes of new species are provided.

Key words: Biodiversity, cellar spiders, DNA barcode, invertebrate, morphology, new species, taxonomy

Academic editor: Sarah Crews
Received: 30 December 2024
Accepted: 18 February 2025
Published: 19 March 2025

ZooBank: https://zoobank.org/CE9ACAC8-0ED2-47EC-AA25-864E630D6D75

Citation: Li J, He Q, Li S, Yao Z (2025) Filling a zoogeographical gap in China: Taxonomic descriptions of six new spider species of the *Pholcus phungiformes* species group (Araneae, Pholcidae). ZooKeys 1232: 285–310. https://doi.org/10.3897/zookeys.1232.145622

Introduction

Pholcus Walckenaer, 1805 is the most diverse genus of the family Pholcidae C.L. Koch, 1850 and is mainly distributed in the Afrotropical, Palaearctic, Indo-Malayan, and Australasian regions (e.g., Huber 2011; Yao and Li 2012, 2025; WSC 2025). This genus comprises 21 species groups and 411 species (Huber 2011; Huber et al. 2018; WSC 2025). The *Pholcus phungiformes* species group is the most speciose with 125 species (e.g., Huber 2011; Wang et al. 2020; Yao et al. 2021; Lu et al. 2022; Zhao et al. 2023a, b; Lee et al. 2024). Almost all of the species in this group have been recorded from four mountain ranges: the Lüliang Mountains (9 spp.) and the Yanshan-Taihang Mountains (35 spp.) in North China, the Changbai Mountains (28 spp.) at the border between northeastern China and North Korea, and the Taebaek-Sobaek Mountains (53 spp.) on the Korean Peninsula. The only exception is *P. phungiformes* Oliger, 1983, which is known from the Maritime Territory, Sakhalin Island, and the Kurile Islands, Russia (Huber 2011).

The records from the Lüliang Mountains represent the westernmost distribution limit of the *P. phungiformes* species group. Furthermore, this group is only distributed north of the Qinling Mountains. These conclusions are supported by the fact that Yao et al. did not find any specimens of this group during their sampling in Shaanxi Province in 2013, 2016, and 2019, nor was any found during a 2022 expedition in the Qinling Mountains, whose range extends from the southern part of Shaanxi Province to the western part of Henan Province (Zhao et al. 2023b; Yang et al. 2024a, b).

In China, 71 species of the *P. phungiformes* species group have been recorded, accounting for 57% of the global total for this group. Nevertheless, the distribution of this group within China is noticeably patchy, due to the lack of surveys targeting this group in mountainous regions situated between the Yanshan-Taihang and Changbai Mountains. For this reason, in 2024, we conducted a survey in these regions for the first time and report herein six new species (Figs 1, 2).

Material and methods

Specimens were examined and measured with a Leica M205 C stereomicroscope. Left male palps were photographed. Epigynes were photographed before dissection. Vulvae were photographed after treatment in a warm 10% solution of potassium hydroxide (KOH) to dissolve soft tissues. Images were captured with a Canon EOS 750D wide zoom digital camera (24.2 megapixels) mounted on the stereomicroscope mentioned above and assembled using Helicon Focus v. 3.10.3 image stacking software (Khmelik et al. 2005). All measurements are given in millimeters (mm). Leg measurements are shown as: total length (femur, patella, tibia, metatarsus, tarsus). Leg segments were measured on their dorsal side. The distribution map was generated with ArcGIS v. 10.2 (ESRI Inc.). The specimens studied are preserved in 75% ethanol and are deposited in the College of Life Science, Shenyang Normal University (SYNU), Liaoning, China.

Terminology and taxonomic descriptions follow Huber (2011) and Yao et al. (2015, 2021). The following abbreviations are used:

aa	anterior arch,	**kn**	knob,
ALE	anterior lateral eye,	**L/d**	length/diameter ratio,
AME	anterior median eye,	**pa**	proximo-lateral apophysis,
b	bulb,	**PME**	posterior median eye,
da	distal apophysis,	**pp**	pore plate,
e	embolus,	**pr**	procursus,
fa	frontal apophysis,	**u**	uncus.

DNA barcode sequences of five new species were obtained. A partial fragment of the mitochondrial cytochrome *c* oxidase subunit I (COI) gene was targeted using the following primers: forward: LCO1490 (5’-GGTCAACAAATCATAAAGATATTGG-3’) and reverse: HCO2198 (5’-TAAACTTCAGGGTGACCAAAAAATCA-3’) (Folmer et al. 1994). Additional information on extraction, amplification and sequencing procedures is provided in Yao et al. (2016). Sequences are deposited in GenBank (accession numbers provided below, Table 1).

Table 1. Voucher specimen information.

New species	Voucher code	GenBank accession number	Sequence length	Collection locality
P. chaoyang sp. nov.	W354	PV056134	634 bp	Liaoning, Chaoyang, Chaoyang County
P. hebei sp. nov.	W358	PV056135	634 bp	Hebei, Chengde, Longhua County
P. huludao sp. nov.	W356	N/A	N/A	Liaoning, Huludao, Jianchang County
P. jinzhou sp. nov.	W350	PV056132	634 bp	Liaoning, Jinzhou, Guta District
P. liaoning sp. nov.	W352	PV056133	634 bp	Liaoning, Chaoyang, Beipiao
P. qin sp. nov.	W359	PV056136	634 bp	Hebei, Qinhuangdao, Funing District

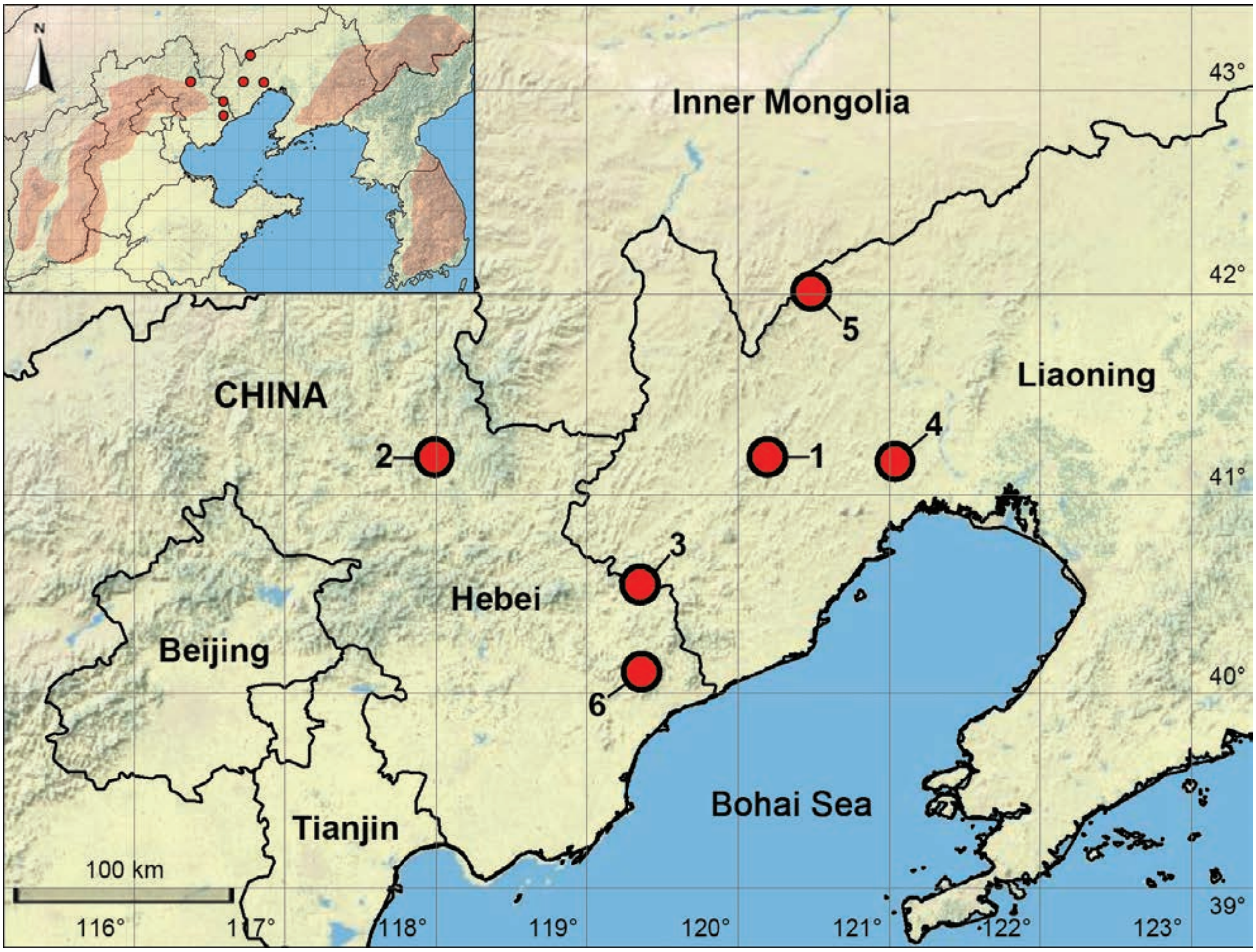

Figure 1. Distribution records of new species of the *Pholcus phungiformes* species group. 1. *P. chaoyang* sp. nov. 2. *P. hebei* sp. nov. 3. *P. huludao* sp. nov. 4. *P. jinzhou* sp. nov. 5. *P. liaoning* sp. nov. 6. *P. qin* sp. nov. Red shading from left to right in the insert indicates the Lüliang Mountains, the Yanshan-Taihang Mountains, the Changbai Mountains, and the Taebaek-Sobaek Mountains.

Taxonomy

Family Pholcidae C.L. Koch, 1850
Subfamily Pholcinae C.L. Koch, 1850

Genus *Pholcus* Walckenaer, 1805

Type species. *Aranea phalangioides* Fuesslin, 1775.

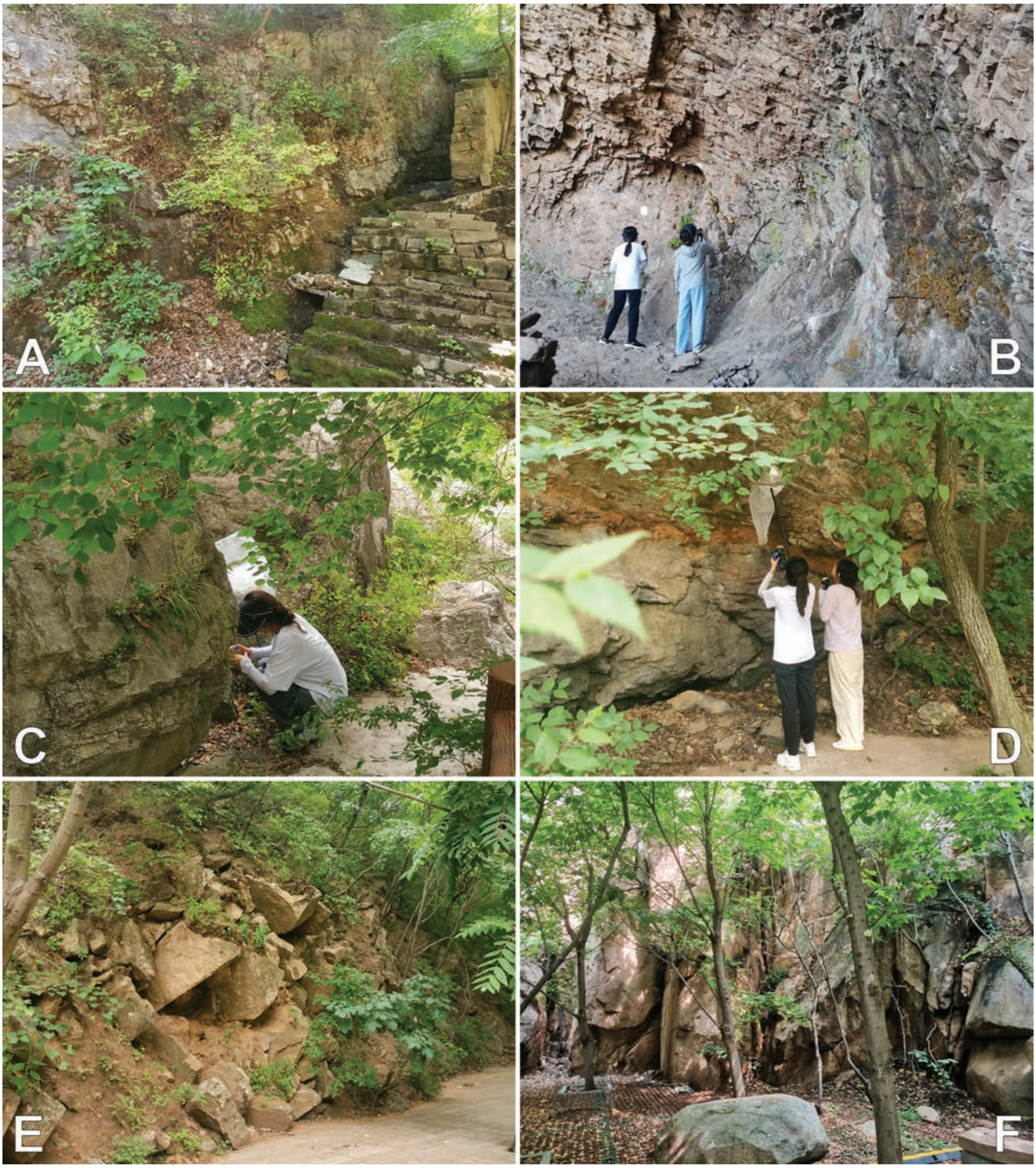

Figure 2. Typical habitats of the new species of the *Pholcus phungiformes* species group. **A** Qingfengling (type locality of *P. chaoyang* sp. nov.) **B** Longfengdong (type locality of *P. hebei* sp. nov.) **C** Longtan Grand Canyon (type locality of *P. huludao* sp. nov.) **D** Beiputuoshan (type locality of *P. jinzhou* sp. nov.) **E** Daheishan (type locality of *P. liaoning* sp. nov.) **F** Bingtangyu (type locality of *P. qin* sp. nov.).

Pholcus phungiformes species group

This species group was recognized by Huber (2011). The six new species described below are assigned to this group by the following combination of characters: male chelicerae with frontal apophyses, male palpal tibia with a prolatero-ventral projection, uncus with a "pseudo-appendix", and epigyne with a knob.

Pholcus chaoyang **S. Li & Yao, sp. nov.**

https://zoobank.org/404BD282-8958-457B-B7B9-B699C681BDFC

Figs 3, 4

Type material. ***Holotype*:** China • ♂; Liaoning, Chaoyang, Chaoyang County, Qingfengling Town, Qingfengling Scenic Spot; 41.186698°N, 120.190401°E; alt. 486 m; 17 Jul. 2024; Z. Yao, J. Li & M. Yan leg.; SYNU-Ar00415. ***Paratypes*:** China • 1♂; same data as for the holotype; SYNU-Ar00416 • 2♀; same data as for the holotype; SYNU-Ar00417–18.

Etymology. The specific name refers to the type locality; noun in apposition.

Diagnosis. The new species resembles *Pholcus huailai* Yao, Li & Lu, 2022 (Lu et al. 2022: 534, S18, figs S17A–D, S18A–H) by having a similar uncus (Fig. 4C) and male chelicerae (Fig. 4D), but it can be distinguished by the: procursus with a raised, prolatero-subdistal membranous edge (arrow 1 in Fig. 3C vs. absent), the straight distal edge of the sclerotized distal apophysis on the procursus (arrow 1 in Fig. 3D vs. curved), epigynal knob column shaped (kn in Fig. 4A vs. wedge shaped), vulval anterior arch curved (aa in Fig. 4B vs. nearly trapezoidal).

Description. Male (***holotype***): Total length 4.95 (5.14 with clypeus), carapace 1.55 long, 1.88 wide, opisthosoma 3.40 long, 1.60 wide. Leg **I**: 36.07 (9.29, 0.76, 9.10, 14.62, 2.30), leg **II**: 25.27 (7.12, 0.72, 6.35, 9.55, 1.53), leg **III**: 18.79 (5.45, 0.67, 4.55, 6.99, 1.13), leg IV: 24.69 (7.24, 0.68, 6.22, 9.10, 1.45); tibia **I** L/d: 55. Eye interdistances and diameters: PME–PME 0.21, PME 0.14, PME–ALE 0.04, AME–AME 0.04, AME 0.09. Sternum width/length: 1.19/0.98. Habitus as in Fig. 4E, F. Carapace yellowish, with brown radiating marks and marginal brown bands; ocular area yellowish, with median and lateral brown bands; clypeus yellowish, with brown marks; sternum brown. Legs yellowish, dark brown on patellae and whitish on distal parts of femora and tibiae, with darker rings on subdistal parts of femora and proximal and subdistal parts of tibiae. Opisthosoma yellowish, with dorsal and lateral brown spots. Chelicerae with pair of proximo-lateral apophyses (pa in Fig. 4D), pair of distal apophyses (da in Fig. 4D) with two teeth each, and pair of frontal apophyses (fa in Fig. 4D). Palps as in Fig. 3A, B; trochanter with long (3 × longer than wide), retrolaterally bulged ventral apophysis; femur with retrolatero-proximal protrusion (arrow in Fig. 3B) and indistinct ventral protrusion; tibia with prolatero-ventral protrusion (arrow in Fig. 3A); procursus simple proximally but complex distally, with raised, prolatero-subdistal membranous edge bearing sclerotized apophysis (arrows 1, 2 in Fig. 3C), sclerotized distal apophysis (arrow 3 in Fig. 3C), and one slender and one strong dorsal spines (arrows 2, 3 in Fig. 3D); uncus with scaly edge (u in Fig. 4C); "pseudo-appendix" curved (arrow in Fig. 4C); embolus weakly sclerotized, with transparent distal projections (e in Fig. 4C). Retrolateral trichobothrium on tibia **I** at 6% proximally; legs with short, vertical setae on tibiae, metatarsi, and tarsi; tarsus **I** with 31 distinct pseudosegments.

Female (***paratype***, SYNU-Ar00417): Similar to male, habitus as in Fig. 4G, H. Total length 5.12 (5.26 with clypeus), carapace 1.44 long, 1.66 wide, opisthosoma 3.68 long, 2.08 wide; tibia **I**: 7.18; tibia **I** L/d: 48. Eye interdistances and diameters: PME–PME 0.23, PME 0.12, PME–ALE 0.05, AME–AME 0.04, AME 0.08. Sternum width/length: 1.05/0.94. Clypeus brown. Epigyne posteriorly strongly curved, with lateral brown marks and knob (kn in Fig. 4A). Vulva with curved, sclerotized anterior arch (aa in Fig. 4B) and pair of nearly elliptical pore plates (pp in Fig. 4B).

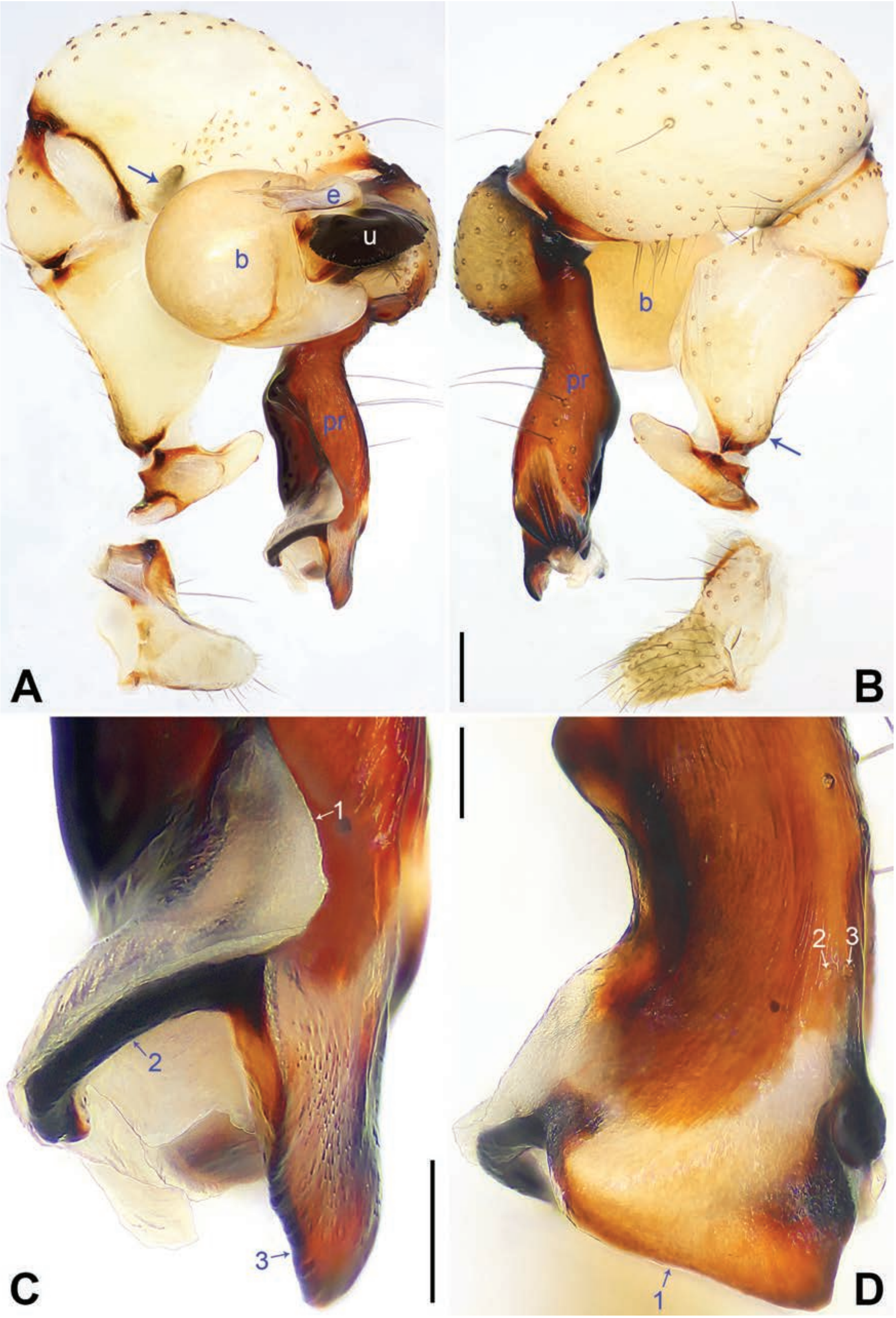

Figure 3. *Pholcus chaoyang* sp. nov., holotype male. **A, B** Palp (**A** prolateral view, arrow points at prolatero-ventral protrusion **B** retrolateral view, arrow points at retrolatero-proximal protrusion) **C, D** distal part of procursus (**C** prolateral view, arrow 1 points at prolatero-subdistal membranous edge, arrow 2 points at sclerotized apophysis, arrow 3 points at distal apophysis **D** dorsal view, arrow 1 points at distal edge, arrows 2, 3 point at dorsal spines). Abbreviations: b = bulb, e = embolus, pr = procursus, u = uncus. Scale bars: 0.20 mm (**A, B**); 0.10 mm (**C, D**).

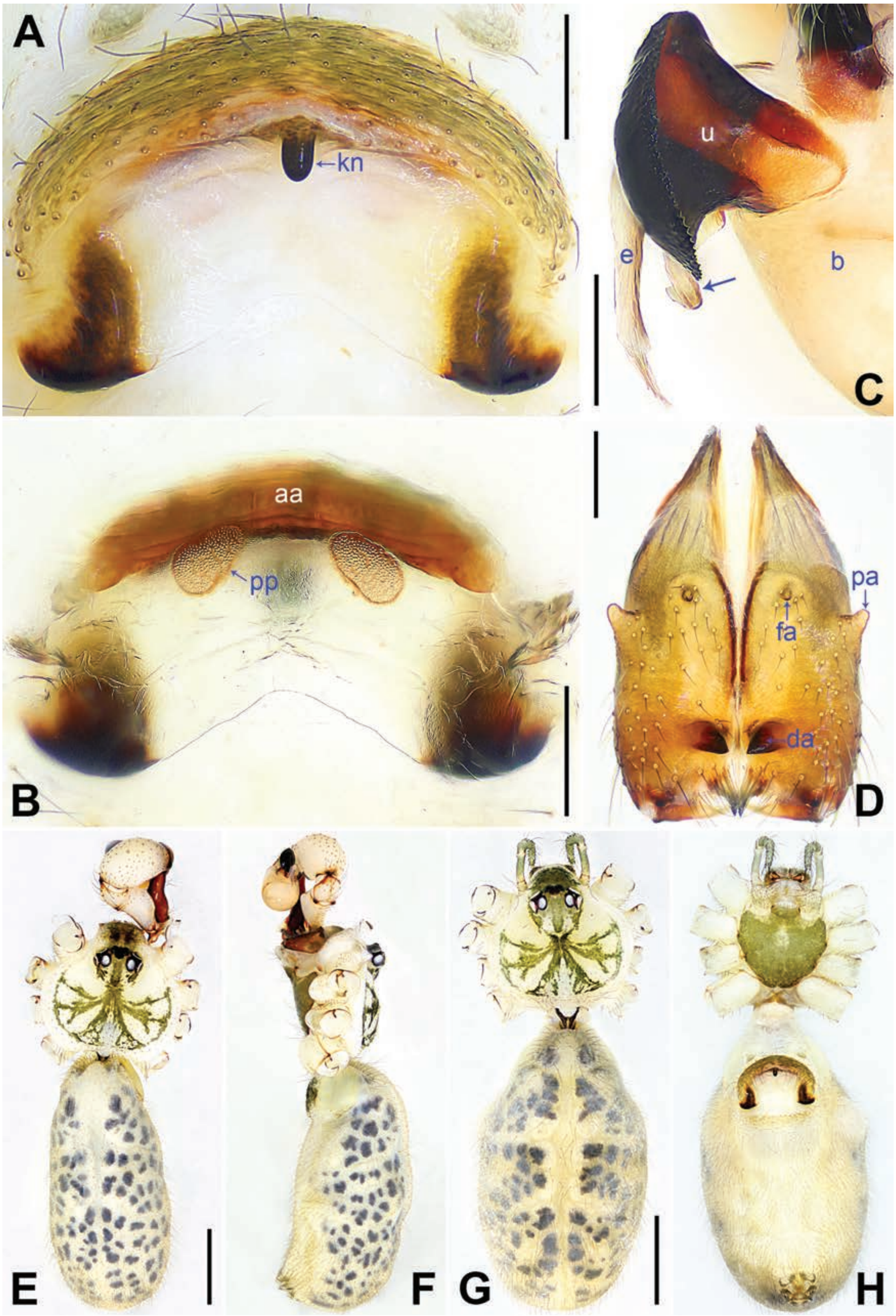

Figure 4. *Pholcus chaoyang* sp. nov., holotype male (**C–F**) and paratype female (**A, B, G, H**). **A** Epigyne, ventral view **B** vulva, dorsal view **C** bulbal apophyses, prolateral view, arrow points at "pseudo-appendix" **D** chelicerae, frontal view **E–H** habitus (**E, G** dorsal view **F** lateral view **H** ventral view). Abbreviations: aa = anterior arch, b = bulb, da = distal apophysis, e = embolus, fa = frontal apophysis, kn = knob, pa = proximo-lateral apophysis, pp = pore plate, u = uncus. Scale bars: 0.20 mm (**A–D**); 1.00 mm (**E–H**).

Variation. Tibia I in paratype male (SYNU-Ar00416): 9.23. Tibia I in another paratype female (SYNU-Ar00418): 7.24.

Habitat. Underside of overhang on rocky cliffs in mountainous area.

Distribution. Liaoning; known only from the type locality (Figs 1, 2A).

Pholcus hebei **S. Li & Yao, sp. nov.**

https://zoobank.org/094C644B-DC6B-4776-983B-767069BD3DFD
Figs 5, 6

Type material. ***Holotype*****:** China • ♂; Hebei, Chengde, Longhua County, Zhongguan Town, Longfengdong Scenic Spot; 41.186398°N, 117.988977°E; alt. 496 m; 19 Jul. 2024; Z. Yao, J. Li & M. Yan leg.; SYNU-Ar00419. ***Paratypes*****:** China • 1♂; same data as for the holotype; SYNU-Ar00420 • 2♀; same data as for the holotype; SYNU-Ar00421–22.

Etymology. The specific name refers to the type locality; noun in apposition.

Diagnosis. The new species resembles *Pholcus zhuolu* Zhang & Zhu, 2009 (Zhang and Zhu 2009: 108, figs 64A–I, 65A–L, Yao and Li 2012: 43, figs 225A–D, 226A–C) by having a similar uncus (Fig. 6C) and male chelicerae (Fig. 6D), but it can be distinguished by the: procursus with a bifurcated prolatero-subdistal apophysis (arrow 1 in Fig. 5C vs. not bifurcated), the large distal membranous lamella (arrow 2 in Fig. 5C vs. indistinct), epigynal plate anteriorly straight (Fig. 6A vs. strongly curved), vulval pore plates long, 4 × longer than wide (pp in Fig. 6B vs. 2 ×).

Description. Male (*holotype*): Total length 5.37 (5.67 with clypeus), carapace 1.52 long, 1.83 wide, opisthosoma 3.85 long, 1.80 wide. Leg I: 43.25 (10.96, 0.75, 11.03, 17.88, 2.63), leg II: 29.18 (8.01, 0.72, 7.31, 11.41, 1.73), leg III: 20.24 (5.83, 0.69, 4.81, 7.63, 1.28), leg IV: 26.48 (7.56, 0.71, 6.41, 10.26, 1.54); tibia I L/d: 74. Eye interdistances and diameters: PME–PME 0.24, PME 0.16, PME–ALE 0.04, AME–AME 0.05, AME 0.09. Sternum width/length: 1.25/1.03. Habitus as in Fig. 6E, F. Carapace yellowish, with brown radiating marks and marginal brown bands; ocular area yellowish, with median and lateral brown bands; clypeus and sternum yellowish, with brown marks. Legs yellowish, dark brown on patellae and whitish on distal parts of femora and tibiae, with darker rings on subdistal parts of femora and proximal and subdistal parts of tibiae. Opisthosoma yellowish, with dorsal and lateral brown spots. Chelicerae with pair of proximo-lateral apophyses (pa in Fig. 6D), pair of distal apophyses (da in Fig. 6D) with two teeth each, and pair of frontal apophyses (fa in Fig. 6D). Palps as in Fig. 5A, B; trochanter with long (4 × longer than wide), retrolaterally strongly bulged ventral apophysis; femur with retrolatero-proximal protrusion (arrow in Fig. 5B) and indistinct ventral protrusion; tibia with prolatero-ventral protrusion (arrow in Fig. 5A); procursus simple proximally but complex distally, with raised prolatero-subdistal edge bearing bifurcated apophysis (arrow 1 in Fig. 5C), distal membranous lamella (arrow 2 in Fig. 5C), distal apophysis (arrow 3 in Fig. 5C), and one slender and three strong dorsal spines (arrows 4–7 in Fig. 5C); uncus nearly elliptical, with scales (u in Fig. 6C); "pseudo-appendix" semi-transparent (not visible in Fig. 6C; cf. Fig. 8C); embolus weakly sclerotized, with transparent distal projections (e in Fig. 6C). Retrolateral trichobothrium on tibia I at 5% proximally; legs with short, vertical setae on tibiae, metatarsi, and tarsi; tarsus I with 36 distinct pseudosegments.

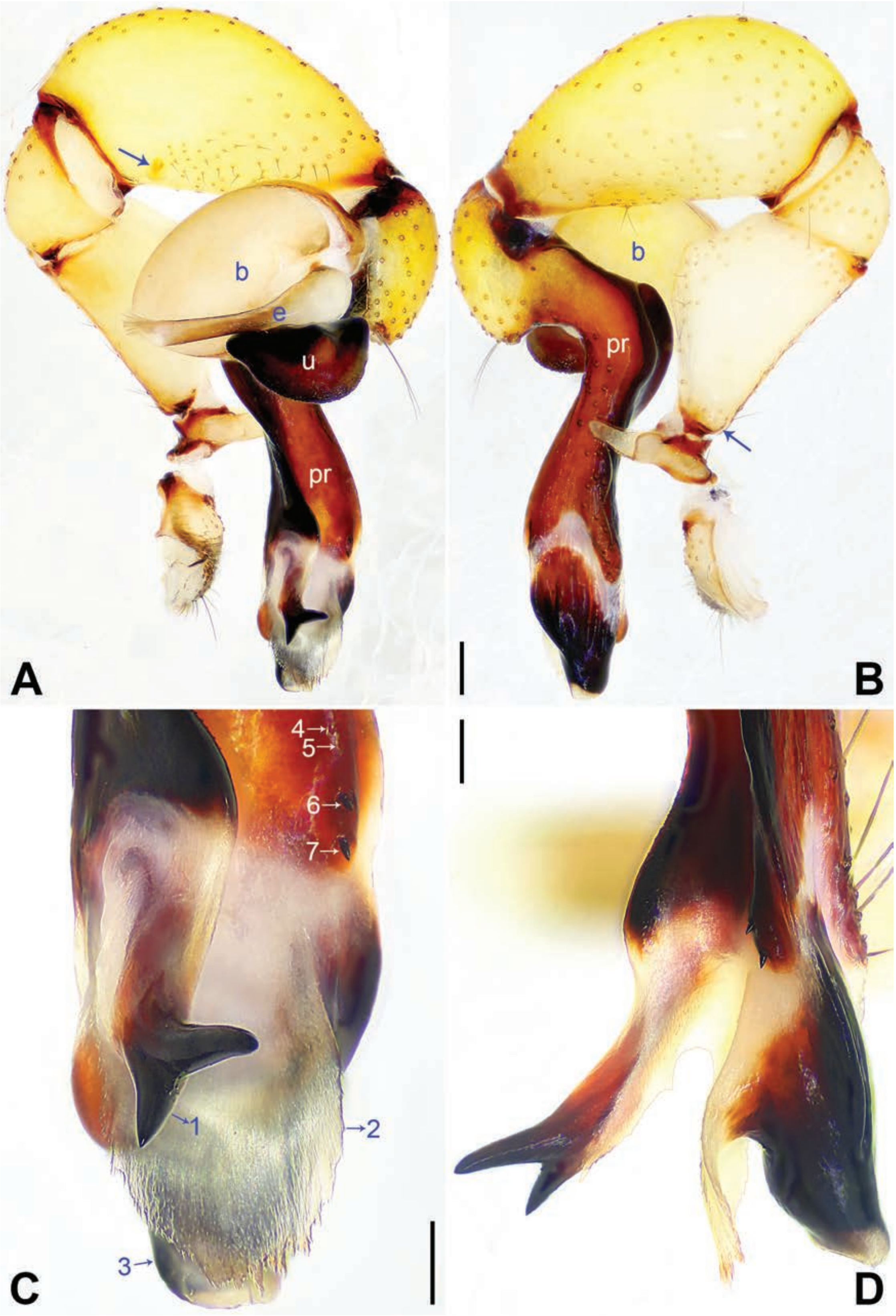

Figure 5. *Pholcus hebei* sp. nov., holotype male. **A, B** Palp (**A** prolateral view, arrow points at prolatero-ventral protrusion **B** retrolateral view, arrow points at retrolatero-proximal protrusion) **C, D** distal part of procursus (**C** prolateral view, arrow 1 points at bifurcated apophysis, arrow 2 points at distal membranous lamella, arrow 3 points at distal apophysis, arrows 4–7 point at dorsal spines **D** dorsal view). Abbreviations: b = bulb, e = embolus, pr = procursus, u = uncus. Scale bars: 0.20 mm (**A, B**); 0.10 mm (**C, D**).

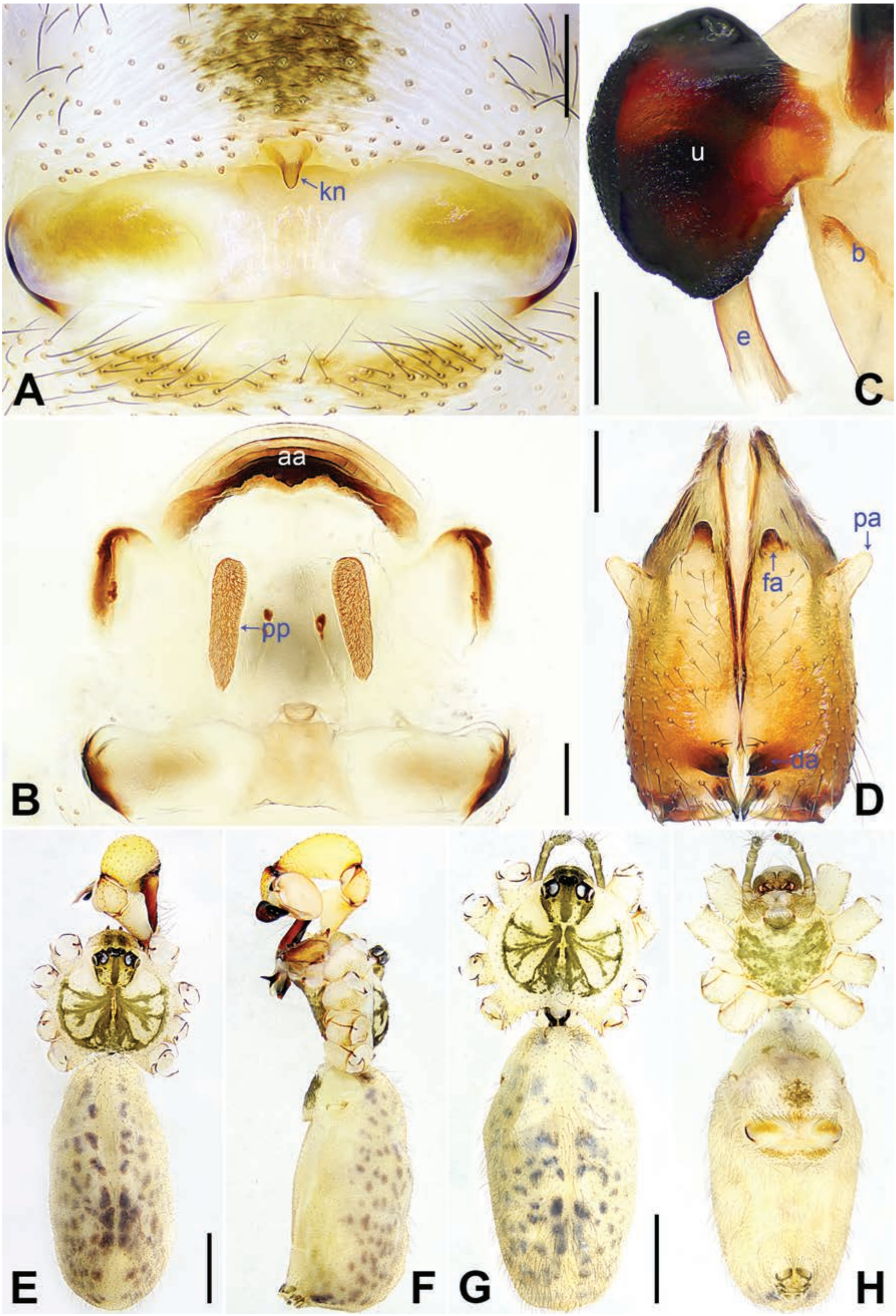

Figure 6. *Pholcus hebei* sp. nov., holotype (**D–F**) and paratype (**C**) males, paratype female (**A, B, G, H**). **A** Epigyne, ventral view **B** vulva, dorsal view **C** bulbal apophyses, prolateral view **D** chelicerae, frontal view **E–H** habitus (**E, G** dorsal view **F** lateral view **H** ventral view). Abbreviations: aa = anterior arch, b = bulb, da = distal apophysis, e = embolus, fa = frontal apophysis, kn = knob, pa = proximo-lateral apophysis, pp = pore plate, u = uncus. Scale bars: 0.20 mm (**A–D**); 1.00 mm (**E–H**).

Female (***paratype***, SYNU-Ar00421): Similar to male, habitus as in Fig. 6G, H. Total length 4.83 (5.01 with clypeus), carapace 1.48 long, 1.70 wide, opisthosoma 3.35 long, 1.84 wide; tibia I: 8.01; tibia I L/d: 53. Eye interdistances and diameters: PME–PME 0.20, PME 0.13, PME–ALE 0.05, AME–AME 0.04, AME 0.08. Sternum width/length: 1.16/0.91. Clypeus brown. Epigyne posteriorly straight, with lateral and median brown marks and knob (kn in Fig. 6A). Vulva with curved, sclerotized anterior arch (aa in Fig. 6B) and pair of long, elliptical pore plates (4 × longer than wide, pp in Fig. 6B).

Variation. Tibia I in paratype male (SYNU-Ar00420): 11.54. Tibia I in another paratype female (SYNU-Ar00422): 7.56.

Habitat. Underside of overhang on rocky cliffs in mountainous area.

Distribution. Hebei; known only from the type locality (Figs 1, 2B).

Pholcus huludao **S. Li & Yao, sp. nov.**

https://zoobank.org/A1DDEF77-6E27-4935-B248-22B7819E8711
Figs 7, 8

Type material. ***Holotype***: CHINA • ♂; Liaoning, Huludao, Jianchang County, Laodazhangzi Town, Longtan Grand Canyon Scenic Spot; 40.554405°N, 119.349993°E; alt. 504 m; 21 Jul. 2024; Z. Yao, J. Li & M. Yan leg.; SYNU-Ar00423. ***Paratypes***: CHINA • 1♂; same data as for the holotype; SYNU-Ar00424 • 2♀; same data as for the holotype; SYNU-Ar00425–26.

Etymology. The specific name refers to the type locality; noun in apposition.

Diagnosis. The new species resembles known congeners from the Lüliang Mountains (e.g., *Pholcus wenshui* Zhao, Li & Yao, 2023, *P. jiaocheng* Zhao, Li & Yao, 2023, *P. luliang* Zhao, Li & Yao, 2023, *P. zhongyang* Zhao, Li & Yao, 2023; Zhao et al. 2023b: 7, figs 2B, 4C, D, 10C, D, 12C, D, 18C, D) by having similar male chelicerae (Fig. 8D) and a curved uncus (Fig. 8C), but it can be distinguished by the following combination of characters: ventro-distal membranous lamella of procursus distally blunt and strongly curved (arrow 2 in Fig. 7C vs. distally pointed and straight), dorso-distal membranous lamella of procursus strongly curved (arrow 3 in Fig. 7C vs. straight), uncus proximally wide and distally narrow, and dorso-medially strongly protruding (arrow 1 in Fig. 8C vs. wide and pointed, not protruding), epigyne posteriorly slightly curved (Fig. 8A vs. strongly curved), vulval pore plates nearly semi-circular (pp in Fig. 8B vs. elliptical).

Description. Male (***holotype***): Total length 4.68 (4.80 with clypeus), carapace 1.44 long, 1.72 wide, opisthosoma 3.24 long, 1.27 wide. Leg I: 39.99 (9.94, 0.75, 10.13, 16.67, 2.50), leg II: 27.14 (7.45, 0.67, 6.73, 10.64, 1.65), leg III: 18.98 (5.58, 0.64, 4.62, 7.05, 1.09), leg IV: 25.51 (7.40, 0.66, 6.35, 9.62, 1.48); tibia I L/d: 68. Eye interdistances and diameters: PME–PME 0.23, PME 0.15, PME–ALE 0.04, AME–AME 0.05, AME 0.10. Sternum width/length: 1.17/0.98. Habitus as in Fig. 8E, F. Carapace yellowish, with brown radiating marks and marginal brown bands; ocular area yellowish, with median and lateral brown bands; clypeus brown; sternum yellowish, with brown marks. Legs yellowish, dark brown on patellae and whitish on distal parts of femora and tibiae, with darker rings on subdistal parts of femora and proximal and subdistal parts of tibiae. Opisthosoma yellowish, with dorsal and lateral brown spots. Chelicerae with pair of proximo-lateral apophyses (pa in Fig. 8D), pair of distal apophyses

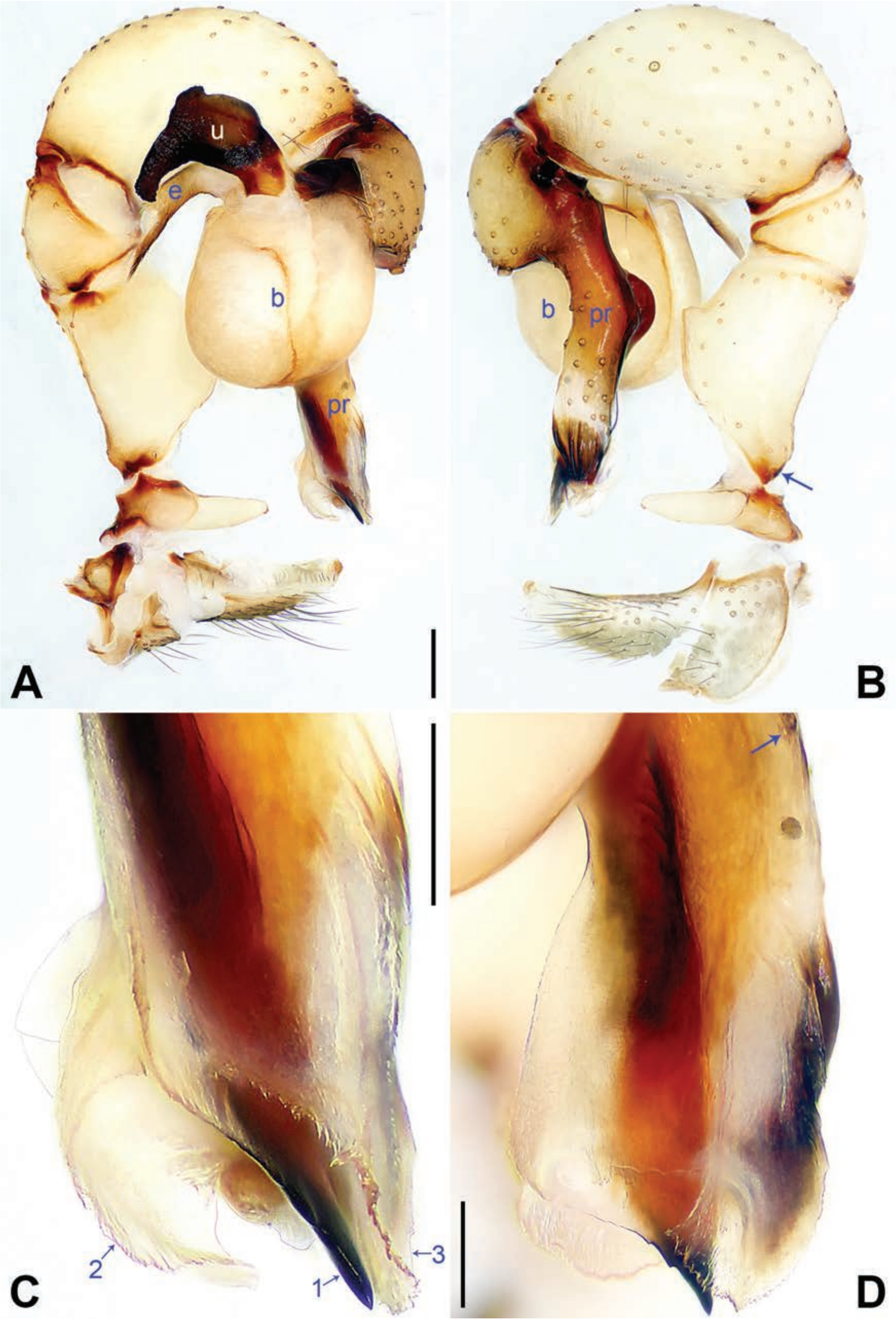

Figure 7. *Pholcus huludao* sp. nov., holotype male. **A, B** Palp (**A** prolateral view **B** retrolateral view, arrow points at retrolatero-proximal protrusion) **C, D** distal part of procursus (**C** prolateral view, arrow 1 points at pointed sclerotized apophysis, arrow 2 points at ventro-distal membranous lamella, arrow 3 points at dorso-distal membranous lamella **D** dorsal view, arrow points at dorsal spine). Abbreviations: b = bulb, e = embolus, pr = procursus, u = uncus. Scale bars: 0.20 mm (**A, B**); 0.10 mm (**C, D**).

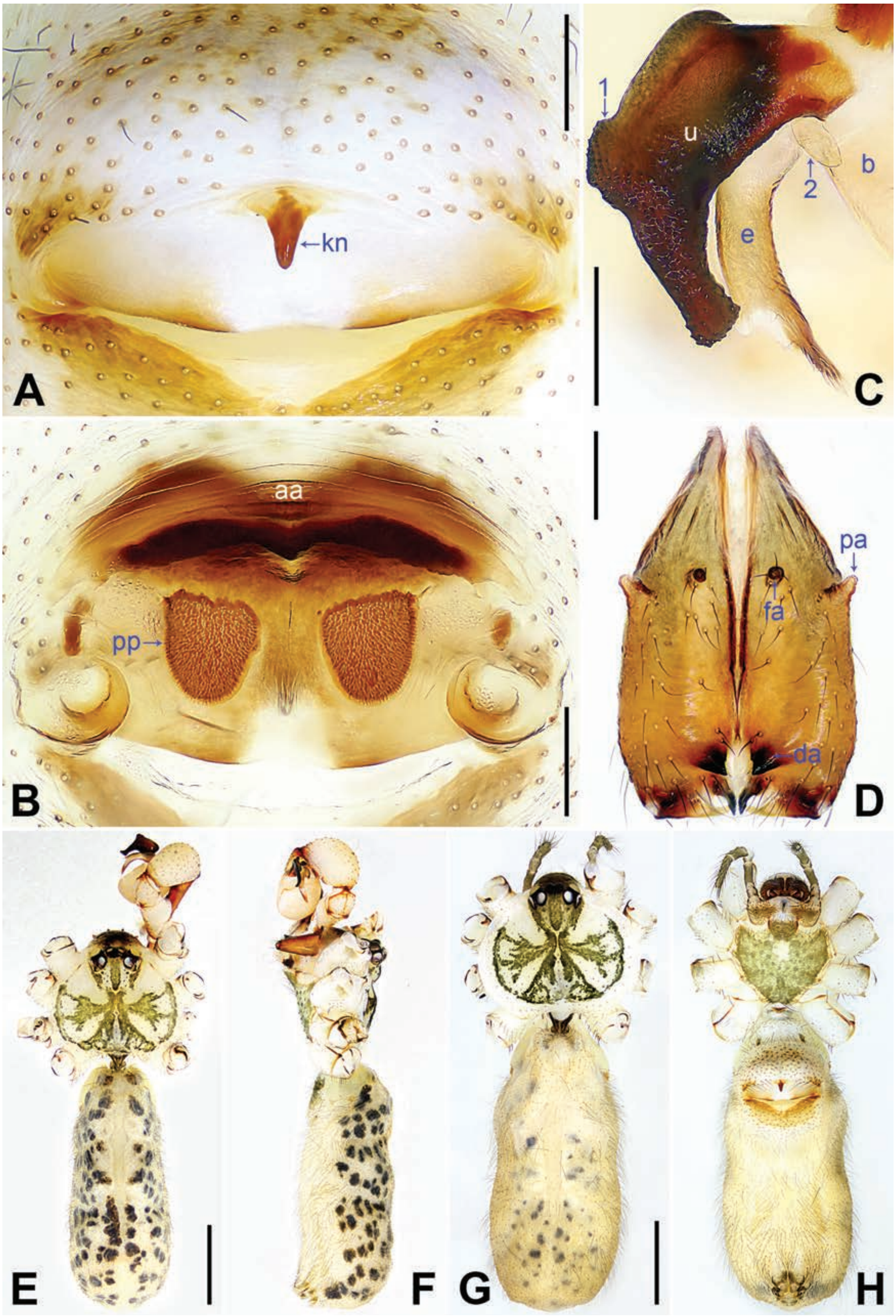

Figure 8. *Pholcus huludao* sp. nov., holotype male (**C–F**) and paratype female (**A, B, G, H**). **A** Epigyne, ventral view **B** vulva, dorsal view **C** bulbal apophyses, prolateral view, arrow 1 points at dorso-median protrusion, arrow 2 points at "pseudo-appendix" **D** chelicerae, frontal view **E–H** habitus (**E, G** dorsal view **F** lateral view **H** ventral view). Abbreviations: aa = anterior arch, b = bulb, da = distal apophysis, e = embolus, fa = frontal apophysis, kn = knob, pa = proximo-lateral apophysis, pp = pore plate, u = uncus. Scale bars: 0.20 mm (**A–D**); 1.00 mm (**E–H**).

(da in Fig. 8D) with two teeth each, and pair of frontal apophyses (fa in Fig. 8D). Palps as in Fig. 7A, B; trochanter with long (4 × longer than wide), retrolaterally bulged ventral apophysis; femur with retrolatero-proximal protrusion (arrow in Fig. 7B) and distinct ventral protrusion; tibia with prolatero-ventral protrusion; procursus simple proximally but complex distally, with raised, prolatero-subdistal membranous edge bearing pointed, sclerotized apophysis (arrow 1 in Fig. 7C), curved, ventro-distal membranous lamella (arrow 2 in Fig. 7C), curved, dorso-distal membranous lamella (arrow 3 in Fig. 7C), and one slender dorsal spine (arrow in Fig. 7D); uncus curved, proximally wide and distally narrow, with scales (u in Fig. 8C); “pseudo-appendix” semi-transparent (arrow 2 in Fig. 8C); embolus weakly sclerotized, with transparent distal projections (e in Fig. 8C). Retrolateral trichobothrium on tibia I at 2% proximally; legs with short, vertical setae on tibiae, metatarsi, and tarsi; tarsus I with 30 distinct pseudosegments.

Female (***paratype***, SYNU-Ar00425): Similar to male, habitus as in Fig. 8G, H. Total length 5.13 (5.26 with clypeus), carapace 1.53 long, 1.95 wide, opisthosoma 3.60 long, 1.60 wide; tibia I: 8.78; tibia I L/d: 59. Eye interdistances and diameters: PME–PME 0.21, PME 0.14, PME–ALE 0.05, AME–AME 0.05, AME 0.10. Sternum width/length: 1.11/0.97. Epigyne posteriorly slightly curved, with lateral brown marks and knob (kn in Fig. 8A). Vulva with curved, sclerotized anterior arch (aa in Fig. 8B) and pair of nearly semi-circular pore plates (pp in Fig. 8B).

Variation. Tibia I in paratype male (SYNU-Ar00424): 9.80. Tibia I in another paratype female (SYNU-Ar00426): 9.25.

Habitat. Underside of overhang on rocky cliffs in mountainous area.

Distribution. Liaoning; known only from the type locality (Figs 1, 2C).

Pholcus jinzhou **S. Li & Yao, sp. nov.**

https://zoobank.org/8C1DC153-00D3-4BDF-8301-F675291E3479
Figs 9, 10

Type material. ***Holotype*****:** China • ♂; Liaoning, Jinzhou, Guta District, Beiputuoshan Scenic Spot; 41.173150°N, 121.042606°E; alt. 163 m; 15 Jul. 2024; Z. Yao, J. Li & M. Yan leg.; SYNU-Ar00427. ***Paratypes*****:** China • 2♂; same data as for the holotype; SYNU-Ar00428–29 • 3♀; same data as for the holotype; SYNU-Ar00430–32.

Etymology. The specific name refers to the type locality; noun in apposition.

Diagnosis. The new species can be easily distinguished from all known congeners in the *Pholcus phungiformes* species group by the following combination of characters: procursus with curved prolatero-subdistal apophysis (arrow 1 in Fig. 9C vs. absent) and comb-like, sclerotized prolatero-distal apophysis (arrow 3 in Fig. 9C vs. absent), proximal apophysis of uncus on retrolateral part of uncus (arrow 1 in Fig. 10C vs. same plane or absent), epigyne with pair of lateral protrusions anterior to epigynal plate (arrow in Fig. 10A vs. absent).

Description. Male (***holotype***): Total length 5.78 (6.01 with clypeus), carapace 1.73 long, 1.95 wide, opisthosoma 4.05 long, 1.93 wide. Leg I: 43.34 (11.09, 0.78, 11.54, 17.56, 2.37), leg II: 30.61 (8.27, 0.83, 7.82, 12.05, 1.64), leg III: 21.87 (6.35, 0.73, 5.32, 8.21, 1.26), leg IV: 28.41 (8.08, 0.73, 7.24, 10.77, 1.59); tibia I L/d: 68. Eye interdistances and diameters: PME–PME 0.28, PME 0.16, PME–ALE 0.03, AME–AME 0.05, AME 0.11. Sternum width/length: 1.30/0.94. Habitus as in Fig. 10E, F.

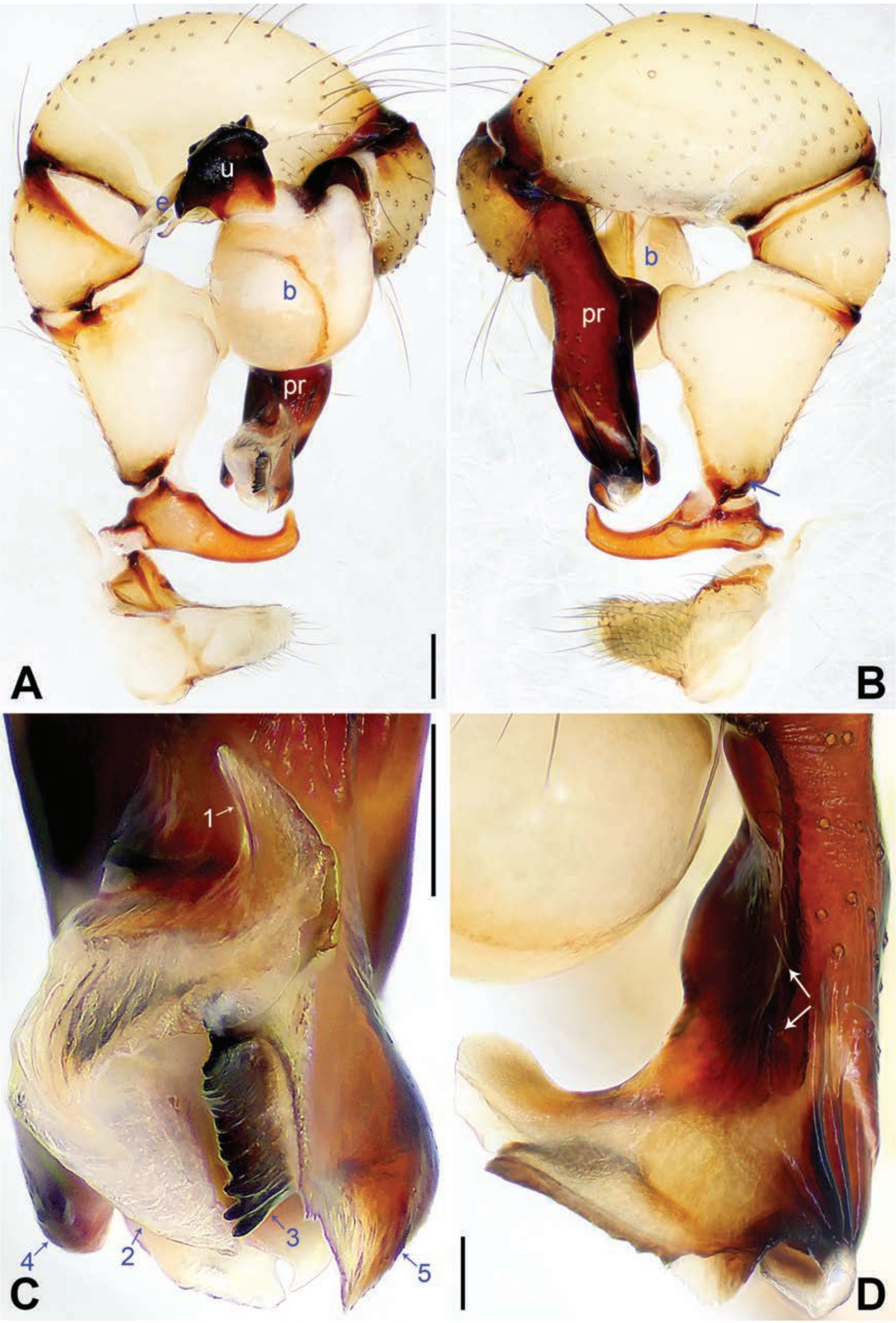

Figure 9. *Pholcus jinzhou* sp. nov., holotype male. **A, B** Palp (**A** prolateral view **B** retrolateral view, arrow points at retrolatero-proximal protrusion) **C, D** distal part of procursus (**C** prolateral view, arrow 1 points at curved apophysis, arrow 2 points at membranous process, arrow 3 points at comb-like sclerotized apophysis, arrow 4 points at ventro-distal apophysis, arrow 5 points at dorso-distal apophysis **D** dorsal view, arrows point at dorsal spines). Abbreviations: b = bulb, e = embolus, pr = procursus, u = uncus. Scale bars: 0.20 mm (**A, B**); 0.10 mm (**C, D**).

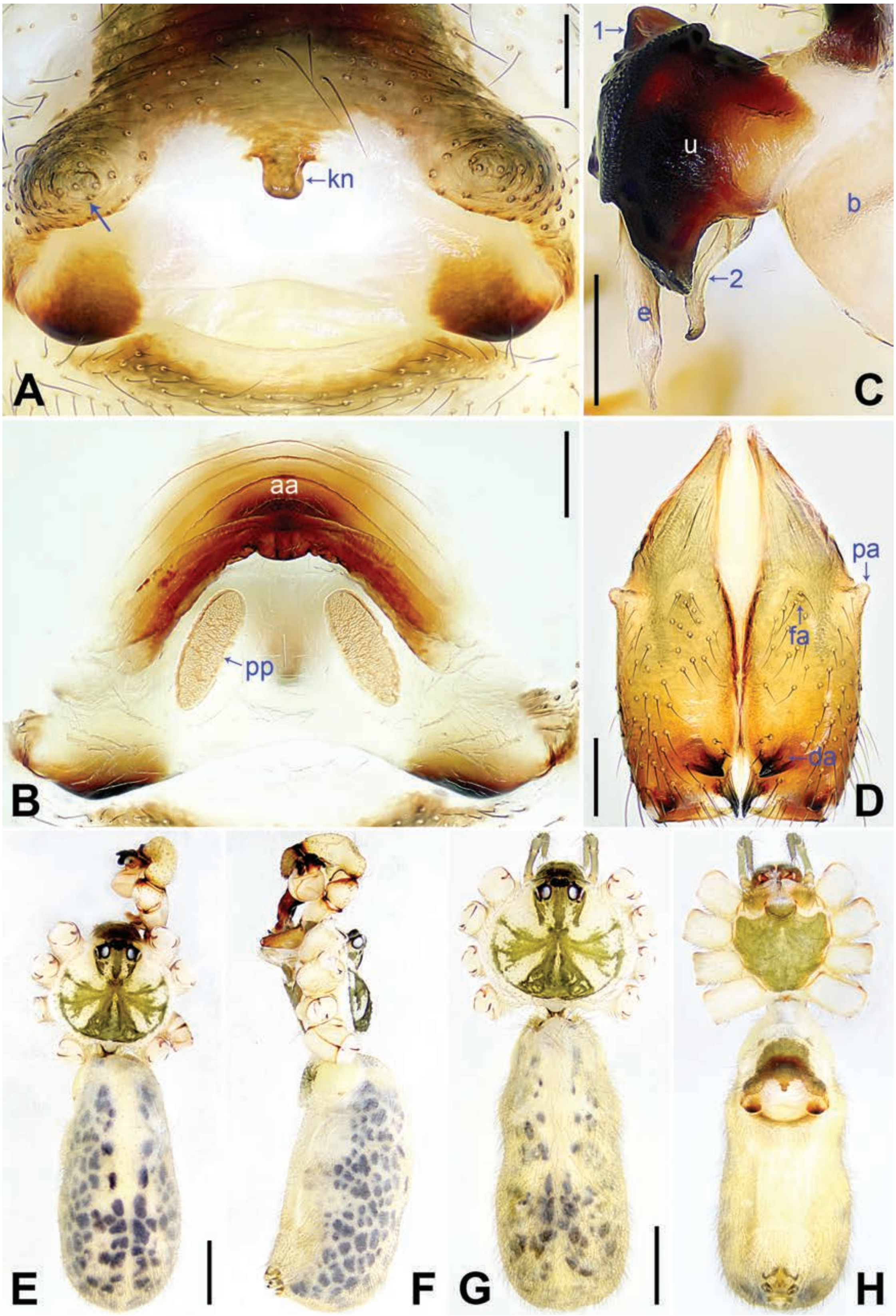

Figure 10. *Pholcus jinzhou* sp. nov., holotype male (**C–F**) and paratype female (**A, B, G, H**). **A** Epigyne, ventral view, arrow points at lateral protrusion **B** vulva, dorsal view **C** bulbal apophyses, prolateral view, arrow 1 points at retrolatero-proximal apophysis, arrow 2 points at "pseudo-appendix" **D** chelicerae, frontal view **E–H** habitus (**E, G** dorsal view **F** lateral view **H** ventral view). Abbreviations: aa = anterior arch, b = bulb, da = distal apophysis, e = embolus, fa = frontal apophysis, kn = knob, pa = proximo-lateral apophysis, pp = pore plate, u = uncus. Scale bars: 0.20 mm (**A–D**); 1.00 mm (**E–H**).

Carapace brown, with brown radiating marks and marginal brown bands; ocular area yellowish, with median and lateral brown bands; clypeus and sternum brown. Legs yellowish, dark brown on patellae and whitish on distal parts of femora and tibiae, with darker rings on subdistal parts of femora and proximal and subdistal parts of tibiae. Opisthosoma yellowish, with dorsal and lateral brown spots. Chelicerae with pair of proximo-lateral apophyses (pa in Fig. 10D), pair of distal apophyses (da in Fig. 10D) with two teeth each, and pair of frontal apophyses (fa in Fig. 10D). Palps as in Fig. 9A, B; trochanter with long (6 × longer than wide), retrolaterally strongly bulged ventral apophysis; femur with retrolatero-proximal protrusion (arrow in Fig. 9B) and distinct ventral protrusion; tibia with prolatero-ventral protrusion; procursus simple proximally but complex distally, with raised prolatero-subdistal edge bearing curved apophysis (arrow 1 in Fig. 9C), membranous process (arrow 2 in Fig. 9C) and comb-like sclerotized apophysis (arrow 3 in Fig. 9C), ventro-distal apophysis (arrow 4 in Fig. 9C), dorso-distal apophysis (arrow 5 in Fig. 9C), and two slender dorsal spines (arrows in Fig. 9D); uncus with distinct retrolatero-proximal apophysis (arrow 1 in Fig. 10C) and scaly edge; “pseudo-appendix” curved, distally sclerotized (arrow 2 in Fig. 10C); embolus weakly sclerotized, with transparent distal projections (e in Fig. 10C). Retrolateral trichobothrium on tibia I at 3% proximally; legs with short, vertical setae on tibiae, metatarsi, and tarsi; tarsus I with 35 distinct pseudosegments.

Female (***paratype***, SYNU-Ar00430): Similar to male, habitus as in Fig. 10G, H. Total length 5.56 (5.80 with clypeus), carapace 1.66 long, 2.05 wide, opisthosoma 3.90 long, 1.70 wide; tibia I: 9.94; tibia I L/d: 55. Eye interdistances and diameters: PME–PME 0.25, PME 0.15, PME–ALE 0.05, AME–AME 0.05, AME 0.09. Sternum width/length: 1.24/1.12. Epigyne posteriorly curved, with lateral brown marks, knob (kn in Fig. 10A), and pair of lateral protrusions anterior to epigynal plate (arrow in Fig. 10A). Vulva with curved, sclerotized anterior arch (aa in Fig. 10B) and pair of long, elliptical pore plates (3 × longer than wide, pp in Fig. 10B).

Variation. Tibia I in two paratype males (SYNU-Ar00428–29): 11.15, 11.54. Tibia I in the other two paratype females (SYNU-Ar00431–32): 9.36, 9.42.

Habitat. Underside of overhang on rocky cliffs in mountainous area.

Distribution. Liaoning; known only from the type locality (Figs 1, 2D).

Pholcus liaoning **S. Li & Yao, sp. nov.**

https://zoobank.org/D0822275-FCA9-404D-81C2-D7C108277EB6
Figs 11, 12

Type material. ***Holotype*:** China • ♂; Liaoning, Chaoyang, Beipiao, Daheishan Scenic Spot; 42.006997°N, 120.484051°E; alt. 609 m; 16 Jul. 2024; Z. Yao, J. Li & M. Yan leg.; SYNU-Ar00433. ***Paratypes*:** China • 1♂; same data as for the holotype; SYNU-Ar00434 • 2♀; same data as for the holotype; SYNU-Ar00435–36.

Etymology. The specific name refers to the type locality; noun in apposition.

Diagnosis. The new species resembles *Pholcus wangjiang* Yao & Li, 2021 (Yao et al. 2021: S22, figs 2B.20, S21A–D, S22A–H) by having a similar uncus (Fig. 12C) and male chelicerae (Fig. 12D), but it can be distinguished by the: procursus with a ventro-distal apophysis (arrow 2 in Fig. 11C vs. absent) and nearly semi-circular, dorso-distal membranous lamella (arrow 1 in Fig. 11D vs.

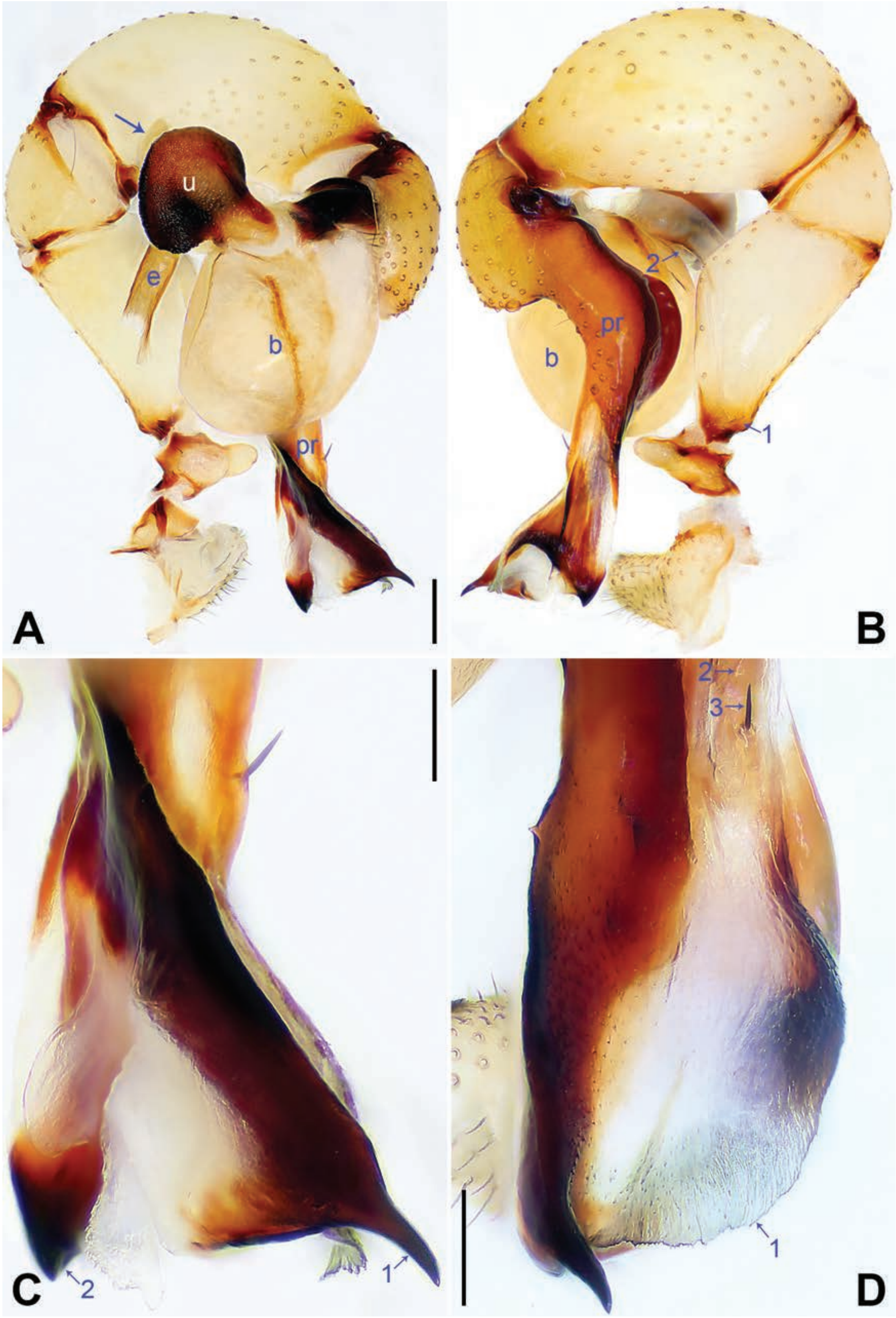

Figure 11. *Pholcus liaoning* sp. nov., holotype male. **A, B** Palp (**A** prolateral view, arrow points at prolatero-ventral protrusion **B** retrolateral view, arrow 1 points at retrolatero-proximal protrusion, arrow 2 points at "pseudo-appendix") **C, D** distal part of procursus (**C** prolateral view, arrow 1 points at pointed apophysis, arrow 2 points at ventro-distal apophysis **D** dorsal view, arrow 1 points at dorso-distal membranous lamella, arrows 2, 3 point at dorsal spines). Abbreviations: b = bulb, e = embolus, pr = procursus, u = uncus. Scale bars: 0.20 mm (**A, B**); 0.10 mm (**C, D**).

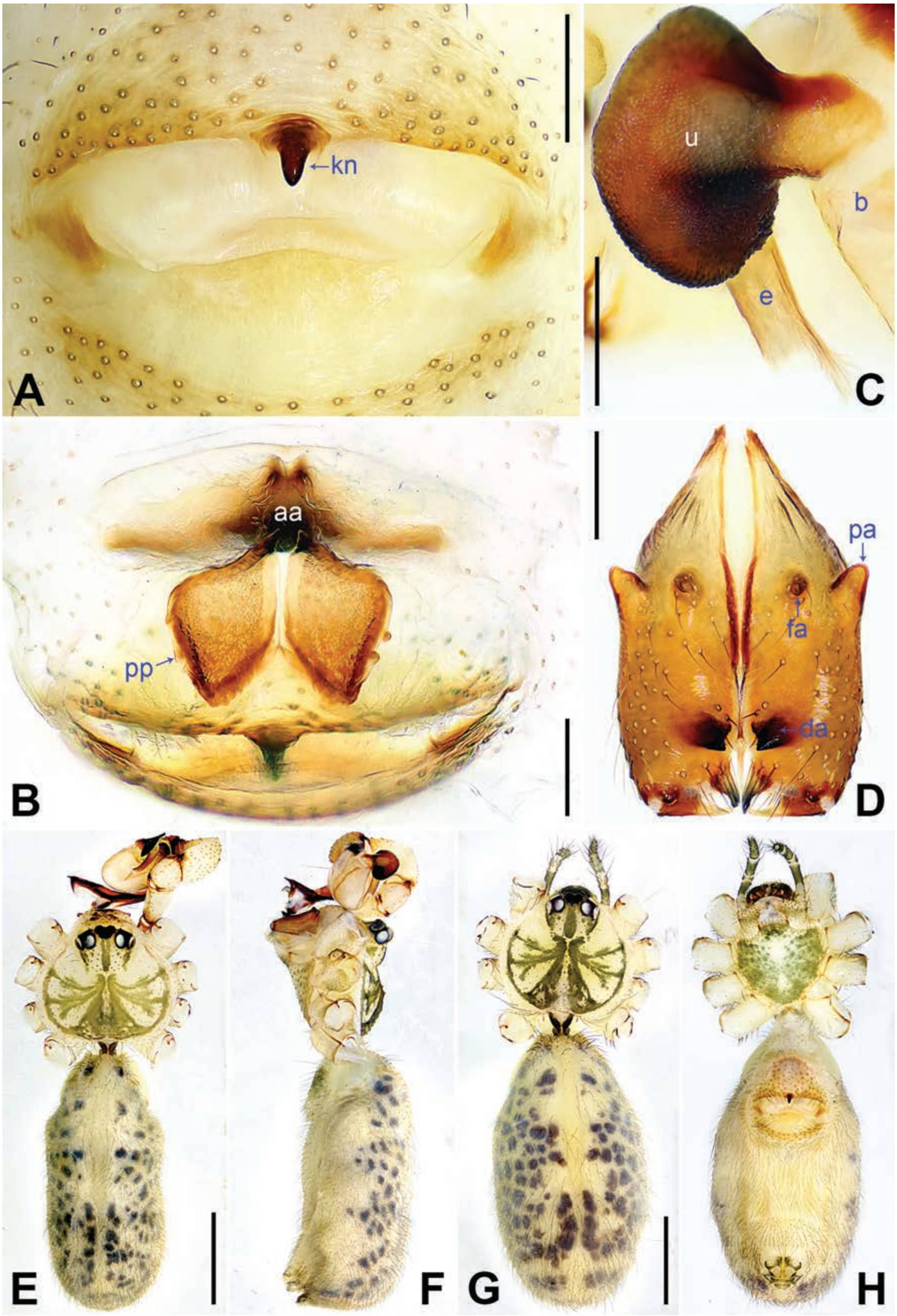

Figure 12. *Pholcus liaoning* sp. nov., holotype male (**C–F**) and paratype female (**A, B, G, H**). **A** Epigyne, ventral view **B** vulva, dorsal view **C** bulbal apophyses, prolateral view **D** chelicerae, frontal view **E–H** habitus (**E, G** dorsal view **F** lateral view **H** ventral view). Abbreviations: aa = anterior arch, b = bulb, da = distal apophysis, e = embolus, fa = frontal apophysis, kn = knob, pa = proximo-lateral apophysis, pp = pore plate, u = uncus. Scale bars: 0.20 mm (**A–D**); 1.00 mm (**E–H**).

absent), epigynal plate without brown marks (Fig. 12A vs. with distinct lateral brown marks), vulval pore plates quadrilateral (pp in Fig. 12B vs. elliptical).

Description. Male (*holotype*): Total length 4.37 (4.49 with clypeus), carapace 1.34 long, 1.50 wide, opisthosoma 3.03 long, 1.41 wide. Leg **I**: 37.15 (9.36, 0.70, 9.49, 15.32, 2.28), leg **II**: 25.89 (7.12, 0.67, 6.47, 10.13, 1.50), leg **III**: 18.46 (5.38, 0.63, 4.49, 6.79, 1.17), leg **IV**: 24.22 (6.99, 0.63, 6.20, 9.04, 1.36); tibia **I** L/d: 67. Eye interdistances and diameters: PME–PME 0.21, PME 0.14, PME–ALE 0.04, AME–AME 0.06, AME 0.08. Sternum width/length: 1.04/0.86. Habitus as in Fig. 12E, F. Carapace yellowish, with brown radiating marks and marginal brown bands; ocular area yellowish, with median and lateral brown bands; clypeus and sternum yellowish, with brown marks. Legs yellowish, dark brown on patellae and whitish on distal parts of femora and tibiae, with darker rings on subdistal parts of femora and proximal and subdistal parts of tibiae. Opisthosoma yellowish, with dorsal and lateral brown spots. Chelicerae with pair of proximo-lateral apophyses (pa in Fig. 12D), pair of distal apophyses (da in Fig. 12D) with two teeth each, and pair of frontal apophyses (fa in Fig. 12D). Palps as in Fig. 11A, B; trochanter with retrolaterally strongly bulged ventral apophysis; femur with retrolatero-proximal protrusion (arrow 1 in Fig. 11B) and indistinct ventral protrusion; tibia with prolatero-ventral protrusion (arrow in Fig. 11A); procursus simple proximally but complex distally, with raised prolatero-subdistal edge bearing pointed apophysis (arrow 1 in Fig. 11C), ventro-distal apophysis (arrow 2 in Fig. 11C), dorso-distal membranous lamella (arrow 1 in Fig. 11D), and two strong dorsal spines (arrows 2, 3 in Fig. 11D); uncus nearly elliptical, with scales (u in Fig. 12C); “pseudo-appendix” semi-transparent (arrow 2 in Fig. 11B); embolus weakly sclerotized, with transparent distal projections (e in Fig. 12C). Retrolateral trichobothrium on tibia **I** at 5% proximally; legs with short, vertical setae on tibiae, metatarsi, and tarsi; tarsus **I** with 30 distinct pseudosegments.

Female (*paratype*, SYNU-Ar00435): Similar to male, habitus as in Fig. 12G, H. Total length 4.68 (4.81 with clypeus), carapace 1.40 long, 1.52 wide, opisthosoma 3.28 long, 1.86 wide; tibia **I**: 8.01; tibia **I** L/d: 57. Eye interdistances and diameters: PME–PME 0.19, PME 0.13, PME–ALE 0.04, AME–AME 0.04, AME 0.08. Sternum width/length: 0.99/0.90. Clypeus brown. Epigyne posteriorly slightly curved, with knob (kn in Fig. 12A). Vulva with ridge-shaped anterior arch (aa in Fig. 12B) and pair of quadrilateral pore plates (pp in Fig. 12B).

Variation. Tibia **I** in paratype male (SYNU-Ar00434): 8.84. Tibia **I** in another paratype female (SYNU-Ar00436): 8.33.

Habitat. Underside of overhang on rocky cliffs in mountainous area.

Distribution. Liaoning; known only from the type locality (Figs 1, 2E).

Pholcus qin S. Li & Yao, sp. nov.

https://zoobank.org/49F606E5-B2C4-4265-8757-3377DA59AB49
Figs 13, 14

Type material. *Holotype*: China • ♂; Hebei, Qinhuangdao, Funing District, Daxinzhai Town, Bingtangyu Scenic Spot; 40.106112°N, 119.356216°E; alt. 250 m; 20 Jul. 2024; Z. Yao, J. Li & M. Yan leg.; SYNU-Ar00437. ***Paratypes***: China • 2♂; same data as for the holotype; SYNU-Ar00438–39 • 3♀; same data as for the holotype; SYNU-Ar00440–42.

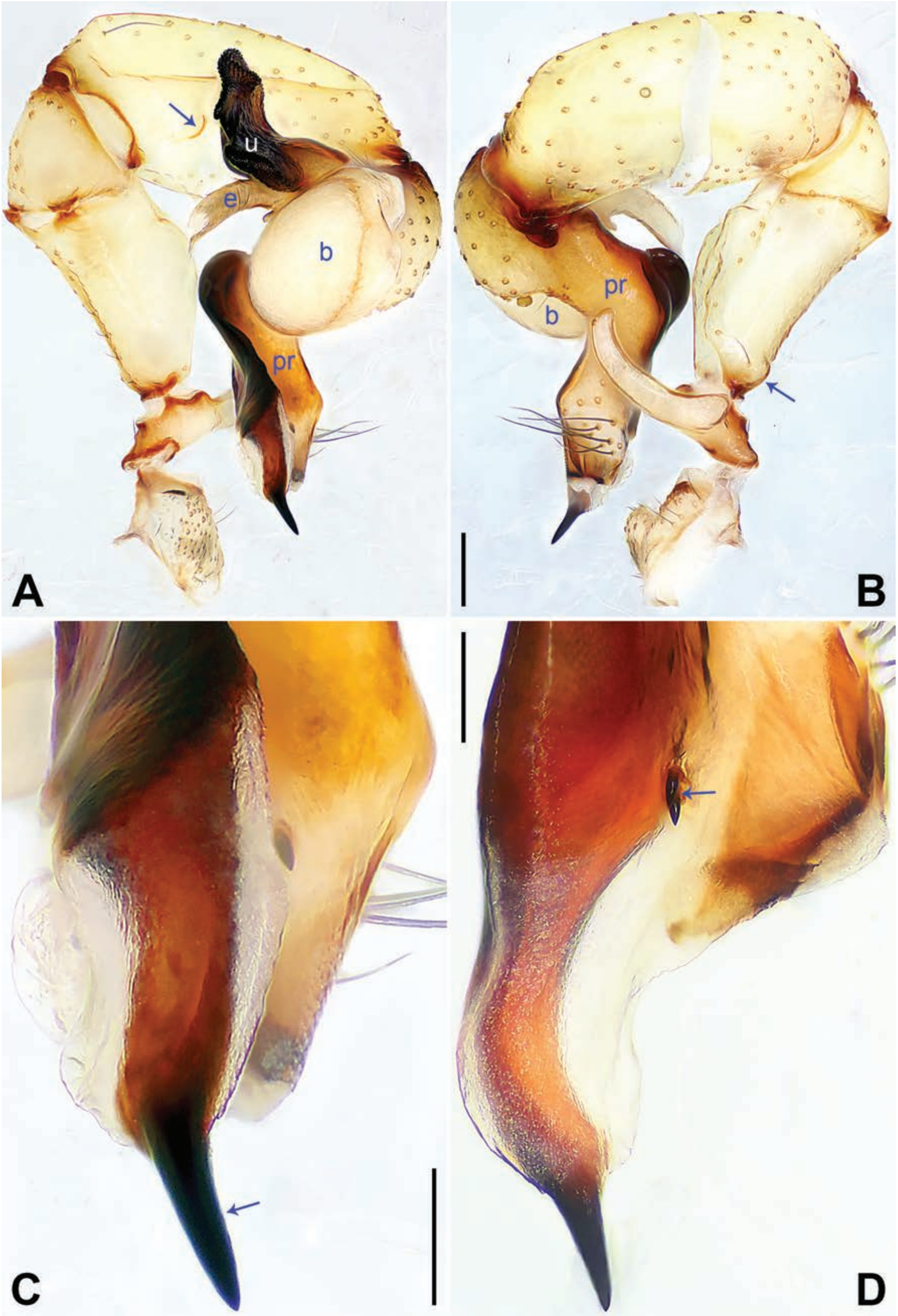

Figure 13. *Pholcus qin* sp. nov., holotype male. **A, B** Palp (**A** prolateral view, arrow points at prolatero-ventral protrusion **B** retrolateral view, arrow points at retrolatero-proximal protrusion) **C, D** distal part of procursus (**C** prolateral view, arrow points at spine-shaped apophysis **D** dorsal view, arrow points at dorsal spines). Abbreviations: b = bulb, e = embolus, pr = procursus, u = uncus. Scale bars: 0.20 mm (**A, B**); 0.10 mm (**C, D**).

Etymology. The specific name refers to the type locality (Qin is a short name for Qinhuangdao); noun in apposition.

Diagnosis. The new species resembles *Pholcus kuaile* Yao, Li & Lu, 2022 (Lu et al. 2022: 534, S21, figs S22A–D, S23A–H) by having similar male chelicerae (Fig. 14D) and a vulval anterior arch (Fig. 14B), but it can be distinguished by the: procursus without an angular ventral sclerite (Fig. 13B vs. present) and without a distal membranous process (Fig. 13C vs. present), uncus with two distal apophyses (arrows 2, 3 in Fig. 14C vs. one), epigynal plate 3 × longer than wide (Fig. 14A vs. 8 ×), vulval pore plates widely separated and same size as knob (pp in Fig. 14B vs. close to each other and 8 × larger than knob).

Description. Male (***holotype***): Total length 4.64 (4.80 with clypeus), carapace 1.28 long, 1.60 wide, opisthosoma 3.36 long, 1.42 wide. Leg I: 40.72 (10.06, 0.75, 10.00, 17.25, 2.66), leg II: 26.95 (7.31, 0.63, 6.47, 10.96, 1.58), leg III: 18.78 (5.32, 0.58, 4.50, 7.25, 1.13), leg IV: 24.34 (6.60, 0.59, 6.09, 9.68, 1.38); tibia I L/d: 77. Eye interdistances and diameters: PME–PME 0.20, PME 0.13, PME–ALE 0.04, AME–AME 0.05, AME 0.08. Sternum width/length: 1.05/0.93. Habitus as in Fig. 14E, F. Carapace yellowish, with brown radiating marks and marginal brown bands; ocular area yellowish, with median and lateral brown bands; clypeus brownish; sternum yellowish, with brown marks. Legs yellowish, dark brown on patellae and whitish on distal parts of femora and tibiae, with darker rings on subdistal parts of femora and proximal and subdistal parts of tibiae. Opisthosoma yellowish, with dorsal and lateral brown spots. Chelicerae with pair of proximo-lateral apophyses (pa in Fig. 14D), pair of distal apophyses (da in Fig. 14D) with two teeth each, and pair of frontal apophyses (fa in Fig. 14D). Palps as in Fig. 13A, B; trochanter with long (8 × longer than wide), retrolaterally strongly bulged ventral apophysis; femur with retrolatero-proximal protrusion (arrow in Fig. 13B) and distinct ventral protrusion; tibia with prolatero-ventral protrusion (arrow in Fig. 13A); procursus simple proximally but complex distally, with raised prolatero-subdistal edge bearing spine-shaped apophysis (arrow in Fig. 13C), and two strong dorsal spines (arrow in Fig. 13D); uncus with scales, proximal apophysis (arrow 1 in Fig. 14C), and two distal apophyses (arrows 2, 3 in Fig. 14C); “pseudo-appendix” semi-transparent (arrow 4 in Fig. 14C); embolus weakly sclerotized, with transparent distal projections (e in Fig. 14C). Retrolateral trichobothrium on tibia I at 3% proximally; legs with short, vertical setae on tibiae, metatarsi, and tarsi; tarsus I with 40 distinct pseudosegments.

Female (***paratype***, SYNU-Ar00440): Similar to male, habitus as in Fig. 14G, H. Total length 4.71 (4.85 with clypeus), carapace 1.39 long, 1.56 wide, opisthosoma 3.32 long, 1.76 wide; tibia I: 8.15; tibia I L/d: 54. Eye interdistances and diameters: PME–PME 0.18, PME 0.14, PME–ALE 0.04, AME–AME 0.05, AME 0.08. Sternum width/length: 0.96/0.90. Clypeus brown. Epigyne posteriorly straight, with knob (kn in Fig. 14A). Vulva with nearly U-shaped, sclerotized anterior arch (aa in Fig. 14B) and pair of nearly elliptical pore plates (pp in Fig. 14B).

Variation. Tibia I in two paratype males (SYNU-Ar00438–39): 10.26, 10.64. Tibia I in the other two paratype females (SYNU-Ar00441–42): 8.08, 8.33.

Habitat. Underside of overhang on rocky cliffs in mountainous area.

Distribution. Hebei; known only from the type locality (Figs 1, 2F).

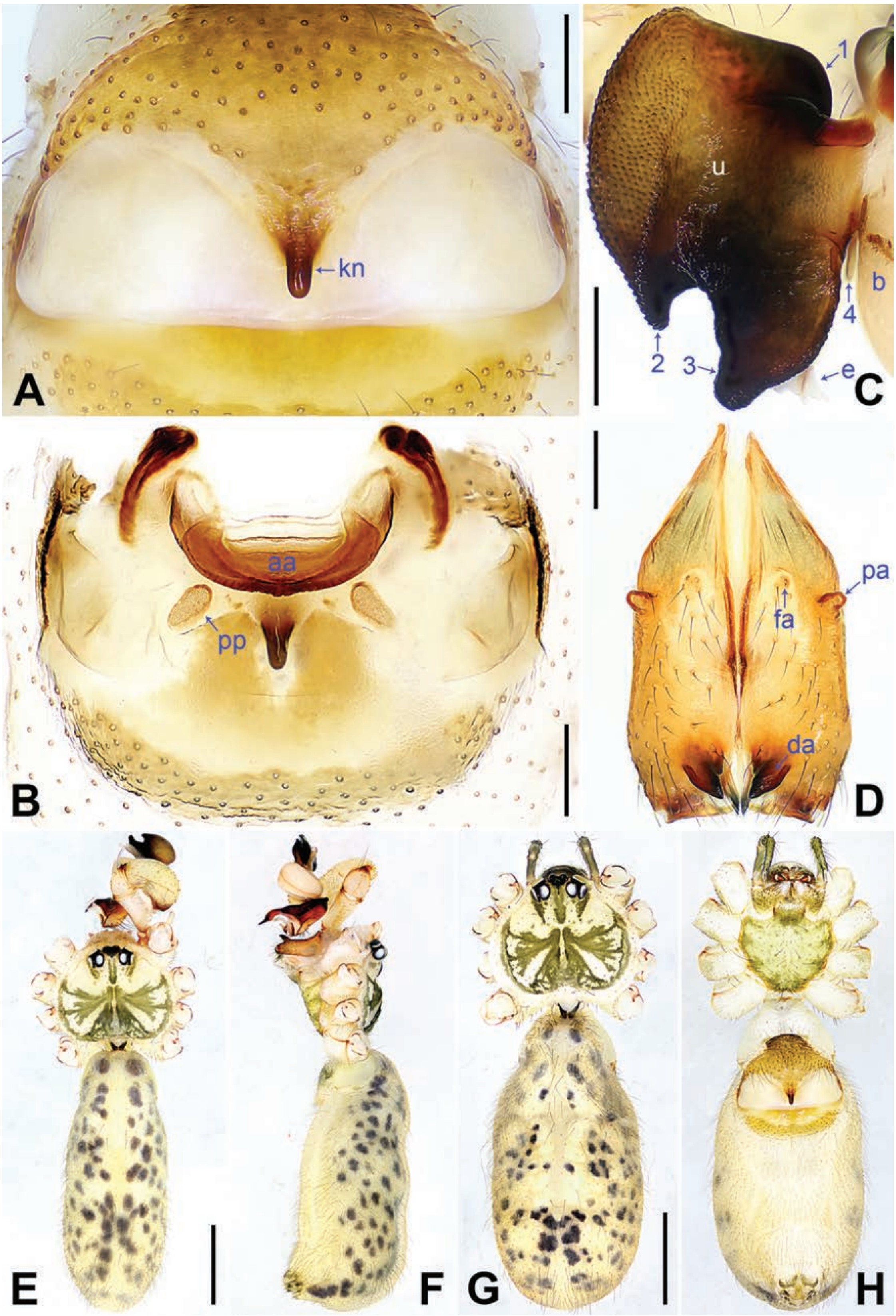

Figure 14. *Pholcus qin* sp. nov., holotype male (**C–F**) and paratype female (**A, B, G, H**). **A** Epigyne, ventral view **B** vulva, dorsal view **C** bulbal apophyses, prolateral view, arrow 1 points at proximal apophysis, arrows 2, 3 point at distal apophyses, arrow 4 points at "pseudo-appendix" **D** chelicerae, frontal view **E–H** habitus (**E, G** dorsal view **F** lateral view **H** ventral view). Abbreviations: aa = anterior arch, b = bulb, da = distal apophysis, e = embolus, fa = frontal apophysis, kn = knob, pa = proximo-lateral apophysis, pp = pore plate, u = uncus. Scale bars: 0.20 mm (**A–D**); 1.00 mm (**E–H**).

Discussion

This study fills a zoogeographical gap in China by collecting, for the first time, species belonging to the *Pholcus phungiformes* species group from the mountainous regions between the Yanshan-Taihang and Changbai Mountains. Nevertheless, there remains another unexplored region: North Korea. Currently, only one species, *P. parkyeonensis* Kim & Yoo, 2009, has been recorded from the southernmost part of North Korea (Kim and Yoo 2009). Given the high diversity of the *P. phungiformes* species group in the Changbai and Taebaek-Sobaek Mountains, as well as the similar landforms and habitats in neighboring North Korea, we anticipate that at least 20–30 species could be discovered if an investigation were to be conducted there. Unfortunately, it is currently difficult to conduct such an investigation in North Korea, as the country lacks experts in this field (Zhang et al. 2022; Yang et al. 2023; WSC 2025) and foreign experts face challenges in surveying there.

Acknowledgements

The manuscript benefited greatly from comments by Sarah Crews and Chang Moon Jang.

Additional information

Conflict of interest

The authors have declared that no competing interests exist.

Ethical statement

No ethical statement was reported.

Funding

This study was supported by the National Natural Science Foundation of China (NSFC-32170461, 31872193). Part of the laboratory work was supported by the Research Fund for the Doctoral Program of Shenyang Normal University (BS201841).

Author contributions

ZY designed the study. ZY and SL performed morphological species identification. JL finished the descriptions and took the photos. ZY performed the molecular experiments. ZY, QH, and JL drafted and revised the manuscript.

Author ORCIDs

Jinglin Li https://orcid.org/0009-0008-3932-309X
Qiaoqiao He https://orcid.org/0000-0002-9381-7444
Shuqiang Li https://orcid.org/0000-0002-3290-5416
Zhiyuan Yao https://orcid.org/0000-0002-1631-0949

Data availability

All of the data that support the findings of this study are available in the main text.

References

Folmer O, Black M, Hoeh W, Lutz R, Vrijenhoek R (1994) DNA primers for amplification of mitochondrial cytochrome c oxidase subunit I from diverse metazoan invertebrates. Molecular Marine Biology and Biotechnology 3(5): 294–299.

Huber BA (2011) Revision and cladistic analysis of *Pholcus* and closely related taxa (Araneae, Pholcidae). Bonner Zoologische Monographien 58: 1–509.

Huber BA, Eberle J, Dimitrov D (2018) The phylogeny of pholcid spiders: a critical evaluation of relationships suggested by molecular data (Araneae, Pholcidae). ZooKeys 789: 51–101. https://doi.org/10.3897/zookeys.789.22781

Khmelik VV, Kozub D, Glazunov A (2005) Helicon Focus 3.10.3. https://www.heliconsoft.com/heliconsoft-products/helicon-focus/ [accessed 13 September 2024]

Kim JP, Yoo SH (2009) One new species of genus *Pholcus* (Araneae: Pholcidae) from Korea. Korean Arachnology 25: 41–46.

Lee JG, Lee JH, Choi DY, Park SJ, Baek MJ, Kim SK (2024) Nine new species of the genus *Pholcus* Walckenaer (Araneae: Pholcidae) from South Korea. Zootaxa 5432(2): 179–212. https://doi.org/10.11646/zootaxa.5432.2.3

Lu Y, Chu C, Zhang X, Li S, Yao Z (2022) Europe vs. China: *Pholcus* (Araneae, Pholcidae) from Yanshan-Taihang Mountains confirms uneven distribution of spiders in Eurasia. Zoological Research 43(4): 532–534 [& Suppl. 1–78]. https://doi.org/10.24272/j.issn.2095-8137.2022.103

Wang X, Shaheen S, He Q, Yao Z (2020) Notes on two closely related spider species of the *Pholcus phungiformes* species group (Araneae, Pholcidae) from Beijing, China. ZooKeys 965: 1–16. https://doi.org/10.3897/zookeys.965.56199

WSC (2025) World Spider Catalog. Version 26. Natural History Museum Bern. http://wsc.nmbe.ch [accessed 19 February 2025]

Yang R, Yan M, Zhang L, Liu H, Koh JKH, He Q, Yao Z (2023) New taxa of spiders (Araneae) from the world in 2022. Biodiversity Science 31(10): 23175 [1–7]. https://doi.org/10.17520/biods.2023175

Yang L, Fu C, Zhang Y, He Q, Yao Z (2024a) A survey of *Pholcus* spiders (Araneae, Pholcidae) from the Qinling Mountains of central China, with descriptions of seven new species. Zoosystematics and Evolution 100(1): 199–221. https://doi.org/10.3897/zse.100.116759

Yang L, He Q, Yao Z (2024b) Taxonomic study of four closely-related species of the *Pholcus yichengicus* species group (Araneae, Pholcidae) from China's Qinling Mountains: an integrated morphological and molecular approach. Zoosystematics and Evolution 100(1): 279–289. https://doi.org/10.3897/zse.100.115633

Yao Z, Li S (2012) New species of the spider genus *Pholcus* (Araneae: Pholcidae) from China. Zootaxa 3289: 1–271. https://doi.org/10.11646/zootaxa.3289.1.1

Yao Z, Li S (2025) Evolutionary history of Old World cellar spiders in the context of Neo-Tethyan sea-land transformations. Zoological Research [in press]. https://doi.org/10.24272/j.issn.2095-8137.2024.395

Yao Z, Pham DS, Li S (2015) Pholcid spiders (Araneae: Pholcidae) from northern Vietnam, with descriptions of nineteen new species. Zootaxa 3909(1): 1–82. https://doi.org/10.11646/zootaxa.3909.1.1

Yao Z, Dong T, Zheng G, Fu J, Li S (2016) High endemism at cave entrances: a case study of spiders of the genus *Uthina*. Scientific Reports 6: 35757 [1–9 & Suppl. 1–52]. https://doi.org/10.1038/srep35757

Yao Z, Wang X, Li S (2021) Tip of the iceberg: species diversity of *Pholcus* spiders (Araneae, Pholcidae) in the Changbai Mountains, Northeast China. Zoological Research 42(3): 267–271 [& Suppl. 1–60]. https://doi.org/10.24272/j.issn.2095-8137.2021.037

Zhang F, Zhu M (2009) A review of the genus *Pholcus* (Araneae: Pholcidae) from China. Zootaxa 2037: 1–114. https://doi.org/10.11646/zootaxa.2037.1.1

Zhang L, Lu Y, Chu C, He Q, Yao Z (2022) New spider taxa of the world in 2021. Biodiversity Science 30(8): 22163 [1–8]. https://doi.org/10.17520/biods.2022163

Zhao F, Jiang T, Yang L, He Q, Zheng G, Yao Z (2023a) Pholcid spiders of the *Pholcus phungiformes* species-group (Araneae, Pholcidae) from Liaoning Province, China: an overview, with description of a new species. ZooKeys 1156: 1–14. https://doi.org/10.3897/zookeys.1156.98331

Zhao F, Yang L, Zou Q, Ali A, Li S, Yao Z (2023b) Diversity of *Pholcus* spiders (Araneae: Pholcidae) in China's Lüliang Mountains: an integrated morphological and molecular approach. Insects 14(4): 364 [1–34]. https://doi.org/10.3390/insects14040364

ZooKeys 1232: 311–341 (2025)
DOI: 10.3897/zookeys.1232.142494

Research Article

A taxonomic synopsis and identification key to the genera of the *Myaptex* group (Diptera, Asilidae, Asilinae), with description of a remarkable new genus and three new species from the South American Chaco

Matheus M. M. Soares[1], Alexssandro Camargo[2], Carlos J. E. Lamas[1]

1 *Museu de Zoologia da Universidade de São Paulo, Laboratório de Diptera, Av. Nazaré, 481, 04263-000 - Ipiranga, São Paulo, São Paulo, Brazil*
2 *Natural History Museum Vienna, 2nd Zoological Department. Burgring 7, 1010 Vienna, Austria*
Corresponding author: Matheus M. M. Soares (matheusmmsoares@gmail.com)

Abstract

Cardiasilus **gen. nov.** is erected to include the following three new species from Brazil and Paraguay: *C. aysu* **sp. nov.** and *C. dangeloi* **sp. nov.** (both from Mato Grosso do Sul, Brazil) and *C. ruda* **sp. nov.** (Paraguay), which are herein described and illustrated. The new genus is placed into the *Myaptex* group of the subfamily Asilinae based on the following set of characters: wing with cells r_{2+3} and r_4 not separated by a recurrent vein (i.e., only two submarginal cells); costal section between tips of veins R_5 and M_1 much shorter than costal section between tips of R_4 and R_5, with R_5 ending bellow wing apex; scutellum tumid, with no sign of an impressed rim and with at least one pair of well-developed apical scutellar macrosetae; claws acute; and abdominal tergites with lateral marginal macrosetae. It can be differentiated from the other genera of the group by the scutum lacking anterior dorsocentral setae, male epandrium inflated (which resembles the ideogram of a heart in dorsal view), male and female sternites 2–6 with lateral macrosetae, and the male sternite 8 with a long digitiform projection at middle of posterior margin. An illustrated identification key to the genera of the *Myaptex* group, as well as to the males of *Cardiasilus* **gen. nov.**, are also provided.

Key words: Assassin flies, Chaco biome, Linnaean shortfall, Pantanal biome, robber flies

Academic editor: Torsten Dikow
Received: 22 November 2024
Accepted: 10 February 2025
Published: 20 March 2025

ZooBank: https://zoobank.org/67DBBE51-5990-4842-AF0F-141CB0AFA4D2

Citation: Soares MMM, Camargo A, Lamas CJE (2025) A taxonomic synopsis and identification key to the genera of the *Myaptex* group (Diptera, Asilidae, Asilinae), with description of a remarkable new genus and three new species from the South American Chaco. ZooKeys 1232: 311–341. https://doi.org/10.3897/zookeys.1232.142494

Introduction

Among the Asilidae subfamilies, Asilinae Latreille, 1802 is one of the most diverse, comprising 186 valid extant genera distributed in all biogeographic regions, except Antarctica (Dikow 2020; Camargo et al. 2022, 2023). In the Neotropical region, 69 genera are recognized (Papavero 2009; Camargo et al. 2022, 2023).

To facilitate the identification of the Neotropical Asilinae genera, Artigas and Papavero (1997) proposed several generic groups delimited by morphology, including internal characters of male and female terminalia. The *Myaptex* group (Artigas and Papavero 1995) comprises nine genera (*Apulvillasilus* Camargo, Vieira & Fisher, 2022; *Atractocoma* Artigas, 1970; *Martintella* Artigas, 1996; *Myaptex* Hull, 1962; *Myaptexaria* Artigas & Papavero, 1995; *Papaverellus* Artigas & Vieira, 2014; *Rhadinosoma* Artigas, 1970; *Scarbroughia* Papavero, 2009; *Wilcoxius* Martin, 1975) and 26 species, with a somewhat disjointed distribution primarily in Central America, the Caribbean, northeastern Brazil, Chile and Argentina (Artigas and Papavero 1995; Papavero 2009; Artigas and Vieira 2014; Vieira et al. 2014; Camargo et al. 2022).

Several areas in the Neotropical region remain inadequately surveyed, particularly for Diptera, which exacerbates the Linnaean and Wallacean shortfalls. To address this gap – especially in certain regions of the Midwest and northern Brazil – the SISBIOTA-Diptera Brazilian Network research program was developed. This program aimed to document the diversity of flies in endangered and understudied areas and biomes in Brazil (Lamas et al. 2023). Most of the material examined in this study was collected during the SISBIOTA-Diptera survey, highlighting the project's significant contribution to reducing the Linnaean and Wallacean shortfalls. It particularly aids in the revision of genera, the description of new taxa, and the recording of new distribution data.

The purpose of this paper is to describe and illustrate a new genus of Asilinae (*Myaptex* group), with three new species from Brazil and Paraguay. Additionally, we provided a taxonomic synopsis of fauna, together with remarks for the genera, an illustrated identification key for the *Myaptex* group genera and a key to species for the males of the new established genus *Cardiasilus* gen. nov.

Materials and methods

The studied specimens are housed at Museu de Zoologia da Universidade de São Paulo (**MZUSP**) and Natural History Museum Vienna (**NHMW**), with photographs of specimens held at the California Academy of Sciences (**CAS**). Terminology follows mainly Cumming and Wood (2017). Male terminalia were dissected with the abdomen cut at the beginning of the sixth segment. The dissected parts were macerated with potassium hydroxide (KOH at 10%) and left at room temperature for seven days. Subsequently, they were neutralized in baths of tap water for 10 min and acetic acid at 10% for 30 min. Then, the dissected parts were transferred to an excavated slide containing glycerin for visualization, analyses, and imaging of its structures under a stereomicroscope. After being examined, the terminalia pieces were placed in a microvial with glycerin and pinned under the corresponding specimen.

Photographs were obtained using the Zeiss® Discovery V20 stereomicroscope with a Zeiss AxioCam Mrc5 camera attached, connected to a desktop computer through Zeiss AxioVs40 v. 4.8.2.0 software. Image sequences were assembled in Helicon Focus 6.7.1 software, with some further editing with Adobe Photoshop. Label data for the primary types are cited verbatim in quotation marks (each line separated by a vertical line "|" and each label by a semicolon ";"), with annotations in square brackets. Distribution map was created with Simplemappr (Shorthouse 2010), using the data present on the specimen labels.

Results

Identification key to the genera of the *Myaptex* group (Asilinae)

1 Wings with bifurcation of R_4 and R_5 before the apex of discal cell (*d*) (Figs 2G, 6F, 9F) **2**

– Wings with bifurcation of R_4 and R_5 at or after the apex of discal cell (*d*) (Figs 13B, 17B) **3**

2 Abdominal sternites with at least 3 pairs of macrosetae (Figs 2H, 6E, 9E); epandria inflated, resembling the ideogram of a heart (i.e., Figs 2B, H, 3A, C). Length, 10–13 mm (Brazil, state of Mato Grosso do Sul and Paraguay). ....***Cardiasilus* gen. nov.**

– Abdominal sternites without macrosetae (Artigas and Vieira 2014: fig. 1); epandria not inflated and flat ventrally, resembling a goat hoof (Artigas and Vieira 2014: fig. 1). Length, 15 mm (Brazil, states of Pará and Piauí)........... ....***Papaverellus* Artigas & Vieira, 2014**

3 Body covered with abundant squamiform-fusiform setae (Fig. 1A, B; Camargo et al. 2022: figs 1, 2)..**4**

– Body without squamiform-fusiform setae (i.e., Fig. 2A, B)...........................**5**

4 Frons with divergent slopes (Camargo et al. 2022: fig. 3); empodium and pulvillus absent (Camargo et al. 2022: fig. 4). Length, 6–9 mm (Argentina) ....***Apulvillasilus* Camargo, Vieira & Fisher, 2022**

– Frons with parallel slopes (Fig. 1D); empodium and pulvillus present (Fig. 1A). Length, 12 mm (Chile)......................... ***Atractocoma* Artigas, 1970**

5 Sternites with macrosetae (Figs 13E, 15E, 18E)..**6**

– Sternites without macrosetae (Fig. 16E) **8**

6 Postpedicel lanceolate, approximately as long as scape and pedicel combined (Fig. 18A, C); mystax restricted to lower 1/2 of face, composed by long and sparse macrosetae (Fig. 18C, D); sternites with 2 pairs of macrosetae (Fig. 18E); phallus exposed (Fig. 18F) Length, 10–11 mm (Cuba, Mexico, Dominican Republic, Guatemala, Honduras, El Salvador, Nicaragua) ..***Wilcoxius* Martin, 1975**

– Postpedicel oval, shorter than scape and pedicel combined (Figs 13C, 15C); mystax occupying almost the entire face, composed by long and dense macrosetae (Figs 13C, D, 15C, D); sternites with abundant setae (Figs 13E, 15E); phallus completely concealed (Figs 13F, 15F)....................................**7**

7 Scutellar disc only with scattered, long setae (Fig. 13B); normally 2–4 black apical scutellar macrosetae; male terminalia with epandria strongly inflated, their apices curved in apically (Fig. 13F). Length, 8–13 mm (Chile) .. .. ***Myaptex* Hull, 1962**

– Scutellar disc with two tufts of abundant, proclinate, long setae (Fig. 15B, C); from 2 to several apical scutellar macrosetae (sometimes mixed black and white) (Fig. 15C); male terminalia with epandria not inflated, their apices blunt and not curved in at apex (Fig. 15F). Length, 17–19 mm (Chile)... ....***Myaptexaria* Artigas & Papavero, 1995**

8 Frons with converging slopes in anterior view (Fig. 12A); mystax restricted to middle of face, resembling a mohawk (Fig. 12A, B); base of vein R_4 usually nearly straight (Vieira et al. 2014: figs 19, 31) (Costa Rica, Mexico, and Trinidad and Tobago) ....***Martintella* Artigas, 1996**

– Frons with parallel slopes in anterior view (Figs 16C, 17E); mystax not restricted to the middle of face and not resembling a mohawk (Figs 16C, 17D); base of vein R_4 angulated (Fig. 17B) **9**

9 Mystax composed of few sparse macrosetae (Fig. 16C, D); at least one pair of well-developed anterior dorsocentral macrosetae (Fig. 16A, D); vein R_4 ending at wing apex (Fig. 16B) (Chile) ....***Rhadinosoma* Artigas, 1970**

– Mystax composed of abundant and dense macrosetae (Fig. 17C, D); well-developed anterior dorsocentral macrosetae absent (Fig. 17A); vein R_4 ending before wing apex (Fig. 17B) (Mexico).............. ***Scarbroughia* Papavero, 2009**

Taxonomic synopsis

Apulvillasilus Camargo, Vieira & Fisher

Apulvillasilus Camargo, Vieira & Fisher, 2022. Type species: *Apulvillasilus boharti* Camargo, Vieira & Fisher, 2022 (original designation). Type locality: Argentina, Catamarca Province, Belén.

Remarks. The monotypic genus *Apulvillasilus* was recently described and illustrated from Argentina. The genus shares with *Atractocoma* Artigas the body covered with abundant squamiform-fusiform setae but can be easily differentiated by the frons with divergent slopes and the legs lacking empodium and pulvillus (a unique condition among the *Myaptex* group).

Distribution. Argentina.

Atractocoma Artigas

Fig. 1

Atractocoma Artigas, 1970. Type species: *Atractocoma nivosa* Artigas, 1970 (original designation). Type locality: Chile, Aysén.

Remarks. The monotypic genus *Atractocoma* is known only from Chile. It shares with *Apulvillasilus* the body covered with abundant squamiform-fusiform setae (as mentioned above) (Fig. 1A, B) but can be easily differentiated by the dense mystax, occupying almost the entirely face (Fig. 1C, D); scutum lacking distinct rows of acrostichal setae and anterior dorsocentral setae absent (Fig. 1A, B); scutellum with three pairs of apical macrosetae and dorsally covered with long and abundant white setae; tergites 2–6 in dorsal view with V-shaped pattern formed by squamiform-fusiform setae (Fig. 1B) and sternites lacking macrosetae (Fig. 1E).

Examined material. Chile, Chico, Lag. Buenos Aires, Aysen, CHILE, 24–31. xii.1960, Pena (1 ♂, 1 ♀, MZUSP).

Distribution. Chile.

Cardiasilus gen. nov.

https://zoobank.org/CC0B7CD3-B621-45A9-8B0A-1852110EE91C

Figs 2–11, 19

Type species. *Cardiasilus aysu* sp. nov. by present designation.

Etymology. From the Greek feminine word *kardia* = heart + *asilus* = common epithet of robber flies. The name refers to the distinct inflated epandria, somewhat heart ideogram-shaped in dorsal view. The gender is masculine.

Diagnosis. *Head*. Antenna ~ 3/4 as long as eye height (Fig. 2A). Scape and pedicel subequally long (Fig. 2E). Postpedicel lanceolate, laterally compressed and slightly tapering towards apex, about as long as scape and pedicel combined (Fig. 2E). Stylus slightly longer than postpedicel, composed of two elements (Fig. 2E). Face wide, slightly narrowing at antennal level and slightly

Figure 1. *Atractocoma nivosa* Artigas, 1970 (identified male from Chile) **A, B** habitus lateral and dorsal, respectively **C** head and thorax, lateral view **D** head, anterior view **E** abdomen, ventral view **F** terminalia, lateral view.

gibbous at lower 1/3, mystax restricted to gibbosity (Fig. 2D). Frons with parallel slopes, slightly concave at antennal level, twice wider than higher (Fig. 2D). Palpus one-segmented, short, ~ 1/5 length of proboscis. Proboscis ~ 3.5/5 as long as eye height (Fig. 2C). ***Thorax***. Acrostichal setae indistinct (Fig. 2C). Anterior dorsocentral macrosetae absent, scutum with three to four pairs of posterior dorsocentral macrosetae (Fig. 2C). Scutellum tumid with pair of marginal macrosetae (Fig. 2B). Anatergite bare. Postmetacoxal area membranous.

Legs. Femora swollen. ***Wing.*** Distinctly shorter than abdomen, with bifurcation of veins R_4 and R_5 placed before apex of discal cell by approx. length of *r-m* cross vein (Fig. 2G). Distance between apex of veins R_4 and R_5 ~ 1.5–2× longer than distance between apex of veins R_5 and M_1 (Fig. 2G). Cells m_3 and *cua* closed and petiolate before wing margin (Fig. 2G). ***Abdomen***. Abdominal sternites 2–6 with two to three pairs of pale yellow macrosetae mid-laterally (Figs 2H, 6E, 9E). Sternite 8 with mid-posterior digitiform projection almost as long as sternite 8 length (Figs 3E, 7E, 10E). ***Terminalia***. Epandria inflated laterally and posteriorly, resembling the ideogram of heart in dorsal view. Phallus long and thin, longer than length of hypandrium plus gonocoxite, divided into two prongs along its entire length (i.e., Fig. 3A–C, F–I).

Remarks. *Cardiasilus* gen. nov. is similar to *Myaptex* Hull by the inflated male epandria (Fig. 14A–D), but can be easily distinguished by the following set of characters: postpedicel lanceolate, approx. as long as length of scape and pedicel combined (Fig. 2E, F); face slightly gibbous at lower 1/3 (Fig. 2C); scutum lacking distinct rows of acrostichal setae; anterior dorsocentral setae absent; femora mostly covered with short black setae (Fig. 2C); male sternite 8 with a long digitiform projection at posterior margin (Figs 2H, 3C, E); gonocoxite L-shaped, with rounded apex and covering the gonostylus versus postpedicel oval, shorter than scape and pedicel combined (Fig. 13C); face distinctly gibbous at lower 2/3 (Fig. 13C); scutum with two distinct rows of acrostichal setae (Fig. 13A, C); three to four pairs of anterior dorsocentral macrosetae; femora mostly covered with long vestiture of white setae (Fig. 13A); male sternite 8 without projections at posterior margin; gonocoxite squared at base, with a digitiform apicoventral projection acute apically (Fig. 14F) in *Myaptex*. It is also similar to some undescribed *Lecania* Macquart species, including *Nerax eurylabis* (Wiedemann, 1828) a species that belongs in *Lecania* (unpublished data) with inflated male epandria, but can be easily distinguished by the scutellum with one pair of apical macrosetae and the abdominal sternites with macrosetae (scutellum bare in *Lecania* or at most bearing tiny, short setulae and sternites only with sparse setae).

Distribution. The new genus is known to occur only in the state of Mato Grosso do Sul (Central-West Brazil) and department of Cordillera (Central-West of the Oriental Region of Paraguay), in biomes of Pantanal and Chaco, respectively (Fig. 19).

Key to species of *Cardiasilus* gen. nov. (males)

1 Inner dorsal margin of epandrium with a short, sub-triangular, pre-apical, process followed by a short, ventral, sub-rectangular, anteriorly curved, apical process (Fig. 10A, F, G). Subepandrial sclerite goblet-shaped (Figs 10F, G, 11D) (Paraguay: Cordillera)........................***Cardiasilus ruda* sp. nov.**

– Inner dorsal margin of epandrium lacking processes, only ventral margin with a short, pre-apical process (Figs 3A, F–I, 7A, F–I). Subepandrial sclerite somewhat trapezoidal or diamond-shaped (Figs 4D, 8D) (Brazil: Mato Grosso do Sul) **2**

2 Anterior row of macrosetae on mid femur wholly white (rarely with 1 or 2 black macrosetae at apical 1/2); postalar macrosetae yellow (Fig. 2C) (sometimes 1 postalar macroseta black); epandrium weakly excavated

at mid-inner dorsal margin (Fig. 3A, H); subepandrial sclerite somewhat diamond-shaped near its middle (Fig. 4D) .... ***Cardiasilus aysu*** **sp. nov.**

– Anterior row of macrosetae on mid femur wholly black, only the basal-most macroseta white (Fig. 6A); postalar macrosetae black (Fig. 6B); epandrium strongly excavated at mid-inner dorsal margin (Fig. 7A, 7F); subepandrial sclerite somewhat trapezoidal at its middle (Fig. 8D)...***Cardiasilus dangeloi*** **sp. nov.**

Cardiasilus aysu **sp. nov.**

https://zoobank.org/FD78363D-6751-4BEC-BC76-F3AD67423224

Figs 2–5, 19

Diagnosis (males). The new species can be easily distinguished from the congenerics by the yellow postalar macrosetae (Fig. 2B, C), inner dorsal margin of epandrium weakly excavated, and lacking processes (Fig. 3A, F, H) and subepandrial sclerite somewhat diamond-shaped near its middle (Fig. 4D).

Description. Male holotype (Fig. 2A). Body Length 12.3 mm; wing length 6.8 mm. ***Head*** (Fig. 2A–F). Scape and pedicel orange-yellow, slightly darker at apex; postpedicel dark brown, lanceolate; stylus dark brown, bare, first element very short, second element long and abruptly narrowed at apex. Face golden pruinose, except gibbosity with mixed silvery and golden pruinosity; mystax with few upper slender black macrosetae and strong golden macrosetae below, extending along oral margin. Frons, golden pruinose, with long black orbital macrosetae. Ocellar tubercle dark brown, with one to two pairs of proclinate long and slender ocellar macrosetae; vertex golden pruinose, almost bare of major setae, only with few slender black setae posteriorly; upper-most four to five postocular macrosetae black, remaining macrosetae yellowish-white. Postcranium golden pruinose, with long, slender, and dense white lower occipital setae. Palpus dark brown, with few short white setae. Proboscis black, ventral surface with long white setae, apex with short white setae. ***Thorax*** (Fig. 2A–C). Antepronotum with few strong golden macrosetae, covered with golden pruinosity and sparse short and white setae. Scutum wholly covered with short vestiture of black setae and golden pruinosity, except notopleural, supra-alar, and acrostichal area close to scutellum with short white setae, in anterior view with U-shaped dark brown median stripe along acrostichal area, followed by L-shaped dark brown paramedian stripe along dorsocentral and intra-alar areas, with both stripes extending slightly beyond transverse suture. Three to four pairs of black, postsutural dorsocentral macrosetae, two black notopleural macrosetae, one black supra-alar macroseta, two yellow postalar macrosetae (anterior one shorter). Scutellum with one pair of apical pale yellow macrosetae, dorsal surface covered with short white setae. Pleuron mostly silvery pruinose, except anepisternum and katepisternum with golden pruinosity anteriorly, anepisternum, katepisternum, anepimeron and meron with few long white setae posteriorly, katatergite with vertical row of yellow macrosetae. ***Legs*** (Fig. 2A). Mostly yellow, except all coxae with dense silvery pruinosity, all femora dorsally with short black setae, apex of mid and hind femora dorsally, apex of all tibiae, apex of all tarsomeres one to four and all tarsomeres five dark brown. Legs with white or golden macrosetae, except when as noted. **Leg I.** Coxa with long and dense white macrosetae anteriorly. Femur with one posterior black macroseta at

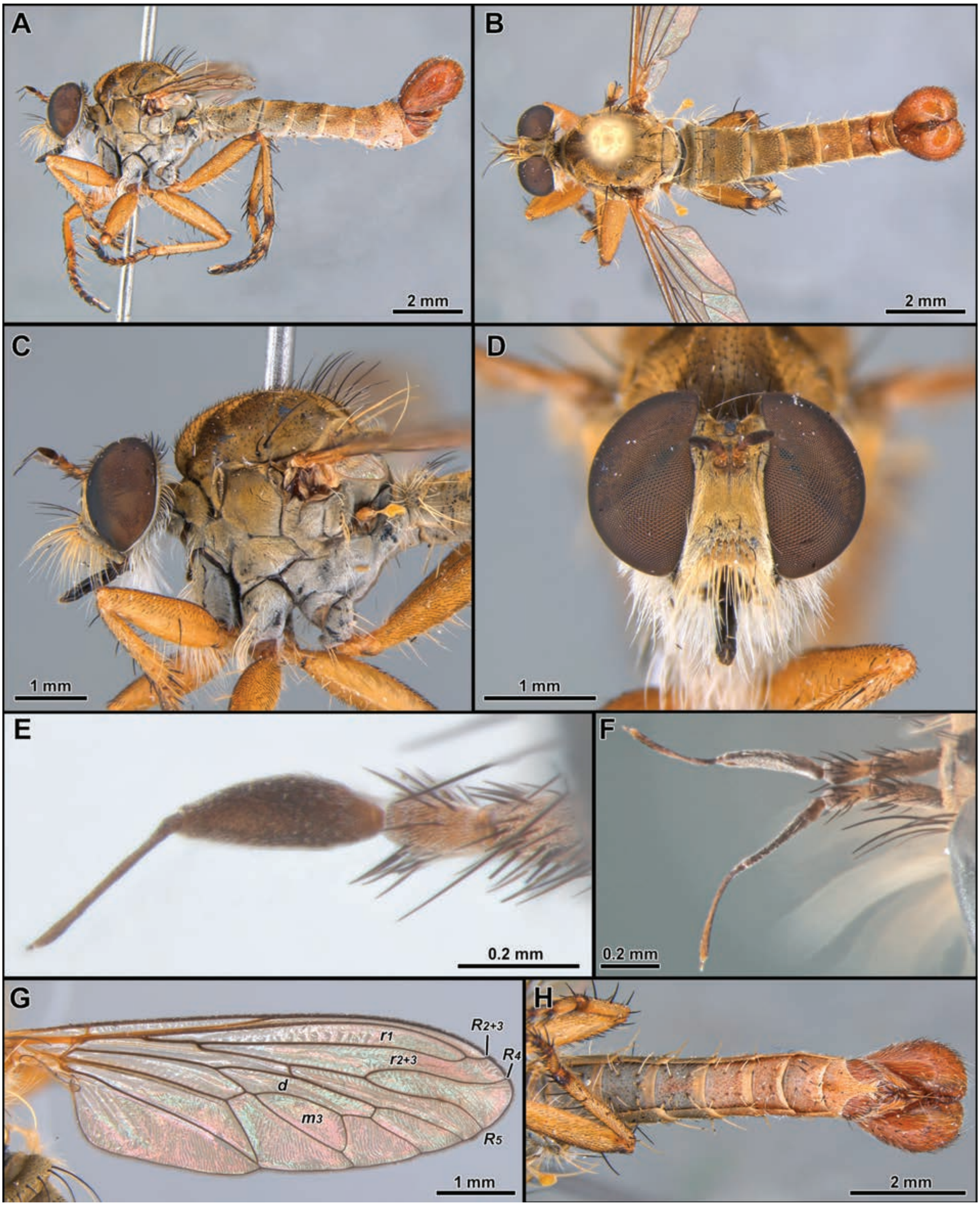

Figure 2. *Cardiasilus aysu* sp. nov. (male holotype) **A, B** habitus lateral and dorsal, respectively **C** head and thorax, lateral view **D** head, anterior view **E, F** antenna, lateral and dorsal views, respectively **G** wing **H** abdomen, ventral view. Abbreviations: *d* = discal cell; *m3* = third medial cell; *r1* = first radial cell; *r2+3* = second + third radial cell; *R2+3* = second branch of radius; *R4* = upper branch of third branch of radius; *R5* = lower branch of third branch of radius.

middle, ventral surface with long setae at basal 1/2. Tibia with one anterodorsal black macroseta at basal 1/4, three dorsal black macrosetae, one near middle and two at apical 1/2, one antero, one dorsal, one posterodorsal, and one ventral black macrosetae at apex, two anterior long macrosetae at apex (~ 2× longer than remaining apical macrosetae), posterior row of four long macrosetae from basal 1/4 to apex, three ventral long black setae near middle. Basitarsus with one antero and one posteroventral short black macrosetae at apex, one posteroventral long macroseta near base, tarsomeres one to three with crown of long macrosetae at apex: one antero and one posteroventral, one antero and one posterodorsal. **Leg II.** Coxa with long and slender macrosetae at apical 1/2, some of them reaching lateral surface. Ventral surface of femur with short vestiture of white setae and five to six long ventral macrosetae at basal 1/2, one anterodorsal apical short black macroseta, one posterodorsal preapical short macroseta, anterior row of four macrosetae from base to apex, anteroventral row of short intermixed black and white macrosetae. Tibia with two to three short dorsal black macrosetae at apical 1/2, one ventral long black macroseta at middle, ventral row of short and slender black setae from basal 2/4 to apex, one posterior long and slender black seta at basal 1/3, two ventral strong macrosetae, one black at middle and one white preapical, one posterior strong macroseta at apical 1/3, crown of long intermixed black and white macrosetae at apex: one antero and one posteroventral, one antero and one posterodorsal, one anterior and one posterior. Tarsus with chaetotaxy similar to fore tarsus. **Leg III.** Coxa laterally with two posterior macrosetae. Femur with two to three anterior macrosetae, anteroventral row of short macrosetae, posteroventral row of long and slender setae at basal 1/2, few long and slender posterodorsal setae near base, one anterodorsal black preapical macroseta, one dorsal preapical macroseta. Tibia with one antero and one posterodorsal short black macrosetae near base, two long anterodorsal black macrosetae: one near middle and one at apical 1/2, two long anteroventral black macrosetae at apical 1/2, crown of black macrosetae at apex: one antero and one posteroventral, one ventral, one anterior and one dorsal. Tarsus with chaetotaxy similar to fore and mid tarsus. ***Wing*** (Fig. 2G). Hyaline, veins brown, orangish at base and Sc. Membrane with sparse dark brown microtrichia at apex of cells r_1, r_{2+3}, r_4 and bordering the veins R_4 and R_5. Halter: yellow. ***Abdomen*** (Fig. 2A, B, H). Mostly brown, becoming orange from segments five to eight, densely covered with golden pruinosity, except lateral margins of tergites one to four, silvery pruinose. Posterior margin of tergite one with six to seven long black macrosetae, lateral margin with seven to eight white lateral marginal macrosetae, lateral margins of tergites two to six with two strong white lateral marginal macrosetae, tergites mostly clothed by short vestiture of black setae, becoming white laterally. Sternites one to four densely silvery pruinose, sternites five to eight mostly orange, with weak silvery pruinosity, sternites two to six with two to three pairs of pale yellow macrosetae mid-laterally and clothed with short, sparse, white setae. ***Terminalia*** (Figs 3, 4). Orange-brown. Tergite eight somewhat saddle-shaped, narrowing at middle of anterior and posterior margins, posterior 1/2 with two to three rows of short setae, longer at posterior corners (Fig. 3D). Sternite eight with short and slender white setae at posterior 1/3, with long digitiform projection at middle of posterior margin, ~ 2/3 as long as sternite eight length, with conspicuous yellow setae (Fig. 3E). Epandrium inflated laterally and posteriorly, resembling the ideogram of a heart in dorsal view, lacking inner and apical projections dorsally, inner ventral margin with a short preapical dentiform process, mostly with short vestiture of brownish setae, except apex with slightly longer yellowish setae (Fig. 3A–C, F–I). Cercus short, digitiform, laterally compressed, covered with short setae (Fig. 3A). Subepandrial sclerite long and narrowing towards apex, with a median subtriangular lateral process

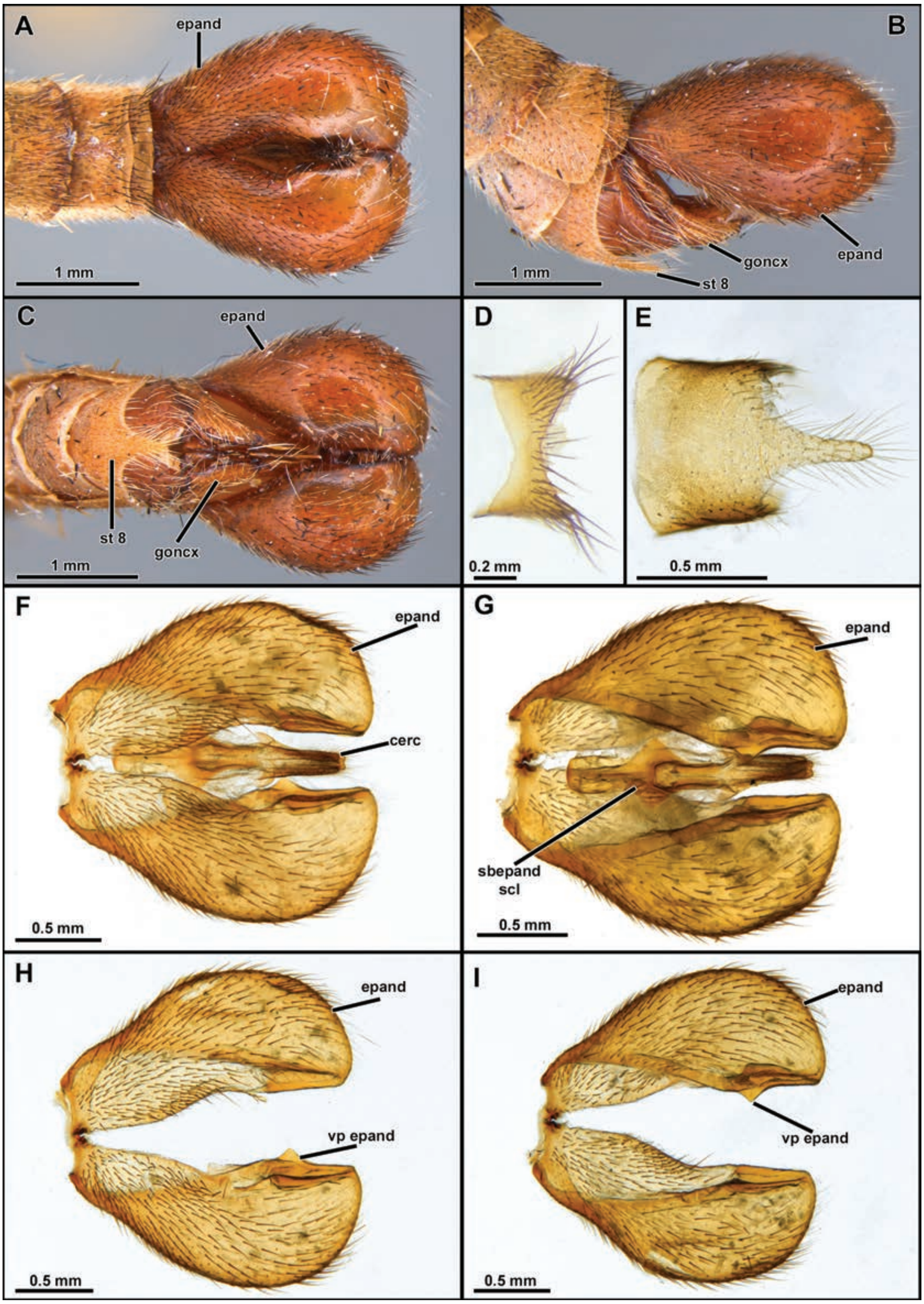

Figure 3. *Cardiasilus aysu* sp. nov. (**A–C** male holotype **D–I** male paratype) **A–C** terminalia in dorsal, lateral, and ventral views, respectively **D** tergite 8 **E** sternite 8 **F, G** dissected terminalia in dorsal and ventral views, respectively **H, I** dissected terminalia without inner appendages in dorsal and ventral views, respectively. Abbreviations: cerc = cercus; epand = epandrium; goncx = gonocoxite; sbepand scl = subepandrial sclerite; st 8 = sternite 8; vp epand = ventral process of epandrium.

(somewhat diamond-shaped near its middle), almost at the same level, internally, with a pair of short, tooth-like processes directed anteriorly, and with a short dentiform preapical process, apex dorsoventrally flattened and covered with short setae (Fig. 4D). Hypandrium subrectangular, with a short concavity at posterior

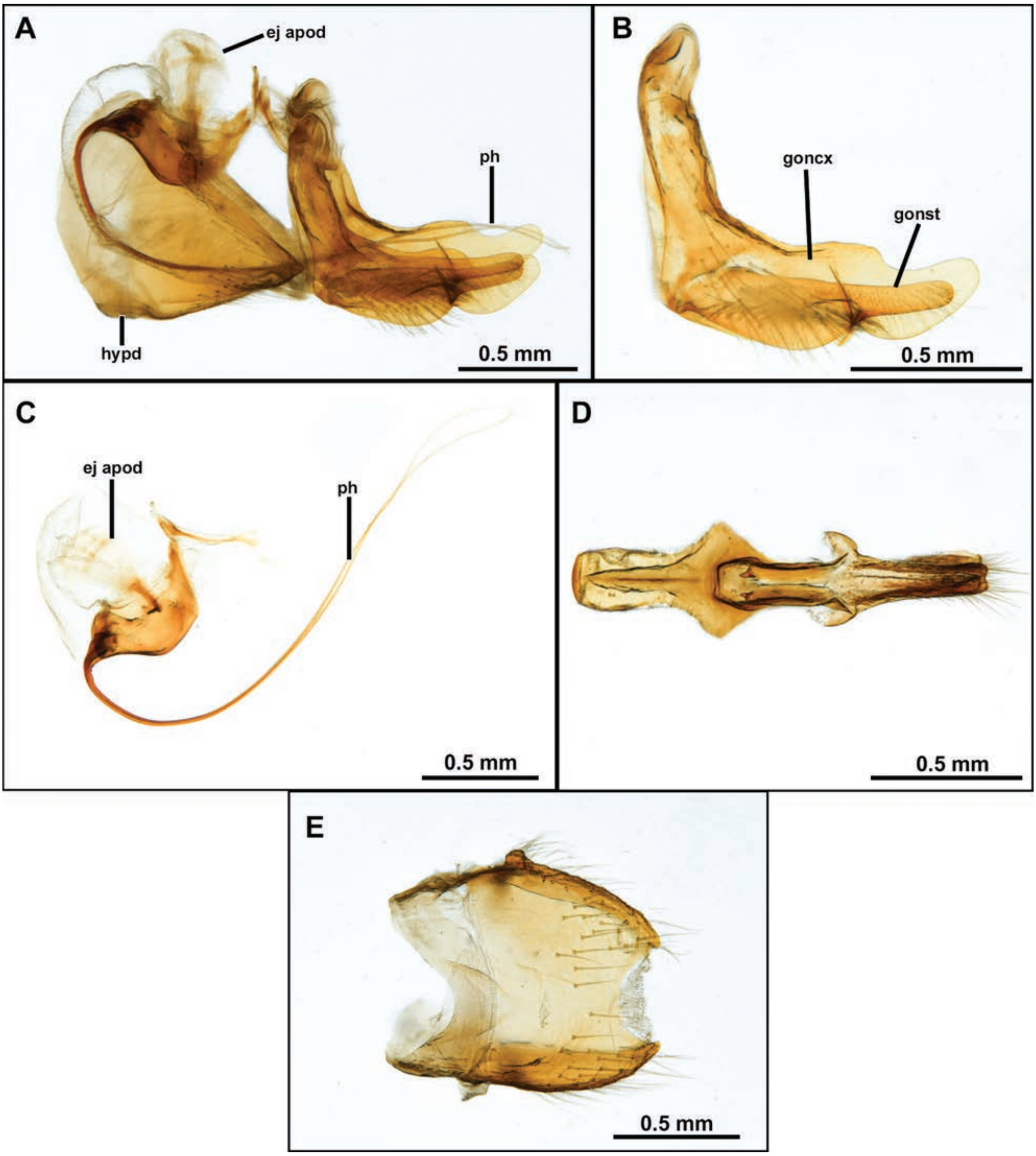

Figure 4. *Cardiasilus aysu* sp. nov. (male paratype) **A** inner appendages **B** gonocoxite and gonostylus **C** phallus and ejaculatory apodeme **D** subepandrial sclerite **E** hypandrium. Abbreviations: ej apod = ejaculatory apodeme; hypd = hypandrium; goncx = gonocoxite; gonst = gonostylus; ph = phallus.

margin, covered with short setae at posterior 1/2 (Fig. 4E). Gonocoxite L-shaped, pointed at base and rounded at apex, with slightly preapical concavity at dorsal margin, few short setae at basal 2/3 of external surface (Fig. 4A, B). Gonostylus ~ 1/2 as long as gonocoxite, somewhat digitiform, with ventral indentation at apical 1/3, apex rounded (Fig. 4A, B). Ejaculatory apodeme fan-shaped (Fig. 4C). Phallus long and thin, longer than length of hypandrium plus gonocoxite, divided into two prongs along the entire length (Fig. 4C).

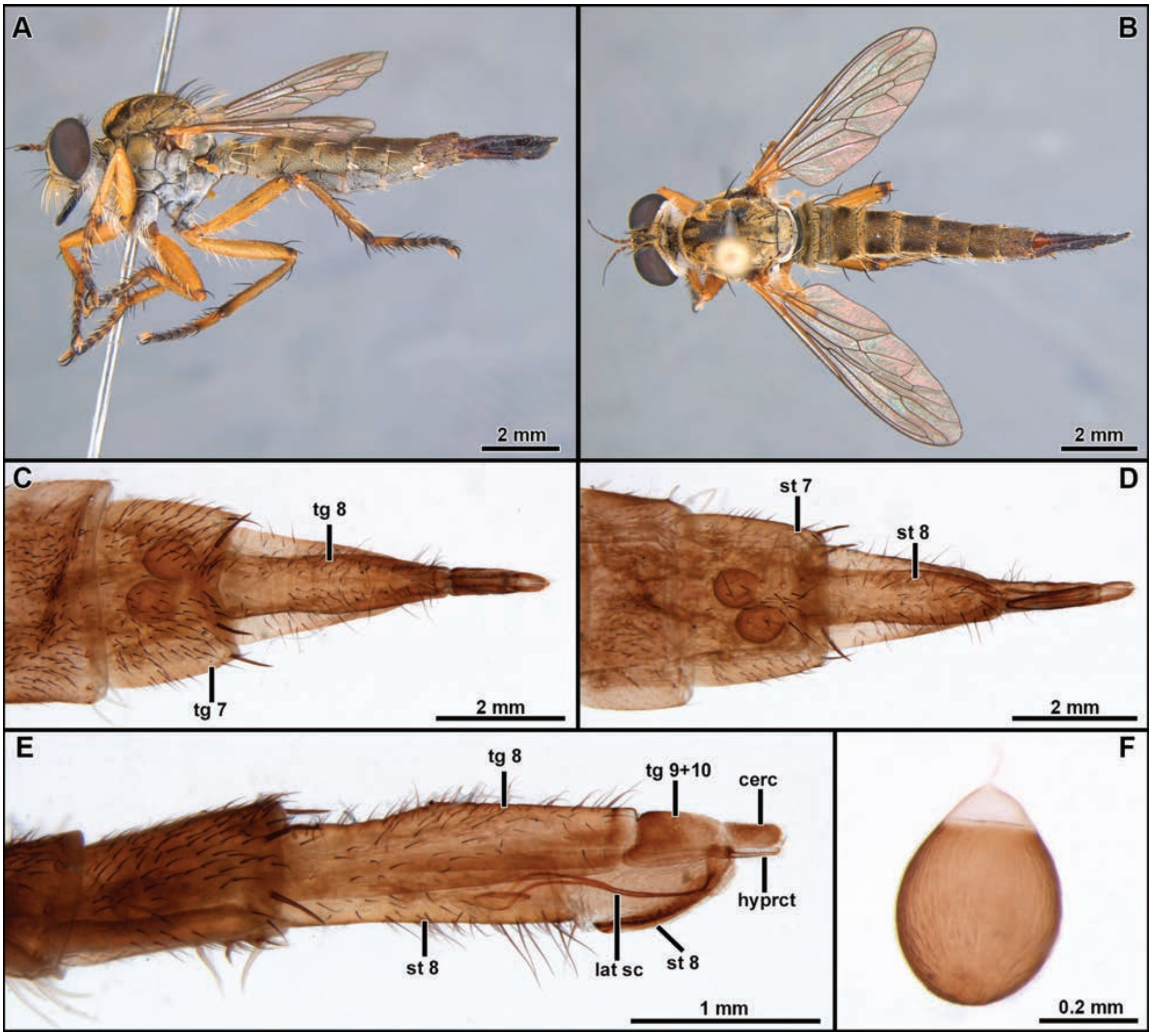

Figure 5. *Cardiasilus aysu* sp. nov. (identified female) **A, B** habitus lateral and dorsal, respectively **C–E** terminalia in dorsal, ventral, and lateral views, respectively **F** spermathecae. Abbreviations: cerc = cercus; hyprct = hypoproct; lat sc = lateral sclerite of genital fork; st = sternite; tg = tergite.

Female (Fig. 5). Similar to male, except as noted: Body length 13.5 mm; wing length 6.8 mm. Abdomen wholly brown, only the segment seven and the basal 1/2 of ovipositor sometimes orange, tergite seven with dark brown macrosetae posteriorly, sternite seven with white macrosetae laterally and posteriorly. ***Terminalia*** (Fig. 5C–F). Laterally compressed from middle of tergite and sternite eight, long and slender, almost two times the length of tergite seven, covered with short black setae, longer before the opening of the genital fork, apex of sternite eight curved ventrally, weakly sclerotized, bare, and strongly striated. Tergite 9+10 slightly longer than cercus, mostly bare and shiny, only covered with few short and sparse white setae. Cercus short, digitiform, covered with short and slender white setae. Hypoproct short, V-shaped. Two sclerotized and rugose spermathecae present, membranous at base.

Type examined material. ***Holotype***: • ♂ (MZUSP) labelled: "Brasil: MS [state of Mato Grosso do Sul]: Porto Murtinho | Trilha Fazenda Campo

Florido | 21°41'52,0"S, 57°45'57,1"W | Ativa | 11.xii.2013 | Lamas & eq. cols. | SISBIOTA | CNPq/FAPESP" "HOLOTYPE | *Cardiasilus aysu* | Soares, Camargo & Lamas [red label]". Holotype condition: Good, not dissected. ***Paratypes*:** • same data as holotype (2 ♂, one dissected, MZUSP); same data, except: 21°38'15,07"S, 57°42'10,2"W | Coleta manual (rede) | 12.xii.2011 | Lamas, Nihei & eq. col. (1 ♂, MZUSP); same data, except: Fazenda Retiro Conceição – Trilha | da Espinhadeira | 21°40'59,7"S, 57°46'42,5"W | Malaise 31 | 10–25.i.2012 | Lamas, Nihei & eq. col. (2 ♂, MZUSP); same data, except: 21°41'06.2"S, 57°46'35.7"W | coleta manual (rede) | 11.xii.2011 (1 ♂, MZUSP; 2 ♂, NHMW); • Porto Murtinho (norte) | Estrada para Pirizal, km18 | 21°33'05"S, 57°45'35"W | 19–31.i.2008 | Nihei, S.; Figueiredo, R. & Almeida, J. (col.) (2 ♂, MZUSP; 2 ♂, NHMW); • same data, except: 21–30.i.2008 (2 ♂, one dissected, MZUSP); same data, except: 24.i.2008 | F.A. Esteves col. (1 ♂, MZUSP); • same data, except: Faz. São Fernando, km12 | 21°36'30"S, 57º49'02"W | 19–31.i.2008 | Nihei, S.; Figueiredo, R. & Almeida, J. | (col.) (1 ♂, MZUSP); same data, except: Arredores do Hotel dos Camalotes | 21°42'28"S, 57°35'00"W | 21–30.i.2008 (1 ♂, MZUSP).

Additional examined material. BRAZIL, MS [state of Mato Grosso do Sul]: Porto Murtinho (norte), Estrada para Pirizal, km18, 21°33'05"S, 57°45'35"W, 19–31.i.2008, Nihei, S.; • Figueiredo, R. & Almeida, J. (col.) (2 ♀, MZUSP; 2 ♀, NHMW); same data, except: Trilha Fazenda Campo Florido, 21°41'52,0"S, 57°45'57,1"W, Ativa, 11.xii.2013, Lamas & eq. cols. (4 ♀, two dissected, MZUSP).

Remarks. The new species is easily recognized by the characters presented in the key and diagnosis (see above).

Distribution. Brazil (state of Mato Grosso do Sul) (Fig. 19).

Etymology. From the Tupi-guarani *aysú* = love, referring to the male terminalia, which resembles an ideogram of a heart in dorsal view. The species' name is treated as a noun in apposition.

Cardiasilus dangeloi sp. nov.

https://zoobank.org/1CF4F823-5199-4E5D-9B5F-5145385C99E3

Figs 6–8, 19

Diagnosis. The black postalar macrosetae (Fig. 6B), the epandrium strongly excavated at mid-inner dorsal margin (Fig. 7A, F, H), and the subepandrial sclerite somewhat trapezoidal at middle (Fig. 8D) should promptly distinguish this species from its congeners.

Description. Male (Fig. 6A). Body Length: 13.2 mm; wing length: 7.1 mm. ***Head*** (Fig. 6A–D). Similar to *C. aysu* sp. nov. except as noted: ***Thorax*** (Fig. 6A, B, D) postalar macrosetae black. ***Legs*** (Fig. 6B). **Leg I.** Tibia with posterior row of four long black macrosetae from basal 1/4 to apex. **Leg II.** Femur with anterior row of four strong black macrosetae (basalmost white). Tibia with macrosetae wholly black. **Leg III.** Femur with anteroventral row of short, strong, and sparse black macrosetae (basalmost white). ***Terminalia*** (Figs 7, 8). Similar to *C. aysu* sp. nov., except as noted: Epandrium strongly excavated at mid-inner dorsal margin (Fig. 7A, F); subepandrial sclerite somewhat trapezoidal at its middle (Fig. 8D).

Female. Unknown.

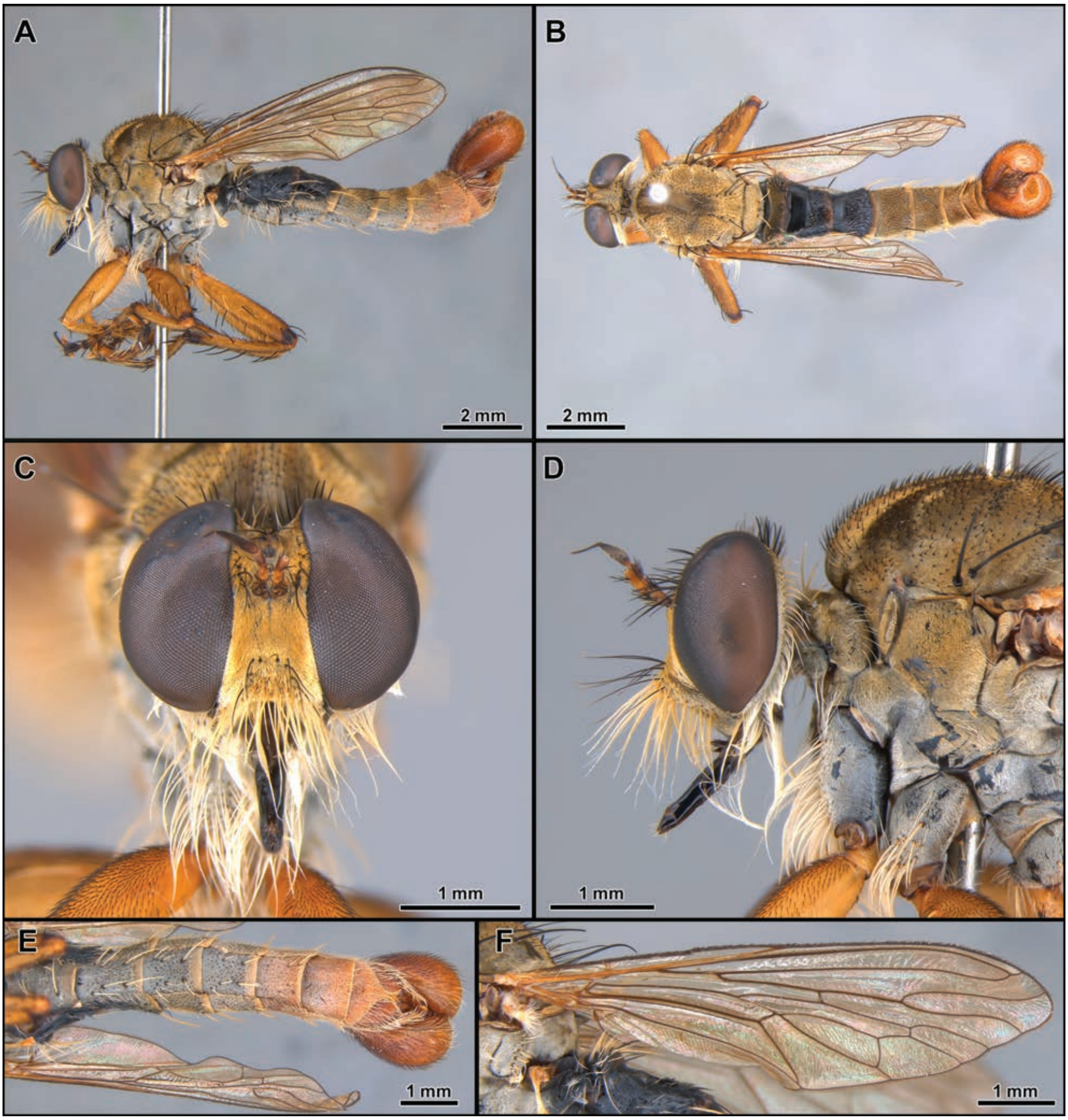

Figure 6. *Cardiasilus dangeloi* sp. nov. (male holotype, before dissection) **A**, **B** habitus lateral and dorsal, respectively **C** head, anterior view **D** head and thorax, lateral view **E** abdomen, ventral view **F** wing.

Type examined material. ***Holotype*** • ♂ (MZUSP) labelled: "BRASIL: MS [state of Mato Grosso do Sul]: Porto Murtinho | Faz. São Fernando – km12 | 21°36'30"S, 57°49'02"W | 19–31.I.2008 | Nihei, S., Figueiredo, R. & Almeida, J. | (col.)" "HOLOTYPE | *Cardiasilus dangeloi* | Soares, Camargo & Lamas [red label]". Holotype condition: Good, left postpedicel broken off, abdomen glued to thorax with remains of glue obscuring pruinosity of tergites one to three, terminalia dissected and stored in microvial at the same pin.

Remarks. The new species is remarkably similar to *C. aysu* sp. nov., differing only in the color of postalar macrosetae black (Fig. 6B), anterior row of macrosetae on mid femur wholly black, only the basalmost macroseta white (Fig. 6A),

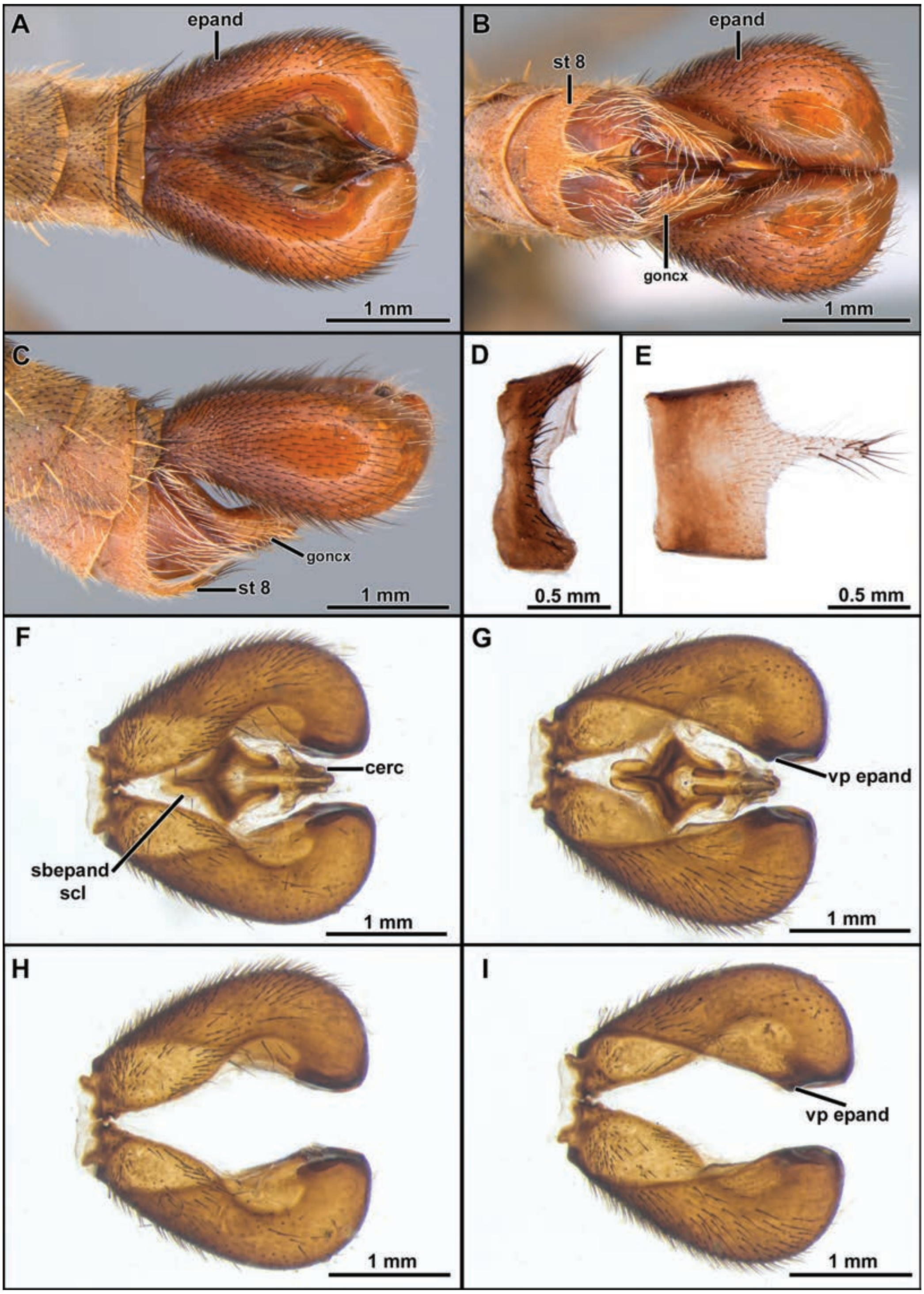

Figure 7. *Cardiasilus dangeloi* sp. nov. (male holotype) **A–C** terminalia in dorsal, ventral, and lateral views, respectively **D** tergite 8 **E** sternite 8 **F, G** dissected terminalia in dorsal and ventral views, respectively **H, I** dissected terminalia without inner appendages in dorsal and ventral views, respectively. Abbreviations: cerc = cercus; epand = epandrium; goncx = gonocoxite; sbepand scl = subepandrial sclerite; st 8 = sternite 8; vp epand = ventral process of epandrium.

epandrium strongly excavated at mid-inner dorsal margin (Fig. 7A, F, H) and subepandrial sclerite somewhat trapezoidal at middle (Fig. 8D). In *C. aysu* sp. nov. the postalar macrosetae are yellow (Fig. 2C), the anterior row of macrosetae on the mid femur is white, the mid-inner dorsal margin of the epandrium is weakly excavated (Fig. 3A) and the subepandrial sclerite is somewhat diamond-shaped

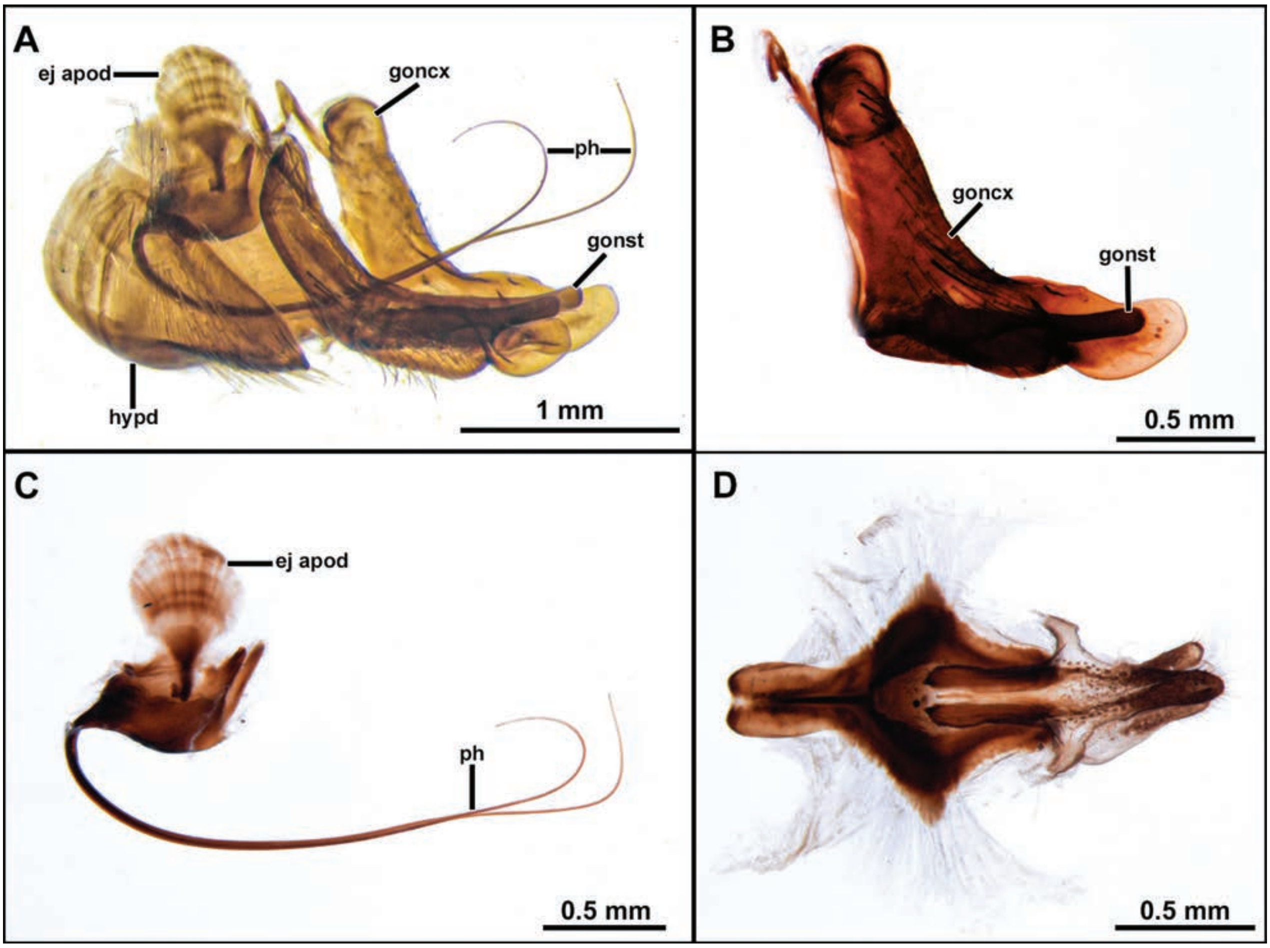

Figure 8. *Cardiasilus dangeloi* sp. nov. (male holotype) **A** inner appendages **B** gonocoxite and gonostylus **C** phallus and ejaculatory apodeme **D** subepandrial sclerite. Abbreviations: ej apod = ejaculatory apodeme; hypd = hypandrium; goncx = gonocoxite; gonst = gonostylus; ph = phallus.

(Fig. 4D). The epandrium strongly excavated medially at inner margin and the lack of a dorsal preapical process also differs *C. dangeloi* sp. nov. from *C. ruda* sp. nov.

Distribution. Brazil (state of Mato Grosso do Sul) (Fig. 19).

Etymology. The new species is named after Gio D'Angelo (INPA), an artist, photographer, and myrmecologist who is the partner of the first author and deeply passionate about scientific illustration. Gio also kindly created the illustration for Fig. 20.

Cardiasilus ruda sp. nov.

https://zoobank.org/00CEB9B1-E2CF-4C9B-B998-C8305DA907BB
Figs 9–11, 19

Diagnosis. The inner margin of epandrium with a short, dorsal, sub-triangular, pre-apical process followed by a short, ventral, sub-rectangular, anteriorly curved, apical process (Fig. 10A, F, G) separates this species from its congeners.

Description. Male (Fig. 9A). Body Length: 10.3 mm; wing length: 5.7 mm. ***Head*** (Fig. 9A–D). Similar to *C. aysu* sp. nov. except as noted: ***Thorax*** (Fig. 9A, B, D). Two pairs of dorsocentral macrosetae. ***Terminalia*** (Figs 10, 11). Epandrium with a short, dorsal, sub-triangular, pre-apical process followed by a short,

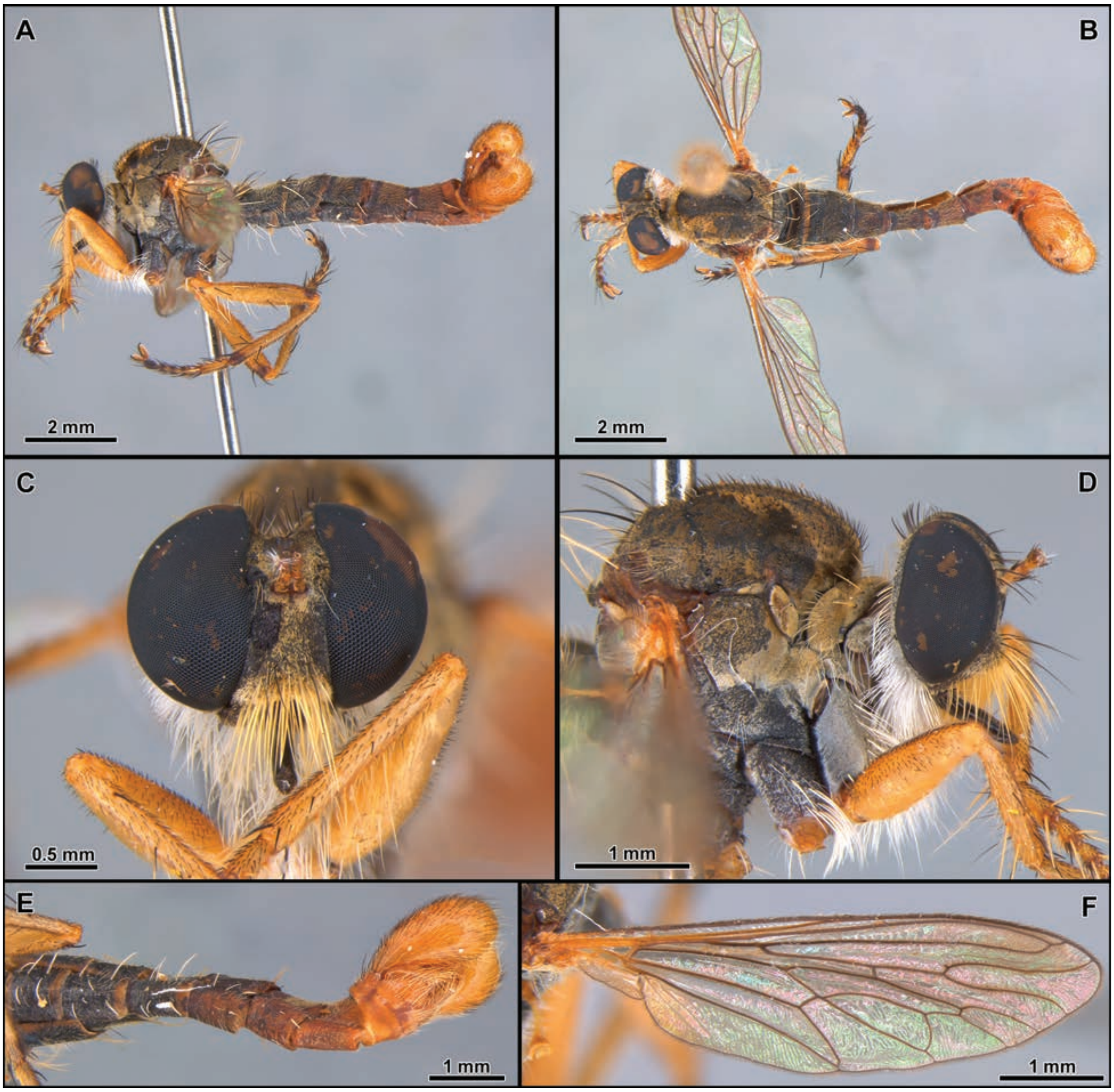

Figure 9. *Cardiasilus ruda* sp. nov. (male holotype, before dissection) **A, B** habitus lateral and dorsal, respectively **C** head, anterior view **D** head and thorax, lateral view **E** abdomen, ventral view **F** wing.

ventral, sub-rectangular, anteriorly curved, apical process (Fig. 10A, F, G). Subepandrial sclerite goblet-shaped (Fig. 11D).

Female. Unknown.

Type examined material. ***Holotype*** • ♂ (MZUSP) labelled: “PARAGUAI | Colônia Pireretá [ca 25°30'09.2"S, 56°59'00.1"W] | 25.xii.1971” “HOLOTYPE | *Cardiasilus ruda* | Soares, Camargo & Lamas [red label]”. Holotype condition: Both postpedicel and mid legs broken off, terminalia dissected and stored in microvial at the same pin.

Remarks. The new species is remarkably similar to *C. aysu* sp. nov., differing only in the shape of epandrium with a short, dorsal, sub-triangular, pre-apical process followed by a short, ventral, sub-rectangular, anteriorly curved, apical process (Fig. 10A, F, G). The epandrium lacks such processes at dorsal inner margin in *C. aysu* sp. nov., and *C. dangeloi* sp. nov.

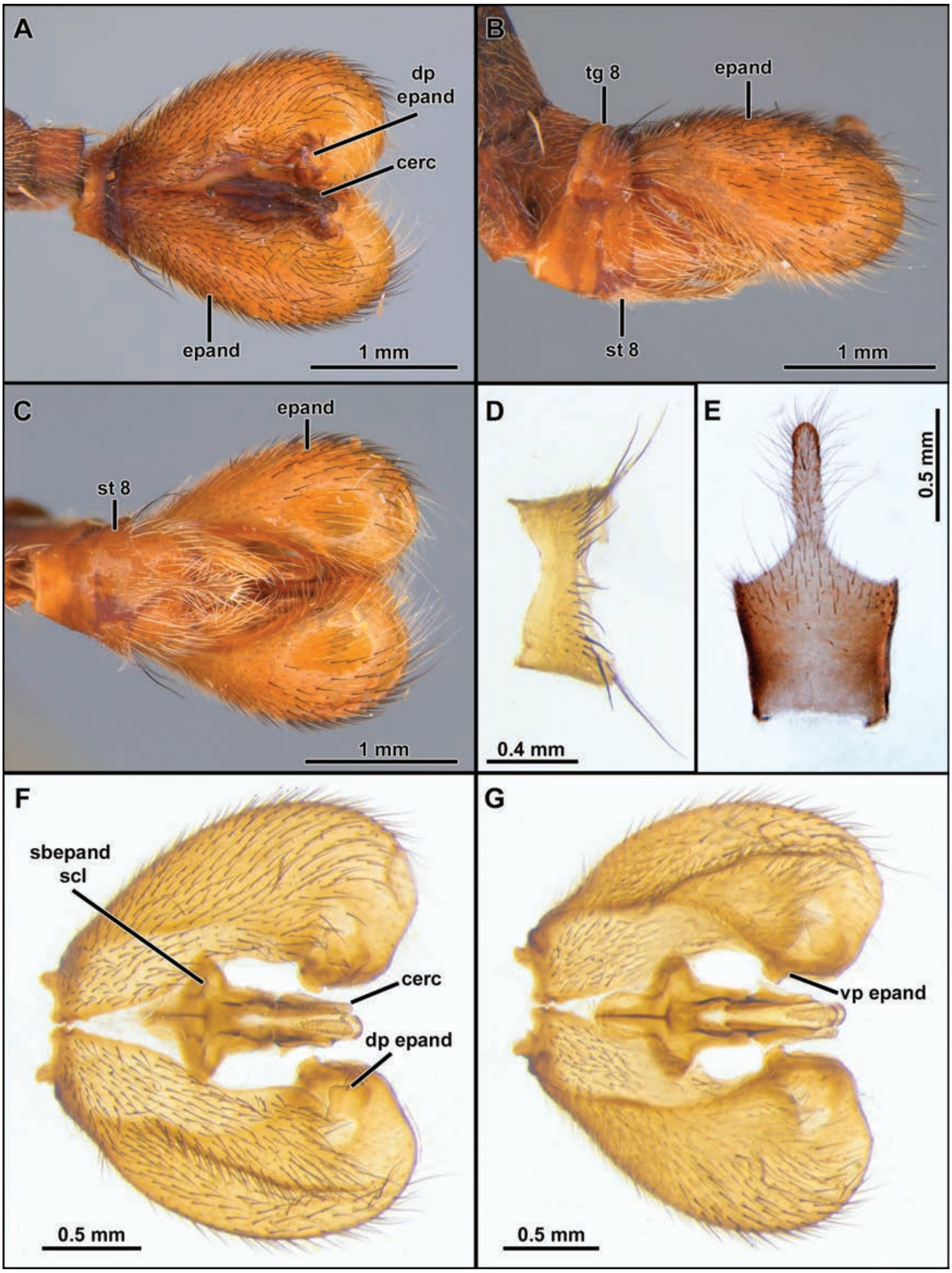

Figure 10. *Cardiasilus ruda* sp. nov. (male holotype) **A–C** terminalia in dorsal, lateral, and ventral views, respectively **D** tergite 8, **E** sternite 8 **F, G** dissected terminalia in dorsal and ventral views, respectively. Abbreviations: cerc = cercus; epand = epandrium; dp epand = dorsal process of epandrium; goncx = gonocoxite; sbepand scl = subepandrial sclerite; st 8 = sternite 8; tg 8 = tergite 8; vp epand = ventral process of epandrium.

Distribution. Paraguay (department of Cordillera) (Fig. 19).

Etymology. Rudá is the deity of love in the pantheon of deities of Tupi-Guarani culture. It alludes to the male epandria that resembles an ideogram of a heart (Fig. 10A). Treated as a noun in apposition.

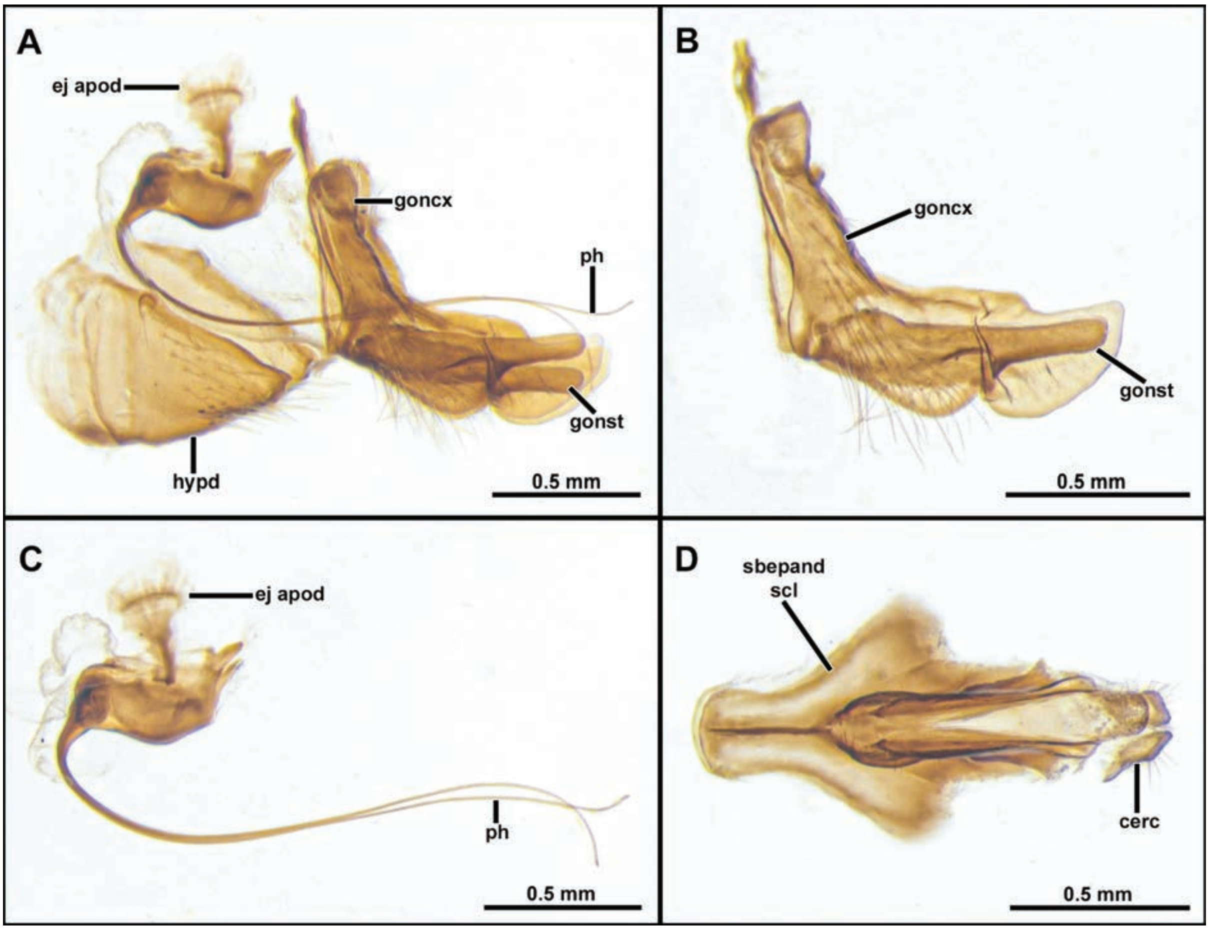

Figure 11. *Cardiasilus ruda* sp. nov. (male holotype) **A** inner appendages **B** gonocoxite and gonostylus **C** phallus and ejaculatory apodeme **D** subepandrial sclerite. Abbreviations: cerc = cercus; ej apod = ejaculatory apodeme; hypd = hypandrium; goncx = gonocoxite; gonst = gonostylus; ph = phallus.

Martintella **Artigas**
Fig. 12

Martintella Artigas, 1996: 75 (*nomen novum* for *Martinella* Artigas & Papavero, 1995). Type species: *Asilus lestes* Williston, 1901 (original designation). Type locality: Mexico, Guerreiro, Chilpancingo

Remarks. The genus *Martintella* was erected to accommodate the species *Asilus lestes* Williston, 1901, at the time placed in *Wilcoxius*. Subsequently, Scarbrough (2010) described the second species, *Martintella elliptica* Scarbrough, 2010, from Trinidad and Tobago. Finally, Vieira et al. (2014) described two new species from Costa Rica, and commented on the possibly dubious position of *Martintella elliptica* in the genus. According to Fisher (2009), species of *Martintella* are similar to those of *Wilcoxius*. However, *Martintella* is easily recognized by the frons with convergent slopes (Fig. 12A), mystax restricted to middle of face, resembling a mohawk (Fig. 12A, B), sternites lacking macrosetae, and phallus completely concealed versus frons with parallel slopes (Fig. 18D), mystax not restricted to the middle of face and not resembling a mohawk (Fig. 18D), sternites two to five with one to two pairs of macrosetae (Fig. 18E), and phallus exposed (Fig. 18F).

Distribution. Costa Rica, Mexico, and Trinidad and Tobago.

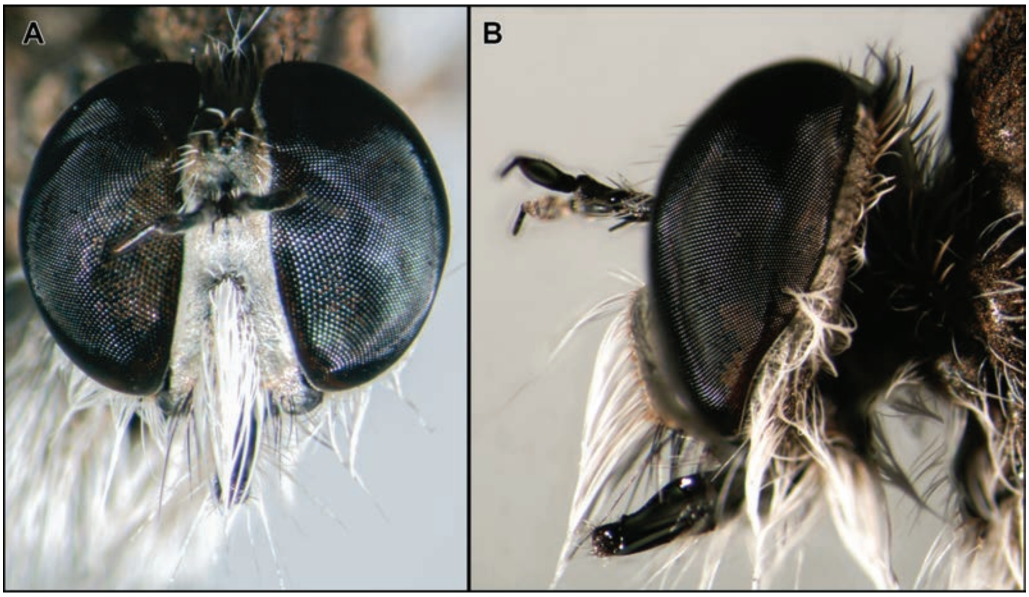

Figure 12. *Martintella* sp. (male from Mexico) **A, B** Head in anterior and lateral views, respectively. Photographs provided by Frida Bello (INECOL).

Myaptex Hull

Figs 13, 14

Myaptex Hull, 1962 (2): 508. Type species, *Myaptex hermanni* Hull, 1962 (original designation). Type locality: Chile, Concepción.

Remarks. *Myaptex* is endemic to Chile and comprises only two species (Papavero 2009). The genus resembles *Myaptexaria* by the face distinctly gibbous, scutum with conspicuous rows of acrostichal setae and anterior dorsocentral macrosetae present, but can be easily segregated by the scutellar disc only with scattered, long setae (Fig. 13B); normally two to four black apical scutellar macrosetae; male terminalia with epandria strongly inflated, their apices curved in apically (Figs 13F, 14A–D) in *Myaptex* versus scutellar disc with two tufts of abundant, proclinate, long setae (Fig. 15B, C), from two to several apical scutellar macrosetae (sometimes mixed black and white) (Fig. 15C), male terminalia with epandria not inflated, their apices blunt and not curved at apex (Fig. 15F) in *Myaptexaria*. *Myaptex* is also superficially similar to *Cardiasilus* gen. nov. (see remarks under *Cardiasilus* gen. nov.), but the only feature they both share is the inflated male epandria (a feature that probably arose independently *de novo* in both genera).

Distribution. Chile.

Examined material. CHILE, Maule, Cauquenes, 25.i.1955, L.E. PENA (1 ♂, dissected MZUSP).

Myaptexaria Artigas & Papavero

Fig. 15

Myaptexaria Artigas & Papavero, 1995: 58. Type species: *Myaptex vexillaria* Artigas, 1970 (original designation). Type locality: Chile, Coquimbo, Vicuña.

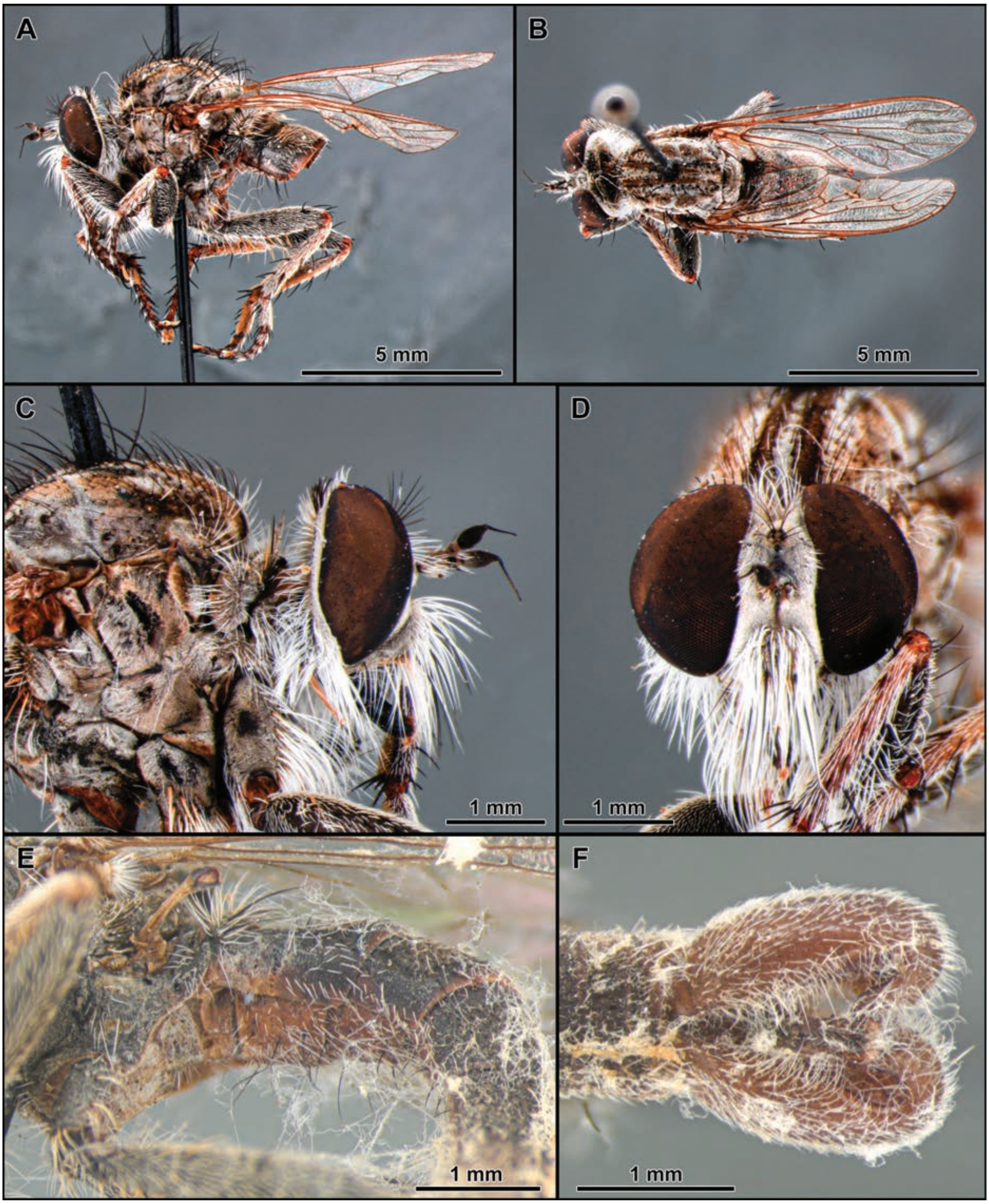

Figure 13. *Myaptex brachyptera* (Philippi, 1865) (identified male from Chile) **A, B** habitus lateral and dorsal, respectively, **C** head and thorax, lateral view **D** head, anterior view **E** abdomen, lateroventral view **F** terminalia, dorsal view.

Remarks. *Myaptexaria* was erect to accommodate three species placed in *Myaptex*: *M. acuta* (Artigas), *M. vexillaria* (Artigas) (type-species) and *M. virilis* (Artigas). Both genera can be easily segregated by the shape of male epandria (as discussed above under remarks of *Myaptex*).

Distribution. Chile.

Examined material. Chile, Coquim. [Coquimbo] Had [Hacienda] Illapel, 600–1000 m, 24–25.x.1954, L.E. PENA (1 ♂, 2 ♀, MZUSP).

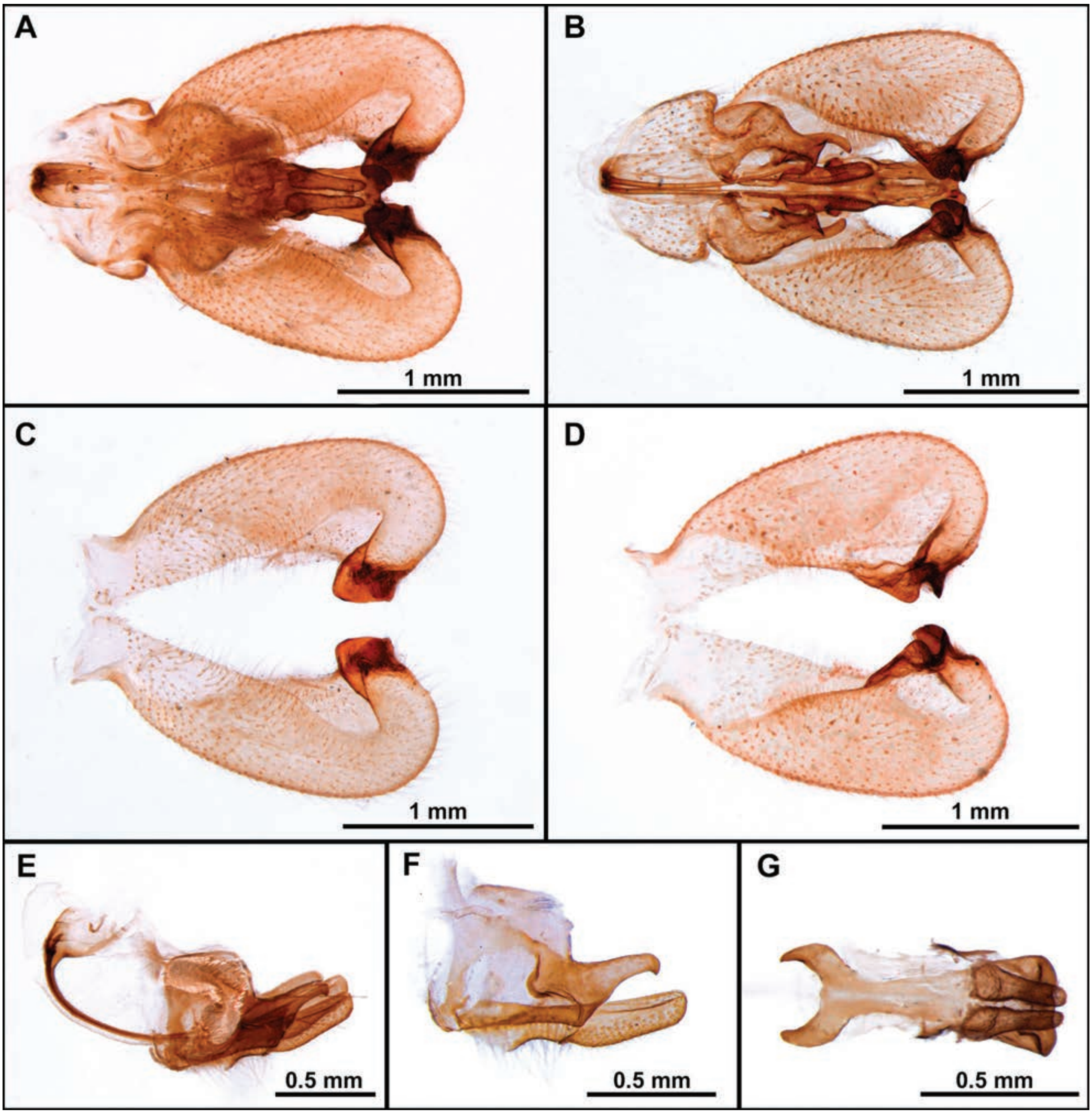

Figure 14. *Myaptex brachyptera* (Philippi, 1865) (identified male from Chile) **A, B** Terminalia in dorsal and ventral views, respectively **C, D** terminalia without inner appendages in dorsal and ventral views, respectively **E** inner appendages, lateral view **F** gonocoxite and gonostylus, lateral view **G** cercus and subepandrial sclerite, dorsal view.

Papaverellus Artigas & Vieira

Papaverellus Artigas & Vieira, 2014: 283. Type species: *Papaverellus aureocingulatus* Artigas & Vieira, 2014 (original designation). Type locality: Brazil, state of Pará, Belém.

Remarks. The monotypic genus *Papaverellus* shares one similarity with *Cardiasilus* gen. nov., the bifurcation of veins R_4 and R_5 before the apex of discal cell (Artigas and Vieira 2014: fig. 5). However, both genera can be distinguished by the abdominal sternites without macrosetae (Artigas and Vieira 2014: fig. 1)

Figure 15. *Myaptexaria vexillaria* Artigas, 1970 (male paratype) **A, B** habitus lateral and dorsal, respectively **C** head and thorax, lateral view **D** head, anterior view **E** abdomen, ventral view **F** terminalia, lateral view.

and epandria not inflated and flat ventrally, resembling a goat hoof (Artigas and Vieira 2014: fig. 1) in *Papaverellus*, whereas *Cardiasilus* gen. nov. has the abdominal sternites with at least three pairs of macrosetae (Figs 2H, 6E, 9E) and male epandria inflated resembling the ideogram of a heart (i.e., Figs 2B, H, 3A, C).

Distribution. Brazil (states of Pará and Piauí).

Rhadinosoma **Artigas**
Fig. 16

Rhadinosoma Artigas, 1970: 346. Type species: *Rhadinosoma calderense* Artigas, 1970 (original designation). Type locality: Chile, Atacama.

Remarks. The monotypic genus *Rhadinosoma* is also known to occur only in Chile. It can be easily segregated from the other genera of the *Myaptex* group by the characteristics presented in the key above, mainly the mystax composed of few sparse macrosetae (Fig. 16C, D) and the vein R_4 ending at wing apex (Fig. 16B).

Distribution. Chile.

Examined material (based on photographs). CHILE, Atacama, Prov. 70 km. S. Copiapo, X–5–1966, E.I. Schlinger, M.E. Irwin, dune Assoc. (1 ♀, CAS).

Scarbroughia **Papavero**
Fig. 17

Scarbroughia Papavero, 2009: 46 (nomen novum for *Furcilla* Martin, 1975). Type species: *Furcilla dorothyae* Martin, 1975 (original designation). Type locality: Mexico, Sonora.

Remarks. The genus *Scarbroughia* comprises two species from Sonora, Mexico, and can be segregated by the mystax composed of abundant and dense macrosetae (Fig. 17C, D), face flat (Fig. 17C), well-developed anterior dorsocentral macrosetae absent (Fig. 17A) and the vein R_4 ending above wing apex (Fig. 17B).

Distribution. Mexico.

Examined material (based on photographs). Mexico, 11 mi. South Navojos, Sonora, Hy. 15 Km. 1766, Sept. 3, 1962, Holotype Furcilla dorothyae Cash. H. Martin, California Academy of Sciences, Type No. 12579 (1 ♂, CAS).

Wilcoxius **Martin**
Fig. 18

Wilcoxius Martin, 1975: 71. Type species: *Wilcoxius truncus* Martin, 1975 (original designation). Type locality: Mexico, Veracruz.

Remarks. According to Fisher (2009) the genus *Wilcoxius* is similar to *Martintella* (see remarks under *Martintella*), but both genera can be promptly distinguished by frons with parallel slopes (Fig. 18D), mystax restricted to the lower 1/2 of face and composed of sparse setae (Fig. 18C, D), abdominal sternites with macrosetae (Fig. 18E) and phallus exposed (Fig. 18F) versus frons with convergent slopes (Fig. 12A), mystax occupying 2/3 of face and restricted to the middle of face, resembling a mohawk (Fig. 12A, B), abdominal sternites

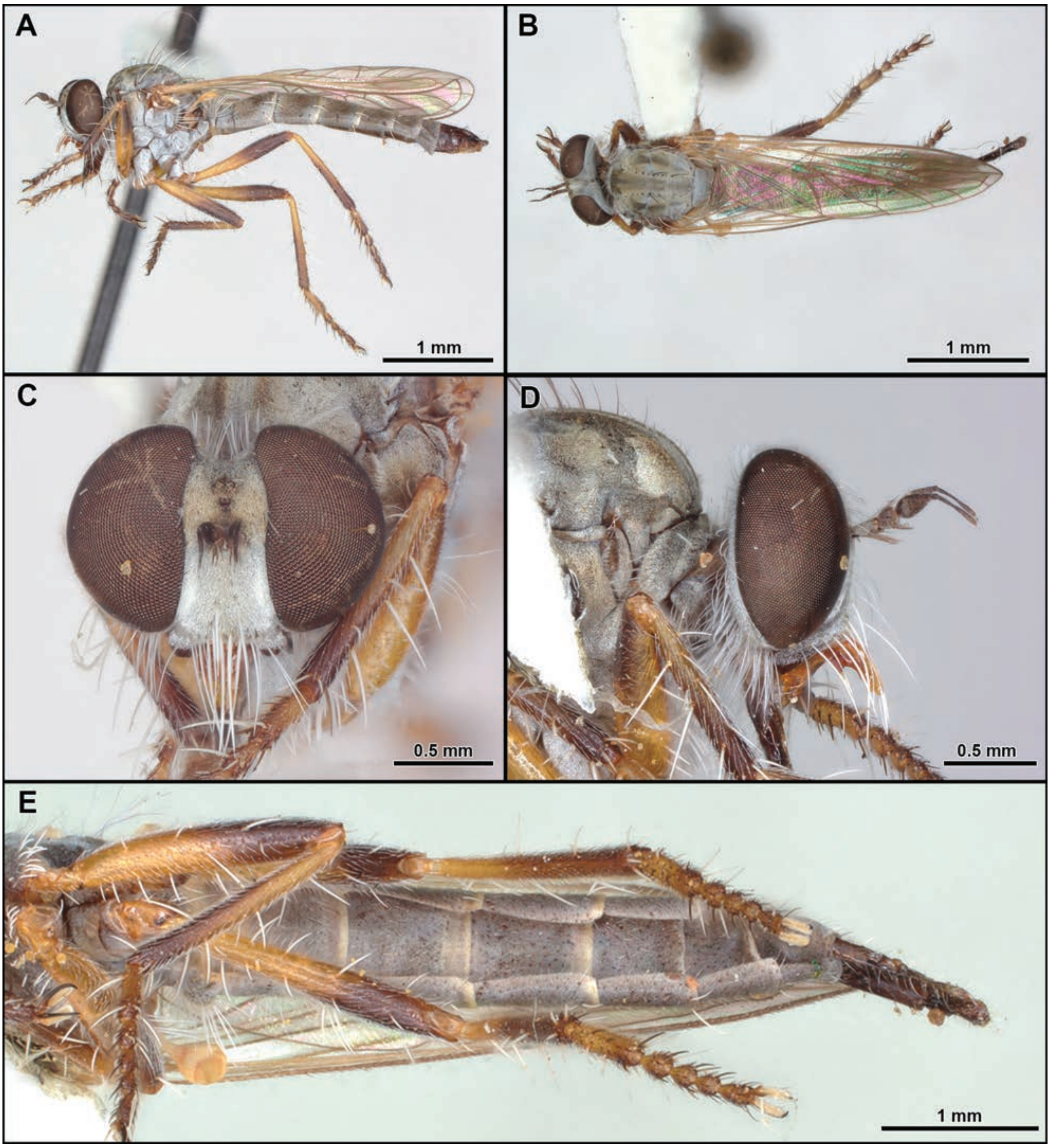

Figure 16. *Rhadinosoma* sp. (female from Chile) **A, B** habitus lateral and dorsal, respectively **C** head, anterior view **D** head and thorax, lateral view **E** abdomen, ventral view. Photographs provided by Denise Montelongo (CAS).

without macrosetae (Vieira et al. 2014: figs 1, 17, 29) and phallus concealed (Vieira et al. 2014: figs 1, 17, 29) in *Martintella*.

Distribution. Cuba, Dominican Republic, El Salvador, Guatemala, Honduras, Mexico, and Nicaragua.

Examined material. Mexico, 40 mi E, Tehuantepec, Oax. 3.viii.1967, Altitude 500ft., RH & EM Painter collectors, PARATYPE, Wilcoxius truncus, Chas. H. Martin (1 ♂, MZUSP).

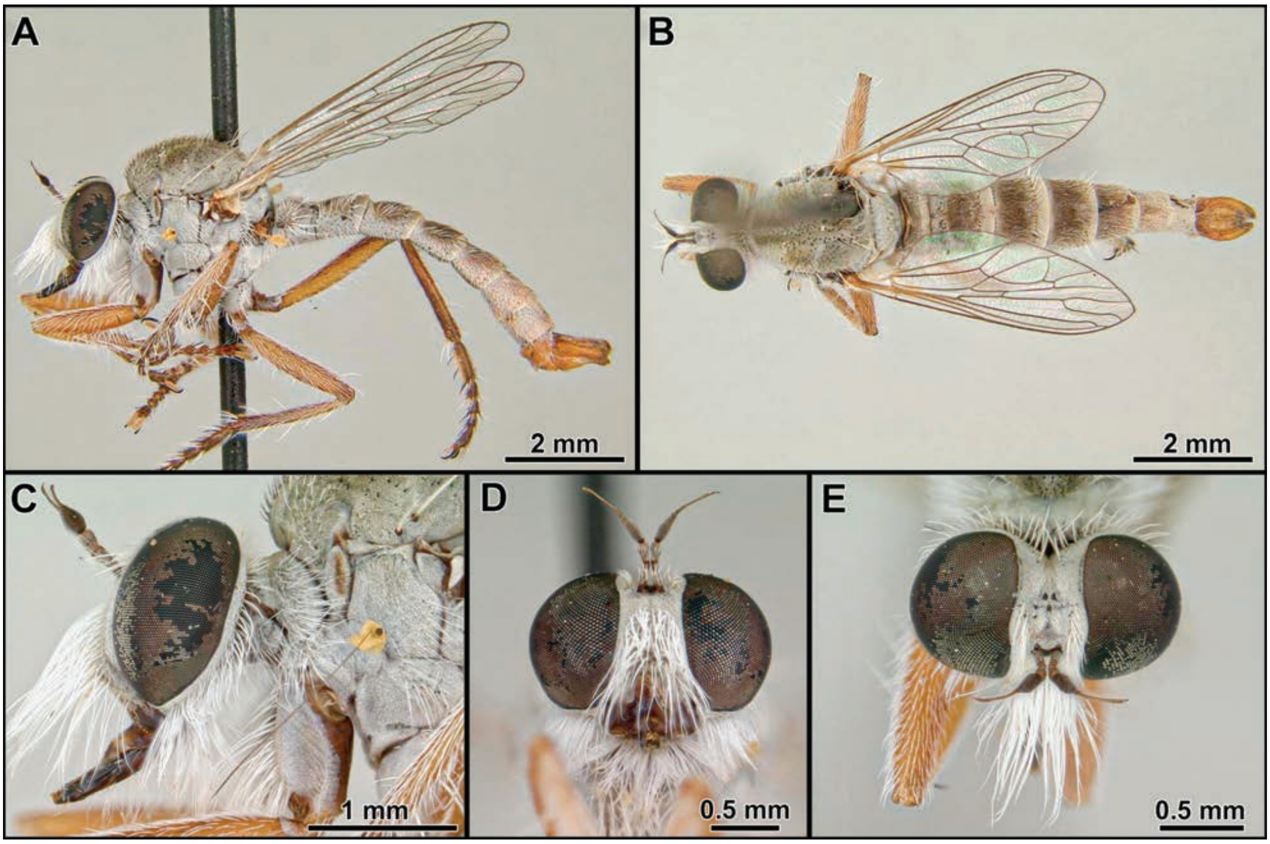

Figure 17. *Scarbroughia dorothyae* (Martin, 1975) (male holotype) **A, B** habitus lateral and dorsal, respectively **C** head, lateral view **D** face, anterior view **E** frons, anterior view. Photographs provided by Christopher Grinter (CAS).

Discussion

Using the adapted key for genera of the *Myaptex* group provided in Camargo et al. (2022) *Cardiasilus* gen. nov. will key out to *Papaverellus* due to the bifurcation of the veins R_4 and R_5 before the apex of the discal cell (on couplet 5 of Camargo et al. (2022) key, where it says "Mystax with abundant bristles occupying 3/4 of face" it should be "Mystax occupying the entire facial gibbosity"). Despite of this similarity on the wing pattern, specimens herein studied can be easily segregated from *Papaverellus* due to the inflated heart ideogram-shaped epandria (flat ventrally, and resembling a goat hoof in *Papaverellus*) and the presence of paired well-developed macrosetae on the sternites 2–7 (sternites without well-developed macrosetae in *Papaverellus*).

Regarding the short recurrent (stump) vein on R_4 that arises close to the origin of R_5 and is presented here as a diagnostic character for *C. ruda* sp. nov., caution is warranted in interpreting this feature. Additional specimens should be collected and examined to verify the diagnostic significance of this character, as the presence or absence of stump veins often demonstrates high variation within the Asilinae genera or species. To illustrate this scenario in the *Myaptex* group, the male paratype of *Martintella elliptica*, provides an example where the recurrent vein is present on the right wing but absent on the left wing (see Vieira et al. 2014: 453, fig. 8). Similarly, in *Apulvillasilus*, the recurrent vein is absent on the male holotype but present on the female paratype (see Camargo et al. 2022: 4, 7, figs 2, 6, 19).

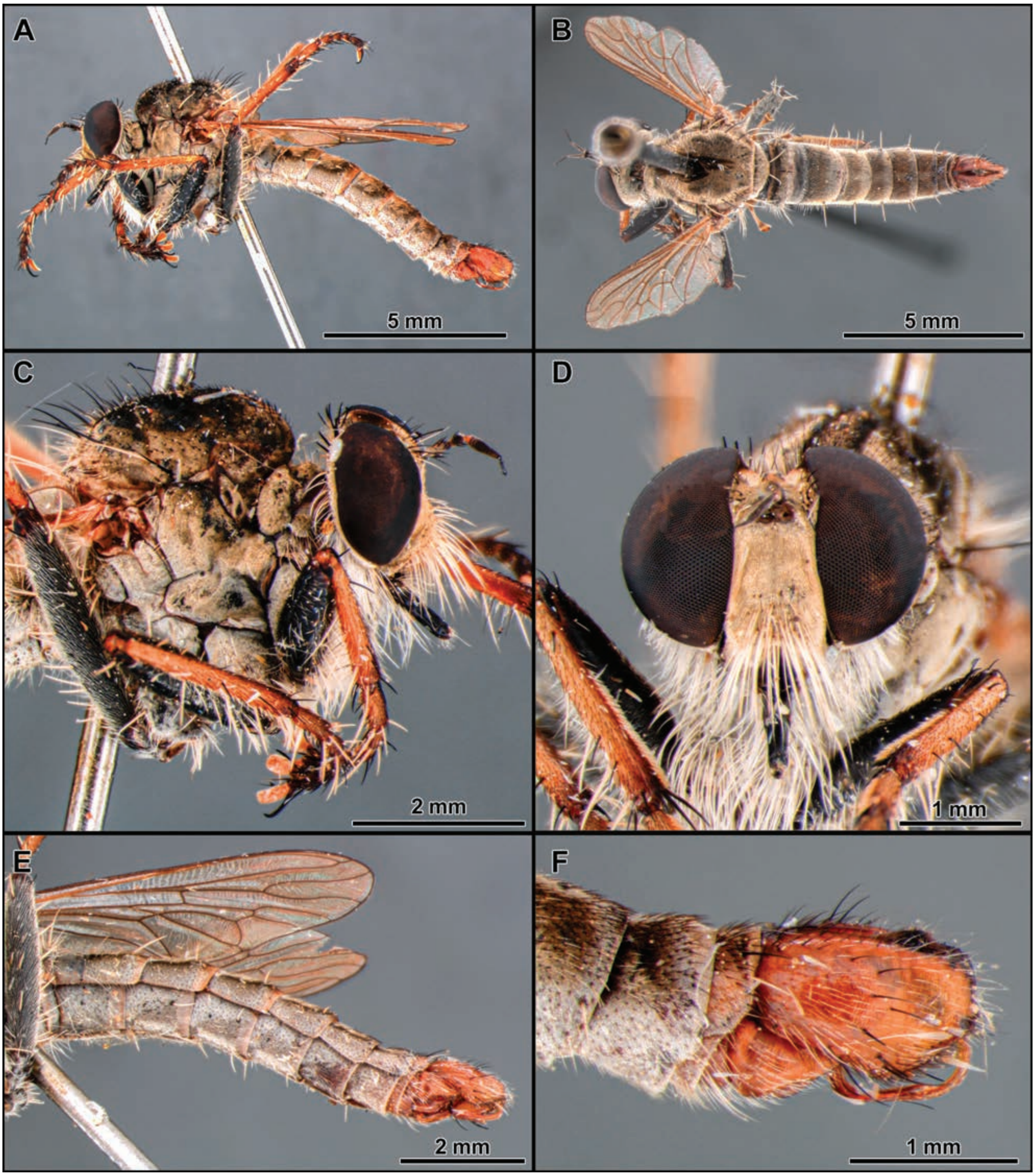

Figure 18. *Wilcoxius truncus* (Martin, 1975) (male holotype) **A, B** habitus lateral and dorsal, respectively **C** head and thorax, lateral view **D** head, anterior view **E** abdomen, lateroventral view **F** terminalia, lateral view.

Cardiasilus gen. nov. is until now known only from the localities of Porto Murtinho, Mato Grosso do Sul state, Brazil, and Colonia Piraretã, Cordillera Department, Paraguay. Both localities are in the eastern side of the Paraguay river in a region that has been historically denominated as part of the "eastern" or "humid chaco". This terminology is currently being considered an unsuitable designation that does not reflect the reality of this region, shaped of a mosaic of ecoregions with a number of widely different florist communities dominated by semi-dry and

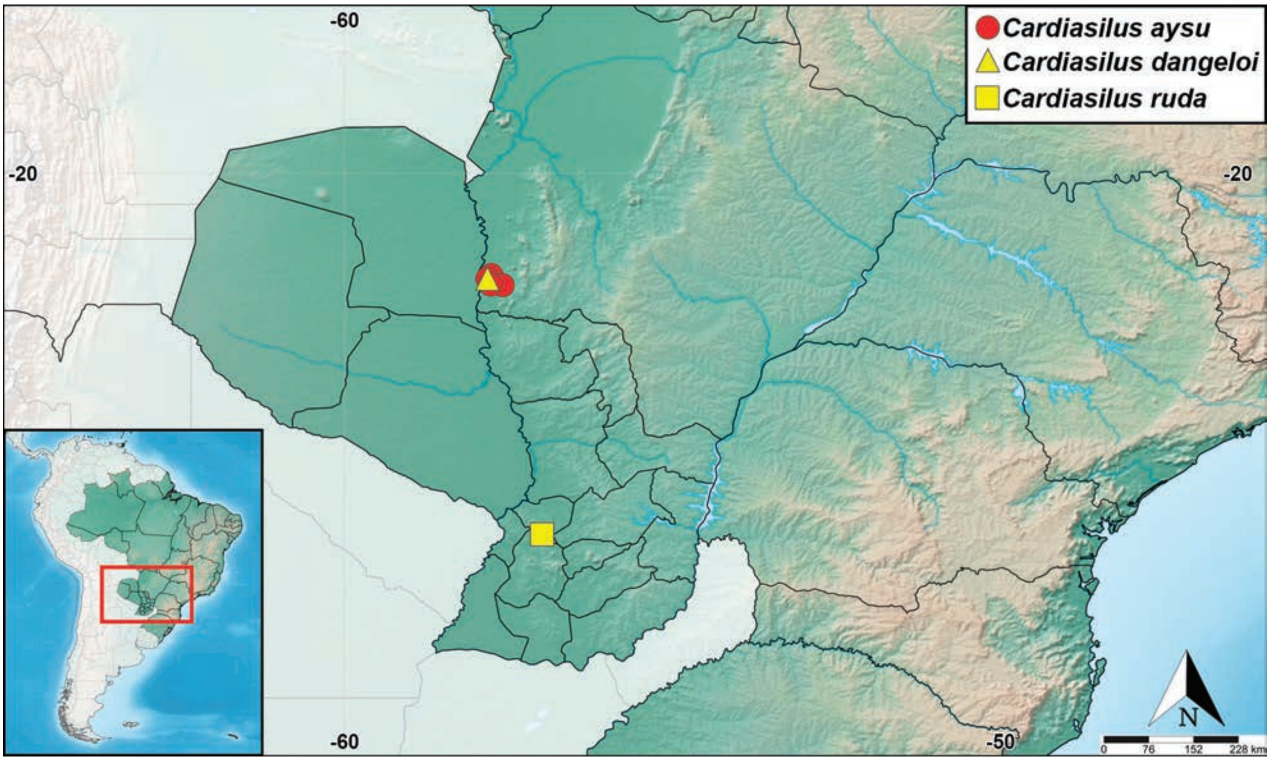

Figure 19. Known geographical distribution of *Cardiasilus* gen. nov. species.

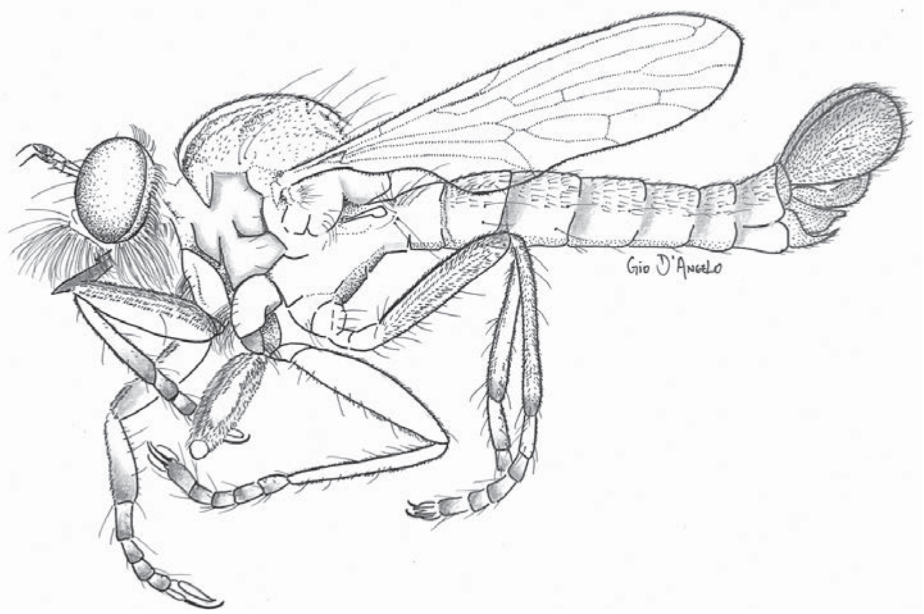

Figure 20. Illustration of *Cardiasilus dangeloi* gen. nov. et sp. nov.

semi-deciduous seasonal forests with interspersed intrusions and islands of "chaquenian", vegetation elements delimited mainly by the different types of soil (Prado et al. 1992; Prado 1993; Avila et al. 2018; Garcete-Barrett *in litt.*).

The Piraretã region is located in the "Cordillera de Los Altos" ecoregion (Avila et al. 2018) and is currently highly anthropized. However, its original vegetation must have been composed mainly of elements from the semi-deciduous Paraná forest, with rocky outcrops in the Saltos de Piraretã region and with "chaquenian" influence in the lower parts (Garcete-Barrett *in litt.*). The portion of the “humid chaco” assigned to Brazil is restricted to the surroundings of Porto Murtinho, which is also a place where different floristic stocks meet (Prado et al. 1992; Prado 1993). In the present study, specimens were collected in areas with open Arborized Stepic Savannah. It is herein postulated that the new genus might be endemic of the mosaic “humid chaco” region along the Paraguay river. Additionally, several Malaise samples collected in localities in Goiás state (which borders) Mato Grosso do Sul state containing huge amounts of Asilidae specimens were analyzed by the first author and not even a single specimen of the new genus was found reinforcing the endemism assumption.

The present paper represents an important contribution to the knowledge of the Chaco biome biodiversity. Recent taxonomic studies of the Diptera fauna in the Chaco domain (Lamas et al. 2015; Riccardi et al. 2018; Quevedo et al. 2024) in Porto Murtinho (Mato Grosso do Sul, Brazil) have revealed a high degree of endemism among Diptera in this region. Many of the samples collected (Lamas et al. 2023) represent new taxa that are not merely new species within known genera; their striking divergence in certain morphological traits suggests the establishment of new genera. This study includes the first recorded instance for the family Asilidae, with all examined material sourced from the humid chaco regions of Brazil and Paraguay. The identification of these previously unknown and unusual Diptera emphasizes the urgent need for international efforts to study and preserve the South American Chaco.

Acknowledgments

We thank Bolivar Rafael Garcete-Barrett for the sharing his knowledge and information regarding the ecoregions of Oriental Paraguay. We are grateful to Christopher Grinter and Denise Montelongo (CAS) for photographs of *Rhadinosoma* sp. and *Scarbroughia dorothyae* housed at CAS collection and Frida Bello (INECOL) for photographs of *Martintella* sp. from Mexico. Rodrigo Vieira (SEDUC/AM) and Pável Sánchez (MUSM) offered useful suggestions to earlier versions of the manuscript.

Additional information

Conflict of interest

The authors have declared that no competing interests exist.

Ethical statement

No ethical statement was reported.

Funding

We thank Fundação de Amparo à Pesquisa do Estado de São Paulo (FAPESP, Brazil) (proc. n. 2023/17951-0 (post-doctoral fellowship grant to MMMS); 2010/52314-0 and 2022/12640-3 to CJEL) and the Conselho Nacional de Desenvolvimento Científico e Tecnológico (CNPq, Brazil) for financial support to CJEL (proc. n. 563256/2010-9 and 310997/2023-2).

Author contributions

Conceptualization: MMMS, AC. Funding acquisition: CJEL. Investigation: MMMS. Methodology: MMMS. Resources: CJEL. Writing - original draft: CJEL, AC, MMMS. Writing - review and editing: MMMS, AC, CJEL.

Author ORCIDs

Matheus M. M. Soares https://orcid.org/0000-0002-2355-1441
Alexssandro Camargo https://orcid.org/0000-0001-7408-7223
Carlos J. E. Lamas https://orcid.org/0000-0002-7750-590X

Data availability

All of the data that support the findings of this study are available in the main text.

References

Artigas JN (1970) Los asilidos de Chile (Diptera – Asilidae). Gayana Zoología 17: 1–472. https://biostor.org/reference/100772

Artigas JN (1996) *Martintella*, a new name for *Martinella* Artigas & Papavero, 1995 (Diptera, Asilidae). Boletín de la Sociedad de Biología de Concepción 67: 75. https://biostor.org/reference/128079

Artigas JN, Papavero N (1995) The American genera of Asilidae (Diptera): Keys for identification with an atlas of female spermathecae and other morphological details. IX.9. Subfamily Asilinae leach—*Myaptex*—group, with the proposal of two new genera and a catalogue of the Neotropical species. Revista Chilena de Entomología 22: 55–73. https://biostor.org/reference/106237

Artigas JN, Papavero N (1997) The American genera of Asilidae (Diptera): Keys for identification with an atlas of female spermathecae and other morphological details. IX.1. Subfamily Asilinae leach (including Apocleinae Lehr): key to generic group. Arquivos de Zoologia Do Estado de São Paulo 34(2): 57–63. https://doi.org/10.11606/issn.2176-7793.v34i1-4p57-63

Artigas JN, Vieira R (2014) New genus and species of Neotropical robber flies (Diptera, Asilidae, Asilinae). Zootaxa 3774(3): 282–288. https://doi.org/10.11646/zootaxa.3774.3.5

Avila TI, D'Elía G, Vogt C, Garcete-Barrett BR (2018). Análisis crítico de la biogeografía del Paraguay. Reportes Científicos de la FACEN 9(1): 42–50. https://doi.org/10.18004/rcfacen.2018.9.1.42

Camargo A, Vieira R, Fisher E (2022) A unique robber fly species and genus of Asilinae from Argentina (Diptera: Asilidae). Austral Entomology 61(4): 407–419. https://doi.org/10.1111/aen.12619

Camargo A, Vieira R, Rafael JA (2023) Taxonomic review of *Ctenodontina* Enderlein, 1914 with the revalidation of *Catostola* Hull, 1958 (Diptera: Asilidae: Asilinae) and description of a new species. Zootaxa 5276(1): 1–71. https://doi.org/10.11646/zootaxa.5276.1.1

Cumming JM, Wood DM (2017) Adult morphology and terminology. In: Kirk-Spriggs AH, Sinclair BJ (Eds) Manual of Afrotropical Diptera. Volume 1. Introductory chapters and keys to Diptera families, Suricata, Vol. 4. South African National Biodiversity Institute, Pretoria, 89–133.

Dikow T (2020) Asiloid Flies. Asilidae generic classification sensu Dikow 2009. https://asiloidflies.si.edu/asilidae-generic-classification-dikow2009 [accessed 20 November 2024]

Fisher E (2009) Asilidae (Robber flies, Assassin flies, Moscas Cazadoras, Moscas Ladronas) [Chapter] 45. In: Brown BV, Borkent A, Cumming JM, Wood DM, Woodley NE, Zumbado MA (Eds) Manual of Central American Diptera. Volume 1. National Research Council Research Press, Ottawa, Ontario, Canada, 585–632.

Hull FM (1962) Robber flies of the world. The genera of the family Asilidae. Bulletin of the United States National Museum 294(1): 1–432, (2): 433–907. https://doi.org/10.5479/si.03629236.224

Lamas CJE, Falaschi RL, Evenhuis NL (2015) A new genus and species of micro bee flies from Brazil (Diptera: Mythicomyiidae: Psiloderoidinae). Zootaxa 3955(3): 403–416. https://doi.org/10.11646/zootaxa.3955.3.7

Lamas CJE, Fachin DA, Falaschi RL, Alcantara DMC, Ale-Rocha R, Amorim DS, Araújo MX, Ascendino S, Baldassio L, Bellodi CF, Bravo F, Calhau J, Capellari RS, Carmo-Neto AM, Cegolin BM, Couri MS, Carvalho CJB, Dios RVP, Falcon AVG, Fusari LM, Garcia CA, Gil-Azevedo LH, Gomes MM, Graciolli G, Gudin FM, Henriques AL, Krolow TK, Mendes LL, Limeira-de-Oliveira F, Maia VC, Marinoni L, Mello RL, Mello-Patiu CA, Morales MN, Oliveira SS, Patiu C, Proença B, Pujol-Luz CVA, Pujol-Luz JR, Rafael JA, Riccardi PR, Rodrigues, JPV, Roque FO, Sallum MAM, Santis MD, Santos CMD, Santos JR, Savaris M, Shimabukuro PHF, Silva VC, Schelesky-Prado DC, Silva-Neto AM, Camargo A, Sousa VR, Urso-Guimarães MV, Wiedenbrug S, Yamaguchi C, Nihei SS (2023) The SISBIOTA-Diptera Brazilian Network: A long-term survey of Diptera from unexplored Brazilian Western Arc of Amazon, Cerrado and Pantanal. Revista Brasileira de Entomologia 67(4): 1–19. https://doi.org/10.1590/1806-9665-rbent-2023-0051

Latreille PA (1802) Histoire naturelle, générale et particulière, des crustacés et des insectes. Tome troisième. Dufart, Paris, xii + 13–467 + 1 pp. https://doi.org/10.5962/bhl.title.15764

Martin CH (1975) The generic and specific characters of four old and six new Asilini genera in the western United States, Mexico and Central America (Diptera: Asilidae). Occasional papers of the California Academy of Sciences 119: 1–107. https://biostor.org/reference/105234

Papavero N (2009) Catalogue of Neotropical Diptera. Asilidae. Neotropical Diptera 17: 1–178.

Prado DE (1993) What is the Gran Chaco vegetation in South America? I. A review. Contributions to the study of flora and vegetation of the Chaco. V. Candollea 48: 145–172.

Prado DE, Gibbs PE, Pott A, Pott VJ (1992) The Chaco-Pantanal transition in southern Mato Grosso, Brazil. In: Furley PA, Proctor J, Ratter JA (Eds) Nature and dynamics of forest-savanna boundaries. Chapman & Hall, London, xxi + 616 pp.

Quevedo L, Capellari RS, Lamas CJE (2024) A new monotypic genus of Dactylomyiini (Diptera: Dolichopodidae: Neurigoninae) from the Brazilian Chaco, with a discussion on the evolution of the lateral epandrial lobe. Zootaxa 5403(3): 346–356. https://doi.org/10.11646/zootaxa.5403.3.4

Riccardi PR, Bazyar Z, Lamas CJE (2018) New genus of the subfamily Oscinellinae from Brazil (Diptera: Chloropidae). Zootaxa 4438(2): 394–400. https://doi.org/10.11646/zootaxa.4438.2.13

Scarbrough AG (2010) A new species of *Martintella* Artigas, 1996 from the islands of Tobago and Trinidad (Diptera: Asilidae). Transactions of the American Entomological Society 136 (1+2): 193–198. https://doi.org/10.3157/061.136.0206

Shorthouse DP (2010) SimpleMappr, a web-enabled tool to produce publication-quality point maps. Online. http://www.simplemappr.net [accessed 20 November 2024]

Vieira R, Rafael JA, Fisher EM (2014) Two new species of *Martintella* Artigas, 1996 (Diptera, Asilidae, Asilinae) from Costa Rica. Zootaxa 3878(5): 451–461. https://doi.org/10.11646/zootaxa.3878.5.3

Williston SW (1901) Supplement (part), 249–332 pp. In: Godman FD, Salvin O (Eds) Biologia centraliamericana. Zoologia-Insecta-Diptera, London, 378 pp. [6 pls]

ZooKeys 1232: 343–355 (2025)
DOI: 10.3897/zookeys.1232.146855

Research Article

Description of three new species of Spartaeini (Araneae, Salticidae, Spartaeinae) from China and Malaysia

Yi Ni[1,2], Kun Yu[1,2], Junxia Zhang[1,2]

1 Key Laboratory of Zoological Systematics and Application, College of Life Sciences, Hebei University, Baoding, Hebei 071002, China
2 Hebei Basic Science Center for Biotic Interaction, Hebei University, Baoding, Hebei 071002, China
Corresponding author: Junxia Zhang (jxzhang1976@163.com)

Abstract

Three new species of Spartaeini from China and Malaysia are described: *Calxattus dengba* **sp. nov.** (♂), *Spartaeus siloi* **sp. nov.** (♂♀), and *Taraxella chrisfehni* **sp. nov.** (♂♀). *Calxattus dengba* is the second discovered species of the genus in the world. The genus *Taraxella* is illustrated with a colour plate for the first time.

Key words: Basal lineages, jumping spider, morphology, taxonomy

Academic editor: Zhiyuan Yao
Received: 15 January 2025
Accepted: 25 February 2025
Published: 20 March 2025

ZooBank: https://zoobank.org/5778FBF6-2A76-4E42-A5A7-FA79CBAF56B9

Citation: Ni Y, Yu K, Zhang J (2025) Description of three new species of Spartaeini (Araneae, Salticidae, Spartaeinae) from China and Malaysia. ZooKeys 1232: 343–355. https://doi.org/10.3897/zookeys.1232.146855

Introduction

The family Salticidae is renowned for its remarkable species diversity, largely attributed to the subfamily Salticinae, which comprises over 6000 of the nearly 7000 known salticid species (WSC 2025). In contrast, the remaining six salticid subfamilies, often referred to as the “basal lineages”, consist of only a few hundred species across approximately 50 genera (Maddison 2015; WSC 2025). Among these, the tribe Spartaeini of the subfamily Spartaeinae is the most diverse, yet it only includes 134 species in 19 genera, all restricted to the Old World (WSC 2025). Notably, 11 of these genera have not had any new species discovered in the last decade (WSC 2025), likely due to insufficient exploration of those areas. The latest species described for the genera *Taraxella* Wanless, 1984 and *Holcolaetis* Simon, 1886 date back to the 1980s (Wanless 1985, 1987). Furthermore, most genera within this tribe exhibit relatively low species diversity, with about one-third being oligotypic or monotypic. Examples include *Wanlessia* Wijesinghe, 1992 (2 spp.), *Veissella* Wanless, 1984 (2 spp.), *Sparbambus* Zhang, Woon & Li, 2006 (2 spp.), *Sonoita* Peckham & Peckham, 1903 (2 spp.), *Paracyrba* Żabka & Kovac, 1996 (1 sp.), and *Calxattus* Wang, Yu & Zhang, 2023 (1 sp.) (WSC 2025).

Here, we describe three new species of Spartaeini: *Calxattus dengba* sp. nov. (male from Xizang, China), *Spartaeus siloi* sp. nov. (both sexes from Guangxi, China), and *Taraxella chrisfehni* sp. nov. (both sexes from Peninsular Malaysia). Notably, *C. dengba* marks the second species of *Calxattus* to be described. Additionally, it has been 38 years since a new species of *Taraxella* was last documented, and this study provides the first colour figure plate for the genus. This study aims to advance our knowledge of the species diversity of Spartaeini.

Material and methods

Specimens preserved in 75% or 95% ethanol were examined under a Nikon SMZ 1500 stereomicroscope and measured using a Leica M205A stereomicroscope. All measurements were taken in millimeters with the dedicated measurement tool in Leica LAS v. 4.3 software. Female genitalia were cleared in a pancreatin solution (Álvarez-Padilla and Hormiga 2007). The setae of male palp were mostly removed using a Chinese acupuncture needle to ensure that its complex palpal structures were not obscured. Photographs of the ethanol-immersed bodies were captured using a Leica M205A stereomicroscope equipped with a Leica DFC550 CCD camera and stacked using LAS v. 4.3 software. Images of the genitalia and other details were captured using an Olympus BX53 microscope equipped with a Kuy Nice CCD camera. The resulting image stacks were then processed using Helicon Focus v. 8 software. Final images were retouched in Adobe Photoshop CC ©2023. All specimens examined are deposited in the Museum of Hebei University (MHBU; Baoding, China).

Terminology in this study mainly followed Wanless (1984, 1987) and Wang et al. (2023), with a few exceptions (see comments for *Spartaeus siloi* sp. nov. and *Taraxella chrisfehni* sp. nov.). Abbreviations used in this study: **AG**, accessory gland; **ALE**, anterior lateral eye; **AME**, anterior median eye; **C**, functional conductor; **CD**, copulatory duct; **CO**, copulatory opening; **Cy**, cymbium; **DH**, distal haematodocha; **dITA**, dorsal intermediate tibial apophysis; **E**, embolus; **EG**, embolic guide; **FD**, fertilization duct; **ITA**, intermediate tibial apophysis; **M**, membrane of distal haematodocha; **MA**, median apophysis; **MTA**, membranous tegular apophysis; **PLE**, posterior lateral eye; **PME**, posterior median eye; **RTA**, retrolateral tibial apophysis; **SD**, sperm duct; **St**, subtegulum; **T**, tegulum; **TA**, tegular apophysis; **TD**, tegular depression; **vITA**, ventral intermediate tibial apophysis; **VTA**, ventral tibial apophysis; **X**, tegular apophysis ‘X’; **Y**, tegular apophysis ‘Y’.

Taxonomy

Calxattus **Wang, Yu & Zhang, 2023**

Calxattus Wang, Yu & Zhang, 2023: 9.

Type species. *Spartaeus serratus* Yang, Liu, Liu & Peng, 2017, by original designation.

Calxattus dengba **sp. nov.**

https://zoobank.org/655EF590-7FF4-4ED5-AFEF-52392536DE9F
Figs 1, 2
Common name. 僜巴岩跳蛛

Type material. ***Holotype*:** China • ♂ (MHBU-ARA-00027415); Xizang Autonomous Region: Nyingchi City, Zayu County, Xia Zayu Town; 9.VIII.2002; M. Zhu leg.

Etymology. The specific epithet is derived from the Dengba people, who live in Zayu County, the type locality of the new species. Noun in apposition.

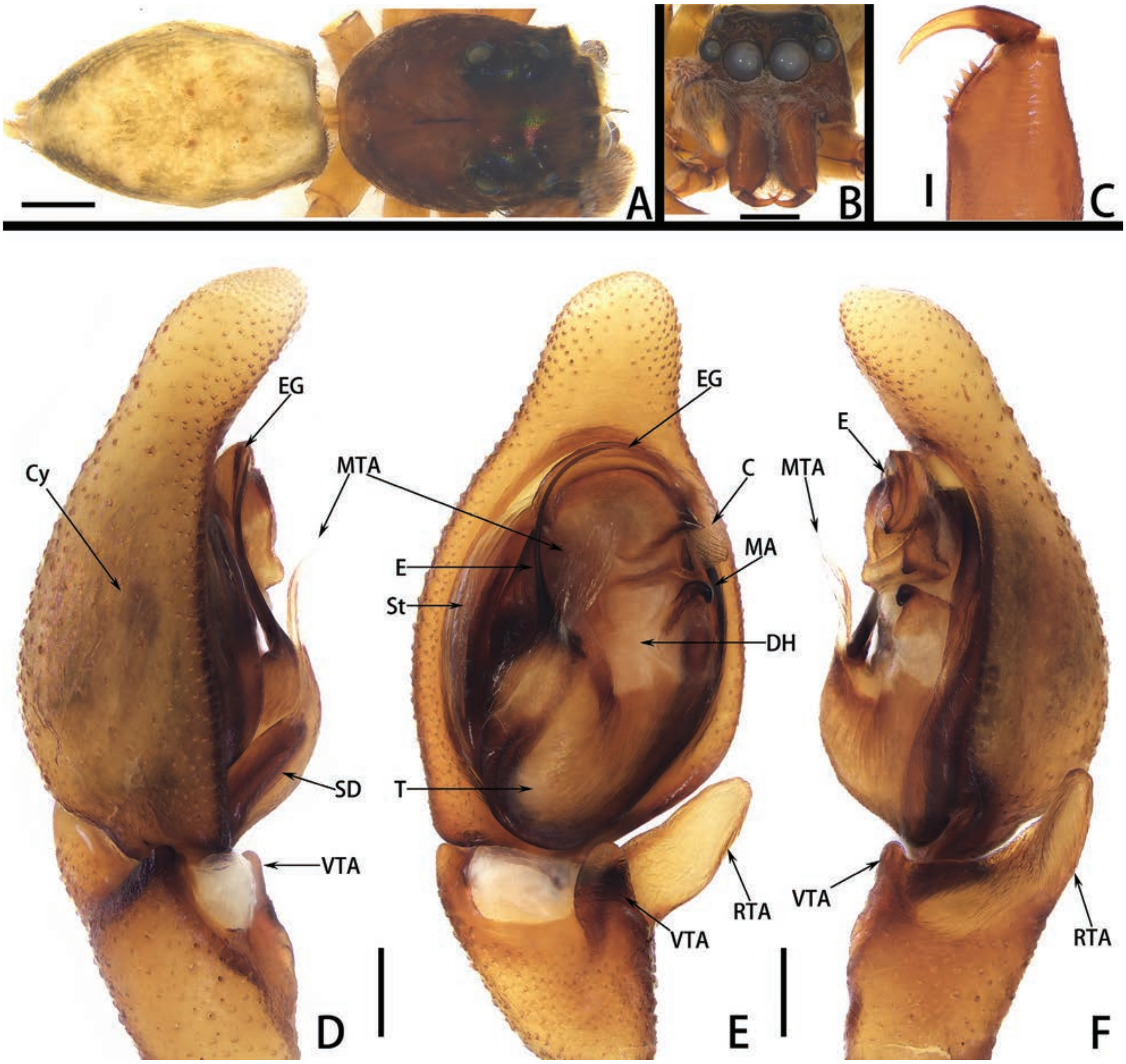

Figure 1. *Calxattus dengba* sp. nov., habitus of holotype male (**A, B**), cheliceral teeth (**C**), palp of holotype male (**D–F**); in dorsal (**A**), front (**B**), prolateral (**D**), ventral (**E**), retrolateral (**F**) and back (**C**) view. Scale bars: 1 mm (**A, B**); 0.2 mm (**C–F**).

Diagnosis. The male of the new species can be distinguished from its sole congeneric species, *C. serratus*, by the following: (1) the RTA lacks processes on its prolateral and retrolateral edges (Figs 1E, 2B; vs. in *C. serratus*, the RTA carries median processes on both prolateral and retrolateral edges; see Wang et al. 2023: figs 5B, 7B); (2) the embolus is relatively short, originates from the median portion of the palpal bulb and terminates near the midpoint of the lower edge of the groove-shaped embolic guide (Figs 1E, 2B; vs. in *C. serratus*, the embolus is long, originates from the lower portion of the bulb and terminates through the groove-shaped embolic guide near the functional conductor; see Wang et al. 2023: figs 5B, 7B); and (3) the median apophysis is located in the upper half of the retrolateral part of the bulb (Figs 1E, 2B; vs. in *C. serratus*, the median apophysis is located in the lower half of the retrolateral part of the bulb; see Wang et al. 2023: figs 5B, 7B).

Description. Male. Measurements of holotype: total length 7.26. Carapace 3.52 long, 2.47 wide. Abdomen 3.34 long, 2.28 wide. Eye measurements:

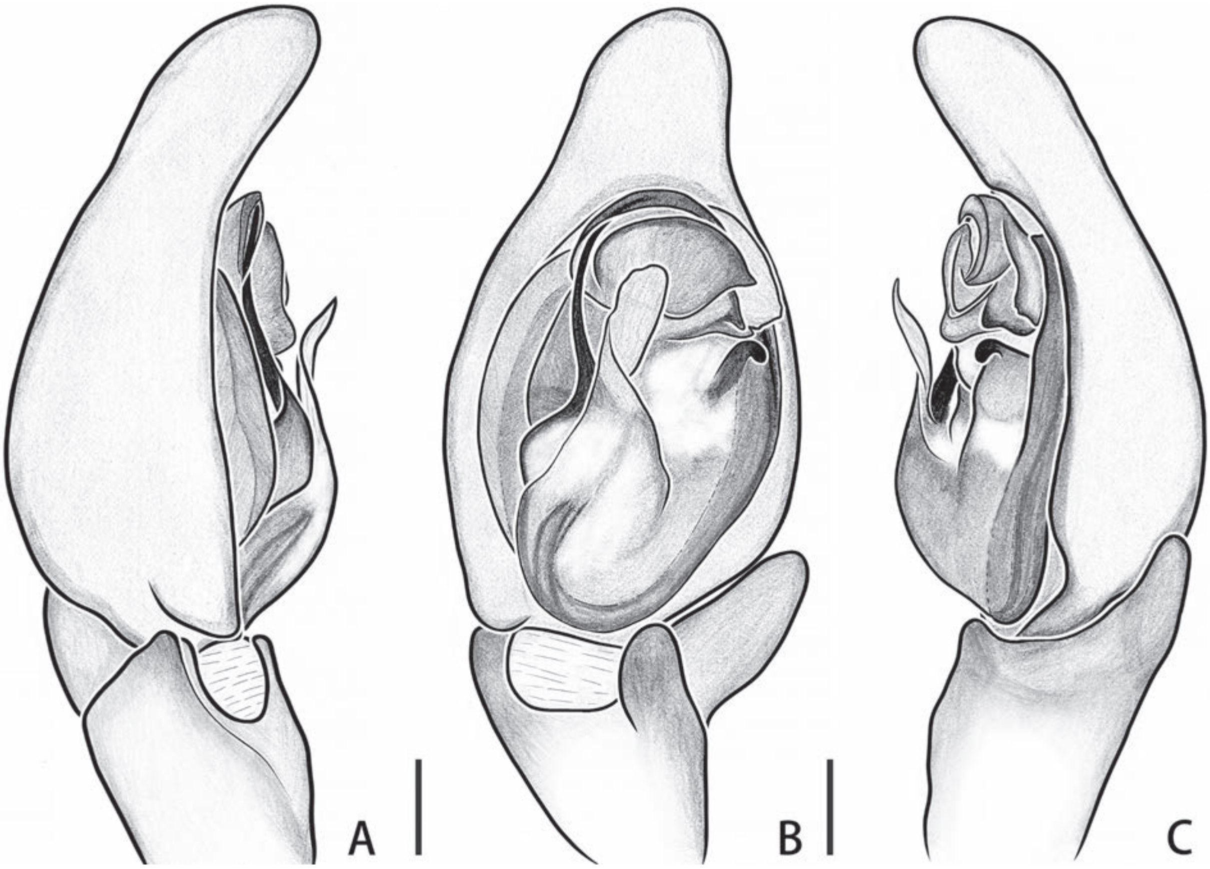

Figure 2. *Calxattus dengba* sp. nov., palp of holotype male (**A–C**); in prolateral (**A**), ventral (**B**) and retrolateral (**C**) view. Scale bars: 0.2 mm (**A–C**).

AME 0.63, ALE 0.26, PME 0.43, PLE 0.37. Leg measurements: I 14.18 (3.78, 1.35, 4.47, 2.91, 1.67), II 7.89 (2.80, 0.96, 2.28, 1.35, 0.50), III 7.74 (2.41, 0.87, 1.86, 1.84, 0.76), IV 11.39 (3.07, 0.83, 3.04, 3.27, 1.18); leg formula 1423. Chelicera (Fig. 1C) brown, with six promarginal and seven retromarginal teeth. Carapace (Fig. 1A, B) reddish-brown, eye surroundings black, clypeus and eye surroundings covered by sparse white setae, fovea dark and longitudinal slit-like. Endites and labium yellowish-brown, with brown setae at distal end; sternum flat and creamy yellow, covered with white and brown setae. Legs (Fig. 1A) dark yellow, bearing long and thin spines; leg I extra long. Abdomen (Fig. 1A) pale yellow and elongated oval, surface faded; dorsal side with visible grey bands at edge, ending near spinnerets; short yellow setae covered on dorsal lateral sides of anterior half; ventral side with fine or flattened setae in middle part. Spinnerets (Fig. 1A) yellow, covered with white setae.

Palp (Figs 1D–F, 2A–C): embolus thread-like, terminating near midpoint of embolic guide in ventral view; median apophysis black, hook-like in ventral view, located in upper half of retrolateral part of bulb, near functional conductor; functional conductor fan-shaped, with plow-like furrows on surface; membranous tegular apophysis transparent, curved in middle portion, originating from tegular apex and covering half of basal embolus; retrolateral and ventral tibial apophyses finger-like in ventral view, surface of retrolateral tibial apophysis with fingerprint-like patterns.

Female. Unknown.

Distribution. China (Xizang).

Spartaeus **Thorell, 1891**

Spartaeus Thorell, 1891: 137.

Type species. *Boethus spinimanus* Thorell, 1878, by original designation.

Spartaeus siloi **sp. nov.**

https://zoobank.org/531DF00D-0A70-4AB3-B507-89B1EEC6A5AE
Figs 3–5
Common name. 诗雷散蛛

Type material. *Holotype*: China • ♂ (MHBU-ARA-00027416); Guangxi Zhuang Autonomous Region, Chongzuo City, Daxin County, Longdian; 22.6931°N, 107.036975°E, 211 m elev.; 27.IV. 2024; W. Wang leg. ***Paratypes*:** China • 1♀ (MHBU-ARA-00027417); same data as holotype; 1♂ (MHBU-ARA-00027538); Guangxi Zhuang Autonomous Region Autonomous Region, Chongzuo City, Daxin County, Xinkang; 22.6538°N, 107.0755°E, 145 m elev.; 12.V.2024; J. Zhang, K. Yu, Z. Yang, Y. Ni & Y. Li leg.

Etymology. The specific epithet is derived from “Si Loi”, which is a unique artistic style of Zhuang folk songs in Daxin County (the type locality). Noun in apposition.

Diagnosis. The new species resembles *S. platnicki* Song, Chen & Gong, 1991 in the shape of the palpal bulb and copulatory duct, but it can be distinguished by the following: (1) the length of the embolus is much less than half of the bulb width (Figs 4B, 5B; vs. in *S. platnicki*, the length of the embolus is more than half of bulb width; see Lin et al. 2023: fig. 18A); (2) the end of the retrolateral tibial apophysis is relatively straight (Figs 4B, 5B; vs. in *S. platnicki*, the end of the retrolateral tibial apophysis is strongly curved; see Lin et al. 2023: fig. 18A); (3) the ventral intermediate tibial apophysis is rounded at the distal end in ventral view (Figs 4B, 5B; vs. in *S. platnicki*, the ventral intermediate tibial apophysis is sharp at the distal end in ventral view; see Lin et al. 2023: fig. 18A); and (4) the two copulatory ducts are nearly parallel (Figs 4D, 5D; vs. curved posteriorly in *S. platnicki*; see Lin et al. 2023: fig. 19A).

Description. Male. Measurements of holotype: total length 7.19. Carapace 3.42 long, 2.37 wide. Abdomen 3.58 long, 1.56 wide. Eye measurements: AME 0.81, ALE 0.45, PME 0.30, PLE 0.30. Leg measurements: I 15.55 (4.43, 1.28, 4.70, 3.7, 1.44), II 9.29 (2.30, 0.91, 2.61, 2.40, 1.07), III 10.05 (2.67, 0.89, 2.38, 2.53, 1.58), IV 13 (3.16, 1.07, 3.39, 4.19, 1.19); leg formula 1432. Chelicera (Fig. 3D) dark brown, with seven promarginal and eight retromarginal teeth. Carapace (Fig. 3B, C) yellow, margin and eye surroundings blackish-brown, anterior lateral margin deep black, eye field with black setae, eye surroundings covered by yellow and white setae, fovea dark and slit-like; endites and labium yellowish-brown, with black setae at distal end, endites slender. Legs (Fig. 3B) with long and thin spines, coxa and trochanter off-white, femur to tibia with obvious grey stripes on anterior and posterior sides. Abdomen (Fig. 3B) yellow, black strips interspersed with white setae around margins, broken near spinnerets; dorsal side with tawny patches and black setae; ventral side off-white, with white setae on both sides, center covered with greyish-white scales.

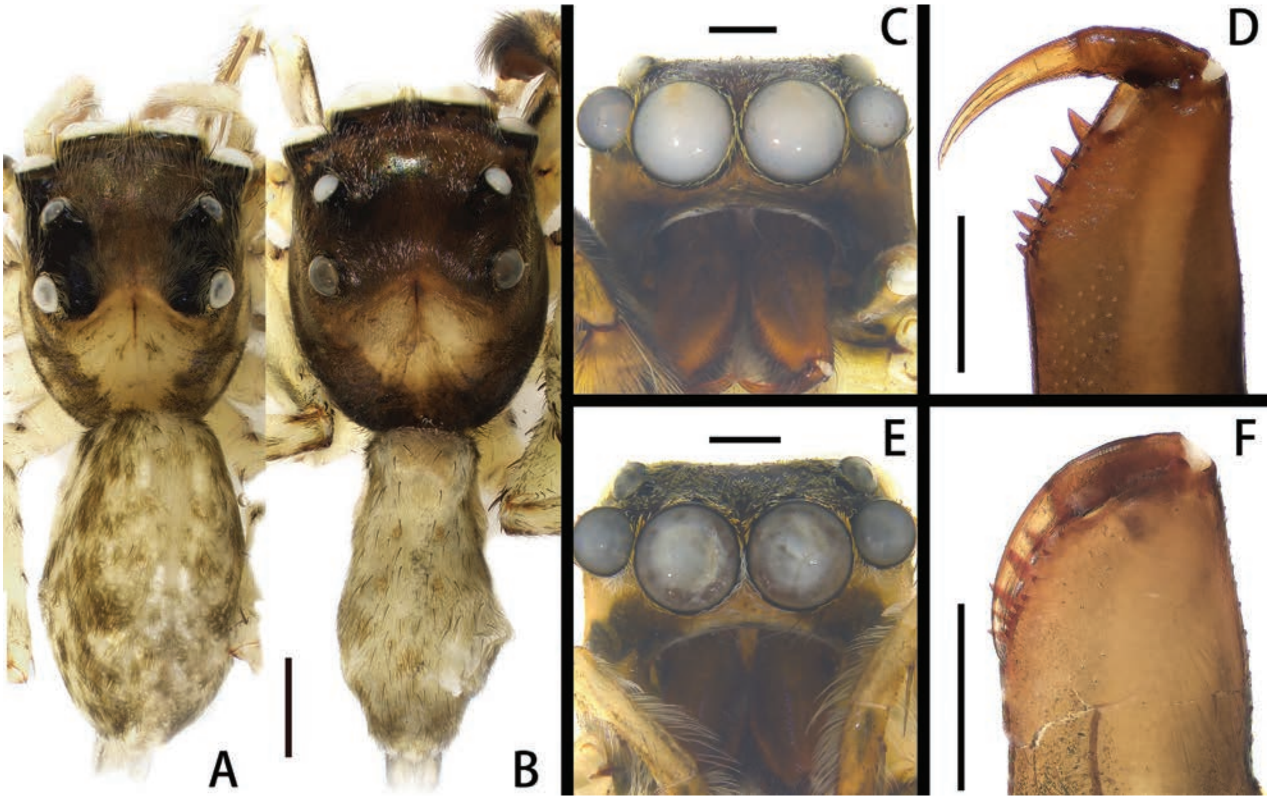

Figure 3. *Spartaeus siloi* sp. nov., habitus of holotype male (**B, C**) and paratype female (**A, E**), cheliceral teeth of holotype male (**D**) and paratype female (**F**); in dorsal (**A, B**), front (**C, E**) and back (**D, F**) view. Scale bars: 0.1 mm (**A, B**); 0.5 mm (**C–F**).

Spinnerets (Fig. 3B) white, spinnerets lateral inward white, lateral exterior with dark brown patches, covered with white setae.

Palp (Figs 4A–C, 5A–C): embolus thin and short, sheep-horn-like in retrolateral view, base of embolus hidden behind membrane formed by distal haematodocha; tegular oval, surface smooth; tegular apophysis triangular, weakly sclerotized in ventral view; ventral tibial apophysis thick, triangular in ventral view; retrolateral tibial apophysis soft and movable, long and flat in ventral view, with small processes on distal end; dorsal intermediate tibial apophysis blackish-brown, with snake-scale-like processes on outer surface, edge wide and flat; ventral intermediate tibial apophysis yellowish-brown, rounded at distal end in ventral view; distal end of cymbium with grey hair tuft.

Female. Measurements of paratype: total length 6.55. Carapace 2.92 long, 2.31 wide. Abdomen 3.33 long, 2.07 wide. Eye measurements: AME 0.68, ALE 0.40, PME 0.28, PLE 0.39. Leg measurements: I 9.15 (2.72, 1.03, 2.70, 1.84, 0.86), II 7.16 (2.25, 0.76, 1.88, 1.53, 0.74), III 7.45 (2.19, 074, 1.84, 1.83, 0.85), IV 8.68 (2.85, 0.72, 2.67, 1.52, 0.92); leg formula 1432. Chelicera (Fig. 3F) brown, with six promarginal and eight retromarginal teeth. Habitus (Fig. 3A, E) similar to that of male, but different in: carapace paler at margin forming a black band from anterior lateral eyes to rear edge of carapace; with a black band in lower position between the anterior median eyes and the posterior lateral eyes; black strips on lateral dorsal side of abdomen not continuous, but with intermittent small black bands.

Epigyne (Figs 4D, E, 5D, E): epigynal plate oval, slightly raised in a mound-like shape; copulatory openings small, slit-shaped in ventral view, anteriorly located; copulatory ducts extending to posterior part, dark and slender; spermathecae

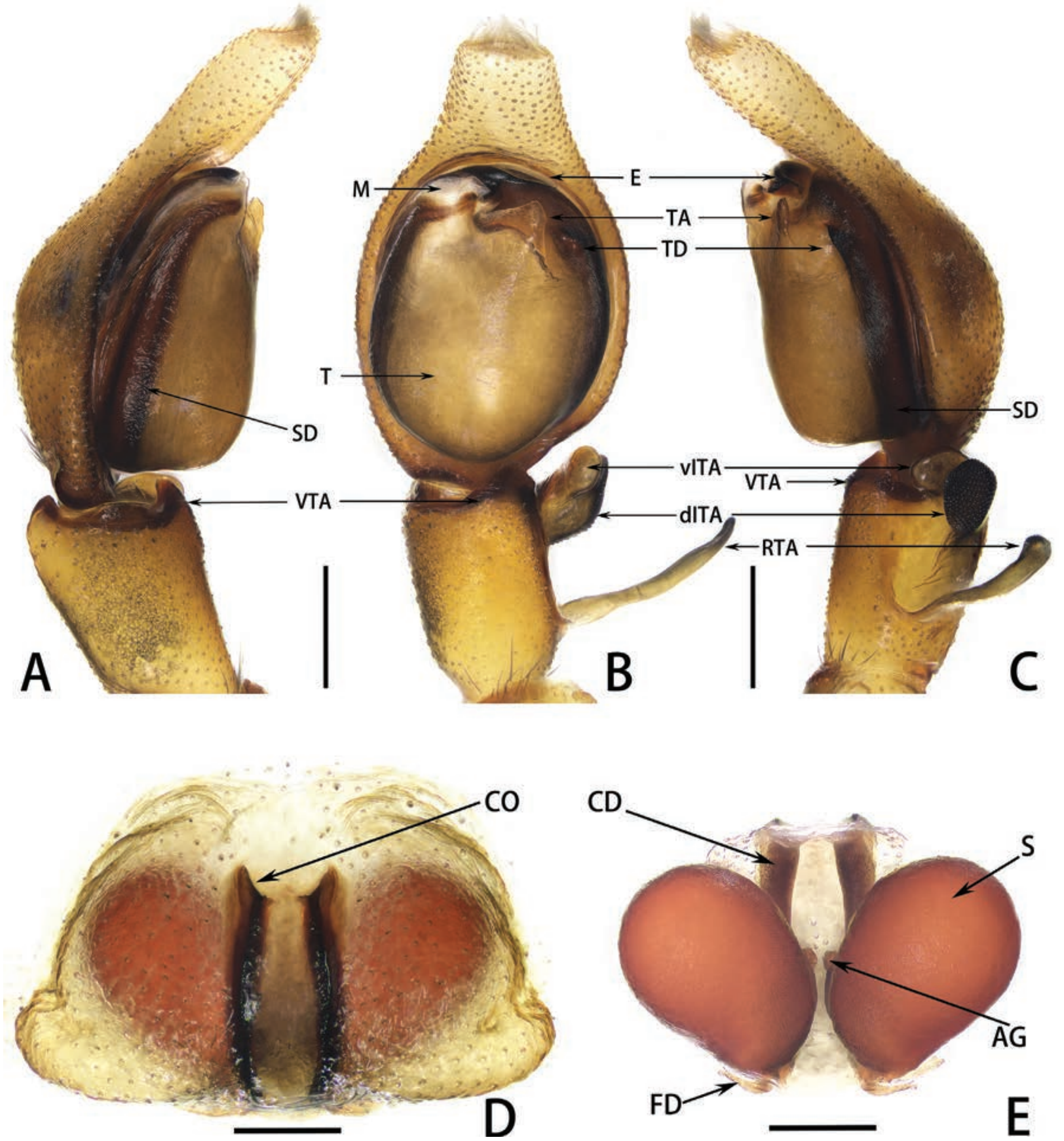

Figure 4. *Spartaeus siloi* sp. nov., palp of holotype male (**A–C**), epigyne (**D**) and vulva (**E**) of paratype female; in prolateral (**A**), ventral (**B, D**), retrolateral (**C**) and dorsal (**E**) view. Scale bars: 0.2 mm (**A–E**).

reddish-brown, large and kidney-shaped; fertilization ducts short, connecting with spermathecae at posterior part; accessory glands located centrally at inner margins of spermathecae, partly hidden by spermathecae in dorsal view.

Distribution. China (Guangxi).

Comments. Following a previous study on *Spartaeus* (Yang et al. 2017: figs 4, 8, 10), we labelled the weekly sclerotized apophysis derived from the tegulum of male palpal bulb as TA. This structure was identified as M_3 in Wanless (1984). Additionally, the membranous patch of the distal haematodocha at the base of embolus is referred to here as M, aligning with the designation of M_1 in Wanless's (1984) study on *Spartaeus*. In the redescription of *S. platnicki* Song, Chen & Gong, 1991, the marked TA (Lin et al. 2023: fig. 18) is likely mislabelled and probably should be M in this study, considering its position at the base of embolus.

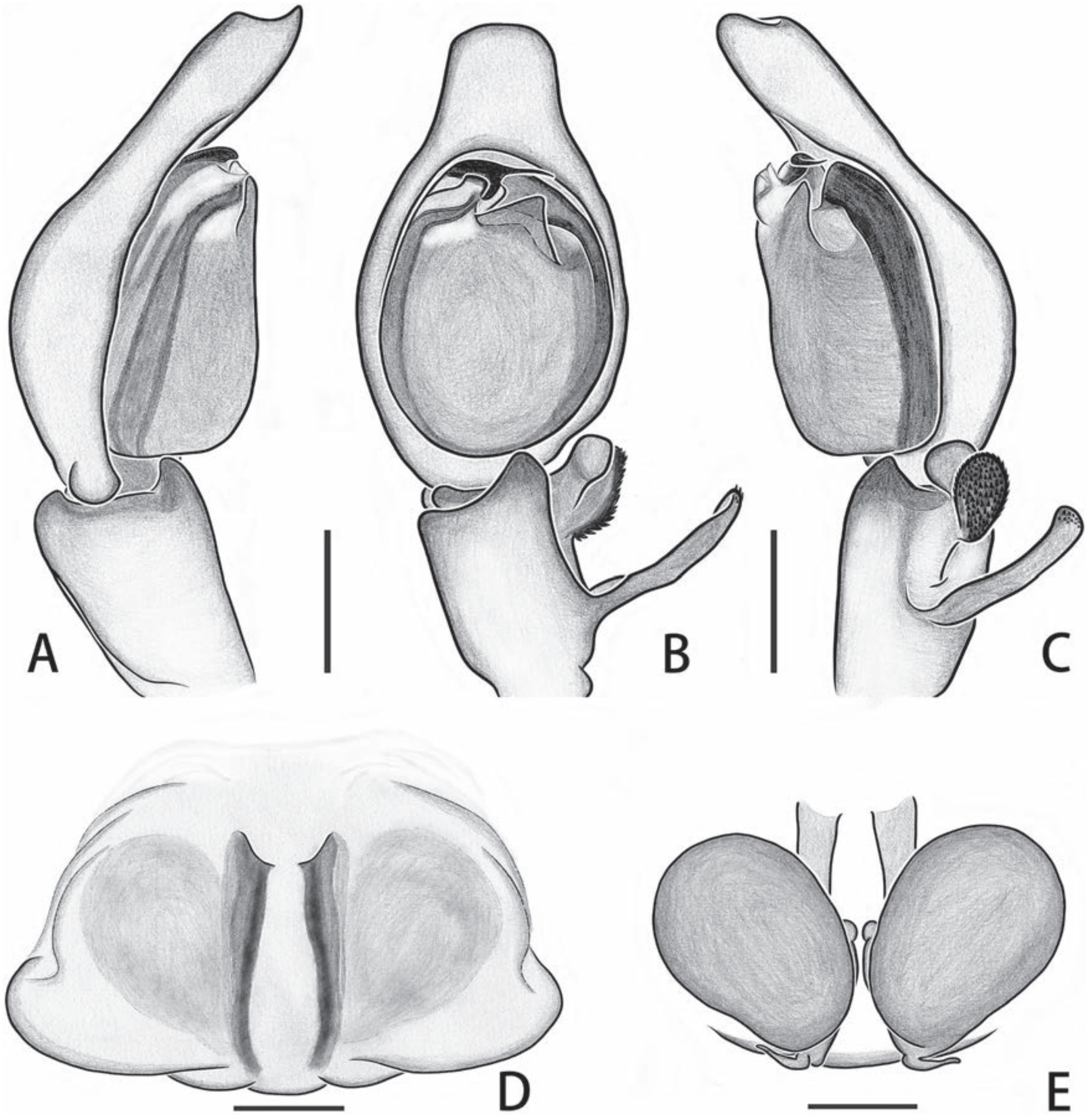

Figure 5. *Spartaeus siloi* sp. nov., palp of holotype male (**A–C**), epigyne (**D**) and vulva (**E**) of paratype female; in prolateral (**A**), ventral (**B, D**), retrolateral (**C**) and dorsal (**E**) view. Scale bars: 0.2 mm (**A–E**).

Taraxella Wanless, 1984

Taraxella Wanless, 1984: 155.

Type species. *Taraxella solitaria* Wanless, 1984, by original designation.

Taraxella chrisfehni sp. nov.

https://zoobank.org/C96EB08B-A1FB-4E1C-A05F-787B5147C599
Figs 6–8
Common name. 克氏塔蛛

Type material. ***Holotype***: Malaysia • ♂ (MHBU-ARA-00021518); Kelantan, Gua Musang; 4.7635°N, 102.0055°E, 199 m elev.; 26.X.2015; Z. Gao, G. Huang & L. Wang leg. ***Paratype***: Malaysia • 1♀ (MHBU-ARA-00027418); same data as the holotype.

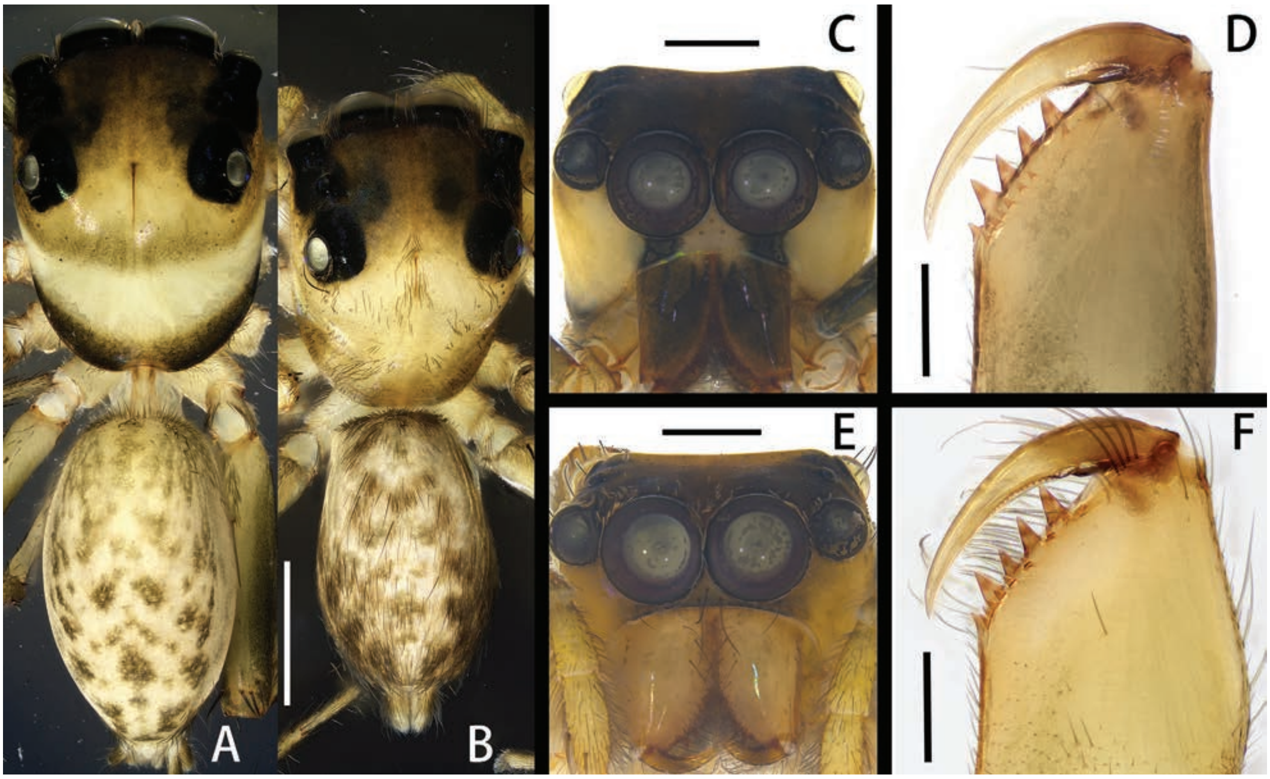

Figure 6. *Taraxella chrisfehni* sp. nov., habitus of holotype male (**A, C**) and paratype female (**B**, **E**), cheliceral teeth of holotype male (**D**) and paratype female (**F**); in dorsal (**A, B**), front (**C, E**) and back (**D, F**) view. Scale bars: 1 mm (**A, B**); 0.5 mm (**C, E**); 0.2 mm (**D, F**).

Etymology. The specific epithet is derived from Chris Fehn, the percussionist and backing vocalist for the heavy metal band Slipknot from 1998 to 2019; the Pinocchio-style mask that Chris Fehn usually wears during his performances resembles the tegular apophysis 'Y' on the palpal bulb of the new species.

Diagnosis. The new species resembles *T. solitaria* in the pattern of tegular apophyses 'X' and 'Y', but it can be distinguished from *T. solitaria* by the following: (1) the 'Y' apophysis is slender, originates from the center of the palpal bulb, protrudes at a 45° angle toward the ventral distal end, bent in proximal 1/3 position from tip (Figs 7A–C, 8A–C; vs. in *T. solitaria*, the apophysis 'Y' is short and stout, originates from the prolateral part of the palpal bulb; see Wanless 1984: fig. 7G, F); (2) the sharp prong is short and slightly curved, positioned between the retrolateral tibial apophysis and the ventral tibial apophysis (Figs 7B, C, 8B, C; vs. in *T. solitaria*, the sharp prong is long and curved in an "S" shape, located dorsally to the retrolateral tibial apophysis; see Wanless 1984: fig. 7G, F); and (3) the membrane of distal haematodocha forms a fan-shaped structure that resembles an inverted trapezoid in ventral view (Figs 7B, 8B; vs. in *T. solitaria*, the fan-shaped structure resembles a rhomboid in ventral view; see Wanless 1984: fig. 7G)

Description. Male. Measurements of holotype: total length 4.75. Carapace 2.24 long, 1.68 wide. Abdomen 2.16 long, 1.28 wide. Eye measurements: AME 0.55, ALE 0.28, PME 0.09, PLE 0.28. Leg measurements: I 5.28 (1.50, 0.50, 1.48, 1.22, 0.58), II 4.12 (1.18, 0.48, 1.17, 0.93, 0.36), III 4.49 (1.21, 0.45, 1.10, 1.25, 0.49), IV 4.44 (1.35, 0.41, 1.10, 1.05, 0.53); leg formula 1342. Chelicera (Fig. 6D) brown, bearing large black patch in anterior region, with five promarginal and nine retromarginal teeth. Carapace (Fig. 6A, C) with dark margins, and an off-white encircling band,

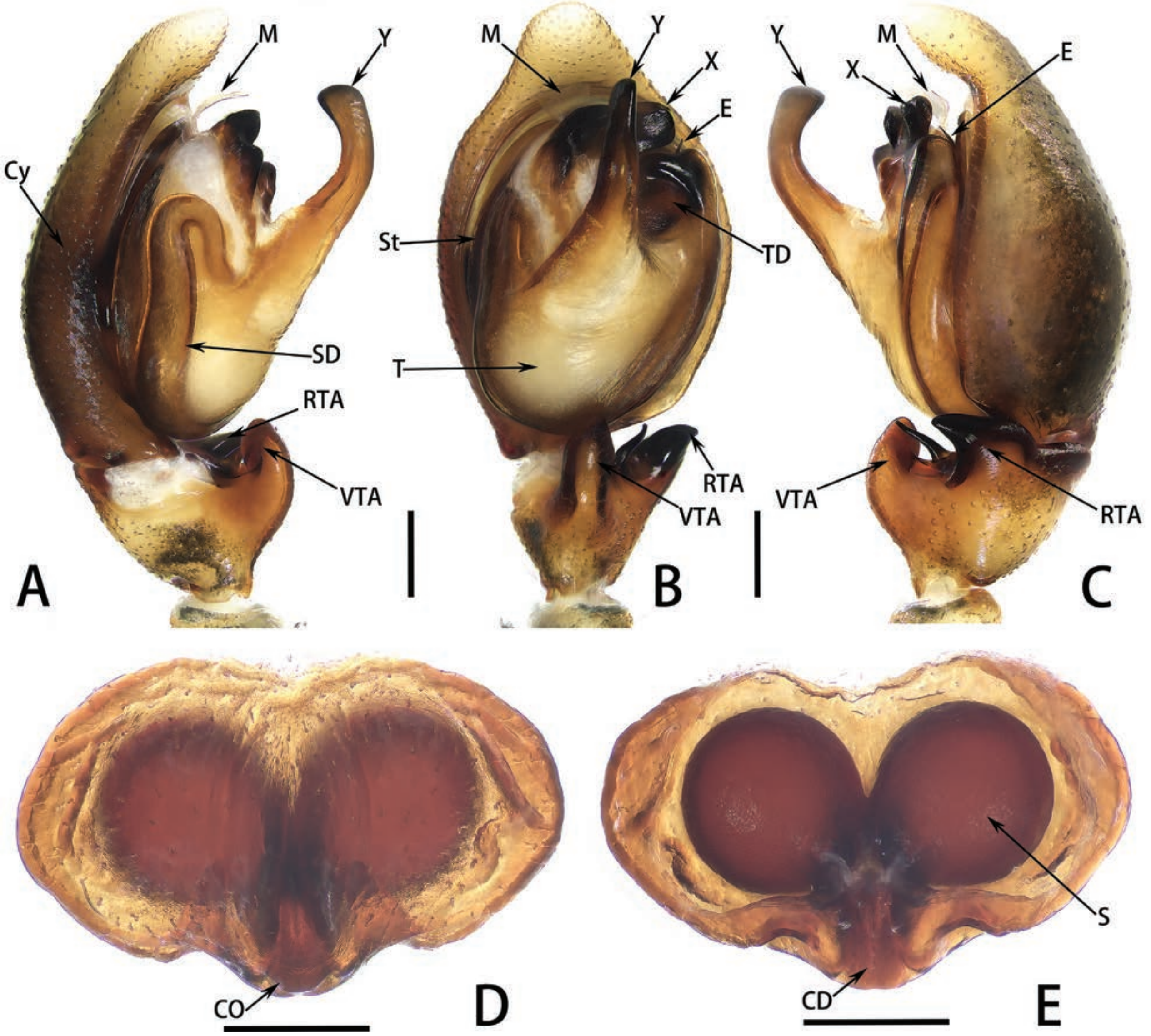

Figure 7. *Taraxella chrisfehni* sp. nov., palp of holotype male (**A–C**), epigyne (**D**) and vulva (**E**) of paratype female; in prolateral (**A**), ventral (**B, D**), retrolateral (**C**) and dorsal (**E**) view. Scale bars: 0.2 mm (**A–E**).

eye field light brown; eye surroundings dark, with black strips beneath anterior median eyes connecting to carapace margin resembling tear stains; fovea brown and longitudinal slit-like; endites light brown, with black setae at distal end; labium pale yellow, with a black spot on surface. Legs (Fig. 6A) bearing long and thin spines, coxa and trochanter off-white, femur and tibia olive-brown. Abdomen (Fig. 6A) off-white on dorsal side, with mottled long black setae; clusters of dark brown setae adorning lateral sides; herringbone patterned lines arranged longitudinally, gradually decreasing in size from front to back in middle; ventral side off-white. Spinnerets (Fig. 6A) pale yellow, covered with black setae.

Palp (Figs 7A–C, 8A–C): embolus partly hidden by tegular apophysis ‘X’ and tegulum in ventral view; tegular apophysis ‘X’ dark, located at distal end of bulb, extending to retrolateral direction, forming three hill-like protrusions on surface in retrolateral view; tegular apophysis ‘Y’ long, bent in proximal 1/3 position from tip; membrane of distal haematodocha forming a transparent fan-like structure, bent ventrally; ventral tibial apophysis thick, bent dorsally, finger-like in ventral

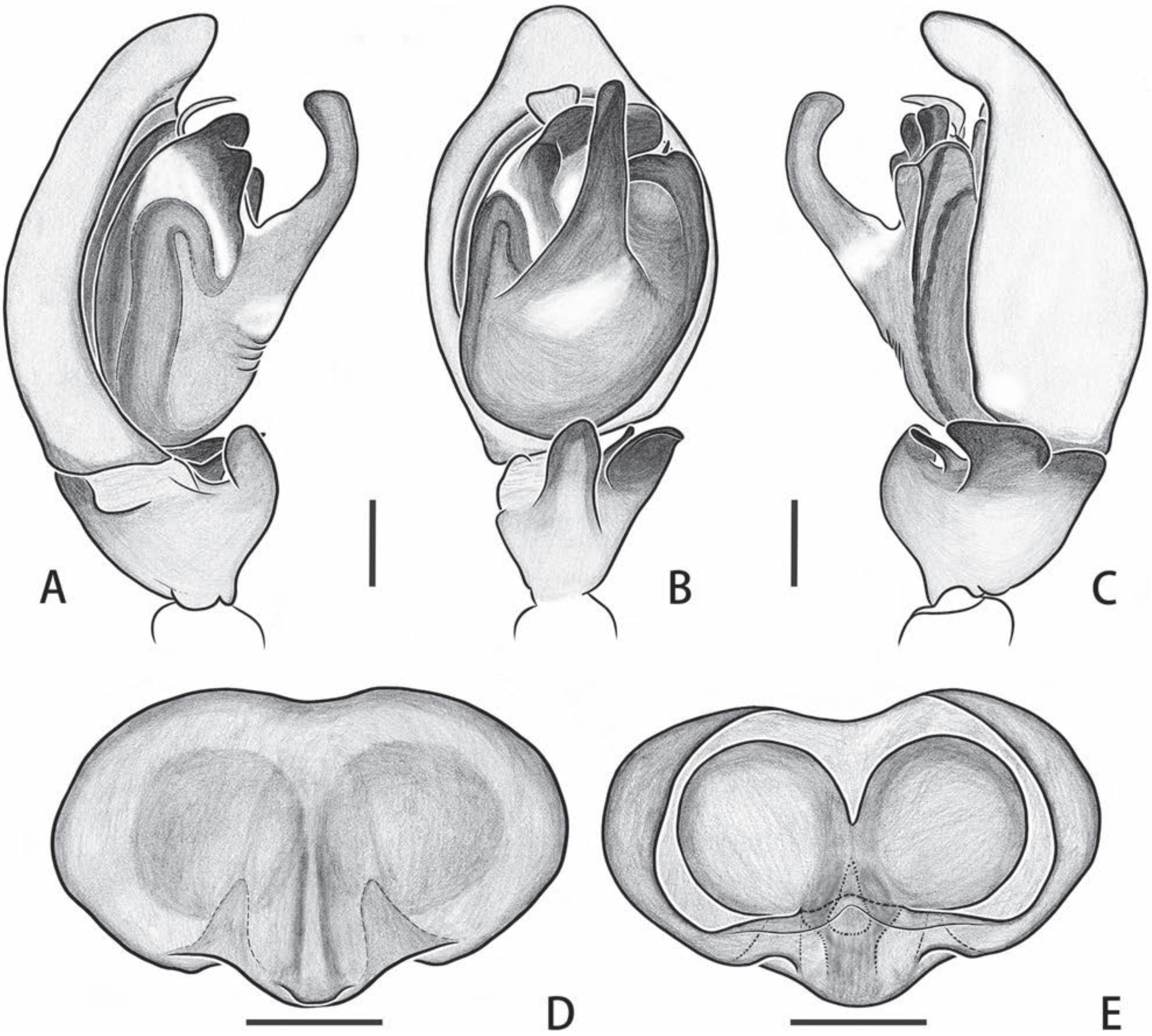

Figure 8. *Taraxella chrisfehni* sp. nov., palp of holotype male (**A–C**), epigyne (**D**) and vulva (**E**) of paratype female; in prolateral (**A**), ventral (**B, D**), retrolateral (**C**) and dorsal (**E**) view. Scale bars: 0.2 mm (**A–E**).

view, edge dark; retrolateral tibial apophysis dark, with a ventral depression, sheep-ear-like in ventral view; prong between VTA and RTA sharp, petiole-like.

Female. Measurements of paratype: total length 4.07. Carapace 1.90 long, 1.53 wide. Abdomen 2.09 long, 1.20 wide. Eye measurements: AME 0.50, ALE 0.06, PME 0.29, PLE 0.27. Leg measurements: **I** 3.76 (1.38, 0.46, 0.99, 0.66, 0.27), **II** 3.38 (1.17, 0.46, 0.90, 0.62, 0.23), **III** 4.03 (1.20, 0.39, 0.98, 0.87, 0.59), **IV** 5.49 (1.54, 0.48, 1.52, 1.49, 0.46); leg formula 4312. Chelicera pale yellow, with five promarginal and eight retromarginal teeth (Fig. 6F). Habitus (Fig. 6B, E) similar to that of male, but different in: carapace paler at margin, lacking obvious off-white band, clypeus narrow, faint black, lacking obvious black strips beneath anterior median eyes; femur and tibia consistent in colour with other leg segments.

Epigyne (Figs 7D, E, 8D, E): epigynal plate heart-shaped, equipped with a longitudinal furrow at posterior-middle part; two triangular concave cavities (possible epigynal pockets) at posterior end facing rearward; copulatory openings slit-shaped, located behind longitudinal furrow; copulatory ducts hidden beneath sclerotized integument and inconspicuous at dorsal view; spermathecae large and spherical, with middle parts closely adhering to each other; fertilization ducts and accessory glands not visible.

Distribution. Malaysia (Kelantan).

Comments. *Taraxella* has the peculiar tegular apophyses 'X' and 'Y', as well as the nearly concealed embolus (Wanless 1987). Tegular apophysis 'Y' is likely homologous to M_3, which may also be denoted as TA (Wanless 1984). Nevertheless, the structure homologous to 'X' remains unclear, and the homology of different apophyses on male palpal bulb in Spartaeinae remains to be investigated. In this study, we followed the terminology in Wanless (1984) and employed 'X' and 'Y' to represent the two massive apophyses of the male palp.

Acknowledgements

We extend our sincere gratitude to all collectors of the specimens utilized in this study; to Weihang Wang (Guangdong, China) for providing the type specimens of *Spartaeus siloi* sp. nov.; to the two reviewers, Dr Cheng Wang and Dr Tamás Szűts, and the editor, Dr Zhiyuan Yao, for their valuable comments and suggestions to improve the manuscript.

Additional information

Conflict of interest

The authors have declared that no competing interests exist.

Ethical statement

No ethical statement was reported.

Funding

This work was funded by the Natural Science Foundation of Hebei Province (grant no. C2024201017) to Junxia Zhang.

Author contributions

Original draft: YN. Drawing and Photography: YN. Review and editing: JZ, KY.

Author ORCIDs

Yi Ni https://orcid.org/0009-0003-3239-3697
Kun Yu https://orcid.org/0000-0002-5517-4484
Junxia Zhang https://orcid.org/0000-0003-2179-3954

Data availability

All of the data that support the findings of this study are available in the main text.

References

Álvarez-Padilla F, Hormiga G (2007) A protocol for digesting internal soft tissues and mounting spiders for scanning electron microscopy. Journal of Arachnology 35(3): 538–542. https://doi.org/10.1636/Sh06-55.1

Lin Y, Xin Y, Wang C, Li S (2023) On ten jumping spider species described by Song and Chai (1992) based on type specimens (Araneae, Salticidae). Zootaxa 5389(1): 1–33. https://doi.org/10.11646/zootaxa.5389.1.1

Maddison WP (2015) A phylogenetic classification of jumping spiders (Araneae: Salticidae). Journal of Arachnology 43(3): 231–292. https://doi.org/10.1636/arac-43-03-231-292

Peckham GW, Peckham EG (1903) New species of the family Attidae from South Africa, with notes on the distribution of the genera found in the Ethiopian region. Transactions of the Wisconsin Academy of Sciences, Arts and Letters 14(1): 173–278 [pl. 19–29].

Simon E (1886) Etudes arachnologiques. 18e Mémoire. XXVI. Matériaux pour servir à la faune des Arachnides du Sénégal. (Suivi d'une appendice intitulé: Descriptions de plusieurs espèces africaines nouvelles). Annales de la Société Entomologique de France (6)5: 345–396.

Song DX, Chen ZQ, Gong LS (1991) A new species of the genus *Spartaeus* from China (Araneae: Salticidae). Acta Zootaxonomica Sinica 16: 424–427.

Thorell T (1878) Studi sui ragni Malesi e Papuani. II. Ragni di Amboina raccolti Prof. O. Beccari. Annali del Museo Civico di Storia Naturale di Genova 13: 5–317.

Thorell T (1891) Spindlar från Nikobarerna och andra delar af södra Asien. Kongliga Svenska Vetenskaps-Akademiens Handlingar 24(2): 1–149.

Wang WH, Yu K, Zhang JX (2023) *Calxattus* gen. nov. from China (Araneae: Salticidae: Spartaeinae: Spartaeini), with redescription of the type species. Acta Arachnologica Sinica 32(1): 8–15. https://doi.org/10.3969/j.issn.1005-9628.2023.01.002

Wanless FR (1984) A review of the spider subfamily Spartaeinae nom. n. (Araneae: Salticidae) with descriptions of six new genera. Bulletin of the British Museum of Natural History (Zool.) 46: 135–205. https://doi.org/10.5962/bhl.part.15964

Wanless FR (1985) A revision of the spider genera *Holcolaetis* and *Sonoita* (Araneae: Salticidae). Bulletin of the British Museum of Natural History (Zool.) 48: 249–278. https://doi.org/10.5962/bhl.part.23463

Wanless FR (1987) Notes on spiders of the family Salticidae. 1. The genera *Spartaeus*, *Mintonia* and *Taraxella*. Bulletin of the British Museum of Natural History (Zool.) 52: 107–137. https://doi.org/10.5962/p.18302

Wijesinghe DP (1992) A new genus of jumping spider from Borneo with notes on the spartaeine palp (Araneae: Salticidae). Raffles Bulletin of Zoology 40(1): 9–19.

World Spider Catalog (2025) World Spider Catalog. Version 25.5. Natural History Museum Bern. https://doi.org/10.24436/2 [Accessed on 2 January 2025]

Yang SF, Liu W, Liu P, Peng XJ (2017) Five new species of *Spartaeus* Thorell, 1891 from China (Araneae: Salticidae). Zootaxa 4303(3): 379–394. https://doi.org/10.11646/zootaxa.4303.3.4

Żabka M, Kovac D (1996) *Paracyrba wanlessi* - a new genus and species of Spartaeinae from peninsular Malaysia, with notes on its biology (Arachnida: Araneae: Salticidae). Senckenbergiana Biologica 76: 153–161.

Zhang JX, Woon JRW, Li D (2006) A new genus and species of jumping spiders (Araneae: Salticidae: Spartaeinae) from Malaysia. Raffles Bulletin of Zoology 54: 241–244.

ZooKeys

ZooKeys 1232: 357–378 (2025)
DOI: 10.3897/zookeys.1232.140688

Research Article

Genus *Hainanphasma* Ho, 2013: taxonomic notes and two new species from Hainan in China (Phasmida, Heteropterygidae)

Yi-Fan Liu[1], Jun-Jie Gu[1], Hai-Jian Wang[1]

1 *College of Agronomy, Sichuan Agricultural University, Chengdu 611130, China*
Corresponding authors: Jun-Jie Gu (orthoptera_gu@aliyun.com); Hai-Jian Wang (wanghaijian2005@sina.com)

Abstract

Two new species of *Hainanphasma* Ho, 2013, *Hainanphasma longiacuta* **sp. nov.** and *H. longidentata* **sp. nov.**, are described and illustrated based on specimens of both sexes from Hainan, China. The heads of *H. cristata* Ho, 2013, based on both sexes, and *H. diaoluoshanensis* Ho, 2013, based on females, are redescribed from new materials. The generic diagnosis of *Hainanphasma* is improved, and the distinction from *Orestes* Redtenbacher, 1906 is clarified. The male and egg of *H. diaoluoshanensis* are described and illustrated for the first time. A key to species of *Hainanphasma* is provided.

Key words: Datamini, key, Phasmatodea, Stick insects, taxonomy

---

Academic editor: Marco Gottardo
Received: 1 November 2024
Accepted: 17 February 2025
Published: 25 March 2025

ZooBank: https://zoobank.org/4C79C7BC-9E3F-429A-A766-D896EBF86575

Citation: Liu Y-F, Gu J-J, Wang H-J (2025) Genus *Hainanphasma* Ho, 2013: taxonomic notes and two new species from Hainan in China (Phasmida, Heteropterygidae). ZooKeys 1232: 357–378. https://doi.org/10.3897/zookeys.1232.140688

Introduction

The Datamini Rehn & Rehn, 1939 currently consists of five genera distributed in China, with two in Hainan Province: *Hainanphasma* Ho, 2013 and *Planispectrum* Rehn & Rehn, 1939 (Ho 2016; Brock et al. 2024). The genus *Hainanphasma*, which is endemic to Hainan, was described in 2013 and attributed to the tribe Datamini, subfamily Dataminae, of the Heteropterygidae (Ho 2013; Brock et al. 2024). This genus includes two species, characterized by the following characters (Ho 2013). In both sexes, the antennae are slender and thin. In females there is a posteriorly projecting and punctulate occipital crest, and the thorax is parallel-sided, with a faint median carina. In males, the occipital crest is strongly elevated, there is a fin-like lamella on the postero-dorsal carina of the meso- and metafemora, the fourth and fifth abdominal terga have distinctive humps, and the thorax is unarmed but with an indistinct median carina. Nonetheless, differentiating *Hainanphasma* from other genera in Datamini, particularly *Orestes* Redtenbacher, 1906 is challenging based on the existing characters.

Bresseel and Constant (2018) have previously examined this genus, presenting specific examples that highlight challenges with diagnostic characters. Gao and Xie (2022) also noted the limited generic differentiation of this genus. The monophyly of *Orestes* has been confirmed by phylogenetic analyses (Bank et al. 2021), but the phylogenetic relationship between *Orestes* and *Hainanphasma* is currently unclear due to the lack of *Hainanphasma* material.

In this paper, we describe two new species and new materials of *H. diaoluoshanensis* Ho, 2013. These findings refine our understanding and clarify its generic status. The paper provides images of female of *O. guangxiensis* (Bi & Li, 1994) collected from Guangxi province, China and *O. mouhotii* (Bates, 1865) collected in Chiang Rai, Thailand to ensure the representative and stable characters used for comparison with *Hainanphasma* in this paper (Fig. 1). *Orestes mouhotii* is the type species of *Orestes*, and *O. guangxiensis* is distributed in Guangxi and Guangdong in China, which are the closest provinces to Hainan. During collection in different areas of Hainan, two new species, *H. longiacuta* sp. nov., *H. longidentata* sp. nov., and the male and egg of *H. diaoluoshanensis* Ho, 2013 were discovered. The arrangement of cephalic armature is figured (Fig. 2), showing similarities to *Microrestes* Bresseel & Constant, 2020, but the cephalic armature differs in having supra-orbitals absent or indistinct and a central coronal present. The heads of *H. cristata* Ho, 2013, based on both sexes, and *H. diaoluoshanensis* Ho, 2013, based on females, are redescribed. A key to species of *Hainanphasma* is provided.

Materials and methods

Specimens were preserved in ethanol in the field, pinned, and dry-preserved in the laboratory. The holotype and some paratypes are deposited at Department of Plant Protection of Sichuan Agricultural University (SICAU), Chengdu, China.

The habitus picture of the specimens were photographed with a Canon EOS550D camera equipped with a Canon EF 100 mm f/2.8L IS USM and a Canon SPEEDLITE 470EX-AI flash (Canon China, Beijing, China). The other images were taken with a SZX16 microscope system and cell Sens Dimension 3.2 software (Olympus, Tokyo, Japan) or a Leica M205A digital imaging system (Leica, Wetzlar, Germany) in the State Key Laboratory of Crop Gene Exploration and Utilization in Southwest China, Sichuan Agricultural University. Measurements were taken under a stereomicroscope with vernier calipers or eyepiece micrometer.

The morphological terms were followed Bragg (2001), Zompro (2004), and Bradler (2009). The nomenclature of the cephalic armature were followed Bresseel and Constant (2020) and Hennemann et al. (2016).

Results

Genus *Hainanphasma* Ho, 2013

Type species. *Hainanphasma cristata* Ho, 2013, by original designation.

Included species. *H. cristata* Ho, 2013, *H. diaoluoshanensis* Ho, 2013, *H. longiacuta* sp. nov., *H. longidentata* sp. nov.

Revised diagnosis. The genus *Hainanphasma* differs from other genera of the Datamini Rehn & Rehn, 1939 by the following combination of characters:

The arrangement of cephalic armature (Fig. 2): supra-occipitals present as blunt spines or small elevations, not split into anterior and posterior supra-occipitals; supra-orbitals absent or indistinct; central coronal present.

In female, body cylindrical; third to fourth abdominal terga slightly increasing in width; postero-dorsal carina of meso- and metafemora with fin-like lamellae or teeth; antero-dorsal and ventral carinae of meso- and metafemora with

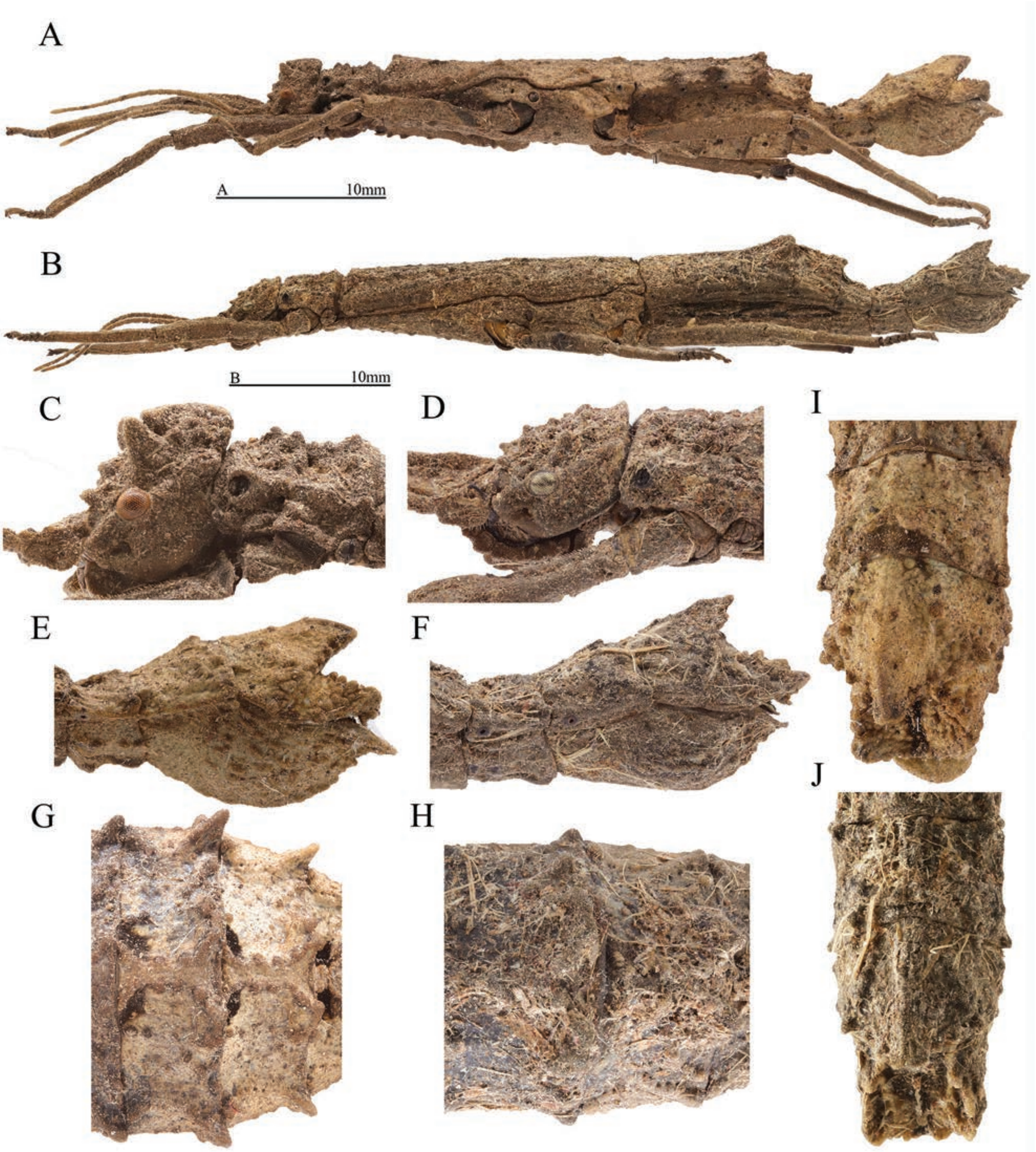

Figure 1. Female of *Orestes guangxiensis* (Bi & Li, 1994) from China, Guangxi, Bobai, 15 Jul. 2022, Yunxiang Zhang leg.; female of *Orestes mouhotii* (Bates, 1865) from Thailand, Chiang Rai, Ban Nanglae Nai, 11 May. 2024, Jie Su leg. **A, B** lateral view of habitus **A** *O. guangxiensis* (Bi & Li, 1994) **B** *O. mouhotii* (Bates, 1865) **C, D** lateral view of head **C** *O. guangxiensis* (Bi & Li, 1994) **D** *O. mouhotii* (Bates, 1865) **E, F** lateral view of terminalia **E** *O. guangxiensis* (Bi & Li, 1994) **F** *O. mouhotii* (Bates, 1865) **G, H** dorsal view of fourth to fifth abdominal terga **G** *O. guangxiensis* (Bi & Li, 1994) **H** *O. mouhotii* (Bates, 1865) **I, J** dorsal view of terminalia **I** *O. guangxiensis* (Bi & Li, 1994) **J** *O. mouhotii* (Bates, 1865). Scale bars: 10 mm (**A, B**); **C–J** not to scale.

small teeth of irregular sizes; fifth abdominal tergum with distinct tubercles and lamellae posteriorly, higher than fourth abdominal tergum; ninth abdominal tergum with distinct posteromedian crest, from slightly shorter to distinctly longer than anal segment.

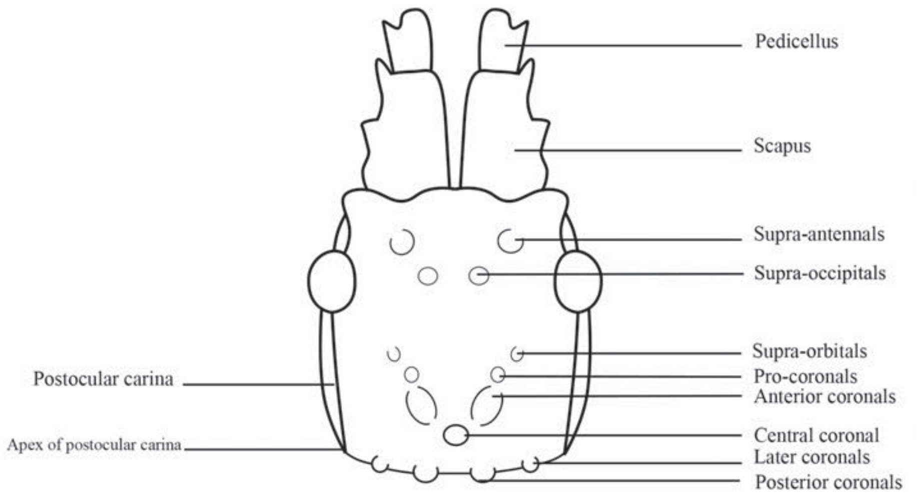

Figure 2. *Hainanphasma* Ho, 2013, nomenclature of cephalic armature.

In male, second abdominal tergum rectangle, longer than wide; dorsal and ventral carinae of meso- and metafemora with fin-like or semi-circle teeth of irregular sizes; posterior margin of fifth abdominal tergum with a pair of humps.

Eggs capsule brown to darker brown, bearing very sparse setae; micropylar plate with margin elevated and broadened; operculum subcircular, elevated centrally; ventral margin oblique in lateral view.

The most closely related genus is *Orestes*. But in *Orestes*, supra-occipitals split into anterior and posterior supra-occipitals; supra-orbitals distinct, present as blunt spines or lamellae (Fig. 1C, D). In female, body robust with widest part at the posterior margin of fourth abdominal tergum or fourth and fifth terga parallel-sided; fourth and fifth abdominal terga with tubercles posteriorly, anterior one larger and higher (Fig. 1G, H); ninth abdominal tergum with small posteromedian crest, not reaching posterior margin of anal segment, shorter than anal segment (Fig. 1E, F, I, J). Eggs can be distinguished by capsule and operculum covered with long and dense setae; operculum shape variable elongated to circular, without distinct elevations.

Distribution. China, Hainan province.

Key to species of *Hainanphasma*

Figs 3, 4

Females

1 Posteromedian crest on ninth abdominal tergum notched apically (Fig. 3I, K, L) **2**
– Posteromedian crest on ninth abdominal tergum tectiform apically (Fig. 3J) .... ***H. longiacuta* sp. nov.**
2 Pedicellus without spine on outer lateral margin (Fig. 3F–H); eighth abdominal tergum not longer than wide (Fig. 3J–L).......... **3**
– Pedicellus with a blunt spine on outer lateral margin (Fig. 3E); eighth abdominal tergum slighty longer than wide (Fig. 3I) .... ***H. longidentata* sp. nov.**

3 Posteromedian crest on ninth abdominal tergum larger, reaching posterior margin of anal segment (Fig, 3L) .... ***H. cristata* Ho, 2013**

– Posteromedian crest on ninth abdominal tergum smaller, not reaching posterior margin of anal segment (Fig. 3K).........***H. diaoluoshanensis* Ho, 2013**

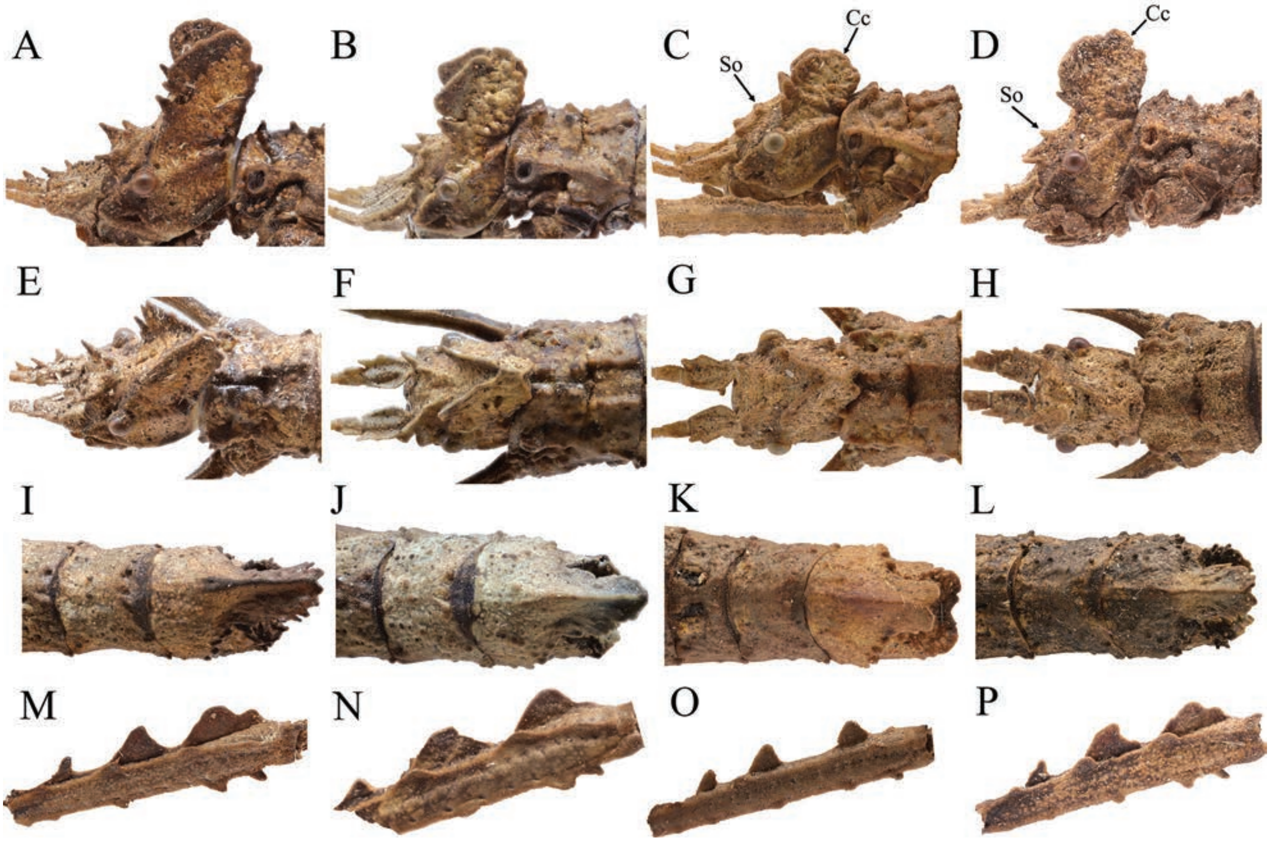

Figure 3. *Hainanphasma* spp., diagnostic characters of females **A–D** lateral view of head **A** *H. longidentata* sp. nov. **B** *H. longiacuta* sp. nov. **C** *H. diaoluoshanensis* Ho, 2013 **D** *H. cristata* Ho, 2013 **E–H** dorsal view of head **E** *H. longidentata* sp. nov. **F** *H. longiacuta* sp. nov. **G** *H. diaoluoshanensis* Ho, 2013 **H** *H. cristata* Ho, 2013 **I–L** dorsal view of terminalia **I** *H. longidentata* sp. nov. **J** *H. longiacuta* sp. nov. **K** *H. diaoluoshanensis* Ho, 2013 **L** *H. cristata* Ho, 2013 **M–P** lateral view of metafemur **M** *H. longidentata* sp. nov. **N** *H. longiacuta* sp. nov. **O** *H. diaoluoshanensis* Ho, 2013 **P** *H. cristata* Ho, 2013. So = supra-occipitals; Cc = central coronal. Not to scale.

Males

1 Anterior coronals lamellate (Fig. 4A, B, D); eighth abdominal tergum longer than wide...**2**

– Anterior coronals subcylindrical (Fig. 4C); eighth abdominal tergum wider than long (Fig. 4M).......................................***H. diaoluoshanensis* Ho, 2013**

2 Supra-occipitals and pro-coronals present as blunt spines (Fig. 4A, D)....**3**

– Supra-occipitals present as indistinct elevations; pro-coronals present as slender spines (Fig. 4B) ....***H. longiacuta* sp. nov.**

3 Central coronal subcylindrical and slender (Fig. 4A) ....
.... ***H. longidentata* sp. nov.**

– Central coronal carinate (Fig. 4D) .... ***H. cristata* Ho, 2013**

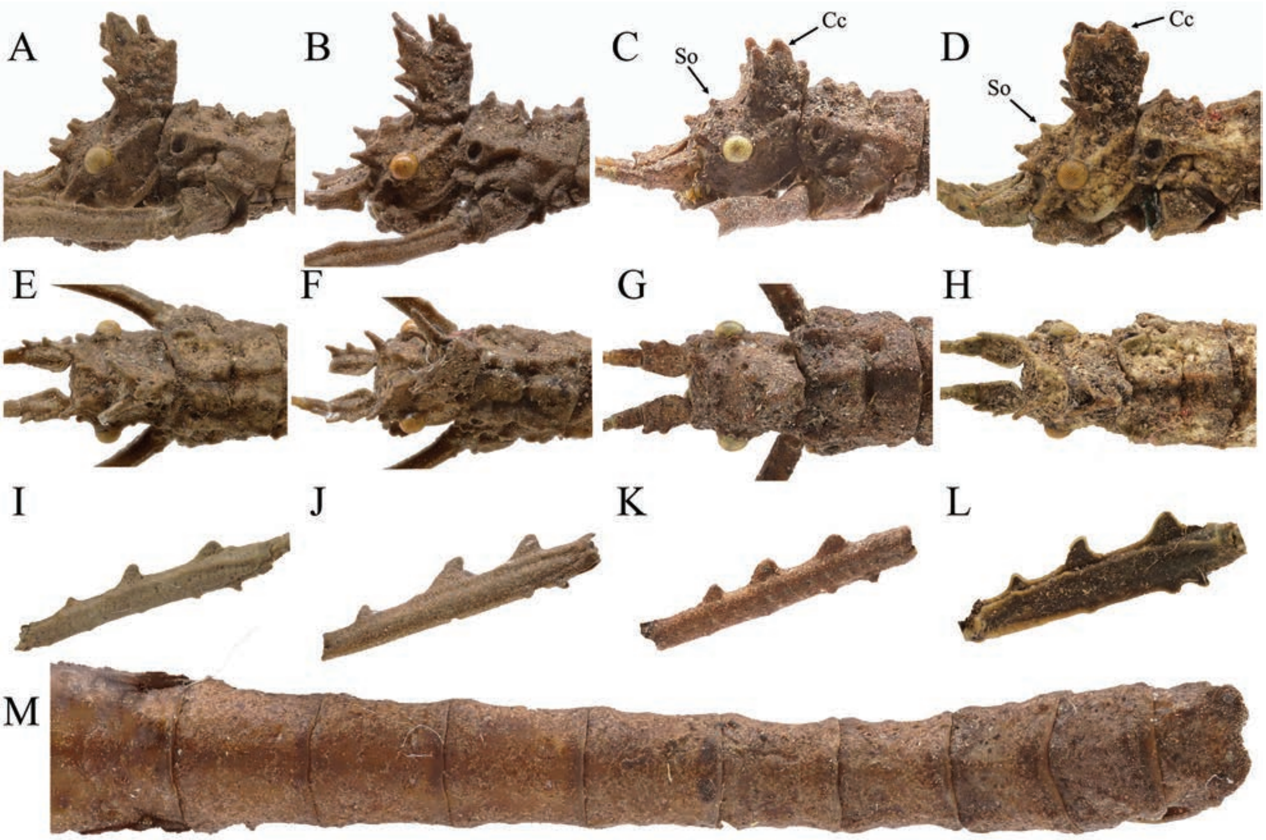

Figure 4. *Hainanphasma* spp., diagnostic characters of males. **A–D** lateral view of head **A** *H. longidentata* sp. nov. **B** *H. longiacuta* sp. nov. **C** *H. diaoluoshanensis* Ho, 2013 **D** *H. cristata* Ho, 2013 **E–H** dorsal view of head **E** *H. longidentata* sp. nov. **F** *H. longiacuta* sp. nov. **G** *H. diaoluoshanensis* Ho, 2013 **H** *H. cristata* Ho, 2013 **I–L** lateral view of metafemur **I** *H. longidentata* sp. nov. **J** *H. longiacuta* sp. nov. **K** *H. diaoluoshanensis* Ho, 2013 **L** *H. cristata* Ho, 2013 **M** *H. diaoluoshanensis* Ho, 2013, dorsal view of abdomen. So = supra-occipitals; Cc = central coronal. Not to scale.

***Hainanphasma longidentata* sp. nov.**

https://zoobank.org/B40561A6-4568-4B43-82CF-5D0D61EFDF5D
Figs 5, 6

Type material. ***Holotype*.** China • ♀; Hainan Province, Lingshui County, Diaoluoshan National Nature Reserve; 19 Aug. 2023; Yifan Liu leg.; SICAHN 23011. ***Paratype*.** China • 1♂; same data as for holotype; SICAHN 23012 (all deposited in SICAU).

Diagnosis. In female, scapus with two blunt spines and pedicellus with a blunt spine on outer lateral margin (Fig. 5C); crest of head distinctly raised and elongated, with posterior margin truncate in lateral view (Fig. 5E); eighth abdominal tergum rectangular, slightly longer than wide (Fig. 5A); posteromedian crest on ninth abdominal tergum distinctly surpassing posterior margin of anal segment, with lateral margins with three to four small lamellate teeth, notched apically (Fig. 5A, I).

In male, supra-antennals, supra-occipitals and pro-coronals present as blunt spines; anterior coronals consisting of a subtriangular lamella and a small blunt spine; central coronal slender and subcylindrical (Fig. 6I); abdominal terga with median longitudinal carina (Fig. 6A); ninth abdominal tergum with a posteromedian ridge-like structure elongated (Fig. 6G); poculum with posterior rim deeply notched posteromedially.

Description. Female (Fig. 5).

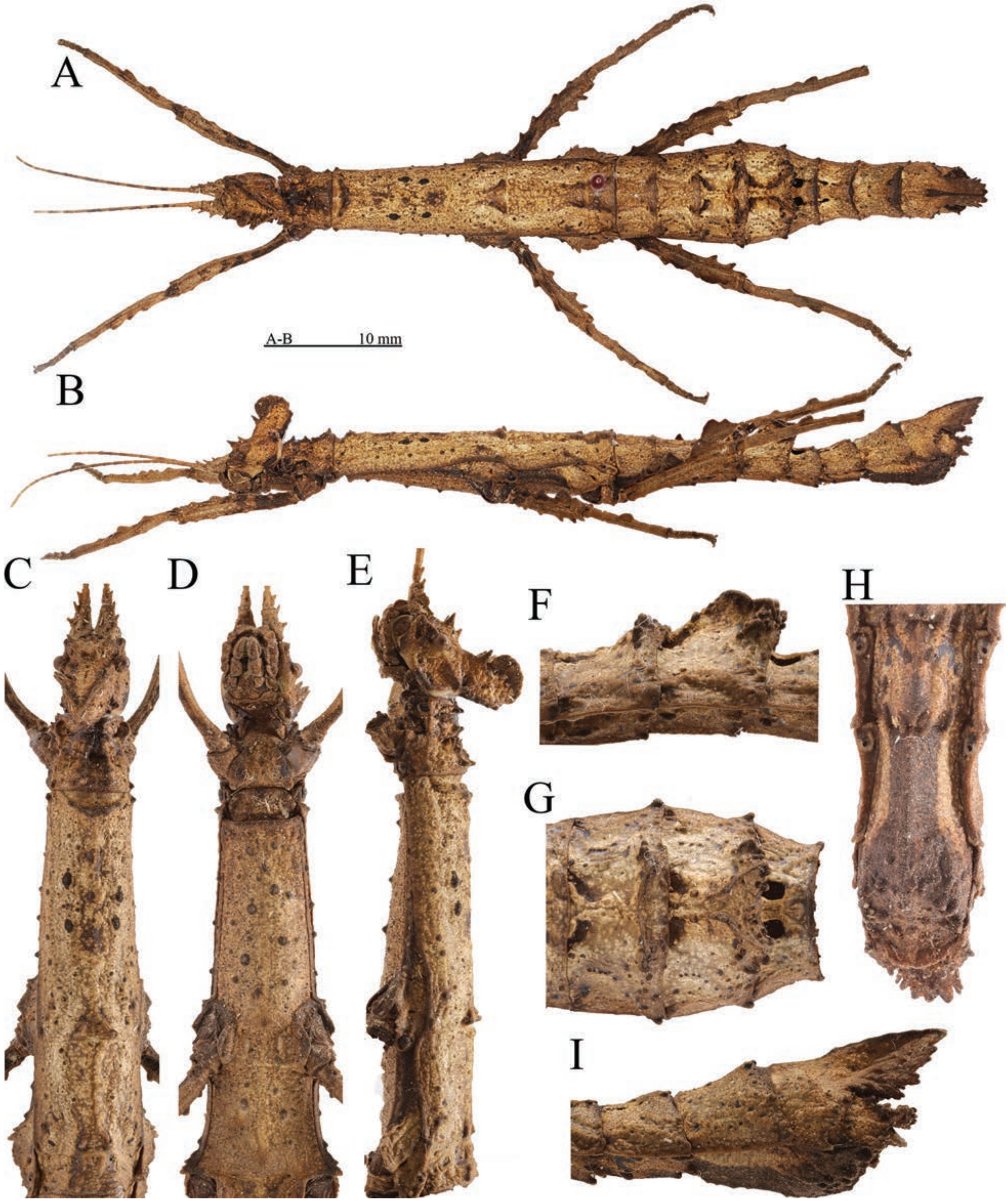

Figure 5. Female (HT) of *Hainanphasma longidentata* sp. nov. **A** dorsal view of habitus **B** lateral view of habitus **C** dorsal view of head and thorax **D** ventral view of head and thorax **E** lateral view of head and thorax **F** lateral view of fourth to fifth abdominal terga **G** dorsal view of fourth to fifth abdominal terga **H** ventral view of terminalia **I** lateral view of terminalia. Scale bars: 10 mm (**A, B**).

Head. Supra-antennals elongated and blunt, slightly flattened laterally and pointed outwards, about equal in length to pro-coronals, followed by two smaller supra-occipitals present as blunt spines. Supra-orbitals absent. Pro-coronals and anterior, central and posterior coronals fused basally and raised. Pro-coronals present as blunt spines. Anterior and central coronals almost continuous, merged into two carinae, strongly compressed laterally and lamellate, V-shaped in dorsal view. Posterior and lateral coronals present as small granules. Eyes dark brown, rounded. Postocular carina distinct, reaching posterior margin of head, with a conical tubercle apically. Antennae brown, darker in some segments, shorter than forelegs. Scapus strongly flattened dorsally, longer than pedicellus, with a central and subapical blunt spine on outer lateral margin; pedicellus slightly flattened dorsoventrally, shorter than third segment, with a central blunt spine on outer lateral margin; third segment cylindrical, slightly shorter than scapus.

Thorax. Pronotum trapezoidal, slightly widening towards the posterior, shorter than head; anterior margin slightly concave and posterior margin nearly truncate; anterolateral angles granulose. Transverse sulcus distinct and incurved, not reaching lateral margins. Prozona with two pairs of granules along distinct longitudinal sulcus. Metazona with three pairs of granules on two indistinct longitudinal carinae, along indistinct longitudinal sulcus. Mesonotum subtrapezoidal, widening towards the posterior; median longitudinal carina indistinct, bifurcated and thickened posteriorly; anterior margin thickened and broadly concave; lateral margins with a small granule near anterior margin. Mesopleura with three or four small granules, widened above coxae; widened portion separated by an indistinct short transverse sulcus; anterior portion subtriangular, with two small granules medially on outer lateral margin; posterior portion with two small elevations anteriorly on outer lateral margin. Metanotum rectangular in outline, about 3 times as long as median segment; median longitudinal carina distinct, bifurcated posteriorly. Metapleura widened above coxae; widened portion separated by a short oblique sulcus; anterior portion with two granules medially on outer lateral margin; posterior portion with a granule medially on outer lateral margin. Mesosternum and metasternum with dispersed conical black elevations.

Abdomen. Median segment to fourth terga with an x-shaped carina medially. Median segment transverse, with anterior and posterior margins nearly truncate. Second tergum parallel-sided, longer than median segment. Third to fourth terga gradually increased in width. Fourth tergum with median longitudinal carina distinct, bifurcated and lamellate posteriorly. Fifth tergum obliquely ascending, with two distinct trapezoidal tubercles posteromedially; tubercles projecting over posterior margin, covered with granules of irregular sizes; median longitudinal carina distinct, bifurcated posteriorly, with curled lamellae. Fifth to eighth terga gradually decreased in width. Eighth tergum rectangular, slightly longer than wide, with lateral margins slightly concave. Ninth tergum equal in width to anal segment, with a distinct posteromedial crest; crest elongated posteriorly, notched apically, distinctly surpassing posterior margin of anal segment; lateral margins with three or four teeth of irregular sizes. Anal segment obliquely descending and dorsally flattened, slightly narrower than ninth tergum, with two granules on oblique longitudinal carinae; dorsal surface covered with dense granules; posterolateral angles elevated and extended; posterior margin with two small granules medially. Subgenital plate boat-shaped, with distinct median carina and dense granules of irregular sizes; posterior rim dorsoventrally flattened and rounded apically, not reaching posterior margin of anal segment. Cerci flattened, hidden inside the anal segment, with apex rounded.

Legs. Profemora slightly curved basally; antero-dorsal carina distinct and undulate; postero-dorsal carina indistinct, with four indistinct elevations; ventral carinae indistinct except for medio-ventral carina, with indistinct elevations. Antero-dorsal carina of meso- and metafemora with four small teeth, almost equal in size. Postero-dorsal carina of meso- and metafemora with three distinct fin-like lamellae, increasing in size towards the apex. Antero-ventral and postero-ventral carinae of meso- and metafemora with four to five teeth, two ones larger subapically. Tibiae with carinae, shorter than corresponding femora; ventral carinae unarmed. Protibiae with distinct dorsal carinae with three lamellate elevations. Meso- and metatibiae with indistinct carinae; antero-dorsal carina with a small elevation; postero-dorsal carina with a fin-like lamella medially.

Male (Fig. 6).

Head. Supra-antennals distinct, slightly flattened laterally, blunt and slightly pointed outwards. Supra-occipitals smaller than supra-antennals, present as conical blunt spines. Pro-coronals and anterior, central and posterior coronals fused basally and distinctly raised. Pro-coronals present as blunt spines, about equal in length to supra-antennals. Anterior coronals consisting of two portions; the upper portion subtriangular and lamellate; the lower portion present as blunt spines, pointed forwards. Central coronal subcylindrical and slender, with apex rounded. Posterior and lateral coronals present as small granules. Eyes yellowish brown, rounded. Postocular carina distinct, with a small conical tubercle apically. Antennae grayish brown to dark brown, darker in some segments, shorter than forelegs. Scapus flattened dorsally, longer than pedicellus, with a central and a subapical blunt spine on outer lateral margin, the latter larger; pedicellus subcylindrical, shorter than third segment; third segment cylindrical, shorter than scapus.

Thorax. Pronotum slightly widening towards the posterior, longer than head; anterior margin concave and posterior margin convex. Transverse sulcus distinct and incurved, not reaching lateral margins. Prozona distinctly elevated centrally, with two pairs of granules alone indistinct longitudinal sulcus. Metazona with two pairs of elevations and a pair of granules on two longitudinal carinae, along indistinct longitudinal sulcus. Mesonotum with indistinct median longitudinal carina, bifurcated and thickened posteriorly; anterior margin thickened and broadly concave, with three indistinct elevations; lateral margins with a row of small pits; anterolateral angles with a small granule. Mesopleura widened above coxae; widened portion separated by an indistinct transverse sulcus, with outer lateral margin undulate. Metanotum rectangular, about 2.8 times as long as median segment, with posterior margin with two elevations; median longitudinal carina distinct. Metapleura widened above coxae; widened portion separated by a short oblique sulcus; anterior portion with outer lateral margin notched medially; posterior portion subtriangular, with a small triangular lamella medially on outer lateral margin.

Abdomen. Abdominal terga rough, slightly varying in length, with median longitudinal carina. Median segment with anterior margin slightly convex and posterior margin truncate. Second to third terga gradually decreasing in width, with a pair of elevations posteromedially. Second tergum rectangle, longer than wide, about 1.5 times as long as median segment. Fourth to sixth terga equal in width, with lateral margins broadly concave. Fourth and fifth terga raised posteromedially and with a pair of humps, posterior one larger. Sixth to eighth terga with a pair of granules posteromedially. Seventh tergum narrowest of abdominal terga. Eighth tergum widening towards the posterior. Ninth tergum with a ridge-like and elongated structure posteromedially. Anal segment transverse, shortest among three terminal terga, notched posteromedially; posterolateral angles

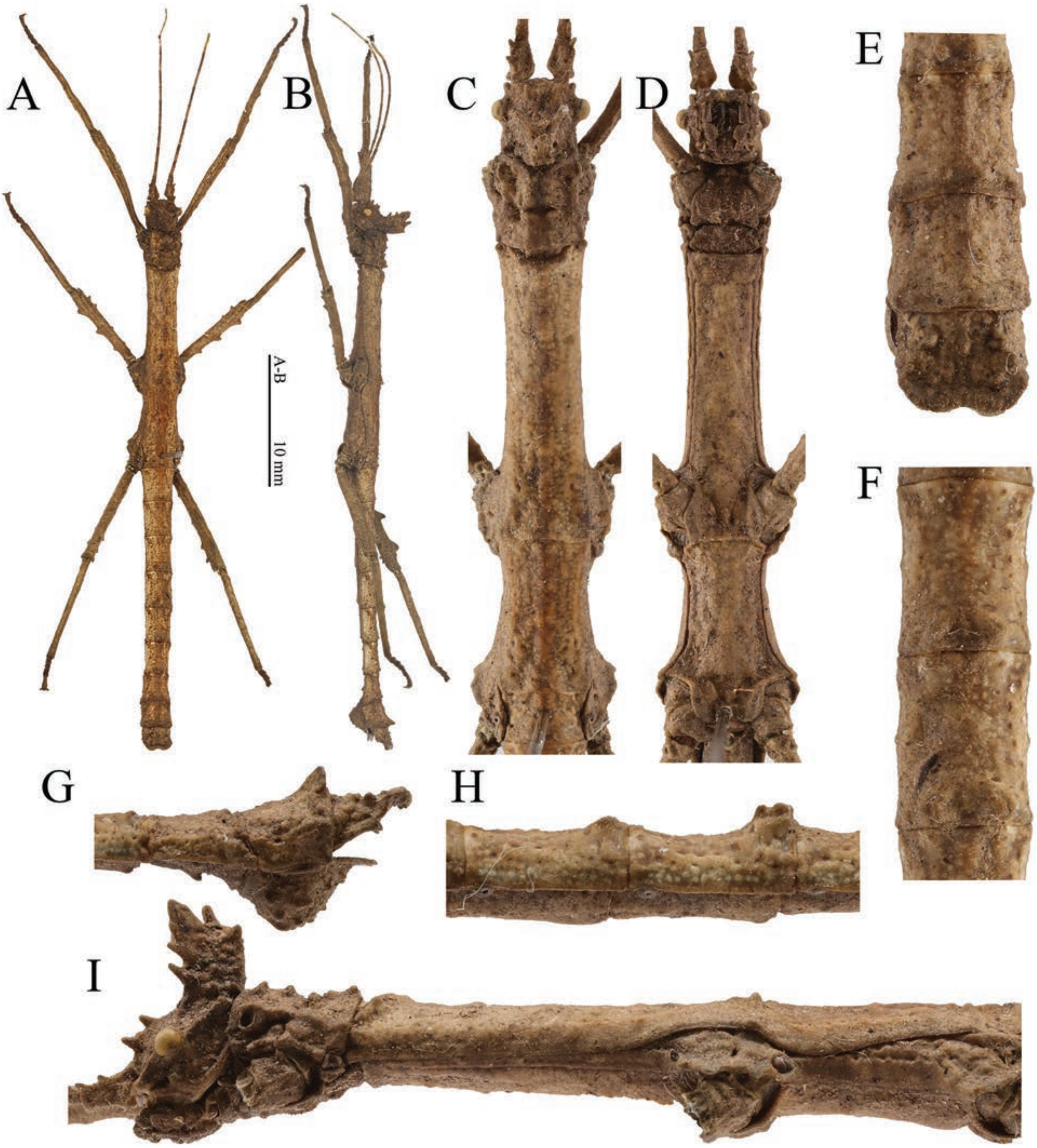

Figure 6. Male (paratype) of *Hainanphasma longidentata* sp. nov. **A** dorsal view of habitus **B** lateral view of habitus **C** dorsal view of head and thorax **D** ventral view of head and thorax **E** dorsal view of terminalia **F** dorsal view of fourth to fifth abdominal terga **G** lateral view of terminalia **H** lateral view of fourth to fifth abdominal terga **I** lateral view of head and thorax. Scale bars: 10 mm (**A, B**).

rounded. Poculum more or less triangular in lateral view, with numerous granules of irregular sizes; posterior rim dorsoventrally flattened and deeply notched posteromedially; posterolateral angles rounded. Cerci small and flattened, not reaching posterior margin of the anal segment, with apex rounded.

Legs. Profemora slightly curved basally; antero-dorsal carina distinct and undulate; postero-ventral carina with four indistinct elevations. Postero-dorsal carina of meso- and metafemora with three fin-like teeth, increasing in size towards the apex. Antero-dorsal carina of meso- and metafemora indistinct and unarmed. Antero-ventral and postero-ventral carinae of meso- and metafemora with two small teeth subapically, and with two indistinct elevations medially and basally. Tibiae with indistinct carinae except for protibiae, shorter than corresponding femora. Protibiae with distinct dorsal carinae with indistinct elevations. Meso- and metatibiae with carinae indistinct and unarmed.

Measurements (mm). Body length: ♀56.60, ♂43.39; length of head: ♀5.22, ♂3.11; length of pronotum: ♀4.10, ♂2.85; length of mesonotum: ♀12.89, ♂9.08; length of metanotum: ♀6.55, ♂5.15; length of median segment: ♀2.13, ♂1.84; length of profemora: ♀9.98, ♂8.71; length of mesofemora: ♀8.09, ♂7.44; length of metafemora: ♀10.64, ♂9.62; length of protibiae: ♀8.32, ♂8.21; length of mesotibiae: ♀6.94, ♂6.75; length of metatibiae: ♀10.27, ♂7.96.

Etymology. The name is derived from the Latin words *longi* (long) and *dentata* (toothed) and refers to the elongated posteromedian crest with dentate margins on the ninth abdominal tergum in female.

Distribution. Known only from the type locality.

Hainanphasma longiacuta sp. nov.

https://zoobank.org/F21F3C0D-2819-4202-A496-9B062551C527
Figs 7, 8, 10A–C

Type material. ***Holotype*.** China • ♀; Hainan Province, Ledong County, Jianfengling National Nature Reserve; 2 Aug. 2023; Yifan Liu leg.; SICAHN 23022. ***Paratype*.** China • 1♂; same data as for holotype; SICAHN 23023 (all deposited in SICAU).

Diagnosis. In female, scapus with a subapical blunt spine and a central indistinct elevation on outer lateral margin (Fig. 7C); pro-coronals present as subtriangular lamellae; central coronal carinate (Fig. 7E); eighth abdominal tergum wider than long (Fig. 7A); posteromedian crest on ninth abdominal tergum distinctly surpassing posterior margin of anal segment, tapering apically, with apex blunt. (Fig. 7A, H, I).

In male, supra-antennals distinct, present as blunt spines; supra-occipitals just present as small elevations; pro-coronals elongated and present as slender spines; anterior coronals consisting of a subtriangular lamella and a blunt spine; central coronal robust, with two granules apically (Fig. 8I); anal segment square in outline, about equal in length to ninth abdominal tergum (Fig. 8E).

Description. Female (Fig. 7).

***Head*.** Supra-antennals slightly flattened laterally, larger than supra-occipitals; apices blunt and slightly pointed outwards. Supra-occipitals present as conical spines. Pro-coronals and anterior, central and posterior coronals fused basally and raised. Supra-orbitals absent. Pro-coronals present as subtriangular lamellae, with apices blunt, about as long as supra-antennals. Anterior coronals strongly compressed laterally and lamellate, lower than central coronal. Central coronal carinate. Posterior coronals present as small granules. Lateral coronals indistinct. Eyes brown to black brown, rounded. Postocular carina distinct, reaching posterior margin of head, with an indistinct granule apically. Antennae brown, darker in some segments, slightly shorter than forelegs. Scapus strongly flattened dorsally, longer than pedicellus, with a subapical blunt spine and a central indistinct elevation on outer lateral margin; pedicellus slightly flat-

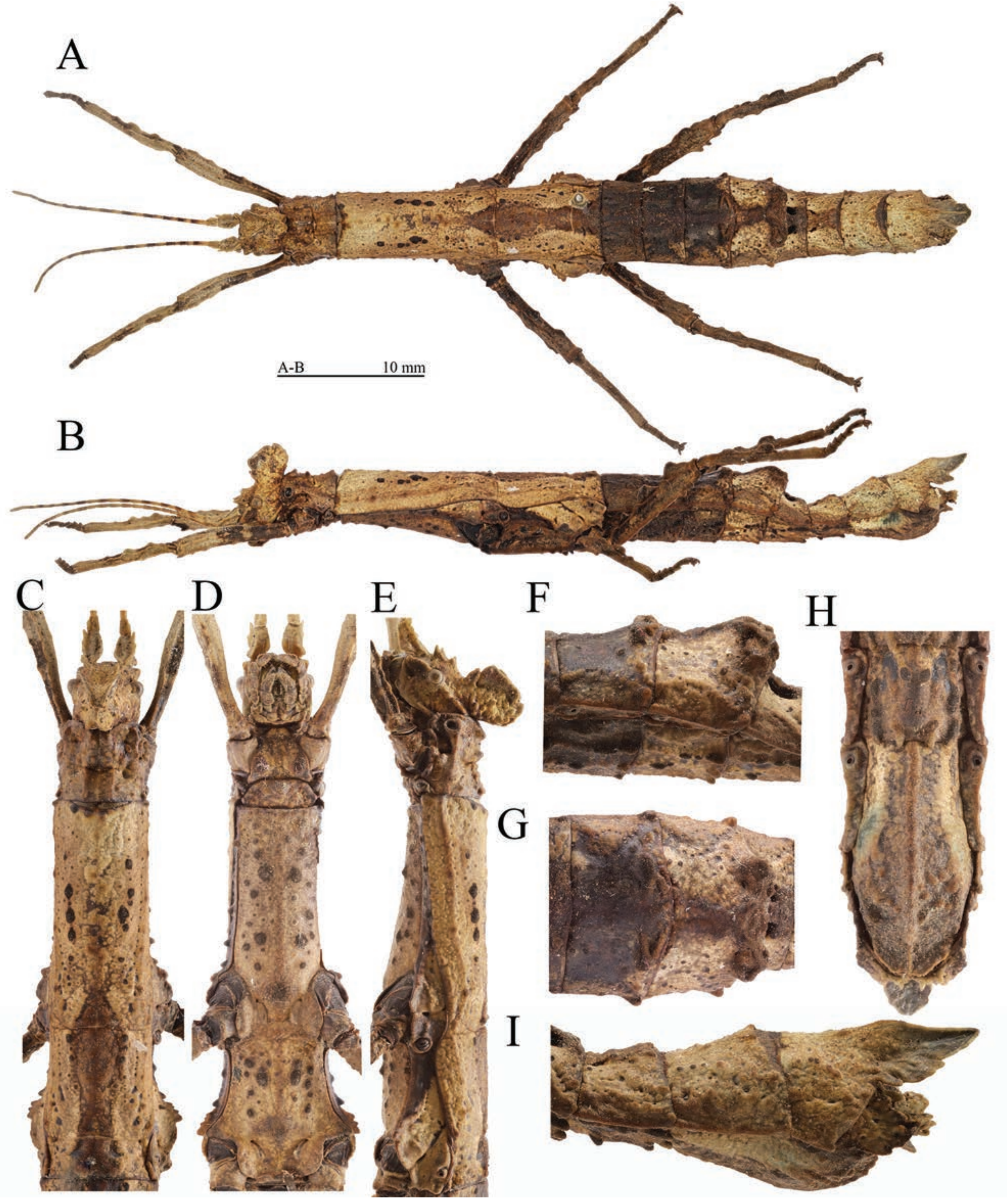

Figure 7. Female (HT) of *Hainanphasma longiacuta* sp. nov. **A** dorsal view of habitus **B** lateral view of habitus **C** dorsal view of head and thorax **D** ventral view of head and thorax **E** lateral view of head and thorax **F** lateral view of fourth to fifth abdominal terga **G** dorsal view of fourth to fifth abdominal terga **H** ventral view of terminalia **I** lateral view of terminalia. Scale bars: 10 mm (**A, B**); **C–I** not to scale.

tened dorsoventrally, carinate laterally, shorter than third segment; third segment cylindrical, shorter than scapus.

Thorax. Pronotum trapezoidal, slightly increasing in width posteriorly, about equal in length to head; anterior margin concave and posterior margin nearly truncate; lateral margins with four dispersed small granules; anterolateral angles rounded and granulose. Transverse sulcus distinct and incurved, not reaching lateral margins. Prozona with two pairs of granules along distinct longitudinal sulcus. Metazona with three pairs of small granules on two longitudinal carinae, along indistinct longitudinal sulcus. Mesonotum almost parallel-sided, with dispersed dark spots of irregular sizes; median longitudinal carina indistinct, bifurcated and thickened posteriorly; anterior margin thickened and incurved; anterolateral angles with a small granule. Mesopleura with five small granules, widened above coxae; widened portion separated by a short transverse sulcus; anterior portion subtriangular, with a small granule anteriorly and a subtriangular elevation medially on outer lateral margin; posterior portion with outer lateral margin undulate. Metanotum rectangular, about 2.5 times as long as median segment; median longitudinal carina distinct, bifurcated posteriorly. Metapleura widened above coxae; widened portion separated by a short oblique sulcus; anterior portion with consecutive three elevations medially on outer lateral margin; posterior portion with a granule medially on outer lateral margin. Mesosternum and metasternum with rounded dark elevations.

Abdomen. Median segment transverse, with anterior and posterior margins nearly truncate. Second tergum parallel-sided, longer than median segment. Third and fourth terga gradually increasing in width. Fourth tergum with two pairs of oblique and short carinae posteriorly. Fifth tergum obliquely ascending, with two distinct trapezoidal tubercles posteromedially; tubercles projecting over posterior margin, covered with small granules; median longitudinal carina distinct, bifurcated and curled posteriorly. Fifth to seventh terga gradually decreased in width. Eighth tergum transverse, wider than long, equal in width to ninth tergum. Ninth tergum wider than anal segment, with a distinct posteromedian crest; crest distinctly surpassing posterior margin of anal segment, tapering apically, with apex blunt; lateral margins with one triangular lamella or three small elevations. Anal segment parallel-sided, obliquely descending, with two granules on oblique longitudinal carinae; dorsal surface covered with dense granules; posterolateral angles elevated and extended; posterior margin with two granules medially. Subgenital plate boat-shaped, with distinct median carina and dense granules of irregular sizes; posterior rim dorsoventrally flattened, notched posteromedially, not reaching posterior margin of anal segment. Cerci flattened, hidden inside the anal segment.

Legs. Profemora slightly curved basally; antero-dorsal carina distinct and undulate; postero-dorsal and ventral carinae indistinct, with indistinct lamellate elevations. Antero-dorsal carina of meso- and metafemora with three to four small lamellae. Postero-dorsal carina of mesofemora with three fin-like lamellae, increasing in size towards the apex. Postero-dorsal carina of metafemora with three fin-like lamellae, median one largest. Antero-ventral and postero-ventral carinae of meso- and metafemora with four to six teeth of irregular sizes, subapical two ones larger and adjacent. Tibiae with carinae, shorter than corresponding femora; ventral carinae indistinct and unarmed. Protibiae with distinct dorsal carinae with three lamellate elevations. Meso- and metatibiae with indistinct dorsal carinae with one to two lamellate elevations anteriorly and medially.

Male (Fig. 8).

Head. Supra-antennals distinctly elongated, blunt and spinose, slightly flattened laterally, pointed outwards. Supra-occipitals indistinct, present as small elevations. Pro-coronals and anterior, central and posterior coronals fused basally and distinctly raised. Pro-coronals distinctly elongated, present as slender spines, with apices pointed. Anterior coronals laterally compressed, consisting of a subtriangular lamella tapering apically and a spine. Central coronal robust, with two granules apically. Posterior and lateral coronals present as small granules. Eyes yellowish brown, rounded. Postocular carina indistinct, with a minute granule apically. Antennae yellowish brown to grayish brown, darker in some segments, shorter than forelegs. Scapus flattened dorsally, longer than pedicellus, with a central elevation and a subapical blunt spine on outer lateral margin; pedicellus subcylindrical, shorter than third segment, laterally carinated; third segment cylindrical, equal in length to scapus.

Thorax. Pronotum rectangular, about equal in length to head; lateral margins undulate; anterior margin concave and posterior margin slightly convex. Transverse sulcus distinct and incurved, not reaching lateral margins. Prozona distinctly elevated centrally, with two pairs of granules; longitudinal sulcus absent. Metazona with two pairs of elevations and a pair of granules posteriorly on two longitudinal carinae, along indistinct longitudinal sulcus. Mesonotum slightly widening towards the posterior, with indistinct median longitudinal carina; anterior margin thickened and broadly concave; anterolateral angles with a small granule; posterior margin truncate, with two small granules medially. Mesopleura widened above coxae; widened portion separated by an indistinct transverse sulcus; anterior portion subtriangular, with a small granule anteriorly on outer lateral margin; posterior portion with outer lateral margin undulate. Metanotum approximately rectangular, about 3 times as long as median segment; median longitudinal carina distinct, with two small granules posteriorly. Metapleura widened above coxae; widened portion separated by an indistinct and oblique sulcus; anterior and posterior portion with a small granule medially on outer lateral margin.

Abdomen. Abdominal terga rough, slightly varying in length. Median segment with anterior margin convex and posterior margin almost truncate. Second tergum longer than wide, slightly narrowing towards the posterior, about 1.3 times as long as median segment. Third to fifth terga equal in length, with indistinct median longitudinal carina and lateral margins broadly concave. Fourth and fifth terga thickened and with a pair of humps posteromedially, posterior one larger. Sixth to seventh terga equal in width, shorter than fifth tergum, with median longitudinal carina and lateral margins broadly concave. Eighth to ninth terga gradually increasing in width. Ninth tergum with distinct median longitudinal carina gradually ascending, present as ridge-like structure posteromedially. Anal segment square in outline, dorsoventrally flattened, notched posteromedially, equal in length to ninth tergum; posterolateral angles rounded. Poculum more or less triangular in lateral view, with numerous granules of irregular sizes; posterior rim flattened dorsoventrally and notched posteromedially; posterolateral angles rounded. Cerci small and flattened, not reaching posterior margin of the anal segment, with apex rounded.

Legs. Profemora slightly curved basally; antero-dorsal carina distinct and undulate; postero-ventral carina with three indistinct elevations. Postero-dorsal carina of mesofemora with two fin-like teeth; postero-dorsal carina of metafemora with three fin-like teeth, median one largest. Antero-dorsal carina of meso- and metafemora indistinct and unarmed. Antero-ventral and postero-ventral carinae of meso- and metafemora with two small teeth subapically, and with two indistinct elevations medially and basally. Tibiae with indistinct carinae except for protibiae, shorter than corresponding femora. Protibiae with distinct dorsal

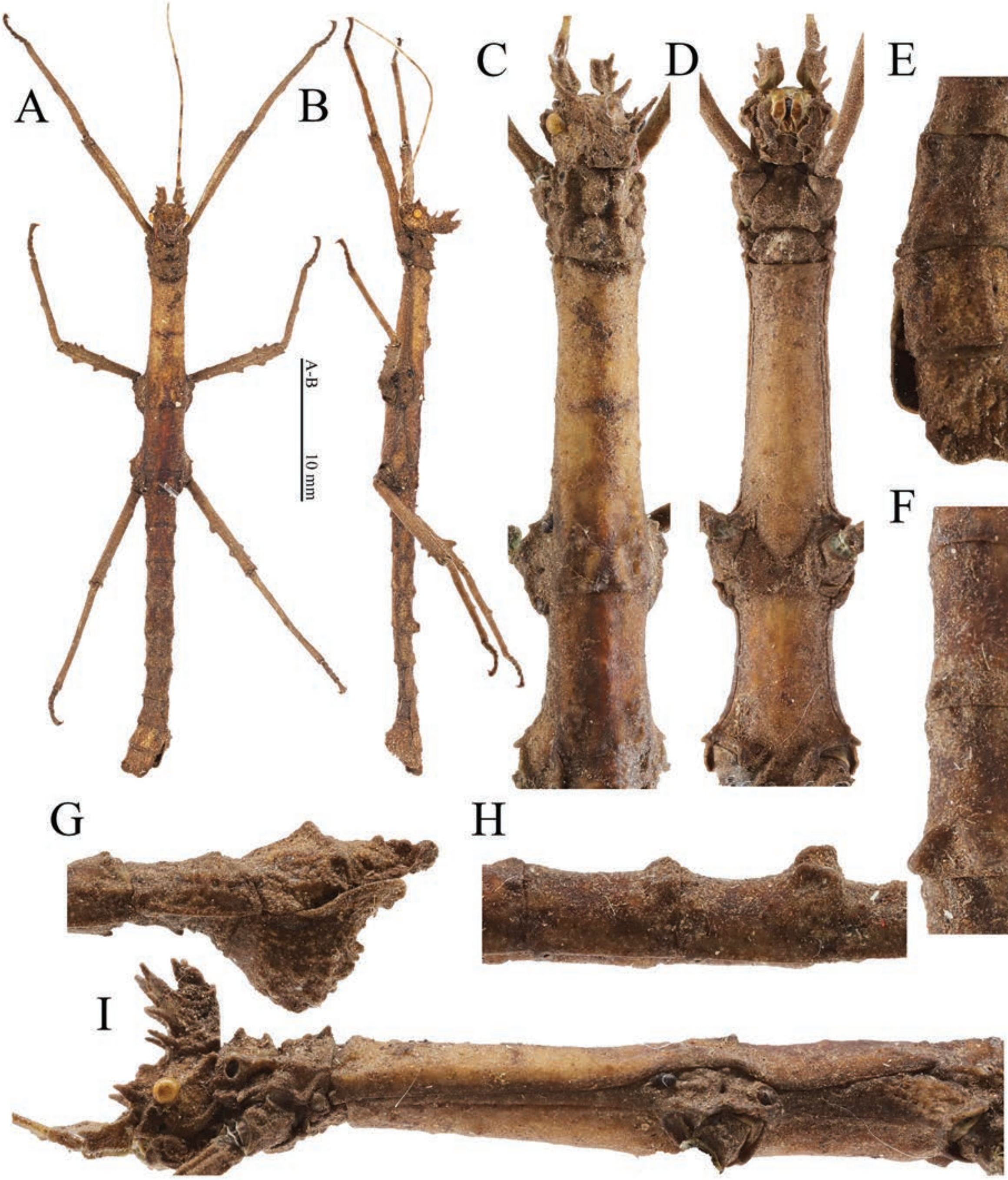

Figure 8. Male (paratype) of *Hainanphasma longiacuta* sp. nov. **A** dorsal view of habitus **B** lateral view of habitus **C** dorsal view of head and thorax **D** ventral view of head and thorax **E** dorsal view of terminalia **F** dorsal view of fourth to fifth abdominal terga **G** lateral view of terminalia **H** lateral view of fourth to fifth abdominal terga **I** lateral view of head and thorax. Scale bars: 10 mm (**A, B**); **C–I** not to scale.

carinae with an indistinct elevation medially. Meso- and metatibiae with indistinct postero-dorsal carina with an indistinct elevation medially.

Eggs (Fig. 10A–C). Capsule brown to dark brown, with small brownish elevations. Capsule and operculum covered with very sparse, short dark setae and densely punctulate. Micropylar plate trilobate with one anterior expansion and with two posterior expansions; anterior expansion slightly widening towards the capsule; posterior arms laterally directed and faded, not reaching ventral margin. Margin of micropylar plate elevated and widened. Micropylar cup distinct, placed near the posterior end of the micropylar plate. Operculum oval, elevated centrally; outer rim dark, with brownish elevations of irregular shape. Median line dark and indistinctly raised. Ventral margin oblique in lateral view.

Measurements (mm). Body length: ♀51.89, ♂41.46; length of head: ♀4.55, ♂3.05; length of pronotum: ♀4.27, ♂2.95; length of mesonotum: ♀11.29, ♂9.24; length of metanotum: ♀5.59, ♂4.96; length of median segment: ♀2.10, ♂1.65; length of profemora: ♀8.92, ♂8.66; length of mesofemora: ♀8.67, ♂6.73; length of metafemora: ♀10.33, ♂9.28; length of protibiae: ♀7.47, ♂7.61; length of mesotibiae: ♀6.72, ♂6.17; length of metatibiae: ♀8.21, ♂7.74.

Etymology. The name is derived from the Latin words *longi* (long) and *acuta* (sharpened) and refers to the posteromedian crest on ninth tergum elongated and tapering apically in female.

Distribution. Known only from the type locality.

Hainanphasma diaoluoshanensis **Ho, 2013**
Figs 9, 10D–F

Hainanphasma diaoluoshanensis Ho, 2013: 203: figs 7–9, 11, 14, 16.

Material examined. China • 1♀1♂; Hainan Province, Lingshui County, Diaoluoshan National Nature Reserve; 20 Aug. 2023; Yifan Liu leg.; SICAHN 23038 • 2♀; Hainan Province, Lingshui County, Diaoluoshan National Nature Reserve; 9 Jul. 2024; Yifan Liu leg.; SICAHN 24041 (all deposited in SICAU).

Revised diagnosis. Smallest in size compared to other species of *Hainanphasma*.

Females can be separated from the other species by the following combination of characters: Armature of head small; supra-orbitals present; eighth abdominal tergum wider than long; posteromedian crest on ninth abdominal tergum small, not reaching posterior margin of anal segment; legs with indistinct carinae.

Males can be separated from the other species by the following combination of characters: Armature of head small; anterior coronals subcylindrical (Fig. 9E); second to seventh abdominal terga without median longitudinal carina (Fig. 9A); fifth abdominal tergum with a pair of small humps posteromedially, fourth abdominal tergum absent (Fig. 9G, I); eighth abdominal tergum trapezoidal, wider than long (Fig. 9F); posterior rim of poculum truncate posteriorly.

Description. Male (Fig. 9). ***Head.*** Supra-antennals present as small and blunt spines, pointed outwards. Supra-occipitals indistinct, present as small granules. Pro-coronals and anterior, central and posterior coronals fused basally and raised. Pro-coronals and posterior coronals present as small elevations. Anterior coronals subcylindrical, larger than supra-antennals, with apices blunt. Central coronal robust and subtriangular, with apex rounded. Lateral coronals almost absent. Eyes yellowish brown, circular and strongly projecting hemispherically. Postocular carina indistinct, with a small granule apically. Antennae yellowish brown to darker brown, shorter than forelegs. Scapus flattened dorsally, longer than pedicellus, with two adjacent and spine-like tubercles placed before the middle on outer lateral margin; pedicellus subcylindrical, shorter than third segment; third segment cylindrical, shorter than scapus.

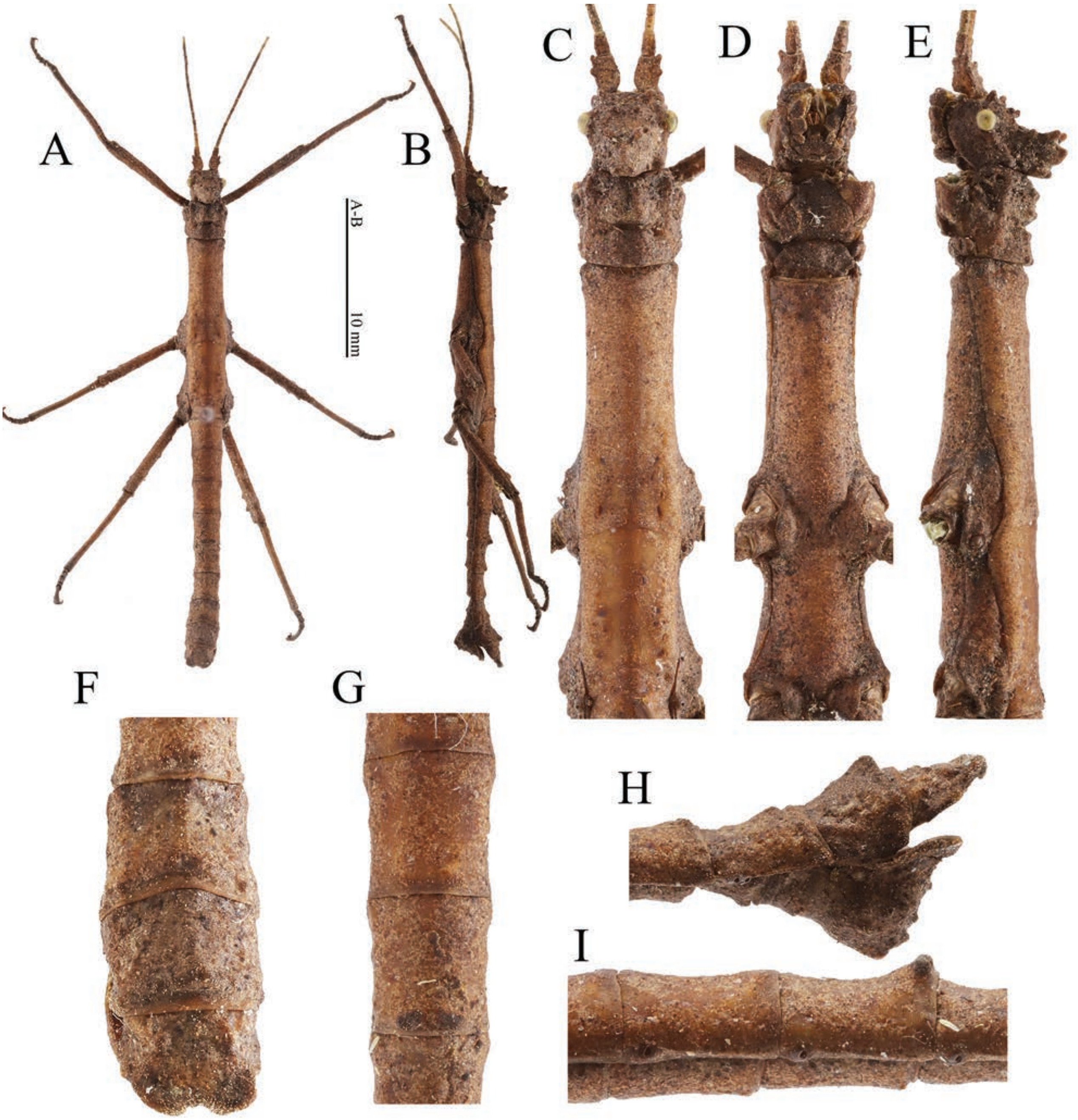

Figure 9. Male of *Hainanphasma diaoluoshanensis* Ho, 2013, from China, Hainan, Lingshui, 20 Aug. 2023, Yifan Liu leg. **A** dorsal view of habitus **B** lateral view of habitus **C** dorsal view of head and thorax **D** ventral view of head and thorax **E** lateral view of head and thorax **F** dorsal view of terminalia **G** dorsal view of fourth to fifth abdominal terga **H** lateral view of terminalia **I** lateral view of fourth to fifth abdominal terga. Scale bars: 10 mm (**A, B**); **C–I** not to scale.

Thorax. Pronotum rectangular, slightly longer than head; anterior margin concave and posterior margin convex; anterolateral angles rounded. Transverse sulcus distinct, not reaching lateral margins. Prozona elevated centrally, with two pairs of small conical elevations along indistinct longitudinal sulcus. Metazona with two pairs of granules on two longitudinal carinae along indistinct longitudinal sulcus. Mesonotum about rectangular, without median longitudinal carina; anterior margin thickened and broadly concave, equal in width to posterior margin; anterolateral angles rounded; posterior margin with two indistinct granules. Mesopleura widened above coxae; widened portion separated by a short transverse sulcus; anterior portion subtriangular, with a small granule medially on outer lateral margin; posterior portion with outer lateral margin truncate. Metanotum approximately rectangular, about 2.5 times as long as median segment, without median longitudinal carina. Metapleura widened above coxae; widened portion triangular, with a small granule posteriorly on outer lateral margin.

Abdomen. Abdominal terga rough, slightly varying in length, with posterior margin thickened. Median segment with anterior margin distinctly convex and posterior margin slightly concave. Second to seventh terga slightly decreasing in width, without median longitudinal carina. Second tergum rectangle, longer than wide, about 1.4 times as long as median segment. Fifth tergum with a pair of small humps posteromedially; fourth tergum absent. Sixth to seventh terga with posterior margin with a pair of granules. Sixth to eighth terga gradually increasing in width. Three terminal terga transverse, wider than long. Eighth abdominal tergum trapezoidal. Ninth tergum with distinct median longitudinal carina gradually ascending, present as ridge-like structure posteromedially. Anal segment transverse, dorsoventrally flattened, notched posteromedially, shortest and narrowest among three terminal terga; posterolateral angles rounded. Poculum about triangular in lateral view, with numerous granules of irregular sizes; posterior rim flattened dorsoventrally and truncate posteriorly; posterolateral angles rounded. Cerci small and flattened, not reaching posterior margin of the anal segment, with apex rounded.

Legs. Legs with carinae indistinct. Profemora slightly curved basally; antero-dorsal and postero-dorsal carinae with three indistinct elevations. Postero-dorsal carina of meso- and metafemora with three thickened and fin-like teeth, increasing in size towards the apex. Antero-dorsal carina of meso- and metafemora indistinct and unarmed. Antero-ventral and postero-ventral carinae of meso- and metafemora with two apical small elevations, posterior one larger. Tibiae unarmed, shorter than corresponding femora.

Eggs (Fig. 10D–F). Capsule brown, with small brownish elevations. Capsule and operculum bearing very sparse, short pale setae and densely punctulate. Micropylar plate trilobate with one anterior expansion and with two posterior expansions; anterior expansion slightly widening towards the capsule; posterior arms laterally directed, almost reaching ventral margin. Margin of micropylar plate elevated and widened. Micropylar cup distinct, placed near the posterior end of the micropylar plate. Operculum subcircular, elevated centrally, with irregularly shaped dense brownish elevations. Median line indistinctly raised. Ventral margin oblique in lateral view.

Redescription of female. *Head.* Supra-antennals present as conical spines, slightly larger than supra-occipitals. Supra-occipitals present, small and conical. Pro-coronals and anterior, central and posterior coronals fused basally and raised. Supra-orbitals and pro-coronals present as conical spines, posterior one larger. Anterior coronals slightly flattened laterally. Central coronal carinate, almost fused with anterior coronals. Posterior and lateral coronals just present as small granules. Postocular carina present, reaching posterior margin of head, with an indistinct granule apically. Antennae brown, darker in some segments, shorter than forelegs, with dense and minute brownish setae. Scapus flattened dorsally, with two adjacent and spine-like tubercles placed before the middle on outer lateral margin; pedicellus subcylindrical, shorter than third segment; third segment cylindrical, shorter than scapus.

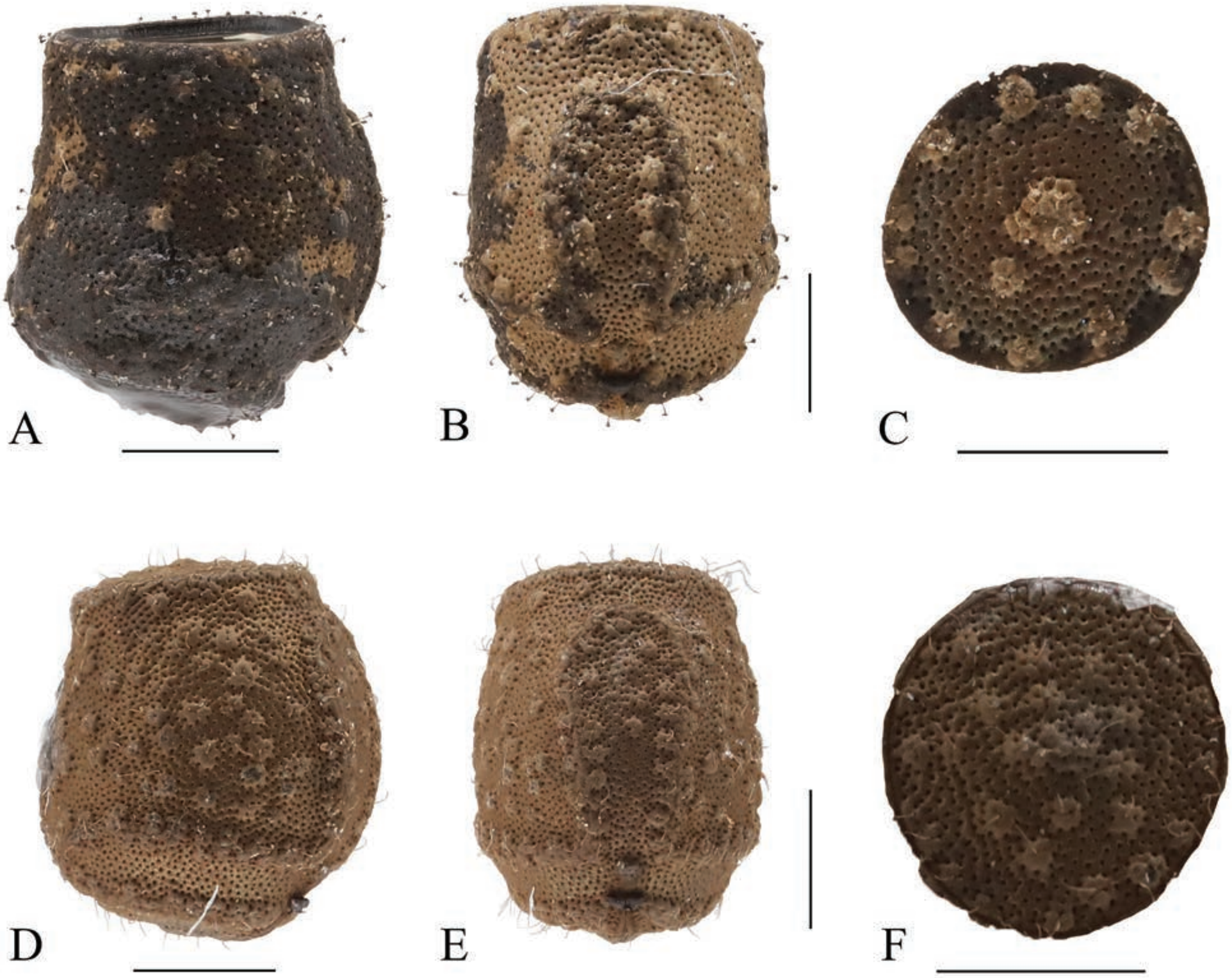

Figure 10. *Hainanphasma* spp., eggs. **A–C** *H. longiacuta* sp. nov. **A** lateral view **B** dorsal view **C** operculum **D–F** *H. diaoluoshanensis* Ho, 2013 **D** lateral view **E** dorsal view **F** operculum. Scale bars: 1 mm.

Measurements (mm). Body length: ♀44.24–46.25, ♂33.46; length of head: ♀4.15–4.35, ♂2.45; length of pronotum: ♀3.52–3.74, ♂2.72; length of mesonotum: ♀9.33–10.2, ♂7.12; length of metanotum: ♀4.70–4.98, ♂3.82; length of median segment: ♀1.87–1.91, ♂1.55; length of profemora: ♀8.01–8.43, ♂7.48; length of mesofemora: ♀7.39–7.78, ♂6.36; length of metafemora: ♀9.71–9.89, ♂8.04; length of protibiae: ♀7.09–7.35, ♂6.77; length of mesotibiae: ♀5.84–6.76, ♂5.22 length of metatibiae: ♀8.62–8.66, ♂6.49.

Distribution. China, Hainan Province, Lingshui County.

Hainanphasma cristata Ho, 2013

Hainanphasma cristata Ho, 2013: 203: figs 1–6, 10, 12, 13, 15, 17, 18.

Material examined. China • 1♀1♂; Hainan Province, Ledong County, Jianfengling National Nature Reserve, 28 Jul. 2023, Yifan Liu leg.; SICAHN 23052 • 2♀; Hainan Province, Ledong County, Jianfengling National Nature Reserve; 13 Jul. 2024, Yifan Liu leg.; SICAHN 24031 (all deposited in SICAU).

Redescription. Female. *Head.* Supra-antennals flattened laterally, distinctly larger than supra-occipitals; apices blunt and slightly pointed outwards.

Supra-occipitals present as conical spines. Pro-coronals and anterior, central and posterior coronals fused basally and raised. Supra-orbitals concial or invisible. Pro-coronals present as blunt spines, very close to anterior coronals. Anterior coronals compressed laterally and lamellate. Central coronal carinate. Posterior coronals present as small granules; lateral coronals distinct. Eyes brown, rounded. Postocular carina distinct, reaching posterior margin of head, with a distinct granule apically. Antennae brown, darker in some segments, slightly longer than forelegs, with dense and minute brownish setae. Scapus strongly flattened dorsally, about equal in length to the combined of pedicellus and third segments, with a subapical elongated spine and a central spine on outer lateral margin; pedicellus slightly flattened dorsoventrally, carinate laterally, shorter than third segment; third segment cylindrical, shorter than scapus.

Male. ***Head.*** Supra-antennals slightly flattened laterally, present as blunt spines, pointed outwards. Supra-occipitals indistinct, present as small granules. Pro-coronals and anterior, central and posterior coronals fused basally and raised. Pro-coronals present as blunt spines. Anterior coronals compressed laterally and lamellate, with anterior margins truncate in lateral view. Central coronal carinate. Posterior and lateral coronals present as distinct granules. Eyes yellowish brown, circular and strongly projecting hemispherically. Postocular carina distinct, with a small granule apically. Antennae yellowish brown to darker brown, with dense and minute brownish setae. Scapus strongly flattened dorsally, longer than pedicellus, with a central elevation and a subapical blunt spine on outer lateral margin; pedicellus slightly flattened dorsoventrally, shorter than third segment; third segment cylindrical, shorter than scapus.

Distribution. China, Hainan province, Ledong, Baisha, Wuzhishan and Wanning counties.

Remarks. This species was collected in similar location as *H. longiacuta* sp. nov., which is characterized by pedicellus carinate laterally and lacking blunt spine on outer lateral margin in female; fourth and fifth abdominal terga with a pair of humps on posterior margin in male, but differs in females with posteromedian crest of ninth abdominal tergum not surpassing posterior margin of anal segment, notched apically; pro-coronals present as blunt spines; eighth abdominal tergum about with the same length and width, differs in males with pro-coronals blunt; anterior coronals lamellate and not divided into two portions; central coronal carinate; anal segment wider than long.

Discussion

Hainanphasma is closely related to *Orestes* and was originally differentiated by body characters, but according to Bresseel and Constant (2018), these generic distinctions are weak and need additional assessment, although the eggs of *Hainanphasma* are notably different from those of *Orestes*. Morphological analysis based on new materials found distinct body characteristics that differentiate *Hainanphasma* from *Orestes*, besides the obvious differences in their eggs. *Hainanphasma* exhibits distinctive arrangements of cephalic armature, with supra-occipitals appearing as blunt spines or small elevations that are not divided into anterior and posterior supra-occipitals, and supra-orbitals are either absent or indistinct. Additionally, in female *Hainanphasma*, the fifth abdominal tergum is consistently higher than the fourth, and a larger posteromedian crest is found on the ninth abdominal tergum. These characteristics are not observed in *Orestes*.

We included the shape and size of the cephalic armature as part of the diagnosis and keys, based on the idea that the number and arrangement of the cephalic armature seem to represent useful generic characters of Datamini, whereas their shape and size seem to be species-specific (Bresseel and Constant 2018, 2020). Some species of *Orestes* with less-marked morphological differences were confirmed as distinct species (Bank et al. 2021), such as *Orestes mouhotii* and *Orestes draegeri* Bresseel & Constant, 2018, with the main differences being only by the proportionally shorter legs and the posteromedian crest on the ninth abdominal tergum in female.

Orestes guangxiensis was previously thought to be distributed in Hainan, but there is a lack of conclusive evidence (Chen et al. 2002; Hennemann et al. 2008). Ho (2013) suggested it should refer to a species from *Hainanphasma*. After examining numerous specimens and making collection from Hainan, in our opinion, key evidence for the distribution of *Orestes* in Hainan is lacking.

Hainan Province, geographically isolated from southern mainland China, is the largest tropical island in China. Its complex and unique habitats are rich in biodiversity, suggesting the likelihood of undiscovered species in Hainan. More material is needed to provide a more comprehensive knowledge of the position and relationship of *Hainanphasma*.

Acknowledgements

Many thank to the subject editor, Marco Gottardo (University of Siena, Italy), and the two reviewers for their valuable comments and suggestions, which greatly improved the quality of this manuscript. We sincerely thank Su Jie from Hebei University for his invaluable help with field surveys, and the staff of Bawangling National Nature Reserve, Diaoluoshan National Nature Reserve, Jianfengling National Nature Reserve, and Wuzhishan National Nature Reserve in Hainan for their field assistance.

Additional information

Conflict of interest

The authors have declared that no competing interests exist.

Ethical statement

No ethical statement was reported.

Funding

This study was supported by the National Natural Science Foundation of China (No. 32270488).

Author contributions

All authors have contributed equally.

Author ORCIDs

Yi-Fan Liu https://orcid.org/0009-0001-1649-969X

Jun-Jie Gu https://orcid.org/0000-0003-1931-4424
Hai-Jian Wang https://orcid.org/0000-0003-4858-5813

Data availability

All of the data that support the findings of this study are available in the main text.

References

Bank S, Buckley TR, Büscher TH, Bresseel J, Constant J, de Haan M, Dittmar D, Dräger H, Kahar RS, Kang A, Kneubühler B, Langton Myers SS, Bradler S (2021) Reconstructing the nonadaptive radiation of an ancient lineage of ground-dwelling stick insects (Phasmatodea: Heteropterygidae). Systematic Entomology 46: 487–507. https://doi.org/10.1111/syen.12472

Bradler S (2009) Die Phylogenie der Stab- und Gespenstschrecken (Insecta: Phasmatodea). Species, Phylogeny and Evolution 2: 3–139. https://doi.org/10.17875/gup2009-710

Bragg PE (2001) Phasmids of Borneo. Natural History Publications (Borneo), Kota Kinabalu, 49–63 + 345–353 pp.

Bresseel J, Constant J (2018) The Oriental stick insect genus *Orestes* Redtenbacher, 1906: taxonomical notes and six new species from Vietnam (Phasmida: Heteropterygidae: Dataminae). Belgian Journal of Entomology 58: 1–62.

Bresseel J, Constant J (2020) *Microrestes* gen. nov., a new genus in the Oriental stick insect tribe Datamini Rehn & Rehn, 1939 with a new species and a new combination (Phasmida: Heteropterygidae: Dataminae). Belgian Journal of Entomology 106: 1–19.

Brock PD, Büscher T, Baker E (2024) Phasmida Species File Online. Version 5.0/5.0. http://PhasmidaSpeciesfile.org [accessed on 1 September 2024]

Chen SC, He YH, Li Y (2002) Phasmatodea. In: Huang FS (Ed.) Forest insects of Hainan. Science Press, Beijing, 100–116 pp.

Gao HR, Xie CX (2022) *Pylaemenes gulinqingensis* sp. nov., a new species of subfamily Dataminae (Phasmida, Heteropterygidae) from Yunnan Province, China. Journal of Orthoptera Research 31(2): 125–129. https://doi.org/10.3897/jor.31.79783

Hennemann FH, Conle OV, Zhang W (2008) Catalogue of the Stick and Leaf-insects (Phasmatodea) of China, with a faunistic analysis, review of recent ecological and biological studies and bibliography (Insecta: Orthoptera: Phasmatodea). Zootaxa 1735: 1–76. https://doi.org/10.11646/zootaxa.1735.1.1

Hennemann FH, Conle OV, Brock PD, Seow-choen F (2016) Revision of the Oriental subfamily Heteropteryginae Kirby, 1896, with a re-arrangement of the family Heteropterygidae and the descriptions of five new species of *Haaniella* Kirby, 1904. (Phasmatodea: Areolatae: Heteropterygidae). Zootaxa 4159(1): 1–219. https://doi.org/10.11646/zootaxa.4159.1.1

Ho GWC (2013) Contribution to the knowledge of Chinese Phasmatodea II: review of the Dataminae Rehn & Rehn, 1939 (Phasmatodea: Heteropterygidae) of China, with descriptions of one new genus and four new species. Zootaxa 3669(3): 201–222. https://doi.org/10.11646/zootaxa.3669.3.1

Ho GWC (2016) Contribution to the knowledge of Chinese Phasmatodea III: catalogue of the phasmids of Hainan Island, China, with descriptions of one new genus, one new species and two new subspecies and proposals of three new combinations. Zootaxa 4150(3): 314–40. https://doi.org/10.11646/zootaxa.4150.3.4

Zompro O (2004) Revision of the genera of the Areolatae, including the status of *Timema* and *Agathemera* (Insecta, Phasmatodea). Abhandlungen des Naturwissenschaftlichen Vereins Hamburg (N.F.) 37: 1–327.

ZooKeys 1232: 379–412 (2025)
DOI: 10.3897/zookeys.1232.141810

Research Article

A checklist of Mantodea for Myanmar with the first record of *Schizocephala bicornis* (Mantodea, Eremiaphilidae) for the country

Zohreh Mirzaee[1], Martin Wiemers[1], Thomas Schmitt[1,2]

1 *Senckenberg Deutsches Entomologisches Institut, Eberswalder Str. 90, 15374 Müncheberg, Germany*
2 *Entomology and Biogeography, Institute of Biochemistry and Biology, Faculty of Science, University of Potsdam, D-14476 Potsdam, Germany*
Corresponding author: Zohreh Mirzaee (zmirzaee1988@gmail.com)

Abstract

This paper presents the first comprehensive checklist of Mantodea species in Myanmar, reporting a total of 54 species belonging to 11 families and 32 genera, one of which (i.e., *Schizocephala bicornis*) constitutes a new record for the country. Four species, *Creobroter urbanus*, *Gonypeta brunneri*, *Theopompa servillei*, and *Rhombodera laticollis*, are considered doubtful within Myanmar's fauna and require further investigation to confirm their presence. Additionally, *Aethalochroa ashmoliana*, *Gonypeta punctata*, and *Toxoderopsis taurus* are regarded as erroneous records.

Key words: Distribution, mantids, Schizocephalini, taxonomy

Academic editor:
Christian Jürgen Schwarz
Received: 16 November 2024
Accepted: 21 February 2025
Published: 25 March 2025

ZooBank: https://zoobank.org/BDDBA8CD-77CE-4400-B640-63260EA89CCE

Citation: Mirzaee Z, Wiemers M, Schmitt T (2025) A checklist of Mantodea for Myanmar with the first record of *Schizocephala bicornis* (Mantodea, Eremiaphilidae) for the country. ZooKeys 1232: 379–412. https://doi.org/10.3897/zookeys.1232.141810

Introduction

The study of Mantodea in Myanmar has been largely neglected, with most records being scattered across various publications that primarily focus on the Mantodea of other regions (e.g., Borneo, India) or the catalogue of Mantodea of the world (Ehrmann 2002; Schwarz et al. 2018; Sathe and Vaishali 2014; Mukherjee et al. 2014; Ehrmann and Borer 2015; Ghate et al. 2021; Yadav and Painkra 2021; Wu and Liu 2021; Kamila and Sureshan 2022). These studies often mention species that also occur in Myanmar. However, until now, there has been no comprehensive checklist dedicated to the Mantodea of Myanmar. This study closes this gap and presents the first such checklist of Mantodea from Myanmar, by using all the relevant literature in order to provide a comprehensive view of the species present in this region. The creation of a checklist is crucial for several reasons. First, a checklist facilitates taxonomic research by providing a reliable reference that can be used to compare species distributions and identify gaps in current knowledge (Margules and Pressey 2000). Second, it serves as a basic resource for biodiversity assessment and conservation planning, helping to identify species that may be endemic or at risk (Costello et al. 2013). By compiling this checklist, we aim to facilitate and encourage further research on Myanmar's Mantodea diversity.

Materials and methods

To compile the checklist, we utilized a range of literature including Wood-Mason (1889), Ehrmann (2002), Roy (2009), Sureshan and Sambath (2009), Schwarz et al. (2018), Mukherjee et al. (2014), Sathe and Vaishali (2014), Ehrmann and Borer (2015), Yadav and Painkra (2021), Wu and Liu (2021), Kamila and Sureshan 2022, as well as the Mantodea Species File website (Otte et al. 2023). These sources are well established and widely regarded as authoritative references in Mantodea research, frequently cited by experts in the field. In addition to the primary sources, data from the iNaturalist and GBIF platforms were also utilized. The term "Mantodea" was searched using a regional filter set to "Myanmar" to extract relevant records. Since citizen science platforms like GBIF may contain misidentifications, each record, along with its associated photographs when available, was individually reviewed.

The assessments followed specific criteria: If key morphological features could be clearly identified from the photographs, the species record was included in this study. However, if identification required the examination of male genitalia or other characteristics not visible in the photographs, the species was either excluded from the checklist or classified as potentially present. Such records were marked for further verification through future surveys to confirm their presence. This systematic approach improved the reliability of the species records while acknowledging the limitations of photographic evidence in certain cases. The taxonomy employed in this study adheres to the framework proposed by Schwarz and Roy (2019), with classification levels – family, subfamily, tribe, subtribe, genus, and species – structured according to the system detailed by Otte et al. (2023).

For the assignment of faunal elements, we first distinguished species apparently endemic to Myanmar from all the others. Second, we selected the species with a Bengal distribution, i.e., adjoining the Gulf of Bengal, being distributed along the coast of east India, as well as in Bangladesh and Myanmar. For the remaining species, the Oriental realm sensu Wallace (1876) was dissected into three parts: India, Indochina, and Sundaland. While India and Indochina are more or less separated by the Ganges delta, Indochina and Sundaland are separated by the Isthmus of Kra in Thailand (Schmitt 2020). If a species is marginally penetrating one adjoining sub-region, it is not considered part of this subregion; thus, Indochinese species also entering north-eastern India are not considered Indian elements, while Indian elements marginally entering Myanmar are not considered as Indochinese elements. As adjoining regions to the Oriental realm, we consider the two transition regions towards East Palearctic and Australis (i.e., Wallacea) and the two regions East Palearctic and New Guinea. Species occurring beyond these regions are classified as such.

Among the unidentified Mantodea specimens housed at the Senckenberg German Entomological Institute (**SDEI**), one specimen was identified by the first author as *Schizocephala bicornis* (Linné, 1758). This identification was achieved through a detailed examination of morphological characteristics, comparing the specimen with other *S. bicornis* specimens from Sri Lanka and India available in the collection. The method for preparing male genitalia followed Brannoch et al. (2017). The final segments of the male abdomen were dissected under a microscope, with the genitalia separated from the terminalia. The genitalia were then macerated in a 10% KOH solution for 24 h. After maceration, the sample was rinsed in distilled water for 24 h, followed by treatment in 70% ethanol, and finally, placed in glycerin to eliminate any remaining ethanol. The genitalia were photographed and stored in a vial with glycerin drops for further analysis. Photographs were taken using a set-up that included the Stone Master Stack Unit, an Olympus OM-D E-M1 Mark II camera, and Zeiss Luminar lenses (40 mm). The software used included Olympus Capture, Stone Master v. 3.8, Helicon Focus 7 for photo stacking, and ImageJ 1.53t for adding scale bars.

To create the distribution map, occurrence records of *S. bicornis* were gathered from previous studies (Sureshan and Sambath 2009; Sathe and Vaishali 2014; Yadav and Painkra 2021), as well as from the GBIF database (https://doi.org/10.15468/dl.vh8rf8), the iNaturalist portal (https://www.inaturalist.org/taxa/52101-Schizocephala-bicornis), and various museum collections (State Museum of Natural History, Karlsruhe (SMNK); Cleveland Museum of Natural History (CMNH); Lund University Biological Museum—Insect Collections Inventory, Entomological Collections (LUZM); Swedish Museum of Natural History (NHRM); and Royal Ontario Museum—Entomology Collection (ROMT)). All records available in GBIF were initially sourced either from iNaturalist or various museum collections. Upon reviewing iNaturalist records, we examined the associated photographs and excluded a few that were incorrectly identified. Subsequently, we contacted the museums to request photographs and the coordinates of the specimens, allowing us to verify that museum records corresponded to *S. bicornis*. A total of 180 records were obtained and mapped using QGIS v. 3.22.

Abbreviations of the zoological institutes and museums mentioned in this study:

ANSP	Academy of Natural Sciences, Philadelphia, USA
CNMS	National Museum, Colombo, Sri Lanka
DBUC	Dipartimento di Biologia Animale, Università di Catania, Catania, Sicily, Italy
FRID	Forest Research Institute, Dehra-Dun, India
HNHM	Hungarian Natural History Museum, Budapest, Hungary
IEAS	Academia Sinica, Shanghai, China
IFRI	Indian Forest Research Institute, Dehra Dun, Uttar Pradesh, India
LNHSM	Lingnan Natural History Survey and Museum, Lingnan University, China
LSUK	Linnean Society, London, United Kingdom
MEUU	Museum of Evolution of Uppsala University, Uppsala, Sweden
MHNG	Muséum d’histoire naturelle, Geneva, Switzerland
MNHN	Muséum national d’Histoire naturelle, Paris, France
MRSN	Natural History Museum, Turin, Italy
MSNG	Museo civico di Storia naturale G. Doria, Genoa, Italy
NHML	Natural History Museum of Los Angeles, USA
NHMUK	Natural History Museum, London, Great Britain
NHMW	Natural History Museum, Vienna, Austria
NHRS	Naturhistoriska Riksmuseet, Stockholm, Sweden
OXUM	University Museum, Oxford, Great Britain
RMNH	Nationaal Natuurhistorisch Museum, Leiden, Netherlands
SDEI	Senckenberg German Entomological Institute, Müncheberg, Germany

SEM	Shanghai Entomological Museum, Chinese Academy of Sciences, Shanghai, China
SMNK	State Museum of Natural History, Karlsruhe, Germany
UZIU	Universitets Zoologiska Institut, Uppsala, Sweden
ZMAS	Saint-Petersburg, Zoological Institute of the Russian Academy of Sciences, St. Petersburg, Russia
ZMB	Museum für Naturkunde der Humboldt-Universität zu Berlin, Berlin, Germany
ZMUH	Zoological Museum and University, Copenhagen, Denmark
ZSIC	Zoological Survey of India, Calcutta, India
ZSM	Zoological State Collection, Munich, Germany

Results

Checklist of the Mantodea of Myanmar

The checklist presented in this study includes a total of 54 species across 11 families and 32 genera. A review of observational records from iNaturalist and GBIF yielded approximately 102 records for 24 species from iNaturalist and 293 records from 47 species from GBIF. The GBIF data consisted of records from multiple sources, including:

- SMNK Mantid Collection: 236 records
- iNaturalist Research-grade Observations: 19 records
- NMNH Material Samples (USNM): 9 records
- NHMUK (London) Collection Specimens: 8 records
- NMNH Extant Specimen Records (USNM): 7 records
- International Barcode of Life project (iBOL): 4 records
- Cleveland Museum of Natural History: 4 records
- Paleobiology Database: 3 records
- INSDC Sequences: 3 records

In total, these platforms provided records for 47 species, including three extinct species of Mantodea (*Burmantis asiatica* Grimaldi, 2003, *Burmantis burmitica* Grimaldi, 2003, *Burmantis zherikhini* Delclos, Penalver, Arillo, Engel, Nel, Azar & Ross, 2016) discovered in Myanmar from amber fossils. Most of the recorded specimens are housed in museums and are included in the literature used for this study. However, some species were identified from Myanmar in museum collections, mostly at SMNK, Germany. Based on the known distribution of these species, it is plausible to classify the following species as expected taxa for Myanmar:

Anaxarcha graminea Stål, 1877
Hierodula tenuidentata Saussure, 1869
Hierodula pistillinota Wang, Zhou & Zhang, 2020
Hierodula confusa Vermeersch & Unnahachote, 2020
Tropidomantis gressitti Tinkham, 1937
Tropidomantis tenera (Stål, 1858)
Creobroter apicalis Saussure, 1869

Leptomantella tonkinae Hebard, 1920
Acromantis gestri Giglio-Tos, 1915

Additionally, the following species are regarded as doubtful and require verification:

Gonypeta brunneri Giglio-Tos, 1915 (Ehrmann 2002)
Theopompa servillei (De Haan, 1842) (Mukherjee et al. 2014; Kamila and Sureshan 2022)
Rhombodera laticollis Burmeister, 1838 (Ehrmann 2002)
Creobroter urbanus (Fabricius, 1775) (Ehrmann and Borer 2015; Kamila and Sureshan 2022).

Furthermore, the species *Aethalochroa ashmoliana* (https://www.inaturalist.org/taxa/750709-Aethalochroa-ashmoliana/browse_photos?place_id=6992), *Gonypeta punctata* (De Haan, 1842) reported in regional checklists (Mukherjee et al. 2014; Kamila and Sureshan 2022), and *Toxoderopsis taurus* (https://www.inaturalist.org/taxa/750765-Toxoderopsis-taurus/browse_photos?place_id=6992) are considered erroneous in this study. The presence of *Gonypeta punctata* (Evgeny Shcherbakov, pers. comm. Dec. 2024), *Aethalochroa ashmoliana*, and *Toxoderopsis taurus* in Myanmar is uncertain due to the lack of confirmed specimens, potential misidentifications, and gaps in verified distribution data. Further fieldwork and examination of museum specimens are recommended to confirm the occurrence of these species in Myanmar. This checklist provides a comprehensive compilation based on current knowledge and a thorough review of the literature, with all relevant records carefully examined.

Order Mantodea Latreille, 1802
Family Metallyticidae Giglio-Tos, 1917
Genus *Metallyticus* Westwood, 1835

1. *Metallyticus violaceus* (Burmeister, 1838)

Metalleutica violacea Burmeister, 1838: 527.
= *Metallyticus splendidus* var. Westwood, 1835: 442.
= *Metallyticus splendidus* var. *purpureus* Westwood, 1837: 359. Westwood 1889: 1.
= *Metalleutica vitripennis* Burmeister, 1838: 527.
= *Mantis chalybea* Serville, 1839: 202–203.
= *Metalleutica violacea* Burmeister, 1838: Charpentier 1841: 287–288. Saussure 1871: 267–268. Borre 1883: 62. Wood-Mason 1889: 1.
= *Mantis* (*Metalleutica*) *splendida* Westwood, 1835: De Haan 1842: 83.

Type material. Paratypes ♂ ♀ ZMB.

Type locality. Java.

Distribution. India (?), Myanmar (Giglio-Tos 1927; Wieland 2008), Malay Peninsula, Sumatra (Singkep Island), Borneo, Java, Davao (S Mindanao, Philippines) (Ehrmann 2002).

Faunal element. Oriental.

Remark. Historical records of *M. violaceus* from Myanmar and neighboring regions contain certain ambiguities. Giglio-Tos (1927) documented a single specimen from Tavoy, Myanmar, now known as Dawei, a city in southeastern Myanmar. This record is considered reliable, as it aligns well with the known distribution of the species. However, Wieland (2008) reported the existence of two specimens collected in 1836, currently housed in the Musée National d'Histoire Naturelle, Paris. These specimens are labelled as originating from "Mari, Indes orientales," a term that Wieland found ambiguous. His research indicated that "Mari" could refer to several locations, including sites in Pakistan, Myanmar, and Papua New Guinea. Ultimately, Wieland speculated that the location might be in northern Myanmar or Pakistan. Based on the known distribution of this species, we believe that its occurrence in northern Myanmar is unlikely. Instead, it is more plausible that the term "Mari" refers to a location in Indonesia, where species of this genus are commonly found. Further research and clarification of historical records are necessary to accurately determine the origin of these specimens.

Family Amorphoscelidae Stål, 1877
Subfamily Amorphoscelinae Stål, 1877
Genus *Amorphoscelis* Stål, 1871

2. *Amorphoscelis* sp.

Remark. In July 2024, a nymph was spotted and recorded on iNaturalist (https://www.inaturalist.org/observations/233030975) from Shan, Myanmar (21.929'N, 99.840'E). This specimen may belong to *Amorphoscelis singaporana* Giglio-Tos, 1915; however, accurate identification of *Amorphoscelis* species currently relies on examining male genitalia. Consequently, additional research is needed to confirm and verify the presence of this species in Myanmar. Additionally, a specimen of *Amorphoscelis* is housed in the Cleveland Museum of Natural History. It was collected by D. Brzoska from Thaung Dut, Sagaing, Myanmar, in 2013 and identified as *Amorphoscelis borneana* Giglio-Tos, 1914. However, due to the lack of access to these specimens and the need for male genitalia examination for definitive identification, we recommend future surveys to validate the occurrence of one or both species in Myanmar.

Family Nanomantidae Brunner de Wattenwyl, 1893
Subfamily Tropidomantinae Giglio-Tos, 1915
Tribe Tropidomantini Giglio-Tos, 1915
Genus *Eomantis* Giglio-Tos, 1915

3. *Eomantis guttatipennis* (Stål, 1877)

Tropidomantis guttatipennis Stål, 1877: 51.
= *Eomantis* [*Tropidomantis*] *guttatipennis* Stål, 1877: Giglio-Tos 1915: 47.

Type material. Holotype ♂ NHRS, paratype: ♀ NHMW.

Type locality. Nepal: Himalaya.

Distribution. India, Nepal, Tibet (China), Myanmar (Mukherjee et al. 2014; Schwarz et al. 2018), N Vietnam (Ehrmann and Borer 2015).

Faunal element. North Oriental.

Family Gonypetidae Westwood, 1889
Subfamily Iridopteryginae Giglio-Tos, 1915
Tribe Amantini Schwarz & Roy, 2019
Genus *Amantis* Giglio-Tos, 1915

4. *Amantis aliena* Beier, 1930

Amantis aliena Beier, 1930: 439.

Type material. Holotype ♀ NHMUK.

Type locality. Myanmar-SW: Tenasserim.

Distribution. Myanmar.

Faunal element. Endemic in Myanmar.

5. *Amantis biroi* Giglio-Tos, 1915

Amantis biroi Giglio-Tos, 1915: 153.

Type material. Holotype ♂ HNHM, paratype ♀ MHNG.

Type locality. India E: Martheran 800 m, Carin Cheba.

Distribution. India, Myanmar (Mukherjee et al. 2014; Schwarz and Konopik 2014).

Faunal element. Indian.

6. *Amantis bolivarii* Giglio-Tos, 1915

Amantis bolivarii Giglio-Tos, 1915: 153.

Type material. Syntypes ♂ MHNG, ♀ MSNG.

Type localities. Myanmar-SW: Tenasserim, Nepal: Himalaya-Kurseong.

Distribution. India, Nepal, Myanmar, Vietnam (Ehrmann and Borer 2015).

Faunal element. North Oriental.

Remark. Ehrmann (2002) listed the following type material for the species: a male holotype in MHNG, a female paratype in MSNG, a male paratype in HNHM, and a possible (para)type male in MRSN. However, according to the original description, there are only two syntypes, a male from Kurseong and a female from Tenasserim, with no holotype originally designated. Therefore, there are still only two syntypes in MHNG and MSNG, with no holotypes or paratypes nor lectotypes and paralectotypes being designated at this moment.

7. *Amantis fuliginosa* (Werner, 1931)

Cimantis fuliginosa Werner, 1931: 1330.

Type material. Holotype ♂ NHMUK.

Type locality. India: Madras-Anamalai Hills, 700 m a.s.l.
Distribution. India, Nepal, Myanmar (Mukherjee et al. 2014).
Faunal element. Indian.

8. *Amantis irina* (Saussure, 1870)

Gonypeta irina Saussure, 1870: 244. Saussure 1871: 56–57.
= *Iridopteryx*? [*Gonypeta*] *irina* (Saussure, 1870): Kirby 1904: 223.

Type material. Holotype ♂ MHNG.
Type locality. Maluku Islands.
Distribution. Myanmar, Malay Peninsula, Sumatra, Maluku Islands (Ehrmann 2002).
Faunal element. Indochinese and Sundaian.

9. *Amantis reticulata* (De Haan, 1842)

Mantis (*Oxypilus*) *reticulata* De Haan, 1842: 87. Stål 1860: 313–314. Kirby 1904: 223. Rehn 1912: 122.
= *Iridopteryx infumata* Bolivar, 1897: 305–306. Rehn 1903: 702.
= *Amantis gestri* Giglio-Tos, 1915: Herbard 1920: 30–31. Giglio-Tos 1927: 171. Beier 1935: 28: Beier 1966: 361 (Syn.?).

Type material. Holotype ♂ RMNH.
Type locality. Java: Karawang.
Distribution. Myanmar, Malay Peninsula, Sumatra, Borneo, Palawan, Java (Ehrmann 2002).
Faunal element. Indochinese and Sundaian.

Subfamily Gonypetinae Westwood, 1889
Tribe Gonypetini Westwood, 1889
Subtribe Gonypetina Westwood, 1889
Genus *Memantis* Giglio-Tos, 1915

10. *Memantis fuliginosa* (Thunberg, 1815)

Mantis fuliginosa Thunberg, 1815: 291–292.
= *Gonypeta femorata* Saussure, 1870: 230. Saussure 1871: 58–59.
= *Humbertiella consobrina* Saussure, 1871: 273–274.
= *Gonypeta* [*Mantis*] *fuliginosa* (Thunberg, 1815): Wood-Mason 1891. Kirby 1904: 224.
= *Elaea* [*Humbertiella*] *consobrina* (Saussure, 1871): Kirby 1904: 214.

Type material. Holotype ♀ MEUU.
Type locality. Sri Lanka.
Distribution. India, Sri Lanka, Nepal, Myanmar (Ehrmann and Borer 2015).

Faunal element. Indian.

Remark. Recent research has revealed inaccuracies in the previously documented information about this species. Kris Anderson conducted a thorough investigation into Thunberg's publications and uncovered key details. Contrary to earlier reports, the holotype is not housed at ZMAS, but at Uppsala University. Additionally, while the type locality was originally recorded as "India E," Anderson's research has clarified that the correct location is actually Sri Lanka. This updated information, verified through personal communication with Kris Anderson (Nov. 2024), corrects the inaccuracies presented in the earlier literature.

Genus *Gimantis* Giglio-Tos, 1915

11. *Gimantis authaemon* (Wood-Mason, 1882)

Gonypeta authaemon Wood-Mason, 1882: 21–27.
= *Iridopteryx marmorata* Brunner Von Wattenwyl, 1893: 65–66.

Type material. Holotype ♀ ZSIC.

Type locality. Myanmar-SW: Tenasserim, on the Mergui River, Minthantoung.

Distribution. India, Myanmar, Thailand, Malay Peninsula (Ehrmann 2002).

Faunal element. Oriental.

Subtribe Humbertiellina Brunner de Wattenwyl, 1893

Genus *Humbertiella* Saussure, 1869

12. *Humbertiella ceylonica* Saussure, 1869

Humbertiella ceylonica Saussure, 1869: 62.
= *Theopompa septentrionum* Wood-Mason, 1891: 64–66.
= *Humbertiella* [*Theopompa*] *septentrionum* (Wood-Mason, 1891): Kirby 1904: 214.

Type material. Holotype ♂ MHNG.

Type locality. Sri Lanka.

Distribution. Sri Lanka, NE India, Nepal, Myanmar (Schwarz et al. 2018).

Faunal element. Bengal.

13. *Humbertiella indica* Saussure, 1869

Humbertiella indica Saussure, 1869: 62.
= *Humbertiella africana* Rehn, 1912: 106–108. Giglio-Tos 1927: 66.

Type material. Holotype ♀ MHNG.

Type locality. India.

Distribution. Pakistan, India, Sri Lanka, Nepal, S Myanmar (Ehrmann and Borer 2015).

Faunal element. Indian.

Family Rivetinidae Ehrmann & Roy, 2002
Subfamily Deiphobinae Schwarz & Roy, 2019
Tribe Deiphobini Schwarz & Roy, 2019
Genus *Deiphobe* Stal, 1877

14. *Deiphobe mesomelas* (Manuel, 1797)

Mantis mesomelas Manuel, 1797: 635–636.
= *Mantis mesomelas* Olivier, 1792, attributio erroris.
= *Mantis conspurcata* Lichtenstein, 1802, partim.
= *Deiphobe mesomelas*: Giglio-Tos 1927: 487. Patel and Singh 2016: 41.
= *Deiphobe infuscata*: Ehrmann and Borer 2015: 230–231, 249, ♂ (India, Nepal, Sri Lanka).
= *Deiphobe brunneri*: Ehrmann and Borer 2015: 230, 248, ♂.
= *Deiphobe incisa*: Werner, 1933: 900–901, ♂. Roonwal and Bhasin 1951: 313, 315 (♂) (type catalogue). Marshall 1975: 316 (♂) (type catalogue).
= *Deiphobe* prope *incisa*: Lombardo 1991: 379–380 (♀) (Myanmar-NE). Lombardo 1993: 197–198 (Nepal). Mukherjee et al. 1995: 200, 278, 279–280, 281 (India-NW). Ehrmann 2002: 118, ♂ (India, Nepal?). Mukherjee et al. 2014: 40–41 (India, Myanmar, Nepal). Ehrmann and Borer 2015: 230, partim (India, Nepal, Myanmar?). Patel and Singh 2016: 41 (India, Myanmar, Nepal).
= *Deiphobe yunnanensis* Tinkham, 1937: 561–562, ♀ (China: Yunnan). Wang 1993: 105–106. Hua 2000: 21. Ehrmann 2002: 118 (China). Otte and Spearman 2005: 229. Zhu et al. 2012: 184.
= *Sphendale infuscata*: Bolivar 1897: 312 (31), ♂, ♀ (India or.). Bolivar 1899: 809.
= *Sphendale robusta* Kirby, 1904: 86 (Nepal). Kirby 1904: 269. Marshall 1975: 323 (type catalogue).

Type material. Holotype ♀, India, depository unknown.

Type localities. India, India-NW, China.

Distribution. India, Nepal, Myanmar, SW China (Schwarz et al. 2018).

Faunal element. North Oriental.

Family Eremiaphilidae Saussure, 1869
Subfamily Iridinae Westwood, 1889
Tribe Schizocephalini Saussure, 1869
Genus *Schizocephala* Serville, 1831

15. *Schizocephala bicornis* (Linné, 1758)

Gryllus (*Mantis*) *bicornis* Linné, 1758: 426. Linné 1764: 116.
= *Mantis bicornis* Linné, 1758: Linné 1767: 691.
= *Mantis oculata* Fabricius, 1781: 348. Fabricius 1787: 228. Stoll 1787: 32–33, 43. Olivier 1792: 632. Fabricius 1793: 19. Lichtenstein 1802: 20.
= *Mantis stricta* Manuel, 1797: 641.
= *Schizocephala stricta* Olivier, 1792: Serville 1831: 56, attributio erroris
= *Schizocephala oculata* Fabricius, 1781: Burmeister 1838: 552.
= *Mantis* (*Schizocephala*) *oculata* Fabricius, 1781: Blanchard 1840: 13. Blanchard 1845: 226–227. Blanchard 1850: 13.

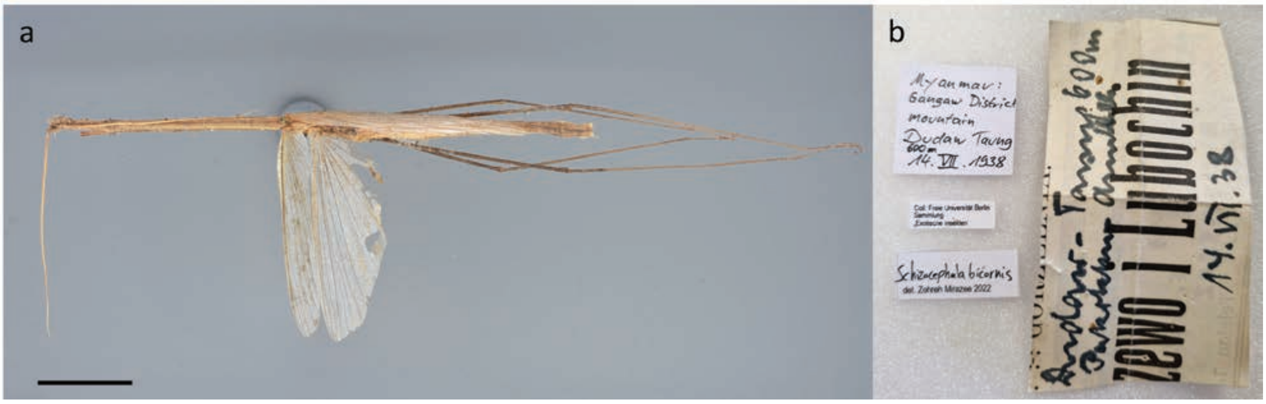

Figure 1. a *Schizocephala bicornis* male **b** labels. Scale bar: 30 mm (**a**).

Type material. Holotype ♀ UZIU.

Type locality. India.

Material examined. 1 ♂, Gangaw District Mountain, Dudaw Taung, Myanmar, 600 m. 4.07.1938), SDEI.

Distribution. India, Nepal, Sri Lanka, Myanmar (this work, new record deposited in SDEI: Gangaw District Mountain, Dudaw Taung, 600 m, 14 July 1938), Thailand, Vietnam.

Faunal element. North Oriental.

Remark. This study provides the first occurrence record of *S. bicornis* in Myanmar (Fig. 1). This mantid is characterized by its long and slender body, with coloration ranging from green to pale cream. It has antennae thickened near the base and anteriorly extended eyes that form a cone shape. The fore femur has four posteroventral spines and three discoidal spines, with the second being the longest. The fore tibia is shortened and equipped with six posteroventral spines. In females, the forewing is very small and opaque (Majumder et al. 2015).

Family Toxoderidae Saussure, 1869
Subfamily Toxoderinae Saussure, 1869
Tribe Toxoderini Saussure, 1869
Genus *Metatoxodera* Roy, 2009

16. *Metatoxodera subparallela* Roy, 2009

Metatoxodera subparallela Roy, 2009: 93–183.

Type material. Holotype MNHN, paratypes: MNHN (“allotype”), paratypes: NHML, SMNK.

Type localities. Myanmar S, Malaysia W.

Distribution. Myanmar, Malay Peninsula (Roy 2009).

Faunal element. Indochinese and Sundaian.

Genus *Paratoxodera* Wood-Mason, 1889

17. *Paratoxodera meggitti* Uvarov, 1927

Paratoxodera meggitti Uvarov, 1927: 658–659.

Type material. Holotype ♂ NHMUK.

Type localities. Burma (Myanmar).

Distribution. Myanmar, S China, Malay Peninsula, Borneo (Roy 2009).

Faunal element. Indochinese and Sundaian.

Genus *Toxodera* Serville, 1837

18. *Toxodera beieri* Roy, 2009

Toxodera beieri Roy, 2009: 111–117.

Type material. Holotype ♂ MHNG, paratypes: ♀ MHNG ("allotype"), ♂ MHNG, ♂ MNHN, ♂ SMNK, ♂ ZSM, ♀ NHML.

Type localities. West Malaysia.

Distribution. Myanmar, Laos, Malay Peninsula, NW Sumatra, Java, Bali (Roy 2009).

Faunal element. Indochinese and Sundaian.

Remark. Paratypes have no locality data.

19. *Toxodera denticulata* Serville, 1837

Toxodera denticulata Serville, 1837: 28–29.
= *Toxodera gigas* Ouwens, 1913: 123.

Type material. Holotype ♂ MNHN.

Type locality. Java.

Distribution. India, S China, Myanmar, Thailand, Laos, Malay Peninsula, Sumatra, Borneo, Java (Roy 2009).

Faunal element. Oriental.

20. *Toxodera fimbriata* Werner, 1930

Toxodera fimbriata Werner, 1930: 9.
= *Toxodera spinigera* Beier, 1931: 20–21.

Type material. Holotype ♂ NHRS.

Type locality. Sumatra.

Faunal element. Indochinese and Sundaian.

Distribution. Myanmar, Malay Peninsula, Sumatra, Borneo (Roy 2009).

21. *Toxodera integrifolia* Werner, 1925

Toxodera integrifolia Werner, 1925: 485–486.

Type material. Holotype ♀ NHRS.

Type locality. Java.

Distribution. Myanmar, Thailand, Malay Peninsula, Java (Roy 2009).

Faunal element. Indochinese and Sundaian.

Family Empusidae Burmeister, 1838
Subfamily Empusinae Burmeister, 1838
Tribe Empusini Burmeister, 1838
Subtribe Empusina Burmeister, 1838
Genus *Gongylus* Thunberg, 1815

22. *Gongylus gongylodes* (Linné, 1758)

Gryllus (*Mantis*) *gongylodes* Linné, 1758: 426. Linné 1764: 112.
= *Mantis gongylodes* Linné, 1758: Linné 1767: 690. Drury 1770: 129–130. Fabricius 1775: 275. Goeze 1778: 22. Fabricius 1781: 346. Fabricius 1787: 227. Gmelin-Linné 1790: 2049. Olivier 1792: 626–627. Fabricius 1793: 17. Lichtenstein 1802: 21–22. Brullé 1835: 78–79.
= *Mantis flabellicornis* Fabricius, 1793: 16–17. Lichtenstein 1802: 22. Latreille 1802: 90. Stoll 1813: 49–50.
= *Empusa* [*Gryllus* (*Mantis*)] *gongylodes* (Linné, 1758): Latreille 1807: 90. Stoll 1813: 46–48. Serville 1831: 48. Westwood 1837: 121–122. Serville 1839: 141–142. Charpentier 1841: 296–297.
= *Empusa flabellicornis* (Fabricius, 1793): Serville 1831: 48.
= *Empusa* (*Gongylodes*) [*Gryllus* (*Mantis*)] *gongylodes* (Linné, 1758): Burmeister 1838: 545.
= *Empusa* (*Empusa*) [*Gryllus* (*Mantis*)] *gongylodes* (Linné, 1758): Blanchard 1840: 10–11.
= *Gongylus* [*Gryllus* (*Mantis*)] *gongyloides* (Linné, 1758): Brunner Von Wattenwyl 1892: 76. Bolivar 1897: 316.

Type material. Holotype ♂ UZIU.

Type locality. India.

Distribution. India, Sri Lanka, Myanmar, Thailand, Java (Schwarz et al. 2018).

Faunal element. Oriental.

23. *Gongylus trachelophyllus* Burmeister, 1838

Empusa (*Gongylus*) *trachelophylla* Burmeister, 1838: 545.
= *Empusa [Gongylus] trachelophylla* Burmeister, 1838: Charpentier 1841: 297.

Type material. Type? 2♀♀ ZMB.

Type locality. India-E: Bengal, Lamar, Picot.

Distribution. India, Myanmar (Wood-Mason 1878).

Faunal element. Oriental.

Remark. In 1871, Wood-Mason received a specimen from Pegu (now Bago), Myanmar, collected by Mr. S. Kurz during a botanical expedition. He noted that the specimen has only slight differences from the typical form of the species, and its prothoracic shield displayed a striking bright blue-violet coloration. Further investigation is required to verify the presence of this species in Myanmar and determine whether it truly belongs to this species or represents a different one.

Family Hymenopodidae Giglio-Tos, 1915
Subfamily Hymenopodinae Giglio-Tos, 1915
Tribe Anaxarchini Giglio-Tos 1919
Genus *Odontomantis* Saussure, 1871

24. *Odontomantis planiceps* (De Haan, 1842)

Mantis (*Oxypilus*) *planiceps* De Haan, 1842: 88.
= *Mantis* (*Oxypilus*) *planiceps* De Haan, 1842: Giebel 1861: 112–113.
= *Acromantis javana* Giglio-Tos, 1915: Saussure 1870: 230.
= *Odontomantis javana* (Giglio-Tos, 1915): Saussure 1871: 33. Stål 1877: 87.

Type material. Holotype ♂ RMNH, paratypes: ♀ RMNH.

Type locality. Holotype: Java (♂), paratype: Borneo (♀).

Distribution. Myanmar (this work), Sumatra, Borneo, Java (Ehrmann 2002).

Faunal element. Indochinese and Sundaian.

Remark. This study documents the presence of this species in Myanmar, i.e., Yangon (16.842°N, 96.174°E), Pyin Oo Lwin (22.039°N, 96.472°E), Ye-U (22.763°N, 95.428°E), based on observations from iNaturalist (https://www.inaturalist.org/observations/139537130, https://www.inaturalist.org/observations/132144778, https://www.inaturalist.org/observations/147323093). However, additional research is required to confirm and validate these records. Additionally, two specimens housed at SMNK in Germany, identified as *Odontomantis* sp. from Myanmar, require further research to determine whether they belong to *Odontomantis planiceps*.

Tribe Hymenopodini Giglio-Tos, 1915
Subtribe Hymenopodina Giglio-Tos, 1915
Genus *Theopropus* Saussure, 1898

25. *Theopropus elegans* (Westwood, 1832)

Blepharis elegans Westwood, 1832: 190–191.
= *Creobotra* [*Blepharis*] *elegans* (Westwood, 1832): Saussure 1871: 145. Brunner Von Wattenwyl 1898: 215.
= *Theopropus praecontatrix* Saussure, 1898: 205 (♀).
= *Theopropus elegans* var. *flavicans* Giglio-Tos, 1927: 562.
= *Theopropus elegans* var. *rubrobrunneus* Beier, 1931: 153.

Type material. Holotype ♀ ZSIC.

Type locality. Tanesserim coast (Myanmar).

Distribution. Myanmar, Malay Peninsula, Sumatra, Borneo, Java (Ehrmann 2002).

Faunal element. Indochinese and Sundaian.

Genus *Hymenopus* Audinet-Serville, 1831

26. *Hymenopus coronatus* (Olivier, 1792)

Mantis coronata Olivier, 1792: 638.

= *Mantis cornuta* Olivier, 1792: Lichtenstein 1802: 24–25.
= *Empusa bicornis* Stoll, 1787: Latreille 1807: 90.
= *Mantis bicornis* Stoll, 1787: Stoll 1813: 38.
= *Hymenopa* [*Mantis*] *coronata* (Olivier, 1792): Serville 1839: 163.
= *Hymenopus* [*Mantis*] *bicornis* (Stoll, 1787): Saussure 1871: 143. Wood-Mason 1878: 586. Saussure 1898: 209–210. Annandale 1901: 839–848. Shelford 1902: 232. Shelford 1903: 299–304. Pocock 1910: 839. Meade-Waldo 1910: 50–52.

Type material. Holotype ♀ ZMB.

Type locality. Ambon Island (Amboina), Java.

Distribution. NE India, Myanmar (this study), S China, Vietnam, Thailand, Sumatra, Nias, Borneo, Java, Ambon, Flores (Hebard 1920; Werner 1921, 1933; Beier 1942).

Faunal element. Indochinese and Sundaian.

Remark. This species is documented for the first time in Myanmar through observational records available on iNaturalist (https://www.inaturalist.org/observations/165655863, https://www.inaturalist.org/observations/165655863, https://www.inaturalist.org/observations/143420594) and ten specimens housed in SMNK, Germany.

Subtribe Pseudocreobotrina Brunner de Wattenwyl, 1893
Genus *Creobroter* Westwood, 1889

27. *Creobroter gemmatus* (Houttuyn in Stoll, 1813)

Mantis gemmata Houttuyn in Stoll, 1813: 71.
= *Creobotra* [*Mantis*] *gemmata* (Stoll, 1813): Saussure 1869: 72–73, attributio erroris
= *Creobotra* [*Mantis*] *urbana* (Fabricius, 1775): Saussure 1871: 144–145. Brunner Von WattenwyL 1893: 73. Bolivar 1897: 315.
= *Creoboter* [*Mantis*] *gemmata* (Stoll, 1813): Kirby 1904: 291, attributio erroris
= *Creobroter gemmatus*: Beier 1929: 251–252. Ingrisch 1987: 136 (Nepal). Ehrmann 2002: 112. Otte and Spearman 2005: 89. Zhu et al. 2012: 47–49, ♂ and ♀. Ehrmann and Borer 2015: 230, 247, ♀. Patel et al. 2016c: 42051.

Type material. Holotype ♂ (lost).

Type locality. Unknown.

Distribution. India, Nepal, Myanmar (Ehrmann and Borer 2015; Kamila and Sureshan 2022), Thailand, S China, Vietnam, Sunda Islands (Ehrmann 2002).

Faunal element. Oriental.

Remark. Regarding the large disjunction and broad distribution of species within the *Creobroter* genus, it is probable that the extensive ranges reported for some species in the literature are artifacts of misidentification. We propose that this may have occurred due to the distributions of several closely related species being mistakenly combined into the range of a single species. The genus *Creobroter* includes 23 described species (Ehrmann 2002; Zhu et al. 2012), most of which exhibit considerable morphological similarity. Notably, *C. gemmatus* has often been used as a “standard identification” for any *Creobroter* specimen that could not be classified into another species, which may have led to subsequent descriptions referencing material originally assigned to *C. gemmatus*. Moreover, the genus has never been comprehensively revised, and many type specimens of early-described species are either lost or irreparably damaged. As a result, the taxonomy of this genus remains problematic until these issues are thoroughly addressed.

Subfamily Phyllothelyinae
Tribe Parablepharini
Genus *Parablepharis* Saussure, 1870

28. *Parablepharis kuhlii* (De Haan, 1842)

Mantis (*Blepharis*) *kuhlii* De Haan, 1842: 93–94.

Type material. Holotype ♀ RMNH.

Type locality. Java.

Distribution. NE India, Myanmar, Vietnam, Borneo, Java (Ehrmann 2002; Mukherjee et al. 2014; Ehrmann and Borer 2015; Kamila and Sureshan 2022).

Faunal element. Indochinese and Sundaian.

Tribe Phyllothelyini Brunner de Wattenwyl 1893
Genus *Phyllothelys* Wood-Mason, 1877

29. *Phyllothelys breve* (Wang, 1993)

Kishinouyeum breve Wang, 1993: Ehrmann and Roy 2009: 74.

Type material. Holotype ♂ SEM.

Type locality. Yunnan, Damenglong.

Distribution. Myanmar, China, Laos (Shcherbakov and Anisyutkin 2018; Wu and Liu 2021).

Faunal element. Indochinese.

30. *Phyllothelys paradoxum* Wood-Mason, 1885

Phyllothelys paradoxum Wood-Mason, 1884: 209–210.

Type material. Holotype ZSIC.

Type locality. Burmah (Myanmar).

Distribution. Myanmar.

Faunal element. Endemic in Myanmar.

31. *Phyllothelys westwoodi* (Wood-Mason, 1876)

Phyllocrania westwoodi Wood-Mason, 1876: 176. Reprint: 1876: 506–507.
= *Phyllothelis* [*Phyllocrania*] *westwoodii* (Wood-Mason, 1876): Westwood 1889: 44.

Type material. Syntypes: ♂ ♀ ZSIC, ♂ NHMUK.

Type locality. India: (Assam, Bhutan), Myanmar: Tenasserim.

Distribution. NE India, SW Myanmar (Roy 2009).

Faunal element. Bengal.

Subfamily Oxypilinae Saussure, 1871
Tribe Oxypilini Saussure, 1871
Genus *Ceratomantis* Wood-Mason, 1876

32. *Ceratomantis saussurii* Wood-Mason, 1876

Ceratomantis saussurii Wood-Mason, 1876: 175. Reprint: 1876: 506–507.
= *Oxypilus* [*Ceratomantis*] *saussurii* (Wood-Mason, 1876): Wood-Mason 1879: 259.

Type material. Holotype ♂ ZSIC.

Type locality. Pegu (Myanmar).

Distribution. Myanmar, Thailand, S China, Laos, Malay Peninsula (Ehrmann 2002).

Faunal element. Indochinese and Sundaian.

Tribe Hestiasulini Giglio-Tos, 1915
Genus *Catestiasula* Giglio-Tos, 1915

33. *Catestiasula nitida* (Brunner, 1893)

Pachymantis nitida Brunner von Wattenwyl, 1892: 72–73.
= *Catestiasula nitidae* Brunner von Wattenwyl, 1892: Giglio-Tos 1915: 101. Giglio-Tos 1927: 547.
= *Catestiasula nitida* (Brunner von Wattenwyl, 1892): Beier 1958: 247.

Type material. Holotype ♂ NHMW.

Type localities. Myanmar-SW: Tenasserim near Mount Mooleyit, 1800–1900 m.

Distribution. S Myanmar, Malay Peninsula, Sumatra, Borneo, Java (Ehrmann 2002).

Faunal element. Indochinese and Sundaian.

Subfamily Acromantinae Brunner de Wattenwyl, 1893
Tribe Acromantini Brunner de Wattenwyl, 1893
Genus *Ambivia* Stål, 1877

34. *Ambivia popa* Stål, 1877

Ambivia popa Stål, 1877: 88. Westwood 1889: 22, 26.
= *Popa* [*Mantis*] *undata* (Fabricius, 1793): Rehn 1903: 718. Werner 1908: 123–124. Rehn 1911: 25–26.
= *Ambivia popa* Stål, 1877: Giglio-Tos 1914: 86. Giglio-Tos 1915: 8. Werner 1922: 125. Giglio-Tos 1927: 529–530. Uvarov 1927: 90. Rehn 1927: 51–52. Sjöstedt 1930: 13. Werner 1933: 901. Beier 1956: 40. Mukherjee and Hazra 1982: 464. Lombardo 1993: 204. Mukherjee and Hazra 1993: 497, 500, 506. Lombardo 1995: 258–260. Mukherjee et al. 1995: 212–213.

Type material. Holotype ♂ NHRS.

Type locality. India: Tranquebar (Kalkutta).

Distribution. India, Nepal, Sri Lanka, Myanmar, Thailand, Laos, Vietnam, Malay Peninsula, Sumatra, Borneo (Schwarz et al. 2018).

Faunal element. Oriental.

Genus *Acromantis* Saussure, 1870

35. *Acromantis indica* Giglio-Tos, 1915

Acromantis indica Giglio-Tos, 1915: 7.

Type material. Holotype ♀ ZSIC.

Type locality. Myanmar: Thngannyinaung, Myavadi.

Distribution. S Myanmar (Ehrmann 2002).

Faunal element. Endemic in Myanmar.

Family Deroplatyidae Westwood, 1889
Subfamily Deroplatyinae Westwood, 1889
Tribe Deroplatyini Westwood, 1889
Subtribe Pseudempusina Rehn, 1911
Genus *Pseudempusa* Brunner von Wattenwyl, 1893

36. *Pseudempusa pavonina* Giglio-Tos, 1916

Pseudempusa pavonina Giglio-Tos, 1916: 3.

Type material. Holotype ♀ MSNG?

Type locality. Myanmar-NE: Carin Chebà, 900–1100 m.

Distribution. N Myanmar, N Thailand (Ehrmann 2002).

Faunal element. Indochinese.

Remark. The holotype might be lost.

37. *Pseudempusa pinnapavonis* Brunner von Wattenwyl, 1892

Pseudempusa pinnapavonis Brunner von Wattenwyl, 1892: 75.

Type material. Holotype ♀ MSNG.

Type locality. Myanmar-NE: Mount Catcin: east of the city, Bhamo, Myanmar: Carin Chebà. 900–1100 m.

Distribution. India, Myanmar, Thailand (Ehrmann 2002).

Faunal element. North Oriental.

Subtribe Deroplatyina Westwood, 1889
Genus *Deroplatys* Westwood, 1839

38. *Deroplatys angustata* Westwood, 1841

Deroplatys angustata Westwood, 1841: 34.

= *Deroplatys horrifica* Westwood, 1889: 40. Kirby 1904: 282.

Type material. Holotype ♂ OXUM.

Type locality. Java.

Distribution. Myanmar, Malay Peninsula, Sumatra, Borneo, Java (Ehrmann 2002).

Faunal element. Indochinese and Sundaian.

39. ***Deroplatys trigonodera*** Westwood, 1889

Deroplatys trigonodera Westwood, 1889: 40.

Type material. Holotype ♀ OXUM.

Type locality. Burmah (Myanmar).

Distribution. Myanmar, Sumatra, Borneo (Ehrmann 2002).

Faunal element. Indochinese and Sundaian.

Family Mantidae Latreille, 1802
Subfamily Choeradodinae Saussure, 1869
Genus *Asiadodis* Roy, 2004

40. ***Asiadodis yunnanensis*** (Wang & Liang, 1995)

Choeradodis yunnanensis Wang & Liang, 1995: 84.

Type material. Holotype ♂ IEAS.

Type locality. Yunnan.

Distribution. S China, Myanmar, N Thailand (Roy 2004).

Faunal element. Indochinese.

Remark. In Asia, *Asiadodis squilla* is broadly distributed across central and southern India as well as Sri Lanka, whereas *A. yunnanensis* is found in southern China, Myanmar, and northern Thailand. However, these areas have not been fully surveyed (Roy 2004).

Subfamily Mantinae Latreille, 1802
Genus *Mantis* Linné, 1758

41. ***Mantis religiosa*** Linné, 1758

Gryllus (*Mantis*) *religiosus* Linné, 1758: 426. Scopoli 1763: 105. Seba 1765, 4: 29, 75. Linné 1767: 690.
= *Mantis oratoria* Fabricius, 1775: 276–277. Lichtenstein 1802: 28–29.
= *Mantis sancta* Fabricius, 1787: 228. Olivier 1792: 628–629.
= *Mantis religiosa* var. *striata* Fabricius, 1793: 20.
= *Mantis maroccana* Thunberg, 1815: 287–299.
= *Mantis pia* Audinet-Serville, 1839: 193. Kirby 1899: 348.
= *Mantis prasina* Audinet-Serville, 1839: 195. Stål 1877: 61.
= *Mantis radiata* Motchoulsky: Fischer-Waldheim 1846: 101.
= *Mantis capensis* Saussure, 1872: 46–47. Stål 1877: 60–61.

= *Mantis religiosa* var. *major* Gerstaecker, 1873: 12.
= *Mantis macroura*: Brunner de Wattenwyl 1882: 60.
= *Mantis carinata* Cosmovici, 1888: 172–173.
= *Mantis religiosa* ab. *flava* Padewieth, 1900: 20.
= *Mantis religiosa* ab. *brunnea* Padewieth, 1900: 20.

Type material. Holotype ♂, paratypes 3 ♀ LSUK.

Type locality. Africa.

Distribution. Africa, Asia, Europe, North America (introduced) (Ehrmann 2002).

Faunal element. Old world.

Remark. Originally found in Africa, Europe, and Asia, it has also been introduced to North America.

Genus *Statilia* Stål, 1877

42. *Statilia* sp.

Remark. In the present study, a specimen from Myanmar is documented as *Statilia* sp. (potentially *Statilia maculata*), based on an observation from iNaturalist (https://www.inaturalist.org/observations/198274625). Additionally, five specimens identified as *Statilia* and collected from Myanmar are housed at SMNK in Germany, requiring further research for species-level identification. The preliminary identification of *Statilia* sp. by the first author remains provisional, as accurate identification of this genus currently necessitates the examination of male genitalia.

43. *Statilia nobilis* (Brunner von Wattenwyl, 1893)

Mantis nobilis Brunner von Wattenwyl, 1893: 70. Beier 1935: 92. Beier 1942: 142. Mathur 1946: 101. Roonwal and Bhasin 1951: 317. Roy 1967: 127, 148. Roy 1968: 175 (syn. of *Statilia nemoralis*).
= *Statilia nemoralis*: Chatterjee and Mukherjee 2013: 4907–4909. Ehrmann and Borer 2015: 242, 268. Otte and Spearman 2005: 193. Patel and Singh 2016: 31. Ingrisch 1987: 114, 136, L3 = ♂ (Nepal). Chatterjee and Mukherjee 2013: 4907–4909.
= *Mantis indica* Mukherjee, 1995: 185, 201, 300–301, 357. Roy 2000: 163. Mukherjee and Shishodia 2000: 64, 65. Ehrmann 2002: 215. Mukherjee et al. 2005: 147, #35–36 (type catalog). Otte and Spearman 2005: 185. Vyjayandi 2007: 95. Berg et al. 2011: 44. Ghate et al. 2012: 22. Chatterjee and Mukherjee 2013: 4907–4909. Mukherjee et al. 2014: 3, 38–39. Ehrmann and Borer 2015: 242, 268. Schwarz et al. 2017: 7.

Type material. Holotype ♀ MSNG.

Type locality. Myanmar; Synonym: *S. indica*: holotype and paratype: India-NE.

Distribution. India, Nepal, Myanmar, Thailand (Ehrmann 2002; Kamila and Sureshan 2022).

Faunal element. North Oriental.

Subfamily Tenoderinae Brunner de Wattenwyl, 1893
Tribe Tenoderini Brunner de Wattenwyl, 1893
Subtribe Tenoderina Brunner de Wattenwyl, 1893
Genus *Tenodera* Burmeister, 1838

44. *Tenodera aridifolia* (Houttuyn in Stoll, 1813)

Mantis aridifolia Houttuyn in Stoll, 1813: 65–66. Audinet-Serville 1839: 178–179, ♂.
= *Paratenodera aridifolia*: Rehn 1903: 705. Rehn 1909: 180.
= *Tenodera aridifolia*: Giglio-Tos 1927: 414, ♂ and ♀ (Asia orientalis). Ehrmann 2002: 349. Ehrmann 2002: 349. Zhu et al. 2012: 221, ♂. Schwarz and Konopik 2014: 151. Ehrmann and Borer 2015: 242, 268, ♀. Patel and Singh 2016a: 37. Mukherjee et al. 2017: 9835–9836, ♂.
= *Tenodera aridifolia aridifolia*: Beier 1935: 93. Ingrisch 1987: 114, 136, ♂ and ♀ (Nepal). Otte and Spearman 2005: 200.
= *Mantis chloreudeta* Burmeister, 1838: 535 (Java, East India). Saussure 1869: 69. Giglio-Tos 1912: 37.

Type material. Holotype ♂ ZMUH.

Type locality. India-E.

Distribution. India, Nepal, S China, Taiwan, Japan, Myanmar, Thailand, Malay Peninsula (Penang, Perak), Philippines, Sumatra, Borneo, Sulawesi, Java, Lesser Sunda Islands (Lombok, Flores, Sumba); introduced: Florida (USA) (Ehrmann 2002; Mukherjee et al. 2014; Ehrmann and Borer 2015; Schwarz et al. 2018; Kamila and Sureshan 2022).

Faunal element. Oriental; Wallacean.

45. *Tenodera fasciata* (Manuel, 1787)

Mantis fasciata Manuel, 1787: 640 (Surinam) (err.).
= *Thespis fasciata*: Audinet-Serville 1831: 46, 55 (Surinam) (err.).
= *Mantis* (*Tenodera*) *fasciata*: Burmeister 1838: 534–535 (Amboina, Java, Tranquebar).
= *Tenodera fasciata*: Giglio-Tos 1912: 45–46. Giglio-Tos 1927: 416. Ingrisch 1987: 114, 136, ♂ (Nepal). Ehrmann 2002: 350. Schwarz and Konopik 2014: 151. Ehrmann and Borer 2015: 243, 269. Patel and Singh 2016a: 38.
= *Tenodera fasciata fasciata*: Otte and Spearman 2005: 202.
= *Mesopteryx fasciata*: Kirby 1904: 238.
= *Mantis leptelytra* Lichtenstein, 1802: 20 (Surinam) (err.). Balderson 1984: 11 (type catalog).
= *Mantis attenuata* Stoll, 1813: 13♂ (Surinam) (err.).
= *Tenodera attenuata*: Hebard 1920: 51, ♂ (Java). Werner 1922: 152. Balderson 1984: 11 (type catalog)
= *Mantis exsiccata* Audinet-Serville, 1839: 176 (Java). Balderson 1984: 11 (type catalog)
= *Tenodera intermedia* Saussure, 1870: 233. Balderson 1984: 11 (type catalog)
= *Tenodera superstitiosa*: Saussure 1871a: 99. Westwood 1889: 13. Rehn 1903: 705. Werner 1908: 118. Rehn 1909: 180.

Type material. See remark.

Type locality. Unknown.

Distribution. India, Sri Lanka, Nepal, S China, Myanmar, Thailand, Malay Peninsula, Borneo, Sulawesi, Java, Flores, Sumba, Moluccas (Ehrmann 2002; Mukherjee et al. 2014; Ehrmann and Borer 2015; Schwarz et al. 2018; Kamila and Sureshan 2022).

Faunal element. Oriental; Wallacean.

Remark. The holotype male of '*M. leptelytra*' (erroneously reported from Surinam) is housed in the MNHN, with the depository of the holotype male (*M. fasciata*) remaining unknown. '*Mantis attenuata*' is represented by a holotype male and paratype female from Indonesia (Maluku Islands), with their depository also unknown. Similarly, the holotype female of '*M. exsiccatal'* is from Java, possibly held at MIZT, while *T. intermedia*, based on a holotype female from New Zealand (erroneously reported), also lacks a known depository.

Genus *Mesopteryx* Saussure, 1870

46. *Mesopteryx platycephala* (Stål, 1877)

= *Tenodera platycephala* Stål, 1877: 56. Brunner de Wattenwyl 1893: 67, ♀ and ♂ (Myanmar). Sjöstedt 1930: 10, 42, ♀ (type catalog).

= *Mesopteryx platycephala*: Wood-Mason 1882: 34–35, ♂ and ♀. Westwood 1889: 14. Kirby 1904b: 237 (India-N, Myanmar). Giglio-Tos 1912: 55–56, ♂and ♀ (Myanmar). Giglio-Tos 1927: 420 (India-E, Myanmar). Beier 1935: 94 (India, Myanmar). Ehrmann 2002: 220, ♀ (Cambodia, India, Myanmar). Ehrmann 2002: 220, ♀ (Cambodia, India, Myanmar). Otte and Spearman 2005: 188, ♀ (Indomalaya). Zhu et al. 2012: 214–215, 1–8, ♀. Mukherjee et al. 2014: 34, ♂ and ♀ (Cambodia, India, Myanmar, Nepal). Ehrmann and Borer 2015: 238, 265, ♂. Patel and Singh 2016: 30.

Type material. Holotype female, NHRS.

Type locality. Unknown.

Distribution. NE India, Nepal, Myanmar, Cambodia (Ehrmann 2002; Mukherjee et al. 2014; Ehrmann and Borer 2015; Schwarz et al. 2018; Kamila and Sureshan 2022).

Faunal element. Indochinese.

Subfamily Hierodulinae Brunner von Wattenwyl, 1893
Tribe Hierodulini Brunner de Wattenwyl, 1893
Genus *Rhombomantis* Ehrmann & Borer, 2015

47. *Rhombomantis tectiformis* (Saussure, 1870)

Rhombodera tectiformis Saussure, 1870: 232–233.

Type material. Holotype ♀ MHNG.

Type locality. India: Bombay.

Distribution. Pakistan, India, Nepal, Myanmar (Schwarz et al. 2018; Kamila and Sureshan 2022).

Faunal element. Indian.

48. *Rhombomantis fusca* (Lombardo, 1992)

Rhombodera fusca Lombardo, 1992: 97–100. Ehrmann 2002: 307. Otte and Spearman 2005: 268. Koçak and Kemal 2008: 46.
= *Hierodula brachynota* Wang and Dong 1993: 205, 207.
= *Rhombodera brachynota*: Ehrmann 2002: 306. Otte and Spearman 2005: 267.
= *Hierodula brachynota*: Koçak and Kemal 2008: 46. Zhu Xiao-Yu. et al. 2012: 246.

Type material. Holotype ♂, paratype ♀ Thailand-N: Prov. Chiang Mai-Samoeng, Maetaeng, DBUC.

Type locality. Thailand-N: Prov Chiang Mai: Samoeng, Maetaeng.

Distribution. China (Yunnan), Myanmar, Thailand, Laos, Malay Peninsula (Ehrmann and Borer 2015; Liu et al. 2021).

Faunal element. Indochinese.

Genus *Hierodula* Burmeister, 1838

49. *Hierodula bhamoana* Giglio-Tos, 1912

Hierodula bhamoana Giglio-Tos, 1912: 92–93.
= *Hierodula* [*Mantis*] *simulacrum* (Fabricius, 1793): Brunner von Wattenwyl 1893: 68.

Type material. Holotype ♀ MSNG.

Type locality. Myanmar-N: Bhamò.

Distribution. Myanmar (Ehrmann 2002).

Faunal element. Endemic in Myanmar.

50. *Hierodula grandis* Saussure, 1870

Hierodula grandis Saussure, 1870: 233.

Type material. Holotype ♂ MHNG, paratype ♀ MHNG.

Type locality. Bangladesh: Sylhit.

Distribution. NE India, Bangladesh, Myanmar, China (Ehrmann 2002; Mukherjee et al. 2014; Wang et al. 2020; Kamila and Sureshan 2022).

Faunal element. Bengal.

51. *Hierodula latipennis* Brunner von Wattenwyl, 1893

Hierodula latipennis Brunner von Wattenwyl, 1892: 69.
= *Hierodula unimaculata* nec Olivier, 1792: Zhu et al. 2012: 249–251.
= *Hierodula latipennis* Brunner von Wattenwyl, 1893: 69. Holotype (♀): Myanmar (Burma),
Carin Ghecù, MSNG.
= *Hierodula macrodentata* Wang, Zhou & Zhang, 2020: 6. Holotype (♂): China, Yunnan, SEM.

Type material. Holotype ♀ MSNG.

Type locality. Myanmar: Carin Ghecù, 1300–1400 m.

Distribution. China (Yunnan), Myanmar (Ehrmann 2002).

Faunal element. Indochinese.

52. *Hierodula multispinulosa* Brunner von Wattenwyl, 1893

Hierodula multispinulosa Brunner von Wattenwyl, 1893: 68–69.

Type material. Holotype ♀ NHMW?

Type locality. Myanmar-C: Mandalay.

Distribution. Myanmar (Ehrmann 2002).

Faunal element. Endemic in Myanmar.

Remark. The holotype might be lost.

53. *Hierodula patellifera* (Audinet-Serville, 1838)

Mantis patellifera Audinet-Serville, 1838: 185–186.
= *Mantis* (*Mantis*) *patellifera*: De Haan 1842: 70.
= *Hierodula patellifera*: Westwood 1889: 12, 27, 35.
= *Hierodula* (*Hierodula*) *patellifera*: Beier 1935: 203: 83.
= *Hierodula patellifera patellifera*: Ehrmann 2002: 180. Chatterjee and Srinivasan 2013: 131–135.
= *Mantis bipapilla* Audinet-Serville, 1839: 188–189 (synonymized by Hebard 1920: 58–59). Charpentier 1841: 291–292.
= *Mantis* (*Mantis*) *bipapilla*: De Haan 1842: 70.
= *Hierodula bipapilla*: Saussure 1871: 79–80. Borre 1883: 68. Westwood 1889: 12, 27, 34–35. Kirby 1904: 245. Shiraki 1911: 324–326. Giglio-Tos 1912: 96–98.
= *Hierodula* (*Hierodula*) *bipapilla*: Giglio-Tos 1927: 448. Vyjayandi and Narendran 2003: 315, 317.
= *Hierodula simulacrum*: Saussure 1869: 68. Saussure 1871: 77–78. Wood-Mason 1882: 30.
= *Hierodula simulacrum*: Borre 1883: 68.
= *Hierodula manillensis* Saussure, 1870: 233 (synonymized by Hebard 1920: 58–59). Ehrmann 2002: 180.
= *Hierodula* (*H.*) *manillensis*: Giglio-Tos 1912: 95–96. Giglio-Tos 1927: 447–448.
= *Hierodula raptoria* Stål, 1877: 38 (female) (synonymized by Giglio-Tos 1927: 447–448).
= *Hierodula dispar* Kirby, 1900: 146–147 (synonymized by Giglio-Tos 1927: 448).
= *Hierodula* (*H.*) *manillana* Giglio-Tos, 1912: 96 (synonymized by Hebard 1920: 58–49). Werner 1926: 228–229. Giglio-Tos 1927: 448. Ehrmann 2002: 180.
= *Hierodula* (*H.*) *patellifera manillana*: Beier 1935: 83.
= *Hierodula patellifera manillana*? Giglio-Tos, 1912: Ehrmann 2002: 180.
= *Hierodula saussurei* Kirby, 1904: 245 (synonymized by Hebard 1920). Werner 1926: 228–229.
= *Hierodula* (*H.*) *saussurei*: Giglio-Tos 1912: 94–95. Giglio-Tos 1927: 447.
= *Hierodula saussurei*: Werner 1930: 4. Ehrmann 2002: 180.
= *Hierodula* (*H.*) *assamensis* Mukherjee et al. 1995: 185, 201, 290–291.

Type material. Holotype ♂ MNHN, paratype ♀ MNHN.

Type locality. Java.

Distribution. India, China-S, Korea, Japan, Taiwan, Myanmar (this study), Philippines, Java, Sumba, New Guinea; introduced: Hawaii (Big Island; Ehrmann 2002).

Faunal element. Oriental; Wallacean; New Guinean; East Palearctic.

Remark. This species is documented for the first time in Myanmar through observational records available on iNaturalist (https://www.inaturalist.org/observations/142558577, https://www.inaturalist.org/observations/250140183) and two specimens collected from Myanmar housed in Natural History Museum (London).

54. *Hierodula venosa* Manuel, 1797

Mantis venosa Manuel, 1797: 639.
= *Mantis conspurcata* Lichtenstein, 1796: 79–80.
= *Mantis punctata* Stoll, 1813: 49.
= *Mantis vitrea* Stoll, 1813: 15.
= *Mantis* (*Hierodula*) *hybrida* Burmeister, 1838: 536.
= *Mantis bankae* Giebel, 1861: 111.
= *Mantis similis* Giebel, 1861: 112.
= *Hierodula novemdentata* Saussure, 1869: 68.
= *Hierodula daphne* Stål, 1877: 38.
= *Hierodula athene* Rehn, 1909: 180–182.

Type material. Type? ♀ ZMB.

Type locality. India-E: Tranquebar.

Distribution. India, Myanmar, Philippines, Sumatra, Borneo, Java.

Faunal element. Oriental.

Discussion

Of the 54 species assigned to a faunal element, only five were endemics of Myanmar and three had a typical Bengalese distribution, one of these also occurring in the East Palearctic. The most common pattern was the combination of an Indochinese and Sundaian distribution (15 species), while pure Indian and pure Indochinese distribution patterns with five and six species, respectively, were relatively rare. The same applies to six species for the combination of Indian and Indochinese distributions (i.e., North Oriental). While all these species had few cases of distributions beyond the Oriental realm, this was commonly observed for the 12 species widely distributed across the three major regions of the Oriental realm (Table 1).

The checklist provided here aims to build a foundation for future research, offering a comprehensive overview of currently known mantid species in Myanmar. It may facilitate comparative studies with neighboring regions, potentially revealing patterns of species distribution and endemism. It may also help to identify areas where further research is needed, guiding future survey efforts.

The data compiled here, for example, allow a biogeographic assessment of Myanmar and beyond. Thus, the entire mantid fauna of Myanmar clearly belongs to the Oriental realm sensu Wallace (1876). No Palearctic elements enter the country and, considering mantids, also its northernmost parts are clearly Oriental with no Palearctic influences. Interestingly, in the majority of cases the species found in Myanmar are restricted to the Oriental realm. The species passing the Wallace line, hereby entering the transition zone of Wallacea, is limited to three, supporting the general relevance of this biogeographic border (Mayr 1944; Simpson 1977). Only one species advances to New Guinea and hence to Australis, supporting the eastern border of Wallacea (i.e., the Lydekker line) as another important biogeographical border. These findings offer more support to the "old" biogeographical classifications (Wallace 1876; Müller 1980) and align with the multi-taxa study by Holt et al. (2013) classifying southern China as part of the Oriental realm and not as transition zone; these authors did not verify the Wallace line but only the Lydekker line.

Looking at the biogeographic structuring of these mantids within the Oriental realm reveals a rate of close to 10% Myanmar endemics. This is relatively low compared with islands (Kier et al. 2009), but is noteworthy in a country not really geographically isolated from the adjoining areas. This finding also underlies the Myanmar faunal element erected on analyses of distribution data of odonates (Heiser and Schmitt 2013). The more widespread species clearly assigned Myanmar to the Indochinese and not to the Indian sub-region (20 vs 5 species). Interestingly, elements widespread in both these sub-regions (i.e., 6 species) are relatively few, underlining the assumed split between these two regions (Schmitt 2020), in the case of mantids maybe be fostered by the Ganges delta. On the contrary, a common distribution in Indochina and Sundaland was observed for as many as 15 mantid species. Thus, the Isthmus of Kra, which has been demonstrated as an important biogeographic breaking-point in many species, including mammals, birds, and plants (Schmitt 2020), apparently is not of major importance for the distribution pattern of mantids. This might be explained by the drying of the sea during glacial periods and the complete exposure of the shelf area, which first was flooded only ca 500 ky ago (Salles et al. 2021). Apparently, mantids had good dispersal conditions via the dried Sunda shelf so that the recent geographic impediment via the Isthmus of Kra seems to be mostly irrelevant for their extant distributions. How this pattern might be reflected in the phylogeographic patterns within species is still awaiting resolution in future research. With a total of 12 species, taxa widely distributed all over the Oriental

Table 1. Numbers of mantid species endemic to Myanmar or present in four distinguished sub-regions of the Oriental realm and their combinations.

Faunal Element	Number of Species
Endemic in Myanmar	5
Bengal	3
Indian	5
Indochinese	6
Indochinese & Sundaian	15
North Oriental (Indian & Indochinese)	6
Oriental (Widespread in Oriental Realm)	12
Oriental & Wallacean	3
Oriental & East Palearctic	5
Old World	1

realm are only a small proportion of all species, thus again underlining the known strong sub-structuring within this realm (Heiser and Schmitt 2013; Schmitt 2020), which also holds true for mantids.

Based on known distributions and ecological factors, several mantid species are expected to occur in Myanmar, although their presence has yet to be confirmed. Species such as *Anaxarcha graminea*, *Hierodula tenuidentata*, *Tropidomantis gressitti*, and *Leptomantella tonkinae* are likely to inhabit the country's diverse ecosystems, given their presence in neighboring regions with similar environmental conditions. Recent discoveries like *Hierodula pistillinota* and *Hierodula confusa* further support the potential for new records with continued research, particularly in underexplored areas. However, some previously reported species, such as *Gonypeta brunneri*, *Theopompa servillei*, and *Rhombodera laticollis*, remain doubtful due to uncertainties in identification and the lack of confirmed specimens. Similarly, records of *Aethalochroa ashmoliana*, *Gonypeta punctata*, and *Toxoderopsis taurus* require further verification, as they may be the result of misidentifications or gaps in distribution data. The use of multiple data sources, including literature, museum collections, and online databases like GBIF and iNaturalist, provides a comprehensive approach to biodiversity documentation. This methodology enhances the reliability of findings and highlights the importance of integrating traditional taxonomic work (Marques et al. 2024). While online platforms offer valuable data, rigorous field studies and examination of museum specimens remain essential to confirm expected species and reassess doubtful records.

We recommend field studies to confirm the presence and evaluate the population status of the species listed in the checklist. Incorporating genetic studies might provide deeper insights into the biogeography of species, on the one hand maybe uncovering cryptic diversity and differentiation, or, on the other hand, potentially confirming population connectivity across entire ranges. Given the evolving nature of taxonomic research and the continuous emergence of new discoveries, regular updates to the checklist are crucial to maintain its relevance and accuracy (Marques et al. 2024).

One highlight of our checklist is the discovery of *Schizocephala bicornis* (Linné, 1758) in Myanmar expanding our understanding of the species' distribution in south-eastern Asia. This species is commonly known as the Indian grass mantid, as it is widespread particularly in southern India. It is a large species, with females up to 14.5 cm in length (Yadav and Painkra 2021) and belongs to the monotypic tribe Schizocephalini (Schwarz and Roy 2019). This mantis is a long, slender species that mimics grass, characterized by a narrow head with forward-protruding conical eyes, a triangular metazona, elongated slender legs, shortened fore coxae, and a long, triangular supra-anal plate (Fig. 1; Majumder et al. 2015). Its natural habitat consists of wet savannahs and high-growing grass layers, in which individuals can optimally camouflage themselves (Mukherjee et al. 1995). Although the presence of *S. bicornis* in Myanmar is not unexpected, given its known distribution in neighboring countries (Fig. 2; Mukherjee et al. 2017), this new record fills the hitherto assumed distribution gap, suggesting a more continuous distribution across the Indian subcontinent and south-eastern Asia. This discovery also underlines the need for more surveys and biodiversity assessments in this region to better understand the extant distributions of Mantodea species.

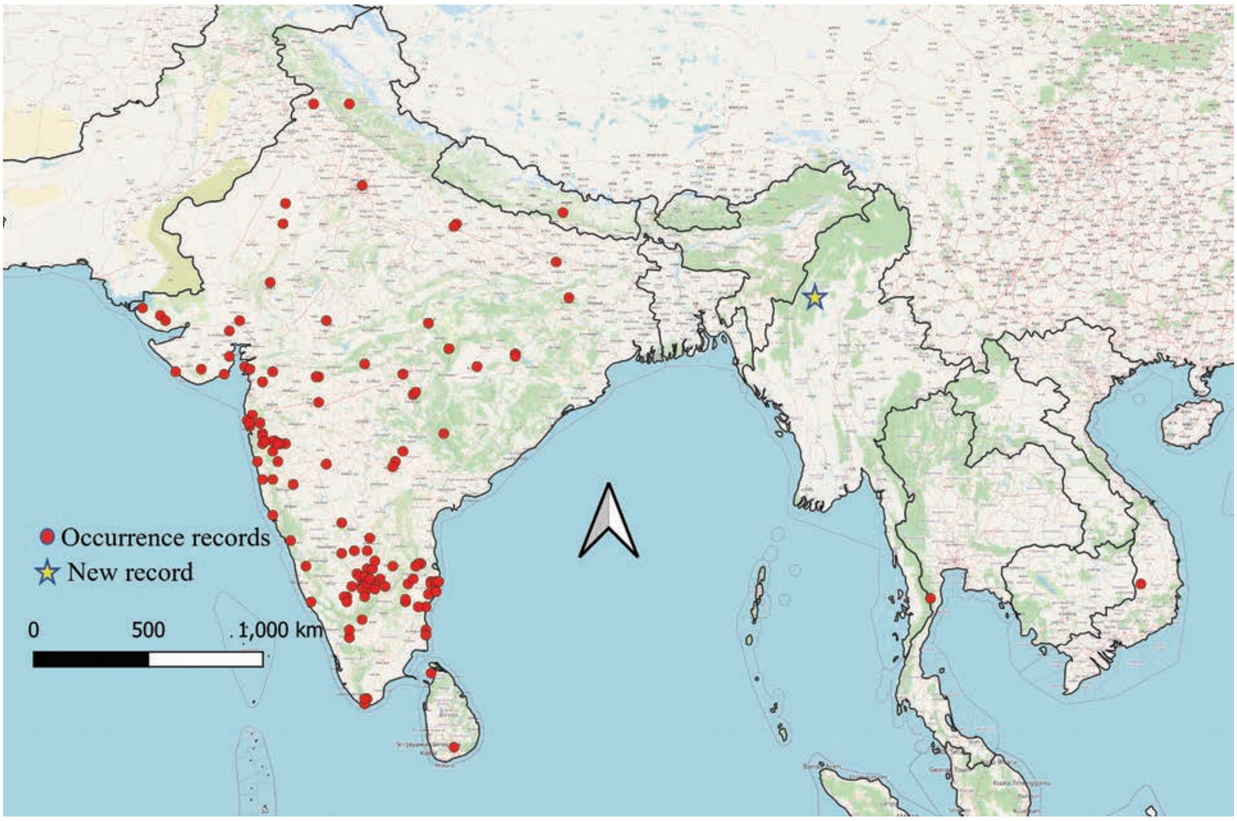

Figure 2. Distribution records of *Schizocephala bicornis*. Red circles representing previously documented locations, while the blue star highlights the newly identified record from Myanmar reported in this study and partly closing the formerly existing gap in the distribution.

In summary, this study not only broadens our understanding of Mantodea distribution in south-eastern Asia but also serves as a valuable resource for future entomological research in Myanmar. The combination of new distribution records and a comprehensive species checklist lays the basis for more detailed studies of Myanmar's rich insect fauna, thereby contributing to broader efforts in biodiversity conservation and taxonomic research in this region.

Acknowledgments

We are grateful to Evgeny Shcherbakov (Lomonosov Moscow State University, Russia) for his valuable feedback on the initial draft, which enhanced the quality of the manuscript. Our sincere thanks also go to Kris Anderson (alumnus at Cornell University, Las Vegas, USA) for generously sharing his research findings, which have been invaluable in updating and correcting the information on *Memantis fuliginosa* (Thunberg, 1815).We also express our gratitude to Tobias Malm, curator at the Swedish Museum of Natural History, Christoffer Fägerström, curator at the Lund Museum of Zoology (Sweden), and Alexander Riedel, curator at the Staatliches Museum für Naturkunde, Karlsruhe (Germany), for sharing important coordinates and data on *S. bicornis*. Lastly, we would like to thank Roberto Poggi (Civic Museum of Natural History "Giacomo Doria," Genoa, Italy) and Roberto Batiston (Museum of Archaeology and Natural Sciences "G. Zannato," Montecchio Maggiore, Italy) for their assistance with information on the type material of *Pseudempusa pavonina*.

Additional information

Conflict of interest

The authors have declared that no competing interests exist.

Ethical statement

No ethical statement was reported.

Funding

No funding was reported.

Author contributions

Study conception and design: Z. Mirzaee; data collection: Z. Mirzaee; data analysis: Z. Mirzaee; interpretation of results: Z. Mirzaee; draft manuscript preparation: Z. Mirzaee; visualization: Z. Mirzaee; critical feedback on the manuscript: T. Schmitt, M. Wiemers.

Author ORCIDs

Zohreh Mirzaee https://orcid.org/0000-0002-1496-8253
Martin Wiemers https://orcid.org/0000-0001-5272-3903
Thomas Schmitt https://orcid.org/0000-0002-1389-8396

Data availability

All of the data that support the findings of this study are available in the main text.

References

Audinet-Serville JGA (1838) Histoire naturelle des Insects Orthopteres. Roret, Paris, 776 pp. https://doi.org/10.5962/bhl.title.95609

Audinet-Serville JG (1839) Histoire naturelle des Insectes Orthoptères. Roret, Paris, 776 pp. https://doi.org/10.5962/bhl.title.16081

Aung TS, Hughes AC, Khine PK, Liu B, Shen XL, Ma KP (2023) Patterns of floristic inventory and plant collections in Myanmar. Plant Divers 45(3): 302–308. https://doi.org/10.1016/j.pld.2023.01.008

Beier M (1931) Neue und seltene Mantodeen aus dem Zoologischen Staatsinstitut und Zoologischen Museum in Hamburg. Mitteilungen aus dem Zoologischen Staatsinstitut und Zoologischen Museum in Hamburg 45: 1–21.

Beier M (1935) Mantodea, Fam. Mantidae, Subfam. Mantinae. Genera Insectorum, Fascicule 203: 1–146.

Beier M (1942) Beiträge zur Kenntnis der Insektenfauna Deutsch-Ostafrikas, insbesondere des MatengoHochlandes. V. Mantodea. – Annalen des Naturhistorischen Museums in Wien 52(1941):117–125.

Beier M (1966) Die Mantiden der Noona Dan Expedition nach den Philippinen und Bismarck Inseln. Noona Dan Papers 29: 361–370.

Blanchard CE (1840) Mantodea (8–13). In: Castelnau FLL (Ed.) Histoire naturelle des Insectes. Duméni 3 Paris, 672 pp.

Blanchard CE (1845) Mantodea (221–233). – Histoire des Insectes. Mantodea and Phasmodea. Librairie de Frimin Didot Frères, Paris, 524 pp.

Blanchard CE (1850) Histoire naturelle des Insectes (Mantodea and Phasmodea). Imprimerie Lacour, Paris, 1: 4 + 128 pp. [Mantodea: 1–19]

Bolivar I (1897) Les Orthoptères de St.-Joseph`s College à Trichinopoly (Sud de l`Inde). Annales de la Société Entomologique de France 66 (2): 282–316.

Borre de Preudhomme C (1883) Liste des Mantides du Musée Royal d'Histoire Naturelle de Belgique. Annales de la Société Entomologique de Belgique 27: 60–81. [Mantodea: 3–24]

Brannoch SK, Svenson GJ (2016) Leveraging female genitalic characters for generic and species delimitation in *Nilomantis* Werner, 1907 and *Ilomantis* Giglio-Tos, 1915 (Mantodea, Nilomantinae). Insect Systematics & Evolution 47(3): 209–244. https://doi.org/10.1163/1876312X-47032141

Brannoch SK, Wieland F, Rivera J, Klass K, Bethoux O, Svenson GJ (2017) Manual of praying mantis morphology, nomenclature and practices (Insecta, Mantodea) ZooKeys 696: 1–100. https://doi.org/10.3897/zookeys.696.12542

Brunner de Wattenwyl KB (1893) Révision du système des Orthoptères et description des espèces rapportées par M. Leonardo Fea de Birmanie. Annali del Museo di Storia Naturale di Genova 13: 1–230. https://doi.org/10.5962/bhl.title.5121

Burmeister H (1838) Fangheuschrecken. Mantodea. In: Handbuch der Entomologie. Zweiter Band. Besondere Entomologie. Zweite Abtheilung. Kaukerfe, Gymnognatha (Erste Hälfte; vulgo Orthoptera). Enslin, Berlin, 517–552.

Charpentier T von (1841) Einige Bemerkungen die Orthopteren betreffend, besonders in Bezug auf Burmeister's und Serville's Schriften über diese Insektenabtheilung (VII). Zeitschrift für die Entomologie 3 (2): 283–305.

Chatterjee P, Srinivasan G (2013) Morphological variation in *Hierodula patellifera patellifera* Serville, 1839 from India. Prommalia 1: 131–135.

Costello MJ, Michener WK, Gahegan M, Zhang ZQ, Bourne PE (2013) Biodiversity data should be published, cited, and peer reviewed. Trends in Ecology & Evolution 28(8): 454–61. https://doi.org/10.1016/j.tree.2013.05.002

De Haan W (1842) Bijdragen tot de Kennis der Orthoptera, Zoologie. Leyden, erhandelingen over de natuurlijke Geschiedenis der Nederlandsche overzeesche Bezittingen 45 + 248 pp.

Drury D (1770) Illustrations of Natural History of exotic Insects. White, London, 30 + 130 pp.

Ehrmann R (2002) Mantodea: Gottesanbeterinnen der Welt. Münster, Natur und Tier Verlag, Münster, 700 pp.

Ehrmann R, and Borer M (2015) Mantodea (Insecta) of Nepal: an annotated checklist. In Biodiversity and Environment of the Himalaya 5: 227–274.

Fabricius JC (1775) Systema Entomologiae. Mantodea & Phasmodea. Korte, Flensburgi et Lipsiae, 30 + 832 pp. [Mantodea: 268–279]

Fabricius JC (1781) Species Insectorum Mantodea & Phasmodea. Bohn, Hamburgi et Kilonii, 1: 8 + 552 pp. [Mantodea: 340–351]

Fabricius JC (1787) Mantissa Insectorum Mantodea & Phasmodea. - Prost, Hafniae 1: 20 + 348 pp. [Mantodea: 224–231]

GBIF.org (2024) GBIF Occurrence Download [accessed 21 August 2024]

Ghate HV, Jadhav SS, Sureshan PM, and Sharma RM (2021) Updated checklist of Indian Mantodea (Insecta). Journal of Threatened Taxa 13(6): 18578–18587. https://doi.org/10.11609/jott.5958.13.6.18578-18587

Giebel CGA (1861) Neue ostindische Schrecken. Zeitschrift für die gesammten Naturwissenschaften 18: 111–121.

Giglio-Tos E (1912) Mantidi esotici. V. Mantes, Tenoderae, Hierodulae et Rhomboderae. Bullettino della Società Entomologica Italiana 43: 3–167.

Giglio-Tos E (1914) Mantidi Raccolti da S. A. R. la Duchessa d'Aosta nella regione dei grandi laghi dell'Africa equatoriale. Revisione della sottofamiglia dei Toxoderini. Annuario del Museo Zoologico della Università di Napoli 4(15): 1–17.

Giglio-Tos E (1915) Mantidi esotici. Generi e specie nuove. Bullettino della Società Entomologica Italiana 46: 134–200.

Giglio-Tos E (1927) Das Tierreich. 50. Lfg. – Orthoptera Mantidae. Walter de Gruyter & Co., Berlin & Leipzig, xl + 707 pp. https://doi.org/10.1515/9783111430669

Hebard M (1920) Studies in Malayan, Papuan, and Australian Mantidae. Proceedings of the Academy of Natural Sciences of Philadelphia 71: 14–82.

Heiser M, Schmitt T (2013) Tracking the boundary between the Palaearctic and the Oriental region: new insights from dragonflies and damselflies (Odonata). Journal of Biogeography 40: 2047–2058. https://doi.org/10.1111/jbi.12133

Holt BG, Lessard JP, Borregaard MK, Fritz SA, Araújo MB, Dimitrov D, Fabre PH, Graham CH, Graves GR, Jønsson KA, Nogués-Bravo D, Wang Z, Whittaker RJ, Fjeldså J, Rahbek C (2013) An update of Wallace's zoogeographic regions of the world. Science 339: 74–78. https://doi.org/10.1126/science.1228282

Kamila AP, Sureshan PM (2022) An updated checklist of mantid fauna (Insecta: Mantodea) of India. Halteres 13: 15–34.

Kier G, Kreft H, Lee TM, Jetz W, Ibisch PL, Nowicki C, MutkeJ, Barthlott W (2009) A global assessment of endemism and species richness across island and mainland regions. Proceedings of the National Academy of Sciences 106(23): 9322–9327. https://doi.org/10.1073/pnas.0810306106

Kirby WF (1900) A monograph of Christmas Island (Indian Ocean). In: Charles W (Ed.) Andrews with descriptions of the fauna and flora by numerous contributors. Annals and Magazine of Natural History, London, 146–147.

Kirby WF (1903) Description of a new species of Mantidae referred to in the above paper. Zoologist 7 (4): 304.

Kirby WF (1904) A synonymic catalogue of Orthoptera. Vol. I. Orthoptera Euplexoptera, Cursoria, et Gressoria. British Museum (Natural History), London, x + 501 pp.

Koçak AÖ, Kemal M (2008) New synonyms and replacement names in the genus group taxa of Araneida. Centre for Entomological Studies Ankara, Miscellaneous Papers 139(140): 1–4.

Lichtenstein AAH (1796) Insekt. Ordo II. Hemiptera; Insekt. Class. II. Ulonata. In: Catalogus musei zoologici ditissimi Hamburgi, d III. Auktionis lege distrahendi. Sektio tertia continens Insekta. Schniebes, Hamburg, 77–85.

Linné C (1758) Systema naturae per regna tria naturae, secundum classes, ordines, genera, species, cum characteribus, differentiis, synonymis, locis. Tomus 1, editio decima, reformata. Laurentii Salvii, Holmiae, Stockholm, 824 pp. https://doi.org/10.5962/bhl.title.542

Liu QP, Liu ZJ, Wang GL, Yin ZX (2021) Taxonomic revision of the praying mantis subfamily Hierodulinae of China (Mantodea: Mantidae). Zootaxa 4951(3): 401–433. https://doi.org/10.11646/zootaxa.4951.3.1

Majumder A, Raha A, Mukherjee TK, Chandra K, Srinivasan G (2015) Mantis (Insecta: Mantodea) fauna of Chhattisgarh, India. Records of the Zoological Survey of India 115(4): 365–383. https://doi.org/10.26515/rzsi/v115/i4/2015/120700

Manuel BE, Olivier GA (1797) Histoire Naturelle, Insectes – Mantes. Encyclopédie Méthodique 7: 619–642.

Margules CR, Pressey RL (2000) Systematic conservation planning. Nature 405(6783): 243–53. https://doi.org/10.1038/35012251

Marques N, Soares CDM, Casali DM, Guimarães EC, Fava FG, Abreu JMDS, Moras LM, da Silva LG, Matias R, de Assis RL, Fraga R, Almeida SM, Lopes VG, Oliveira V, Missagia R, Carvalho EC, Carneiro NJ, Alves R, Souza-Filho P, Oliveira G, Miranda M, Tavares VDC (2024) Retrieving biodiversity data from multiple sources: making secondary data standardised and accessible. Biodiversity Data Journal 12: e133775. https://doi.org/10.3897/BDJ.12.e133775

Mayr E (1944) Wallace's line in the light of recent zoogeographic studies. The Quarterly Review of Biology 19(1): 1–14. https://doi.org/10.1086/394684

Mukherjee TK, Ghosh A, Hazra AK (1995) The mantid fauna of India (Insecta: Mantodea). Oriental Insects 29(1): 185–358. https://doi.org/10.1080/00305316.1995.10433744

Mukherjee TK, Ehrmann R, Chatterjee P (2014) Checklist of Mantodea (Insecta) from India. Priamus 30: 1015–8243.

Mukherjee TK, Iyer G, Chatterjee P (2017) Twenty-three new records of Mantodea (Insecta) from some states of India. Journal of Threatened Taxa 9(2): 9829–9839. https://doi.org/10.11609/jott.1936.9.2.9829-9839

Müller P (1980) Biogeographie. UTB, Verlag Eugen Ulmer, Stuttgart, 414 pp.

Olivier GA (1792) Encyclopedie Méthodique. Histoire Naturelle, ou Histoire Naturelle des Crustaces, des Arachnides et des Insectes (Paris) 7: 635–641.

Otte, D, Spearman L, Stiewe MBD (2023) Mantodea Species File Online. Version 5.0/5.0. [accessed 30 August 2024]

Patel S, Singh R (2016) Updated checklist and distribution of Mantidae (Mantodea: Insecta) of the world. International Journal of Research Studies in Zoology 2(4): 17–54. https://doi.org/10.20431/2454-941X.0204003

Rehn JAG (1909) A contribution to the knowledge of the Orthoptera of Sumatra. Bulletin of the American Museum of Natural History 26: 177–186.

Roonwal ML, Bhasin GD (1951) A systematic catalogue of the main identified entomological collections at the Forest Research Institute, Dehra Dun. Indian Forester 77(5): 313–318.

Roy R (2004) Révision et phylogénie des Choeradodini Kirby, 1904 (Dictyoptera, Mantidae). In: Bulletin de la Société entomologique de France 109(2): 113–128. https://doi.org/10.3406/bsef.2004.16095

Roy R (2009) Révision des Toxoderini sensu novo (Mantodea, Toxoderidae). Revue Suisse de Zoologie 116(1): 93–183. https://doi.org/10.5962/bhl.part.79491

Salles T, Mallard C, Husson L, Zahirovic S, Sarr AC, Sepulchre P (2021) Quaternary landscape dynamics boosted species dispersal across Southeast Asia. Communications Earth & Environment 2(1): 240. https://doi.org/10.1038/s43247-021-00311-7

Sathe TV, Vaishali PJ (2014) Report on nine new species of mantids (Insecta: Mantodea) and their insect pest predatory potential from agroecosystems of Kolhapur region. Journal of Entomology and Zoology Studies 2(5): 304–307.

Saussure H de (1869) Essai d'un Système des Mantides. Mittheilungen der Schweizerischen entomologischen Gesellschaft 3: 49–73.

Saussure H de (1870) Additions au système des Mantides. Mittheilungen der Schweizerischen entomologischen Gesellschaft 3: 221–244.

Saussure H de (1871) Mélanges orthoptérologiques. IIIme Fascicule. IV. Mantides. Mémoires de la Société de physique et d'Histoire naturelle de Genève 21(2): 1–214.

Schmitt T (2020) Molekulare Biogeographie: Gene in Raum und Zeit. UTB. Haupt Verlag, Bern, 504 pp. https://doi.org/10.36198/9783838586793

Schwarz CJ, Konopik O (2014) An annotated checklist of the praying mantises (Mantodea) of Borneo, including the results of the 2008 scientific expedition to Lanjak Entimau Wildlife Sanctuary, Sarawak. Zootaxa 3797(1): 130–168. https://doi.org/10.11646/zootaxa.3797.1.12

Schwarz CJ, Roy R (2019) The systematics of Mantodea revisited: an updated classification incorporating multiple data sources (Insecta: Dictyoptera). Annales de la Société entomologique de France (NS) 55(2): 101–196. https://doi.org/10.1080/00379271.2018.1556567

Schwarz CJ, Ehrmann R, Borer M, Monnerat C (2018) Mantodea (Insecta) of Nepal: corrections and annotations to the checklist. Biodiversität und Naturausstattung im Himalaya 6: 201–47.

Seba A (1765) Description exacte des principales curiositez naturelles du magnifique Cabinet d'Albert Seba. Amsterdam, Thesaurus 4: 42 + 226 pp. [108 pls.]

Shcherbakov E, Anisyutkin L (2018) Update on the praying mantises (Insecta: Mantodea) of South-East Vietnam. In Annales de la Société entomologique de France (NS) 54(2): 119–140. https://doi.org/10.1080/00379271.2018.1447394

Simpson GG (1977) Too many lines; the limits of the Oriental and Australian zoogeographic regions. Proceedings of the American Philosophical Society 121(2): 107–120.

Sjöstedt Y (1930) Orthopterentypen im Naturhistorischen Reichsmuseum zu Stockholm. Arkiv för Zoologi 21A: 1–43.

Stål C (1877) Systema Mantodeorum: essai d'une systématisation nouvelle des Mantodées. Bihang till Kongliga Svenska Vetenskaps Akademiens Handlingar 4: 1–91.

Stoll C (1787) Represéntation exactement colorée d'après nature des spectres, des mantes, des sauterelles, des grillons, des criquets et des blattes. Qui se trouvent dans les quatre parties du monde, l'Europe, l'Asie, l'Afrique et l'Amérique. J. C. Sepp, Amsterdam, 9 + 56 pp. [18 pls]

Stoll C (1813) Représentation exactement colorée d'après nature des Spectres ou Phasmes, des Mantes, des Sauterelles, des Grillons, des Criquets et des Blattes. Qui se trouvent dans les quatre parties du monde, l'Europe, l'Asie, l'Afrique et l'Amérique. J. C. Sepp, Amsterdam, 9 + 79 pp. [25 pls.]

Sureshan PM, Sambath S (2009) Mantid (Insecta: Mantodea) fauna of old Bihar (Bihar and Jharkhand) with some new records for the state. Records of the Zoological Survey of India 11–26. https://doi.org/10.26515/rzsi/v109/i3/2009/158988

Thunberg CP (1815) Hemipterorum maxillosorum genera illustrata – plurimisque novis speciebus ditata ac descripta. Mémoires de l'Académie 5: 211–301. [1 pl.]

Tinkham ER (1937) Studies in Chinese Mantidae (Orthoptera). Lingnan Science Journal 16(4): 551–572. [pl. 17]

Uvarov BP (1927) A new mantid from Burma. Annals and Magazine of Natural History 9(19): 658–659. https://doi.org/10.1080/00222932708655557

Wallace AR (1876) The geographical distribution of animals. McMillian & Co, London, 576 pp.

Wang T, Dong D (1993) Three new species of mantids from Yunnan Province, China (Mantodea). Zoological Research 14(3): 203–207.

Wang Y, Zhou S, Zhang YL (2020) Revision of the genus *Hierodula* Burmeister (Mantodea: Mantidae) in China. Entomotaxonomia 42(2): 1–20. https://doi.org/10.11680/entomotax.202010

Werner F (1921) Über Mantodeen aus Niederländisch-Indien. Treubia. 2(1): 125–135.

Werner F (1925) Vierter Beitrag zur Kenntnis der Mantodeen von Niederländisch-Indien. Treubia 6 (3–4): 476–486. [pl. 24]

Werner F (1926) Zur Kenntnis der Mantodeen der Philippinen. Konowia 5(3): 227–232.

Werner F (1930) Über asiatische Mantideen aus dem naturhistorischen Reichsmuseum in Stockholm. Arkiv för Zoologi 21 A(34): 1–10. [3 pls.] https://doi.org/10.5962/bhl.part.1498

Werner F (1933) Neue Orthopteren im Naturhistorischen Museum zu Basel. Verhandlungen der Naturforschenden Gesellschaft in Basel 43: 1–3.

Westwood JO (1835) Insectorum arachnoidumque novorum decades duo. Zoological Journal 5: 440–453. [pl. 22]

Westwood JO (1837) Illustrations of Exotic Entomology. Bohn 3: 58–59.

Westwood JO (1889) Revisio Insectorum Familiae Mantidarum, speciebus novis aut minus cognitis descriptis et delineates. Gurney & Jackson, London, 53 pp.

Wieland F (2008) The genus *Metallyticus* reviewed (Insecta: Mantodea). Species, Phylogeny and Evolution 1(3): 147–170.

Wood-Mason J (1876) On the geographical distribution of *Schizocephala*, a genus of Mantidæ. Journal of Natural History 18(107): 439–439. https://doi.org/10.1080/00222937608682072

Wood-Mason J (1878) XVI.–Notes on new and little-known Mantidæ. Journal of Natural History 1(2): 143–147. https://doi.org/10.1080/00222937808682304

Wood-Mason J (1882) On new and little-known Mantodea. Journal of the Asiatic Society of Bengal 51(2): 21–36.

Wood-Mason J (1889) A catalogue of the Mantodea, with descriptions of new genera and species, and an enumeration of the specimens, in the collection of the Indian Museum, Calcutta. Annals and Magazine of Natural History 4(23): 365–368. https://doi.org/10.1080/00222938909460543

Wood-Mason J (1891) A Catalogue of the Mantodea, with descriptions of new genera and species, and an enumeration of the specimens, in the Collection of the Indian Museum, Calcutta 2: 49–66.

Wu C, Liu CX (2021) Taxonomic revision of the genus *Phyllothelys* Wood-Mason (Mantodea: Hymenopodidae) from China. Annales de La Société Entomologique de France (NS) 57(5): 449–480. https://doi.org/10.1080/00379271.2021.1973560

Yadav RS, Painkra GP (2021) Mantids (Insecta: Mantodea) of Uttar Pradesh, India. Journal of Threatened Taxa 13(6): 18578–18587. https://doi.org/10.11609/jott.5958.13.6.18578-18587

Zhu XY, Wu C, Yuan QZ (2012) Mantodea in China. Xiyuan Publishing House, Beijing, 331 pp.